# University of Oslo

Vittoria Mallia

# Potential endocrine disrupting activity of cyanobacteria – possible roles for microcystins

**Thesis submitted for the degree of Philosophiae Doctor**

Department of Chemistry

Faculty of Mathematics and Natural Sciences

Norwegian Veterinary Institute of Oslo

MSCA-ITN-2016 PROTECTED

2020

*To my Dad,*

*The best human being I have ever met.*

*"Life is not easy for any of us. But what of that? We must have perseverance and above all confidence in ourselves. We must believe that we are gifted for something and that this thing must be attained."*

*Marie Curie*

# TABLE OF CONTENTS

# ACKNOWLEDGMENTS

This is the hardest chapter to write for me, but I am deeply grateful and I will do my best to put this gratitude in a few honest and informal words. Much more thoughts and "thank you", already said or still to say, deserve to be better expressed in private.

This thesis comes from three years of work (June 2017-July 2020), mainly spent in the Chemistry and Toxinology Research Group of the Norwegian Veterinary Institute of Oslo. I would like to start with a big thank you to all the people of this group, naming Ida above all, for these years together. I learnt a lot with you. Time has flown.

A big thanks to the University of Oslo. I met great people and learnt many things there.

I would like to thank the Marie Skłodowska-Curie PROTECTED ITN, for funding my PhD, for teaching me so many things and giving me so many possibilities. I am deeply grateful to Lisa and Katie, to all the people involved in the project, especially those ones I could work with during my secondments. A big thought for my friends, the wonderful ESRs. Thanks for the moments we shared. You have been a real and precious family for me. Thanks to the people I have worked with in Belfast. A special thanks to Maeve. And a special thanks to Emma, for her friendship and support during the secondment and for the paper. Thanks to those ones who made my papers and my thesis becoming something real.

I would like to thank (in advance) the opponents, for the time they will spend on this thesis.

A huge thank you to my main supervisor Silvio (Dr Uhlig), who supported my work with no rest from the beginning, managing also my winter moods, deeply affected by the lack of light. Another huge thank you to my co-supervisors in Oslo, Gunnar (Dr Eriksen), Morten (Dr Sandvik) and Frode (Prof. Rise), for their help and support, different in quantity, but always of absolute quality. And thank you to Chris (Dr Miles), who co-supervised me from the other side of the World as if he was only a few meters far away! All of you gave a real contribution to my scientific and personal growth and I feel very lucky for that.

Thanks to my dear Amritha. We shared the office, the "miserable PhD-life", food, laughs, complaining, stress and fun. It wouldn't have been the same without you. Thanks to Ana for bringing into my Norwegian life so much light (or maybe it was the red of your hair…), fun, chocolate, shitty music, and that Southern spirit I needed. My sarcasm found its comfort zone together with yours. Thanks to Carlos and Ynthe, to complete the group of my wonderful office-mates.

Thank you Norway, Oslo and my peaceful place, Vigelandsparken. I can call "home" more than once place now, and this is a great privilege. Thanks to my Italian friends in Oslo, who helped fighting the "nostalgia canaglia". Thanks to Andrea and Tiziano, for their continuous help and a bit of "donca" (always appreciated).

Thanks to all those people that (more or less) recently, even without knowing it, supported me with unexpected precious words, thoughts, smiles, but also live workouts, zoom chats, texts on social networks, so powerful for surviving this crazy 2020.

Thanks again and again to Prof. Cruciani, for many precious advices during these years.

Thanks to my Friends in Italy. I am deeply grateful to have you in my life and it is not possible to express in few words how much important your friendship has been to make me feel better any time I was struggling with my PhD and my "up & down" mood in these (thirty)three years. You are my biggest achievement if I think about my whole life. I would have special words for each of you, but I will simply write your names, to have you impressed not only in my heart, but also in such an important goal. Andrea, Giorgio and Roby, my cetriolini. Chiara, Vale and Stefy, my precious amichenji. Alessia and Susy, my socio Ghianda, Gruccio and Giulia, Lucia, Agnese, Elena, Marta, Chiara; The Bellini's family.

A very special thanks to my "bone e acculturate" women, Mary, Elisa, Chiara and Annarita. I love you all so much that I can even share food with you and you know what this means.

Thanks to my smart, wonderful sisters, Agni, Giorgina and Enrica_"forever5yearsoldObina". I am so proud of you and so grateful I have been and I am so lucky having you growing up around me.

Thanks to my big Italian family and especially to Nonna Enrica and Loretta, for so many things. So many.

A special thanks to my boyfriend, Nicola. I could write another thesis (just kidding, when it's enough it's enough. Four is enough.) on how much lucky and grateful I am to have you in my life, always supporting my ambitions and needs, with so much love and enthusiasm, and excellently overcoming distances…and thank you for considering me such a smart scientist to be likely the next Nobel prize for Chemistry. Well, I will never be of course, but you can believe that if you want to, I don't mind :) 50% of this thesis is yours!

Thank you Norwegian airlines, because you made me think Italy was so close to Norway that I could go whenever I wanted. And "thank you" SARS-CoV-2, to make me understand that… well, first of all I was overestimating the power of Norwegian airlines, and then, that even if being very small you can do huge things in your life. Very HUGE.

I think I should thank myself too, shouldn't I? My heart survived many things in these years, including living in, and traveling, Countries where it is allowed to put pineapple on pizza.

Thank you Dad, my Roni. I name you in the end, but you will be always the first one I must thank for all I can have and do in my life.

*"Grazie a chi*
*Mi ha regalato un movimento*
*Allontanandomi da qualcosa*
*E avvicinandomi a qualcos'altro"*

# SUMMARY

Cyanobacteria are cosmopolitan photosynthetic prokaryotes, which can form dense accumulations in aquatic environments. Some cyanobacterial species are able to synthesize a number of biologically active metabolites, including potent toxins (cyanotoxins), and may release them in the waters. The best known cyanotoxins are the microcystins (MCs), a family of cyclic heptapeptides sharing a common core structure, including about three hundred reported congeners. MCs are produced by several cyanobacterial genera, including *Microcystis* and *Planktothrix*. Cyanobacterial toxins may compromise the water quality and result in harm to invertebrates and vertebrates including humans.

Among the harmful effects cyanobacterial bioactive metabolites may exert on organisms, a relatively poorly investigated one is the potential interference with the endocrine system. Compounds interfering with the endocrine system are called endocrine disruptors (EDs), and represent a current major concern. ED activity can happen through a variety of mechanisms, targeting different steps in the system's functions and result in a variety of unwanted effects. Scientific literature about cyanobacteria as EDs is relatively limited, and mainly focused on the investigation of microcystin-LR (MC-LR), the main and most studied congener of the MC family. Several animal studies reported MC-LR as having estrogenic effect and reproductive toxicity, possibly related to ED activity. However, the role of MC congeners other than MC-LR, as well as the relative role of MCs vs. other cyanobacterial bioactive metabolites, have not been clarified. The major mechanisms of cyanobacterial interference with endocrine pathways deserve clarification, too.

This thesis' work aimed to investigate cyanobacteria as EDs, with a focus on MCs' role and on their mechanisms of action. A parallel aim was the structural elucidation of new MC congeners. Extracts from a collection of 27 cyanobacterial strains belonging to the *Microcystis* and *Planktothrix* genera, including MC-producing and non-MC-producing strains, were used for investigation.

*In vitro* assays were used to investigate ED activity. In particular, reporter gene assays (RGAs) on nuclear estrogen, androgen and glucocorticoid receptors (**Paper II**), a human liver microsome (HLM) assay for 17β-estradiol biotransformation/phase I metabolism (**Paper II**), and the H295R steroidogenesis assay (**Paper III**) were used. The first assay focused on receptor-mediated mechanisms of ED activity, while the other two focused on non-receptor-mediated mechanisms (i.e. interference with hormone metabolism or synthesis, respectively). In addition, a combination of simple and complementary chemical tools, such as liquid chromatography–mass spectrometry (LC–MS), nitrogen-15 ($^{15}$N)-labeling and functional derivatization reactions were used for structural elucidation of MCs (**Paper I**).

Cyanobacteria (both extracts and pure MCs) showed ED activity. Receptor-mediated mechanisms did not appear to be the main mechanisms of action for estrogenic activity, neither in presence nor in absence of MCs in the cyanobacterial extracts. For androgen and glucocorticoid receptors, further studies are needed. Pure MC-LR as well as a *Microcystis*

*aeruginosa* strain that produced MC-LR, showed an effect on 17β-estradiol biotransformation/phase I metabolism products. In particular, while the overall 17β-estradiol depletion was not significantly affected by either MC-LR or the *M. aeruginosa* extract, a significant change in the ratio of biotransformation products/metabolites was observed. The investigation window was limited (in terms of monitored products/metabolites) due to the preliminary nature of this study. However, this constitutes an interesting starting point for further investigation of a wider range of metabolites. Indeed, the ratio imbalance may favor compounds that lead to pathophysiological outcomes. Cyanobacterial extracts from *M. aeruginosa* strains and pure MCs had an effect on steroidogenesis, that is, the process of steroidal hormone biosynthesis. Results suggested an opposite tendency of MCs compared to other bioactive *M. aeruginosa* metabolites on the modulation of steroidal hormone production, although further studies would be necessary to elucidate the mechanism behind this modulation.

Cyanobacterial ED activity effects are real, although further investigation is needed to clarify modes of action. ED activity investigation should go together with structural elucidation of cyanobacterial bioactive metabolites, MCs included, due to the interdependency of metabolite structure and bioactivity.

# ABBREVIATIONS

| | |
|---|---|
| Adda | 3*S*-amino-9*S*-methoxy-2*S*,6,8*S*-trimethyl-10-phenyldeca-4*E*,6*E*-dienoic acid |
| ADMAdda | 9-*O*-acetylDMAdda |
| AIF | All ion fragmentation |
| APCI | Atmospheric-pressure chemical ionization |
| ATP | Adenosine triphosphate |
| CID | Collision-induced dissociation |
| Cit | Citrulline |
| CYP | Cytochrome P450 |
| DC | Direct current |
| Dha | Dehydroalanine |
| Dhb | Dehydrobutyrine |
| DHEA | Dehydroepiandrosterone |
| DIA | Data-independent acquisition |
| DMAdda | 9-*O*-demethylAdda |
| DMSO | Dimethyl sulfoxide |
| DNA | Deoxyribonucleic acid |
| D-Masp | *iso*-linked D-β-methylaspartic acid |
| EC | European Commission |
| ED | Endocrine disruptor/disrupting |
| EDC | Endocrine disrupting chemical |
| EFSA | European Food Safety Authority |
| ESA | European Space Agency |

| | |
|---|---|
| ESI | Electrospray ionization |
| FS | Full scan |
| FSH | Follicle-stimulating hormone |
| FT-ICR | Fourier-transform ion cyclotron resonance |
| GnRH | Gonadotropin-releasing hormone |
| GSH | Glutathione |
| Har | Homoarginine |
| HCD | High-energy collisional dissociation |
| HLM | Human liver microsome |
| HPA | Hypothalamic-pituitary-adrenal |
| HPG | Hypothalamic-pituitary-gonadal |
| HPGL | Hypothalamic-pituitary-gonadal-liver |
| HPI | Hypothalamic-pituitary-interrenal |
| HPLC | High-performance liquid chromatography |
| HPT | Hypothalamic-pituitary-thyroid |
| HRMS | High-resolution mass spectrometry |
| HSD | Hydroxysteroid dehydrogenases |
| IARC | International Agency for Research on Cancer |
| ILO | International Labour Organization |
| IPCS | International Programme on Chemical Safety |
| ip/iv | Intraperitoneal/intravenous |
| ITMS | Ion trap mass spectrometry |
| KC | Key characteristic |
| LC | Liquid chromatography |

| | |
|---|---|
| LH | Luteinizing hormone |
| LC–MS | Liquid chromatography–mass spectrometry |
| LIT | Linear ion trap |
| LTQ | Linear trap quadrupole |
| *luc* | Luciferase (gene) |
| MC | Microcystin |
| MCP | Microchannel plate |
| Mdha | *N*-methyldehydroalanine |
| Mdhb | *N*-methyldehydrobutyrine |
| MRM | Multiple reaction monitoring |
| MS | Mass spectrometry |
| Mser | *N*-methylserine |
| MTT | 3-(4,5-dimethylthiazol-2-yl)-2,5-diphenyltetrazolium bromide |
| $MS^n$ | Multiple-stage mass spectrometry |
| MS/MS | Mass spectrometry/mass spectrometry (same as tandem MS) |
| NADPH | Nicotinamide adenine dinucleotide phosphate |
| NIVA | Norsk institutt for vannforskning/Norwegian institute for water research |
| NMR | Nuclear magnetic resonance |
| NOD | Nodularin |
| NORCCA | Norwegian culture collection of algae |
| NRCC | National Research Council of Canada |
| NRPS | Non-ribosomal peptide synthetase |
| OATP | Organic anion-transporting polypeptide |
| ODS | Octadecylsilane |

| | |
|---|---|
| PKS | Polyketide synthase |
| POP | Persistent organic pollutant |
| PP | Protein phosphatase |
| PRM | Parallel reaction monitoring |
| Q | Quadrupole |
| QqQ | Triple quadrupole |
| RDBE | Ring/double-bond equivalent |
| RF | Radio frequency |
| RGA | Reporter gene assay |
| RP-LC | Reversed-phase liquid chromatography |
| SAR | Structure–activity relationship |
| SRE | Steroid response element |
| SRM | Selected reaction monitoring |
| SIM | Selected ion monitoring |
| StAR | Steroidogenic acute regulatory protein |
| Tandem MS | Tandem-mass spectrometry (same as MS/MS) |
| TDI | Tolerable daily intake |
| TQMS | Triple-quadrupole mass spectrometer |
| TOF | Time of flight |
| UHPLC | Ultrahigh-performance liquid chromatography |
| UNEP | United Nations Environmental Programme |
| VTG | Vitellogenin |
| *vtg1* | Vitellogenin 1 (gene) |
| WHO | World Health Organization |

# PROTEINOGENIC L-AMINO ACID ABBREVIATIONS

| AMINO ACID* | 3-letter abbreviation | 1-letter abbreviation |
|---|---|---|
| Alanine | Ala | A |
| Arginine | Arg | R |
| Asparagine | Asn | N |
| Aspartic acid | Asp | D |
| Cysteine | Cys | C |
| Glutamic acid | Glu | E |
| Glutamine | Gln | Q |
| Glycine | Gly | G |
| Histidine | His | H |
| Isoleucine | Ile | I |
| Leucine | Leu | L |
| Lysine | Lys | K |
| Methionine | Met | M |
| Phenylalanine | Phe | F |
| Proline | Pro | P |

| | | |
|---|---|---|
| Serine | Ser | S |
| Threonine | Thr | T |
| Tryptophan | Trp | W |
| Tyrosine | Tyr | Y |
| Valine | Val | V |

*For completeness, all proteinogenic L-amino acids are listed, including those not mentioned in the thesis.

# 1. AIMS OF THE STUDY

The aim of this work was to investigate the potential role of bioactive metabolites produced by cyanobacteria (photosynthetic prokaryotes, also known as "blue–green algae") as endocrine disruptors (EDs), that is, compounds able to interfere with the endocrine (hormonal) system homeostasis.

Cyanobacteria and EDs represent two global concerns, even independently, in terms of environmental, human and wildlife health. Filling knowledge gaps on both topics, as well as investigating their overlap, helps to assess potential related risks.

This study focused on the *Microcystis* and *Planktothrix* cyanobacterial genera. Some species belonging to these genera are able to produce, among other metabolites, microcystins (MCs), the most known and widespread family of toxins produced by cyanobacteria. A special interest was reserved to the potential role of MCs as EDs. Since structure and activity of a compound are interconnected, a concurrent aim was to structurally describe previously undescribed MC congeners.

The goals of the work were:

1) Investigation of chemical **structures** of new MC congeners (**Paper I**).

2) Investigation of the potential endocrine disrupting **activity** and **related mechanisms** of action, of cyanobacterial extracts and pure MCs (**Paper II**, **Paper III**).

## 2. LIST OF PAPERS

**PAPER I**

**Mallia, V.**; Uhlig, S.; Rafuse, C.; Meija, J.; Miles, C. O., Novel microcystins from *Planktothrix prolifica* NIVA-CYA 544 Identified by LC–MS/MS, functional group derivatization and $^{15}$N-labeling. *Mar. Drugs* **2019**, *17*, 643.

**PAPER II**

**Mallia, V.**; Ivanova, L.; Eriksen, G.S.; Harper, E.; Connolly, L.; Uhlig, S., Investigation of *in vitro* endocrine activities of *Microcystis* and *Planktothrix* cyanobacterial strains. *Toxins* **2020**, *12*, 228.

**PAPER III**

**Mallia, V.**; Verhaegen, S.; Styrishave B.; Eriksen, G.S.; Johannsen, M.L.; Ropstad, E.; Uhlig, S., Microcystins and *Microcystis aeruginosa* extracts modulate steroidogenesis differentially in the human H295R adrenal model *in vitro*.

*Submitted manuscript*

# 3. INTRODUCTION

## 3.1 Cyanobacteria

### 3.1.1 General features

Cyanobacteria are ancient (around 3 billion years old) photosynthetic prokaryotes [1, 2], which are distributed worldwide. They are also commonly known as "blue–green algae", although strictly speaking the term algae refers only to eukaryotes. This way of naming them is mainly related to their appearance when they form massive accumulations on water surfaces and shorelines, and to their ability for oxygenic photosynthesis (which is also true for algae).

In addition, they are not necessarily blue–green, that is "cyano" [3]. Cyanobacteria can exhibit a wide range of colors. The prefix "cyano" refers to their characteristic accessory pigment phycocyanin, often masked by the green chlorophyll *a* or by other accessory pigments [3, 4].

Greenish cyanobacterial mass accumulations are very well visible to the naked eye. Single cells of cyanobacteria, however, have microscopic dimensions with different morphologies depending on the species [5].

Mentioning species, cyanobacterial taxonomy is a topic that is still an open battlefield. Cyanobacteria were established as prokaryotes only in the 1960s [6] and regarding genera and species identification, the debate is still significant, especially because of the not always reconcilable outcomes from the traditional cellular morphology approach, and more recent molecular methods based on gene sequencing. For the reader to have at least an idea, here is the example of the CyanoDB database (http://www.cyanodb.cz/), which includes 387 genera and 1506 species [7, 8], but being aware that these numbers can change depending on the chosen approach for identification. In any case, there are thousands of existing species, including both already recorded species as well as species predicted to exist [9]. Among all genera, *Microcystis* and *Planktothrix* were the two that were included in the collection used for this work (see section 4.1 Cyanobacterial collection). They are briefly described in the following sub-section.

#### 3.1.1.1 *Microcystis* and *Planktothrix* genera

*Microcystis* and *Planktothrix* genera (**Figure 1**) are among the most widespread freshwater cyanobacterial genera. Both include species that can synthetize MCs [10-12].

The genus *Microcystis* has been reported from almost all over the world [13]. This genus includes several species, known to form massive accumulations and produce toxins. The best known is *M. aeruginosa*. *Microcystis* spp. are unicellular, usually forming gelatinous colonies [14]. They can accumulate on the water surface, thanks to their floating ability, as well as moving along the water column of shallow, turbid water systems to absorb phosphorous suspended from sediments [15].

The genus *Planktothrix* is characterized by multicellular filaments [10]. *Planktothrix* spp. are very efficient light harvesters, thanks also to accessory pigment–protein complexes (blue–green phycocyanin and red phycoerythrin). They can grow at low light intensities, like in turbid or

deeper water, at the thermocline (the transition layer between the warmer surface water layer and the colder deep-water layer) [13]. *P. rubescens* and *P. agardhii* are the two most abundant and common species [16]. *P. prolifica* is another species that was a main one in this thesis' work (**Paper I**).
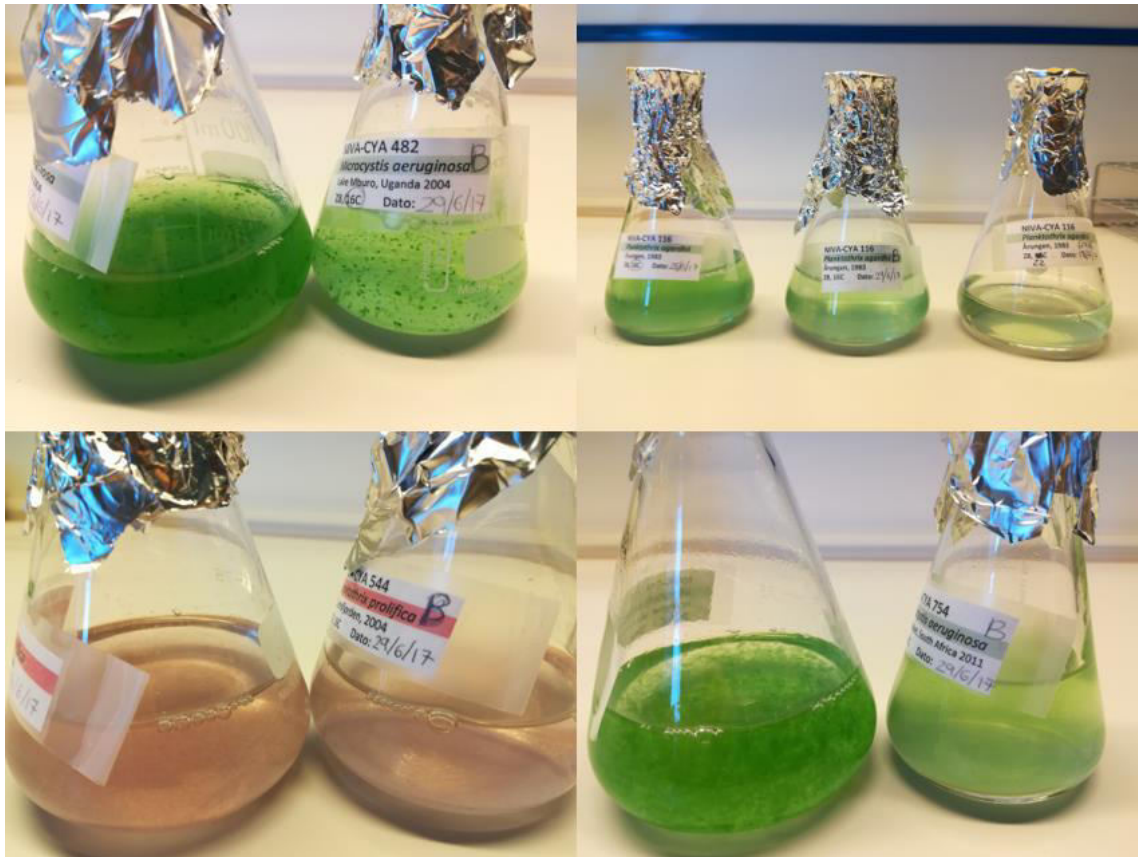


**Figure 1.** Cyanobacterial cultures of species belonging to the *Microcystis* and *Planktothrix* genera, from the collection used for this thesis' work.

### 3.1.2 Cyanobacterial growth, accumulation and metabolites production

Cyanobacteria are highly resistant and resilient and are able to survive and grow in extreme and hostile environments (e.g., with high salinity, very high or very low temperatures, high solar irradiance and low-light) and conditions (e.g., nutrient-limiting conditions) [2]. Cyanobacteria are commonly found in aquatic environments, such as fresh, brackish and marine waters, both on the water surface (planktonic species, in dispersed or aggregated form) and on the bottom sediment (benthic species). They can also be attached to shoreline rocks or sediments, or they can live in symbiosis with fungi or plants (e.g. lichens). Although less studied, terrestrial cyanobacteria exist and show high strain diversity, too [17].

Two main factors affect cyanobacterial growth: the availability of nutrients and the availability of light, both essential to the photosynthetic process of converting minerals and $CO_2$ into biomass, thanks to light energy. The thermal stratification of the water column (according to seasons) is also important. Indeed, buoyant cyanobacteria may adjust their position according to light accessibility, shading and outcompeting other organisms. Competition, predation and parasitism are co-factors affecting their growth as well [18].

In particular, eutrophication (excessive availability of nutrients, especially phosphates) of water bodies such as lakes and ponds, lead to growth becoming overgrowth and excessive accumulation, also known as a "bloom".

### 3.1.2.1 Cyanobacterial blooms

A cyanobacterial bloom is the result of a massive increase in cyanobacterial biomass (**Figure 2**), usually in a relatively short time frame, from between a few days to a couple of weeks [18]. It often causes a marked visible discoloration of the water [3].



**Figure 2.** Cyanobacterial bloom in the Baltic Sea (photo credit: European Space Agency, ESA, 2019).

Depending on the cyanobacterial species composing the blooms, they can be toxic to the aquatic ecosystem and surrounding environment. Toxic cyanobacterial metabolites released in the bloom can kill fish, mammals and birds [19, 20]. They may cause human illness or even death, when contaminated water bodies are sources of drinking water or used for fishing or recreational purposes [13]. Cyanobacteria can coexist in blooms together with other types of algal microorganisms. Blooms' dangerous character goes beyond potential productions of toxic metabolites. The biomass of microorganisms itself may clog gills of fish and invertebrates, smooth and cover corals and submerge aquatic vegetation [21]. The excessive growth of biomass could lead to an extreme oxygen depletion once the biomass decays and this may be problematic for other life forms in the water.

Blooms are increasing in frequency, magnitude and duration on a global scale [3]. They often occur naturally, even in pristine waterbodies, but human activities play a major role in their more frequent occurrence and increasing intensity [22]. Industrial and agricultural activities, as well as urbanization, may increase chemicals released into water bodies. Some of those chemicals become nutrients (i.e. nitrogen and phosphorus from fertilizers used in agriculture or wastewater discharge) which "overfeed" cyanobacteria and other algae, leading to an overgrowth and thus to a bloom [23, 24]. In addition, altered and more intensive agriculture increase the runoff of soil containing nutrients. Climate change, affecting phenomena like, for example, water temperatures and extreme weather events (hurricanes, floods or drought) may also affect blooms' proliferation. In general, blooms tend to occur in eutrophic ecosystems and in conjunction with relatively high temperatures (above 20 °C) [25].

### 3.1.2.2 Cyanobacterial bioactive metabolites

Cyanobacterial (bioactive) metabolites constitute a very heterogeneous group, in terms of chemistry and biological activity, including toxicity [2, 26-29]. They are mainly peptides, but also retinoids, alkaloids, lactones and phospholipids [29-32]. The ability of cyanobacteria to successfully colonize such a variety of ecological niches may be connected to the variety of metabolites they are able to produce [2].

Before describing the main cyanobacterial toxins (cyanotoxins) [2, 26], above all MCs, it is important to emphasize that among all the compounds they are able to synthetize, a large variety of molecules demonstrated beneficial properties and have found applications in several fields, including biotechnology and pharmaceutical drugs [2, 33-35].

### 3.1.3 Microcystins (MCs)

MCs represent the most widespread family of toxins produced by cyanobacteria [28, 36], and are well known hepatotoxins [37, 38]. MCs usually have molecular masses of around 1 kDa. At present, at least 279 MC congeners have been reported in the literature [39], and this number is likely to increase.

### 3.1.3.1 Chemical structure, nomenclature and biosynthesis of MCs

The full structural identification of the first MC congeners dates back to the 1980s [40, 41], when literature still referred to MCs as "cyanoginosins" and "cyanoviridins" [42, 43].

All MC congeners share a general cyclic core structure, made up by seven amino acids, of which five are relatively conserved, while the other two are more variable. This structure includes uncommon amino acids such as the non-proteinogenic (i.e., not protein-forming) 3$S$-amino-9$S$-methoxy-2$S$,6,8$S$-trimethyl-10-phenyldeca-4$E$,6$E$-dienoic acid (Adda), $iso$-linked D-β-methylaspartic acid (D-Masp) and $N$-methyldehydroalanine (Mdha) (**Figure 3**). The common sequence is cyclo(D-Ala$^1$-X$^2$-D-Masp$^3$-Z$^4$-Adda$^5$-γ-D-Glu$^6$-Mdha$^7$), where superscript numbers represent positions in the macrocyclic ring system. X and Z (**Figure 3**), in positions-2 and -4, respectively, are the two variable L-amino acids mainly responsible for the high levels of structural diversity within the class. However, structural variations have been described in all seven positions of the ring, explaining the high and increasing number of reported MC congeners. Other frequently encountered modifications stem from demethylation or methylation at positions-3 (i.e., D-Asp instead of D-Masp) or -7 (i.e., dehydrobutyrine (Dhb) or

dehydroalanine (Dha) instead of Mdha) [44]. The two more common modifications to the Adda group are 9-*O*-demethylation (DMAdda) and 9-*O*-acetylation (ADMAdda) [39]. According to the literature, the most highly conserved amino acid is D-Glu (glutamic acid, denoted also by the 1-letter abbreviation E) at position-6 [39].
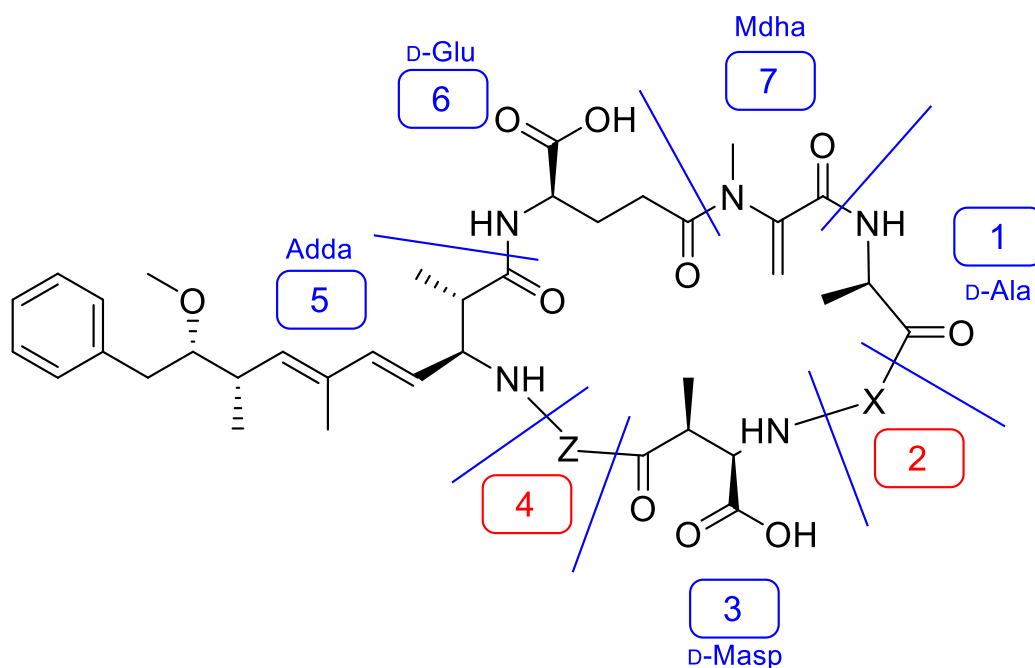


**Figure 3.** General core cyclic structure of MCs (black), with the seven positions highlighted and labelled. X and Z represent generic L-amino acids in the most variable positions, -2 and -4 (red), of the sequence. In all other positions (blue), the most common amino acids are shown.

The generally adopted nomenclature for MCs indicates the amino acid variations present in that specific congener. The term "microcystin-XZ" or "MC-XZ" is used, where X and Z represent positions-2 and 4, as mentioned above (i.e. microcystin-LR or MC-LR has leucine, Leu or L, and arginine, Arg or R, in position-2 and -4, respectively). Variations from the common sequence on other positions are reported in square brackets as a prefix, separated by commas without spaces and in numerical order mentioning the position as superscript number (e.g. in [D-Asp³, DMAdda⁵]MC-LR the desmethylated forms take the places of "classic" D-Masp in position-3 and Adda in position-5).

The substantial MC structural diversity results from both genetic and environmental (e.g., light, nutrient availability, temperature and pH) factors. Indeed, those factors could affect enzymes involved in the MC biosynthetic process, and thus the presence and abundance of MC congeners [45-50]. The gene cluster *mcy* encodes for the large multienzyme machine that is responsible for MC biosynthesis, and it has been characterized in several cyanobacterial genera (including *Microcystis* and *Planktothrix*) [12, 51]. The synthase combines polyketide synthases (PKSs), non-ribosomal peptide-synthetases (NRPSs) and tailoring enzymes [51, 52]. The cluster can spontaneously change following mutations, deletions or insertions, or genetic

recombinations. This may affect the synthesis, thus leading to the naturally observed diversity within the MC family [13].

Among reported congeners, about one fifth do not come from an "original" biosynthesis, but rather from subsequent chemical or biochemical transformations of other variants, which could happen either in the environment or during sample handling/extraction/storage [39, 53-55].

More than ten different cyanobacterial genera are able to produce MCs, including *Microcystis* (the genus from which the name "microcystin" derives since it was the first one where they were found [56]) and *Planktothrix* [51, 52, 57]. Each cyanobacterial strain usually produces one or two dominant congeners, in addition to a number of minor MC analogues [39, 58] (**Paper I**).

### 3.1.3.2 Biological activity (toxicity) of MCs

In this section, it is described the biological activity of MCs, but limited to main toxicity/harmful effects for humans and wildlife. The biological role(s) of MCs for the cyanobacteria themselves is still an open question [59], but outside the focus of the thesis. However, MCs may have a key role in the persistence of algal colonies and the dominance of *Microcystis* spp. in cyanobacterial accumulations [60].

The most infamous human toxicity event related to MCs dates back to 1996, when in Brazil more than fifty patients died because of acute liver failure following hemodialysis with MC-contaminated water [37, 38]. In addition to acute intoxication, chronic exposure to low-concentrations could lead to long-term carcinogenic effects [61, 62]. Several episodes of wildlife toxicity have been documented, as well as for farm and domestic animals [19, 63].

*3.1.3.2.1 The main mechanism of action for MC toxicity*

Regarding the mechanism of action, MC toxicity is primarily and highly connected to the inhibition of eukaryotic protein serine/threonine phosphatases 1 and 2A (PP1 and PP2A), which are ubiquitously expressed in organisms [13, 57, 64-66]. This inhibition results in hyperphosphorylation [57] of cellular proteins regulating a variety of processes including key processes like cell proliferation, apoptosis and differentiation. PP1 and PP2A are also present in plants, which may also suffer adverse outcomes [67].

Structure–activity relationship (SAR) studies have been carried out to understand which chemical and conformational features of MCs make them so toxic. In particular, available crystal structures of MCs complexed with either PP1 or PP2A (**Figure 4**) have been investigated, revealing conformational and binding modes.
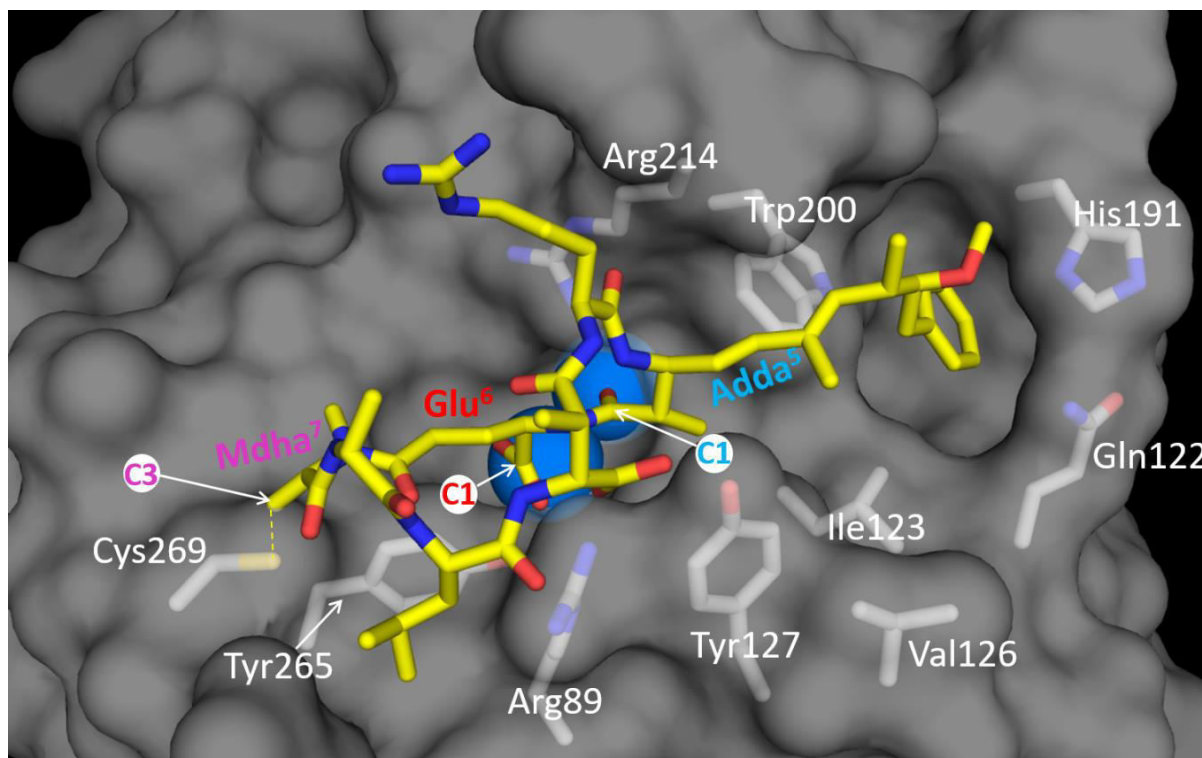
**Figure 4.** X-ray crystal structure of PP2A catalytic subunit bound to MC-LR [68], and the adjacent amino acid side chains interacting with the toxin. Blue spheres represent catalytic metal ions, while C1, and C3 indicate the corresponding atom numbers in the carbon chains of selected amino acids, with colors corresponding to the named amino acid residues. A covalent bond (dashed line) is present between the sulfur atom of cysteine-269 (Cys269) of the protein and C-3 of the Mdha[7]-residue of MC-LR. Figure courtesy of C. O. Miles, NRC Canada.

When in complex with PP1 and PP2A, the heptacycle is not planar but twisted, and blocks potential substrates from entering the active site. The cyclic structure is fundamental for the toxicity. Indeed, it has been reported that opening the ring of MC-LR at any position reduced its toxicity [39, 69].

The lipophilic group of Adda[5] is a key element for binding PP2A (**Figure 4** and **Figure 5**): its side chain creates hydrophobic interactions with four amino acids in the catalytic subunit of PP2A (glycine122, Gln122; isoleucine123, Ile123; histidine191, His191 and tryptophan200, Trp200 in **Figure 4**; the number next to the amino acid abbreviation represents the position in the amino acid sequence of the protein) [70]. Similar interactions with different amino acids happen in PP1 [13, 57]. MCs containing DMAdda and ADMAdda interact with PPs similarly to those containing Adda [39].

The Glu[6] moiety is the other key element for binding PP2A (and PP1) (**Figure 4** and **Figure 5**): its free carboxylic group makes hydrogen bonds with metal-bound water molecules in the active catalytic sites of both PP1 and PP2A. When esterified, this binding potential is lost and toxicity is greatly reduced [39]. The carbonyl group of the Adda-amide, which is adjacent Glu[6], also participates in similar hydrogen binding [39, 57].

The α,β-unsaturated carbonyl of Mdha[7] adds a third important (but not essential) interaction [71, 72]: a covalent linkage forms with a cysteine (Cys) residue in the catalytic subunits of

PP2A, Cys269 in **Figure 4**, and PP1 (**Figure 5**), but the reaction is slow and not required for binding.
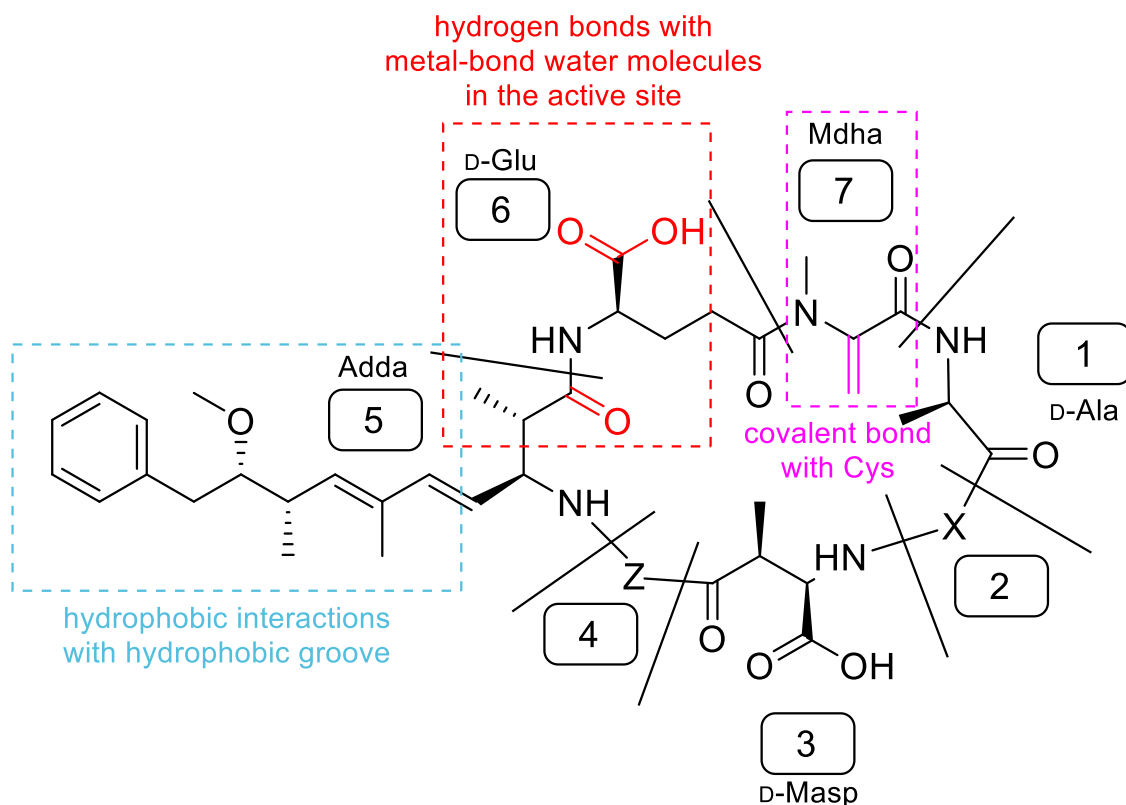


**Figure 5.** Main moieties involved in the inhibition of PP1 and PP2A by MCs.

The catalytic subunit of PP2A is among the most conserved enzymes in species ranging from yeast to mammals [73].

It is interesting that the two most important moieties for PP1 and PP2 inhibition are related to Adda[5] and Glu[6], which are highly conserved in the majority of MC congeners.

Other interactions can contribute to and modulate interactions between different MCs and PP1/PP2A inhibition [39].

Inhibition of PP1 and PP2A may lead to several adverse events besides hepatic damage, that is tumor promotion, formation of reactive oxygen species (and consequent DNA damage), and interference with DNA repair mechanisms [36, 74-76]. Therefore, MCs are considered potential genotoxic carcinogens by the International Agency for Research on Cancer (IARC), which list MC-LR as possible human carcinogen (Group 2B) [77].

Inhibition of PP1 and PP2A is the main and most studied mechanism of MC toxicity, but not the only one. Inhibition of phosphatases such as PP4, PP5 and PP6 is a less studied example [57].

### 3.1.3.2.2 Routes of exposure for MCs

Oral administration of contaminated drinking water is the main route of exposure to MCs for both humans and animals. In 1998, the World Health Organization (WHO) established a provisional guideline value of 1 µg/L for total MC-LR (free and cell-bound toxin), in drinking water, and has established a tolerable daily intake (TDI) of 0.04 µg/kg body mass per day for humans [78]. Concentrations of dissolved MC-LR in aquatic environments is usually within a range of 0.1–10 µg/L, while cell-bound concentrations are several order of magnitude higher [74, 79, 80], and thus potentially harmful both for aquatic animals, wildlife in the environment and for humans. Ingestion through food and food supplements [81], dermal contact and inhalation are other possible routes of exposure [82].

However, WHO is currently reviewing the reports on health effects for cyanobacteria and cyanotoxins in water, with the aim to revise existing guideline values for MC-LR (at present only based on life-time exposure and not considering shorter-term exceedances), but also to establish values for other cyanotoxins [83].

Further caution has to be used when extrapolating values from animal data to humans, from *in vitro* or *in vivo* testing, as well as data from intraperitoneal/intravenous (ip/iv) injections (directly into the bloodstream) to oral exposure (i.e. through the gastrointestinal tract) [39, 84].

Routes of exposures may affect toxicokinetics, that is, the way in which a chemical enters (absorption, distribution) and is processed (metabolism, excretion) by the organism. Thus, as for other xenobiotics (all those chemicals that enter an organism, but which are extrinsic to its normal metabolism), the toxicokinetics of MCs plays a crucial role for their toxicity [13, 39]. MCs are not hydrolysed in the stomach (they are not good substrates for mammalian proteases, because of their peculiar amino acids including D-amino acids and Adda), and are absorbed across the intestine into the bloodstream [26]. MCs are relatively hydrophilic, have a quite high molecular weight, and are unable to permeate cell membranes passively [85, 86]. They can cross them actively, transported by Organic Anion Transporting Polypeptides (OATPs) [87]. OATP1B1 and OATP1B3, which are the most efficient ones for this purpose, are located only in the liver (at least in healthy humans) and this supports hepatotoxicity as a main form of MC toxicity. However, other OATPs (e.g., OATP1A2) less efficient but still able to transport MCs, are present also in other organs, such as kidneys and across the blood–brain barrier, explaining the toxicity in organs other than liver. Indeed, neurotoxicity has also been reported [88, 89].

### 3.1.3.2.3 More than MC-LR

Most studies of *in vitro* and *in vivo* toxicity studied the effects of MC-LR [39]. However, extrapolation of toxicological information from MC-LR to the whole MC group, might be difficult considering the differences among all MC variants, especially the more lipophilic ones for which kinetic parameters can be significantly different [13]. Structural variations of MCs seem to have an impact on toxicity more through toxicokinetics than toxicodynamics. The uptake, tissue distribution and excretion can be very different for different MC variants, affecting toxicity [13]. For example, the more hydrophilic MC-RR showed different affinities for OATP1B1 and 1B3 [87] compared to MC-LR because of more efficient detoxification (it is more efficiently conjugated than MC-LR, especially at low concentrations) [84]. Reported differences in the metabolism of the two MC variants, MC-LR and MC-RR, were more pronounced in rodent cytosol than in human samples [84].

### 3.1.4 Cyanobacterial bioactive metabolites beyond MCs

It is beyond the scope of this work to describe chemical and biological properties of all cyanobacterial bioactive metabolites. However, it is fundamental to have in mind the enormous heterogeneity of what cyanobacteria can synthetize. More than one hundred additional secondary metabolites have been identified yearly, only in the last ten years [90]. Studies on MCs represent the 90% of the total scientific output on cyanopeptides [30]. Peptides represent more than 60% of the known bioactive cyanobacterial metabolites [33]. More than 500 identified other cyanopeptides can be added to the 279 reported MC congeners [30, 39]. Retinoids, alkaloids, lactones and phospholipids are the main other categories of bioactive cyanocompounds [27].

(Harmful) effects of cyanobacteria cannot realistically be linked only to MCs, nor to MC-LR alone, which is nevertheless the only regulated cyanobacterial toxin currently. As mentioned in the previous section, the WHO is working to expand drinking water guidelines available for MC-LR, to other cyanotoxins [83]. However, establishing rules and limits for all known cyanobacterial metabolites would require a proper knowledge of both structures and properties of all these metabolites.

Focusing on cyanopeptides, there are both cyclic and linear ones and they are classified according to conserved molecular substructures [91], as it was described for MCs. Within each class, monomers' variation defines different congeners. Some reported cyanopeptides classes beyond MCs are nodularins (NODs), which are closely related to MCs from the structural point of view, cyanopeptolins, anabaenopeptins, cyclamides, cryptophycins, aeruginosines, microgininins, microviridins and other depsipeptides [30, 90, 91].

Non-peptide metabolites are smaller and without a unique structural feature, thus less easy to classify [90].

Another way to classify cyanobacterial bioactive metabolites, including MCs, is according to their toxic effect, i.e. hepatotoxins (like MCs and NODs), neurotoxins (e.g., anatoxins, saxitoxins), and so on [26, 52, 92].

## 3.2 Endocrine disruptors (EDs)

### 3.2.1 Definition of a contemporary global concern: what are EDs?

Endocrine disruptors (EDs), or endocrine disrupting chemicals (EDCs), are listed among the "*key environment and health challenges of our time*" [93].

In 2002, the International Programme on Chemical Safety (IPCS), a collaboration between the WHO, International Labour Organization (ILO) and United Nations Environmental Programme (UNEP), published the report *Global Assessment of the State-of-the-Science of Endocrine Disruptors* [94], where these two important definitions were given:

"*An **endocrine disruptor** is an exogenous substance or mixture that alters function(s) of the endocrine system and consequently causes adverse health effects in an intact organism, or its progeny, or (sub) populations*";

"*A **potential endocrine disruptor** is an exogenous substance or mixture that possesses properties that might be expected to lead to endocrine disruption in an intact organism, or its progeny, or (sub) populations.*".

In other words, those two groups hold a wide array of chemicals (synthetic and/or natural), which alter or potentially alter the homeostasis of the endocrine (hormonal) system, leading to more or less serious negative effects in an organism or its progeny. Throughout their lives, humans and animals are exposed to a variety of such chemicals.

### 3.2.2 The endocrine system

The endocrine system of an organism is a network of interacting tissues, which uses small molecules as communication tools. These small molecules are called hormones and are released by the endocrine glands [95].

Different glands, distributed throughout the whole body, release different types of hormones. The main glands of the endocrine system are hypothalamus, pineal gland, pituitary gland, thyroid gland, parathyroid gland, thymus, adrenal glands, pancreas and gonads (ovary and testis) [95] (**Figure 6**).
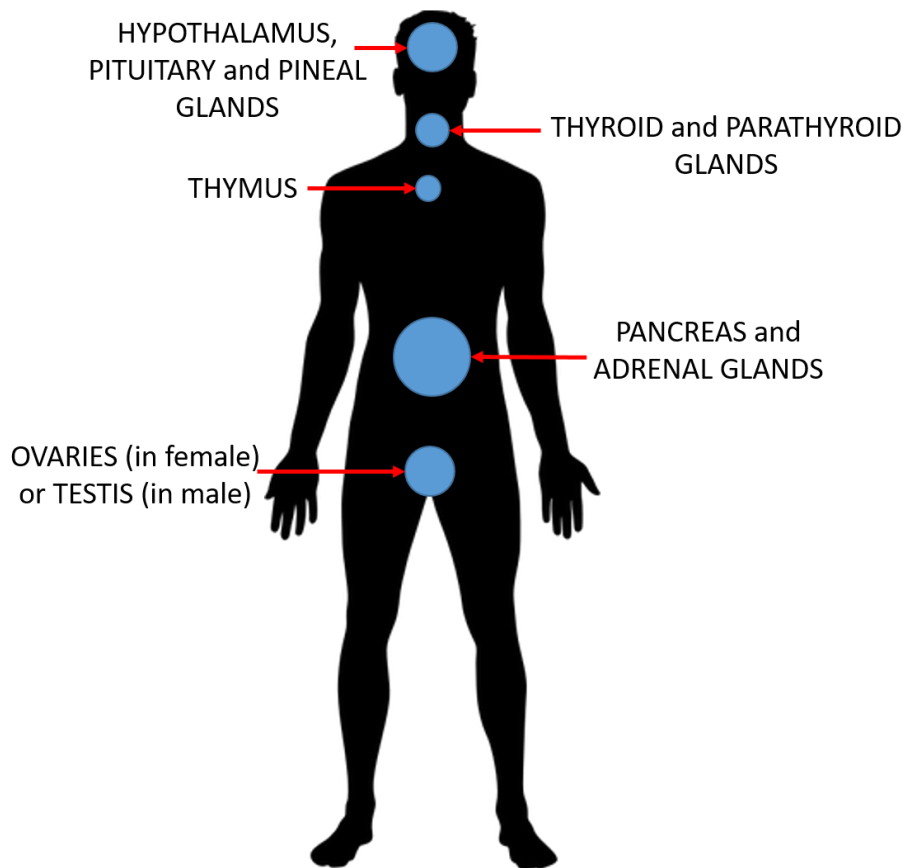
**Figure 6.** Distribution of the main endocrine glands throughout the human body.

Once released by glands, hormones travel through the bloodstream, and reach distant cells and tissues where they bind to specific receptors and thus are able to produce "effects". Through these effects, an organism can regulate very important and critical processes, as for example metabolism, development and growth, reproduction, immunity, and homeostasis [96]. A regular supply of hormones is essential for health. Unwanted sustained increases or decreases in hormone production may lead to diseases. Hormone production and serum hormone concentrations are controlled and maintained by feedback mechanisms, in much the same way as a thermostat regulates the temperature in a room [97].

Although this idea of how the system generally works can be described in a simple and linear scheme (**Figure 7**), complex pathways and feedback mechanisms are behind its functioning.
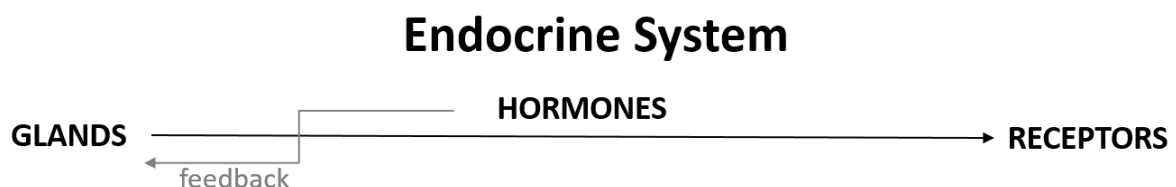
# Endocrine System



**Figure 7.** Schematic representation of the endocrine system functioning.

Endocrine tissues and glands form an unique system, having fundamental interrelationships [98]. When a number of glands signal each other in sequence, they are usually referred to as an "axis". Important examples, both for humans and wildlife, are the hypothalamic-pituitary-thyroid (HPT) axis, the hypothalamic-pituitary-adrenal (HPA) axis and the hypothalamic-pituitary-gonadal (HPG) axis (**Figure 8**). The first axis mainly regulates metabolism and stress response, the second one is the human central stress response system, and the third one plays a critical role in sex development and reproduction [99-101].
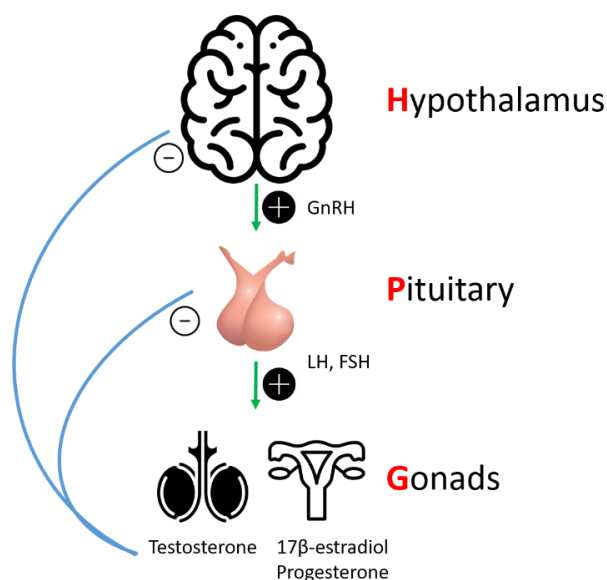


**Figure 8.** HPG axis and its feedback functioning: gonadotropin-releasing hormone (GnRH) is secreted from the hypothalamus, thus the anterior portion of the pituitary gland produces luteinizing hormone (LH) and follicle-stimulating hormone (FSH), and the gonads (testis and ovaries) produce testosterone and estrogens (17β-estradiol, progesterone).

Sex development and reproduction toxicity have been fundamental in research about cyanobacterial compounds interfering with the endocrine system, thus the HPG axis seemed to play a crucial role (see section 3.3 Cyanobacteria and EDs).

Apart from humans, vertebrates such as other mammals, fish, amphibians, reptiles and birds, possess a similar system, although structures and roles may differ. In addition, also invertebrates as molluscs, shellfish and insects possess an endocrine system. Clearly, the complexity of the system scales with the complexity of organisms [102].

### 3.2.3 State-of-the-art on EDs

Colborn and colleagues introduced the concept of "endocrine disruption" (ED) for the first time in 1993 [103]. Since then, concerns about EDs started growing [104-107], and in the last two decades, intensive scientific work has been done to increase the knowledge of their impact both on human and wildlife health [108-112].

The endocrine system controls many processes in the human body, from early stages of development to adulthood [96]. Therefore, various unwanted consequences are possible following exposure to xenobiotics disturbing its homeostasis. A similar picture applies to wildlife.

The topic EDs is complex, and there are many knowledge gaps. Many of the gaps identified in 2018 by the European Commission (EC) [113], are still valid. It is generally recognized that exposure to EDs in certain periods of development (i.e. foetal stage and puberty in case of humans) may increase the susceptibility to diseases later in life. However, the understanding of their contribution compared to other factors (i.e. genetic, environment, lifestyle) is limited and not trivial to investigate. The mixture effect ("cocktail effect") is another cause of concern, i.e. the exposure to a combination of EDs may lead to a more severe adverse effect, even if the individual ED concentrations are below the effect level [107, 114].

It is important to highlight that ED activity can happen in many different ways via affecting various components of the endocrine system (**Figure 9**). Thus, this means that many different chemicals can potentially act as EDs.
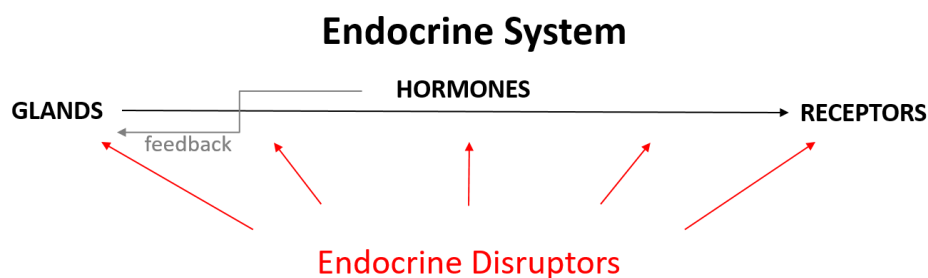


**Figure 9.** Schematic representation of the EDs actions at different levels of the endocrine system functioning.

Among possible mechanisms of disruption, the most studied is probably the direct interference with endocrine receptors. This interference is frequently divided into two main types. The disruptor can bind and activate the receptor, mimicking the biological activity of its natural hormone, but leading to different and often unwanted responses. This type of interference is called "agonistic effect" and it can be either "full", "partial" or "inverse", depending on the biological response efficacy (100%, lower or even negative for inverse agonists) [115]. Alternatively, the disruptor can bind to the receptor without activating it, but preventing the binding of its natural hormone (either in a reversible or irreversible way) and thereby blocking the effect of the hormone. This is called "antagonistic effect" [116]. In addition, there are also the so-called "allosteric modulators", which do not bind to the agonist-binding site of the receptor, but instead on specific allosteric binding sites and modulate the response of the receptor to its natural ligand [117].

However, there are many other possibilities of non-receptor mediated mechanisms of disruption, which are maybe less intuitive but still very important [118-120]. For example, disruptors may interfere with the binding to transport proteins in the blood or the hormone itself, altering the amount of free circulating hormones. They may interfere with enzymes responsible for production (i.e. steroidogenesis, **Paper III**), transformation (e.g., 17β-estradiol metabolism, **Paper II**) and /or elimination of hormones. Again, this may lead to a variety of consequences, for example the modulation of estrogen hydroxylation (i.e., impact on metabolite ratios, **Paper II**) potentially increase the risk of breast or other hormone-related cancers [121].

Since there are many different ways to exert ED activity, reliable tests methods are required to investigate them [122]. In 2013, the European Food Safety Authority (EFSA) summarized existing guidelines for ED testing, underlining the lack of several predictive models [123]. A number of mechanistic assays for ED screening and regulation have been developed. However, they are limited to the interaction with sex steroid nuclear receptors or the alteration of sex steroids synthesis [122]. The variety and complexity of possible mechanisms of action make the identification of reliable tests complex. Furthermore, mechanisms by which hormones and consequently EDs may exert specific actions may depend on what happens at the cellular and tissue levels, as well as on circadian rhythms, seasonal changes, life stage and sex [124]. Therefore, many factors need to be considered and currently it is not possible to replace well-designed *in vivo* studies with *in vitro* models.

An interesting consensus statement on the key characteristics (KCs) of EDs has been published recently [125]. Since there are common features of hormone regulation and action shared by all hormones and that are independent of their diverse roles, it follows that there are also some features shared by those chemicals that interfere with hormone regulation and action. The authors identified 10 KCs for a compound to be classifiable as ED:

KC1.   Interacts with or activates hormone receptors
KC2.   Antagonizes hormone receptors
KC3.   Alters hormone receptor expression
KC4.   Alters signal transduction in hormone-responsive cells
KC5.   Induces epigenetic modifications in hormone-producing or hormone-responsive cells
KC6.   Alters hormone synthesis
KC7.   Alters hormone transport across cell membranes
KC8.   Alters hormone distribution or circulating hormone levels
KC9.   Alters hormone metabolism or clearance
KC10. Alters fate of hormone-producing or hormone-responsive cells

Interference can mean amplifying, reducing or deleting expected outcomes related to those KCs. Furthermore, it has been stated that the number of KCs eventually associated to a potential ED is not predictive of relative hazard. Indeed, a single but critical KC may lead to severe consequences and therefore to a high hazard level [125]. The KCs may help identifying gaps in background data and setting research priorities rather than merely serving as a checklist.

In summary, there are many targets for EDs, many mechanisms by which they may unfold their activity, and many chemicals may fall into the complex ED definition. When this complexity meets the complexity of the cyanobacterial metabolome, understanding potential overlap may be challenging.

Most publications on EDs, and especially those that deal with human exposure, target ED chemicals of anthropogenic origin, e.g. packaging industries products, pesticides, food additives, cosmetics and pharmaceuticals. Among these ED chemicals are, for example, phthalates, bisphenols, parabens, and persistent organic pollutants (POPs) [109]. These are mainly synthetic products. Among compounds of natural origin, the phytoestrogens (so named because of their estrogenic activity) produced by plants and ingested by humans for example through soybeans or other legumes, gained a certain notoriety as well. However, as phytoestrogens are natural products, the perception of associated risk seems lower as compared to synthetic chemicals [126].

## 3.3 Cyanobacteria and EDs

Currently, the majority of research on the ED activity of cyanobacterial compounds has focused on MC-LR. Furthermore, these research studies have been often part of the wider investigation of negative effects exerted by MCs on the reproductive system. Indeed, a strong evidence of reproductive toxicity connected to MC exposure has been provided by a variety of studies, both *in vitro* and *in vivo* [127].

A study from Wu et al. [128] in female mice (given daily i.p. injections for 28 days with 5 and 20 µg/kg MC-LR), reported the impact of MC-LR on the female reproductive system. Results showed pathomorphological changes in ovaries (reduction in weight), decrease in the number of primordial follicles as well as abnormal estrus cycle, with consequent impact on fertility. Progesterone (a steroid hormone) levels in the blood decreased after exposures to MC-LR, but without evident changes on the pituitary hormone levels (i.e., follicle-stimulating hormone, FSH, luteinizing hormone, LH) and 17β-estradiol (a steroid hormone), thus the impact was likely directly on the ovary (gonads) rather than indirectly through the HPG axis (see section 3.2.2 The endocrine system, **Figure 8**).

Several studies on male rats and mice reported that MC-LR affects the male reproductive system [127]. Given daily i.p. injections for up to 28 days (depending on the study) with a range of 3.75–30 µg/kg MC-LR caused sperm abnormality, injury to testis and decreased levels of serum testosterone (a steroid hormone). However, in this case, the decreased levels of serum testosterone came along with modulation of GnRH (gonadotropin-releasing hormone) secretion and either reduced or increased FSH and LH levels [129-131] (see section 3.2.2 The endocrine system, **Figure 8**). Interference with HPG axis seemed to cause indirect dysfunction of Leydig cells in the testis (known to be responsible for testosterone secretion), thus causing lower levels of serum testosterone [131]. The distribution of MC-LR in the gonads and target cells within the gonads remain unclear. MC-LR is unable to easily penetrate biological membranes or bio-accumulate [85, 86]. However, as already mentioned, some cells express specific membrane transporters (OATPs, see section 3.1.3.2.2 Routes of exposure for MCs) that enable MC-LR to accumulate [87], e.g. in ovarian cells (in females) [128] as well as in spermatogonia and Sertoli cells (essential for testis formation and spermatogenesis) in the testis (in males), as shown *in vitro* [131].

Research on how MC-LR affects the fish reproductive system is also available. A study from Zhao et al. [132] reported the disruption of reproductive performance of female zebrafish after being exposed for three weeks to MC-LR (10 and 50 µg/L showed detectable effects). Modulation of 17β-estradiol, testosterone and vitellogenin (VTG), which is a precursor protein of egg yolk synthesized in the fish female liver, was reported in that and in other studies [133]. The serum levels of VTG or the levels of VTG from fish organ homogenates are useful biomarkers for evaluating estrogenic activity. Neither adult male fish nor juvenile fish produce VTG, unless exposed to exogenous estrogens [134]. The decrease of oogenesis (egg production), and thus fertilization and hatching rates were reported. The possibility of trans-generational effects was suggested. Changes in the transcription of steroidogenic (i.e., related to steroid hormones synthesis) pathway genes in zebrafish were also reported, corresponding to the alteration of hormones levels [132]. Su et al. [135] came to similar conclusions, showing that for male zebrafish, a life-cycle exposure to environmentally relevant concentrations of MC-

LR (i.e., 30 µg/L) resulted in testicular damage, sperm maturation delay and imbalanced secretion of sex hormones (testosterone and 17β-estradiol), by disrupting transcriptional responses or related genes in the HPG axis. A recent study on male zebrafish showed the impact of persistent exposure to MC-LR on the hypothalamic-pituitary-interrenal (HPI) axis (which is the analogue of HPA axis in mammals) [136], with extensive upregulation of HPI axis genes and inhibition of specific brain nuclear receptors with consequential increase of serum cortisol levels.

*In vitro* studies on mammalian cell lines have been performed almost exclusively in mouse/rat Sertoli and Leydig cells, reporting findings supporting the zebrafish *in vivo* studies [127, 129]. Hou et al. [137] used the H295R human cell line [138] along with *in vivo* experiments using male zebrafish, to investigate MC-LR effects on steroidogenesis, reporting a non-dose depending estrogenic activity of MC-LR. Extensive up-regulation of steroidogenic genes supported testosterone and 17β-estradiol modulation. In the liver, the vitellogenin 1 gene (*vtg1*) was up-regulated while both the transcriptional and protein levels of the estrogen receptor declined. It is possible to talk about an effect on the hypothalamic-pituitary-gonadal-liver (HPGL) axis. Oziol and Bouaïcha [139] used the transgenic human cell line MELN and reported that MC-LR (and NOD-R) showed estrogenic potential at low concentrations (nM), likely by indirect interaction with estrogen receptors.

Reproductive toxicity of MCs has also been reported in birds and amphibians even though the investigation is more limited than for fish and mammals (mice/rats). However, data on the effects of MCs on human reproduction represents a big knowledge gap [127].

More global investigations into the ED and reproductive toxicity of cyanobacteria mainly focused on the species *M. aeruginosa*, which includes MC-LR producing strains. Damage to the testis and reduction of sperm quality was reported in mice after exposure to MC-producing *M. aeruginosa* cell extracts [140]. Spermatogonia and Sertoli cells were damaged in both rats and rabbits after exposure to MC-containing *M. aeruginosa* extracts [141-143]. Reproductive/endocrine effects on zebrafish embryos exposed to *M. aeruginosa* and *P. agardhii* seemed to exclude a significant role of MCs in a study by Jonas et al. [144]. Studies from Stepankova and collaborators reported cytotoxicity and estrogenic effects (receptor-mediated) from extracts of blooming cyanobacteria containing MCs [145, 146]. The effects were greater than what would be expected from the extracts of pure laboratory cultures. These studies indicated that cyanobacterial compounds other than MCs, or possibly compounds that originated from other organisms (e.g., phytoestrogens from algal species in the water column), were at least partly involved in the reported estrogenic effects. Induction of VTG in zebrafish larvae has been reported as effect of *M. aeruginosa* and MC-LR [147], supporting an estrogenic activity in accordance with other studies [127, 148].

It is important to remember that reproductive toxicity may be exerted by MCs and/or other cyanobacterial bioactive metabolites, through mechanisms other than direct interference with endocrine system pathways (e.g., modulation of PP1 and PP2A activities, oxidative stress, DNA damage, reproductive tumors) [127]. However, the HPG axis is an important pathway for endocrine regulation in the process of development and reproduction, and it seems to play a role in cyanobacterial ED activity, alone or in combination with other mechanisms, as for example liver damage [136, 149].

Cyanobacterial compounds represent a potential contribution to ED effects in aquatic ecosystems, especially in case of high bloom densities [145]. Known and unknown MC congeners, together with other cyanobacterial bioactive compounds, represent themselves a complex mixture. Furthermore, when in the natural environments, cyanobacterial biomass may accumulate a variety of anthropogenic chemical compounds, as well as compounds produced by other species coexisting in the water, thus the total effect they exert may be the result of endogenous plus accumulated substances [145, 150]. It is no obvious way to trace the observed ED effects to specific compounds. The simultaneous exposure to all these compounds together could lead to additive, synergistic or antagonistic toxic effects.

In summary, the available data on cyanobacteria as EDs are mainly related to reproductive toxicity in animals (e.g., mice/rats and fish), studied either using MC-LR or extracts/exudates from *M. aeruginosa*. Despite several negative effects on the endocrine system (e.g., estrogenic) have been documented, some doubts remain about the modes of action. The role of MCs other than MC-LR and of other cyanobacterial bioactive compounds beyond MCs has not been clarified. Cyanobacterial contribution to ED activity in aquatic environments might be underestimated compared to known pollutants of anthropogenic origin.

# 4. METHODOLOGIES

The main methodologies used in the thesis and its associated papers are described in this chapter, ranging from cyanobacterial collection handling, to the chemical and biological tools for the investigations.

## 4.1 Cyanobacterial collection

Twenty-seven cyanobacterial strains were selected for investigation, belonging to *Microcystis* and *Planktothrix* genera. The collection included both MC-producing and non-MC-producing strains (**Table 1**).

Twenty-five strains (19 *Microcystis* spp. and 6 *Planktothrix* spp.) were purchased from The Norwegian Culture Collection of Algae, NORCCA (https://niva-cca.no/), jointly maintained and owned by the Norwegian Institute for Water Research (Norsk institutt for vannforskning, NIVA, Oslo, Norway) and the University of Oslo. In addition, the Pasteur Institute (Paris, France) provided the *M. aeruginosa* PCC7806 strain. For the studies that are summarized in **Paper III**, the PCC7806*mcyB*− strain, which is genetically modified from PCC7806 to be unable to produce MCs [151], was also purchased from the Pasteur Institute (https://catalogue-crbip.pasteur.fr/).

**Table 1.** Cyanobacterial collection's details

| Strain ID | Species | Origin | MCs* |
|---|---|---|---|
| NIVA-CYA 22 | *M. aeruginosa* | L. Mendota, Madison, WI, 1948 | no |
| NIVA-CYA 24 | *P. prolifica* | L. Levrasjön, Kristianstad, Sweden, 1975 | no |
| NIVA-CYA 31 | *M. aeruginosa* | L. Little Rideau, Ontario, Canada, 1954 | yes |
| NIVA-CYA 56/1 | *P. mougeotii* | L. Steinsfjorden, Buskerud, Norway, 1978 | no |
| NIVA-CYA 116 | *P. agardhii* | L. Årungen, Norway,1983 | no |
| NIVA-CYA 123/1 | *M. aeruginosa* | L. Mälaren, Sweden, 1983 | no |
| NIVA-CYA 140 | *M. aeruginosa* | Bendig's Pond, Bruno, Saskatchewan, Canada, 1975 | yes |
| NIVA-CYA 143 | *M. aeruginosa* | L. Akersvatnet. Norway, 1984 | no |
| NIVA-CYA 144 | *M. cf. aeruginosa* | L. Borrevatnet, Vestfold, Norway, 1984 | no |
| NIVA-CYA 166 | *M. aeruginosa* | L. Hellesjøvatnet, Akershus, Norway, 1987 | no |
| NIVA-CYA 264 | *M. botrys* | L. Frøylandsvatnet, Rogaland, Norway, 1990 | yes |
| NIVA-CYA 279 | *M. cf. ichthyoblabe* | L. Østensjøvatnet, Oslo, Norway, 1990 | no |
| NIVA-CYA 431 | *M. novacekii* | L. Victoria, Murchison Bay, Uganda, 2000 | no |
| NIVA-CYA 432 | *M. sp.* | L. Victoria, Murchison Bay, Uganda, 2000 | no |
| NIVA-CYA 475 | *M. aeruginosa* | L. Victoria, Murchison Bay, Uganda, 2000 | no |
| NIVA-CYA 476 | *M. aeruginosa* | L. Victoria, Murchison Bay, Uganda, 2004 | no |

| NIVA-CYA 478 | *M. aeruginosa* | L. Victoria, Murchison Bay, Uganda, 2000 | no |
|---|---|---|---|
| NIVA-CYA 482 | *M. aeruginosa* | L. Mburo, Uganda, 2004 | no |
| NIVA-CYA 544 | *P. prolifica* | L. Steinsfjorden, Buskerud, Norway, 2004 | yes |
| NIVA-CYA 598 | *P. prolifica* | L. Kolbotnvatnet, Akershus, Norway, 2007 | yes |
| NIVA-CYA 613 | *M. botrys* | L. Steinsfjorden, Buskerud, Norway, 2008 | yes |
| NIVA-CYA 632 | *P. rubescens* | L. Lyseren, Østfold, Norway, 2008 | yes |
| NIVA-CYA 754 | *M. aeruginosa* | Roodeplaat, South Africa, 2011 | no |
| NIVA-CYA 842 | *M. aeruginosa* | Hartbeespoort Dam, South Africa, 2013 | no |
| K-0540 | *M. aeruginosa* | Bagsværd Sø, Denmark, ? | no |
| PCC7806 | *M. aeruginosa* | Braakman Reservoirs, The Netherlands, 1972 | yes |
| PCC7806*mcyB*− | *M. aeruginosa* | Braakman Reservoirs, The Netherlands, 1972 | no |

*according to literature/vendor and confirmed by indirect competitive multihapten MC ELISA [152].


### 4.1.1 Culturing of cyanobacteria

All strains were cultivated in Z8 medium [153] in 100 mL glass Erlenmeyer flasks in an incubator (IPP110plus, Memmert GmbH + Co.KG, Schwabach, Germany) at 18 °C with a 14/10 h light/dark photoperiod, using 1% of maximum light intensity. Cultures have been maintained for 3 years, passing from old generations to new ones regularly (every 6–7 weeks) (**Figure 10**).



**Figure 10.** Collection of cyanobacterial strains belonging to *Microcystis* and *Planktothrix* genera.

#### 4.1.1.2 $^{15}$N-labeling of the *P. prolifica* NIVA-CYA 544 strain

An aliquot of the *P. prolifica* NIVA-CYA 544 strain was sent to the National Research Council of Canada (NRCC), which collaborated in **Paper I** work. At NRCC, along with the cultivation in classic Z8 medium [153], the strain was cultivated in a Z8 medium enriched in nitrogen-15 (i.e., the $NaNO_3$ and $Ca(NO_3)_2$ were replaced with $Na^{15}NO_3$ and $Ca(^{15}NO_3)_2$). The enriched culture lead to $^{15}$N-labeling of the MCs produced by the strain. The labeling proved to be extremely helpful for elucidating the elemental compositions of MC congeners, both by comparison of their isotope profiles with theoretical calculations and by examination of the high-resolution mass spectrometry (HRMS) spectra of the labeled and unlabeled MC congeners detected in *P. prolifica* NIVA-CYA 544, as described in detail in **Paper I**.

### 4.1.2 Extraction of cyanobacterial cultures

Extracts were prepared several times, following the same protocol.

For preparation of extracts, 3 mL (or 5 mL) of each culture was transferred to a glass tube and stored at −20 °C overnight. It was then allowed to thaw at ambient temperature, and the same volume of methanol was added (i.e. 3 or 5 mL). The tube was then vortex-mixed for 20 s, sonicated for 5 min and centrifuged for 10 min at 1,000 rcf. The supernatant was collected and aliquots transferred to screw-cap glass liquid chromatography (LC) vials (when directly used for liquid chromatography−mass spectrometry, LC−MS, analysis). Extracts were stored at −20 °C until use and between uses.

## 4.2 Liquid chromatography−mass spectrometry (LC−MS)

LC−MS is a powerful analytical technique. It combines the resolving power (the ability to resolve/separate analytes in time) of LC with the selectivity (separate ionized molecules according to their *m/z*) of MS. In other words, LC separates the sample components and then introduces them to the mass spectrometer for specific detection and identification [154, 155].

LC−MS may provide information about molecular formula, structure, identity and concentration of specific components of a liquid sample [154].

LC−MS played a major role in this thesis' work, especially for structural elucidation of new MC congeners (**Paper I**), but also for ED activity investigations (**Papers II** and **Paper III**). In this section, general information on LC−MS principles and terminology are provided. Some main instrumental components (i.e., those ones that were used for some of the experimental work of this thesis) will be briefly described. Furthermore, some details on LC−MS related to MCs are given.

### 4.2.1. Basic principles of LC

As a chromatographic technique, LC is a method for separation of different components in a liquid solution, based on their different affinity to a stationary phase [156]. A chromatographic column is a device containing the stationary phase, while a mobile phase passes through it driving the solution. Depending on the affinity of each component of the solution to the particles of the stationary phase, the rate of migration of each component may vary from zero (i.e. maximum affinity) to the velocity of the mobile phase [157]. The choice of the type of stationary

phase and of the chromatographic method (e.g. mobile phase composition and elution gradient design) is highly important and inherently connected to chemical-physical properties of the sample analyzed.

### 4.2.1.1 High- and ultrahigh-performance liquid chromatography (HPLC and UHPLC)

The abbreviation HPLC stands for high-performance liquid chromatography, a term that replaces and contains the two concepts of high-speed and high-pressure liquid chromatography. The important improvement coming with HPLC was the use of small (e.g. 3–10 µm) and uniform particles for use as stationary phase. Such a tight packing, usually contained in stainless-steal columns, requires an efficient pumping system to produce sufficient pressure and consequently a high enough flow rate of the mobile phases through the chromatographic column. HPLC performance is better in terms of resolving power, detection, quantitation and speed, compared to classic LC [155, 157]. UHPLC uses even smaller particles as stationary phases ($\leq 2$ µm), thus narrower and shorter columns (e.g., 4.6 mm internal diameter and a length of 150–250 mm for HPLC versus 2.1 mm or less and 30–100 mm for UHPLC). UHPLC runs at lower flow rates than traditional HPLC, for example 0.2–0.7 mL/min against 1–2 mL/min, respectively. UHPLC systems are capable of handling high pressures (over 1000 bar) in comparison to the more traditional analytical range of HPLC (300–400 bar). UHPLC separation produce narrower peaks, improving resolution, and requires high-speed response detection (> 100Hz) [158, 159].

### 4.2.2 Basic principles of MS

The purpose of the MS technique consists in the characterization of matter through separation and detection of gas-phase ions, according to their $m/z$ value [155, 160]. The $m$ represents the mass of the ion divided by the unified atomic mass unit (1 u = 1/12 of the mass of the $^{12}$C-isotope at rest and in its ground state, that is $1.660538921 \times 10^{-27}$ kg. The unit u is also called "Dalton" (Da). The $z$ represents the absolute charge of the ion divided by the elementary charge ($e = 1.602176565 \times 10^{-19}$ C), rounded to the nearest integer number. Both $m$ and $z$ are dimensionless numbers, and so it is $m/z$. The $m/z$ abbreviation is used almost universally as the independent variable in a mass spectrum (described below) [161].

In other words, the mass spectrometer, thanks to its different components (**Figure 11**), creates and then detects electrically charged atomic or molecular species. It "weighs" charged analytes, which must be (or be brought) into the gaseous phase.

The main strength of this technique is its versatility, which allows analyses (qualitatively and/or quantitatively) of a wide range of molecules (from small molecules to biopolymers), by combining different components such as different types of mass analyzers [155, 160].

There are four basic main components in a mass spectrometer (**Figure 11**):

1) INLET SYSTEM, to introduce the sample;
2) ION SOURCE, to ionize the sample;
3) MASS ANALYZER, to sort previously generated ions according to their $m/z$;
4) DETECTOR, to convert sorted ions into a signal for each $m/z$.

While the inlet system (and some ion sources, e.g. for the coupling with LC) commonly operates at atmospheric pressure, the other components require high vacuum to reduce collisions

between ions of interest and other gas-phase molecules, which can compromise ion detection (unwanted reactions which increase results' complexity). Different types of each component can be combined and matched, depending on necessity. An instrument computer with dedicated software controls operations and data acquisition, and may be used for data processing [162].
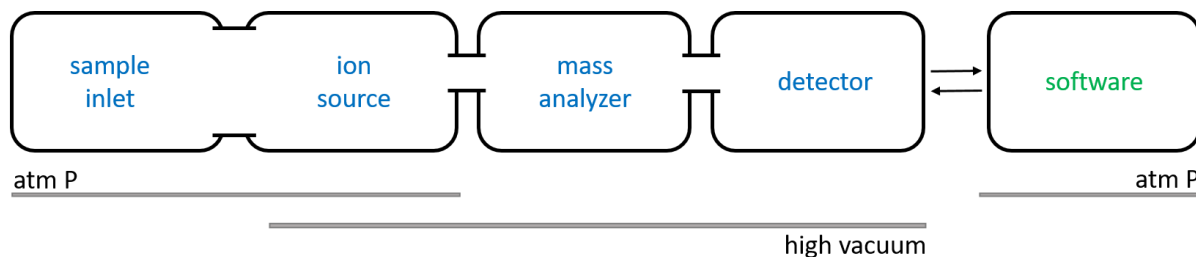


**Figure 11.** Schematic image of basic components of a mass spectrometer.

A further component in the mass spectrometer, the collision cell, can be found in the ion path between mass analyzers, which can be more than one, or between ion source acceleration region and the first analyzer. In the collision cell, selected ions, fragment after collision or interaction with inert gas molecules (e.g., helium, nitrogen or argon) [161]. Fragmentation of a selected ion, followed by the acquisition and the study of fragment ions (or product ions), is the basic idea of tandem mass spectrometry (tandem-MS or MS/MS). Precursor ions of a selected $m/z$ fragment ion or of selected neutral mass loss, may also be studied in tandem-MS experiments. To perform MS/MS, trap instruments (tandem-MS in time) or instruments incorporating more than one analyzer (tandem-MS in space) are used [161]. The multiple stage mass spectrometry ($MS^n$), which involves consecutive collision-activated dissociation reactions to examine fragment ions, is possible in ion trapping instruments [163].

Results from a mass spectrometric analysis, are usually presented as a plot of the relative (less often absolute) intensity (abundance) of the sorted ions versus $m/z$, the so-called "mass spectrum" with different "peaks" corresponding to specific $m/z$ value (**Figure 12**).
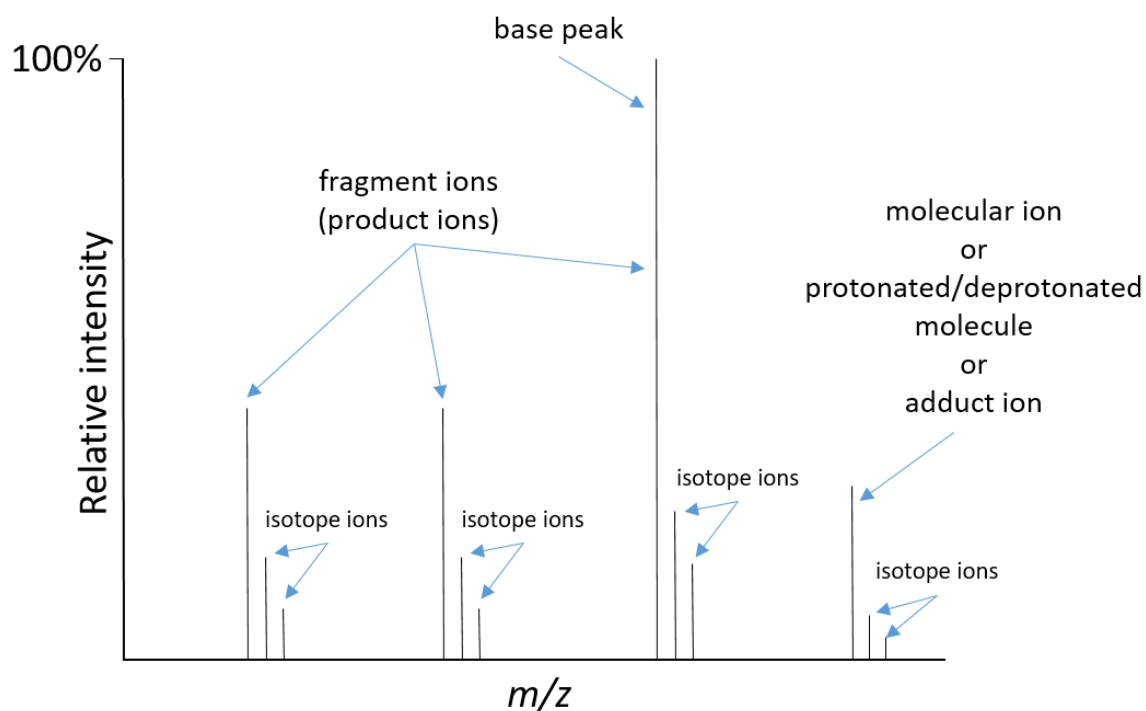
**Figure 12.** Schematic image of a mass spectrum with some common types of peaks observed.

It can be useful to recognize the **molecular ion peak** ($[M]^+$ or $[M]^-$) or the **protonated/deprotonated molecule peak** ($[M + H]^+/[M - H]^-$) (depending on ionization system), that is the peak directly related to the molecule of interest. Since the distribution of energy transferred to molecules during the ionization may break chemical bonds, **fragment ion peaks** (already mentioned in the previous page) may also appear in the spectrum. Fragment ions are a type of product ions, which more generally are formed as the product of a reaction involving a particular precursor ion. Fragment ion peaks show up always on the left side of their precursor molecular ion (i.e. at lower *m/z*). When energies are very high, fragment ions dominate the spectrum at expense of the molecular ion, which may also disappear. Finally, the **base peak** is the most intense (because it is the most stable resulting from the ionization and fragmentation processes) in the spectrum and all other peaks are usually normalized relative to it. **Isotope peaks** may be observed if the analyte molecules contain elements with several isotopic forms (the most commonly observed are isotope peaks arising from the presence of the $^{13}C$ isotope). Some set of isotopic peaks may show a particular pattern deriving from specific elements (i.e. Cl, Br). The isotopic pattern can be helpful for determining the elemental composition of an ion (**Paper I**).

The types of ions that are shown in **Figure 12** are not all the possible ones. Multiply charged ions ($[M \pm nH]^{n\pm}$) and up to several co-occurring adduct ions (e.g. $[M + Na]^+$, $[M + Cl]^-$, $[M + NH_4]^+$) can be observed, depending on the properties of the analyte molecule, but also on the ion source design and on mobile phase components added to "aid" the ionization process (e.g. formic acid as proton donor, which has largely been used in my work).

By definition, the *m/z* ratio is not equivalent to the mass of the ion. The numeric values of mass and *m/z* correspond when the charge is unit ($z = \pm 1$).

Important definitions related to the concept of "mass" in MS are [161]:

- Exact mass (or exact *m/z*): calculated mass (or *m/z*) of an ion or molecule with specified isotopic composition.
- Accurate mass (or *m/z*): experimentally determined mass (or *m/z*) of an ion or molecule of known charge.
- Mono-isotopic mass (or *m/z*): calculated mass (or *m/z*) of an ion or molecule based on the masses of the most common stable isotopes of its constituent elements present.
- Average mass (or *m/z*): calculated mass (or *m/z*) of an ion or molecule weighted for its isotopic composition.
- Most abundant mass (or *m/z*): mass (or *m/z*) of the ion or molecule with the highest signal intensity in the isotope pattern.
- Nominal mass (or *m/z*): calculated mass (or *m/z*) using masses of the elements present, rounded to the nearest integer number (e.g., C = 12, H = 1).
- Isobaric masses (or *m/z*): calculated masses (or *m/z*) coming from empirical formulae that have the same nominal mass, but different exact masses (e.g., CO and $N_2$).

Keeping these definitions in mind is useful when reading the thesis, the papers and especially **Paper I**. It is particularly important to highlight that accurate mass and exact mass are not at all synonymous. The accurate mass comes from experimental determination, while the exact mass from a theoretical calculation. The main purpose of accurate mass measurements is the determination of the elemental composition of a molecule under investigation. The calculated elemental composition is then compared to the exact mass and the mass error calculated, which is a measure for the credibility of the calculated composition. In **Paper I**, there are tangible examples of accurate mass use for determination of new MCs' molecular formulae. MCs' exact masses were calculated using a mass calculator tab of a toxin mass list (publicly available) [164]. The ring/double-bond equivalent (RDBE) calculation, as a mean for determining the degree of unsaturation (number of rings or multiple bonds), gave further information to limit molecular formulae hypothesis (e.g., for the MCs, RDBE ranges from 17 to 22 [39]).

### 4.2.2.1 Sample inlets

No matter which type of inlets, the main function of this component is to introduce a sufficient quantity (to represent its composition properly) of the sample into the ion source [155].

The LC unit can be coupled to the mass spectrometer via an interface that both evaporates the column effluent and ionizes its constituents. LC is compatible, among others, with polar compounds of high molecular mass, e.g. peptides like MCs [162].

In this thesis work, LC was the only method of sample introduction that was used.

### 4.2.2.2 Ion sources

It is necessary to convert neutral analyte molecules into ions, as only ions can be separated and detected by MS. This is because electrically neutral molecules cannot be manipulated using electrical (or magnetic) fields, which are the means used by MS analyzers. Focusing, separation, and detection in MS, require ions. The amount of energy used for ionization affects the types of ions generated, and thus the spectrum appearance. This energy depends on the method of ionization.

The development of ionization methods working at atmospheric pressure has been fundamental for the coupling of LC to MS. Indeed, mobile phases used in LC produce large volumes of vapor, incompatible with MS-components in high vacuum.

*4.2.2.2.1 Electrospray ionization (ESI) source (**Paper I**, **II** and **III**)*

ESI is a popular liquid-based ion source and works at atmospheric pressure. It is the dominant method for ionizing polar and medium polar compounds, and works with small molecules as well as with large biopolymers [165]. The liquid analyte solution from the LC separation and a nebulizing sheath gas (usually nitrogen) "travel" in two concentric steel tubes, which comprise the electrospray needle. A stream of highly charged droplets result from an electrical potential difference (2–5 kV) applied between the spray needle tip and the inlet of the instrument. Residual ions with opposite charge to that of the applied voltage are thus removed. Therefore, the resulting aerosol contains just one charge type, which is the same as the applied voltage. An additional heated drying gas helps to evaporate the charged droplets, and as the charge density increases the droplets disintegrate, releasing ionized analytes into the gas phase [162]. Differential pumping removes the excess gas and solvent molecules before analyte ions reach the analyzer. A series of progressively evacuated chambers connects the ESI source and the mass analyzer. A simple representation of this type of ion source is shown in **Figure 13**.
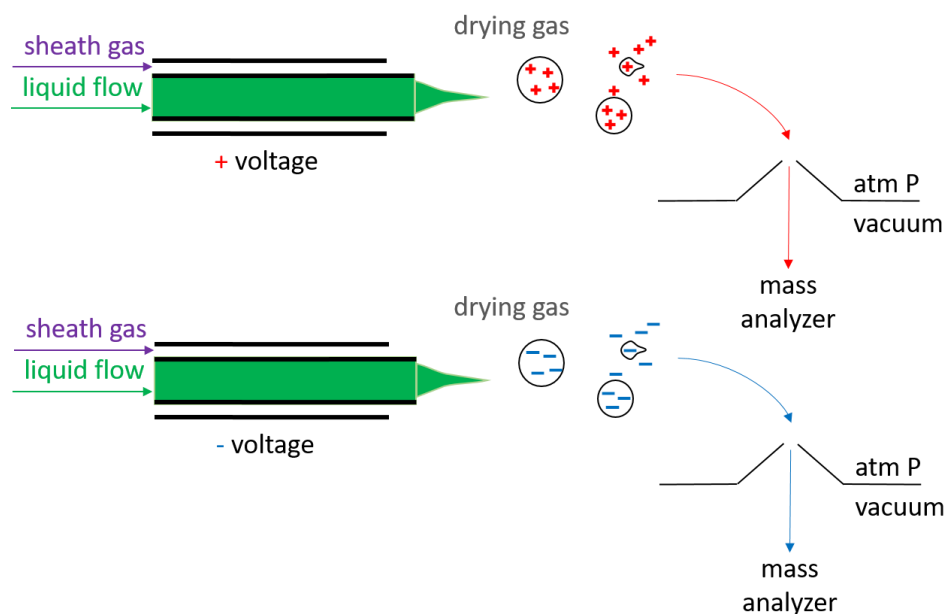


**Figure 13**. ESI source, in positive (above) and negative (below) modes. Applied voltage range is 2–5 kV.

To allow the ESI process, the mobile phase flowing through the needle must be electrically conductive. For this reason, some electrolytes are usually added to mobile phases.

ESI is a "soft" ionization technique, meaning that energies involved are relatively low (but high enough for generating ions). This "softness" helps to reduce the propensity of analyte molecules to fragment during ionization. For further information on fragmentation, it is necessary to perform tandem-MS experiments. Depending on mobile phases and the nature of the analyte, ions formed are predominately protonated and deprotonated molecules or adducts, like for

examples $[M + H]^+$ or [M + alkali metal]$^+$, $[M + NH_4]^+$ or $[M - H]^-$ or $[M + Cl]^-$ in negative mode [166, 167]. A further typical and unique ESI feature is the formation of multiply charged ions $[M \pm nH]^{n\pm}$ as the molecular mass of the analyte increases or if the analyte contains multiple easily ionizable functional groups, e.g. basic amino groups [155]. Acidic and/or basic groups in the analyte molecule influence which ions are formed and therefore determine which polarity mode should be used. Compounds with mainly basic functional groups are generally detected better in positive mode, while the negative ion mode is generally best suited for analyte molecules with acidic groups. Comparison of both positive and negative mass spectra can also be informative (**Paper I**).

*4.2.2.2.2 Atmospheric-pressure chemical ionization (APCI) source (**Paper III**)*

The APCI played a minor role, relative to ESI, in this work (steroid hormone analyses, **Paper III**). Briefly, it is a soft ionization technique (i.e. yields relatively little fragmentation), and it works at atmospheric pressure, as the name suggests. The main difference between ESI and APCI is the ionizing agents: these are electrons, for ESI, and ions, for APCI. Indeed, chemical ionization implies gas-phase (reagent) ion-(analyte) molecule reactions. APCI and ESI are the most commonly used ion sources in quantitative analysis. However, in the case of nonpolar compounds such as steroids (**Paper III**) and some drug molecules, APCI is often more efficient than ESI [168].

### 4.2.2.3 Mass analyzers

Mass analyzers are responsible for sorting ions according to their *m/z*, by using either an electric field or a magnetic field. Those based on the application of an electric field are today more common and could be divided into two groups, beam-type and trapping-type instruments.

In beam-type instruments, the ions travel through the mass analyser in a single beam before reaching the detector. Quadrupole (Q) and Time-of-Flight (TOF) mass analyzers belong to this group.

Trapping-type instruments hold the ions in a spatially confined area (the trap) for a certain period of time before they are ejected towards the detector. Ion trap (IT) (linear or cylindrical) and the Orbitrap, as their names suggest, belong to this group of mass analyzers [162, 168].

Analyzers separate ions either in time (collecting them successively over a period of time, from milliseconds to seconds) or in space (simultaneously or almost simultaneously, on microsecond scale). Qs and ITs scan ions over time. Analyzers with TOF designed analyzers separate ions in space.

For completeness of information, instruments based on magnetic field for ion sorting, are the magnetic sector and the Fourier-transform ion cyclotron resonance (FT-ICR) mass spectrometer.

It is possible to mix-and-match identical or different types of analyzers, obtaining more sophisticated instruments, e.g., Q-Orbitrap (called *hybrid*, because it combines different mass analyzers) or the triple quadrupole (QqQ) [162].

The choice of the analyzer is important, as it determines mass resolution and mass measurement accuracy, as well as the types of tandem-MS experiments that can be performed. Thus, it is a matter of the aim of the study but also the instrument availability. Different types of

instrumentation may also give complementary information about the same analyte, as was the case for our identification of new MC congeners (**Paper I**).

Mass analyzers related to this thesis are briefly described in the sections below. All these mass analyzers separate ions by using electric fields, and all belong to the "in time" separation group.

*4.2.2.3.1 Triple quadrupole (QqQ or TQMS) (**Paper II** and **III**)*

The Q consists of four hyperbolically or cylindrically shaped parallel metal (or metal-coated) rods arranged in two pairs in a square configuration (**Figure 14**).
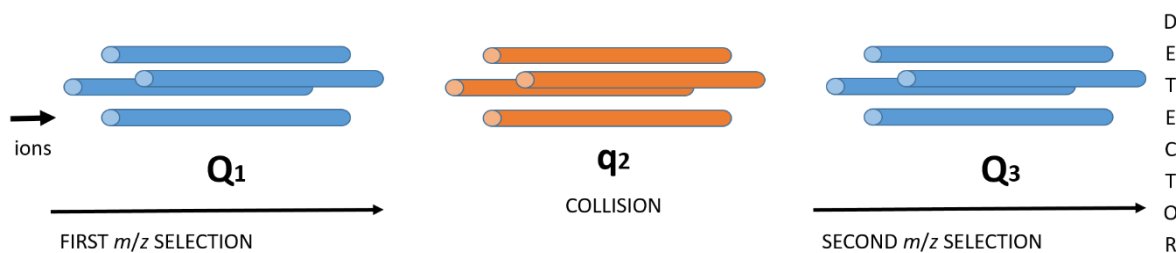


**Figure 14.** Schematic representation of the Q analyzer: two pairs of metal roads (A and B) in square configuration.

One pair of facing roads has an applied voltage comprised of a direct current (DC) component, in combination with an overlapping radio frequency (RF). The other pair has an applied voltage that is opposite to the first one, establishing a two dimensional quadrupole potential.

Ions travelling in the Q during analysis will be, at the same time, attracted by one set of rods and repulsed by the second set of rods. The applied voltages affect the trajectory of ions traveling down the path centered between the four rods.

A Q mass analyzer is widely used as a "filter" device, usually prior fragmentation in the collision cell, in the case of MS/MS analysis. Ions of a single specific *m/z* maintain stable trajectories from the ion source to the collision cell (or the detector), whereas ions with different *m/z* values "fall" into the roads.

A common combination of Q analyzers is the triple quadrupole (QqQ or TQMS). In a QqQ, the first and the third set of quadrupoles (symbolized by an upper case Q) are effectively analyzers, while the central one (q) works as collision cell (often filled with argon) for inducing fragmentation, using only the RF component of the potential, for guiding ions. The design of the collision cell may also be something different from a quadrupole (e.g., a hexapole) (**Figure 15**).



**Figure 15.** Schematic representation of the QqQ analyzer: $Q_1$ and $Q_3$ work as analyzers, while $q_2$ acts as an RF-only collision cell.

A QqQ has four common scan modes:

1) PRODUCT ION SCAN
   $Q_1$ transmits ions with a specific *m/z*, which fragment in $q_2$ followed by subsequent scanning of fragment ions in $Q_3$ ("true" MS/MS).

2) PRECURSOR ION SCAN
   $Q_3$ transmits fragment ions with a specific *m/z*, which have been generated in $q_2$ while scanning in $Q_1$ enables determination of the precursor ions from which the specific fragments arise.

3) NEUTRAL LOSS SCAN
   $Q_1$ and $Q_3$ scan simultaneously, maintaining a constant *m/z* difference (usually corresponding to a neutral loss typical of functional groups to be identified), while $q_2$ is set to fragment all ions.

4) SELECTED REACTION MONITORING (SRM)
   $Q_1$ transmits ions with a specific *m/z*, which fragment in $q_2$ followed by selection of a specific fragment ion *m/z* in $Q_3$. This allows to detect an analyte ion in a selective and sensitive way. When either $Q_1$ or $Q_2$, or both of them, are set perform SRM on more than one *m/z*, this is referred to as multiple reaction monitoring (MRM).
   MRM has been used in **Paper II** for quantification of 17β-estradiol and its biotransformation products, as well as in **Paper III** for steroid analysis.

Furthermore, QqQ could in principle operate as a single mass filter if both $Q_1$ and $q_2$ transmit all ions and $Q_3$ acquires the spectrum.

*4.2.2.3.2 Linear Ion Trap (LIT) (**Paper I**)*

In an LIT (**Figure 16**), the ions are confined radially by a two-dimensional RF field and axially by stopping potentials (DC) applied to end electrodes.
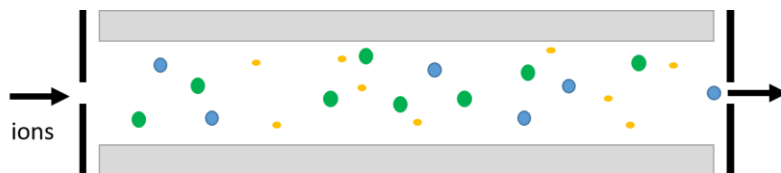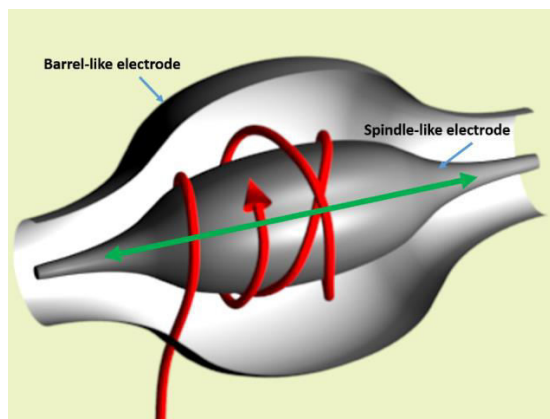


**Figure 16.** Schematic representation of an LIT.

Compared to cylindrically-shaped traps, LITs have higher storage capacity and higher trapping efficiencies, thus higher sensitivity and lower detection limits. [169]. The ion extraction efficiency of LITs is relatively low.

Ions are either injected into or created within the trap. The RF voltage is adjusted and multi-frequency resonance ejection waveforms are applied to the trap to eliminate all but the desired ions in preparation of subsequent analyses. The energy of these stabilized selected ions can be increased allowing collisions with a dampening gas, thereby inducing fragmentation. Scanning the ions inside the trap is possible so their paths become unstable, allowing them to be ejected from the trapping field and direct them towards the detector.

*4.2.2.3.3 Orbitrap (**Paper I, II, III**)*

The Orbitrap analyzer is based on an invention by Alexander A. Makarov [170]. It operates by radially trapping ions about a central spindle electrode. An outer barrel-like electrode is coaxial with the inner spindle-like one. The ion injection happens perpendicularly to the longer axis of the trap. Ions orbit around the central electrode and oscillate axially (**Figure 17**).



**Figure 17.** Schematic representation of the Orbitrap analyzer, showing the inner (spindle-like) electrode and the outer (barrel-like) electrode. The red rolled arrow represents the orbiting of the ions around the central electrode while the green straight arrow with double tips represents the axial oscillation of the ions. Figure modified from Wikipedia (https://en.wikipedia.org/wiki/Orbitrap#/media/File:Orbitrappe.png access date 23/07/2020).

Makarov himself pointed out the necessity of an external ion storage device in front of the Orbitrap [170]. This external ion collection and injection device is in commercially available commonly instruments the so-called C-trap (the name comes from its C-shape). The injection itself, happening through high-speed pulses, provides the excitation of the ions. They are squeezed into a curved trajectory by the modulation of the potential of the inner electrode and are forced towards the wider gap near the equator of the electrode. The *m/z* of individual ions is measured from the frequency of the axial oscillations around the central electrode (**Figure 17**) [171, 172].

### 4.2.2.4 Detectors

MS detectors are very sensitive components, which have the role of detecting and amplifying the signals coming from sorted ions. They will not be described in detail, because this knowledge is more instrumental than functional to comprehension of this thesis' work. However, the most common one are:

- Discrete dynode electron multiplier.
- Continuous dynode electron multiplier (Channeltron).
- Microchannel plate (MCP).

### 4.2.3 LC–MS and MC analysis

MCs, as with most other cyanobacterial toxins, are non-volatile, relatively hydrophilic molecules that possess functional groups that may be ionized and are thus well-suited for

analysis by LC–MS. The types of MS techniques that have been used for their analyses have evolved through the years, according to the development of MS technologies [39, 173, 174]. LC–MS represents a sensitive and selective tool to target and quantify known MCs, but may also be used to elucidate structures of new MC congeners (as in **Paper I**). Indeed, although for unequivocal structural elucidation, isolation and purification of single variants followed by nuclear magnetic resonance (NMR) investigations is usually needed, MS, and especially high-resolution MS, can provide precious information both on molecular formula (full scan, FS) and structure (MS/MS) of an unknown MC, thereby enabling tentative elucidation (**Paper I**).

### 4.2.3.1 LC separation of MCs

Separation of MCs using liquid chromatography LC is today typically done using so-called reversed-phase liquid chromatography (RP-LC) that employs a hydrophobic stationary phase and a relatively polar mobile phase (essentially, mobile phases' polarities are inverted compared to the normal-phase chromatography). UHPLC systems are nowadays the preferred ones [173].

Acidic mobile phases together with an octadecylsilane stationary phase (ODS, or "C18") are commonly used for the separation of MCs. The elution order of MCs in RP-LC depends mainly on the polarity of the molecules: the more hydrophilic (polar) congeners elute earlier, while the more hydrophobic ones elute later. The elution order itself may provide information on relative structural features among different MC congeners.

Hydrophilicity, and consequently elution, are often correlated to the number of Arg residues in the MC structure. Thus, with regard to the most variable positions (-2 and -4) in the heptacycle, the general rule is that congeners containing two Arg, i.e. MC-RR, are the most polar and elute first. These are followed by those containing a single Arg in position-4 (e.g., MC-LR), then analogues with a single Arg in position-2 (e.g., MC-RY) and finally those ones with no Arg residues (e.g., MC-LA) [39, 175]. However, some exceptions from this common order may be due to other amino acids or conjugated groups in the structure, as well as to a different type of chromatographic column used with different selectivity (e.g. the RP-LC pentafluorophenyl propyl column, "F5", used in methods A and C in **Paper I**, which separates molecules by various retention mechanisms including π-π interactions).

### 4.2.3.2 LC–MS for MC structural elucidation

*4.2.3.2.1 MCs in positive and negative ESI mode*

ESI is the most common ionization technique used for LC–MS analysis of MCs and the main one used in my work.

The ionization mechanism tends to be similar for MC congeners with similar polarity. The polarity depends on the amino acid residues in the heptacycle and differences depend especially on the most variable positions (-2 and -4) (see section 3.1.2.1 Chemical structure, nomenclature and biosynthesis of MCs).

In positive ESI mode, MC congeners containing in position-2 and -4 two Arg (or homoarginine, Har) residues that each contain a guanidine group, or congeners that are conjugated to Cys or glutathione (GSH) in position-7, are predominantly double-charged ($[M + H]^{2+}$). All the other MC congeners are mainly single-charged $[M + H]^+$ [173]. In MCs without Arg or guanidinium group, the methoxy group of Adda is the protonated one [173]. The addition of a small percentage of acid (e.g., 0.1% formic acid) to the mobile phases both enhances chromatographic

separation and also supplies protons for the ionization process. Adducts with cations present in the sample, other than protons (e.g., $Na^+$ or $NH_4^+$), are also possible, especially for those congeners with no Arg (or Har), which are comparatively poorly ionizable [39, 164].

In negative ESI mode, all MC congeners show predominantly the singly charged ion $[M - H]^-$ as dominant ion species [39].

*4.2.3.2.2 High-resolution (tandem) mass spectrometry, HRMS(/MS) for MCs*

HRMS allows accurate mass measurements (the high resolution allows separation of isobaric compounds that have the same nominal *m/z*, but different exact *m/z*), which can be used for calculation of elemental composition of new MC congeners (and/or of the fragment ions in HRMS/MS) [176-178]. The elemental composition is an essential starting point for tentative structure elucidation of new MCs [173]. The possible molecular formulae can be calculated starting from the accurate masses. This number can be narrowed down limiting the reasonable number of the main elements (C, H, N, O, S), as well as by the number of RDBEs, which for MCs ranges from 17 to 27 [39]. The comparison of the HRMS(/MS) spectra of $^{15}N$-labeled MCs in labeled cultures (see section 4.1.1.2 $^{15}N$-labeling of the *P. prolifica* NIVA-CYA 544 strain), to their unlabeled counterparts, as in **Paper I**, can give a further confidence in identifying the correct elemental composition of molecular and fragment ions, simply by counting nitrogens [179]. When comparing spectra from labeled and unlabeled cultures, obtained under the same analytical conditions, the profiles are identical, but the *m/z* of peaks are shifted as dictated by the number of N atoms in the peaks. Indeed, $^{14}N$ has a mass of 14.003074 u while $^{15}N$ has a mass of 15.000109 u. The difference is thus 0.997035 u. This "about one unit" difference clearly shows in the spectra how many N atoms are in a specific peak. For example, as shown in **Figure 18**, the molecular ion peak of [D-Asp³]MC-ER (**Paper I**), which according to our hypothesis contained ten nitrogens, is observed at *m/z* 997.4953 and 1007.4670 in the unlabeled and labeled spectra, respectively. The shifted mass confirmed our hypothesis of ten nitrogens. The same reasoning applies to fragment ion peaks and when there is no shift, there are no nitrogens in that fragment (**Figure 18**).

It does not contain N
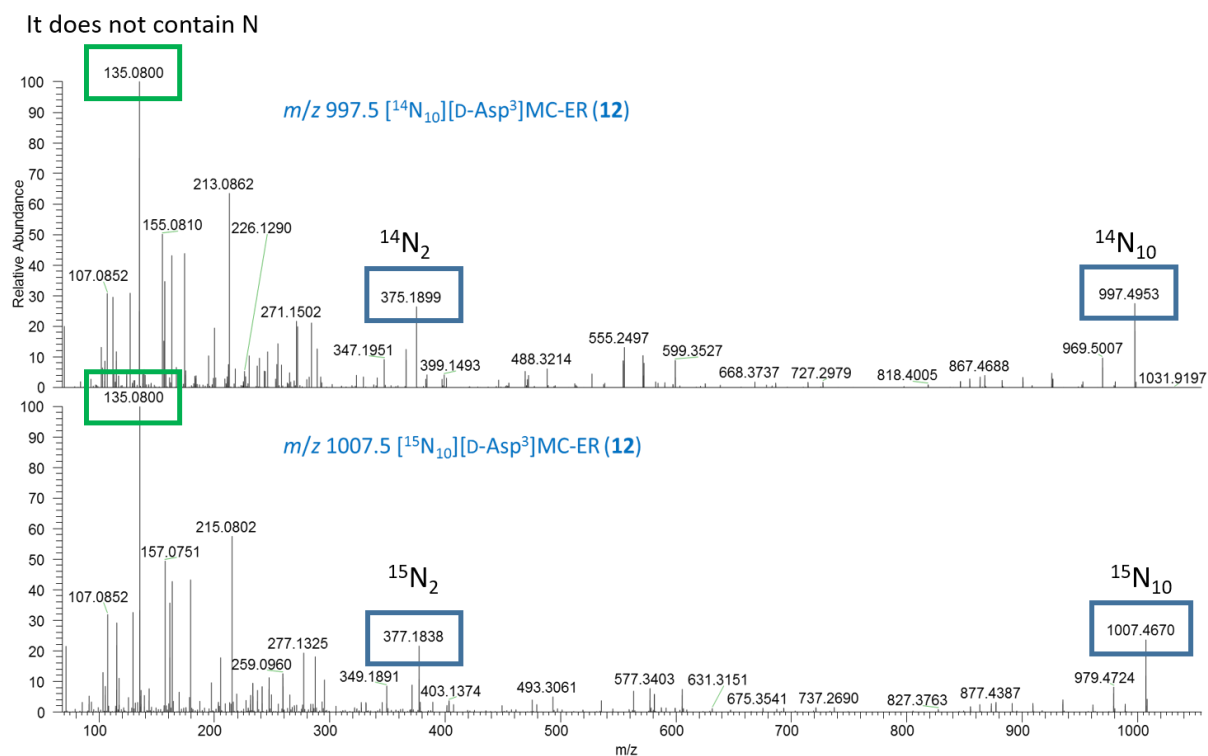
**Figure 18.** LC–HRMS/MS spectra of [M + H]$^+$ of unlabeled (top) and $^{15}$N-labeled [D-Asp$^3$]MC-ER (from **Paper I** Supplementary Material, Figure S20).

However, since isomeric MC congeners (and/or MC fragments), that is, compounds sharing the same molecular formula (but having different structures), are common [39], high-resolution accurate mass measurements alone are usually not enough for structural elucidation of MCs [173]. Thus, further supportive tools are often needed.

Data on characteristic fragmentation pathways, as described in the following section, and functional group derivatization reactions (monitored using LC–HRMS, see section 4.3 Functional group derivatization) can give supportive information to help elucidate chemical structures in general, and are especially useful for the MS-based characterization of MCs. Biosynthetic considerations may also help on narrowing down the number of plausible structures/amino acids hypothesized.

### 4.2.3.2.3 MC dissociation: MC-characteristic fragments and sequence ions

A rather large number of studies on MCs' MS/MS dissociations are available, both in positive and negative ionization modes [179-182]. The way in which MCs fragment gives fundamental structural information.

There are some fragments, which are MC class-characteristic; that is, they provide a sensitive indication that the investigated congener under investigation belongs to the MC family (or the closely related NOD family). The most important are, in positive mode, *m/z* 135.0804, and in negative mode *m/z* 128.0353 (**Figure 19**) [173]. They both arise from highly conserved residues in the MC-macrocycle, Adda$^5$ and Glu$^6$, respectively, and 100% of reported MCs contain either one or the other moiety [164]. Other characteristic fragments are more specific for some MC variants [173, 183].
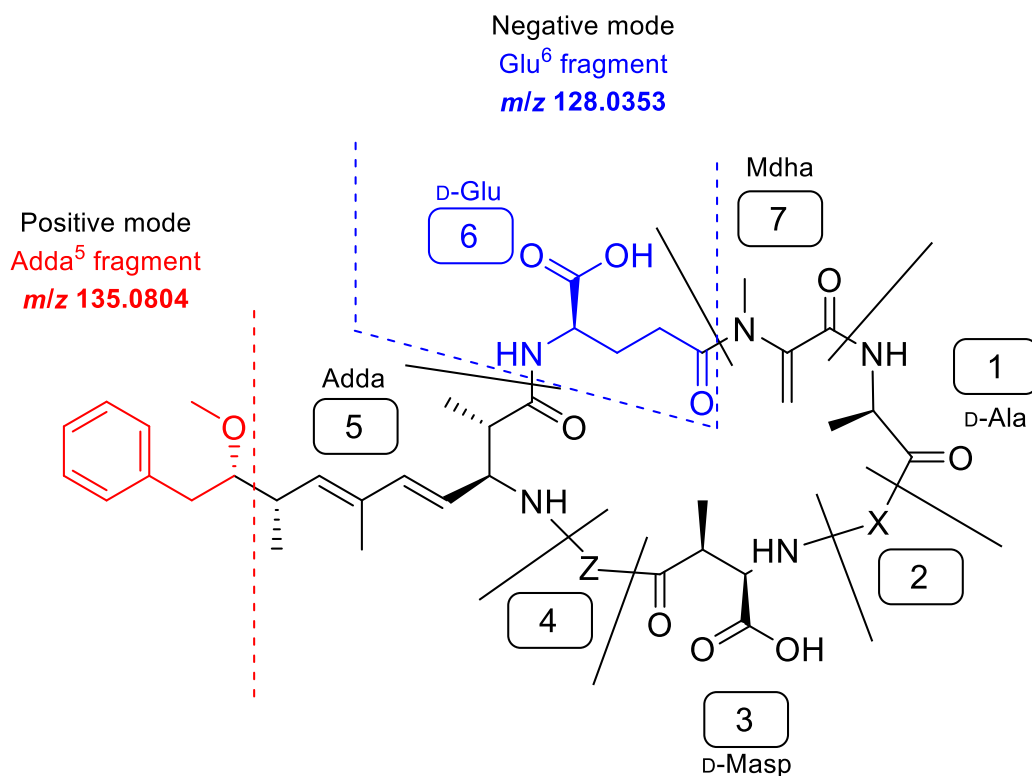
**Figure 19**. MCs class-characteristic fragments detectable in positive mode, *m/z* 135.0804 from Adda[5] residue (red) and, in negative mode, *m/z* 128.0353 from Glu[6] residue (blue). X and Z represent the two most variable positions (-2 and -4) of the seven in the MC-heptacyclic core (see section 3.1.3.1 Chemical structure, nomenclature and biosynthesis of MCs).

Together with these characteristic fragments, there are some sequence ions deriving from cleavages of peptide bonds, during collision-induced dissociation (CID), which open and break the heptacycle. They effectively help in sequencing the original structure, especially when comparing sequence ions from a new congener to the corresponding ones for reference standards of similar congeners (Tables 2–4 and Figure S13–S14 in **Paper I**). Some examples are given in **Figure 20a** and **20b**.
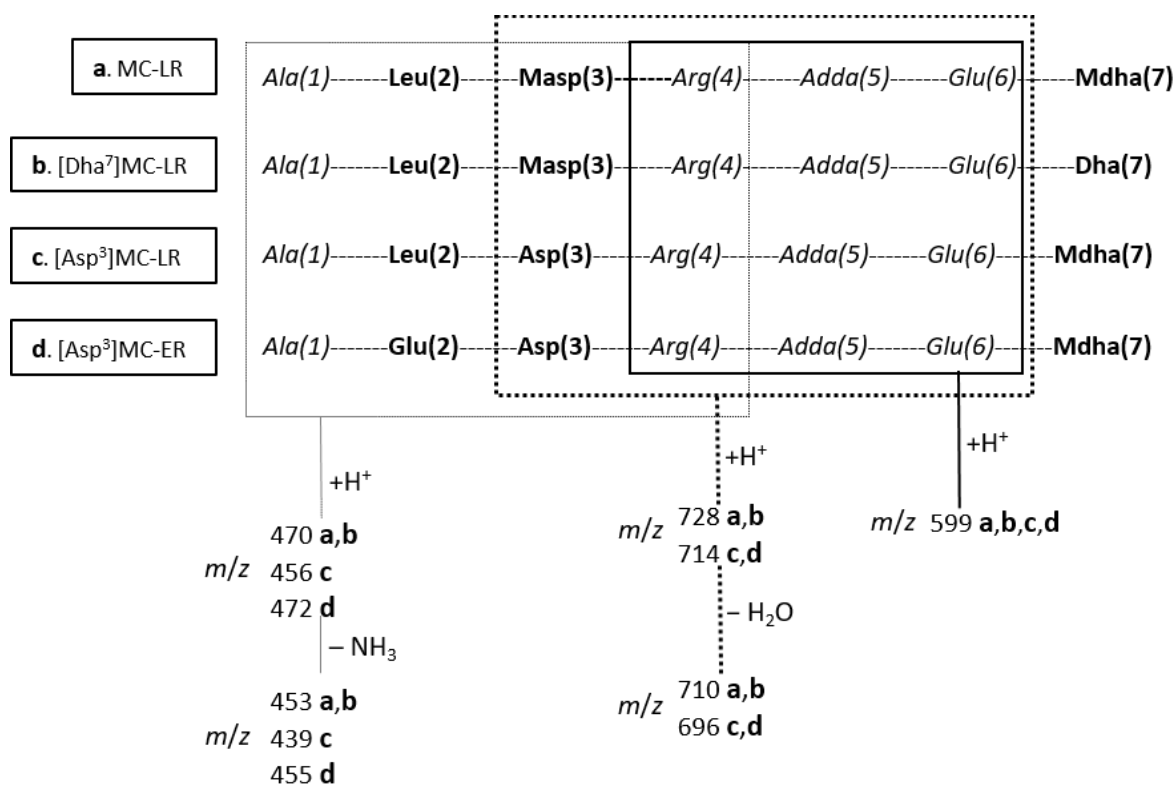
**Figure 20a.** Examples of sequence ions, *m/z* deriving from cleavages of peptide bonds (and eventual neutral loss of ammonia, $NH_3$ or water, $H_2O$), during, for four MC congeners (**a-d**).
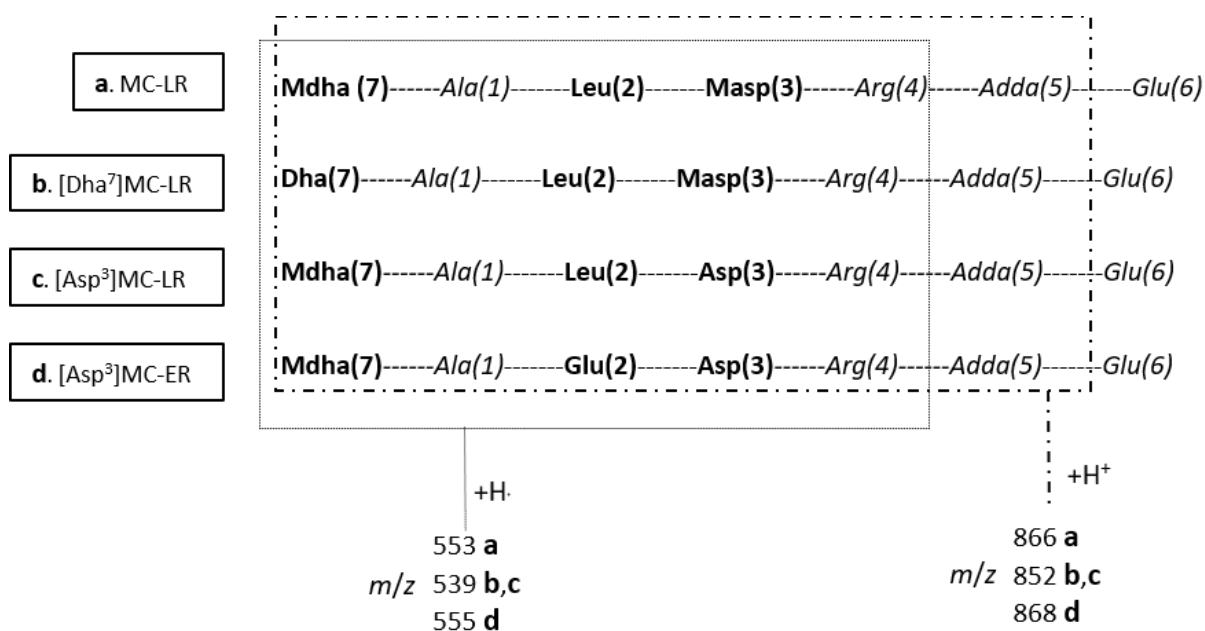


**Figure 20b.** Examples of sequence ions, *m/z* deriving from cleavages of peptide bonds, during CID, for four MC congeners (**a-d**).

Depending on energies involved in the collisions, different and complementary fragmentation information can be obtained. Higher-energy collisional dissociation (HCD) is a single-stage process, which involves a relatively small number of energetic collisions. It allows detection of ions over the full $m/z$ range and does not suffer from the low-mass cut-off that is common for CID. Therefore, HCD in connection with HRMS/MS allows simultaneous detection of characteristic fragments (low $m/z$) and main sequence ions (higher $m/z$ range) simultaneously. HCD is a feature of Orbitrap mass spectrometers (e.g., the hybrid quadrupole-Orbitrap, Q Exactive, instrument in **Paper I**). In contrast, CID, which is commonly performed in ion traps (e.g. the linear trap quadrupole, LTQ, in **Paper I**) involves longer time scales and a larger number of less energetic collisions. The main limitation of CID is due to the so-called 1/3 rule: product ions of less than 1/3 the precursor ion $m/z$ cannot be detected, thus excluding the class-specific fragments for MCs. However, it provides spectra rich in the middle $m/z$ product ions range for MCs (**Paper I**) [182]. Furthermore, allowing multiple stages of MS/MS (MS$^n$), it can be used to establish the origin of lower mass product ions using higher order experiments, e.g. MS$^3$ (this is not possible in the single-stage HCD process) [39]. Different information from different types of dissociation means different mass spectra potentially containing complementary information (Figure S4, **Paper I**) [184].

### 4.2.3.2.4 Scan modes used for MC structural elucidation in *Paper I*

Here a very brief explication of the scan modes used in **Paper I** (Q Exactive instrument), for a better text comprehension.

**FS Full scan:** scanning of ions within a defined mass range.

**AIF All-ion-fragmentation:** all precursor ions are fragmented without pre-selection by the quadrupole.

**DIA Data-independent acquisition:** all precursor ions within a selected $m/z$ window are fragmented and analyzed in a second stage of the MS/MS experiment.

**PRM Parallel reaction monitoring:** unlike the SRM (described in the section 4.2.2.3.1 Triple quadrupole (QqQ or TQMS)), which performs one transition at a time, PRM performs a full product ion scan for each selected precursor ion, that is, parallel monitoring of all fragments from the precursor ion. In a Q Exactive (**Paper I**), the Q is set to select the precursor ion(s) which is/are fragmented in the HCD collision cell. Finally, the Orbitrap scans all product ions with high resolution and high accuracy.

**SIM Selected ion monitoring:** the instrument is set to gather data at masses of interest. Since only a few masses are monitored, more time may be spent looking at these masses, thus increasing in sensitivity.

## 4.3 Functional group derivatization

Functional group derivatization is a tool that efficiently supported this thesis work on the aim "investigation of chemical structures of new MC congeners" in **Paper I**. In simple words, chemical reactions specifically targeting presumed functionalities of the investigated molecule(s) (i.e. novel MC congeners), were used to help to prove the presence (or absence) of certain amino acids in specific positions of the structure(s). The aim was to support structural hypothesis for novel MCs based on LC–(HR)MS/MS) data, supplemented with ^{15}N-labeling and isotopic profile analysis, as described in previous sections. The progress of the derivatization reactions was monitored using LC–HRMS.

Sections below give a general overview of the reactions that were utilized in the work reported in **Paper I**, in order to understand how they can be used to support tentative MC-structures. A further aim of the section is to highlight the specific roles these reactions played in this work.

### 4.3.1 Thiol conjugation

Thiol conjugation helped to clarify the identity of the amino acid in position-7 of the MC-ring [185]. As mentioned in the section on chemical structure of MCs, most congeners include Mdha as the amino acid in that position. Mdha contains an α,β-unsaturated carbonyl group. The electrophilic double bond is reactive towards nucleophilic thiols R–SH (nucleophilic addition). Mdha is the most common, but not the only amino acid found in position-7, as described in section 3.1.3.1 Chemical structure, nomenclature and biosynthesis of MCs. Its *N*-demethylated form, Dha, is one of the alternatives and it also contains an α,β-unsaturated carbonyl group. Both Mdha and Dha react readily with thiols (the *N*-methyl group having minimal effect on this reactivity). When a Dhb[7]-moiety is present, the MC's reactivity strongly decreases (ca. 2 orders of magnitude) compared to when an Mdha[7]-moiety is present, and derivatization may not be detected by LC–MS [186] (**Figure 21**).
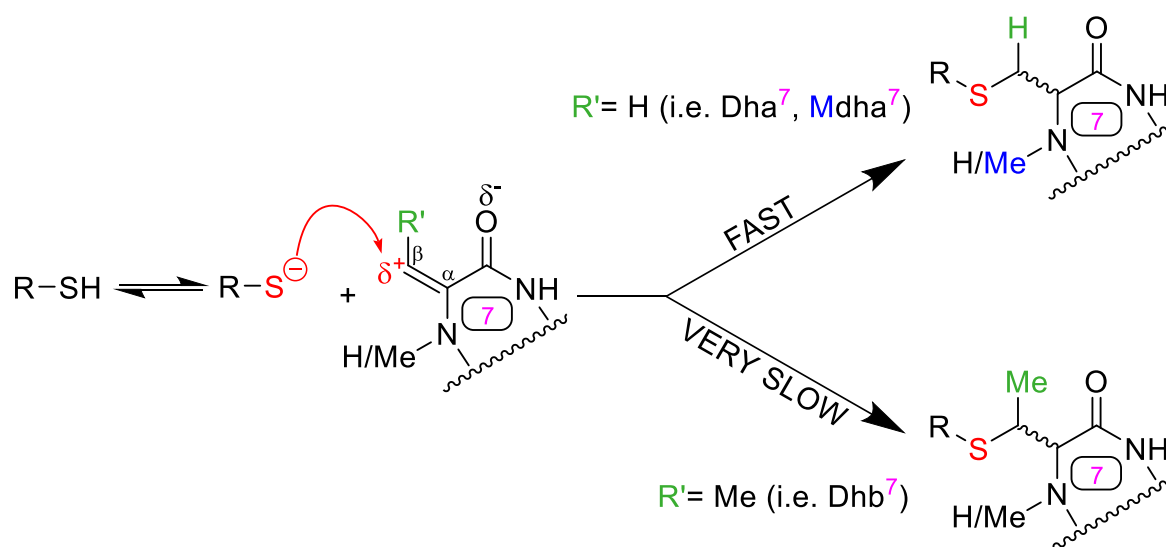


**Figure 21.** Nucleophilic addition of thiols to the electrophilic β-carbon of the α,β-unsaturated carbonyl group of moiety[7] of MC heptacycle. The thiolate, in equilibrium with its thiol, is the reactive nucleophile. The reaction happens easily when R' is a hydrogen (i.e., Dha, Mdha), under weakly basic conditions.

The reaction is comparatively very slow (and often undetectable) when R' is a methyl group (i.e., Dhb) [185].

This behaviour highlights the impact of the methyl group in the β-position, which is the only difference between Dha and Dhb. The same decrease in reactivity could be expected if Mdhb is present in position-7. However, since Mdhb is extremely rare in MCs [39], available data come from reaction of thiols with NOD-R (Mdhb is the dominant amino acid in position-5 for NOD analogues. Position-5 in the NOD-ring corresponds to position-7 for the MC-ring. [186]. A third possible scenario is that the amino acid in position-7 does not possess an α,β-unsaturated carbonyl group available for nucleophilic addition (e.g. *N*-methylserine (Mser), serine (Ser) or a pre-existing thiol-derivative), and thus there is no reaction. To summarize, there are three general groups of moieties that can be found in position-7 (**Figure 22**) of the MC-ring: those showing a "free double bond" ready to react with thiols (**A**); those with a methyl group in the β-position of the double bond, which significantly impedes the reaction (**B**), and moieties not having an α,β-unsaturated carbonyl group available for reaction (**C**).
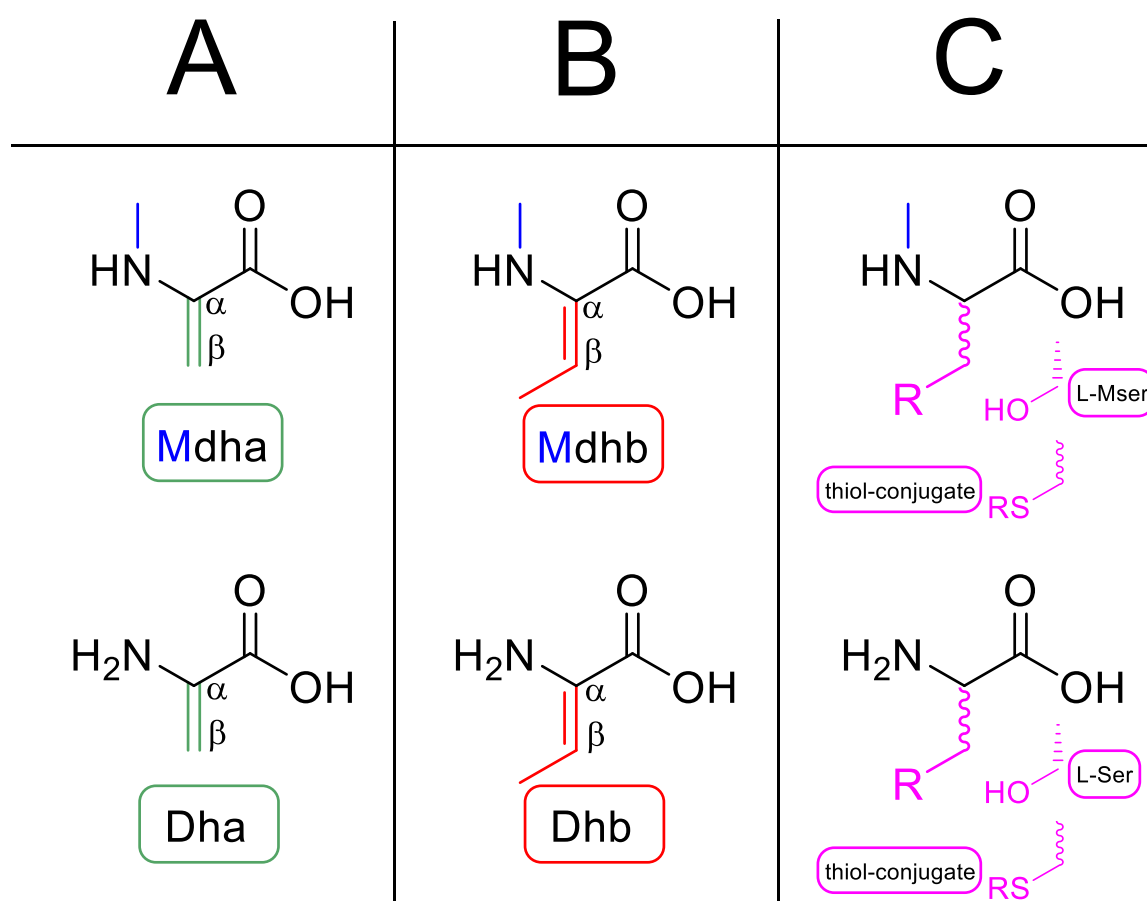


**Figure 22.** Examples of different moieties in position-7 of MC heptacycle, grouped according to their reactivity with thiols: **A)** α,β-unsaturated carbonyl group, readily reactive; **B)** α,β-unsaturated carbonyl group with a methyl group in β-position, which impedes reactivity; **C)** no α,β-unsaturated carbonyl group available.

Therefore, thiol derivatization represents a convenient practical tool to demonstrate the presence of Mdha or Dha in position-7, but also an easy way to differentiate between isobaric and isomeric amino acids like Mdha and Dhb [185] (Mdha and Dhb have the same molecular formula, thus not even HRMS methods alone can differentiate them), simply by observing their reactivity towards thiols.

Literature reports the reaction of several thiols (e.g. 2-mercaptoethanol, GSH, aminoethanthiol) with MCs [71, 186, 187]. The choice of the thiol needs to be appropriate and depends on the aim of the study. Thiol derivatization performed with 2-mercaptoethanol (herein simply referred to as mercaptoethanol) under weakly basic conditions was described by Miles and co-authors [186] as a simple and effective tool to help detect candidate MC analogues by LC–MS, especially in complex mixtures. The reaction is simple to perform and products of the nucleophilic addition are easily identifiable by LC–HRMS, because of the predictable increase in mass associated with the thiol (78.0139 in case of mercaptoethanol). Resulting derivatives from mercaptoethanol addition have similar retention times, ionization and fragmentation properties compared to their underivatized precursors. Thus, the study of MS/MS spectra of both underivatized precursors and derivatives may help with tentative identification of putative MCs, especially when reference standards are not available. In addition, the addition of the thiol moiety places the MC derivatives in a LC–MS mass window slightly, but significantly, shifted from the original MCs, with fewer interferences [186].

In **Paper I**, we performed two separate series of thiol derivatization experiments, using mercaptoethanol, or using a 1:1 mixture of mercaptoethanol and $d_4$-mercaptoethanol, as reactive thiols. The progress of the reaction was followed by two different LC–HRMS methods (see Experimental section, **Paper I**). The advantage of using the 1:1 mixture of mercaptoethanol and $d_4$-mercaptoethanol is that it results in a distinctive isotope pattern in the thiol derivatives, allowing their presence and identities to be determined with greater certainty.

Thanks to those derivatizations, we identified 8 of the 12 candidate MC peaks detected in *P. prolifica* NIVA-CYA 544 potentially containing Dha[7] or Mdha[7] (examples in **Figure 23**). The other four peaks were from MC congeners in which the double bond was already "occupied" from conjugations with biological thiols such as GSH (**Paper I**). Experimental conditions were based on Miles et al. [186] and can be found in the Experimental section of **Paper I**.
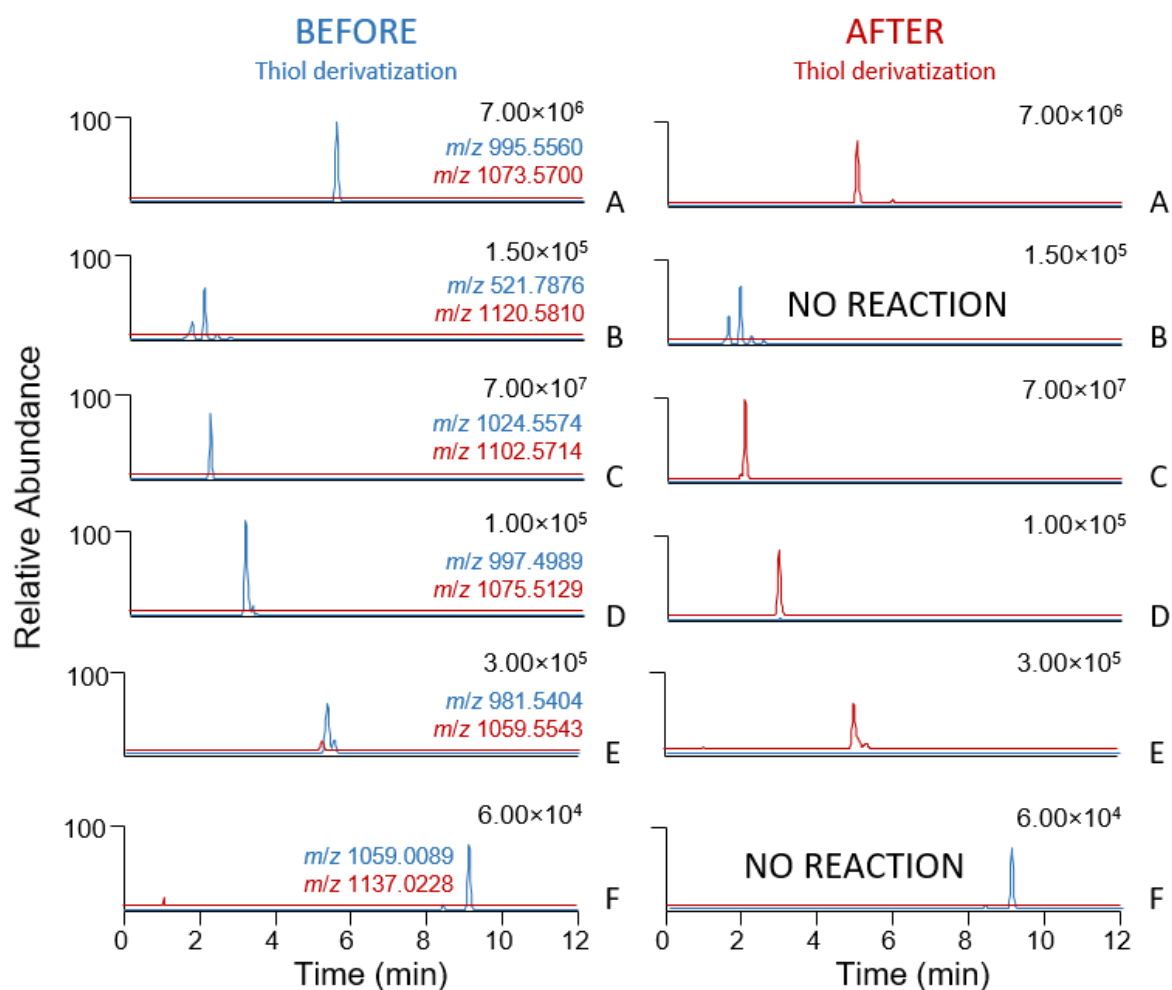
**Figure 23.** Extracted positive ion LC–HRMS chromatograms (± 5 ppm) before (**left**), and after (**right**), thiol derivatization with 2-mercaptoethanol. Blue lines represent underivatized MCs (*m/z* above) while red lines represent their mercaptoethanol derivatives (m/z below). (**A**) standard of MC-LR, and five examples among MC congeners from *P. prolifica* NIVA-CYA 544; (**B**) [D-Asp³,Mser⁷]MC-RR; (**C**) [D-Asp³]MC-RR; (**D**) [D-Asp³]MC-ER; (**E**) [D-Asp³]MC-LR and; (**F**) the heavy [D-Asp³]MC-RR conjugate. Pairs of chromatograms are on the same fixed scale (number in the top right-hand corner of each chromatogram).

In addition to aid structural elucidation of putative MC congeners, the mercaptoethanol reaction helped us to identify a mis-identified commercial standard, supplied (incorrectly) as [D-Asp³]MC-RR, but which was shown to be [D-Asp³,Dhb⁷]MC-RR. The standard did not react noticeably with mercaptoethanol (**Figure 24**), but was expected to do so if it would be [D-Asp³]MC-RR). This non-detectable reactivity [185], together with comparison of retention times of reference standards, allowed the correct identification of these structural isomers (**Figure 24**). At about the same time, Birbeck et al. [188] independently reached the same conclusion regarding their standard of [D-Asp³]MC-RR obtained from the same supplier.
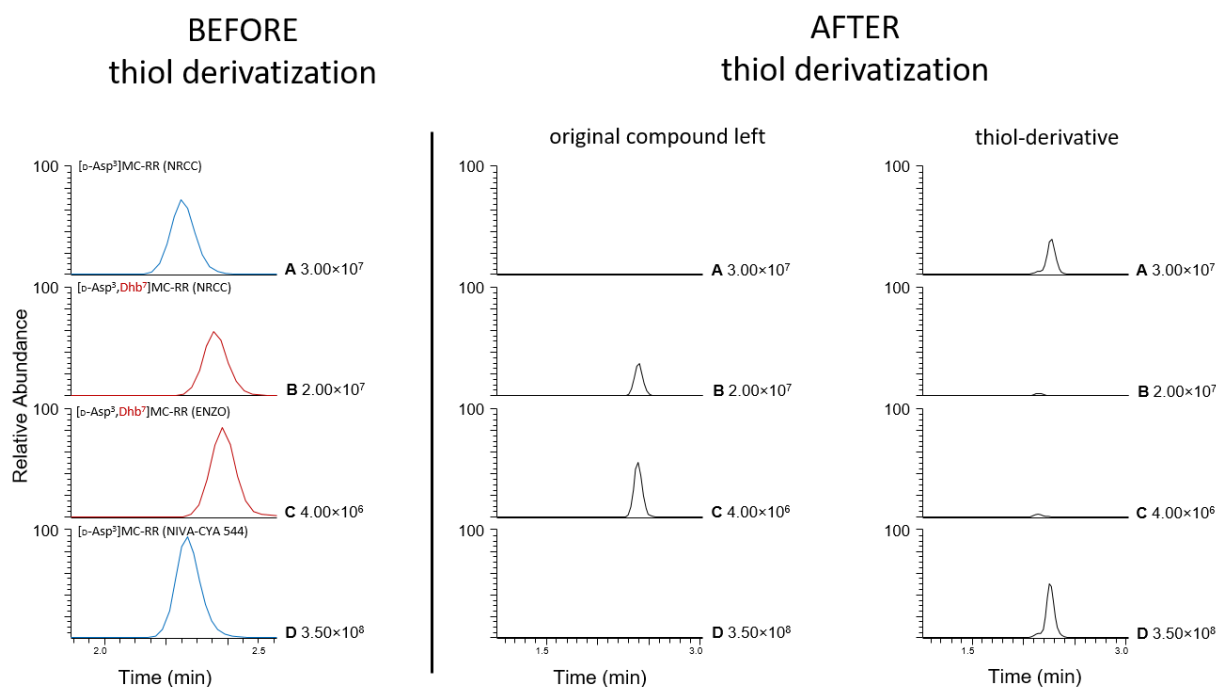
**Figure 24.** Extracted positive ion LC–HRMS chromatograms (± 5 ppm) before (**left**), and after (**right**), thiol derivatization with mercaptoethanol (thiol) of (**A**) reference standard of [D-Asp³]MC-RR from National Research Council of Canada (NRCC); (**B**) reference standard of [D-Asp³,Dhb⁷]MC-RR from NRCC; (**C**) commercial standard of [D-Asp³,Dhb⁷]MC-RR from ENZO mis-identified as [D-Asp³]MC-RR; [D-Asp³]MC-RR in *P. prolifica* NIVA-CYA 544. [D-Asp³,Dhb⁷]MC-RR, which contains Dhb in position-7, does not react detectably with mercaptoethanol under the conditions used. Chromatograms for each compound are on the same fixed scale (number in the bottom right-hand corner of each chromatogram). Peaks after thiol derivatization have reduced intensities (ca 2-fold) compared to those ones before the reaction, due to dilution with sodium carbonate buffer.

Derivatization with GSH falls in this category of reactions, too. We converted a standard of [D-Asp³]MC-RR to its GSH-conjugate to support the identification of the first reported GSH conjugate (Figure S15 of **Paper I**) of MCs in a cyanobacterial culture ([D-Asp³]MC-RR–GSH conjugate), through comparison of its retention time, accurate mass and LC–HRMS/MS spectra.

### 4.3.2 Methylation of carboxylic acid functionalities

Extracts of *P. prolifica* NIVA-CYA 544 were treated with diazomethane ($CH_2N_2$) to methylate and thereby count the number of reactive carboxylic acid groups present in each MC. The reaction was monitored by LC–HRMS/MS. Details of the method are described in the Experimental section of **Paper I**.

Diazomethane is a popular esterifying agent for laboratory use. It allows mild conversion of a carboxylic acid group to its methyl ester (**Figure 25**).
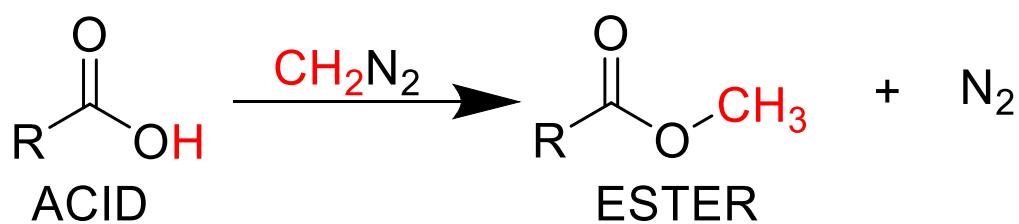
**Figure 25.** Methylation of carboxylic acid group with diazomethane ($CH_2N_2$).

Most MC congeners contain two carboxylic acids groups. These belong to the D-Glu[6] moiety, which is the most highly conserved in the MC cycle, and to D-Masp[3] or D-Asp[3], the most common moieties in position-3 [39]. Among the new congeners tentatively identified in **Paper I**, two were thought to contain Glu in position-2 and/or position-4, in addition to D-Glu being present in position-6 (i.e., [D-Asp[3]]MC-ER and [D-Asp[3]]MC-EE), based on LC–ITMS and –HRMS/MS data as well as ^{15}N isotope labelling. Thus, the final number of carboxylic acid groups were thought to be three and four, respectively, in these congeners (**Figure 26**).
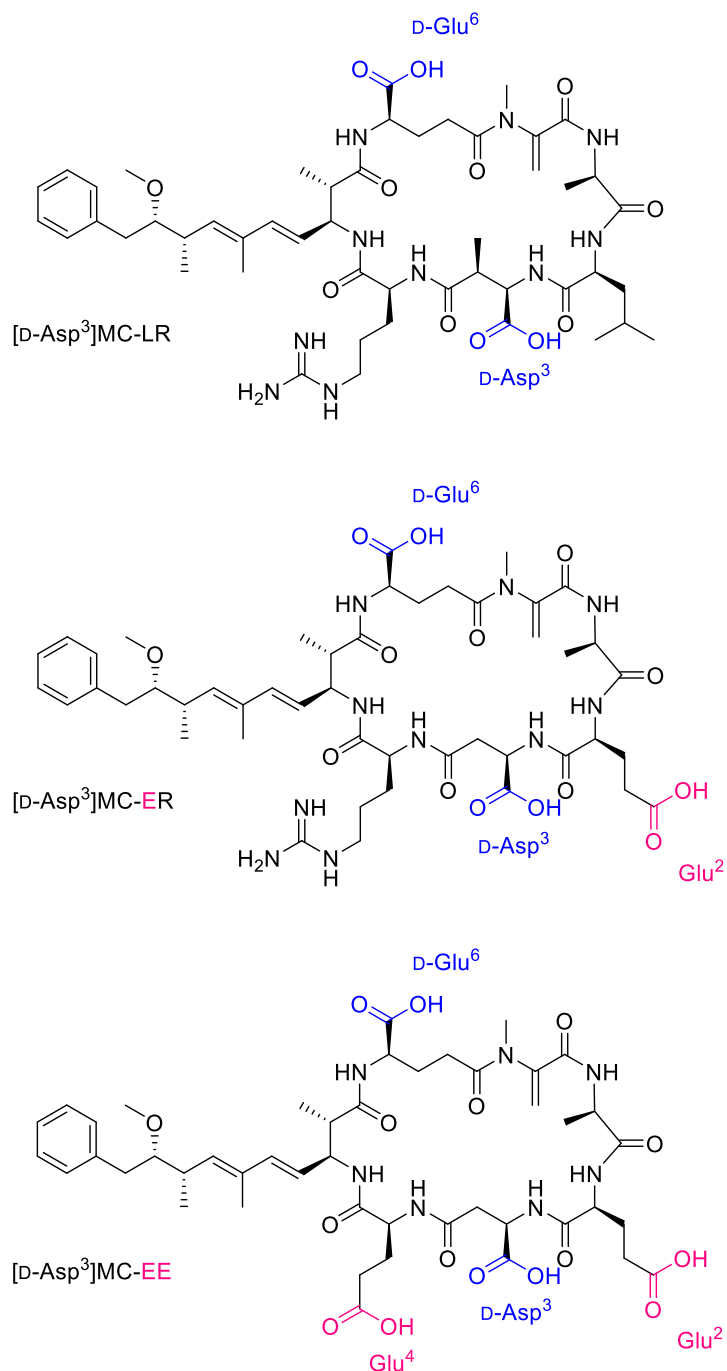
**Figure 26.** [D-Asp³]MC-ER and [D-Asp³]MC-EE contain one or two additional carboxylic acid groups compared to [D-Asp³]MC-LR, respectively (the pink Glu² and/or Glu⁴), in addition to the two carboxylic acids (the blue D-Asp³ and Glu⁶) found in [D-Asp³]MC-LR and most other MCs.

Esterification with diazomethane was used in this work, as a means of counting the total number of reactive carboxylic acid functionalities and thereby verifying the presence of additional Glu moieties. It was a complementary tool, to support the tentative identification of new MC congeners as [D-Asp³]MC-ER and [D-Asp³]MC-EE. In fact, HRMS/MS methods alone could not prove the specific presence of Glu even though they could provide accurate masses of fragments, and thus only the probable elemental composition of moieties in position-2 and/or -4. **Figure27** shows some examples that would have the same elemental composition as Glu.

However, both structures on the right do not contain the carboxylic functionality and would be unreactive towards a methylation agent as mild as diazomethane.
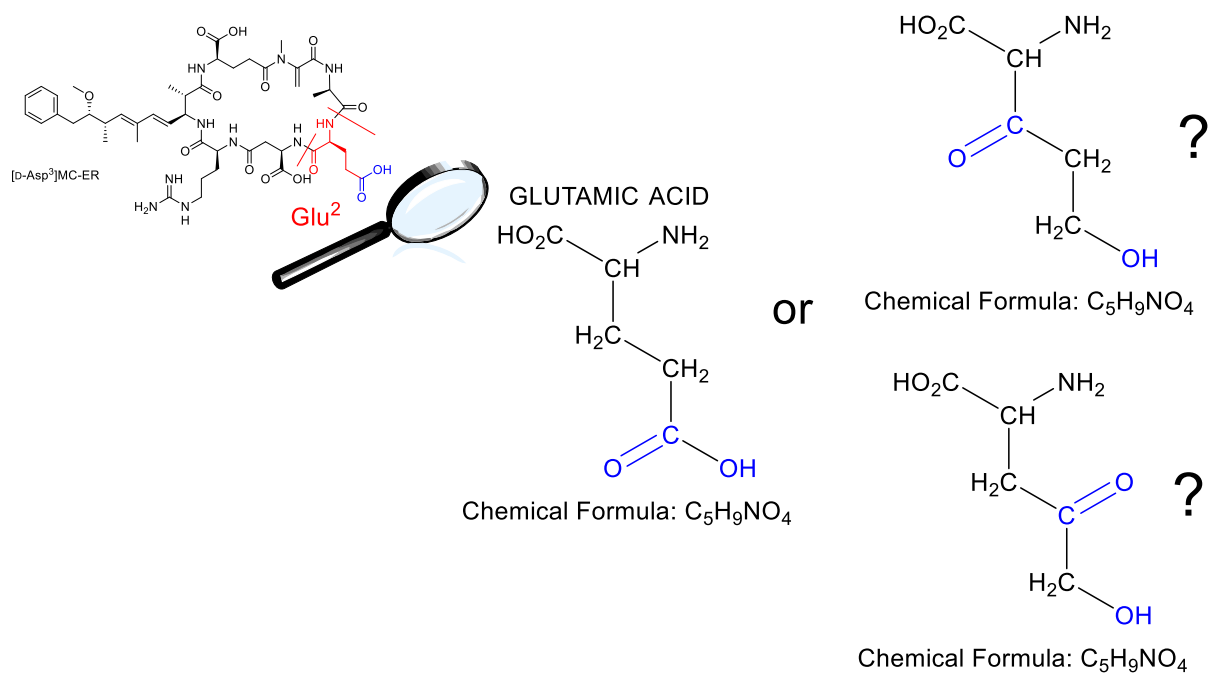


**Figure 27.** Left-hand side: structure of [D-Asp³]MC-ER with Glu² moiety highlighted in red and the carboxylic functionality highlighted in blue. Center and right-hand side: structures of glutamic acid and two structural isomers. Glu-isomers can be excluded as moiety in position-2 in [D-Asp3]MC-ER, using esterification with diazomethane.

Methylation could then confirm whether or not those elements were arranged to form a carboxylic acid, and if so then the structural formula likely corresponded to Glu (**Figure 28** and **Figure 29**).
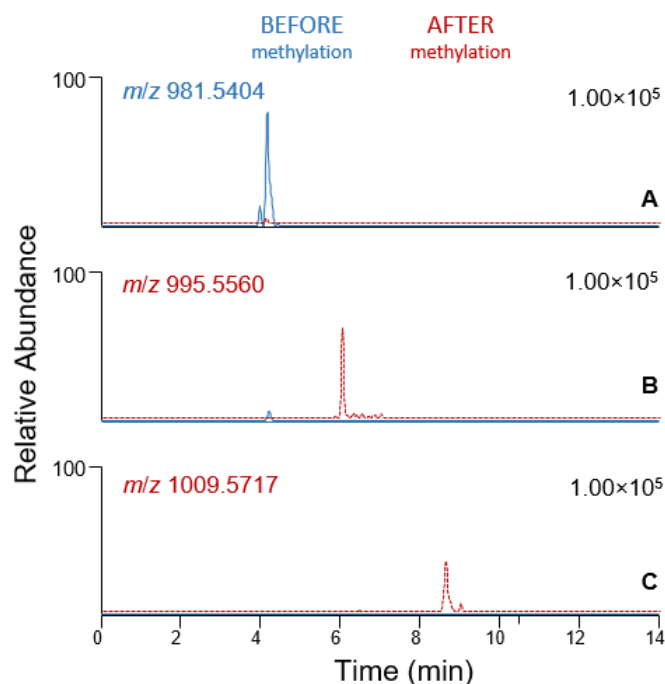
**Figure 28.** Extracted positive ion LC–HRMS chromatograms (± 5 ppm) of: (**A**) a [D-Asp³]MC-LR reference standard and its; (**B**) monomethyl esters, and; (**C**) dimethyl ester (exact *m/z* reported in the left-hand corner) obtained by reaction with diazomethane. Chromatograms are on a fixed scale (number in the top right-hand corner of each chromatogram). Full light-blue lines are chromatograms prior to reaction; dashed red lines are from analysis of the reaction mixture.
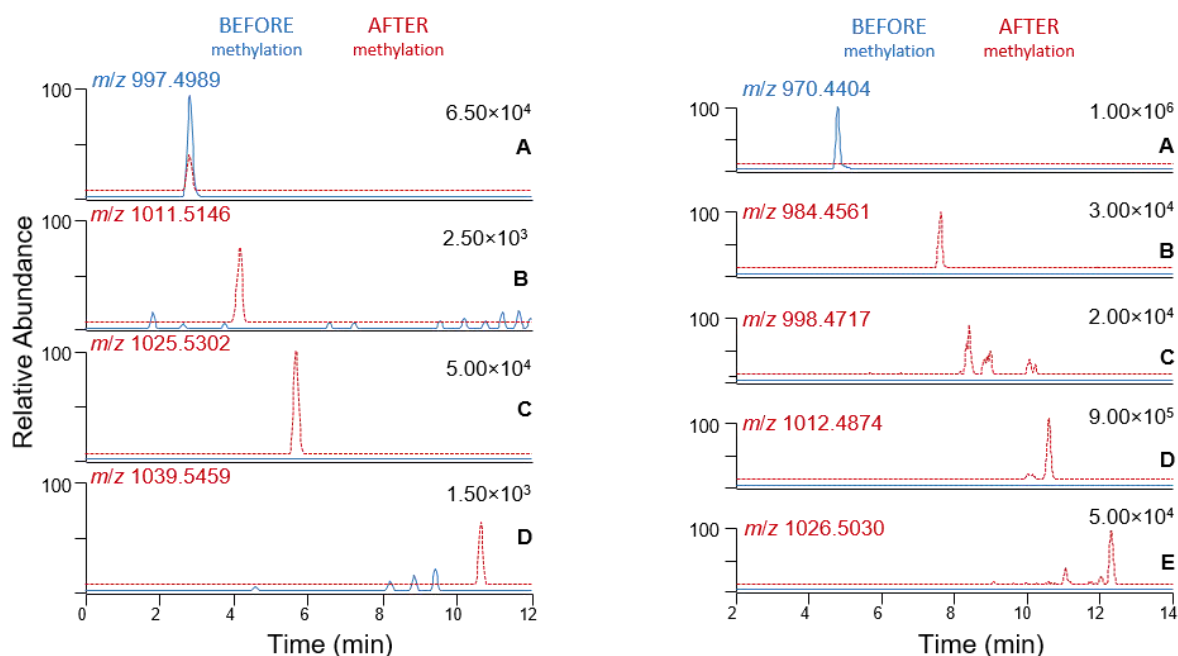


**Figure 29.** Extracted positive ion LC–HRMS chromatograms (± 5 ppm) of [D-Asp³]MC-ER (**left**, **A**) and [D-Asp³]MC-EE (**right**, **A**) from NIVA-CYA 544 and its monomethyl esters (**B**), dimethyl esters (**C**) trimethyl ester(s) (**D**) and tetramethyl ester (**E**) (exact *m/z* reported on the left-hand corner) obtained by reaction with diazomethane. Chromatograms are on a fixed scale (number in the top right-hand corner

47

of each chromatogram). Full light-blue lines are chromatograms prior to reaction; dashed red lines are from analysis of the reaction mixture.

Esterification is a common reaction (usually acid-catalysed) between carboxylic acids and alcohols. Thus, acidic methanol-containing solutions, which are often used for extraction, isolation and/or storage of MCs, can create favourable conditions for esterification of carboxylic acid groups. The D-Glu[6] carboxylic acid is readily esterified by acidic methanol [189] or by (trimethylsilyl)diazomethane/ethanol [177], and it has been suggested that all reported D-Glu(OMe)-containing MCs are artefacts generated through esterification rather than being biosynthesized by cyanobacteria [39]. Namikoshi et al. [190] reported seven MCs that all contained -E(OMe), i.e. methyl esters of Glu in position-2 and/or -4. With hindsight, these were all probably artefacts originally biosynthesized as -EE congeners. Since methyl ester artefacts have been reported at position-2 and -4 [190], but not at position-3 and -6, it seems likely that the conditions were sufficiently favourable for Glu[2] and/or Glu[4] esterification, but not for D-Asp[3] and D-Glu[6] esterification. This suggests that Glu[2] and/or Glu[4] are more easily esterified than D-Asp[3] and D-Glu[6] moieties.

### 4.3.3 Oxidation with sodium periodate

Extracts were also treated with sodium periodate to identify compounds containing sulfide linkages via oxidation to their sulfoxides. This reaction was performed at the NRCC and it was monitored by LC–HRMS/MS, as described in the Experimental section of **Paper I**.

Periodate is a mild oxidant and it is well known to oxidize sulfides to sulfoxides [191]. On the other hand, sulfoxides are not expected to further oxidize to sulfones (too mild oxidant) (**Figure 30**). In **Paper I**, sodium periodate has been used.
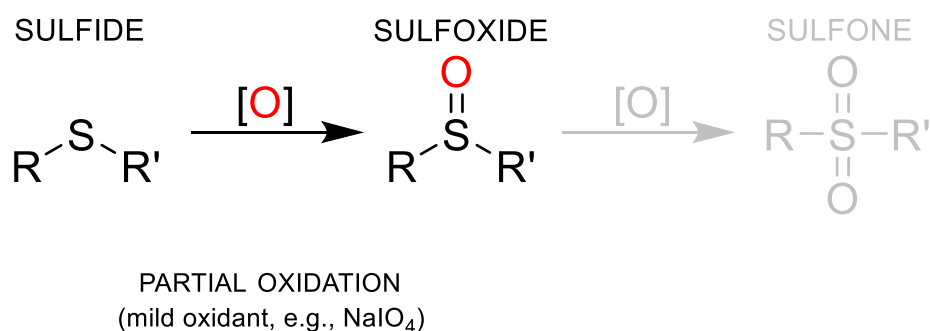


**Figure 30**. Oxidation of a sulfide group to a sulfoxide group with a mild oxidant, e.g. sodium periodate (NaIO$_4$).

The reaction supported the tentative identification of a MC congener with a surprising (considering the usual range of MCs) high-molecular-mass (2116 Da) in *P. prolifica* NIVA-CYA 544, which was a sulfide conjugate of [D-Asp[3]]MC-RR. Its sulfoxide was also present in the strain, likely as an autoxidation [54] product (**Paper I**). The sulfide was quantitatively converted into its sulfoxide by the reaction with periodate, establishing the sulfoxide nature at the same time (Figure S2-S3 of **Paper I**). The sulfoxide itself did not react detectably to give the sulfone, as expected because of the mild oxidation power of periodate. We did not investigate the structure of the *S*-conjugate further at this stage.

## 4.4 *In vitro* assays for ED activity investigation

*In vitro* assays for studying ED activities represent simple-to-use tools. They can be well-suited for the screening of EDs based on their toxicological mechanisms. Such assays are complementary to analytical-chemical methods [192].

EDs can be identified according to some characteristics they share, the KCs [125] described in section 3.2.3 State of the science on EDs). These KCs reflect the variety of modes of action through which a compound can interfere with the endocrine system's pathways. Different mechanisms require different assays. The lack of a complete *in vitro* array of predictive models for each mode of action is one of the gaps for the hazard assessment of EDs [123].

In this thesis work, three types of *in vitro* assays to study the potential ED activity of cyanobacteria have been used (**Figure 31**). Two of the assays are based on mammalian cell line models: reporter gene assays (RGAs) (**Paper II**), and the H295R steroidogenesis assay (**Paper III**). While the purpose of the former is to measure effects (of cyanobacterial compounds) on steroid nuclear receptor(s) signaling, the latter investigates effects on steroid hormones production. The third assay, which aimed to investigate effects on 17β-estradiol biotransformation (in particular Phase I metabolism modulation), was based on the human liver microsome (HLM) model (**Paper II**).
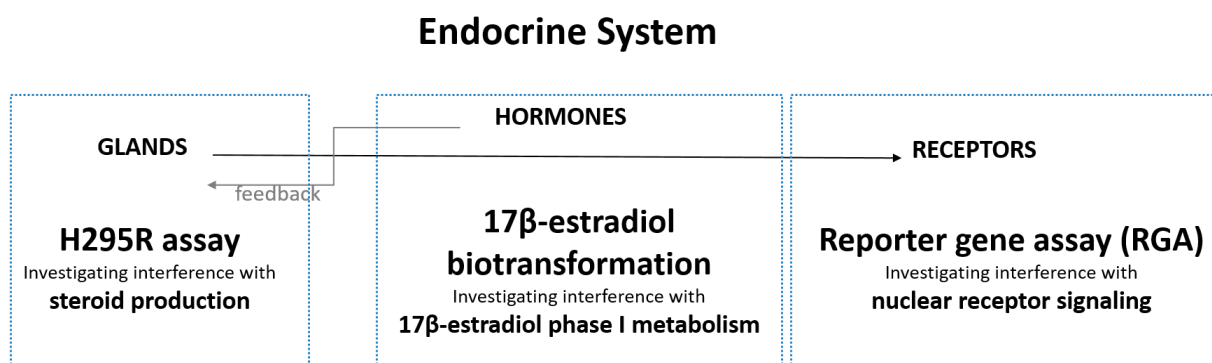


**Figure 31.** *In vitro* assays used for investigation of ED activity of cyanobacterial compounds.

These three assays assess effects on different aspects of the endocrine system (see the section 3.2.2 The endocrine system) from the biosynthesis of hormones at the glandular level, to hormone-receptor interactions, passing through hormones' metabolism. In the following sections, the basic principles of these assays are described, highlighting their use in this thesis. Experimental details are described in **Paper II** (RGAs and HLM assay) and **Paper III** (H295R assay).

**4.4.1 Cell based bioassays**

**4.4.1.1 Reporter gene assays (RGAs)**

Receptor-mediated mechanisms are the most widely investigated with regards to ED activity. They are the most intuitive mechanisms, since receptors represent the targets of individual hormones [95]. In this work, RGAs were the first *in vitro* bioassays that were used to investigate the effects of cyanobacterial extracts on the receptor level (**Paper II**).

RGAs can measure agonistic and antagonistic effects (of tested compounds) on specific cellular receptors. These are nuclear (intracellular, located in the nucleus) receptor proteins, reached by their specific steroid hormones. Thus, steroid hormones are molecules that are sufficiently small and hydrophobic to diffuse across cell membranes in order to bind at the nuclear receptors. In unstimulated cells (i.e. when the hormone is absent), steroid receptors are in an inactive form and often part of a multi-protein complex in the cell. Upon hormone binding, the receptor undergoes a conformational change and acts as transcription regulator in the nucleus. It binds to DNA on specific steroid response elements (SRE) and activates the transcription of its target genes [193, 194]. RGAs are designed to detect exactly such an activation, using a so-called "reporter gene", a gene that can be fused to regulatory sequences or genes of interest, to report expression location or levels by producing proteins that enables detection and measurement of gene expression [192, 195, 196] (**Figure 32**).

In this work, cell lines that respond to specific types of steroid hormones were used as RGAs: MMV-Luc (estrogen-responsive), TARM-Luc (androgen-responsive) and TGRM-Luc (glucocorticoid-responsive). These cell lines were originally developed by transfecting human mammary gland cell lines with relevant receptors and incorporating a transactivation step with a signaling protein, the luciferase [193]. The luciferase gene (*luc*) is a commonly used reporter gene in such assays [197]. It is one of the two types of *luc* genes, cloned from either fireflies, as in this case, or bacteria. It encodes a 61-kDa enzyme able to oxidize the substrate D-luciferin, in the presence of adenosine triphosphate (ATP), oxygen, and $Mg^{2+}$, yielding a fluorescent product that can be quantified by measuring the released light [198].
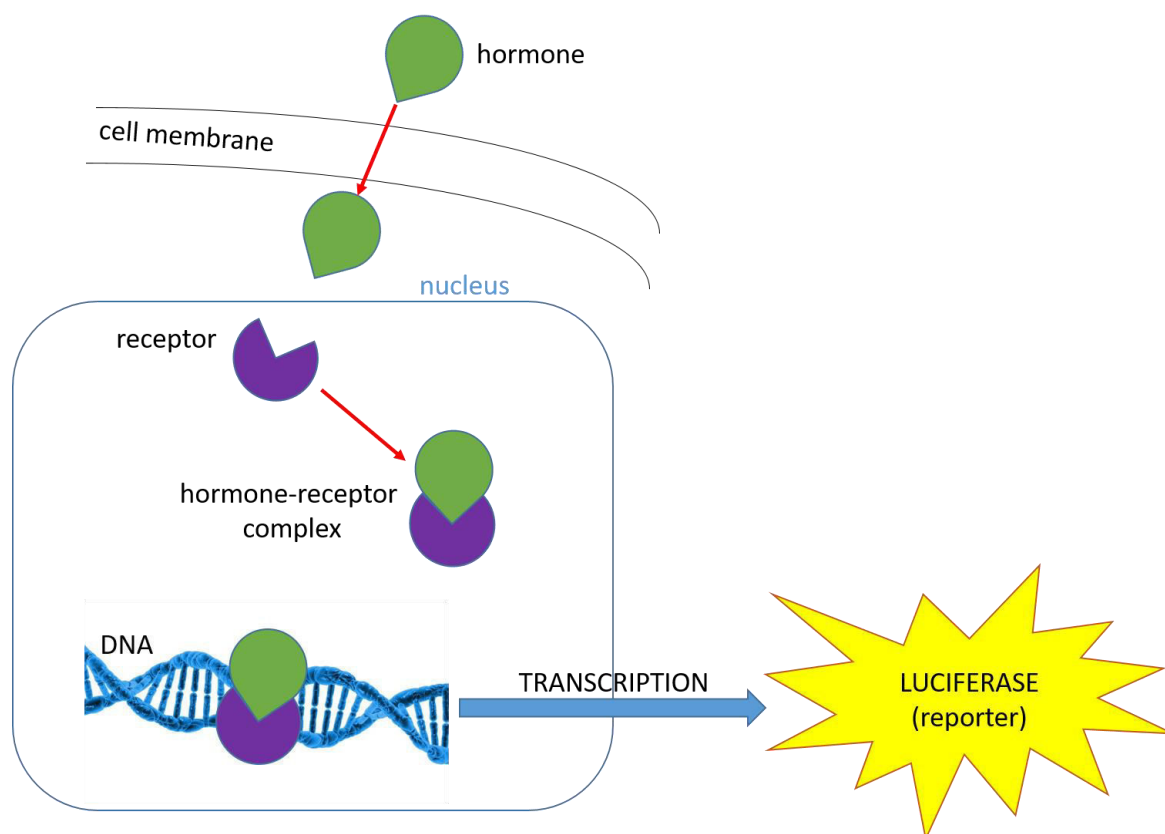
**Figure 32.** Scheme of (reporter gene) luciferase gene assay functioning.

Compared to simple receptor-binding assays, which can only determine binding — but not the activation, RGAs are able to measure receptor activation through the measurement of the signaling protein luciferase. Thus, RGAs can discriminate receptor agonists and antagonist compounds (compounds able to respectively mimic or block natural transcriptional activation of steroids by binding to their nuclear receptors, see section 3.2.3 State of the science on EDs), providing a specific and sensitive means for ED activity screening [192].

In this work, RGAs were used to screen extracts from the whole cyanobacterial collection, both for agonistic and antagonistic effects (see the section 3.2.3 State of the science on EDs) on estrogen, androgen and glucocorticoid receptors (**Paper II**).

### 4.4.1.2 H295R steroidogenesis assay

The human adrenocortical carcinoma cell line, H295R (also referred to as NCI-H295R), originated from an excised adrenocortical carcinoma [199]. The initial cells obtained from the patients' tumor were cultured and the resultant cell line was called NCI-H295. Further efforts were made to select a population of cells with better monolayer attachment and more rapid growth, which are the (NCI-)H295R (three different strains are available) [199, 200].

The H295R cell line is a model for studies on adrenal steroidogenesis and its disruption [138, 201]. Steroidogenesis is the overall process of steroid hormones production.

The adrenal cortex is the outer part of the adrenal gland, which is one of the main endocrine glands (located above the kidneys), where steroidogenesis takes place. It is divided into three

zones: zona glomerulosa, zona fasciculate and zona reticularis [202]. The adrenal cortex is a major target organ affected by EDs [108, 203]. H295R cells conserve physiological characteristics of the undifferentiated adrenal cortex gland. Thus, these cells have the unique property of expressing genes that encode for all the key steroidogenesis enzymes and represent a powerful tool for ED activity investigation [201].

Steroidal hormones include corticosteroids (glucocorticoids and mineralocorticoids) produced mainly in the adrenal cortex and sex steroids (estrogens, androgens and progestogens, produced mainly in the gonads [204]. The distinction in production site is not exclusive, however, because the adrenal cortex also secretes sex hormones, albeit to a lesser extent than the gonads, and also the ovaries may produce adrenal steroids under abnormal conditions [205, 206]. All steroid hormones have a common precursor, cholesterol. Steroidogenic acute regulatory protein (StAR) transport cholesterol to the inner mitochondrial membrane in steroidogenic cells. This rate-limiting step is followed by the action of several key enzymes that modify cholesterol into other steroidal hormones [206] (**Figure 33**).
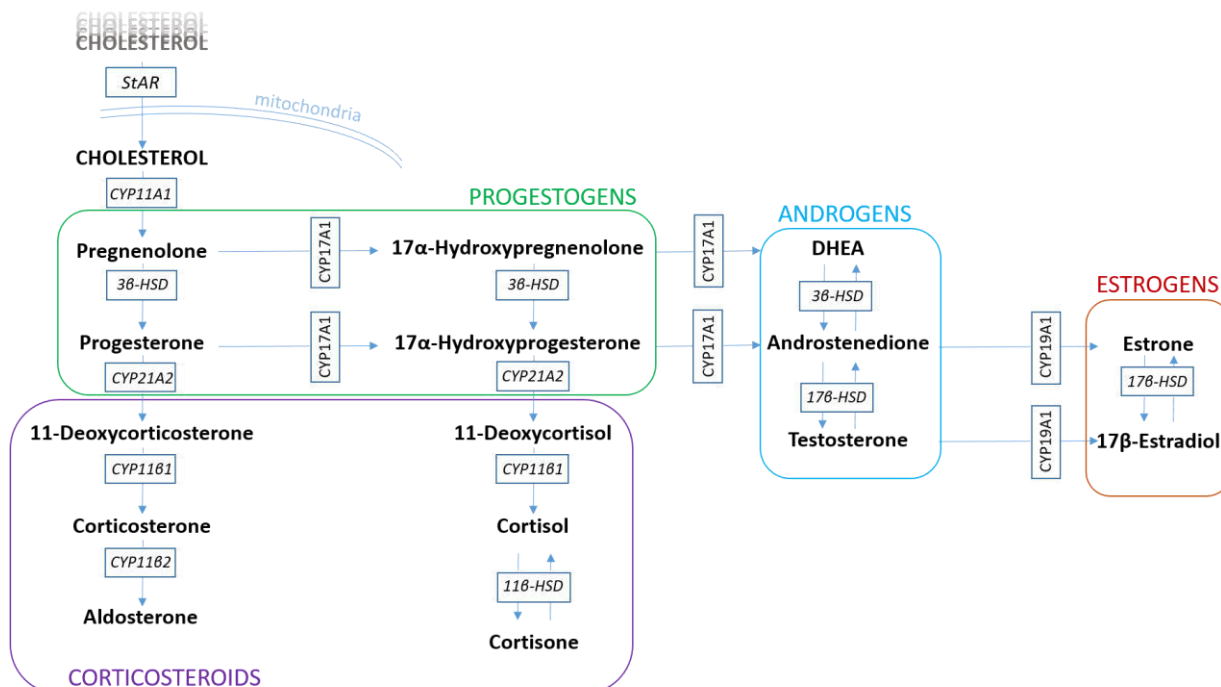


**Figure 33.** The steroidogenesis pathways including steroidal hormones (in bold black). Enzymes that catalyse the interconversion of individual hormones are in shown in italics.

Steroidal hormones regulate several important functions, including growth and development, metabolism and reproduction [207].

A variety of xenobiotics can alter the gene expression or activity of enzymes that are of importance for steroidogenesis. By altering the production or catalytic activity of steroidogenic or steroid-catabolizing enzymes, these chemicals have the potential to alter the steroid balance in organisms, with potentially major adverse effects [205, 208].

The H295R steroidogenesis assay has been used at the last stage of the investigations on cyanobacterial ED activity. The aim was to clarify the potential impact of MCs, and MC-LR in

particular, on steroidal hormones production, as well as to discriminate MCs' role from that one of other cyanobacterial active metabolites. To do that, 14 hormones of the steroidogenesis pathways were quantified by LC–MS/MS after exposing H295R cells to cyanobacterial compounds (**Paper III**).

### 4.4.1.3 *In vitro* cell viability and cytotoxicity assays (MTT and AlamarBlue)

Cell viability and cytotoxicity (i.e., being toxic to cells) assays are important tools for biological evaluation of *in vitro* studies. Cell viability assays measure live and healthy cells within a population and/or their survival following treatment with compounds, to guarantee cell performance when used for *in vitro* bioassays while cytotoxicity assays measure dead cells. Either cells health is evaluated through measurement of their metabolic activity, ATP content, cell proliferation or using cell toxicity assays that provide a readout on markers of cell death, such as a loss of membrane integrity.

*4.4.1.3.1 MTT assay*

MTT (3-(4,5-dimethylthiazol-2-yl)-2–5-diphenyltetrazolium bromide) assay is a common colorimetric assay. Reagents used in colorimetric assays develop a color in response to the viability of cells, quantifiable by spectrophotometer measurements. In viable cells with active metabolism, the yellow MTT is reduced to the purple formazan by NADH and quantified by light absorbance at specific wavelength. MTT formazan is insoluble in water, and it forms purple needle-shaped crystals in the cells. Therefore, prior to measuring the absorbance, an organic solvent such as dimethyl sulfoxide (DMSO) is used to solubilize the crystals [209, 210].

MTT assay has been used along with RGAs (details in **Paper II**).

*4.4.1.3.2 AlamarBlue assay*

AlamarBlue assay (or resazurin reduction assay) is based on enzymatic activity measurement. It is a widely used fluorimetric assay. It is based on the conversion of the blue non-fluorescent dye resazurin ((7-hydroxy-3H-phenoxazin-3-one-10-oxide) non-toxic and cell permeable compound), to the pink fluorescent resorufin by mitochondrial and other enzymes such as diaphorases, after entering cells. Viable cells convert continuously resazurin to resorufin, thus the amount of produced resorufin is related to the number of viable cells and it can be quantified using a microplate reader fluorimeter. The resazurin incubation period needed for a sufficient fluorescent signal above background is usually about 1–4 hours.

AlamarBlue assay has been used along with H295R assay (details in **Paper III**).

### 4.4.2 HLM biotransformation assay

Liver microsomes (in this study human liver microsomes) are just one among several possible liver preparations (i.e. liver slices, hepatocytes, etc.) that can be used to study the biotransformation of chemical substances [211, 212].

Biotransformation is a metabolic process, which takes places mainly (but not exclusively) in the liver. This process consists of a series of different reactions, which commonly aim to increase the hydrophilicity of a compound (both exogenous and endogenous) to facilitate its excretion [213]. These reactions either can occur simultaneously or sequentially, or even in reverse and are usually grouped into two main phases, depending on the chemistry involved. Phase I involves functionalization reactions (e.g. oxidative, reductive, hydrolytic). Phase II

biotransformation consists of conjugation with polar molecules (e.g. glucuronidation, acetylation and sulfation, conjugation with GSH or with amino acids). A phase 0, corresponding to the uptake of the compound through transporters, and a phase III, which refers to transporter-mediated elimination, have also been defined [214]. **Paper II** focused on the effect of cyanobacterial compounds on phase I biotransformation of 17β-estradiol.

The enzymes catalyzing biotransformation reactions can give biotransformation products that render the substrate compound inactive, active, or even (more) toxic or bioactive [213, 215]. The major enzyme metabolizing activity is preserved in microsomal *in vitro* models, although microsomes are artefacts, i.e. they are not present in living cells. Indeed, they are concentrated and separated from other cellular debris by differential centrifugation on homogenized hepatic cells [212]. The microsomal fraction consists primarily of soluble enzymes from the endoplasmic reticulum that are isolated and concentrated. The cytochrome P450 system (or CYPs) [216] is the family of membrane-bound enzymes found within the endoplasmic reticulum of hepatocytes, and is thus one of the types of enzymes concentrated in the microsomes, which mainly catalyze phase I oxidation reactions [212]. Microsomes containing high amounts of specific CYPs can be prepared via heterologous expression [217]. Microsomal model require exogenous cofactors for enzymes to be active. For phase I oxidations this is a nicotinamide adenine dinucleotide phosphate (NADPH)-regenerating system (**Paper II**).

The HLM model is widely used in drug metabolism research. It is a relatively cheap model, easy to use and microsomes may be stored (–80 °C, or below) for several years [218, 219].

In this thesis, the HLM model has been used to evaluate the impact of cyanobacterial compounds, i.e. MC-LR and an extract from an MC-LR-producing strain of *M. aeruginosa*) on 17β-estradiol phase I biotransformation. The aim was to investigate a possible estrogenic effect through a non-receptor mediated mechanism, 17β-estradiol was incubated either alone or in the presence of MC-LR or *M. aeruginosa* extract. 17β-estradiol depletion as well as the concurrent production of the main oxidative metabolites were investigated by LC–MS/MS (**Paper II**).

### 4.4.3 MC ELISA

An indirect competitive multihapten MC ELISA was used (**Paper II**), along with LC–MS and literature data, to confirm MC production by cyanobacterial strains in the collection of *Microcystis* and *Planktothrix* spp. used for this thesis' work. This assay played a minor role in the thesis, as a supportive screening tool. However, it is an interesting and useful tool for MC analysis in general. Further details can be found in Samdal et al. (2014) [152].

# 5. DISCUSSION OF MAIN RESULTS

This project aimed to investigate the potential role of cyanobacterial metabolites, in particular MCs, as EDs. It was a rather broad aim that may be approached in many ways. However, this general aim was translated into specific goals, which lead to the achievement of results described in **Paper I**, **Paper II** and **Paper III**.

The goals were:

1. **Structural investigation** of (new) MC congeners (**Paper I**).

2. **Investigation of ED activity** (and **related mechanisms** of action) of MCs and cyanobacterial extracts (**Paper II**, **Paper III**).

This chapter does not aim to replace the detailed discussions in the attached publications, but rather to summarize and provide an overview of the overall relevance and interconnection of the findings.

In hindsight, the findings reported in this thesis are generally mostly related to research that was performed using two cyanobacterial strains from the collection of 27. These were *P. prolifica* NIVA-CYA 544 (isolated in Norway in 2004) and *M. aeruginosa* PCC7806 (isolated in the Netherlands in 1972). They represent the two genera investigated in this work, and both strains were able to synthesize MCs. The two strains had previously been used in several studies. The *M. aeruginosa* strain has been used also for studies on cyanobacterial ED activity [144, 147]. They represented established starting points for this work and could still provide interesting data and results. In addition, this work focused on the most studied cyanotoxins, the MCs, including exploring their structural variability (**Paper I**), their potential ED activity *in vitro*, and especially the potential ED activity of the well-studied congener MC-LR (**Paper II** and **Paper III**). Overall, it was a well-balanced approach for exploring a field so wide but at the same time as little studied as cyanobacteria and EDs.

## 5.1 Structural investigation: new MC congeners from *P. prolifica* NIVA-CYA 544 (Paper I)

In *P. prolifica* NIVA-CYA 544 extracts, we could identify up to seven unreported MC congeners. This strain was supposed to be tested for endocrine effects on nuclear receptors in RGAs, as part of the ED activity investigation (**Paper II**). During the original low-resolution LC–ITMS screening, which aimed merely to confirm MC production before performing RGAs, a potential MC of unreported molecular mass was detected (*m/z* 997) during this strain's analysis, suggesting the presence of a possible new MC variant. Indeed, this congener was later on tentatively identified as [D-Asp³]MC-ER.

This discovery was the starting point of a deeper investigation of the strain extracts, utilizing a combination of analytical tools (described in the 4. Methodologies chapter and discussed in the

last part of this section), which eventually led to the (tentative) identification of the new MC congeners that are described in **Paper I**. The tools and especially their combination played a crucial role.

**Table 2** on the next page summarizes some of the principal data for new MCs reported in **Paper I**, including their neutral formulae, number of nitrogen atoms as measured from $^{15}$N-labeling, exact $m/z$ for protonated and deprotonated molecules, reactivity to thiol and number of carboxylic acid functionalities (derived from methylation with diazomethane).

**Table 2.** Properties of new MC congeners identified in *P. prolifica* NIVA-CYA 544 (**Paper I**)

| | Microcystin analogue | Status | Neutral Formula | Number of Nitrogens | $m/z$ for $[M+zH]^{z+}$ (+z) | $m/z$ for $[M-zH]^{z-}$ (-z) | Thiol-reactive | Number of carboxylic acid groups |
|---|---|---|---|---|---|---|---|---|
| 1 | [D-Asp$^3$]MC-EE | probable | $C_{46}H_{63}N_7O_{16}$ | 7 | 970.4404 (1) | 968.4259 (1) | yes | 4 |
| 2 | [D-Asp$^3$]MC-ER | probable | $C_{47}H_{68}N_{10}O_{14}$ | 10 | 997.4989 (1) | 995.4844 (1) | yes | 3 |
| 3 | [D-Asp$^3$]MC-RW | probable | $C_{53}H_{71}N_{11}O_{12}$ | 11 | 1054.5356 (1) | 1052.5211 (1) | yes | not determined |
| 4 | [D-Asp$^3$]MC-RCit | probable | $C_{48}H_{72}N_{12}O_{13}$ | 12 | 1025.5415 (1) | 1023.5269 (1) | yes | not determined |
| 5 | GSH-conjugate of [D-Asp$^3$]MC-RR | confirmed | $C_{58}H_{90}N_{16}O_{18}S$ | 16 | 666.3243 (2) | 1329.6267 (1) | no | not determined |
| 6 | Sulfide conjugate of [D-Asp$^3$]MC-RR | tentative | $C_{93}H_{145}N_{21}O_{33}S$ | 21 | 1059.0088 (2) | 1056.9950 (2) | no | not determined |
| 7 | Sulfoxide of **6** | tentative | $C_{93}H_{145}N_{21}O_{34}S$ | 21 | 1067.0060 (2) | 1064.9919 (2) | no | not determined |

57

These new compounds (**Table 2**) have some interesting characteristics that are worth discussing in more detail.

- [D-Asp³]MC-EE (**1**) and [D-Asp³]MC-ER (**2**) were the first reported MCs containing Glu in positions-2 and -4.

The identification of these congeners helped, with hindsight, recognizing previously reported MCs [190] containing methyl esters of Glu in positions-2 and/or -4, as artefacts (see also the section 4.3.2 Methylation of carboxylic acid functionalities). Furthermore, this may help in the future to target congeners biosynthesized as Glu-containing in positions-2 and/or -4, when their methyl esters are detected in blooms or other samples. Among all reported MC congeners, about 20% are the result of chemical/biochemical transformation in the environment or during sample extraction and preparation [39].

- [D-Asp³]MC-RW (**3**) was reported as a new congener, containing Trp (denoted also by the 1-letter abbreviation W) in position-4. It was present at low levels, and it would likely go unnoticed without a thorough analysis of concentrated extracts and without the combination of analytical tools as was used in this study (the same applies to [D-Asp³]MC-EE, which was also present at low relative concentration).

Low-level MCs can present some interesting food for thought about MC biosynthesis, which may be produced by a strain, and which may be overlooked especially with targeted analysis. Low abundance in one strain does not imply that a specific congener cannot be dominant in another strain. Thus, the identification of a new congener is always important, as another piece of knowledge about the complex structural variability of MCs and cyanotoxins in general. For example, [D-Asp³]MC-EE (**1**) and [D-Asp³]MC-ER (**2**), which were minor congeners in *P. prolifica* NIVA-CYA 544, were shown to be major components in a culture from Myanmar, as recently published by Ballot et al. [220]. When discussing toxicological properties of MCs, the degree of amino acid variability was demonstrated to have a fundamental impact on toxicity [39, 92]. Thus, as there will be differences in toxin profiles between strains, the net-toxicity can be hard to predict. Another aspect are species differences among exposed animals meaning that while some toxin mixtures might be harmful for one species, they might not for another.

- [D-Asp³]MC-RCit (**4**) was the first reported congener containing citrulline (Cit).

This result was interesting not only because it represented a new congener, but also because Cit is an amino acid that is involved in both the biosynthesis and catabolism of Arg in bacteria. This means that it could be a minor by-product from the biosynthesis or the breakdown of [D-Asp³]MC-RR (the most abundant congener detected in *P. prolifica* NIVA-CYA 544) and, on a larger scale, this means that similar analogues could in general accompany congeners containing Arg in blooms and cultures. Their abundance could be substantially smaller than the Arg-related analogues (i.e., in this case [D-Asp³]MC-RR), and thus, it could be important to look specifically for them if interested in their detection. Another important detail to discuss related to [D-Asp³]MC-RCit (**4**) is the strong evidence that the amino acid in position-4 is Cit and not argininic acid, which has the same molecular formula ($C_6H_{13}N_3O_3$) (**Figure 34**).
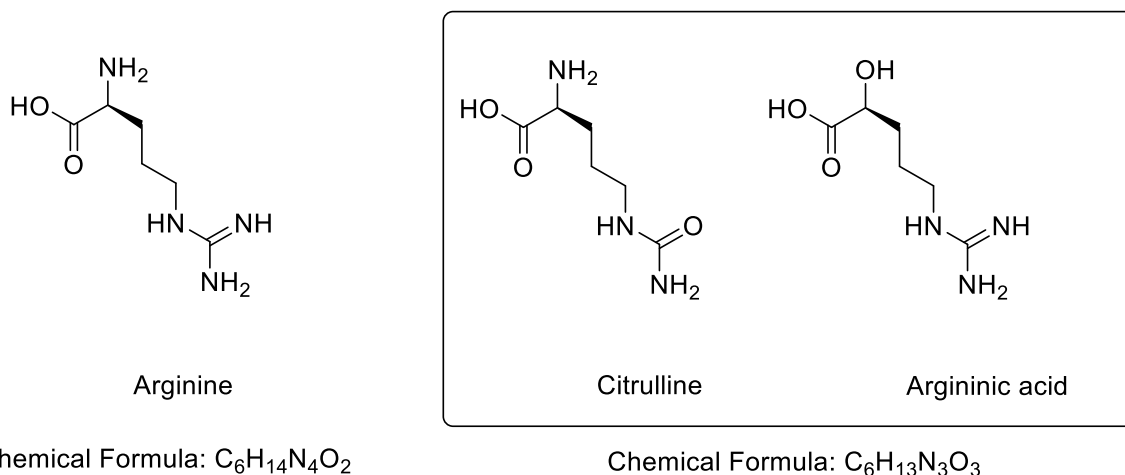
**Figure 34.** Arginine (Arg), citrulline (Cit), argininic acid structures and chemical formulae.

Both biosynthetic considerations, and the combination of tools used in this study, supported that the amino acid in position-4 in **4** was Cit and not argininic acid, highlighting again the importance of complementary approaches. From a biosynthetic point of view, the presence of argininic acid would require an unprecedented structural feature, which is an ester linkage within the MC-macrocycle (**Figure 35**). This would also result in different MS/MS fragmentation patterns. In addition, the argininic acid would imply a guanidinium group terminating the side chain in position-4 (**Figure 35**). Such a molecule would possess two guanidinium groups (in positions-2 and -4), which is expected to afford doubly-charged ions during ESI (in accordance to –RR type of MCs). It would also elute at a short retention time and show a fragmentation pattern similar to [D-Asp³]MC-RR. Instead, the compound was singly charged, eluted closely to and fragmented similarly to [D-Asp³]MC-LR (Supplementary Material of **Paper I**).
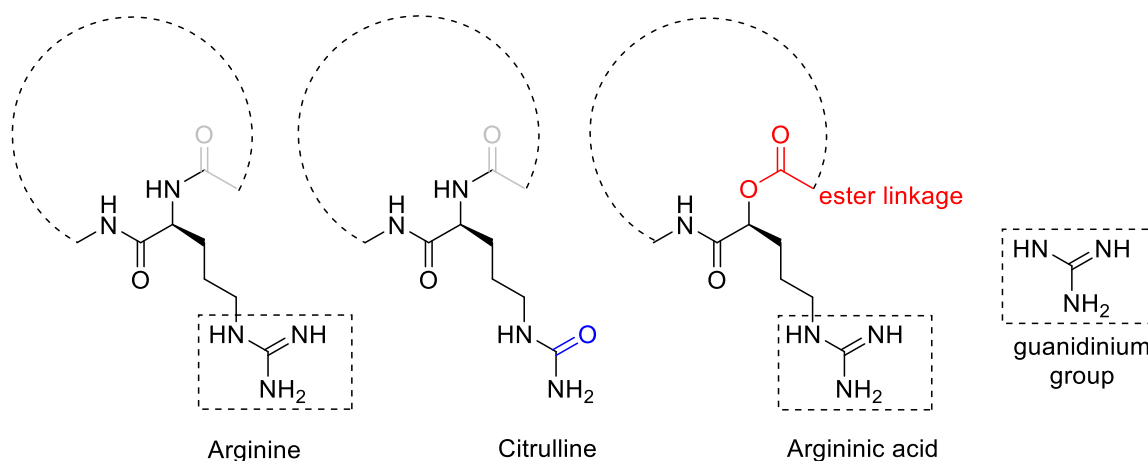


**Figure 35.** Arginine, citrulline and argininic acid in a MC-macrocycle. Argininic acid would imply an ester linkage, which is biosynthetically unlikely. The guanidinium group in the argininic acid moiety would imply chromatographic and mass spectral behaviour similar to congeners containing arginine both in position-2 and -4.

In addition, LC–HRMS/MS data showed that the side-chain of the amino acid at position-4 of this compound contained $C_4H_9ON_2$, and must include exactly one ring or double bond. Given that neither of the two nitrogen atoms can be basic (given the molecule's charge-state, retention time, and fragmentation pattern), both nitrogen atoms must therefore be either side of a carbonyl group, thereby indicating the presence of a carbamide group R-NH-C=O(NH$_2$). Furthermore, HRMS/MS spectra of the unlabeled and ^{15}N-labeled compound (Figure S64, **Paper I**) unambiguously demonstrated that the most prominent product ion in the HRMS/MS spectrum is due to a neutral loss of HNCO (isocyanic acid), which is a characteristic neutral loss from Cit-containing peptides [221]. In summary, this is an example of how both biosynthetic considerations and the combination of analytical tools was used to used provide structural evidence, highlighting again the importance of complementary approaches.

- The GSH-conjugate of [D-Asp[3]]MC-RR (**5**) appears to be the first report of a MC–GSH conjugate in a cyanobacterial culture.

The semi-synthetic conversion of a standard of [D-Asp[3]]MC-RR to its GSH-conjugate (see section 4.3.1 Thiol conjugation), confirmed this identification. This finding suggests that the GSH-derived conjugates identified previously in a *Microcystis* bloom [222] may be produced by the cyanobacteria in the bloom without the involvement of other organisms coexisting in the water.

- A sulfide conjugate of [D-Asp[3]]MC-RR (**6**) (and its sulfoxide (**7**)), comprising a molecular mass of 2116 Da made this type of MC variant unprecedented (the second largest MCs are GSH conjugates with molecular masses of ca. 1300 Da).

This conjugate is more than 50% more massive than the common MCs' mass range. The reported molecule was a doubly-charged (both in positive and negative ion mode) conjugate of the well-known [D-Asp[3]]MC-RR, even though further studies will be required to fully elucidate what is conjugated to the MC-core. The corresponding sulfoxide was also present in the strain, likely as a result of autoxidation. The reaction with periodate was a key tool for establishing the sulfide and sulfoxide nature of the congeners at the same time (as described in the section 4.3.3 Oxidation with sodium periodate). The sulfide conjugate consisted of a diastereomeric pair of major and minor isomers (Figure 2 of **Paper I**), just like all other MC-thiol conjugates. The sulfur atom in the sulfide becomes a chiral centre when oxidized to a sulfoxide. Consequently, each of the two sulfide diastereoisomers is converted to a pair of sulfoxide diastereoisomers by oxidation to the sulfoxide form, giving rise to four isomers (Figure 2 of **Paper I**).

In addition to "merely" elucidating the structures of new MCs, which is of inherent importance for research on MC chemistry and biosynthesis, special focus was on the combination of complementary analytical tools to establish the chemical structures.

These tools were:

1. LC–MS/MS, to target fundamental MC moieties such as Adda[5] or Glu[6] (characteristic fragments in positive and negative ionization mode, respectively), as well as other single or combined moieties, which give characteristic fragments.
2. ^{15}N-labeling, to establish the exact number of nitrogen atoms and aid in the interpretation of high-resolution mass spectra.
3. Thiol derivatization using mercaptoethanol (followed by LC–HRMS), to target Mdha[7] or Dha[7] moieties.

4. Esterification with diazomethane (followed by LC–HRMS), to target carboxylic acid groups.
5. Oxidation with sodium periodate (followed by LC–HRMS), to target sulfide groups.
6. Application of isotope-profile analysis to support correct identification of molecular formulae.

The pool of selective chemical derivatization reactions, as well as isotope pattern analysis for $^{15}$N-labelled isotopologues (relative to unlabeled variants), supported structural hypotheses based on accurate mass measurements and characteristic MS fragmentation achieved by multiple LC–MS/MS analyses (both CID–ITMS/MS and HCD–HRMS/MS), in positive and negative ionization modes. This set of tools allowed the collection of strong lines of evidence complementing each other, i.e. complementary structural information.

Showing the power of simultaneously applying these multiple approaches that all are based on various LC–MS analysis to this research problem was not an aim of the project in itself. However, it demonstrates that in some cases it is possible to overcome the use of other resource-demanding techniques such as NMR, or peptide degradation followed by amino acid analysis. The presented approach is not an absolute replacement for these techniques that may give information to unequivocally establish chemical structures (i.e., stereochemistry), but a valuable option that may work easily for this family of toxins. Indeed, the knowledge of their core structure and how they fragment and react, is well established and may give trustable starting clues for realistic structural hypotheses of new putative congeners. Thus, these hypotheses can be confirmed (or not) by using the tools listed above.

Considerations on how MCs are biosynthesized may help further on narrowing down the list of plausible structures produced by the same strain. Indeed, all congeners are produced by the same synthase in a strain and therefore may tend to keep some common features, such as a demethylation of a specific moiety like D-Asp$^3$ in all reported congeners in *P. prolifica* NIVA-CYA 544, Table 1 of **Paper I**).

## 5.2 ED activity investigation: cyanobacteria and steroid hormones (Paper II and Paper III)

*In vitro* models represented the best starting point for the ED activity investigations. They are easy to set up, cost effective, reproducible and generally ethically unproblematic compared to experiments *in vivo*. Monolayer cell cultures can be maintained for an extended period, up to several weeks. HLM are a very good model for prediction of *in vivo* toxicokinetics and biotransformation, and are widely used in the pharma industry.

The findings from the ED activity investigations of this work are summarized in **Paper II** and **Paper III**. The experiments targeted one or more steroid hormones, using methodologies that studied ED effects at different levels (**Figure 36**).

The first step to approach cyanobacterial ED activity investigations was a screening of *Microcystis* and *Planktothrix* spp. culture extracts, from the whole in-house cyanobacterial collection (with the exception of the MC-deficient PCC7806*mcyB*−, which joined the collection at a later stage), in RGAs. Special focus was on estrogen-responsive RGA. In a next step, a HLM biotransformation assay was used to investigate estrogenic effects through modulation of 17β-estradiol phase I metabolism, by co-incubation of 17β-estradiol with a MC-producing *M. aeruginosa* culture extract and pure MC-LR. Finally, the H295R steroidogenesis assay was used to assess the impact of MC-LR either alone or as a natural part of a *M. aeruginosa* culture extract on the biosynthesis of steroid hormones. Furthermore, modulation of steroidogenesis was also studied following exposure of H295R with a mixture of MC-LR and other pure MCs or with a MC-deficient *M. aeruginosa* culture extract.
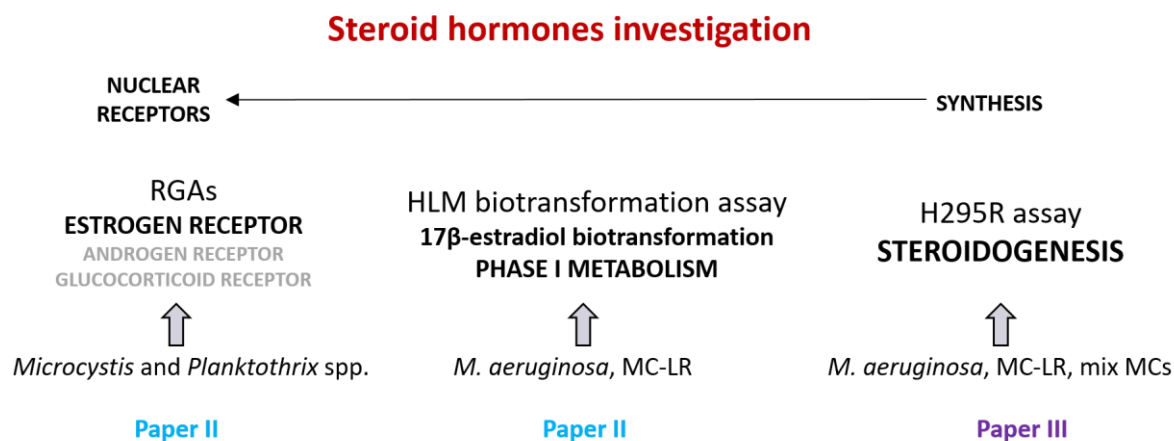


**Figure 36.** Overview of the *in vitro* assays used for investigation of ED activity of cyanobacterial compounds, results of which are summarized in **Paper II** and **Paper III**.

As described in the section 3.3 Cyanobacteria and EDs, existing literature on ED activity of cyanobacteria is mainly focused on MC-LR and MC-LR-producing *M. aeruginosa* cyanobacterial strains, and are mainly based on animal models [127].

Several studies on zebrafish reported modulation of VTG levels following exposure to MC-LR [127]. Since VTG is considered a biomarker for estrogenic activity [134], estrogen-responsive RGAs [193] were expected to be a good start to narrow down the number of cultures with estrogen activity among those ones composing the collection (see section 4.1 Cyanobacterial collection), with the aim to select the most bioactive for further investigations. At this stage, indications if MC-producing strains were more or less responsive in the RGAs compared to non-MC-producing strains were expected, thus giving a first indication for a possible role of MCs regarding estrogenic activity. Indeed, their role is rather controversial according to the scientific literature.

However, none of the culture extracts showed substantial agonist or antagonist activity at the estrogen receptor level (**Paper II**). Furthermore, the cyanobacterial culture medium Z8 [153], which was also tested in the estrogen-responsive RGAs, unexpectedly showed a weak estrogen agonist activity. This response created a background effect for all extracts, which made it very difficult to draw clear conclusions about the extract responses. Probably, the Z8 interference came from contaminants introduced during the production of the medium itself, rather than from its components. However, despite the effects of the cultivation medium itself, it was clear that none of the extracts had a strong agonist or antagonist activity in the RGAs. The rather marginal effect of the cyanobacterial extracts in the estrogen-responsive RGAs was unexpected given that estrogenic effects exerted by MCs and/or *M. aeruginosa* extracts are supported in the literature. This could imply that the estrogenic effect exerted by MCs and/or *M. aeruginosa* as shown in the VTG induction assays, might mainly derive from mechanisms other than direct interaction with estrogen receptors.

The initial RGA screening also included androgen- and glucocorticoid-responsive RGAs, and provided preliminary data on the interference with androgen and glucocorticoid receptors. Possible effects were observed, especially in the glucocorticoid RGAs, but the replicate variability was high and would require further verification (**Paper II**). It was decided to move towards further studies on non-receptor mediated mechanisms of estrogen activity. Regardless of this, modulation of androgen and glucocorticoid receptors constitute an unexplored field on cyanobacterial potential ED activity, which deserves to be studied in more detail in the future.

With respect to the KCs identified for a compound to be classified as ED [125] (see section 3.2.3 State of the science on EDs), our interest moved from investigation of KC1 "Interacts with or activates hormone receptors" and KC2 "Antagonizes hormone receptors" with the RGAs, to the study of KC9 "Alters hormone metabolism or clearance". Thus, an HLM assay was employed for the CYP-mediated biotransformation of 17β-estradiol. The aim was to investigate if and how cyanobacterial compounds could affect phase I metabolism of 17β-estradiol.

The experiment aimed to study the potential interference with 17β-estradiol phase I metabolism by co-incubation of 17β-estradiol with either pure MC-LR or an extract of *M. aeruginosa* PCC7806, which produces MC-LR as main MC variant. Modulation of the 17β-estradiol main biotransformation products, 2-hydroxyestradiol and 4-hydroxyestradiol (conversion catalyzed by CYPs), as well as levels of estrone and estriol (linked to 17β-estradiol via reduction and oxidation biotransformation reactions) were monitored. However, only 2-hydroxyestradiol and estrone were produced in concentrations that allowed quantification in the HLM assay, and only these could thus be compared when 17β-estradiol was incubated either alone or together with

cyanobacterial components. Estrone is a natural weak estrogen that is in equilibrium with 17β-estradiol. It can be a metabolic intermediate in the synthesis of 17β-estradiol. The enzyme 17β-hydroxysteroid dehydrogenases (17β-HSD) catalyzes interconversion of 17β-estradiol and estrone [223] (**Figure 37**).

The overall depletion of 17β-estradiol after 60 min of incubation in HLM was not significantly affected by the presence of cyanobacterial compounds (either MC-LR or *M. aeruginosa* PCC7806 extract). However, changes in the production of 2-hydroxyestradiol and estrone oxidative metabolites were observed after 60 min of 17β-estradiol co-incubation with cyanobacterial compounds in HLM. In particular, 2-hydroxyestradiol production was significantly lower compared to when 17β-estradiol was incubated with HLM alone, both when 17β-estradiol was co-incubated with MC-LR and with the *M. aeruginosa* PCC7806 extract. On the other hand, estrone concentrations increased significantly when 17β-estradiol was co-incubated with *M. aeruginosa* PCC7806 extract. Although drawing strong conclusions (i.e. about the role of MCs vs. other compounds or the impact on the overall 17β-estradiol biotransformation) from these results could sound pretentious, some interesting considerations can be done. Indeed, an endocrine interference was observed, meaning that an ED mechanism of action via modulation of 17β-estradiol biotransformation is plausible. Even though only a few of a range of known 17β-estradiol metabolites were measured, the experiments demonstrated the potential of MCs and *M. aeruginosa* to alter the profile of 17β-estradiol metabolites formed. This work may represent a starting point for a deeper investigation involving the monitoring of other 17β-estradiol metabolites, including phase II metabolites, and thus other enzymatic pathways. Such work could be extended to studies on the impact of cyanotoxins on metabolism of other hormones.

Estrogens, including 17β-estradiol and estrone, undergo extensive oxidative metabolism by specific CYP enzymes [224, 225]. Oxygenated estrogen metabolites exert different biological activities and some of them may have pathophysiological roles (e.g., 16α-hydroxyestrone and 4-hydroxyestrone cause damage to cellular proteins and DNA and may be carcinogenic in specific cells) [121, 226, 227]. Furthermore, different oxygenated metabolites possess different estrogenic potencies. For example, C-2 metabolites (e.g., 2-hydroxyestradiol) tend to have limited or no significant estrogen activity relative to their parent hormones. In contrast to this, C-4 and C-16 metabolites (e.g., 4-hydroxyestradiol) seem to be as or nearly as potent as the parent estrogens [226]. An altered estrogen-metabolite profile may therefore have a significant ED effect.

However, due to the complex network linking hormone and metabolites, some equilibria may be affected indirectly and increased or decreased conversion into a specific metabolite may also imply changes of related pathways. Furthermore, among the variety of different CYP isoforms involved in the oxidative metabolism of estrogens, some possess a selective catalytic activity for regiospecific hydroxylation reactions of endogenous estrogens, meaning that there are specific metabolites produced by different members of the enzyme family [224]. The oxidation product 2-hydroxyestradiol was expected to be the major one in our model, because of the high levels of CYP1A2 and CYP3A4 in HLM [225, 227] (isoforms highly expressed in the liver) (**Figure 37**).

Although CYP isoforms are largely present in the liver, they are also present in extrahepatic estrogen target organs. For example, CYP19A1, also known as aromatase, is a specific isoform

responsible for converting androgens into estrogens, which in females is most active in the ovaries, while in general it is active in brain, placenta, bones and other tissues as well [228]. The latter example of the aromatase shows that CYPs have a critical role not only in an estrogen oxidative metabolism, but also in its biosynthesis. Estrogens formation is part of the complex steroidal hormone biosynthetic process, the so-called steroidogenesis [206] (**Figure 37**).
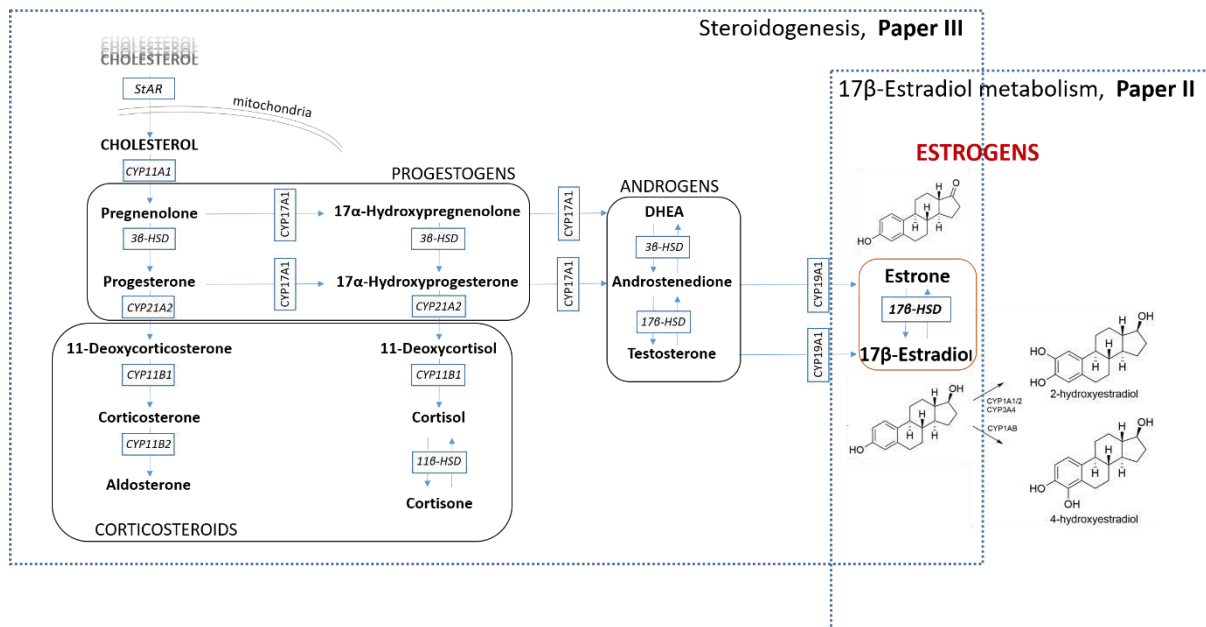


**Figure 37.** Overview over the steroidal hormone biosynthetic and biotransformation pathways investigated for non-receptor mediated mechanisms of action: steroidogenesis (**Paper III**, using H295R model) and 17β-estradiol phase I main metabolites (**Paper II**, using HLM model). Enzymes that catalyze specific reactions are also shown.

Studies into the interference of cyanobacterial compounds with steroidogenesis was the final step of the ED investigation work (**Paper III**). This step refers to KC6 "Alters hormone synthesis", as investigated characteristic [125]. The aim was again to assess a potential non-receptor mediated mechanism through which cyanobacterial compounds can interfere with the endocrine system, and a possible interference with steroidogenesis has already been reported in the literature (see section 3.3 Cyanobacteria and EDs). The specific involvement of MCs in the observed effects was again one of the objectives. Human adrenal cortex-derived cells (H295R) [138, 199] were exposed to either MC-LR alone, a mixture made up of MC-LR together with eight other MCs and NOD-R, or extracts from the MC-LR-producing *M. aeruginosa* PCC7806 strain or its MC-deficient mutant PCC7806*mcyB*−. Concentrations of 14 hormones of the steroidogenesis pathway were quantified in order to find out if and to what extent the different exposures modulate their production/interconversion (see Result section in **Paper III**). A complete discussion about the modulation of hormonal concentrations is reported in **Paper III**. Here, some results are used to make considerations.

While not affecting 17β-estradiol and testosterone concentrations as it was in a previous study using the same model [137], MC-LR significantly increased the levels of 17-hydroxypregnenolone and dehydroepiandrosterone (DHEA) in a concentration-dependent manner. Interestingly, both the *M. aeruginosa* PCC7806 extract and that of its MC-deficient

mutant *M. aeruginosa* PCC7806*mcyB*− showed a dose-dependent effect on 17-hydroxypregnenolone and DHEA, but opposite to pure MC-LR. The MC mixture did not show the same trend, suggesting that the pure MC congeners other than MC-LR might affect steroidogenesis to a lesser extent. An inhibition of the enzyme 3β-HSD (**Figure 37**) could explain the effect of MC-LR, while there appeared to be other metabolites in the *M. aeruginosa* extracts that outcompeted the MC-LR related effect. However, since we did not measure enzyme activities but merely hormone concentrations, this remains just a plausible hypothesis.

Another example of observed effect of H295R exposure with MC-LR or the MCs/NOD-R mixture was the modulation of hormones along the pathway leading from 17-hydroxypregnenolone to cortisol and cortisone, through 17-hydroxyprogesterone and 11-deoxycortisol, thus involving CYP21A2 or CYP11β1 enzymes. While cortisone and cortisol concentrations were reduced for specific concentrations of pure MCs, they were increased for both *M. aeruginosa* extracts. The latter result showed high variability resulting in statistical insignificance. However, as extracts from both PCC7806 strains confirmed the trend of MCs having the opposite effects on steroidal hormones biosynthesis compared to the cyanobacterial extracts, this deserves further investigation.

A statistically significant and concentration-dependent upregulation of 11-deoxycorticosterone was observed for both MC-LR and *M. aeruginosa* extracts. Thus, concentrations of this hormone were increased following exposure with pure MC-LR, and both the PCC7806 wild-type and *mcyB*− extracts. However, a similar effect for the PCC7806 wild-type and *mcyB*− mutant again suggests a role of other metabolites than MCs.

In summary, the above-discussed examples of results, together with other details in **Paper III**, clearly suggest ED activities on steroidal hormones via modulation of their biosynthesis, of both MCs and other cyanobacterial metabolites. However, to translate statistically significant outcomes in this experimental setup into a biological outcome in an intact organism is very difficult. Indeed, the steroidogenic pathway is a complex branched pathway (**Figure 37**). Hormones are highly dependent on each other and the measured effects on one hormone necessarily affect other hormones. Furthermore, it is important to note that the net effect on hormone modulation may depend on different mechanisms either going into the same directions, or into opposite directions, thus with a possible attenuated final effect. This is especially important for interpretation of results from the univariate data analysis, while in this study both univariate and multivariate data analyses gave highly comparable results (Figure 2 of **Paper III**).

Overall, the results of this cyanobacterial ED activity investigation indicate that MCs and other cyanobacterial bioactive metabolites are potential EDs. Knowing the ability of MCs to exert toxicity inhibiting PP1 and PP2A, a similar mechanism can be hypothesized for a direct interaction of MCs with enzymes involved in steroidogenesis. However, the hypothesis of MCs affecting gene expression resulting in up- or down-regulating enzyme levels, is also plausible. Taking into consideration the complexity of both the metabolite composition of cyanobacteria (still largely unknown) and of the endocrine system (no *in vitro* test is currently able to assess the overall effect on the total system), no firm conclusion can be drawn on the overall biological significance of this ED activity in intact organisms. Conducted *in vitro* studies can guide future investigations, though.

# 6. RESEARCH NEEDS AND FUTURE PROSPECTIVE

Since cyanobacteria and their toxins are an enormous field of research including many different aspects, there naturally remain needs for future research both in general terms and as a natural continuation of the research presented in this thesis.

With respect to the research presented in this work, further investigations may be suggested on the following topics:

- Structural clarification of the new heavy thiol-linked [D-Asp³]MC-RR conjugate reported in **Paper I**. This conjugate is an entirely new form of a MC compound and its structural identification could give important clues about the biological chemistry and biosynthesis of these toxins.
- Study the interference of cyanobacterial extracts and/or pure MCs with androgen and glucocorticoid receptors in more detail (**Paper II**). Despite the rather large variances of the androgen- and glucocorticoid-responsive RGA in this work, there were trends that showed possible interferences especially with the glucocorticoid receptor that would be worth investigating in more detail.
- A larger study into the interferences of cyanobacterial extracts and/or pure MCs with 17β-estradiol biotransformation (phase I and phase II metabolism), focusing on a wider range of 17β-estradiol metabolites (**Paper II**).
- The interference of MCs other than MC-LR separately, and not in combination as reported in **Paper III**, as well as cyanobacterial metabolites other than MCs on steroidogenesis, collecting more data on hormone modulation. Supplement the data with studying the interaction of cyanotoxins with specific enzymes that are involved in steroidogenesis in order to understand biological mechanisms behind observed effects better (**Paper III**). Include other known PP2A inhibitors such as okadaic acid in this work.

Regarding more general issues, it has already been discussed in this thesis that there are many gaps in ED investigations as well as the in the structural knowledge of cyanobacterial metabolites, in addition to the very limited investigation on cyanobacterial ED activity. Here, the aim is not to be exhaustive in listing all those gaps, but rather to do some reflections.

The quality of the risk assessment for exposure with cyanobacterial toxins and other metabolites, which is the ultimate goal, is dependent on available toxicological data (in terms of amount and quality of data on occurrence and biological activity). Toxicological profiles can drastically change depending on absorption, tissue distribution, metabolism and excretion that is the toxicokinetics of different MC variants. Structural differences lead to toxicity differences. Thus, a major effort on structure investigation is fundamental and needs to go together with bioactivity investigations. This is true for MCs as well as for all other bioactive cyanobacterial metabolites. It would be important, for both research work and regulations, to move the focus from MC-LR towards the concept of "total MCs", thus "total cyanotoxins". Furthermore, when considering a real situation, which means an environmental sample, the sample matrix may also play a role. This matrix is not just the water, but rather everything that is in the water. Thus,

interactions between different cyanobacterial components, as well as concomitant exposure with other chemicals should be considered.

The inherent complexity of the cyanobacterial metabolome and of the endocrine pathways make it unlikely that a single unique compound would be identified as responsible for observed ED activity effects. Furthermore, a single mechanism of action is equally unlikely. It would be interesting and important to better explore interference of cyanobacterial compounds with endocrine system's axes also through non-receptor-mediated mechanisms. The knowledge of the mechanisms is essential for the possibilities to evaluate potential interactions between different compounds as well as for the extrapolation of data between species. However, for the evaluation of the overall biological outcome of the alterations observed, well-planned *in vivo* studies would be needed for a final assessment. Preliminary *in vitro* data provide information that are useful in the planning, to focus on relevant endpoints and relevant metabolites/extracts.

# 7. CONCLUSIONS

Cyanobacteria and EDs are two major challenging global issues. In general, they are separate fields of research, and both may be harmful for humans, wildlife and environmental health. Despite there is much concern about them as unrelated fields, their interconnection has been poorly investigated, and has mainly been oriented towards possible estrogenic activity of MC-LR, as major congener of the widespread cyanobacterial toxins MCs. However, reported data on ED activity of MCs are in part contradictory, and possible underlying mechanisms are little studied.

The present work aimed to investigate cyanobacterial ED activity, focusing on mechanisms of action and the role of MCs as ED cyanobacterial metabolites. A parallel aim was the structural investigation of new MC congeners. A combination of chemical analytical tools and biological assays were used to fulfil these aims, leading to the following conclusions:

- Cyanobacteria can be a source of endocrine disruption.
- MC-LR (and/or other MCs) may act as ED chemicals, but MCs appear not to be exclusively responsible for ED effects of cyanobacteria. Other cyanobacterial bioactive metabolites also showed the (in part dominating) ability to interfere with the endocrine system.
- Receptor-mediated mechanisms are not crucial for cyanobacteria to exert ED activity. Interference with 17β-estradiol biotransformation and metabolism as well as interference with steroidal hormones biosynthesis was reported, meaning that non-receptor mediated modes of action may play a major role for cyanobacteria to exert ED activity.
- Structural investigation of new MC congeners, which is a closed related field of research, due to structure and activity interdependency, has still an enormous field of action. The combination of LC–HRMS/MS techniques with basic chemical tools as isotopic labeling and selective chemical derivatization is an easy, but powerful approach for studying MC diversity.

# REFERENCES

1. Nutman, A. P.; Bennett, V. C.; Friend, C. R.; Van Kranendonk, M. J.; Chivas, A. R., Rapid emergence of life shown by discovery of 3,700-million-year-old microbial structures. *Nature* **2016,** *537*, 535–538.
2. Codd, G. A.; Meriluoto, J.; Metcalf, J. S., Introduction: Cyanobacteria, Cyanotoxins, their Human Impact, and Risk Management. In *Meriluoto, J., Spoof, L., Codd, G. A. (eds), Handbook of Cyanobacterial Monitoring and Cyanotoxin Analysis, John Wiley & Sons, Ltd, Chichester, UK*, Meriluoto, J.; Spoof, L.; Codd, G. A., Eds. John Wiley & Sons, Ltd.: 2017; pp 1–8.
3. Huisman, J.; Codd, G. A.; Paerl, H. W.; Ibelings, B. W.; Verspagen, J. M. H.; Visser, P. M., Cyanobacterial blooms. *Nat. Rev. Microbiol.* **2018,** *16*, 471–483.
4. Stomp, M.; Huisman, J.; Voros, L.; Pick, F. R.; Laamanen, M.; Haverkamp, T.; Stal, L. J., Colourful coexistence of red and green picocyanobacteria in lakes and seas. *Ecol. Lett.* **2007,** *10*, 290–298.
5. Chorus, I.; Bartram, J., Toxic Cyanobacteria in Water: a Guide to their Public Health Consequences, Monitoring and Management; E&FN Spon: New York, NY, USA. WHO: **1999**.
6. Percival S.L; W., W. D., Cyanobacteria. In *Microbiology of Waterborne Diseases*, Second edition ed.; 2014; pp 65–78.
7. Hauer, T.; Komárek, J., CyanoDB 2.0 - On-line database of cyanobacterial genera. World-wide electronic publication, Univ. of South Bohemia & Inst. of Botany AS CR,. 2020.
8. Komárek, J., A polyphasic approach for the taxonomy of cyanobacteria: principles and applications. *Eur. J. Phycol.* **2016,** *51*, 346–353.
9. Nabout, J.; Rocha, B.; Carneiro, F.; C.L, S. A., How many species of Cyanobacteria are there? Using a discovery curve to predict the species number. *Biodiversity and Conservation* **2013,** *22*.
10. Christiansen, G.; Fastner, J.; Erhard, M.; Börner, T.; Dittmann, E., Microcystin biosynthesis in *Planktothrix*: genes, evolution, and manipulation. *J. Bacteriol.* **2003,** *185*, 564–572.
11. Nishizawa, T.; Asayama, M.; Fujii, K.; Harada, K.; Shirai, M., Genetic analysis of the peptide synthetase genes for a cyclic heptapeptide microcystin in *Microcystis* spp. *J. Biochem.* **1999,** *126*, 520–529.
12. Tillett, D.; Dittmann, E.; Erhard, M.; von Dohren, H.; Borner, T.; Neilan, B. A., Structural organization of microcystin biosynthesis in *Microcystis aeruginosa* PCC7806: an integrated peptide–polyketide synthetase system. *Chem Biol.* **2000,** *7*, 753–764.
13. Buratti, F. M.; Manganelli, M.; Vichi, S.; Stefanelli, M.; Scardala, S.; Testai, E.; Funari, E., Cyanotoxins: producing organisms, occurrence, toxicity, mechanism of action and human health toxicological risk evaluation. *Arch. Toxicol.* **2017,** *91*, 1049–1130.
14. Borowitzka, M. A., Chapter 3 - Biology of Microalgae. In *Microalgae in Health and Disease Prevention*, Academic Press: 2018; pp 23–72.
15. Paerl, H. W., Mitigating harmful cyanobacterial blooms in a human- and climatically-impacted world. *Life (Basel)* **2014,** *4*, 988–1012.
16. Kurmayer, R.; Deng, L.; Entfellner, E., Role of toxic and bioactive secondary metabolites in colonization and bloom formation by filamentous cyanobacteria *Planktothrix*. *Harmful Algae* **2016,** *54*, 69–86.
17. Nguyen, X. H.; Sumimoto, S.; Suda, S., Unexpected high diversity of terrestrial cyanobacteria from the campus of the University of the Ryukyus, Okinawa, Japan. *Microorganisms* **2017,** *5*.
18. Humbert, J. F.; Fastner, J., Ecology of Cyanobacteria. In *Meriluoto, J., Spoof, L., Codd, G. A. (eds), Handbook of Cyanobacterial Monitoring and Cyanotoxin Analysis*, Meriluoto, J.; Spoof, L.; Codd, G. A., Eds. John Wiley & Sons, Ltd., Chichester, UK: 2017; pp 9–18.
19. Miller, M. A.; Kudela, R. M.; Mekebri, A.; Crane, D.; Oates, S. C.; Tinker, M. T.; Staedler, M.; Miller, W. A.; Toy-Choutka, S.; Dominik, C.; Hardin, D.; Langlois, G.; Murray, M.; Ward, K.; Jessup, D. A., Evidence for a novel marine harmful algal bloom: cyanotoxin (microcystin) transfer from land to sea otters. *PLoS One* **2010,** *5*, 1–11.

20. Hilborn, E. D.; Beasley, V. R., One health and cyanobacteria in freshwater systems: animal illnesses and deaths are sentinel events for human health risks. *Toxins (Basel)* **2015,** *7*, 1374–1395.

21. Paerl, H. W.; Otten, T. G., Harmful cyanobacterial blooms: causes, consequences, and controls. *Microb. Ecol.* **2013,** *65*, 995–1010.

22. Sandrini, G.; Ji, X.; Verspagen, J. M.; Tann, R. P.; Slot, P. C.; Luimstra, V. M.; Schuurmans, J. M.; Matthijs, H. C.; Huisman, J., Rapid adaptation of harmful cyanobacteria to rising $CO_2$. *Proc. Natl. Acad. Sci. U. S. A.* **2016,** *113*, 9315–9320.

23. Michalak, A. M.; Anderson, E. J.; Beletsky, D.; Boland, S.; Bosch, N. S.; Bridgeman, T. B.; Chaffin, J. D.; Cho, K.; Confesor, R.; Daloglu, I.; Depinto, J. V.; Evans, M. A.; Fahnenstiel, G. L.; He, L.; Ho, J. C.; Jenkins, L.; Johengen, T. H.; Kuo, K. C.; Laporte, E.; Liu, X.; McWilliams, M. R.; Moore, M. R.; Posselt, D. J.; Richards, R. P.; Scavia, D.; Steiner, A. L.; Verhamme, E.; Wright, D. M.; Zagorski, M. A., Record-setting algal bloom in Lake Erie caused by agricultural and meteorological trends consistent with expected future conditions. *Proc. Natl. Acad. Sci. U. S. A.* **2013,** *110*, 6448–6452.

24. Conley, D. J.; Paerl, H. W.; Howarth, R. W.; Boesch, D. F.; Seitzinger, S. P.; Havens, K. E.; Lancelot, C.; Likens, G. E., Ecology. Controlling eutrophication: nitrogen and phosphorus. *Science* **2009,** *323*, 1014–1015.

25. Paerl, H., Nutrient and other environmental controls of harmful cyanobacterial blooms along the freshwater-marine continuum. *Adv. Exp. Med. Biol.* **2008,** *619*, 217–237.

26. Dow, C. S.; Swoboda, U. K., Cyanotoxins. In *The Ecology of Cyanobacteria: Their Diversity in Time and Space*, 2002; pp 613–632.

27. Elersek, T.; Blaha, L.; Mazur-Marzec, H.; Schmidt, W.; Carmeli, S., Other Cyanobacterial Bioactive Substances. In *Meriluoto, J., Spoof, L., Codd, G. A. (eds), Handbook of Cyanobacterial Monitoring and Cyanotoxin Analysis, John Wiley & Sons, Ltd, Chichester, UK*, Meriluoto, J.; Spoof, L.; Codd, G. A., Eds. John Wiley & Sons, Ltd.: 2017; pp 179-192.

28. Sivonen, K.; Jones, G., Cyanobacterial toxins. In *Toxic cyanobacteria in water: a guide to their public health consequences, monitoring and management. Published on the behalf of WHO by E & FN Spon, London*, Chorus, I.; Bartram, J., Eds. 1999; pp 41–111.

29. Smith, G. D.; Thanh Doan, N., Cyanobacterial metabolites with bioactivity against photosynthesis in cyanobacteria, algae and higher plants. *J. Appl. Phycol.* **1999,** *11*, 337–344.

30. Janssen, E. M., Cyanobacterial peptides beyond microcystins — a review on co-occurrence, toxicity, and challenges for risk assessment. *Water Res.* **2019,** *151*, 488–499.

31. Wu, X.; Jiang, J.; Wan, Y.; Giesy, J. P.; Hu, J., Cyanobacteria blooms produce teratogenic retinoic acids. *Proc. Natl. Acad. Sci. U. S. A.* **2012,** *109*, 9477–9482.

32. Vasas, G.; Borbely, G.; Nanasi, P.; Nanasi, P. P., Alkaloids from Cyanobacteria with diverse powerful bioactivities. *Mini-Rev. Med. Chem.* **2010,** *10*, 946–955.

33. Chlipala, G. E.; Mo, S.; Orjala, J., Chemodiversity in freshwater and terrestrial cyanobacteria — a source for drug discovery. *Curr. Drug Targets* **2011,** *12*, 1654–1673.

34. Demay, J.; Bernard, C.; Reinhardt, A.; Marie, B., Natural products from cyanobacteria: focus on beneficial activities. *Mar. Drugs* **2019,** *17*.

35. Zanchett, G.; Oliveira-Filho, E. C., Cyanobacteria and cyanotoxins: from impacts on aquatic ecosystems and human health to anticarcinogenic effects. *Toxins (Basel)* **2013,** *5*, 1896–1917.

36. Svirčev, Z.; Drobac, D.; Tokodi, N.; Mijovic, B.; Codd, G. A.; Meriluoto, J., Toxicology of microcystins with reference to cases of human intoxications and epidemiological investigations of exposures to cyanobacteria and cyanotoxins. *Arch. Toxicol.* **2017,** *91*, 621–650.

37. Carmichael, W. W.; Azevedo, S. M.; An, J. S.; Molica, R. J.; Jochimsen, E. M.; Lau, S.; Rinehart, K. L.; Shaw, G. R.; Eaglesham, G. K., Human fatalities from cyanobacteria: chemical and biological evidence for cyanotoxins. *Environ. Health Perspect.* **2001,** *109*, 663–668.

38. Jochimsen, E. M.; Carmichael, W. W.; An, J. S.; Cardo, D. M.; Cookson, S. T.; Holmes, C. E.; Antunes, M. B.; de Melo Filho, D. A.; Lyra, T. M.; Barreto, V. S.; Azevedo, S. M.; Jarvis, W. R., Liver failure and death after exposure to microcystins at a hemodialysis center in Brazil. *N. Engl. J. Med.* **1998,** *338*, 873–878.

39. Bouaicha, N.; Miles, C. O.; Beach, D. G.; Labidi, Z.; Djabri, A.; Benayache, N. Y.; Nguyen-Quang, T., Structural diversity, characterization and toxicology of microcystins. *Toxins (Basel)* **2019,** *11*.

40. Botes, D. P.; Kruger, H.; Viljoen, C. C., Isolation and characterization of four toxins from the blue–green alga, *Microcystis aeruginosa. Toxicon* **1982,** *20*, 945–954.

41. Botes, D. P.; Viljoen, C. C.; Kruger, H.; Wessels, P. L.; Williams, D. H., Configuration assignments of the amino acid residues and the presence of *N*-methyldehydroalanine in toxins from the blue–green alga, *Microcystis aeruginosa. Toxicon* **1982,** *20*, 1037–1042.

42. Ooi, T.; Kusumi, T.; Kakisawa, H.; Watanabe, M. M., Structure of cyanoviridin RR, a toxin from the blue–green alga,*Microcystis viridis*. *J. Appl. Phycol.* **1989,** *1*, 31–38.

43. Botes, D. P.; Wessels, P. L.; Kruger, H.; Runnegar, M. T. C.; Santikarn, S.; Smith, R. J.; Barna, J. C. J.; Williams, D. H., Structural studies on cyanoginosins-LR, -YR, -YA, and -YM, peptide toxins from *Microcystis aeruginosa. J. Chem. Soc., Perkin Trans. 1* **1985**, 2747–2748.

44. Qi, Y.; Bortoli, S.; Volmer, D. A., Detailed study of cyanobacterial microcystins using high performance tandem mass spectrometry. *J. Am. Soc. Mass Spectrom.* **2014,** *25*, 1253–1262.

45. Puddick, J.; Prinsep, M. R.; Wood, S. A.; Cary, S. C.; Hamilton, D. P., Modulation of microcystin congener abundance following nitrogen depletion of a *Microcystis* batch culture. *Aquat. Ecol.* **2016,** *50*, 235–246.

46. Sevilla, E.; Martin-Luna, B.; Vela, L.; Bes, M. T.; Fillat, M. F.; Peleato, M. L., Iron availability affects mcyD expression and microcystin-LR synthesis in *Microcystis aeruginosa* PCC7806. *Environ. Microbiol.* **2008,** *10*, 2476–2483.

47. Song, L.; Sano, T.; Li, R.; Watanabe, M. M.; Liu, Y.; Kaya, K., Microcystin production of *Microcystis viridis* (cyanobacteria) under different culture conditions. *Phycol. Res.* **1998,** *46*, 19–23.

48. Tonk, L.; Visser, P. M.; Christiansen, G.; Dittmann, E.; Snelder, E. O.; Wiedner, C.; Mur, L. R.; Huisman, J., The microcystin composition of the cyanobacterium *Planktothrix agardhii* changes toward a more toxic variant with increasing light intensity. *Appl. Environ. Microbiol.* **2005,** *71*, 5177–5181.

49. Van de Waal, D. B.; Verspagen, J. M. H.; Lürling, M.; Van Donk, E.; Visser, P. M.; Huisman, J., The ecological stoichiometry of toxins produced by harmful cyanobacteria: an experimental test of the carbon-nutrient balance hypothesis. *Ecol. Lett.* **2009,** *12*, 1326–1335.

50. Rohrlack, T.; Skulberg, R.; Skulberg, O. M., Distribution of oligopeptide chemotypes of the cyanobacterium *Planktothrix* and their persistence in selected lakes in Fennoscandia[1]. *J. Phycol.* **2009,** *45*, 1259–1265.

51. Christiansen, G.; Fastner, J.; Erhard, M.; Borner, T.; Dittmann, E., Microcystin biosynthesis in *Planktothrix:* genes, evolution, and manipulation. *J. Bacteriol.* **2003,** *185*, 564–572.

52. Dittmann, E.; Fewer, D. P.; Neilan, B. A., Cyanobacterial toxins: biosynthetic routes and evolutionary roots. *FEMS Microbiol. Rev.* **2013,** *37*, 23–43.

53. Bouhaddada, R.; Nelieu, S.; Nasri, H.; Delarue, G.; Bouaicha, N., High diversity of microcystins in a *Microcystis* bloom from an Algerian lake. *Environ. Pollut.* **2016,** *216*, 836–844.

54. Miles, C. O.; Melanson, J. E.; Ballot, A., Sulfide oxidations for LC–MS analysis of methionine-containing microcystins in *Dolichospermum flos-aquae* NIVA-CYA 656. *Environ. Sci. Technol.* **2014,** *48*, 13307–13315.

55. Puddick, J.; Prinsep, M. R.; Wood, S. A.; Miles, C. O.; Rise, F.; Cary, S. C.; Hamilton, D. P.; Wilkins, A. L., Structural characterization of new microcystins containing tryptophan and oxidized tryptophan residues. *Mar. Drugs* **2013,** *11*, 3025–3045.

56. Hughes, E. O.; Gorham, P. R.; Zehnder, A., Toxicity of a unialgal culture of *Microcystis aeruginosa. Can. J. Microbiol.* **1958,** *4*, 225–236.

57. Fontanillo, M.; Kohn, M., Microcystins: synthesis and structure–activity relationship studies toward PP1 and PP2A. *Bioorg. Med. Chem.* **2018,** *26*, 1118–1126.

58. Miles, C. O.; Sandvik, M.; Nonga, H. E.; Rundberget, T.; Wilkins, A. L.; Rise, F.; Ballot, A., Identification of microcystins in a Lake Victoria cyanobacterial bloom using LC–MS with thiol derivatization. *Toxicon* **2013,** *70*, 21–31.

59. Schatz, D.; Keren, Y.; Vardi, A.; Sukenik, A.; Carmeli, S.; Börner, T.; Dittmann, E.; Kaplan, A., Towards clarification of the biological role of microcystins, a family of cyanobacterial toxins. *Environ. Microbiol.* **2007,** *9*, 965–970.

60. Gan, N.; Xiao, Y.; Zhu, L.; Wu, Z.; Liu, J.; Hu, C.; Song, L., The role of microcystins in maintaining colonies of bloom-forming *Microcystis* spp. *Environ. Microbiol.* **2012,** *14*, 730–742.

61. Svirčev, Z.; Krstič, S.; Miladinov-Mikov, M.; Baltič, V.; Vidovič, M., Freshwater cyanobacterial blooms and primary liver cancer epidemiological studies in Serbia. *J. Environ. Sci. Health, Part C: Environ. Carcinog. Ecotoxicol. Rev.* **2009,** *27*, 36–55.

62. Ueno, Y.; Nagata, S.; Tsutsumi, T.; Hasegawa, A.; Watanabe, M. F.; Park, H.-D.; Chen, G.-C.; Chen, G.; Yu, S.-Z., Detection of microcystins, a blue–green algal hepatotoxin, in drinking water sampled in Haimen and Fusui, endemic areas of primary liver cancer in China, by highly sensitive immunoassay. *Carcinogenesis* **1996,** *17*, 1317–1321.

63. Butler, N.; Carlisle, J. C.; Linville, R.; Washburn, B., Microcystins: a brief overview of their toxicity and effects, with special reference to fish, wildlife, and livestock. Department of Water Resources Resources Agency, Ed. 2009; pp 1–21.

64. MacKintosh, C.; Beattie, K. A.; Klumpp, S.; Cohen, P.; Codd, G. A., Cyanobacterial microcystin-LR is a potent and specific inhibitor of protein phosphatases 1 and 2A from both mammals and higher plants. *FEBS Lett.* **1990,** *264*, 187–192.

65. Runnegar, M. T.; Kong, S.; Berndt, N., Protein phosphatase inhibition and in vivo hepatotoxicity of microcystins. *Am. J. Physiol.* **1993,** *265*, G224–G230.

66. Yoshizawa, S.; Matsushima, R.; Watanabe, M. F.; Harada, K.; Ichihara, A.; Carmichael, W. W.; Fujiki, H., Inhibition of protein phosphatases by microcystins and nodularin associated with hepatotoxicity. *J. Cancer Res. Clin. Oncol.* **1990,** *116*, 609–614.

67. Bittencourt-Oliveira, M. C.; Hereman, T. C.; Cordeiro-Araújo, M. K.; Macedo-Silva, I.; Dias, C. T.; Sasaki, F. F.; Moura, A. N., Phytotoxicity associated to microcystins: a review. *Braz. J. Biol.* **2014,** *74*, 753–760.

68. Xu, Y.; Xing, Y.; Chen, Y.; Chao, Y.; Lin, Z.; Fan, E.; Yu, J. W.; Strack, S.; Jeffrey, P. D.; Shi, Y., Structure of the protein phosphatase 2A holoenzyme. *Cell* **2006,** *127*, 1239–1251.

69. Namikoshi, M.; Sun, F.; Choi, B. W.; Rinehart, K. L.; Carmichael, W. W.; Evans, W. R.; Beasley, V. R., Seven more microcystins from Homer Lake cells: application of the general method for structure assignment of peptides containing a,b-dehydroamino acid unit(s). *J. Org. Chem.* **1995,** *60*, 3671–3679.

70. Xing, Y.; Xu, Y.; Chen, Y.; Jeffrey, P. D.; Chao, Y.; Lin, Z.; Li, Z.; Strack, S.; Stock, J. B.; Shi, Y., Structure of protein phosphatase 2A core enzyme bound to tumor-inducing toxins. *Cell* **2006,** *127*, 341–353.

71. Kondo, F.; Ikai, Y.; Oka, H.; Okumura, M.; Ishikawa, N.; Harada, K.; Matsuura, K.; Murata, H.; Suzuki, M., Formation, characterization, and toxicity of the glutathione and cysteine conjugates of toxic heptapeptide microcystins. *Chem. Res. Toxicol.* **1992,** *5*, 591–596.

72. Pereira, S. R.; Vasconcelos, V. M.; Antunes, A., The phosphoprotein phosphatase family of Ser/Thr phosphatases as principal targets of naturally occurring toxins. *Crit. Rev. Toxicol.* **2011,** *41*, 83–110.

73. Cohen, P. T. W.; Brewis, N. D.; Hughes, V.; Mann, D. J., Protein serine/threonine phosphatases; an expanding family. *FEBS Lett.* **1990,** *268*, 355–359.

74. Žegura, B.; Straser, A.; Filipic, M., Genotoxity and potential carcinogenicity of cyanobacterial toxins — a review. *Mutat. Res.* **2011,** *727*, 16–41.

75. Falconer, I. R.; Yeung, D. S., Cytoskeletal changes in hepatocytes induced by *Microcystis* toxins and their relation to hyperphosphorylation of cell proteins. *Chem.-Biol. Interact.* **1992,** *81*, 181–196.

76. Zong, W.; Wang, X.; Du, Y.; Zhang, S.; Zhang, Y.; Teng, Y., Molecular mechanism for the regulation of microcystin toxicity to protein phosphatase1 by glutathione conjugation pathway. *BioMed Res. Int* **2017,** *2017*, 9676504.

77. Grosse, Y.; Baan, R.; Straif, K.; Secretan, B.; El Ghissassi, F.; Cogliano, V. J., Carcinogenicity of nitrate, nitrite, and cyanobacterial peptide toxins. *Lancet Oncol.* **2006,** 628–629.

78.  World Health Organization (WHO), Guidelines for Drinking-Water Quality: Fourth Edition Incorporating the First Addendum, https://www.who.int/water_sanitation_health/publications/drinking-water-quality-guidelines-4-including-1st-addendum/en/. Geneva, Switzerland, **2017**.

79.  Wang, Q.; Niu, Y.; Xie, P.; Chen, J.; Ma, Z.; Tao, M.; Qi, M.; Wu, L.; Guo, L., Factors affecting temporal and spatial variations of microcystins in Gonghu Bay of Lake Taihu, with potential risk of microcystin contamination to human health. *Sci. World J.* **2010,** *10*, 1795–1809.

80.  Hu, X.; Zhang, R.; Ye, J.; Wu, X.; Zhang, Y.; Wu, C., Monitoring and research of microcystins and environmental factors in a typical artificial freshwater aquaculture pond. *Environ. Sci. Pollut. Res.* **2018,** *25*, 5921–5933.

81.  Miller, T. R.; Xiong, A.; Deeds, J. R.; Stutts, W. L.; Samdal, I. A.; Løvberg, K. E.; Miles, C. O., Microcystin toxins at potentially hazardous levels in algal dietary supplements revealed by a combination of bioassay, immunoassay, and mass spectrometric methods. *J. Agric. Food Chem.* **2020**.

82.  Codd, G.; Bell, S.; Kaya, K.; Ward, C.; Beattie, K.; Metcalf, J., Cyanobacterial toxins, exposure routes and human health. *Eur. J. Phycol.* **1999,** *34*, 405–415.

83.  World Health Organization (WHO) Chemical hazards in drinking-water: Microcystin-LR. https://www.who.int/water_sanitation_health/water-quality/guidelines/chemicals/microcystin/en/ (accessed 06/07/2020),

84.  Buratti, F.; Testai, E., Species- and congener-differences in microcystin-LR and -RR GSH conjugation in human, rat, and mouse hepatic cytosol. *Toxicol. Lett.* **2014,** *232*.

85.  Campos, A.; Vasconcelos, V., Molecular mechanisms of microcystin toxicity in animal cells. *Int. J. Mol. Sci.* **2010,** *11*, 268–287.

86.  Eriksson, J. E.; Grönberg, L.; Nygård, S.; Slotte, J. P.; Meriluoto, J. A., Hepatocellular uptake of 3H-dihydromicrocystin-LR, a cyclic peptide toxin. *Biochim. Biophys. Acta* **1990,** *1025*, 60–66.

87.  Fischer, A.; Hoeger, S. J.; Stemmer, K.; Feurstein, D. J.; Knobeloch, D.; Nussler, A.; Dietrich, D. R., The role of organic anion transporting polypeptides (OATPs/SLCOs) in the toxicity of different microcystin congeners *in vitro*: a comparison of primary human hepatocytes and OATP-transfected HEK293 cells. *Toxicol. Appl. Pharmacol.* **2010,** *245*, 9–20.

88.  Feurstein, D.; Stemmer, K.; Kleinteich, J.; Speicher, T.; Dietrich, D. R., Microcystin congener- and concentration-dependent induction of murine neuron apoptosis and neurite degeneration. *Toxicol. Sci.* **2011,** *124*, 424–431.

89.  Díez-Quijada, L.; Prieto, A. I.; Guzmán-Guillén, R.; Jos, A.; Camean, A. M., Occurrence and toxicity of microcystin congeners other than MC-LR and MC-RR: a review. *Food Chem. Toxicol.* **2019,** *125*, 106-132.

90.  Jones, M. R.; Pinto, E.; Torres, M. A.; Dörr, F.; Mazur-Marzec, H.; Szubert, K.; Tartaglione, L.; Dell'Aversano, C.; Miles, C. O.; Beach, D. G.; McCarron, P.; Sivonen, K.; Fewer, D. P.; Jokela, J.; Janssen, E. M.-L., Comprehensive database of secondary metabolites from cyanobacteria. *bioRxiv* **2020**, 2020.04.16.038703.

91.  Welker, M.; von Döhren, H., Cyanobacterial peptides – nature's own combinatorial biosynthesis. *FEMS Microbiol. Rev.* **2006,** *30*, 530–563.

92.  Funari, E.; Testai, E., Human health risk assessment related to cyanotoxins exposure. *Crit. Rev. Toxicol.* **2008,** *38*, 97–125.

93.  World Health Organization (WHO), Parma Declaration on Environment and Health, http://www.euro.who.int/parma2010 Parma, 2010.

94.  International Programme on Chemical Safety (IPCS), *Global assessment of the state-of-the-science of endocrine disruptors* Geneva, Switzerland, **2002**.

95.  European Commission (EC) What is the endocrine system? https://ec.europa.eu/environment/chemicals/endocrine/definitions/definitions_en.htm (accessed 24/06/2020),

96.  European Commission (EC) Why is it important for life? https://ec.europa.eu/environment/chemicals/endocrine/definitions/life_en.htm (accessed 24/06/2020),

97. Utiger, R. D. Human endocrine system. https://www.britannica.com/science/human-endocrine-system (accessed 27/06/2020),

98. U. S. National Institutes of Health, N. C. I. SEER Training Modules, Endocrine Glands & Their Hormones. https://training.seer.cancer.gov/ (24/06/2020),

99. Dattani, M. T.; Gevers, E. F., Endocrinology of Fetal Development. In *Williams Textbook of Endocrinology* 13th ed.; 2016; pp 849–892.

100. Ortiga-Carvalho, T. M.; Chiamolera, M. I.; Pazos-Moura, C. C.; Wondisford, F. E., Hypothalamus-Pituitary-Thyroid Axis. *Compr. Physiol.* **2016,** *6*, 1387–1428.

101. Smith, S. M.; Vale, W. W., The role of the hypothalamic-pituitary-adrenal axis in neuroendocrine responses to stress. *Dialogues Clin. Neurosci.* **2006,** *8*, 383–395.

102. Norris, D. O.; Schwartz, T. B. Endocrine system. https://www.britannica.com/science/endocrine-system (accessed 29/06/2020),

103. Colborn, T.; vom Saal, F. S.; Soto, A. M., Developmental effects of endocrine-disrupting chemicals in wildlife and humans. *Environ. Health Perspect.* **1993,** *101*, 378–384.

104. Bergman, A.; Brandt, I.; Brouwer, A.; Harrison, P. T. C.; Holmes, P.; Humfrey, C. D.; Keiding, N.; Randall, G.; M., S. R.; Skakkebaek, N. E. *European Workshop on the Impact of Endocrine Disrupters on Human Health and Wildlife, 2-4 December 1996, Weybridge, UK: Report of Proceedings. Environment and Climate Research Programme of DG XII of the European Commission (Report EUR 17549).* 1997.

105. Diamanti-Kandarakis, E.; Bourguignon, J. P.; Giudice, L. C.; Hauser, R.; Prins, G. S.; Soto, A. M.; Zoeller, R. T.; Gore, A. C., Endocrine-disrupting chemicals: an Endocrine Society scientific statement. *Endocr. Rev.* **2009,** *30*, 293–342.

106. Kortenkamp, A.; Martin, O.; Evans, R.; Orton, F.; McKinlay, R.; Rosivatz, E.; Faust, M., Response to a critique of the European Commission document, "State of the art assessment of endocrine disrupters" by Rhomberg and colleagues–letter to the editor. *Crit. Rev. Toxicol.* **2012,** *42*, 787–789; author reply 790–791.

107. UN Environmental Programme (UNEP)/World Health Organization (WHO), *State of the science of endocrine disrupting chemicals–2012.* Geneva, Switzerland, **2012.**

108. Bergman, A.; Heindel, J. J.; Kasten, T.; Kidd, K. A.; Jobling, S.; Neira, M.; Zoeller, R. T.; Becher, G.; Bjerregaard, P.; Bornman, R.; Brandt, I.; Kortenkamp, A.; Muir, D.; Drisse, M. N.; Ochieng, R.; Skakkebaek, N. E.; Bylehn, A. S.; Iguchi, T.; Toppari, J.; Woodruff, T. J., The impact of endocrine disruption: a consensus statement on the state of the science. *Environ. Health Perspect.* **2013,** *121*, A104–A106.

109. Giulivo, M.; Lopez de Alda, M.; Capri, E.; Barcelo, D., Human exposure to endocrine disrupting compounds: Their role in reproductive systems, metabolic syndrome and breast cancer. A review. *Environ. Res.* **2016,** *151*, 251–264.

110. Gore, A. C.; Chappell, V. A.; Fenton, S. E.; Flaws, J. A.; Nadal, A.; Prins, G. S.; Toppari, J.; Zoeller, R. T., EDC-2: The Endocrine Society's second scientific statement on endocrine-disrupting chemicals. *Endocr. Rev.* **2015,** *36*, E1–E150.

111. Gore, A. C.; Chappell, V. A.; Fenton, S. E.; Flaws, J. A.; Nadal, A.; Prins, G. S.; Toppari, J.; Zoeller, R. T., Executive summary to EDC-2: The Endocrine Society's second scientific statement on endocrine-disrupting chemicals. *Endocr. Rev.* **2015,** *36*, 593–602.

112. Lauretta, R.; Sansone, A.; Sansone, M.; Romanelli, F.; Appetecchia, M., Endocrine disrupting chemicals: effects on endocrine glands. *Front. Endocrinol.* **2019,** *10*, 178.

113. European Commission (EC), Communication from the Commission to the European Parliament, the Council, the European Economic and Social Committee of the Regions, Towards a comprehensive European Union framework on endocrine disruptors, https://eur-lex.europa.eu/legal-content/en/TXT/?uri=CELEX:52018DC0734. 2018.

114. Kortenkamp, A., Low dose mixture effects of endocrine disrupters and their implications for regulatory thresholds in chemical risk assessment. *Curr. Opin. Pharmacol.* **2014,** *19*, 105–111.

115. Salahudeen, M. S.; Nishtala, P. S., An overview of pharmacodynamic modelling, ligand-binding approach and its application in clinical practice. *Saudi Pharm. J.* **2017,** *25*, 165–175.

116. European Commission (EC) What are endocrine disruptors? https://ec.europa.eu/environment/chemicals/endocrine/definitions/endodis_en.htm (accessed 24/06/2020),

117.   Abdel-Magid, A. F., Allosteric modulators: an emerging concept in drug discovery. *ACS Med. Chem. Lett.* **2015,** *6*, 104–107.

118.   Hecker, M.; Giesy, J. P., Novel trends in endocrine disruptor testing: the H295R Steroidogenesis Assay for identification of inducers and inhibitors of hormone production. *Anal Bioanal Chem* **2008,** *390*, 287–291.

119.   Kiyama, R.; Wada-Kiyama, Y., Estrogenic endocrine disruptors: molecular mechanisms of action. *Environ. Int.* **2015,** *83*, 11–40.

120.   Tabb, M. M.; Blumberg, B., New modes of action for endocrine-disrupting chemicals. *Mol. Endocrinol.* **2006,** *20*, 475–482.

121.   Sepkovic, D. W.; Bradlow, H. L., Estrogen hydroxylation–the good and the bad. *Ann. N. Y. Acad. Sci.* **2009,** *1155*, 57–67.

122.   Organisation for Economic Co-operation and Development (OECD), *Revised Guidance Document 150 on Standardised Test Guidelines for Evaluating Chemicals for Endocrine Disruption.* 2018.

123.   EFSA Scientific Committee, Scientific Opinion on the hazard assessment of endocrine disruptors: Scientific criteria for identification of endocrine disruptors and appropriateness of existing test methods for assessing effects mediated by these substances on human health and the environment. *EFSA J* **2013,** *11*, 3132.

124.   Zoeller, R. T.; Brown, T. R.; Doan, L. L.; Gore, A. C.; Skakkebaek, N. E.; Soto, A. M.; Woodruff, T. J.; Vom Saal, F. S., Endocrine-disrupting chemicals and public health protection: a statement of principles from The Endocrine Society. *Endocrinology* **2012,** *153*, 4097–4110.

125.   La Merrill, M. A.; Vandenberg, L. N.; Smith, M. T.; Goodson, W.; Browne, P.; Patisaul, H. B.; Guyton, K. Z.; Kortenkamp, A.; Cogliano, V. J.; Woodruff, T. J.; Rieswijk, L.; Sone, H.; Korach, K. S.; Gore, A. C.; Zeise, L.; Zoeller, R. T., Consensus on the key characteristics of endocrine-disrupting chemicals as a basis for hazard identification. *Nat. Rev. Endocrinol.* **2020,** *16*, 45–57.

126.   Darbre, P. D., Endocrine disruptors and obesity. *Curr. Obes. Rep.* **2017,** *6*, 18–27.

127.   Chen, L.; Chen, J.; Zhang, X.; Xie, P., A review of reproductive toxicity of microcystins. *J. Hazard. Mater.* **2016,** *301*, 381–399.

128.   Wu, J.; Shao, S.; Zhou, F.; Wen, S.; Chen, F.; Han, X., Reproductive toxicity on female mice induced by microcystin-LR. *Environ. Toxicol. Pharmacol.* **2014,** *37*, 1–6.

129.   Li, Y.; Sheng, J.; Sha, J.; Han, X., The toxic effects of microcystin-LR on the reproductive system of male rats *in vivo* and *in vitro. Reprod. Toxicol.* **2008,** *26*, 239–245.

130.   Chen, Y.; Xu, J.; Li, Y.; Han, X., Decline of sperm quality and testicular function in male mice during chronic low-dose exposure to microcystin-LR. *Reprod. Toxicol.* **2011,** *31*, 551–557.

131.   Wang, L.; Wang, X.; Geng, Z.; Zhou, Y.; Chen, Y.; Wu, J.; Han, X., Distribution of microcystin-LR to testis of male Sprague-Dawley rats. *Ecotoxicology* **2013,** *22*, 1555–1563.

132.   Zhao, Y.; Xie, L.; Yan, Y., Microcystin-LR impairs zebrafish reproduction by affecting oogenesis and endocrine system. *Chemosphere* **2015,** *120*, 115–122.

133.   Qiao, Q.; Liu, W.; Wu, K.; Song, T.; Hu, J.; Huang, X.; Wen, J.; Chen, L.; Zhang, X., Female zebrafish (*Danio rerio*) are more vulnerable than males to microcystin-LR exposure, without exhibiting estrogenic effects. *Aquat. Toxicol.* **2013,** *142–143*, 272-82.

134.   Heppell, S. A.; Denslow, N. D.; Folmar, L. C.; Sullivan, C. V., Universal assay of vitellogenin as a biomarker for environmental estrogens. *Environ. Health Perspect.* **1995,** *103 Suppl 7*, 9–15.

135.   Su, Y.; Li, L.; Hou, J.; Wu, N.; Lin, W.; Li, G., Life-cycle exposure to microcystin-LR interferes with the reproductive endocrine system of male zebrafish. *Aquat. Toxicol.* **2016,** *175*, 205–212.

136.   Wang, L.; Lin, W.; Zha, Q.; Guo, H.; Zhang, D.; Yang, L.; Li, L.; Li, D.; Tang, R., Persistent exposure to environmental levels of microcystin-LR disturbs cortisol production via hypothalamic-pituitary-interrenal (HPI) axis and subsequently liver glucose metabolism in adult male zebrafish (*Danio rerio*). *Toxins (Basel)* **2020,** *12*.

137.   Hou, J.; Li, L.; Wu, N.; Su, Y.; Lin, W.; Li, G.; Gu, Z., Reproduction impairment and endocrine disruption in female zebrafish after long-term exposure to MC-LR: a life cycle assessment. *Environ. Pollut.* **2016,** *208*, 477–485.

138. Gracia, T.; Hilscherova, K.; Jones, P. D.; Newsted, J. L.; Zhang, X.; Hecker, M.; Higley, E. B.; Sanderson, J. T.; Yu, R. M.; Wu, R. S.; Giesy, J. P., The H295R system for evaluation of endocrine-disrupting effects. *Ecotoxicol. Environ. Saf.* **2006,** *65,* 293–305.

139. Oziol, L.; Bouaicha, N., First evidence of estrogenic potential of the cyanobacterial heptotoxins the nodularin-R and the microcystin-LR in cultured mammalian cells. *J. Hazard. Mater.* **2010,** *174,* 610–615.

140. Ding, X. S.; Li, X. Y.; Duan, H. Y.; Chung, I. K.; Lee, J. A., Toxic effects of *Microcystis* cell extracts on the reproductive system of male mice. *Toxicon* **2006,** *48,* 973–979.

141. Li, G.-Y.; Xie, P.; Li, H.-Y.; Hao, L.; Xiong, Q.; Qiu, T., Involment of p53, Bax, and Bcl-2 pathway in microcystins-induced apoptosis in rat testis. *Environ. Toxicol.* **2011,** *26,* 111–117.

142. Xiong, Q.; Xie, P.; Li, H.; Hao, L.; Li, G.; Qiu, T.; Liu, Y., Involvement of Fas/FasL system in apoptotic signaling in testicular germ cells of male Wistar rats injected i.v. with microcystins. *Toxicon* **2009,** *54,* 1–7.

143. Liu, Y.; Xie, P.; Qiu, T.; Li, H.-Y.; Li, G.-Y.; Hao, L.; Xiong, Q., *Microcystin* extracts induce ultrastructural damage and biochemical disturbance in male rabbit testis. *Environ. Toxicol.* **2010,** *25,* 9–17.

144. Jonas, A.; Scholz, S.; Fetter, E.; Sychrova, E.; Novakova, K.; Ortmann, J.; Benisek, M.; Adamovsky, O.; Giesy, J. P.; Hilscherova, K., Endocrine, teratogenic and neurotoxic effects of cyanobacteria detected by cellular in vitro and zebrafish embryos assays. *Chemosphere* **2015,** *120,* 321–327.

145. Stepankova, T.; Ambrozova, L.; Blaha, L.; Giesy, J. P.; Hilscherova, K., *In vitro* modulation of intracellular receptor signaling and cytotoxicity induced by extracts of cyanobacteria, complex water blooms and their fractions. *Aquat. Toxicol.* **2011,** *105,* 497–507.

146. Sychrova, E.; Stepankova, T.; Novakova, K.; Blaha, L.; Giesy, J. P.; Hilscherova, K., Estrogenic activity in extracts and exudates of cyanobacteria and green algae. *Environ. Int.* **2012,** *39,* 134–140.

147. Rogers, E. D.; Henry, T. B.; Twiner, M. J.; Gouffon, J. S.; McPherson, J. T.; Boyer, G. L.; Sayler, G. S.; Wilhelm, S. W., Global gene expression profiling in larval zebrafish exposed to microcystin-LR and microcystis reveals endocrine disrupting effects of cyanobacteria. *Environ. Sci. Technol.* **2011,** *45,* 1962–1969.

148. Liu, G.; Ke, M.; Fan, X.; Zhang, M.; Zhu, Y.; Lu, T.; Sun, L.; Qian, H., Reproductive and endocrine-disrupting toxicity of *Microcystis aeruginosa* in female zebrafish. *Chemosphere* **2018,** *192,* 289–296.

149. Xiong, X.; Zhong, A.; Xu, H., Effect of cyanotoxins on the hypothalamic-pituitary-gonadal axis in male adult mouse. *PLoS One* **2014,** *9,* e106585.

150. Jia, Y.; Chen, Q.; Crawford, S. E.; Song, L.; Chen, W.; Hammers-Wirtz, M.; Strauss, T.; Seiler, T. B.; Schaffer, A.; Hollert, H., Cyanobacterial blooms act as sink and source of endocrine disruptors in the third largest freshwater lake in China. *Environ. Pollut.* **2019,** *245,* 408–418.

151. Dittmann, E.; Neilan, B. A.; Erhard, M.; Von Döhren, H.; Börner, T., Insertional mutagenesis of a peptide synthetase gene that is responsible for hepatotoxin production in the cyanobacterium *Microcystis aeruginosa* PCC 7806. *Mol. Microbiol.* **1997,** *26,* 779–787.

152. Samdal, I. A.; Ballot, A.; Lovberg, K. E.; Miles, C. O., Multihapten approach leading to a sensitive ELISA with broad cross-reactivity to microcystins and nodularin. *Environ Sci Technol* **2014,** *48,* 8035–8043.

153. Kotai, J. *Instructions for preparation of modified nutrient solution Z8 for algae*; Norwegian Institute for Water Research, Oslo, Norway: 1972.

154. Pitt, J. J., Principles and applications of liquid chromatography–mass spectrometry in clinical biochemistry. *Clin. Biochem. Rev* **2009,** *30,* 19–34.

155. Ardrey, R. E., *Liquid Chromatography–Mass Spectrometry: An Introduction*. John Wiley & Sons: 2003.

156. Ardrey, R. E., Liquid Chromatography. In *Liquid Chromatography–Mass Spectrometry: An Introduction*, John Wiley & Sons: 2003.

157. Lough, W. J.; Wainer, I. W., *High Performance Liquid Chromatography: Fundamental Principles and Practice*. Blackie Academic and Professional, London, UK: 2013.

158. Cross, T. Thermoscientific, HPLC or UHPLC? https://analyteguru.com/hplc-or-uhplc/ (accessed 13/07/2020),

159. Deepak, B. lab-training.com: What are the Benefits of UHPLC over normal Analytical HPLC? https://lab-training.com/2014/04/17/what-are-the-benefits-of-uhplc-over-normal-analytical-hplc/ (accessed 13/07/2020),

160. Niessen, W. M. A.; Tinke, A. P., Liquid chromatography–mass spectrometry general principles and instrumentation. *J. Chromatogr. A* **1995,** *703*, 37–57.

161. Murray, K. K.; Boyd, R. K.; Eberlin, M. N.; Langley, G. J.; Li, L.; Naito, Y., Definitions of terms relating to mass spectrometry (IUPAC Recommendations 2013). *Pure Appl. Chem.* **2013,** *85*, 1515.

162. Greaves, J.; Roboz, J., *Mass Spectrometry for the Novice.* Taylor & Francis Group, Boca Raton, FL, US: 2014.

163. Glish, G. L., Multiple stage mass spectrometry: the next generation tandem mass spectrometry experiment. *Analyst* **1994,** *119*, 533–537.

164. Miles, C.; Stirling, D., Toxin mass list COM v16.0 (microcystin and nodularin lists and mass calculators for mass spectrometry of microcystins, nodularins, saxitoxins and anatoxins). 2019.

165. Ho, C. S.; Lam, C. W.; Chan, M. H.; Cheung, R. C.; Law, L. K.; Lit, L. C.; Ng, K. F.; Suen, M. W.; Tai, H. L., Electrospray ionisation mass spectrometry: principles and clinical applications. *Clin. Biochem. Rev* **2003,** *24*, 3–12.

166. Kruve, A.; Kaupmees, K., Adduct formation in ESI/MS by mobile phase additives. *J. Am. Soc. Mass Spectrom.* **2017,** *28*, 887–894.

167. Zhu, J.; Cole, R. B., Formation and decompositions of chloride adduct ions, [M + Cl]⁻, in negative ion electrospray ionization mass spectrometry. *J. Am. Soc. Mass Spectrom.* **2000,** *11*, 932–941.

168. Rockwood, A. L.; Kushnir, M. M.; Clarke, N. J., 2 - Mass Spectrometry. In *Principles and Applications of Clinical Mass Spectrometry – Small Molecules, Peptides, and Pathogens*, Rifai, N.; Horvath, A. R.; Wittwer, C. T., Eds. Elsevier: 2018.

169. Douglas, D. J.; Frank, A. J.; Mao, D., Linear ion traps in mass spectrometry. *Mass Spectrom. Rev.* **2005,** *24*, 1–29.

170. Makarov, A., Electrostatic axially harmonic orbital trapping: a high-performance technique of mass analysis. *Anal. Chem.* **2000,** *72*, 1156–1162.

171. Hu, Q.; Noll, R. J.; Li, H.; Makarov, A.; Hardman, M.; Graham Cooks, R., The Orbitrap: a new mass spectrometer. *J. Mass Spectrom.* **2005,** *40*, 430–443.

172. Makarov, A.; Denisov, E.; Kholomeev, A.; Balschun, W.; Lange, O.; Strupat, K.; Horning, S., Performance evaluation of a hybrid linear ion trap/orbitrap mass spectrometer. *Anal. Chem.* **2006,** *78*, 2113–2120.

173. Caixach, J.; Flores, C.; Spoof, L.; Meriluoto, J.; Schmidt, W.; Mazur-Marzec, H.; Hiskia, A.; Kaloudis, T.; Furey, A., Liquid Chromatography–Mass Spectrometry. In *Handbook of Cyanobacterial Monitoring and Cyanotoxin Analysis,*, Meriluoto, J.; Spoof, L.; Codd, G. A., Eds. John Wiley & Sons, Ltd., Chichester, UK: 2017; pp 218–251.

174. Bortoli, S.; Volmer, D. A., Characterization and identification of microcystins by mass spectrometry. *Eur. J. Mass Spectrom.* **2014,** *20*, 1–19.

175. Kleinteich, J.; Puddick, J.; Wood, S. A.; Hildebrand, F.; Laughinghouse IV, H. D.; Pearce, D. A.; Dietrich, D. R.; Wilmotte, A., Toxic cyanobacteria in Svalbard: chemical diversity of microcystins detected using a liquid chromatography mass spectrometry precursor ion screening method. *Toxins (Basel)* **2018,** *10*.

176. Ortiz, X.; Korenkova, E.; Jobst, K. J.; MacPherson, K. A.; Reiner, E. J., A high throughput targeted and non-targeted method for the analysis of microcystins and anatoxin-A using on-line solid phase extraction coupled to liquid chromatography-quadrupole time-of-flight high resolution mass spectrometry. *Anal. Bioanal. Chem.* **2017,** *409*, 4959–4969.

177. Teta, R.; Della Sala, G.; Glukhov, E.; Gerwick, L.; Gerwick, W. H.; Mangoni, A.; Costantino, V., Combined LC–MS/MS and molecular networking approach reveals new cyanotoxins from the 2014 cyanobacterial bloom in Green Lake, Seattle. *Environ. Sci. Technol.* **2015,** *49*, 14301–14310.

178.	Yilmaz, M.; Foss, A. J.; Miles, C. O.; Özen, M.; Demir, N.; Balci, M.; Beach, D. G., Comprehensive multi-technique approach reveals the high diversity of microcystins in field collections and an associated isolate of *Microcystis aeruginosa* from a Turkish lake. *Toxicon* **2019,** *167*, 87–100.

179.	Stewart, A. K.; Strangman, W. K.; Percy, A.; Wright, J. L. C., The biosynthesis of ^{15}N-labeled microcystins and the comparative MS/MS fragmentation of natural abundance and their ^{15}N-labeled congeners using LC–MS/MS. *Toxicon* **2018,** *144*, 91–102.

180.	Dörr, F. A.; Oliveira-Silva, D.; Lopes, N. P.; Iglesias, J.; Volmer, D. A.; Pinto, E., Dissociation of deprotonated microcystin variants by collision-induced dissociation following electrospray ionization. *Rapid Commun. Mass Spectrom.* **2011,** *25*, 1981–1992.

181.	Ferranti, P.; Fabbrocino, S.; Nasi, A.; Caira, S.; Bruno, M.; Serpe, L.; Gallo, P., Liquid chromatography coupled to quadruple time-of-flight tandem mass spectrometry for microcystin analysis in freshwaters: method performances and characterisation of a novel variant of microcystin-RR. *Rapid Commun. Mass Spectrom.* **2009,** *23*, 1328–1336.

182.	Mayumi, T.; Kato, H.; Imanishi, S.; Kawasaki, Y.; Hasegawa, M.; Harada, K., Structural characterization of microcystins by LC/MS/MS under ion trap conditions. *J. Antibiot.* **2006,** *59*, 710-719.

183.	Benke, P. I.; Vinay Kumar, M. C.; Pan, D.; Swarup, S., A mass spectrometry-based unique fragment approach for the identification of microcystins. *Analyst* **2015,** *140*, 1198–1206.

184.	Attard, T. J.; Carter, M. D.; Fang, M.; Johnson, R. C.; Reid, G. E., Structural characterization and absolute quantification of microcystin peptides using collision-induced and ultraviolet photo-dissociation tandem mass spectrometry. *J. Am. Soc. Mass Spectrom.* **2018**.

185.	Miles, C. O.; Sandvik, M.; Haande, S.; Nonga, H.; Ballot, A., LC–MS analysis with thiol derivatization to differentiate [Dhb[7]]- from [Mdha[7]]-microcystins: analysis of cyanobacterial blooms, *Planktothrix* cultures and European crayfish from Lake Steinsfjorden, Norway. *Environ. Sci. Technol.* **2013,** *47*, 4080–4087.

186.	Miles, C. O.; Sandvik, M.; Nonga, H. E.; Rundberget, T.; Wilkins, A. L.; Rise, F.; Ballot, A., Thiol derivatization for LC–MS identification of microcystins in complex matrices. *Environ. Sci. Technol.* **2012,** *46*, 8937–8944.

187.	Sherlock, I. R.; James, K. J.; Caudwell, F. B.; MacKintosh, C., First identification of microcystins in Irish lakes aided by a new derivatisation procedure for electrospray mass spectrometric analysis. *Nat. Toxins* **1997,** *5*, 247–254.

188.	Birbeck, J. A.; Peraino, N. J.; O'Neill, G. M.; Coady, J.; Westrick, J. A., Dhb microcystins discovered in USA using an online concentration LC–MS/MS platform. *Toxins (Basel)* **2019,** *11*.

189.	Harada, K. I.; Tsuji, K.; Watanabe, M. F.; Kondo, F., Stability of microcystins from cyanobacteria - III. Effect of pH and temperature. *Phycologia* **1996,** *35 (Suppl.)*, 83–88.

190.	Namikoshi, M.; Yuan, M.; Sivonen, K.; Carmichael, W. W.; Rinehart, K. L.; Rouhiainen, L.; Sun, F.; Brittain, S.; Otsuki, A., Seven new microcystins possessing two L-glutamic acid units, isolated from *Anabaena* sp. strain 186. *Chem. Res. Toxicol.* **1998,** *11*, 143–149.

191.	Leonard, N. J.; Johnson, C. R., Periodate oxidation of sulfides to sulfoxides. Scope of the reaction. *J. Org. Chem.* **1962,** *27*, 282–284.

192.	Connolly, L.; Ropstad, E.; Verhaegen, S., In vitro bioassays for the study of endocrine-disrupting food additives and contaminants. *TrAC, Trends Anal. Chem.* **2011,** *30*, 227–238.

193.	Willemsen, P.; Scippo, M. L.; Kausel, G.; Figueroa, J.; Maghuin-Rogister, G.; Martial, J. A.; Muller, M., Use of reporter cell lines for detection of endocrine-disrupter activity. *Anal. Bioanal. Chem.* **2004,** *378*, 655–63.

194.	Alberts, B.; Hopkin, K.; Bray, D.; Johnson, A. D.; Lewis, L.; Roberts, K.; Raff, M.; Walter, P., *Essential Cell Biology*. Taylor & Francis Group: 2009.

195.	https://www.noaa.gov/what-is-harmful-algal-bloom.

196.	https://www.nature.com/subjects/reporter-genes. (Accessed 13/08/2020),

197.	Eun, H.-M., 8 - Marker/Reporter Enzymes. In *Enzymology Primer for Recombinant DNA Technology*, Eun, H.-M., Ed. Academic Press: San Diego, 1996; pp 567–645.

198.	Riggs, P., Fusion Proteins. In *Encyclopedia of Genetics*, Brenner, S.; Miller, J. H., Eds. Academic Press: New York, 2001; pp 739–740.

199. Gazdar, A. F.; Oie, H. K.; Shackleton, C. H.; Chen, T. R.; Triche, T. J.; Myers, C. E.; Chrousos, G. P.; Brennan, M. F.; Stein, C. A.; La Rocca, R. V., Establishment and characterization of a human adrenocortical carcinoma cell line that expresses multiple pathways of steroid biosynthesis. *Cancer Res.* **1990,** *50*, 5488-5496.

200. Wang, T.; Rainey, W. E., Human adrenocortical carcinoma cell lines. *Mol. Cell. Endocrinol.* **2012,** *351*, 58–65.

201. Rainey, W. E.; Bird, I. M.; Mason, J. I., The NCI-H295 cell line: a pluripotent model for human adrenocortical studies. *Mol. Cell. Endocrinol.* **1994,** *100*, 45–50.

202. Willenberg, H. S.; Bornstein, S. R., Adrenal Cortex; Development, Anatomy, Physiology. In *Endotext*, Feingold, K. R.; Anawalt, B.; Boyce, A.; Chrousos, G.; Dungan, K.; Grossman, A.; Hershman, J. M.; Kaltsas, G.; Koch, C.; Kopp, P.; Korbonits, M.; McLachlan, R.; Morley, J. E.; New, M.; Perreault, L.; Purnell, J.; Rebar, R.; Singer, F.; Trence, D. L.; Vinik, A.; Wilson, D. P., Eds. South Dartmouth (MA), 2000.

203. Ullerås, E.; Ohlsson, Å.; Oskarsson, A., Secretion of cortisol and aldosterone as a vulnerable target for adrenal endocrine disruption — screening of 30 selected chemicals in the human H295R cell model. *J. Appl. Toxicol.* **2008,** *28*, 1045–1053.

204. Payne, A. H.; Hales, D. B., Overview of steroidogenic enzymes in the pathway from cholesterol to active steroid hormones. *Endocr. Rev.* **2004,** *25*, 947–970.

205. Miller, W. L.; Auchus, R. J., The molecular biology, biochemistry, and physiology of human steroidogenesis and its disorders. *Endocr. Rev.* **2011,** *32*, 81–151.

206. Miller, W. L., Steroid hormone synthesis in mitochondria. *Mol. Cell. Endocrinol.* **2013,** *379*, 62–73.

207. Ho, C. K. M.; Christenson, L. K.; Strauss, J. F., CHAPTER 6 - Intracellular Cholesterol Dynamics in Steroidogenic Cells. In *The Ovary (Second Edition)*, Leung, P. C. K.; Adashi, E. Y., Eds. Academic Press: San Diego, 2004; pp 93–110.

208. Hilscherova, K.; Jones, P. D.; Gracia, T.; Newsted, J. L.; Zhang, X.; Sanderson, J. T.; Yu, R. M.; Wu, R. S.; Giesy, J. P., Assessment of the effects of chemicals on the expression of ten steroidogenic genes in the H295R cell line using real–time PCR. *Toxicol. Sci.* **2004,** *81*, 78–89.

209. Mosmann, T., Rapid colorimetric assay for cellular growth and survival: application to proliferation and cytotoxicity assays. *J. Immunol. Methods* **1983,** *65*, 55–63.

210. Stone, V.; Johnston, H.; Schins, R. P., Development of *in vitro* systems for nanotoxicology: methodological considerations. *Crit. Rev. Toxicol.* **2009,** *39*, 613–626.

211. Jia, L.; Liu, X., The conduct of drug metabolism studies considered good practice (II): *in vitro* experiments. *Curr. Drug Metab.* **2007,** *8*, 822–829.

212. Asha, S.; Vidyavathi, M., Role of human liver microsomes in *in vitro* metabolism of drugs–a review. *Appl. Biochem. Biotechnol.* **2010,** *160*, 1699–1722.

213. Almazroo, O. A.; Miah, M. K.; Venkataramanan, R., Drug metabolism in the liver. *Clin. Liver Dis.* **2017,** *21*, 1–20.

214. Döring, B.; Petzinger, E., Phase 0 and phase III transport in various organs: combined concept of phases in xenobiotic transport and metabolism. *Drug Metab. Rev.* **2014,** *46*, 261–282.

215. Kulkarni, A. P., Role of biotransformation in conceptal toxicity of drugs and other chemicals. *Curr. Pharm. Des.* **2001,** *7*, 833–857.

216. McDonnell, A. M.; Dang, C. H., Basic review of the cytochrome p450 system. *J. Adv. Pract. Oncol.* **2013,** *4*, 263–268.

217. Pan, Y.; Abd-Rashid, B. A.; Ismail, Z.; Ismail, R.; Mak, J. W.; Ong, C. E., Heterologous expression of human cytochromes P450 2D6 and CYP3A4 in *Escherichia coli* and their functional characterization. *The Protein Journal* **2011,** *30*, 581–591.

218. Donato, M. T.; Castell, J. V., Strategies and molecular probes to investigate the role of cytochrome P450 in drug metabolism: focus on *in vitro* studies. *Clin. Pharmacokinet.* **2003,** *42*, 153–178.

219. Brandon, E. F.; Raap, C. D.; Meijerman, I.; Beijnen, J. H.; Schellens, J. H., An update on *in vitro* test methods in human hepatic drug biotransformation research: pros and cons. *Toxicol. Appl. Pharmacol.* **2003,** *189*, 233–246.

220.  Ballot, A.; Swe, T.; Mjelde, M.; Cerasino, L.; Hostyeva, V.; Miles, C. O., Cylindrospermopsin- and deoxycylindrospermopsin-producing *Raphidiopsis raciborskii* and microcystin-producing *Microcystis* spp. in Meiktila Lake, Myanmar. *Toxins (Basel)* **2020,** *12*.

221.  Hao, G.; Wang, D.; Gu, J.; Shen, Q.; Gross, S. S.; Wang, Y., Neutral loss of isocyanic acid in peptide CID spectra: a novel diagnostic marker for mass spectrometric identification of protein citrullination. *J. Am. Soc. Mass Spectrom.* **2009,** *20*, 723–727.

222.  Foss, A. J.; Miles, C. O.; Samdal, I. A.; Løvberg, K. E.; Wilkins, A. L.; Rise, F.; Jaabaek, J. A. H.; McGowan, P. C.; Aubel, M. T., Analysis of free and metabolized microcystins in samples following a bird mortality event. *Harmful Algae* **2018,** *80*, 117–129.

223.  Labrie, F.; Luu-The, V.; Lin, S. X.; Labrie, C.; Simard, J.; Breton, R.; Belanger, A., The key role of 17β-hydroxysteroid dehydrogenases in sex steroid biology. *Steroids* **1997,** *62*, 148–158.

224.  Badawi, A. F.; Cavalieri, E. L.; Rogan, E. G., Role of human cytochrome P450 1A1, 1A2, 1B1, and 3A4 in the 2-, 4-, and 16a-hydroxylation of 17b-estradiol. *Metabolism* **2001,** *50*, 1001–1003.

225.  Zhu, B. T.; Lee, A. J., NADPH-dependent metabolism of 17b-estradiol and estrone to polar and nonpolar metabolites by human tissues and cytochrome P450 isoforms. *Steroids* **2005,** *70*, 225–244.

226.  Martucci, C. P.; Fishman, J., P450 enzymes of estrogen metabolism. *Pharmacol. Ther.* **1993,** *57*, 237–257.

227.  Tsuchiya, Y.; Nakajima, M.; Yokoi, T., Cytochrome P450-mediated metabolism of estrogens and its regulation in human. *Cancer Lett.* **2005,** *227*, 115–124.

228.  Stocco, C., Tissue physiology and pathology of aromatase. *Steroids* **2012,** *77*, 27–35.

# PAPER I

*Article*

# Novel Microcystins from *Planktothrix prolifica* NIVA-CYA 544 Identified by LC-MS/MS, Functional Group Derivatization and ^{15}N-labeling

**Vittoria Mallia [1,2,\*], Silvio Uhlig [1] , Cheryl Rafuse [3], Juris Meija [4] and Christopher O. Miles [3]**

[1] Toxinology Research Group, Norwegian Veterinary Institute, Ullevålsveien 68, N-0454 Oslo, Norway; silvio.uhlig@vetinst.no

[2] Department of Chemistry, University of Oslo, P.O. Box 1033, N-0315 Oslo, Norway

[3] National Research Council, 1411 Oxford Street, Halifax, NS B3H 3Z1, Canada; cheryl.rafuse@nrc-cnrc.gc.ca (C.R.); christopher.miles@nrc-cnrc.gc.ca (C.O.M.)

[4] National Research Council, 1200 Montreal Road, Ottawa, ON K1A 0R6, Canada; juris.meija@nrc-cnrc.gc.ca

**\*** Correspondence: vittoria.mallia@vetinst.no or vitt-87@hotmail.it; Tel.: +47-23216000

**Abstract:** Microcystins are cyclic heptapeptides from cyanobacteria that are potent inhibitors of protein phosphatases and are toxic to animals and humans. At present, more than 250 microcystin variants are known, with variants reported for all seven peptide moieties. While D-glutamic acid (D-Glu) is highly-conserved at position-6 of microcystins, there has been only one report of a cyanobacterium (*Anabaena*) producing microcystins containing L-Glu at the variable 2- and 4-positions. Liquid chromatography–mass spectrometry analyses of extracts from *Planktothrix prolifica* NIVA-CYA 544 led to the tentative identification of two new Glu-containing microcystins, [D-Asp[3]]MC-ER (**12**) and [D-Asp[3]]MC-EE (**13**). Structure determination was aided by thiol derivatization of the Mdha[7]-moiety and esterification of the carboxylic acid groups, while ^{15}N-labeling of the culture and isotopic profile analysis assisted the determination of the number of nitrogen atoms present and the elemental composition of molecular and product-ions. The major microcystin analog in the extracts was [D-Asp[3]]MC-RR (**1**). A microcystin with an unprecedented high-molecular-mass (2116 Da) was also detected and tentatively identified as a sulfide-linked conjugate of [D-Asp[3]]MC-RR (**15**) by LC–HRMS/MS and sulfide oxidation, together with its sulfoxide (**16**) produced via autoxidation. Low levels of [D-Asp[3]]MC-RW (**14**), [D-Asp[3]]MC-LR (**4**), [D-Asp[3],Mser[7]]MC-RR (**11**), [D-Asp[3]]MC-RY (**17**), [D-Asp[3]]MC-RF (**18**), [D-Asp[3]]MC-RR–glutathione conjugate (**19**), and [D-Asp[3]]MC-RCit (**20**), the first reported microcystin containing citrulline, were also identified in the extract, and an oxidized derivative of [D-Asp[3]]MC-RR and the cysteine conjugate of **1** were partially characterized.

**Keywords:** cyanotoxin; microcystin; hepatotoxin; mass spectrometry; *Planktothrix*

## 1. Introduction

Microcystins (MCs) (Figure 1) are non-ribosomal heptapeptides [1] produced by cyanobacteria, frequently occurring in eutrophic freshwater ecosystems worldwide [2,3]. MCs are potent hepatotoxins implicated in the poisoning of diverse birds, fish, and mammals, including sheep, dogs, cattle, sea otters, and humans [4,5], and one incident with human fatalities has been reported [6,7]. Inhibition of protein phosphatase-1 and -2A (PP1 and PP2A) is believed to be the principal mechanism of toxicity of MCs [8,9]. Some studies show that MCs can also modulate PP activity by regulating their expression [10]. Oxidative stress may also be an important additional biochemical mechanism of MC toxicity in both mammalian and plant cells [11,12]. Recent studies have implicated MCs as reproductive toxins, likely due to endocrine-disrupting effects [10]. They are among the most common cyanotoxins

worldwide and are the most studied. They are synthesized intracellularly by several cyanobacterial genera including *Microcystis* and *Planktothrix* spp., and then released to water bodies via cell lysis following cell death and/or physical stress [2,13–15].



Mdha[7]/Dhb[7] *m/z* 375.1915
Dha[7]  *m/z* 361.1758
Mser[7]  *m/z* 393.2020

*m/z* 128.0353

*m/z* 135.0804

Adda

Microcystin skeleton

Variants at position-7

| R[2],R[3] | Abbrev. | X | Abbrev. |
|---|---|---|---|
| Me,H | Mdha | OH | Mser |
| H,H | Dha | SR | Conj. |
| H,Me | Dhb | | |

| | | ② | ④ | ⑦ | R[1] | +z | [M+zH][z+] *m/z* | -z | [M−zH][z−] *m/z* |
|---|---|---|---|---|---|---|---|---|---|
| **1** | [D-Asp³]MC-RR | Arg | Arg | Mdha | H | 2 | 512.7824 | 1 | 1022.5429 |
| **2** | MC-RR | Arg | Arg | Mdha | Me | 2 | 519.7902 | 1 | 1036.5585 |
| **3** | MC-YR | Tyr | Arg | Mdha | Me | 1 | 1045.5353 | 1 | 1043.5208 |
| **4** | [D-Asp³]MC-LR | Leu | Arg | Mdha | H | 1 | 981.5404 | 1 | 979.5258 |
| **5** | [Dha⁷]MC-LR | Leu | Arg | Dha | Me | 1 | 981.5404 | 1 | 979.5258 |
| **6** | MC-LR | Leu | Arg | Mdha | Me | 1 | 995.5560 | 1 | 993.5415 |
| **7** | MC-LA | Leu | Ala | Mdha | Me | 1 | 910.4920 | 1 | 908.4775 |
| **8** | MC-LY | Leu | Tyr | Mdha | Me | 1 | 1002.5183 | 1 | 1000.5037 |
| **9** | MC-LW | Leu | Trp | Mdha | Me | 1 | 1025.5342 | 1 | 1023.5197 |
| **10** | MC-LF | Leu | Phe | Mdha | Me | 1 | 986.5233 | 1 | 984.5088 |
| **11** | [D-Asp³,Mser⁷]MC-RR | Arg | Arg | Mser | H | 2 | 521.7876 | 1 | 1040.5535 |
| **12** | [D-Asp³]MC-ER | Glu | Arg | Mdha | H | 1 | 997.4989 | 1 | 995.4844 |
| **13** | [D-Asp³]MC-EE | Glu | Glu | Mdha | H | 1 | 970.4404 | 1 | 968.4259 |
| **14** | [D-Asp³]MC-RW | Arg | Trp | Mdha | H | 1 | 1054.5356 | 1 | 1052.5211 |
| **15** | Sulfide conjugate of **1** | Arg | Arg | Conj.(S) | H | 2 | 1059.0088 | 2 | 1056.9950 |
| **16** | Sulfoxide of **15** | Arg | Arg | Conj.(SO) | H | 2 | 1067.0060 | 2 | 1064.9919 |
| **17** | [D-Asp³]MC-RY | Arg | Tyr | Mdha | H | 1 | 1031.5197 | 1 | 1029.5051 |
| **18** | [D-Asp³]MC-RF | Arg | Phe | Mdha | H | 1 | 1015.5247 | 1 | 1013.5102 |
| **19** | GSH conjugate of **1** | Arg | Arg | GSH conj. | H | 2 | 666.3243 | 1 | 1329.6267 |
| **20** | [D-Asp³]MC-RCit | Arg | Cit | Mdha | H | 1 | 1025.5415 | 1 | 1023.5269 |
| **21** | [D-Asp³]MC-LY | Leu | Tyr | Mdha | H | 1 | 988.5026 | 1 | 986.4881 |
| **22** | [D-Asp³]MC-LF | Leu | Phe | Mdha | H | 1 | 972.5077 | 1 | 970.4931 |
| **23** | [D-Asp³,Dhb⁷]MC-RR | Arg | Arg | Dhb | H | 2 | 512.7824 | 1 | 1022.5429 |

**Figure 1.** Structures of microcystins (MCs) mentioned in the abstract and text. Values for *m/z* are exact masses except for **15** and **16**, for which definitive atomic compositions have not yet been established. The origin of the characteristic fragments from Adda⁵ and Glu⁶ (in positive and negative ionization modes, respectively) are also shown. The stereochemistries of **11–16** and **20** are assumed, based on biosynthetic considerations, and amino acid numbering is shown inside the circles. An oxidized derivative of **1** and a cysteine conjugate of **1** was also tentatively identified in NIVA-CYA 544 extracts.

Currently, more than 250 MC variants have been reported [16]. The increasing number of congeners, and the complexity of the sample matrix in environmental samples from mixed cyanobacterial blooms, complicates the detection and identification of MCs [17]. The World Health Organization recommends a provisional guideline value of 1 µg/L for MC-LR, the most studied MC congener, in drinking water and a chronic tolerable daily intake (TDI) of 0.04 µg/kg body mass per day for humans [18]. However, the vast majority of the congeners cannot be monitored in a single targeted LC–MS/MS method (so usually only the most common MCs are targeted), nor are their biological effects well understood [19]. Since the structure of MC congeners influences their toxicities [20], reliable identification of all major MC variants produced by individual cyanobacterial strains or in algal blooms is therefore needed for effective risk assessment and freshwater management [21].

MCs have molecular masses of around 1 kDa and share a general cyclic structure composed of seven D- and L-amino acids, including uncommon amino acids such as 3*S*-amino-9*S*-methoxy-2*S*,6,8*S*-trimethyl-10-phenyldeca-4*E*,6*E*-dienoic acid (Adda), iso-linked D-β-methylaspartic acid (D-Masp) and *N*-methyldehydroalanine (Mdha) (Figure 1). The presence of the Adda residue is crucial for the toxicity of MC molecules with both Adda[5] and γ-linked D-Glu[6] being particularly important for binding to the protein phosphatase enzyme [22,23]. The common amino acid sequence in MCs is cyclo(D-Ala[1]-X[2]- D-Masp[3]-Z[4]-Adda[5]-γ-D-Glu[6]-Mdha[7]) (Figure 1), where X and Z are variable L-amino acids. Other frequently encountered variations stem from demethylation or methylation at positions-3 (i.e., D-Asp instead of D-Masp) or -7 (e.g., dehydrobutyrine (Dhb) or dehydroalanine (Dha) instead of Mdha) [21]. In other cases, the substitution of D-Ala[1] by D-Leu or D-Ser, and methyl esterification at D-Glu[6] (to form D-Glu(OMe)[6]) have also been observed [24], although such methyl esters appear to be artefactual [25,26]. These structural variations can have a major impact on the physical properties of MCs, as well as on their toxicity and fate during algal bloom events [22]. In addition to MCs, cyanobacteria can also produce other cyanotoxins, other oligopeptides, can contain lipopolysaccharides in their cell walls and may produce other metabolites with various bioactivities and potential applications [16,27,28].

As a prelude to investigations into the components responsible for the reported reproductive toxicity of cyanobacteria [10,29,30], we screened a range of cultures of *Microcystis* and *Planktothrix* strains for MCs by LC–MS because the toxicity of MCs might influence results of cell-based bioassays. Several previously unreported putative MC congeners were detected in *P. prolifica* strain NIVA-CYA 544, isolated from Lake Steinsfjorden, Buskerud, Norway, in 2004. Here we report detailed analysis using LC–MS and MS/MS, chemical reactivity tests, and ^{15}N-labeling, leading to the identification of a range of novel and previously known MCs in this culture.

## 2. Results and Discussion

### 2.1. MCs Profiling of P. prolifica NIVA-CYA 544

Prior to the profiling of the *P. prolifica* strain, LC–HRMS (method A) and LC–ITMS/MS (method C) were tested and optimized using a set of nine MC standards as well as a nodularin-R standard. Extracts from the culture were then examined by LC–ITMS/MS and LC–HRMS/MS methods in positive and negative ionization modes, and the chromatograms examined for characteristic precursor- and product-ions (including those shown in Figure 1) corresponding to known MCs. To detect possible MC congeners in the *P. prolifica* extract, we also specifically looked for the Adda[5]-derived product-ion at *m/z* 135.0804 (Figure 1) in the positive mode HRMS/MS spectra, as well as the *m/z* 128.0353 (or 129.0324 in ^{15}N-labeled MCs) product-ion (Figure 1), derived from the D-Glu[6] moiety of MCs, in negative mode HRMS/MS spectra. The positive mode HRMS/MS spectra were also examined for a range of other characteristic product-ions of MCs. All of the candidate MCs displayed product-ions indicative of the presence of Adda[5] and D-Glu[6] in their HRMS/MS mass spectra. In addition, derivatization with mercaptoethanol was used together with LC–HRMS to identify candidate peaks of thiol-reactive compounds potentially containing Dha[7]- or Mdha[7]-groups [31,32], and identified 8 of the 12 candidate MC peaks (Figure 2, Table 1) as potentially containing Dha[7] or Mdha[7] moieties. Together, these screening approaches target three of the MC amino acid residues in closest contact with the binding site of PPs, two of which (Adda[5] and D-Glu[6]) appear to be required for inhibition of PPs by MCs [33]. The resulting candidate peaks from this screening were then matched with possible precursor ions with the same retention time and an appropriate *m/z* in the LC–HRMS chromatograms (Figure 2), and more concentrated extracts were studied by targeted LC–HRMS/MS analysis, chemical reactivity, and ^{15}N-labeling. Extracts were also treated with sodium periodate to identify compounds containing sulfide linkages via oxidation to their sulfoxides [25,33,34] with the reactions monitored by LC–HRMS/MS, and esterified with diazomethane to count the number of reactive carboxylic acid groups present in each MC, with the reactions monitored by LC–HRMS/MS.

**Table 1.** Properties of MCs identified in *P. prolifica* NIVA-CYA 544 (LC–HRMS method A unless specified).

| | Microcystin | Confidence | Neutral Formula [a] | No. N [b] | $t_R$ (min) [c] | Positive [d] m/z | +z | Δm (ppm) | Thiol-Reactive | No. $CO_2H$ [e] |
|---|---|---|---|---|---|---|---|---|---|---|
| 1 | [D-Asp³]MC-RR | confirmed | $C_{48}H_{73}N_{13}O_{12}$ | 13 | 2.81 | 512.7815 | 2 | −1.6 | yes | 2 |
| 4 | [D-Asp³]MC-LR | confirmed | $C_{48}H_{72}N_{10}O_{12}$ | 10 | 5.72 | 981.5419 | 1 | +1.6 | yes | 2 |
| 11 | [D-Asp³,Mser⁷]MC-RR | probable | $C_{48}H_{75}N_{13}O_{13}$ | 13 | 2.59 | 521.7879 | 2 | +0.5 | no | ND |
| 12 | [D-Asp³]MC-ER | probable | $C_{47}H_{68}N_{10}O_{14}$ | 10 | 3.63 | 997.4988 | 1 | −0.2 | yes | 3 |
| 13 | [D-Asp³]MC-EE | probable | $C_{46}H_{63}N_{7}O_{16}$ | 7 | 4.99 | 970.4413 | 1 | +0.9 | yes | 4 |
| 14 | [D-Asp³]MC-RW | probable | $C_{53}H_{71}N_{11}O_{12}$ | 11 | 10.01 | 1054.5387 | 1 | +2.9 | yes | ND |
| 15 | Sulfide conjugate of 1 | tentative | $C_{93}H_{145}N_{21}O_{33}S$ | 21 | 9.85 [f] | 1059.0076 | 2 | −1.3 | no | ND |
| 16 | 15-sulfoxide | tentative | $C_{93}H_{145}N_{21}O_{34}S$ | 21 | 6.50 [g] | 1067.0052 | 2 | −1.2 | no | ND |
| 17 | [D-Asp³]MC-RY | probable | $C_{51}H_{70}N_{10}O_{13}$ | 10 | 7.16 | 1031.5204 | 1 | +0.7 | yes | ND |
| 18 | [D-Asp³]MC-RF | probable | $C_{51}H_{70}N_{10}O_{12}$ | 10 | 9.94 | 1015.5246 | 1 | −0.2 | yes | ND |
| 19 | GSH-conjugate of 1 | confirmed | $C_{58}H_{90}N_{16}O_{18}S$ | 16 | 2.05 | 666.3251 | 2 | +1.3 | no | ND |
| 20 | [D-Asp³]MC-RCit | probable | $C_{48}H_{72}N_{12}O_{13}$ | 12 | 3.44 | 1025.5431 | 1 | +1.6 | yes | ND |

[a] Except for **15** and **16**, only one single viable formula was obtained for each compound via analysis of its isotope patterns obtained from LC–HRMS (method B) in both negative and positive ionization modes using the National Research Council of Canada (NRC) Molecular Formula Calculator. See Figures S40–S57. [b] Number of nitrogen atoms, as measured from ¹⁵N-labeled culture (LC–HRMS method B). [c] Retention times of standards (min): [D-Asp³]MC-RR (**1**), 2.82; MC-RR (**2**), 3.12; MC-YR (**3**), 5.22; [D-Asp³]MC-LR (**4**), 5.71; [Dha⁷]MC-LR (**5**), 4.67 (method C); MC-LR (**6**), 5.84; MC-LA (**7**), 9.35; MC-LY (**8**), 10.65; MC-LW (**9**), 13.83; MC-LF (**10**), 13.91; [D-Asp³Dhb⁷]MC-RR (**23**), 2.97 (Table S1). [d] Measured *m/z* for [M + H]⁺ or [M + 2H]²⁺. [e] Measured by esterification with $CH_2N_2$. ND = not determined. [f] Minor isomer also present at 9.46 min. [g] Minor isomer also present at 5.85 min.
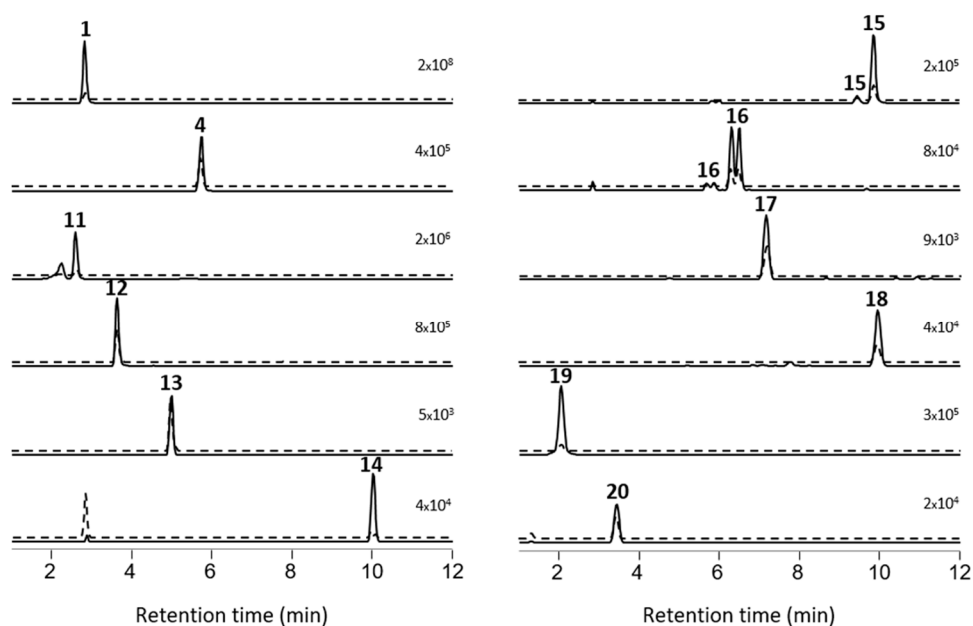
**Figure 2.** Extracted ion LC–HRMS chromatograms (± 5 ppm) of MC congeners obtained with LC-HRMS/MS method A from a concentrated extract of *P. prolifica* NIVA-CYA 544 (from top left): [D-Asp$^3$]MC-RR (**1**), [D-Asp$^3$]MC-LR (**4**), [D-Asp$^3$,Mser$^7$]MC-RR (**11**), [D-Asp$^3$]MC-ER (**12**), [D-Asp$^3$]MC-EE (**13**), [D-Asp$^3$]MC-RW (**14**), sulfide-conjugate of **1** (**15**), sulfoxide of **15** (**16**), [D-Asp$^3$]MC-RY (**17**), [D-Asp$^3$]MC-RF (**18**), GSH-conjugate of **1** (**19**), and [D-Asp$^3$]MC-RCit (**20**). Solid lines are chromatograms from positive ionization ([M + H]$^+$ or [M + 2H]$^{2+}$), while dashed lines are from negative ionization ([M − H]$^-$ or [M − 2H]$^{2-}$). Each pair of the positive and negative chromatogram is on the same fixed intensity scale (number in the top right-hand corner of each chromatogram).

## 2.2. Isotopic Enrichment Calculations

The culture was maintained for 13 months in $^{15}$N-labeled medium and analyzed alongside unlabeled culture, allowing the number of N-atoms in the molecular- and product-ions to be determined [35] using LC–HRMS/MS method B. Isotopic composition of the constituent elements dictates the shape of isotope patterns observed in mass spectrometry. A molecule with elemental formula $C_cH_hN_nO_o$, for example, will contain $(1 + c)(1 + h)(1 + n)(1 + o)(2 + o)/2$ distinct combinations of ions (isotopologues). The abundance (proportion) of all of these isotopologues is governed in accordance with the basic rules of probability. For example, with the lightest of the ions having an abundance of $x(^{12}C)^c x(^1H)^h x(^{14}N)^n x(^{16}O)^o$ where $x(^{12}C)$ is the abundance (proportion) of carbon-12 atoms among all carbon atoms and so on. Thus, knowledge of the molecular formula and the isotopic composition of all makeup elements enables us to establish the expected ('theoretical') isotope patterns of molecules. The full isotopic pattern of the MC [D-Asp$^3$]MC-RR (**1**) ($C_{48}H_{73}N_{13}O_{12}$) contains nearly 5 million components, which necessitates computationally efficient algorithms to be used in practical calculations. When the isotopic composition of nitrogen (the abundance of nitrogen-15, $x(^{15}N)$) is unknown in the analyzed toxins, the theoretical isotopic patterns can be viewed as a function of $x(^{15}N)$ and both the experimental and theoretical patterns are compared for each plausible value of $x(^{15}N)$ until the best fit is obtained. The similarity between the experimental and theoretical spectra is evaluated by comparing the ion intensities at all unique masses. For this, all ions in theoretical spectra are aggregated similar to the data collection process of the mass spectrometer. A good match between the two spectra will exhibit a linear regression, $I_{\text{theor}}(M_i) = bI_{\text{exp}}(M_i)$, and the isotopic enrichment of nitrogen corresponding to the best match between the two spectra was found by means of the correlation coefficient of the above regression as described by MacCoss et al. [36]. Although lighter ions tend to have higher ion transmission efficiencies in mass spectrometers [37], leading to slightly biased isotopic patterns, an effect known as the instrumental mass fractionation, this has little effect

on our calculations. Moreover, the fitness-for-purpose of our approach was established by subjecting our calculation routines to a series of MCs of known identity (molecular formula). The calculations were performed in R using a web-based interface and an example is shown for [D-Asp³]MC-RR (**1**) (Figure 3).
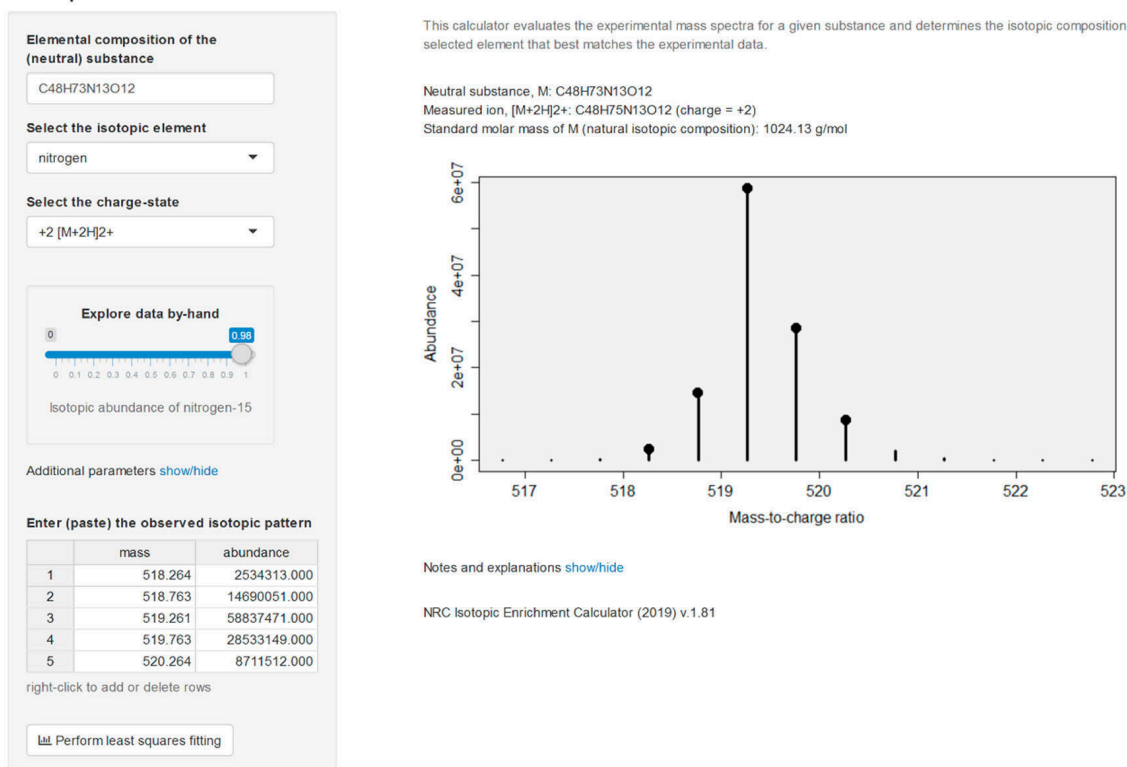


**Figure 3.** Screenshot of the NRC Isotopic Enrichment Calculator (v.1.81) as applied to the positive ionization electrospray mass spectrum for [D-Asp³]MC-RR (**1**) grown in a medium having 98% of nitrogen as nitrogen-15. Data input is in the left panel with output on the right-hand panel including the isotopic abundance with the best fit to the observed *m/z* and intensities, together with a representation of the mass spectrum (circles: observed *m/z* and intensities, vertical bars: calculated values given the molecular formula, charge-state, and isotopic composition of nitrogen).

*2.3. Elemental Composition Elucidation*

The cultures were grown in two distinct media, one having normal isotopic composition and the other enriched in nitrogen-15. Crude extracts from both cultures were then mixed and analyzed by LC–HRMS/MS method B, which provided a set of two mass spectra obtained under identical conditions for each toxin. The molecular formulae were elucidated from this set of data first, by performing mass decomposition of each observed signal using efficient algorithms as implemented in the R packages ecipex [38] and Rdisop [39,40] while taking into account the isotopic enrichment of nitrogen-15 in the MCs as determined from the analysis of **1** present in the same cultures. From the set of obtained matches we retained only the molecular formulae common to all mass signals, and further eliminated those formulae that violated the Senior rules of molecular composition [41]. The theoretical isotopic pattern was generated for each candidate match and formulae whose theoretical isotopic patterns deviated significantly from the observed isotopic patterns were discarded. Last, the two resulting sets of candidates (one from the natural growth medium and one from nitrogen-15 enriched growth medium) were intersected and common matches returned. The entire procedure was then repeated for data acquired under different ionization modes, so that all the data available (e.g., [M + H]⁺, [M + 2H]²⁺, and [M − H]⁻) were used together to constrain the set of molecular formula candidates for

each compound (e.g., Figure 4). The calculations were performed in R using a web-based interface, and a graphical representation of the output is shown for [D-Asp$^3$]MC-RCit (**20**) (Figure 4). In this case, the analysis of *m/z* values of the observed signals from the neutral molecule leads to ca. 2000 candidate formulae which are reduced to ca. 200 by applying Senior rules. The isotopic profile analysis reduces the number of molecular formulae candidates to ca. 100 and then to 5 remaining matches after cross-referencing them with expected isotopic patterns of isotopically labeled analogs.
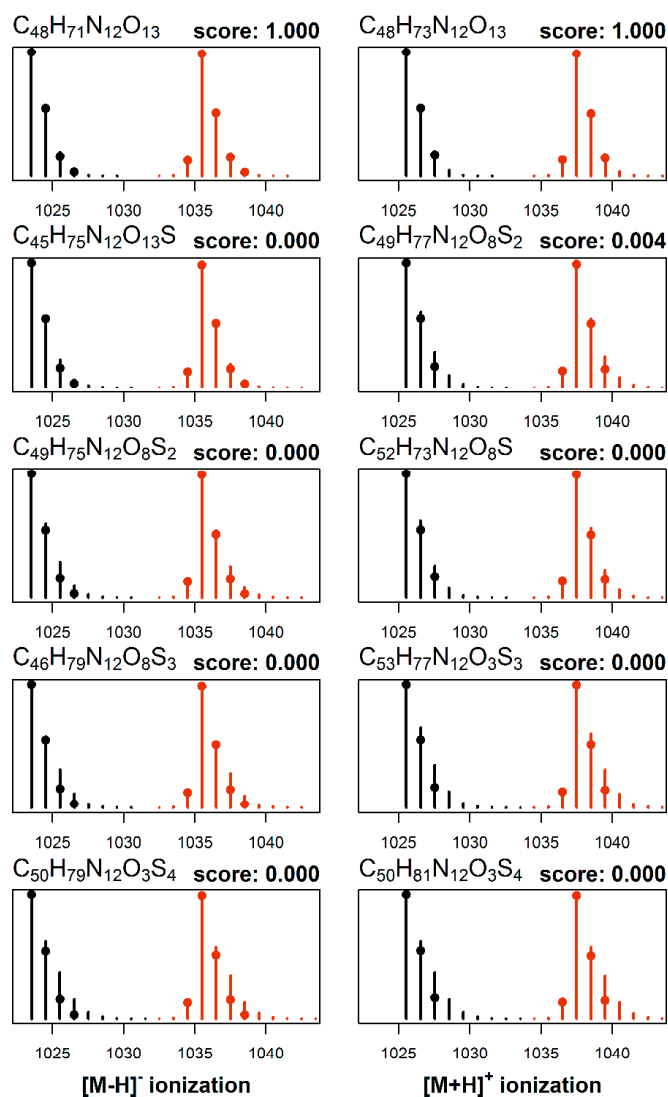


**Figure 4.** Elucidation of the elemental formula from HRMS of an MC using the NRC Molecular Formula Calculator. This example shows normalized mass spectra ([M − H]$^-$ on the left, [M + H]$^+$ on the right) of **20** from a culture cultivated in normal growth medium and in medium whose isotopic composition of nitrogen was altered to 98% nitrogen-15. Each MS measurement mode produced mass spectra (*m/z* and intensities shown with circles) from natural (black) and nitrogen-15 enriched (red) growth media, which were subjected to molecular formula elucidation calculations. Assuming up to 3 ppm mass measurement errors, only five elemental formulae satisfied all constraints (higher scoring formulae shown from top to bottom), and the resulting matches along with their match-scores (from 0.000–1.000) are shown (calculated mass spectra shown as black or red bars). Only one plausible candidate emerged with a high score for both [M − H]$^-$ and [M + H]$^+$ (C$_{48}$H$_{72}$N$_{12}$O$_{13}$), which is the elemental formula for [D-Asp$^3$]MC-RCit (**20**). The remaining candidates showed very low scores for both [M − H]$^-$ and [M + H]$^+$, indicating a poor match to the experimentally observed HRMS spectra, and that they are therefore not viable elemental formulae for **20**.

## 2.4. Identification of MC Congeners

Individual compounds were tentatively identified as MCs based on their MS/MS spectra, retention times relative to authentic standards and thiol reactivity. Tentative structures were then assigned based on the molecular formulae established from LC–HRMS, LC–ITMS/MS, LC–HRMS/MS and ^{15}N-labeling experiments, as well as reactivity towards thiols, diazomethane, and periodate. It should be noted that the stereochemistry of the compounds cannot be determined using MS data alone, and the stereochemistries of novel compounds **12–16** and **20** were assumed to be identical to those of known MCs based on biosynthetic considerations (MCs are produced by MC synthetases, and all MCs whose structures have been fully elucidated possess the amino acid stereochemistry shown in Figure 1).

[D-Asp[3]]MC-RR (**1**): In LC–HRMS, the most abundant compound afforded ions with *m/z* 512.7815 (Table 1) and 1024.5549 (*z* = 2 and 1, respectively) in positive, and *m/z* 1022.5437 in negative ion modes, and contained 13 N atoms by ^{15}N-labeling experiments, corresponding to an elemental composition of $C_{48}H_{73}N_{13}O_{12}$ for the neutral molecule (Table 1, Figure 1). This, as well as its short retention time and the predominance of its double-charged molecular ion in positive ion mode, was indicative of a desmethylated MC-RR congener. In the initial studies, **1** from NIVA-CYA 544 unexpectedly showed a small but consistent difference in retention time compared to a standard of [D-Asp[3]]MC-RR using method A (Figure S1), even though the two compounds gave essentially identical LC–HRMS/MS product-ion spectra. However, comparison of the reactivity of these compounds with mercaptoethanol and LC–HRMS/MS characteristics with reference materials of [D-Asp[3]]MC-RR (**1**) and [D-Asp[3],Dhb[7]]MC-RR (**23**) from NRC, showed that **1** from NIVA-CYA 544 possessed identical retention time, MS and MS/MS spectra and rapid thiol reactivity as **1** from NRC, establishing its identity as **1**. In contrast, the initially-used commercial standard of [D-Asp[3]]MC-RR did not react detectably with mercaptoethanol, characteristic of the presence of a Dhb[7]- or Mdhb[7]-containing MC [31], and its retention time, MS, MS/MS spectra and thiol-reactivity characteristics were identical to those of the [D-Asp[3],Dhb[7]]MC-RR (**23**) reference material from NRC. Product-ions from higher-energy collisional dissociation (HCD) of **1** in positive ion mode at *m/z* 375.1901 ($C_{20}H_{27}O_5N_2^+$, from Adda[5]–D-Glu[6]–Mdha[7] minus $C_9H_{10}O$, Δ*m* = −3.6 ppm, Figure 1) and 426.2077 ($C_{17}H_{28}O_6N_7^+$, from Mdha[7]–D-Ala[1]–Arg[2]–D-Asp[3], Δ*m* = −4.4 ppm) confirmed the site of demethylation as being on position-3 rather than position-7 (i.e., D-Asp[3] rather than Dha[7]). This compound has previously been identified as the predominant MC in this strain [31]. Treatment of an extract of NIVA-CYA 544 with diazomethane resulted in complete esterification of the D-Glu[6] carboxylic acid group of **1**, but no esterification of the D-Asp[3] residue was detected. The D-Asp[3] residue appears to be relatively unreactive to acid-catalyzed esterification with methanol since D-Glu(OMe)[6] but not D-Asp[3] esters have been reported as esterification artifacts thus far [25,26], and the (trimethylsilyl)diazomethane-promoted methyl esterification of MCs was recently shown to display the same selectivity [42]. With the identity of **1** as the most abundant MC in NIVA-CYA 544 firmly established, analysis of the profile of its molecular ion isotope envelope was used to estimate the level of nitrogen-15 incorporation into MCs at *x*(^{15}N) = 0.98 mol/mol (Figure 3) in NIVA-CYA 544 after extended maintenance of the culture in nitrogen-15 enriched medium.

[D-Asp[3],Mser[7]]MC-RR (**11**): The peak of [D-Asp[3]]MC-RR (**1**) was accompanied by an earlier eluting, minor peak (approximately 1% relative peak area) (Figure 2). In LC–HRMS, the compound afforded ions with *m/z* 521.7879 and 1042.5678 (*z* = 2 and 1, respectively) in positive, and *m/z* 1040.5567 in negative ion modes, and contained 13 N atoms by ^{15}N-labeling, and had an elemental composition of $C_{48}H_{75}N_{13}O_{13}$ for the neutral molecule (Table 1). The mass difference was equivalent to addition of $H_2O$ to **1** (Table 1), and the compound afforded almost exclusively double-charged ions in positive ion mode, suggesting it to be a desmethylated congener of [Mser[7]]MC-RR (**11**). Furthermore, **11** did not react with mercaptoethanol, indicating that it did not contain an electrophilic double bond such as is present in the Dha[7] or Mdha[7] moieties found in most MCs [31,32]. In addition, characteristic product-ions at *m/z* 393.2003 ($C_{20}H_{29}O_6N_2^+$, from Adda[5]–D-Glu[6]–Mser[7] minus $C_9H_{10}O$, Δ*m* = −4.4 ppm, Figure 1) and *m/z* 444.2190 ($C_{17}H_{30}O_7N_7^+$, from Mser[7]–Ala[1]–Arg[2]–Asp[3], Δ*m* = −2.5 ppm) indicated the presence of D-Asp[3] and Mser[7] moieties, confirming its identity as [D-Asp[3],Mser[7]]MC-RR (**11**).

[D-Asp$^3$]MC-RR conjugate (**15**): One of the more abundant of the minor MCs in terms of peak area in the LC–HRMS chromatograms (Figure 2) of fresh extracts afforded exclusively double-charged ions in positive and negative ion modes with *m/z* 1059.0076 and *m/z* 1056.9981, respectively (Table 1, Figure 2), which showed weak product-ions at *m/z* 135.0804 and 128.0351 in the positive and negative ion LC–HRMS/MS chromatograms, respectively. These data suggest an MC with a molecular mass of 2116 Da for the corresponding neutral molecule. Furthermore, $^{15}$N-labeling indicated the presence of 21 N atoms in the structure. The compound did not react with mercaptoethanol and was oxidized with periodate to give a product with *m/z* corresponding to addition of one oxygen atom, presumed to be the sulfoxide derivative (see discussion for **16**, below, Table 1, Figure 2, Figure S2). The latter two observations suggest a sulfide linkage at the Mdha moiety, since sulfide-containing MCs are readily oxidized to sulfoxides upon treatment with mild oxidants such as periodate [33] or hydrogen peroxide [25], and the presence of an existing sulfide linkage to a Mdha$^7$/Dha$^7$ would prevent reaction with mercaptoethanol [25,32]. Positive ion LC–HRMS/MS spectra of **15** (and comparison with data from $^{15}$N-labeled **15**) established the presence of product-ions at *m/z* 135.0803 (C$_9$H$_{11}$O$^+$, $\Delta m$ = −1.0 ppm, from Adda$^5$) and 512.7820 (C$_{48}$H$_{75}$O$_{12}$N$_{13}{}^+$, $\Delta m$ = −0.7 ppm, [**1** + 2H]$^{2+}$), 426.2094 (C$_{17}$H$_{28}$O$_6$N$_7{}^+$, $\Delta m$ = −0.4 ppm, from Mdha$^7$–D-Ala$^1$–Arg$^2$–D-Asp$^3$), and 599.3541 (C$_{31}$H$_{47}$O$_6$N$_6{}^+$, $\Delta m$ = −1.8 ppm, from Arg$^4$–Adda$^5$–D-Glu$^6$), indicating that **15** is an unidentified sulfide-linked conjugate of **1** coupled via its Mdha$^7$ moiety and with a molecular mass of 2116 Da. Analysis of the isotope profile for unlabeled and $^{15}$N-labeled **15** suggested a probable elemental composition of C$_{93}$H$_{145}$N$_{21}$O$_{33}$S (Table 1), although C$_{97}$H$_{145}$N$_{21}$O$_{28}$S$_2$ could not be excluded. Assuming conjugation of a sulfide moiety to **1** via its Mdha$^7$-group, the former formula would require the thiol-containing moiety to be C$_{45}$H$_{72}$N$_8$O$_{21}$S (or C$_{49}$H$_{72}$N$_8$O$_{16}$S$_2$ for the latter formula for **15**). While little information is available about the moiety in **15** that is conjugated to **1**, the LC–MS data suggest that it must be relatively non-polar and may contain an acidic functional group and not a strongly basic group, since **15** eluted much later than **1** on a C18 LC column (LC–HRMS method B, Table S1) and was doubly-charged in both positive and negative ion modes.

[D-Asp$^3$]MC-RR conjugate sulfoxide (**16**): A doubly-charged compound showing a major and a minor peak in both positive and negative modes was present at *m/z* 1067.0052 and 1064.9949, respectively, and contained 21 N atoms according to $^{15}$N-labeling, but was not initially recognized as an MC because it was present at low abundance in extracts, had an unusual charge state given its retention time, and it was not affected by thiol derivatization. However, HP-20 extracts contained this compound at levels sufficient for product-ion spectra, and in LC–HRMS/MS **16** gave rise in positive and negative ion modes to product-ions at *m/z* 135.0804 and 128.0351, respectively, that are characteristic of MCs (Figure 1). Furthermore, the mass difference between **16** and **15** corresponded to one oxygen atom, prompting a more detailed examination of **16** and $^{15}$N-labeled **16** by targeted positive ion LC–HRMS/MS. This confirmed the presence of product-ions at *m/z* 135.0804 (C$_9$H$_{11}$O$^+$, $\Delta m$ = −0.3 ppm, from Adda$^5$) and 512.7816 (C$_{48}$H$_{75}$O$_{12}$N$_{13}{}^+$, $\Delta m$ = −1.5 ppm, from [**1** + 2H]$^{2+}$), 426.2088 (C$_{17}$H$_{28}$O$_6$N$_7{}^+$, $\Delta m$ = −1.8 ppm, from Mdha$^7$–Ala$^1$–Arg$^2$–Asp$^3$), and 599.3550 (C$_{31}$H$_{47}$O$_6$N$_6{}^+$, $\Delta m$ = −0.3 ppm, from Arg$^4$–Adda$^5$–D-Glu$^6$), indicating a second conjugate of **1**. At this stage, **15** was tested in a periodate oxidation experiment to ascertain whether it contained a dialkyl sulfide that could be oxidized to a sulfoxide. This experiment showed that **15** was quantitatively converted to **16** by periodate oxidation (Figure S2), establishing **16** as an *S*-oxide of **15**. Both peaks of **16** appeared to be distorted in a way that suggested the presence of a partially resolved pair of diastereomeric sulfoxides. Two product-ions in **16** (*m/z* 404.1629, C$_{20}$H$_{26}$O$_4$N$_3$S$^+$, $\Delta m$ −2.4 ppm, and 243.0795, C$_{10}$H$_{15}$O$_3$N$_2$S$^+$, $\Delta m$ −1.2 ppm) were present at *m/z* values 15.9949 greater than the equivalent product-ions in **15** (*m/z* 388.1681, C$_{20}$H$_{26}$O$_3$N$_3$S$^+$, $\Delta m$ −2.2 ppm, and 227.0845, C$_{10}$H$_{15}$O$_2$N$_2$S$^+$, $\Delta m$ −1.7 ppm) (Figure 5), indicating that these ions contained the sulfide/sulfoxide moiety. Sulfoxide-**16** appears to be an autoxidation product formed through aerial oxidation of **15**, as its concentration relative to **15** increased with time and sample manipulation, and was more abundant in the HP-20 extracts than in simple methanol–water extracts, similar to the situation for Met-containing MCs [34]. Compound-**16** was not affected by the weakly

basic ammonium carbonate buffer (pH ~ 8.6) used for the mercaptoethanol derivatization, unlike the glutathione sulfoxide conjugates of [D-Leu[1]]MC-LR reported by Foss et al. [25], which could indicate that the sulfoxide group in **16** (and, consequently, the sulfide of **15**) might not be involved in the conjugation to the Mdha[7] of **1**.

[D-Asp[3]]MC-RR–glutathione conjugate (**19**): Another predominantly doubly-charged compound, affording positive ions at *m/z* 666.3251 and 1331.6461 for [M + 2H][2+] and [M + H][+], respectively, and negative ions at *m/z* 1329.6289 for [M − H][−], eluted before **11** and was the earliest eluting MC congener identified with certainty in the extract (Figure 2, Table 1). Its calculated elemental composition ($C_{58}H_{90}N_{16}O_{18}S$ for the neutral molecule, Table 1) showed that **19** contained one atom of sulfur and three more nitrogen atoms than **1**. Due to the short retention time and its elemental composition, and that an MC–GSH-conjugate was recently reported in a cyanobacterial bloom [25], we suspected that **19** might be a glutathione conjugate of the major MC congener, **1**. This was verified by reacting a standard of **1** with glutathione and comparing the LC–HRMS characteristics of the products with the culture extract (Figure S15, Figure S39). This appears to be the first report of GSH conjugates of MCs in cyanobacterial culture and suggests that the GSH-derived conjugates identified in a *Microcystis* bloom [25] could have been produced by the cyanobacteria in the bloom without the involvement of other organisms in the water column.
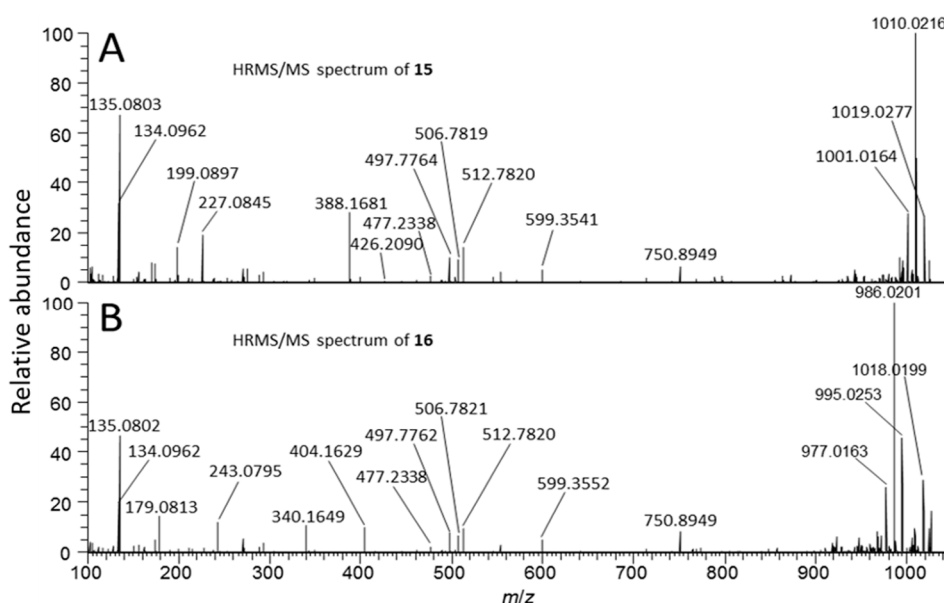


**Figure 5.** Positive mode product-ion spectra ([M + 2H][2+]) of putative [D-Asp[3]]MC-RR conjugate **15** (**A**) and its sulfoxide **16** (**B**) obtained from an extract of NIVA-CYA 544 with LC–HRMS/MS method B.

*[D-Asp[3]]MC-LR (4).* Another MC afforded [M + H][+] and [M − H][−] ions at *m/z* 981.5419 and *m/z* 979.5298 in positive and negative ion modes, respectively (Figure 2, Table 1), while ^{15}N-labeling indicated the presence of 10 N atoms in the structure, and an elemental composition of $C_{48}H_{72}N_{10}O_{12}$ for the neutral molecule (Table 1). This analog has the same elemental composition and eluted with the same retention time as a standard of [D-Asp[3]]MC-LR (**4**). Product-ions at *m/z* 375.1902 (from Adda[5]–D-Glu[6]–Mdha[7] minus $C_9H_{10}O$, Δ*m* = −3.3 ppm, Figure 1), 599.3538 ($C_{31}H_{47}O_6N_6^+$, from Arg[4]–Adda[5]–D-Glu[6], Δ*m* = −2.3 ppm) and 272.1343 ($C_{10}H_{18}O_4N_5^+$, Δ*m* = −3.8 ppm, from D-Asp[3]–Arg[4]) showed that demethylation relative to MC-LR was in position-3 and not in position-7, consistent with **4**, which was previously tentatively identified as a minor MC in this culture [31]. Furthermore, detailed examination of the product-ion spectrum obtained from LC–MS[2] (method C) of **4** (Table 2) showed that it was identical to those reported previously for this compound [32,43,44] and with that of the authentic standard of **4**, and all product-ions containing residue-3 appeared at *m/z* values 14 Da less than the corresponding product-ions of MC-LR (**6**) (Table 2).

**Table 2.** Assignments of observed product-ions and their *m/z* from collision-induced dissociation of [M + H]$^+$ of [D-Asp$^3$]MC-ER (**12**) obtained using LC–ITMS/MS (method C) and comparison to the corresponding product-ions observed for MC-LR (**6**), [Dha$^7$]MC-LR (**5**) and [D-Asp$^3$]MC-LR (**4**).$^a$

| Fragment Ion Assignment | (6) | (5) | (4) | (12) |
|---|---|---|---|---|
| [M + H]$^+$ | 995.6 | 981.5 | 981.5 | 997.5 |
| [M − NH$_3$+ H]$^+$ | 978.6 | 964.5 | 964.5 | 980.5 |
| [M − H$_2$O +H]$^+$ | 977.6 | 963.6 | 963.5 | 979.5 |
| [M − CO + H]$^+$ | 967.6 | 953.6 | 953.6 | 969.5 |
| [M − 48 + H]$^+$ | 946.5 | 932.5 | 932.5 | 948.4 |
| [Arg-Adda-Glu-res$^7$-Ala-X$^2$-NH$_2$ + 2H]$^+$ | 883.6 | 869.6 | 883.5 | 899.5 |
| [Arg-Adda-Glu-res$^7$-Ala-X$^2$ + H]$^+$ | 866.6 | 852.5 | 866.6 | 882.5 |
| [res$^7$-Ala-X$^2$-res$^3$-Arg-Adda + H]$^+$ | 866.6 | 852.5 | 852.5 | 868.5 |
| [M−Addafrag. + H]$^+$ | 861.5 | 847.5 | 847.5 | 863.4 |
| [M−Addafrag. − NH$_3$ + H]$^+$ | 844.5 | 830.4 | 830.4 | 846.4 |
| [Arg-Adda-Glu-res$^7$-Ala- X$^2$-CO + H]$^+$ | 838.6 | 824.6 | 838.6 | 854.5 |
| [Ala-X$^2$-res$^3$-Arg-Adda − Addafrag. + H]$^+$ | 783.5 | 783.5 | 769.6 | 785.4 |
| [Arg-Adda-Glu-res$^7$-Ala + H]$^+$ | 753.5 | 739.5 | 753.5 | 753.5 |
| [res$^3$-Arg-Adda-Glu + H]$^+$ | 728.5 | 728.5 | 714.4 | 714.4 |
| [res$^3$-Arg-Adda-Glu − H$_2$O + H]$^+$ | 710.4 | 710.4 | 696.4 | 696.4 |
| [Arg-Adda-Glu-res$^7$ + H]$^+$ | 682.4 | 668.4 | 682.4 | 696.4 |
| [Glu-res$^7$-Ala-X$^2$-res$^3$-Arg + H]$^+$ | 682.4 | 668.4 | 668.4 | 684.4 |
| [Arg-Adda-Glu + H]$^+$ | 599.4 | 599.4 | 599.4 | 599.4 |
| [Arg-Adda-Glu − NH$_3$ + H]$^+$ | 582.4 | 582.4 | 582.4 | 582.4 |
| [Arg-Adda-Glu − CO + H]$^+$ | 571.4 | 571.4 | 571.4 | 571.4 |
| [res$^7$-Ala-X$^2$-res$^3$-Arg-NH$_2$ + 2H]$^+$ | 570.4 | 556.4 | 556.4 | 572.3 |
| [res$^7$-Ala-X$^2$-res$^3$-Arg + H]$^+$ | 553.4 | 539.4 | 539.4 | 555.3 |
| [Ala-X$^2$-res$^3$-Arg + H]$^+$ | 470.4 | 470.4 | 456.4 | 472.3 |
| [Ala-X$^2$-res$^3$-Arg − NH$_3$ + H]$^+$ | 453.3 | 453.3 | 439.3 | 455.3 |
| [Adda-Glu-res$^7$ − Addafrag. − NH$_3$ + H]$^+$ | 375.3 | 361.2 | 375.3 | 375.3 |
| [res$^3$-Arg-NH$_2$ + H]$^+$ | 303.2 | 303.2 | 289.2 | 289.2 |
| [res$^3$-Arg + H]$^+$ | 285.2 | 285.2 | ND | ND |

$^a$ ND = Not Detected; X$^2$ = Leu (**6**, **5**, **4**) or Glu (**12**); res$^3$ = Masp (**6**, **5**) or Asp (**4**, **12**); res$^7$ = Mdha (**6**, **4**, **12**) or Dha (**5**); Addafrag = C$_9$H$_{10}$O.

[D-Asp$^3$]MC-ER (**12**): An MC that eluted before [D-Asp$^3$]MC-LR (**4**) using LC–MS methods A and B (Table S1), displayed [M + H]$^+$ and [M − H]$^-$ ions at *m/z* 997.4988 and 995.4869 in full-scan positive and negative ion modes, respectively, and contained 10 N atoms by $^{15}$N-labeling, with an elemental composition of C$_{47}$H$_{68}$N$_{10}$O$_{14}$ (Table 1). The elemental composition, retention time, and being singly-charged was consistent with a demethylated MC containing Glu and Arg in the variable 2- and 4-positions (Figure 1). Product-ions at *m/z* 375.1902 (from Adda$^5$–D-Glu$^6$–Mdha$^7$ minus C$_9$H$_{10}$O, Δ*m* = −3.3 ppm, Figure 1), 599.3537 (C$_{31}$H$_{47}$O$_6$N$_6$$^+$, Δ*m* = −2.3 ppm, from Arg$^4$–Adda$^5$–D-Glu$^6$) and 155.0811 (C$_7$H$_{11}$O$_2$N$_2$$^+$, Δ*m* = −3.3 ppm, from Mdha$^7$–D-Ala$^1$) indicated that the compound differed from MC-LR (**6**) only in positions-3 and -4 (Figure 6, Figure S22). A product-ion at *m/z* 272.1342 (C$_{10}$H$_{18}$O$_4$N$_5$$^+$, Δ*m* = −4.4 ppm, from D-Asp$^3$–Arg$^4$) indicated demethylation at position-3, showing that the remaining mass difference was in position-2 and thus that the compound likely contained Glu$^2$ (Figure S23). Consistent with this was the presence of a product-ion at *m/z* 284.1231 (C$_{12}$H$_{18}$O$_5$N$_3$$^+$, Δ*m* = −3.9 ppm, from Mdha$^7$–D-Ala$^1$–Glu$^2$, cf. 268.3365 for Mdha$^7$–D-Ala$^1$–Leu$^2$ for MC-LR (**6**)). In addition, comparison of the product-ion spectrum of **12** with that of [D-Asp$^3$]MC-LR (**4**), obtained by LC–ITMS/MS method C, showed that all product-ions containing residue-4 in **12** were heavier by 16 Da than the corresponding product-ions in **4**, while all other product-ions occurred at identical *m/z* in **12** and **4**, and the expected mass differences to the corresponding product-ions from **5** and **6** were observed (Table 2). The reaction of **12** with diazomethane gave, principally, a dimethyl ester (Figure S38). This establishes the presence of three carboxylic acid groups in **12** (D-Glu$^6$, Glu$^2$, and the unreactive D-Asp$^3$), and thus that the amino acid at position-2 contains a carboxylic acid rather than a

hydroxyketone. Consequently, **12** was determined to be [D-Asp³]MC-ER, although the stereochemistry cannot be established from MS/MS data alone. Congeners of MC-ER have not been reported previously, although EE-type MCs have been reported before, but only as their methyl esters [45].
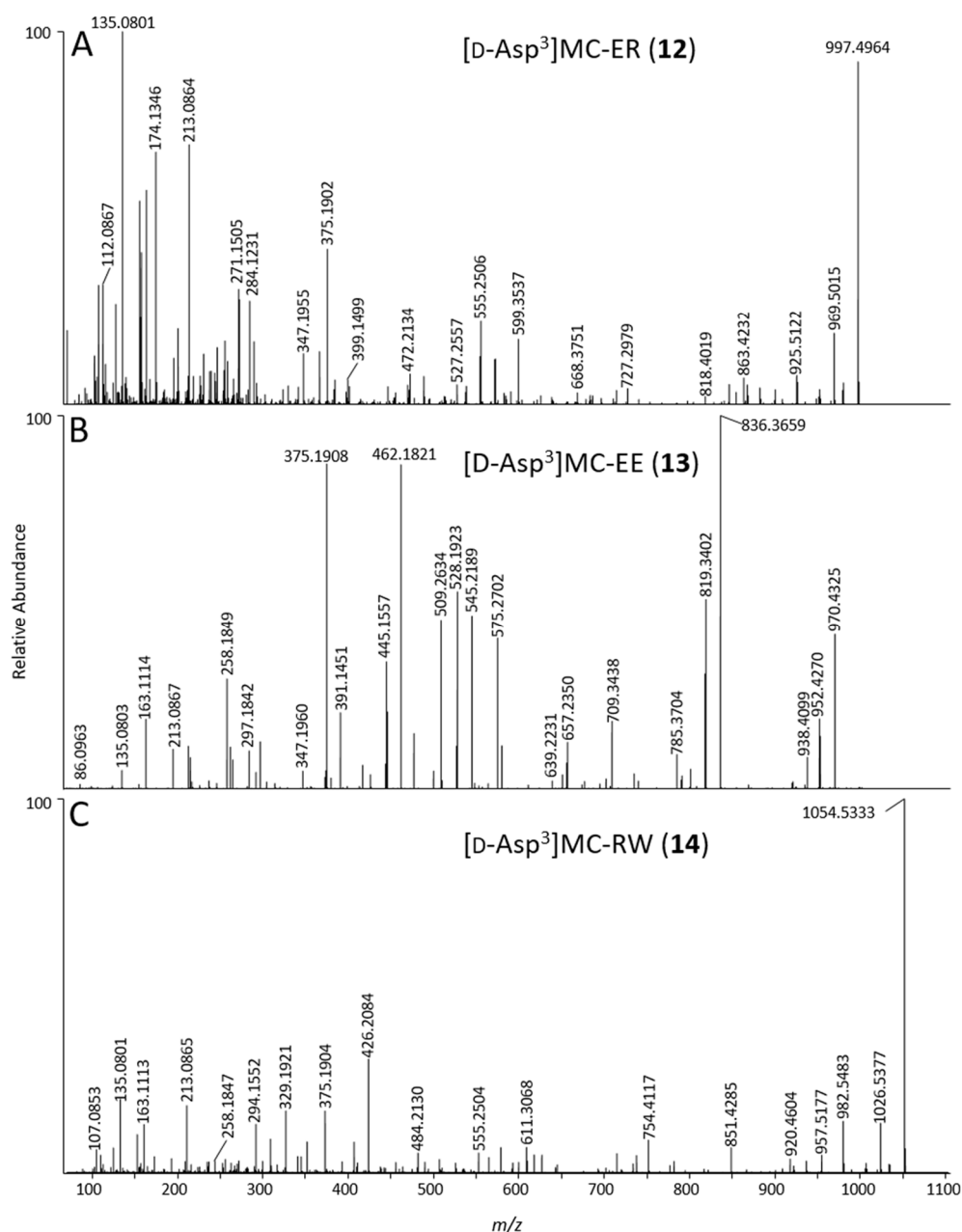


**Figure 6.** Positive mode product-ion spectra of [D-Asp³]MC-ER (**12**) (**A**), [D-Asp³]MC-EE (**13**) (**B**) and [D-Asp³]MC-RW (**14**) (**C**), obtained from an extract of NIVA-CYA 544 using LC–HRMS/MS (method B).

[D-Asp³]MC-EE (**13**): An MC affording $[M + H]^+$ and $[M - H]^-$ ions at *m/z* 970.4413 and 968.4301, and containing 7 N atoms by $^{15}$N-labeling, had a neutral formula of $C_{46}H_{63}N_7O_{16}$ (Table 1), indicating the absence of Arg in the structure despite its retention time is only slightly longer than for the Arg⁴-containing **4** in LC–HRMS method A. However, in LC–HRMS method B (using a C18 column) this compound was the latest-eluting MC in NIVA-CYA 544, eluting 4.6 min later than **4**, but more than 3.5 min earlier than non-Arg-containing MCs such as MC-LA in this system (Table S1). The elemental composition was consistent with [D-Asp³]MC-EE, an MC containing Glu at both the variable 2- and 4-positions (Figure 1). The abundance of [D-Asp³]MC-EE was typically ca. 1:55 relative to

[D-Asp$^3$]MC-ER based on LC–HRMS peak areas, making [D-Asp$^3$]MC-EE difficult to detect even in concentrated culture extracts. Product-ions at *m/z* 375.1906 and 509.2634 (C$_{20}$H$_{27}$O$_5$N$_2$$^+$, and C$_{29}$H$_{37}$O$_6$N$_2$$^+$, $\Delta m$ = −1.7 and −2.4 ppm, both originating from Adda$^5$–D-Glu$^6$–Dha$^7$, see Figure 1), and *m/z* 446.2278 and 580.3006 (C$_{23}$H$_{32}$N$_3$O$_6$$^+$, and C$_{32}$H$_{42}$N$_3$O$_7$$^+$, $\Delta m$ = −2.4 and −1.9 ppm, both originating from Adda$^5$–D-Glu$^6$–Mdha$^7$–D-Ala$^1$) indicated that **13** contained variations only in positions 2–4. Consistent with this, product-ions at *m/z* 262.1026 (C$_9$H$_{16}$O$_6$N$_3$$^+$, $\Delta m$ = −2.1 ppm, from D-Asp$^3$–Glu$^4$), 391.1451 (C$_{14}$H$_{23}$O$_9$N$_4$$^+$, $\Delta m$ = −2.2. ppm, from Glu$^2$–D-Asp$^3$–Glu$^4$), and 575.2702 (C$_{28}$H$_{39}$O$_9$N$_4$$^+$, $\Delta m$ = −1.7 ppm, from Adda$^5$–D-Glu$^6$–Mdha$^7$–D-Ala$^1$–Glu$^2$) were consistent with Glu at positions-2 and -4 and D-Asp$^3$ at position-3 (Figure 6, Figure S28). In addition, examination of the product-ion spectrum of **13** obtained with LC–ITMS/MS method C with published data for [D-Asp$^3$]MC-LY (**21**) and [D-Asp$^3$]MC-LF (**22**) obtained under similar conditions [31], showed only the mass differences that would be expected from replacing residues-2 and -4 of **21** and **22** with Glu (Table 3). Reaction of **13** with diazomethane gave mainly the trimethyl ester (Figure S38), demonstrating the presence of 3 reactive (D-Glu$^6$, Glu$^2$, and Glu$^4$) and one much less reactive (D-Asp$^3$) carboxylic acid groups in **13** and, when taken together with the LC–HRMS/MS data, confirms its identity as [D-Asp$^3$]MC-EE (**13**).

**Table 3.** Assignments of observed product-ions and their *m/z* from collision-induced dissociation of [M + H]$^+$ of [D-Asp$^3$]MC-EE (**13**) and comparison to the corresponding product-ions from [D-Asp$^3$]MC-LY (**21**) and [D-Asp$^3$]MC-LF (**22**). LC–ITMS/MS method C was used for acquisition of the data for **13**, data for **21** and **22** are from Miles et al. [44].[a]

| Fragment Ion Assignment | (21) | (22) | (13) |
|---|---|---|---|
| [M + H]$^+$ | 988 | 972 | 970.4 |
| [M − NH$_3$ + H]$^+$ | 971 | 955 | 953.4 |
| [M − H$_2$O + H]$^+$ | 970 | 954 | 952.5 |
| [M − CO + H]$^+$ | 960 | 944 | 942.6 |
| [M − Addafrag + H]$^+$ | 854 | 838 | 836.4 |
| [M − Addafrag − NH$_3$ + H]$^+$ | 837 | 821 | 819.4 |
| [M − Addafrag − H$_2$O + H]$^+$ | 836 | 820 | 818.5 |
| [Adda-Glu-Mdha-Ala-X$^2$ − NH$_3$+ H]$^+$ | 693 | 693 | 709.3 |
| [M − Adda + H]$^+$ | 675 | 659 | 657.3 |
| [M − Adda − H$_2$O + H]$^+$ | ND | ND | 639.2 |
| [Adda-Glu-Mdha-Ala − NH$_3$ + H]$^+$ | 580 | 580 | 580.3 |
| [Adda-Glu-Mdha-Ala-X$^2$ − Addafrag − NH$_3$+ H]$^+$ | 559 | 559 | 575.2 |
| [Z$^4$-Asp-X$^2$-Ala-Mdha-NH$_2$ + 2H]$^+$ | 563 | 547 | 545.4 |
| [Z$^4$-Asp-X$^2$-Ala-Mdha + H]$^+$ | 546 | 530 | 528.3 |
| [Adda-Glu-Mdha − NH$_3$ + H]$^+$ | 509 | 509 | 509.3 |
| [Z$^4$-Asp-X$^2$-Ala-NH$_2$ + 2H]$^+$ | 480 | 464 | 462.3 |
| [Z$^4$-Asp-X$^2$-Ala + H]$^+$ | 463 | 447 | 445.2 |
| [Z$^4$-Asp-X$^2$ + H]$^+$ | 392 | 376 | 374.3 |
| [Adda-Glu-Mdha − Addafrag − NH$_3$ + H]$^+$ | 375 | 375 | 375.3 |

[a] ND = Not Detected; X$^2$ = Leu (**21**, **22**) or Glu (**13**); Z$^4$ = Tyr (**21**), Phe (**22**) or Glu (**13**); Addafrag = C$_9$H$_{10}$O.

[D-Asp$^3$]MC-RW (**14**): The LC–HRMS and LC–HRMS/MS data revealed a compound that afforded [M + H]$^+$ and [M − H]$^-$ ions with *m/z* 1054.5387 and 1052.5264 in positive and negative ion modes, respectively (Figure 2, Table 1), and $^{15}$N-labeling revealed the presence of 11 N atoms, and an elemental composition for the corresponding neutral molecule of C$_{53}$H$_{71}$N$_{11}$O$_{12}$, consistent with a desmethylated congener of MC-RW or MC-WR (Table 1). Product-ions in positive mode at *m/z* 375.1904 (C$_{20}$H$_{27}$O$_5$N$_2$$^+$, $\Delta m$ = −2.8 ppm, from Adda$^5$–D-Glu$^6$–Mdha$^7$ minus C$_9$H$_{10}$O, Figure 1) and 426.2084 (C$_{17}$H$_{28}$O$_6$N$_7$$^+$, $\Delta m$ = −3.0 ppm, from Mdha$^7$–D-Ala$^1$–Arg$^2$–D-Asp$^3$) confirmed the site of demethylation as being on position-3 rather than position-7 (D-Asp$^3$ rather than Dha$^7$) and, together with the complete absence of a product-ion at *m/z* 599.3552, confirmed the presence of Arg$^2$ rather than Arg$^4$ (Figure 6). Comparison with HRMS/MS data for [D-Asp$^3$]MC-RY [46] revealed other product-ions at 851.4285 (C$_{42}$H$_{59}$O$_{11}$N$_8$$^+$,

$\Delta m = -1.5$ ppm, from Adda[5]–D-Glu[6]–Mdha[7]–D-Ala[1]–Arg[2]–D-Asp[3]) and 302.1125 ($C_{15}H_{16}O_4N_3{}^+$, $\Delta m = -3.4$ ppm, from Asp[3]–Trp[4]) consistent with Trp at position-4, and thus that **14** is [D-Asp[3]]MC-RW. Comparison of the observed product-ions from LC–ITMS/MS of the [D-Asp[3]]MC-RW (**14**) (Figure S12) with literature data for the Arg[2]-containing congeners [D-Asp[3]]MC-RY (**17**) and [D-Asp[3]]MC-RF (**18**) (Table 4) [44] was fully consistent with the proposed structure, with **17** and **18** differing only in the amino acid at position-4 (Tyr and Phe, respectively) from [D-Asp[3]]MC-RW (**14**). Product-ions containing these moieties shifted in relation to mass differences between the three amino acids, while other fragments appeared at the same *m/z* values for all the compounds (Table 4).

**Table 4.** Assignments of observed product-ions and their *m/z* from collision-induced dissociation of [M + H]$^+$ of [D-Asp[3]]MC-RW (**14**) and comparison to the corresponding product-ions from [D-Asp[3]]MC-RY (**17**) and [D-Asp[3]]MC-RF (**18**). LC–MS method C was used for acquisition of the data for **14**, data for **17** and **18** are from Miles et al. [44].[a]

| Fragment Ion Assignment | 17 | 18 | 14 |
|---|---|---|---|
| [M + H]$^+$ | 1031 | 1015 | 1054.8 |
| [M − NH$_3$ + H]$^+$ | 1014 | 998 | 1037.7 |
| [M − H$_2$O + H]$^+$ | 1013 | 997 | 1036.7 |
| [M − CO + H]$^+$ | 1003 | 987 | 1026.7 |
| [Z$^4$-Adda-Glu-Mdha-Ala-Arg − NH$_3$ + H]$^+$ | 916 | 900 | 939.6 |
| [M − Addafrag + H]$^+$ | 897 | 881 | 920.7 |
| [Adda-Glu-Mdha-Ala-Arg-Asp − NH$_3$ + H]$^+$ | 851 | 851 | 851.6 |
| [Ala-Arg-Asp-Z$^4$-Adda + H]$^+$ | 819 | 803 | 842.5 |
| [Adda-Glu-Mdha-Ala-Arg + H]$^+$ | 754 | 754 | 754.6 |
| [Adda-Glu-Mdha-Ala-Arg − H$_2$O + H]$^+$ | 736 | 736 | 736.5 |
| [Adda-Glu-Mdha-Ala-Arg-Asp − Addafrag − NH$_3$ + H]$^+$ | 717 | 717 | 717.5 |
| [Mdha-Ala-Arg-Asp-Z$^4$-NH$_2$ + H]$^+$ | 606 | 590 | 629.5 |
| [Mdha-Ala-Arg-Asp-Z$^4$-NH$_2$ − H$_2$O + H]$^+$ | 588 | 572 | 611.5 |
| [Mdha-Ala-Arg-Asp-Z$^4$ − NH$_3$ + H]$^+$ | 572 | 556 | 595.3 |
| [Glu-Mdha-Ala-Arg-Asp + H]$^+$ | 555 | ND | 555.4 |
| [Arg-Asp-Z$^4$ + H]$^+$ | 435 | 419 | 458.4 |
| [Mdha-Ala-Arg-Asp + H]$^+$ | 426 | 426 | 426.4 |
| [Mdha-Ala-Arg-Asp − NH$_3$ + H]$^+$ | 409 | 409 | 409.3 |
| [Glu-Mdha-Ala-Arg − CO$_2$H + H]$^+$ | 395 | 395 | 395.3 |
| [Adda-Glu-Mdha − Addafrag − NH$_3$ + H]$^+$ | 375 | 375 | 375.3 |
| [Mdha-Ala-Arg + H]$^+$ | 311 | 311 | 311.2 |

[a] ND = Not Detected; Z$^4$ = Tyr (**17**), Phe (**18**), or Trp (**14**); Addafrag = C$_9$H$_{10}$O.

[D-Asp[3]]MC-RY (**17**) and [D-Asp[3]]MC-RF (**18**): These two MCs were minor congeners in the *P. prolifica* NIVA-CYA 544 extract (Figure 2). Their elemental compositions were determined on the basis of the *m/z* of their protonated or deprotonated ions, ^{15}N-labeling, and analysis of their isotope patterns to be $C_{51}H_{70}N_{10}O_{13}$ and $C_{51}H_{70}N_{10}O_{12}$, respectively (Table 1). [D-Asp[3]]MC-RY (**17**) and [D-Asp[3]]MC-RF (**18**) eluted with the same retention times as **17** and **18** in the extract from L. Victoria, and although the HRMS/MS spectrum of **17** was weak, it displayed several product-ions (*m/z* 426.2069, 375.1915, 213.0879, 155.0814, and 135.0801) that were consistent with [D-Asp[3]]MC-RY [46]. The HRMS/MS spectrum of **18** was stronger, and contained product-ions consistent with the proposed structure, including those observed for **17** (above) as well as at *m/z* 851.4282 ($\Delta m = -1.9$ ppm, from Adda[5]–D-Glu[6]–Mdha[7]–D-Ala[1]–Arg[2]–D-Asp[3]) [46] that were consistent with [D-Asp[3]]MC-RF (**18**).

[D-Asp[3]]MC-RCit (**20**): A relatively early eluting MC congener (retention time 3.44 min using LC–HRMS method A) afforded singly-charged ions at *m/z* 1025.5431 and 1023.5311 in positive and negative ionization modes, respectively, corresponding to the [M + H]$^+$ and [M − H]$^-$ ions, respectively. The number of nitrogen atoms was determined to be 12 using ^{15}N-labeling. These data, as well as analysis of the isotope profiles with and without nitrogen-15 labeling (Figure 4) established a

molecular formula of $C_{48}H_{72}N_{12}O_{13}$ for the neutral molecule. The retention time of **20** was only slightly shorter than that of **4** in LC−HRMS method B (Figure S6, Table S1), which together with the charge state and molecular formula suggested that **20** contained one Arg residue. The positive HRMS/MS spectrum of **20** (Figure S36) was very similar to those of [D-Asp³]MC-RW (**14**) and [D-Asp³]MC-RF (**18**) (Figure S37), and in particular displayed prominent product-ions at *m/z* 375.1904 ($C_{20}H_{27}O_5N_2^+$, $\Delta m$ = −2.8 ppm, from Adda⁵–D-Glu⁶–Mdha⁷ minus $C_9H_{10}O$, Figure 1) and 426.2083 ($C_{17}H_{28}O_6N_7^+$, $\Delta m$ = −3.0 ppm, from Mdha⁷–D-Ala¹–Arg²–D-Asp³), confirming demethylation at position-3 rather than position-7 (D-Asp³ rather than Dha⁷) and, together with the complete absence of a product-ion at *m/z* 599.3552, confirmed the presence of Arg² rather than Arg⁴. Furthermore, product-ions at 851.4314 ($C_{42}H_{59}O_{11}N_8^+$, $\Delta m$ = +1.9 ppm, from Adda⁵–D-Glu⁶–Mdha⁷–D-Ala¹–Arg²–D-Asp³) and 273.1193 ($C_{10}H_{17}O_5N_4^+$, $\Delta$ −0.2 ppm, from D-Asp³–Cit⁴) were consistent with Cit at position-4, and thus that **20** is [D-Asp³]MC-RCit. In particular, the LC–HRMS/MS data indicated that the side-chain of the amino acid at position-2 was neutral, and consisted of a $C_4H_9ON_2$ unit that included exactly one ring or double bond. Given that the two nitrogen atoms cannot be basic (due to the molecule's charge state, retention time, and fragmentation pattern), both of the nitrogen atoms must be either side of a carbonyl group, indicating the presence of a carbamide group R-NH-CONH₂. This is consistent with Cit, which is by far the most likely of the possibilities based on biosynthetic and metabolic considerations. Furthermore, **20** showed a prominent product at *m/z* 982.5310 (Figures S36 and S64), which examination of the product-ion spectra from unlabeled and ¹⁵N-labeled **20** (Figure S64) unambiguously showed to be due to neutral loss of HNCO. This neutral loss is a characteristic of Cit-containing peptides [47] and, together with the foregoing observations, establishes **20** as [Asp³]MC-RCit. This is the first Cit-containing MC to be identified. Given that Cit is involved in both the biosynthesis and catabolism of Arg in bacteria [48], **20** may be a minor byproduct from biosynthesis of the much more abundant **1** or originate from the subsequent breakdown of **1** in the cells.

A number of minor MCs were detected by LC–HRMS method B in extracts of NIVA-CYA 544 (Figures S5–S8) but were not sufficiently abundant to be identified with any certainty from the LC–MS data. One of these is believed to be [D-Asp³]MC-RY(OMe) based on its accurate mass ($t_R$ = 8.79 min, *m/z* 1061.5310, $C_{52}H_{73}N_{10}O_{14}^+$ $\Delta m$ = +0.7 ppm) and relative retention time (eluting in the tail of the much more abundant [D-Asp³]MC-RY (**17**) (Figure S8), as has been observed elsewhere [44]). The limited number of product-ions observed (Figure S34) were also fully consistent with **17**. Another appeared to be a major and a minor isomer of the Cys conjugate of **1** (Figure S5, major isomer $t_R$ = 3.74 min, *m/z* 573.2922, $C_{51}H_{82}N_{14}O_{14}S^{2+}$, $\Delta m$ = −1.5 ppm, containing 14 nitrogen atoms by ¹⁵N-labeling and with an excellent isotope pattern match to the proposed structure (Figures S55–S57), the presence of which is unsurprising given the identification of the corresponding GSH conjugate (**19**) in the same extract. An oxidized analog of **1**, containing one extra oxygen atom (Figure S5, $t_R$ = 4.09 min, *m/z* 520.7796, $C_{48}H_{75}N_{13}O_{13}^{2+}$, $\Delta m$ = −0.4 ppm, containing 13 nitrogen atoms by ¹⁵N-labeling and with an excellent isotope pattern match for the proposed structure) was detected, but the location of the additional oxygen atom was not determined.

In summary, multiple LC–MS analyses were applied for the tentative identification of new MC congeners in *P. prolifica* NIVA-CYA 544. We showed the application of different modes of mass spectrometric fragmentation in order to obtain complementary structural information. Further structural elucidation was aided by specific derivatization techniques of functional groups and ¹⁵N-labeling of the peptides, as well as analysis of the isotope patterns observed for the compounds during LC–HRMS analysis of unlabeled and ¹⁵N-labeled culture extracts. This resulted in the characterization of new glutamic acid- (**12** and **13**) and citrulline-containing (**20**) microcystins as well as a tryptophan-containing analog (**14**). The identity of the high molecular weight MC-containing **15** has tentatively been shown to be a sulfide-linked conjugate of [D-Asp³]MC-RR (**1**), with its sulfoxide derivative **16** present as an autoxidation product in the extracts, but further studies are needed for definitive structural determination of **15** and **16**. Nevertheless, the detection of these unusual compounds illustrates the power of the combined chemical and LC–MS analytical methods used in this

study. Furthermore, the presence of **15** and **16** in this culture suggests that similar high-molecular-mass MC conjugates may be produced by other cyanobacterial cultures and blooms, but would be difficult to detect by standard methods due to the combination of their unusual mass, charge-state and retention times. If similar conjugates exist for non-Arg-containing MCs, they are expected to elute very late and be singly-charged in positive ionization mode with $m/z > 2000$.

MCs containing Glu at positions-2 and -4 have been reported [45] as methyl esters at one or both positions. We did not observe any methyl esters of MCs in the NIVA-CYA 544 extracts in this study. Furthermore, during the chemical characterization of the MCs in this strain, we found that the carboxylic acid groups on $Glu^2$, $Glu^4$, D-$Glu^6$ were readily esterified by diazomethane. The above findings for NIVA-CYA 544, taken together with the observation that D-$Glu^6$ in MCs is known to be readily esterified by methanol in the presence of traces of acid [25,26], suggests that the originally-reported esterified MC-EE congeners [45] in *Anabaena* strain 186 may have been artifacts from reaction of the carboxylic acid groups of $Glu^2$ and $Glu^4$ with solvent during extraction and purification in a similar manner to that which has been described for D-$Glu^6$. If so, then the seven MCs in the *Anabaena* strain 186 identified by Namikoshi et al. [45] would originally have been biosynthesized as [$Dha^7$]MC-EE, [D-$Asp^3$,$Dha^7$]MC-EE, [$Ser^7$]MC-EE, [D-$Asp^3$,$Ser^7$]MC-EE and MC-EE in the cyanobacterium. It would appear from this that the carboxylic acid groups in the Glu residues at position-2 and -4 of MC-EE congeners might be even more easily esterified than the carboxylic acid of D-$Glu^6$, as none of the esterified MC-EE congeners reported by Namikoshi et al. contained a D-$Glu(OMe)^6$ residue. The potential presence of artefactual MCs containing methyl esters after exposure to methanol and acids needs to be considered when using LC–MS methods to analyze processed extracts from cyanobacterial blooms or cultures. A Cit-containing MC, [D-$Asp^3$]MC-RCit (**20**), was also detected for the first time. It seems likely that this compound is related to the presence of the much more abundant [D-$Asp^3$]MC-RR (**1**), and therefore that low levels of Cit-containing MCs could be present in other cyanobacterial samples with high levels of Arg-containing MCs. The above findings also illustrate the power of combining LC–HRMS/MS techniques with isotopic labeling and selective chemical derivatization techniques and highlight the unexpected MC diversity that may be present in cyanobacteria and which could be easily overlooked using more conventional analytical approaches.

## 3. Experimental Section

### 3.1. Chemicals and Reagents

LC–MS grade water and acetonitrile were from Fisher Scientific (Oslo, Norway). Methanol (gradient quality) was from Romil (Cambridge, UK). The following MC standards (≥95% purity) were from Enzo Life Sciences (Enzo Biochem, Inc., Farmingdale, NY, USA): Hepatotox Set 1 (containing MC-LR (**6**), MC-RR (**2**), MC-LY (**8**), MC-YR (**3**), MC-LW (**9**), MC-LF (**10**), MC-LA, and NOD-R), [D-$Asp^3$,$Dhb^7$]MC-RR (**23**) (supplied as [D-$Asp^3$]MC-RR (**1**), but subsequently identified as **23** by thiol derivatization and comparison with reference materials of **1** and **23** using LC-MS/MS methods A and B), and [D-$Asp^3$]MC-LR (**4**). A certified reference material of [$Dha^7$]MC-LR (**5**) and reference materials of [D-$Asp^3$]MC-RR (**1**) and [D-$Asp^3$,$Dhb^7$]MC-RR (**23**) were from National Research Council of Canada (NRC, Halifax, NS, Canada). Extracts of a bloom from Lake Victoria that contained [D-$Asp^3$]MC-RY (**17**), [D-$Asp^3$]MC-RF (**18**) and [D-$Asp^3$]MC-LA were available from earlier work [43]. Individual stock solutions of 12.5 µg/mL (MC-LY, MC-LW, MC-LF, MC-LA, [D-$Asp^3$,$Dhb^7$]MC-RR, [D-$Asp^3$]MC-LR, 25 µg/mL (MC-RR), and 50 µg/mL (MC-LR, NOD-R), were prepared in 50% methanol. From those solutions, a pooled working stock of 1 µg/mL (each compound), was prepared in methanol and diluted to 200 ng/mL in 50% methanol. Sodium carbonate (pro analysis), 2-mercaptoethanol (≥99%), diazald (99%), L-glutathione (≥98%) and 2-(2-ethoxyethoxy)ethanol (≥99%) were from Sigma–Aldrich (Steinheim, Germany). Sodium bicarbonate, potassium hydroxide, formic acid and acetic acid (all pro analysis purity) were from Merck KGaA (Darmstadt, Germany). Diaion HP-20 resin was from Supelco Analytical (Bellefonte, PA, USA).

## 3.2. Cultivation of P. prolifica NIVA-CYA 544 and Extraction of MCs

*P. prolifica* strain NIVA-CYA 544 was from The Norwegian Culture Collection of Algae (NORCCA) maintained and owned by the Norwegian Institute for Water Research (NIVA) and the University of Oslo. The strain was originally isolated from Lake Steinsfjorden, Norway, in 2004. It was cultivated in Z8 medium [49] in 100 mL glass Erlenmeyer flasks in an incubator (IPP110plus, Memmert GmbH + Co. KG, Schwabach, Germany) at 18 °C with a 14/10 h light/dark photoperiod, using 1% of maximum light intensity. For general screening of MCs, 3 mL of the culture was transferred to a glass tube and stored at −20 °C overnight, then allowed to thaw at room temperature, and 3 mL of methanol was added. The tube was then vortex-mixed for 20 s, sonicated for 5 min and centrifuged for 10 min at 1000 rcf. The supernatant was transferred to screw-cap vials and stored refrigerated until analysis. A concentrated extract to assist in MS/MS analyses of the minor congeners was obtained with HP-20 as described elsewhere [33].

## 3.3. Cultivation of P. prolifica NIVA-CYA 544 for $^{15}$N-labeling of MCs

In late exponential phase, a culture (15 mL) was concentrated by centrifugation (8000 rcf, swinging bucket rotor, 4 °C, 15 min), and the supernatant removed. Concentrated cells (~3 mL) were inoculated into 17 mL of sterile Z8 medium in which the $NaNO_3$ and $Ca(NO_3)_2$ had been replaced with $Na^{15}NO_3$ and $Ca(^{15}NO_3)_2$ (>98% $^{15}$N, Cambridge Isotope Laboratories, Andover, MA, USA). Cultures were grown at 18 °C under a 14:10 h light/dark photoperiod in a Conviron model E7/2 dual compartment plant growth chamber. An approximate photon flux density of 95–100 µmol m$^{-2}$ s$^{-1}$ cool white light was maintained. The light was measured outside the flask using a Li-Cor Model LI-185B quantum/photometer. Cultures were transferred every 3 weeks at which time small aliquots were examined by LC–HRMS analysis (method B) until maximum $^{15}$N-incorporation (~98%) was observed (~12 weeks and 4 transfers) based on isotopic composition of **1** and **4**. After 20 transfers (~13 months), a concentrated extract was obtained from 15 mL of the labeled and unlabeled cultures for full-scan LC–HRMS (method B) analysis using HP-20 as described elsewhere [33], and the data used for analysis of the isotopic composition of the MCs.

## 3.4. Liquid Chromatography–Mass Spectrometry

### 3.4.1. LC–HRMS and LC–HRMS/MS (Method A)

HPLC was performed using a Kinetex F5 column (150 × 2.1 mm, 2.6 µm, Phenomenex, Torrance, CA, USA) at 30 °C. The flow rate was 0.3 mL/min, and the injection volumes were 5–10 µL. Mobile phase A was 0.1% formic acid in the water, and mobile phase B was 0.1% formic acid in acetonitrile. The separation was performed by isocratic elution using 30% B for 0.5 min, followed by a linear gradient to 50% B over 14.5 min. The column was flushed with 100% B for 2 min before returning to the starting conditions and equilibration for 2 min. A Vanquish Horizon UHPLC (Thermo Fisher Scientific, Waltham, MA, USA) was interfaced with a Q-Exactive Fourier-transform high-resolution mass spectrometer (Thermo Fisher Scientific). A heated electrospray interface (HESI-II) was operated at 300 °C and used for ionization with a spray voltage of 3.8 kV and 3.5 kV in positive and/or negative mode, respectively. The mass spectrometer was run in the positive or negative full-scan mode in the mass range *m/z* 400−2200. The mass resolution was set to 70,000 at *m/z* 200. Other important interface parameters included an ion transfer capillary temperature of 250 °C, a sheath gas flow rate of 55 units, and an auxiliary gas flow rate of 25 units. All-ion-fragmentation (AIF) was performed using a mass resolution of 17,500, a max IT of 200 ms, and an AGC target of $3 \times 10^6$. The normalized collision energy was set to 35%. The mass range during AIF was *m/z* 80−1200. Parallel reaction monitoring (PRM) was performed using a mass resolution of 17,500.

### 3.4.2. LC–HRMS and LC–HRMS/MS (Method B)

LC-HRMS method B used a Q Exactive-HF Orbitrap mass spectrometer equipped with a HESI-II heated electrospray ionization interface (ThermoFisher Scientific, Waltham, MA, USA) using an Agilent 1200 LC system including a binary pump, autosampler and column oven (Agilent, Santa Clara, CA, USA). Analyses were performed with a SymmetryShield C18 column (100 × 2.1 mm, 3.5 μm, Waters, Milford, MA, USA) held at 40 °C with mobile phases A and B of water and acetonitrile, respectively, each of which contained formic acid (0.1% v/v). Gradient elution (0.3 mL/min) was from 20–90% B over 18 min, then to 100% B over 0.1 min and a hold at 100% B (2.9 min), then returned to 20% B over 0.1 min with a hold at 20% B (3.9 min) to equilibrate the column (total run time 25 min). Injection volume was typically 1–5 μL.

The mass spectrometer was operated in positive ion mode and calibrated from *m/z* 74–1622. The spray voltage was 3.7 kV, the capillary temperature was 350 °C, and the sheath and auxiliary gas flow rates were 25 and 8 units, respectively, with MS data acquired from 2–20 min. Mass spectral data was collected using a combined full-scan and data-independent acquisition (DIA) method. Full-scan data was collected over a range from *m/z* 500–1400 using the 60,000-mass resolution setting, an AGC target of $1 \times 10^6$ and a max IT of 100 ms. DIA data was collected using the 15,000-mass resolution setting, an AGC target of $2 \times 10^5$, max IT set to 'auto' and a stepped collision energy of 30, 60 and 80 eV. Precursor isolation windows were 62 *m/z* wide centered at *m/z* 530, 590, 650, 710, 770, 830, 890, 950, 1010, 1070, 1130, 1190, 1250, 1310, and 1370, and DIA chromatograms were typically extracted for the following product-ions: *m/z* 121.1011, 121.0647, 135.0804, 135.1168, 213.0870, 361.1758, 375.1915, 379.1864, 389.2072, 393.2020, 412.1939, 426.2096, 440.2252, 454.2409, 585.3395, 599.3552, 613.3709. Putative MCs detected using the above full-scan/DIA method were further probed in a targeted manner using the PRM mode with a 0.7 *m/z* precursor isolation window, typically using the 30,000-resolution setting, an AGC target of $5 \times 10^5$ and a max IT of 400 ms. Typical collision energies were: stepped CE at 30 and 35 eV for MCs with no Arg, stepped CE at 60, 65 and 70 eV for MCs with one Arg, and CE at 65 eV for $[M + H]^+$ and stepped CE at 20, 25 and 30 eV for $[M + 2H]^{2+}$ of MCs with two Arg groups. Full-scan chromatograms were obtained in MS-SIM mode as above but with mass resolution 120,000 and max IT 300 ms.

In negative mode, the mass spectrometer was calibrated from *m/z* 69–1780 and the spray voltage was −3.7 kV, while the capillary temperature, sheath, and auxiliary gas flow rates were the same as for positive mode. Mass spectrometry data were collected in full-scan/DIA scan mode as above using a scan range of *m/z* 750–1400, a mass resolution setting of 60,000, AGC target of $1 \times 10^6$ and max IT of 100 ms. For DIA, HRMS/MS data were collected from *m/z* 93–1400 using a resolution setting of 15,000, AGC target of $2 \times 10^5$, max IT set to 'auto', and stepped collision energy 65 and 100 V. Isolation windows were 45 *m/z* wide and centered at *m/z* 772, 815, 858, 902, 945, 988, 1032, 1075, 1118, 1162, 1205, 1248, 1294, 1335, and 1378, and DIA chromatograms were extracted for the *m/z* 128.0353 (or *m/z* 129.0324 for ^{15}N-labeled MCs) product-ion. Full-scan chromatograms were obtained over a scan range *m/z* 750–1400 at a mass resolution setting of 120,000 using an AGC target of $1 \times 10^6$ and a max IT of 300 ms.

### 3.4.3. LC–ITMS/MS (Method C)

The HPLC conditions were identical as for LC–HRMS method A. However, a Finnigan Surveyor HPLC system was interfaced with an LTQ linear ion trap mass spectrometer (both Thermo Fisher Scientific) operated in positive or negative ionization mode and fitted with an electrospray ionization interface. The capillary voltage and tube lens offset of the instrument were tuned with continuous infusion of MC-LR (10 μg/mL) in 50% methanol into a mobile phase composed of 50% A. The spray voltage was set to 3.5 kV, the sheath gas and auxiliary gas flow rates were 58 and 3.0 units, respectively, and the capillary temperature was 275 °C. The MS/MS product-ion spectra of the $[M + H]^+$ and $[M − H]^−$ ions were acquired using collision-induced dissociation in the ion trap. The ESI settings were as described above. Individual precursor ions were selected with an isolation width of *m/z* 2, the

activation Q was set to 0.25, and the activation time was set to 30 ms. The normalized collision energy was 35%.

### 3.5. 2-Mercaptoethanol Derivatization for Mdha⁷/Dhb⁷ Differentiation

To an aliquot (100 μL) of the 50% methanol extract of *P. prolifica* was added 16 μL of 5 μg/mL MC-LR as internal standard (in 50% methanol), and then mixed with 60 μL of 0.2 M sodium carbonate buffer (pH = 9.2) in a septum-capped vial, left in the autosampler tray [28,29] at 20 °C for 20 min, and then analyzed by LC–HRMS (method A). Then, 2-mercaptoethanol (1 μL) was added, with brief vortex-mixing, and the vial placed back in the autosampler tray. The reaction was then followed by LC–HRMS method A for 3 h.

Separate derivatization experiments were performed by the addition of ammonium carbonate (0.1 M, 200 μL) to a filtered extract (200 μL), with 200 μL transferred to two LC-MS vials. To one vial was added 1 μL of a 1:1 mixture of mercaptoethanol and $d_4$-mercaptoethanol (Sigma–Aldrich, St. Louis, MO, USA), while 1 μL of water was added to the other vial as a control. The samples were placed in the LC sample tray (15 °C) and the reactions monitored periodically until completion and then analyzed using LC–HRMS method B.

### 3.6. Methylation of Carboxylic Acids

An aliquot of the cyanobacterial extract (200 μL) was transferred to the outer tube of a diazomethane-generator (Aldrich, Steinheim, Germany) and 3 mL of methanol added. The extract was then exposed to diazomethane generated from diazald (*N*-methyl-*N*-nitroso-*p*-toluenesulfonamide) in the apparatus, according to the manufacturer's instructions. After 18 h, 1 mL acetic acid was added to the inner tube to remove unreacted diazomethane, the methanol solution was transferred to a glass tube and evaporated at 60 °C under a gentle stream of nitrogen. The residue was dissolved in 100 μL of methanol, vortex-mixed, and transferred to an LC vial for LC–HRMS analysis using LC–HRMS method A.

### 3.7. ¹⁵N-Incorporation and Molecular Formula Calculations

The incorporation of ¹⁵N into the microcystin with an established molecular formula (**1**) in cultures of *P. prolifica* NIVA-CYA 544 grown in ¹⁵N-labeled media was calculated with NRC Isotopic Enrichment Calculator (https://metrology.shinyapps.io/isotopic-enrichment-calculator/, v.1.81) using intensities of the peaks in the isotope envelopes obtained with LC-HRMS method B (Figures S40 and S41). For MCs where the molecular formula was not established, the number of nitrogen atoms present was determined from the separation of the isotope envelope peaks of the labeled and unlabeled compound, greatly restricting the number of feasible molecular formulae that were consistent with the accurate mass of the compound. A second program, NRC Molecular Formula Calculator (https://metrology.shinyapps.io/molecular-formula-calculator/, v.1.01), the features of which are described in the text, was used to obtain the most likely molecular formula for unknown MCs, based on the accurate masses and relative intensities of the isotope envelope peaks of the labeled and unlabeled MC obtained from a mixture of labeled and unlabeled extracts, and on the isotopic composition of ¹⁵N in MCs as established for labeled **1**. Candidate patterns were ranked using Bayesian statistics as implemented in R package Rdisop [39,40] and except for **15** and **16** (where several viable formulae were obtained), the match with the highest score was chosen (scores were normalized to the best match).

### 3.8. Reaction of **1** with Glutathione to Produce **19**.

Derivatization of **1** with GSH was based on Foss et al. [25] and proceeded by the addition of 200 μL of GSH (2.5 mg/mL in pH 9.4 carbonate buffer) to ca. 40 ng [ᴅ-Asp³]MC-RR (**1**) in methanol (90 μL). The progress of the reaction was followed by LC-HRMS method A (Figure S15).

### 3.9. Oxidation with Sodium Periodate

Periodate oxidations, based on Yilmaz et al. [33], were performed by the addition of aqueous sodium periodate (1 mg/mL) to an equal volume (100 µL) of the filtered extract. Samples and reactions were placed in the sample tray (held at 15 °C) and the reactions monitored periodically until completion and then analyzed.

### References

1. Benke, P.I.; Vinay Kumar, M.C.; Pan, D.; Swarup, S. A mass spectrometry-based unique fragment approach for the identification of microcystins. *Analyst* **2015**, *140*, 1198–1206. [CrossRef] [PubMed]

2. Li, J.; Li, R.; Li, J. Current research scenario for microcystins biodegradation—A review on fundamental knowledge, application prospects and challenges. *Sci. Total Environ.* **2017**, *595*, 615–632. [CrossRef] [PubMed]

3. Paerl, H.W.; Hall, N.S.; Calandrino, E.S. Controlling harmful cyanobacterial blooms in a world experiencing anthropogenic and climatic-induced change. *Sci. Total Environ.* **2011**, *409*, 1739–1745. [CrossRef] [PubMed]

4. Miller, M.A.; Kudela, R.M.; Mekebri, A.; Crane, D.; Oates, S.C.; Tinker, M.T.; Staedler, M.; Miller, W.A.; Toy-Choutka, S.; Dominik, C.; et al. Evidence for a novel marine harmful algal bloom: Cyanotoxin (microcystin) transfer from land to sea otters. *PLoS ONE* **2010**, *5*, e12576. [CrossRef]

5. Fontanillo, M.; Kohn, M. Microcystins: Synthesis and structure-activity relationship studies toward PP1 and PP2A. *Bioorg. Med. Chem.* **2018**, *26*, 1118–1126. [CrossRef]

6. Carmichael, W.W.; Azevedo, S.M.; An, J.S.; Molica, R.J.; Jochimsen, E.M.; Lau, S.; Rinehart, K.L.; Shaw, G.R.; Eaglesham, G.K. Human fatalities from cyanobacteria: Chemical and biological evidence for cyanotoxins. *Environ. Health Perspect.* **2001**, *109*, 663–668. [CrossRef]

7. Jochimsen, E.M.; Carmichael, W.W.; An, J.S.; Cardo, D.M.; Cookson, S.T.; Holmes, C.E.; Antunes, M.B.; de Melo Filho, D.A.; Lyra, T.M.; Barreto, V.S.; et al. Liver failure and death after exposure to microcystins at a hemodialysis center in Brazil. *N. Engl. J. Med.* **1998**, *338*, 873–878. [CrossRef]

8. MacKintosh, C.; Beattie, K.A.; Klumpp, S.; Cohen, P.; Codd, G.A. Cyanobacterial microcystin-LR is a potent and specific inhibitor of protein phosphatases 1 and 2A from both mammals and higher plants. *FEBS Lett.* **1990**, *264*, 187–192. [CrossRef]

9. Yoshizawa, S.; Matsushima, R.; Watanabe, M.F.; Harada, K.; Ichihara, A.; Carmichael, W.W.; Fujiki, H. Inhibition of protein phosphatases by microcystins and nodularin associated with hepatotoxicity. *J. Cancer Res. Clin. Oncol.* **1990**, *116*, 609–614. [CrossRef]

10. Chen, L.; Chen, J.; Zhang, X.; Xie, P. A review of reproductive toxicity of microcystins. *J. Hazard. Mater.* **2016**, *301*, 381–399. [CrossRef]

11. Chen, L.; Li, S.C.; Guo, X.C.; Xie, P.; Chen, J. The role of GSH in microcystin-induced apoptosis in rat liver: Involvement of oxidative stress and NF-κB. *Environ. Toxicol.* **2016**, *31*, 552–560. [CrossRef] [PubMed]

12. Xiong, Q.; Xie, P.; Li, H.; Hao, L.; Li, G.; Qiu, T.; Liu, Y. Acute effects of microcystins exposure on the transcription of antioxidant enzyme genes in three organs (liver, kidney, and testis) of male Wistar rats. *J. Biochem. Mol. Toxicol.* **2010**, *24*, 361–367. [CrossRef] [PubMed]

13. Christiansen, G.; Fastner, J.; Erhard, M.; Borner, T.; Dittmann, E. Microcystin biosynthesis in *Planktothrix*: *Genes*, evolution, and manipulation. *J. Bacteriol.* **2003**, *185*, 564–572. [CrossRef] [PubMed]

14. Ross, C.; Santiago-Vazquez, L.; Paul, V. Toxin release in response to oxidative stress and programmed cell death in the cyanobacterium *Microcystis aeruginosa*. *Aquat. Toxicol.* **2006**, *78*, 66–73. [CrossRef]

15. Botes, D.P.; Kruger, H.; Viljoen, C.C. Isolation and characterization of four toxins from the blue–green alga, *Microcystis aeruginosa*. *Toxicon* **1982**, *20*, 945–954. [CrossRef]

16. Huisman, J.; Codd, G.A.; Paerl, H.W.; Ibelings, B.W.; Verspagen, J.M.H.; Visser, P.M. Cyanobacterial blooms. *Nat. Rev. Microbiol.* **2018**, *16*, 471–483. [CrossRef]

17. Kleinteich, J.; Puddick, J.; Wood, S.A.; Hildebrand, F.; Laughinghouse, H.I.; Pearce, D.A.; Dietrich, D.R.; Wilmotte, A. Toxic cyanobacteria in Svalbard: Chemical diversity of microcystins detected using a liquid chromatography mass spectrometry precursor ion screening method. *Toxins* **2018**, *10*, 147. [CrossRef]

18. WHO. *Guidelines for Drinking-Water Quality: Fourth Edition Incorporating the First Addendum*; WHO: Geneva, Switzerland, 2017.

19. He, H.; Wu, S.; Wahome, P.G.; Bertin, M.J.; Pedone, A.C.; Beauchesne, K.R.; Moeller, P.D.R.; Carter, G.T. Microcystins containing doubly homologated tyrosine residues from a *Microcystis aeruginosa* bloom: Structures and cytotoxicity. *J. Nat. Prod.* **2018**, *81*, 1368–1375. [CrossRef]

20. Feurstein, D.; Stemmer, K.; Kleinteich, J.; Speicher, T.; Dietrich, D.R. Microcystin congener- and concentration-dependent induction of murine neuron apoptosis and neurite degeneration. *Toxicol. Sci.* **2011**, *124*, 424–431. [CrossRef]

21. Qi, Y.; Bortoli, S.; Volmer, D.A. Detailed study of cyanobacterial microcystins using high performance tandem mass spectrometry. *J. Am. Soc. Mass Spectrom.* **2014**, *25*, 1253–1262. [CrossRef]

22. Schmidt, J.R.; Wilhelm, S.W.; Boyer, G.L. The fate of microcystins in the environment and challenges for monitoring. *Toxins* **2014**, *6*, 3354–3387. [CrossRef] [PubMed]

23. Stotts, R.R.; Namikoshi, M.; Haschek, W.M.; Rinehart, K.L.; Carmichael, W.W.; Dahlem, A.M.; Beasley, V.R. Structural modifications imparting reduced toxicity in microcystins from *Microcystis* spp. *Toxicon* **1993**, *31*, 783–789. [CrossRef]

24. Bortoli, S.; Volmer, D.A. Characterization and identification of microcystins by mass spectrometry. *Eur. J. Mass Spectrom.* **2014**, *20*, 1–19. [CrossRef] [PubMed]

25. Foss, A.J.; Miles, C.O.; Samdal, I.A.; Løvberg, K.E.; Wilkins, A.L.; Rise, F.; Jaabaek, J.A.H.; McGowan, P.C.; Aubel, M.T. Analysis of free and metabolized microcystins in samples following a bird mortality event. *Harmful Algae* **2018**, *80*, 117–129. [CrossRef]

26. Harada, K.I.; Tsuji, K.; Watanabe, M.F.; Kondo, F. Stability of microcystins from cyanobacteria—III. Effect of pH and temperature. *Phycologia* **1996**, *35*, 83–88. [CrossRef]

27. Janssen, E.M. Cyanobacterial peptides beyond microcystins—A review on co-occurrence, toxicity, and challenges for risk assessment. *Water Res.* **2019**, *151*, 488–499. [CrossRef]

28. Shah, S.A.A.; Akhter, N.; Auckloo, B.N.; Khan, I.; Lu, Y.; Wang, K.; Wu, B.; Guo, Y.W. Structural diversity, biological properties and applications of natural products from cyanobacteria. A review. *Mar. Drugs* **2017**, *15*, 354. [CrossRef]

29. Rogers, E.D.; Henry, T.B.; Twiner, M.J.; Gouffon, J.S.; McPherson, J.T.; Boyer, G.L.; Sayler, G.S.; Wilhelm, S.W. Global gene expression profiling in larval zebrafish exposed to microcystin-LR and microcystis reveals endocrine disrupting effects of cyanobacteria. *Environ. Sci. Technol.* **2011**, *45*, 1962–1969. [CrossRef]

30. Stepankova, T.; Ambrozova, L.; Blaha, L.; Giesy, J.P.; Hilscherova, K. In vitro modulation of intracellular receptor signaling and cytotoxicity induced by extracts of cyanobacteria, complex water blooms and their fractions. *Aquat. Toxicol.* **2011**, *105*, 497–507. [CrossRef]

31. Miles, C.O.; Sandvik, M.; Haande, S.; Nonga, H.; Ballot, A. LC–MS analysis with thiol derivatization to differentiate [Dhb[7]]- from [Mdha[7]]-microcystins: Analysis of cyanobacterial blooms, *Planktothrix* cultures and European crayfish from Lake Steinsfjorden, Norway. *Environ. Sci. Technol.* **2013**, *47*, 4080–4087. [CrossRef]

32. Miles, C.O.; Sandvik, M.; Nonga, H.E.; Rundberget, T.; Wilkins, A.L.; Rise, F.; Ballot, A. Thiol derivatization for LC–MS identification of microcystins in complex matrices. *Environ. Sci. Technol.* **2012**, *46*, 8937–8944. [CrossRef] [PubMed]

33. Yilmaz, M.; Foss, A.J.; Miles, C.O.; Ozen, M.; Demir, N.; Balci, M.; Beach, D.G. Comprehensive multi-technique approach reveals the high diversity of microcystins in field collections and an associated isolate of Microcystis aeruginosa from a Turkish lake. *Toxicon* **2019**, *167*, 87–100. [CrossRef] [PubMed]

34. Miles, C.O.; Melanson, J.E.; Ballot, A. Sulfide oxidations for LC–MS analysis of methionine-containing microcystins in *Dolichospermum flos-aquae* NIVA-CYA 656. *Environ. Sci. Technol.* **2014**, *48*, 13307–13315. [CrossRef] [PubMed]

35. Stewart, A.K.; Strangman, W.K.; Percy, A.; Wright, J.L.C. The biosynthesis of $^{15}$N-labeled microcystins and the comparative MS/MS fragmentation of natural abundance and their $^{15}$N-labeled congeners using LC–MS/MS. *Toxicon* **2018**, *144*, 91–102. [CrossRef] [PubMed]

36. MacCoss, M.J.; Wu, C.C.; Matthews, D.E.; Yates, J.R., III. Measurement of the isotope enrichment of stable isotope-labeled proteins using high-resolution mass spectra of peptides. *Anal. Chem.* **2005**, *77*, 7646–7653. [CrossRef] [PubMed]

37. Meija, J. An ode to the atomic weights. *Nat. Chem.* **2014**, *6*, 749–750. [CrossRef]

38. Ipsen, A. Efficient calculation of exact fine structure isotope patterns via the multidimensional Fourier transform. *Anal. Chem.* **2014**, *86*, 5316–5322. [CrossRef]

39. Bocker, S.; Letzel, M.C.; Liptak, Z.; Pervukhin, A. SIRIUS: Decomposing isotope patterns for metabolite identification. *Bioinformatics* **2009**, *25*, 218–224. [CrossRef]

40. Pervukhin, A.; Neumann, S. Decomposition of Isotopic Patterns. R package: Rdisop, 1.42. 2017. Available online: https://www.bioconductor.org/packages/release/bioc/html/Rdisop.html (accessed on 7 October 2019).

41. Senior, J.K. Partitions and their representative graphs. *Am. J. Math.* **1951**, *73*, 663–689. [CrossRef]

42. Teta, R.; Della Sala, G.; Glukhov, E.; Gerwick, L.; Gerwick, W.H.; Mangoni, A.; Costantino, V. Combined LC–MS/MS and molecular networking approach reveals new cyanotoxins from the 2014 cyanobacterial bloom in Green Lake, Seattle. *Environ. Sci. Technol.* **2015**, *49*, 14301–14310. [CrossRef]

43. Ballot, A.; Sandvik, M.; Rundberget, T.; Botha, C.J.; Miles, C.O. Diversity of cyanobacteria and cyanotoxins in Hartbeespoort Dam, South Africa. *Mar. Freshwater Res.* **2014**, *65*, 175–189. [CrossRef]

44. Miles, C.O.; Sandvik, M.; Nonga, H.E.; Rundberget, T.; Wilkins, A.L.; Rise, F.; Ballot, A. Identification of microcystins in a Lake Victoria cyanobacterial bloom using LC–MS with thiol derivatization. *Toxicon* **2013**, *70*, 21–31. [CrossRef] [PubMed]

45. Namikoshi, M.; Yuan, M.; Sivonen, K.; Carmichael, W.W.; Rinehart, K.L.; Rouhiainen, L.; Sun, F.; Brittain, S.; Otsuki, A. Seven new microcystins possessing two L-glutamic acid units, isolated from *Anabaena* sp. strain 186. *Chem. Res. Toxicol.* **1998**, *11*, 143–149. [CrossRef] [PubMed]

46. Okello, W.; Portmann, C.; Erhard, M.; Gademann, K.; Kurmayer, R. Occurrence of microcystin-producing cyanobacteria in Ugandan freshwater habitats. *Environ. Toxicol.* **2010**, *25*, 367–380. [CrossRef] [PubMed]

47. Hao, G.; Wang, D.; Gu, J.; Shen, Q.; Gross, S.S.; Wang, Y. Neutral loss of isocyanic acid in peptide CID spectra: A novel diagnostic marker for mass spectrometric identification of protein citrullination. *J. Am. Soc. Mass Spectrom.* **2009**, *20*, 723–727. [CrossRef]

48. Cunin, R.; Glansdorff, N.; Pierard, A.; Stalon, V. Biosynthesis and metabolism of arginine in bacteria. *Microbiol. Rev.* **1986**, *50*, 314–352.

49. Kotai, J. *Instructions for Preparation of Modified Nutrient Solution Z8 for Algae*; Norwegian Institute for Water Research: Oslo, Norway, 1972.

**Supplementary Material**

**Novel microcystins from *Planktothrix prolifica* NIVA-CYA 544 identified by LC-MS/MS, functional group derivatization and ^{15}N-labeling**

Vittoria Mallia,[1,2] Silvio Uhlig,[1] Cheryl Rafuse,[3] Juris Meija,[4] and Christopher O. Miles[3]

[1]*Toxinology Research Group, Norwegian Veterinary Institute, Ullevålsveien 68, N-0454 Oslo, Norway*

[2]*Department of Chemistry, University of Oslo, P.O. Box 1033, N-0315 Oslo, Norway*

[3]*National Research Council, 1411 Oxford Street, Halifax, NS, B3H 3Z1, Canada*

[4]*National Research Council, 1200 Montreal Road, Ottawa, ON, K1A 0R6, Canada*

**Table of contents**

**Table S1**. Retention times of microcystins detected in *P. prolifica* NIVA-CYA 544 or authentic samples analysed using the three LC–MS methods.

| | Microcystin | Confidence | $t_R$ (min) method A | method B | method C |
|---|---|---|---|---|---|
| 1 | [D-Asp³]MC-RR | confirmed | 2.81 | 4.28 | — |
| 4 | [D-Asp³]MC-LR | confirmed | 5.72 | 7.04 | 4.46 |
| 11 | [D-Asp³,Mser⁷]MC-RR | probable | 2.59 | 4.14 | 1.82 |
| 12 | [D-Asp³]MC-ER | probable | 3.63 | 6.24 | 3.53 |
| 13 | [D-Asp³]MC-EE | probable | 4.99 | 11.62 | 3.93 |
| 14 | [D-Asp³]MC-RW | probable | 10.01 | 9.72 | 8.40 |
| 15 | Sulfide conjugate of **1** | tentative | 9.85[e] | 7.50 | 7.47 |
| 16 | **15**-sulfoxide | tentative | 6.50[f] | 6.53 | — |
| 17 | [D-Asp³]MC-RY | probable | 7.16 | 8.73 | — |
| 18 | [D-Asp³]MC-RF | probable | 9.94 | 9.82 | — |
| 19 | GSH-conjugate of **1** | confirmed | 2.05 | 4.09 | — |
| 20 | [D-Asp³]MC-RCit | probable | 3.44 | 6.79 | — |
| — | Cys-conjugate of **1** | tentative | — | 3.74 | — |
| — | oxidized **1** | tentative | — | 4.09 | — |
| 2 | MC-RR | standard | 3.12 | 4.63 | 2.31 |
| 3 | MC-YR | standard | 5.22 | 7.14 | 4.09 |
| 5 | [Dha⁷]MC-LR | standard | — | 7.28 | 4.67 |
| 6 | MC-LR | standard | 5.84 | 7.29 | 4.58 |
| 7 | MC-LA | standard | 9.35 | 15.10 | 8.39 |
| 8 | MC-LY | standard | 10.65 | 15.34 | 9.67 |
| 9 | MC-LW | standard | 13.83 | 17.20 | 12.80 |
| 10 | MC-LF | standard | 13.91 | 17.85 | 12.89 |
| 23 | [D-Asp³,Dhb⁷]MC-RR | standard | 2.97 | — | 2.19 |
| 24 | [D-Asp³]MC-EHar | tentative | — | 6.55 | — |
| 25 | [D-Asp³]MC-RY(OMe) | tentative | — | 8.89 | — |
| 26 | [D-Asp³]MC-HarY | tentative | — | 8.90 | — |
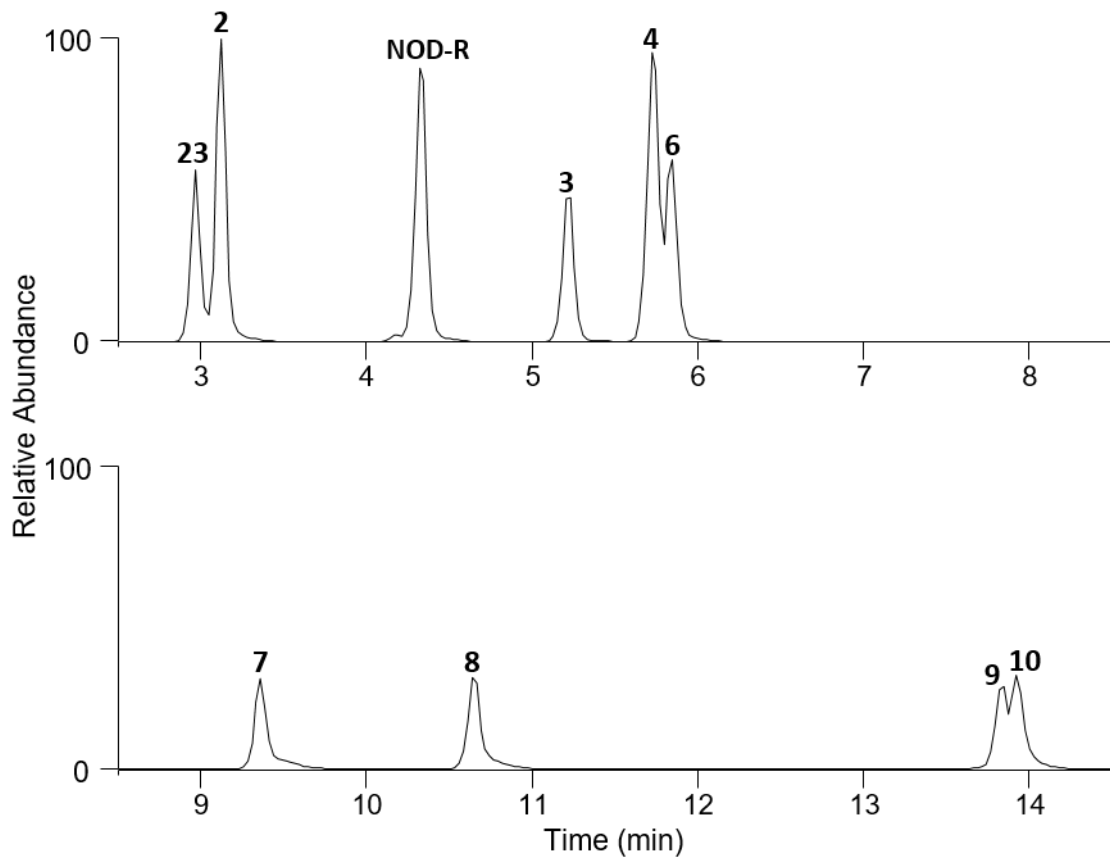
**Figure S1**. LC–HRMS (method A) full scan chromatogram in positive ion mode of a standard mixture (200 ng/mL) of 9 microcystins (MCs) and Nodularin-R, used to optimize the method: [D-Asp$^3$,Dhb$^7$]MC-RR (**23**) (wrongly labelled by Enzo as [D-Asp$^3$]MC-RR), MC-RR (**2**), NOD-R, MC-YR (**3**), [D-Asp$^3$]MC-LR (**4**), MC-LR (**6**), MC-LA (**7**), MC-LY (**8**), MC-LW (**9**), MC-LF (**10**). The chromatogram was extracted at the specified *m/z* of standard compounds, as reported in Figure 1, with 5 ppm tolerance.
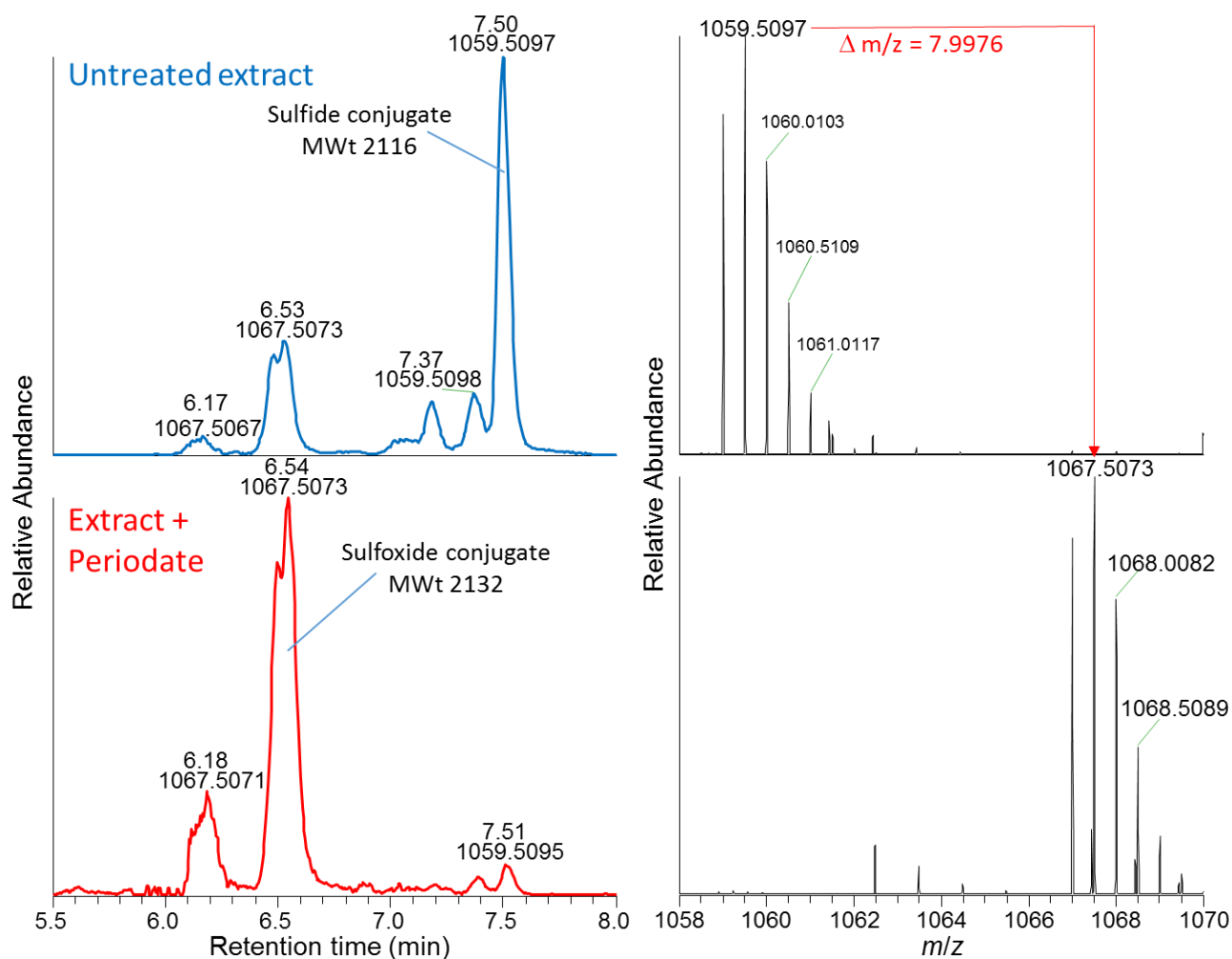
**Figure S2.** Left, LC−HRMS chromatograms (method B) before (top left) and after (bottom left) treatment with sodium periodate. Both chromatograms are extracted at both *m/z* 1059.0088 and 1067.0060, and show complete conversion of sulfide **15** to sulfoxide **16**. To the right are the mass spectra of the main peak the sulfide (top right) and sulfoxide (bottom right), showing a change in *m/z* corresponding to addition of one oxygen atom (theoretical Δ *m/z* = 7.9975).
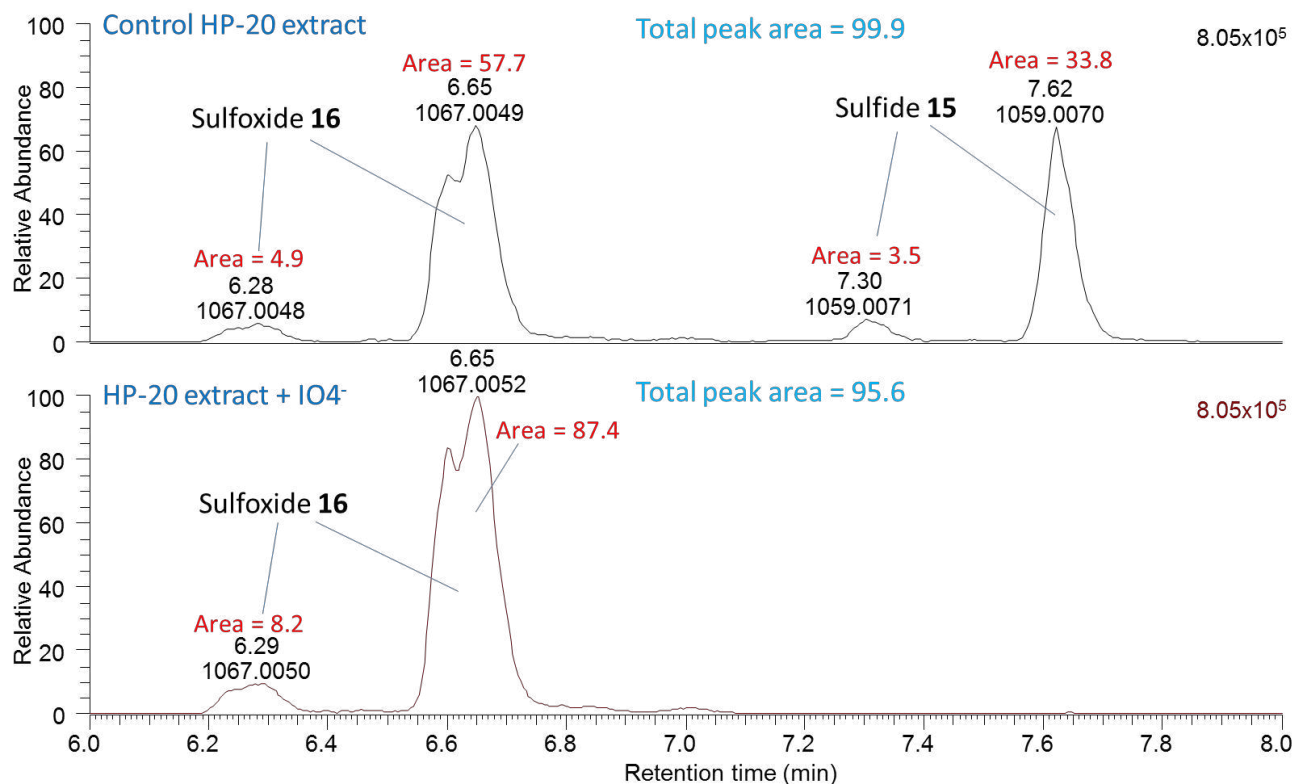
**Figure S3.** LC–HRMS chromatograms before (top) and 15 min after (bottom) treatment with sodium periodate. Both chromatograms are extracted at both *m/z* 1059.0088 and 1067.0060, and displayed with the same vertical scale. Equivalent injection volumes were used for both chromatograms, and integration of the peaks (peak areas in arbitrary units) shows complete conversion of sulfide **15** to sulfoxide **16**.
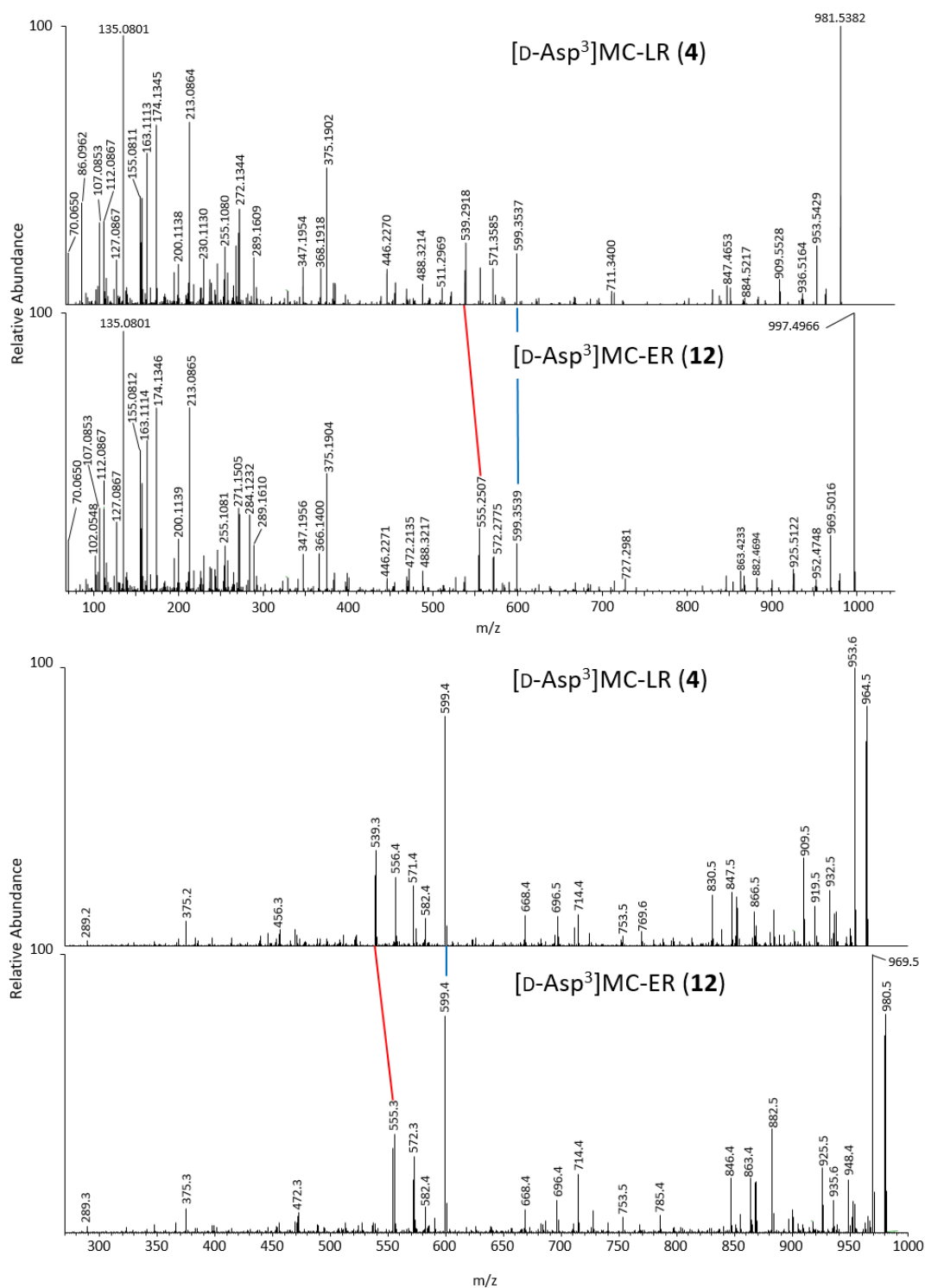
**Figure S4.** Top, LC–HRMS/MS (method A) product ion spectra, and; bottom, LC–MS² (method C) product ion spectra from collision-induced fragmentation of the [M + H]⁺ ions of [D-Asp³]MC-LR (**4**) and [D-Asp³]MC-ER (**12**). The blue lines link examples of conserved fragments while the red lines link examples of fragments shifted by the exact difference between the masses of L and E (15.9585).
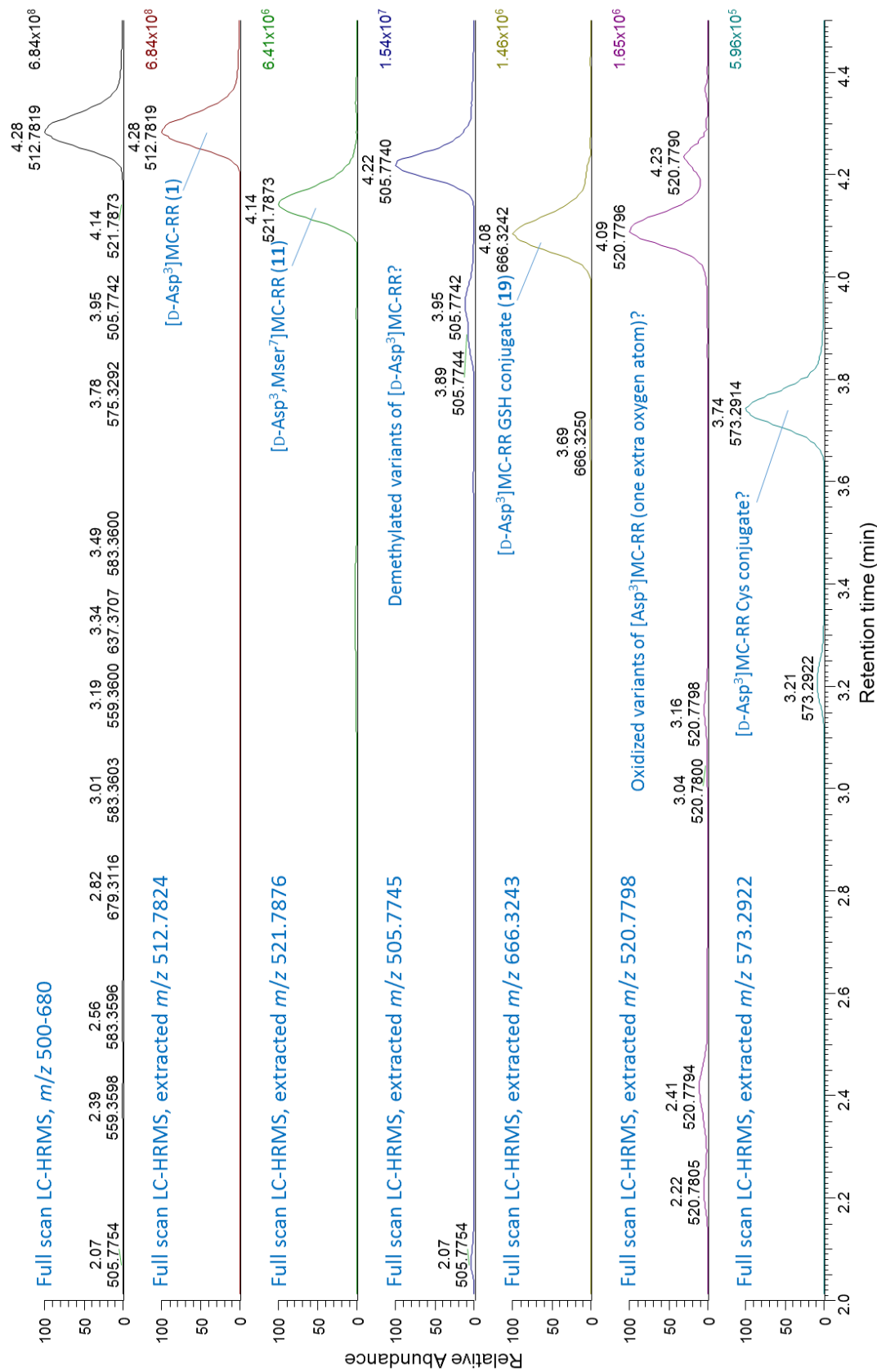
**Figure S5.** LC−HRMS (method B) chromatograms (2.0–4.5 min) in positive ionization mode of an HP-20 extract of NIVA-CYA 544, showing the polar doubly-charged microcystins. Extracted ion chromatograms were at the specified *m/z* with 5 ppm tolerance.

**Figure S6.** LC–HRMS (method B) chromatograms (5.5–7.5 min) in positive ionization mode of an HP-20 extract of NIVA-CYA 544, showing the less polar singly-charged microcystins. Extracted ion chromatograms were at the specified *m/z* with 5 ppm tolerance.
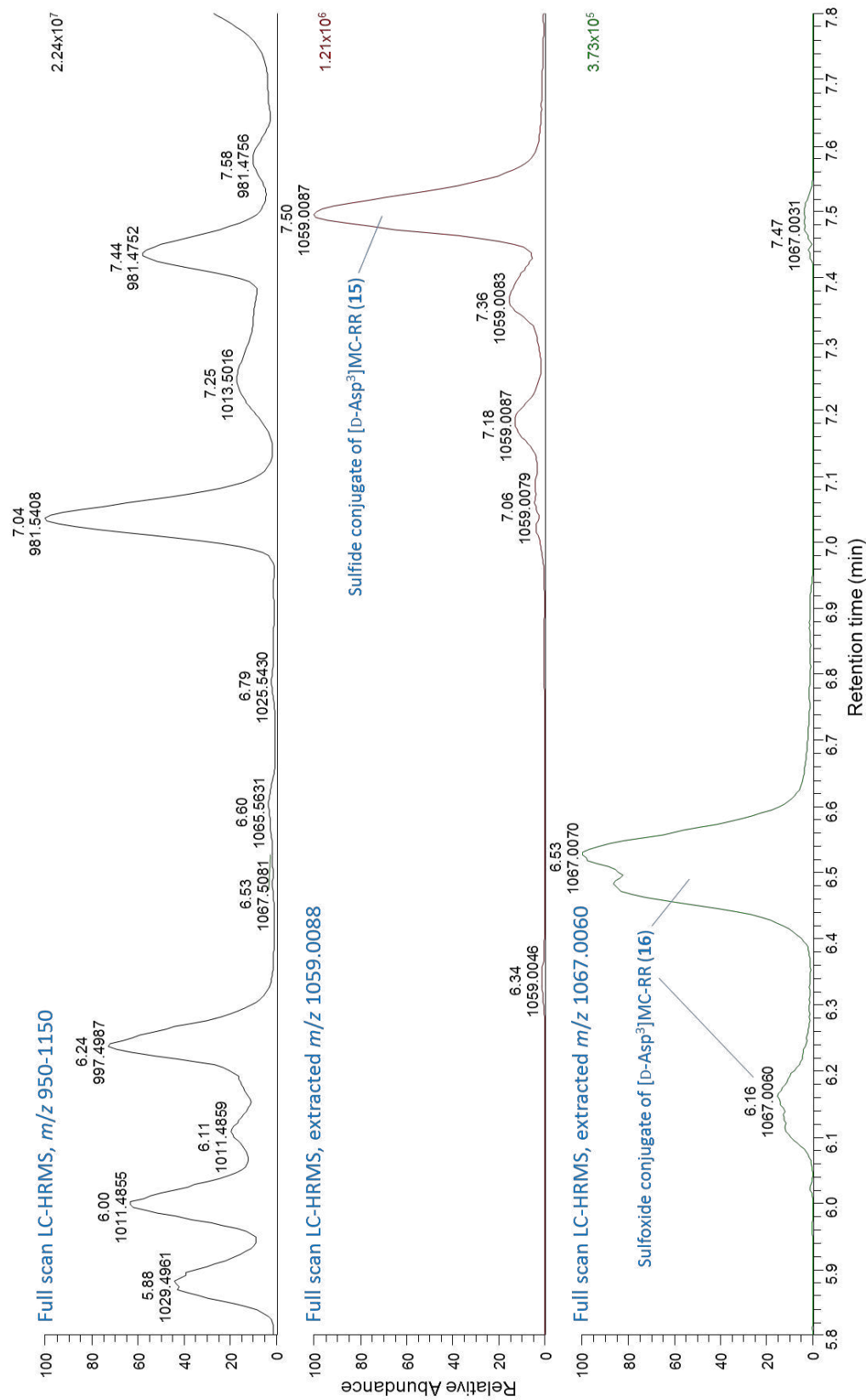
**Figure S7.** LC–HRMS (method B) chromatograms (5.8–7.8 min) in positive ionization mode of an HP-20 extract of NIVA-CYA 544, showing the less polar doubly-charged microcystin conjugates. Extracted ion chromatograms were at the specified *m/z* with 5 ppm tolerance. Note the presence of a major and a minor stereoisomer of **16**, each of which appears to be present as a pair of sulfoxide diastereoisomers.

**Figure S8.** LC−HRMS (method B) chromatograms (8.5−12 min) in positive ionization mode of an HP-20 extract of NIVA-CYA 544, showing the least polar singly-charged microcystins. Extracted ion chromatograms were at the specified *m/z* with 5 ppm tolerance.
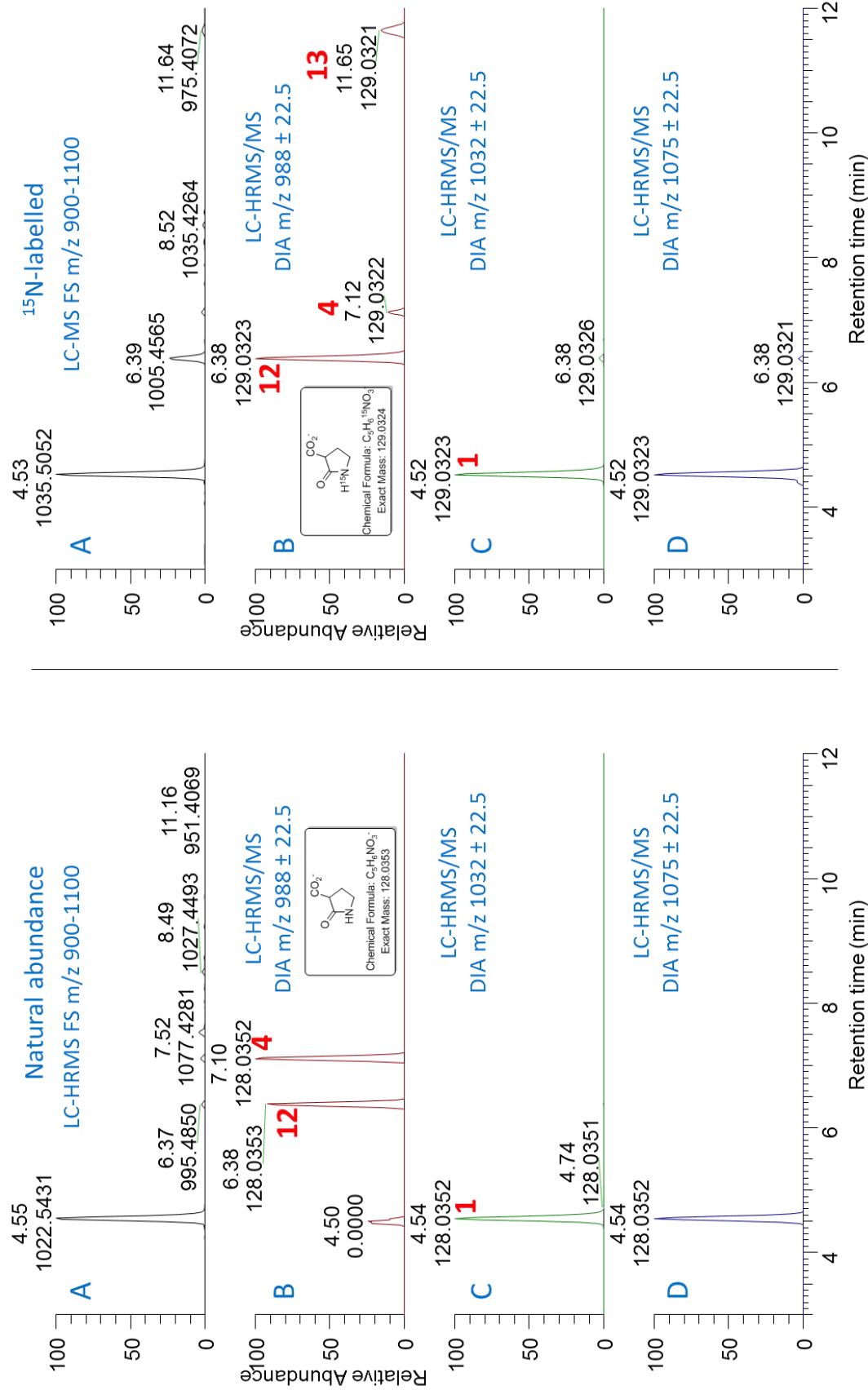
**Figure S9.** Negative ionization LC−MS/MS FS/DIA chromatograms of an extract of NIVA-CYA 544 at natural abundance (left) and in a ^{15}N-labelled culture (right), extracted at *m/z* 128.0353 ($C_5H_6{}^{14}NO_3{}^-$, left) and 129.0324 ($C_5H_6{}^{15}NO_3{}^-$, right) from the Glu[6]-moiety.
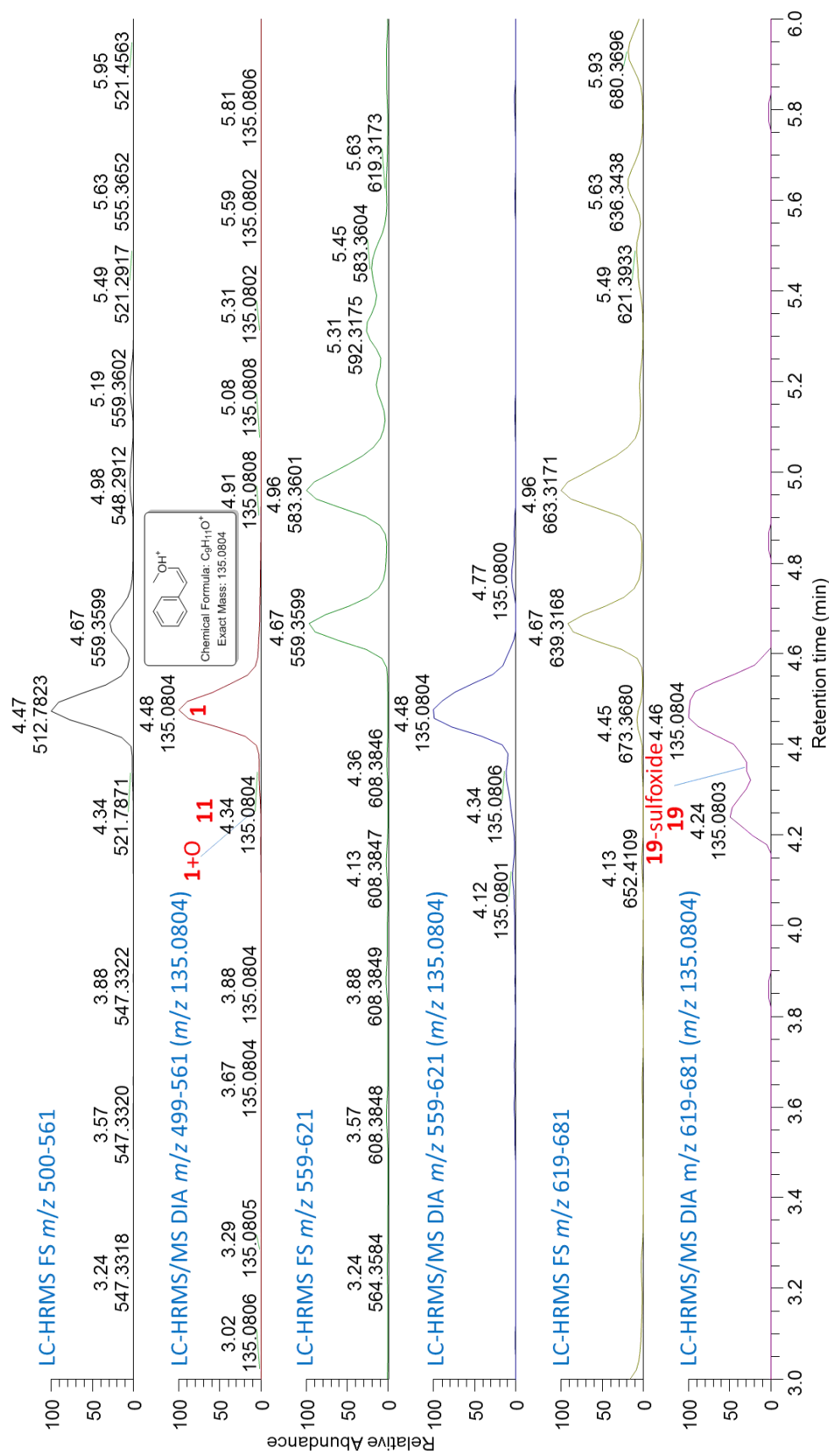
**Figure S10.** Positive ionization LC–MS/MS FS/DIA chromatograms of an extract of NIVA-CYA 544 at natural abundance extracted at *m/z* 135.0804 ($C_9H_{11}O^+$) from the Adda[5]-moiety.
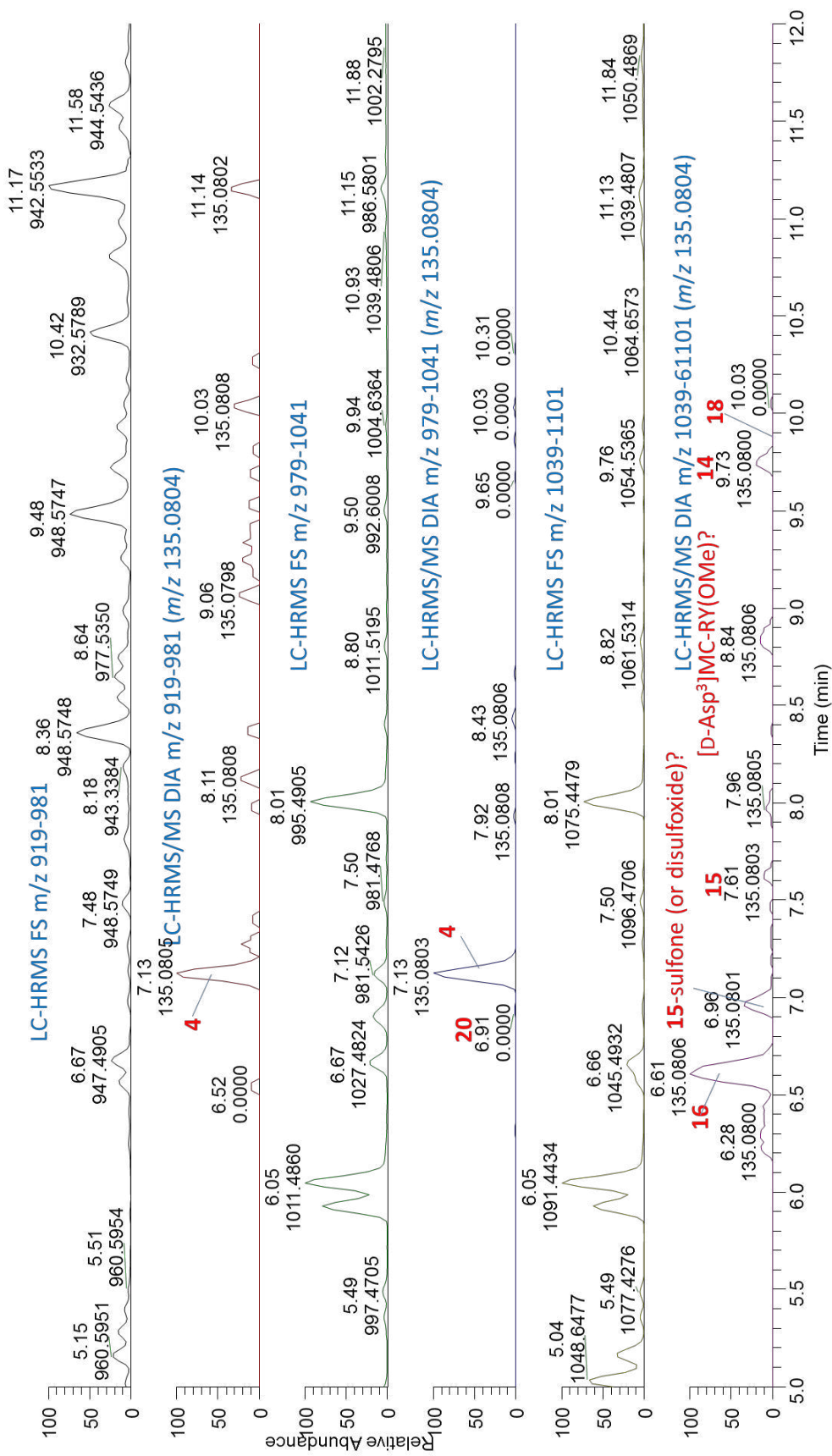
**Figure S11.** Positive ionization LC−MS/MS FS/DIA chromatograms of an extract of NIVA-CYA 544 at natural abundance extracted at $m/z$ 135.0804 ($C_9H_{11}O^+$) from the Adda[5]-moiety.
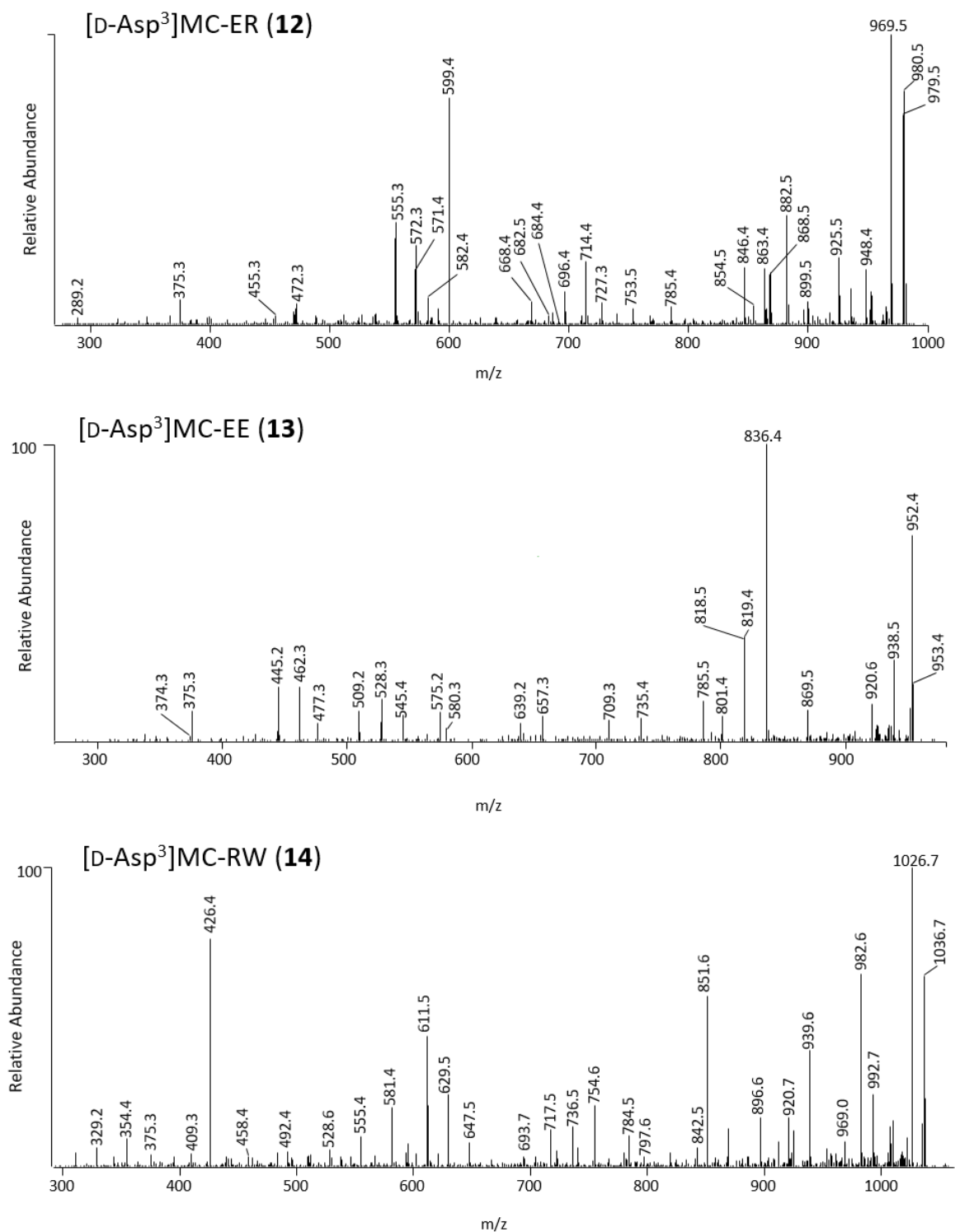
**Figure S12.** LC–MS$^2$ (method C) product ion spectra from collision-induced fragmentation of the [M + H]$^+$ ions of [D-Asp$^3$]MC-ER (**12**), [D-Asp$^3$]MC-EE (**13**) and [D-Asp$^3$]MC-RW (**14**).
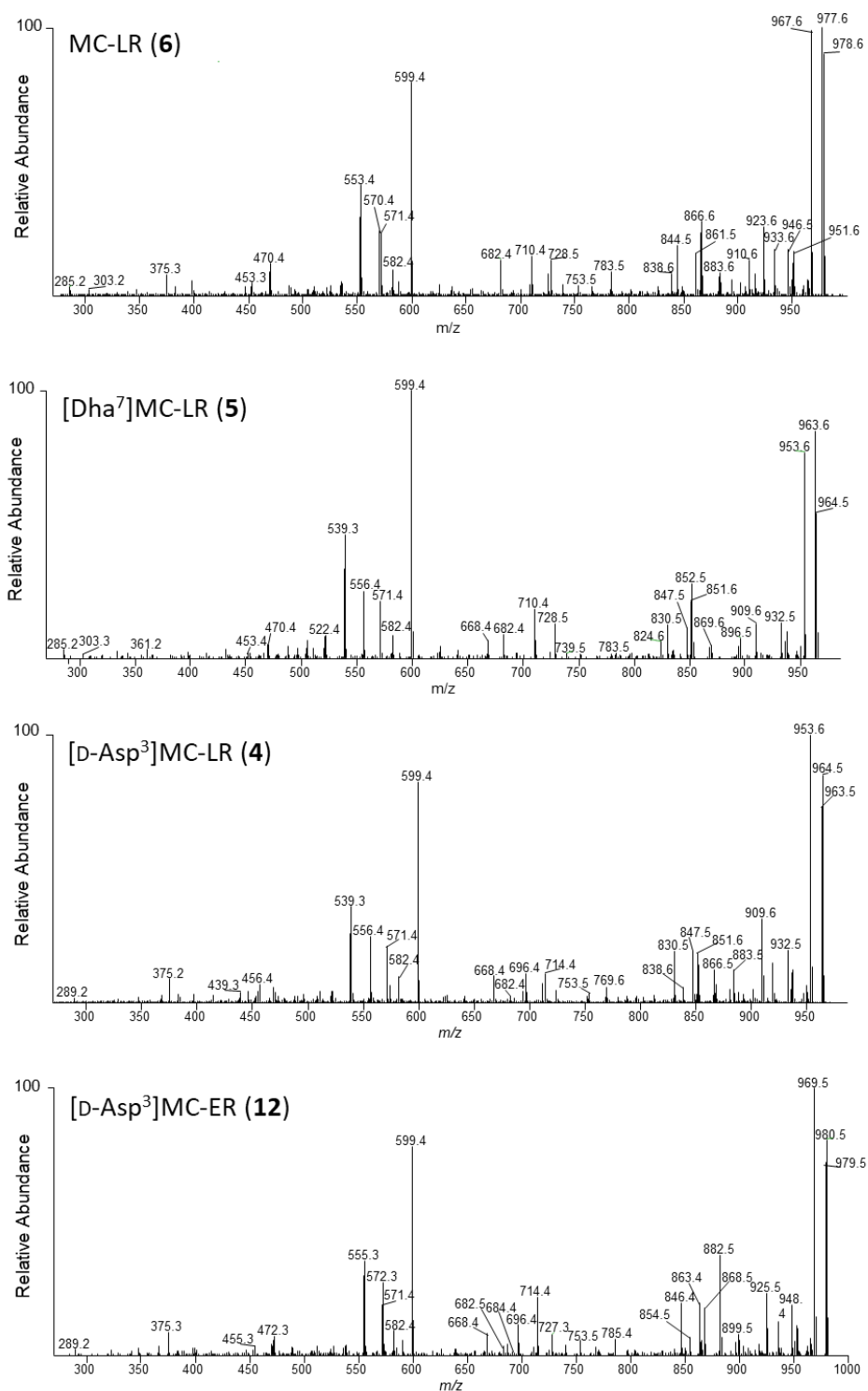
**Figure S13.** LC–MS/MS (method C) positive product ion spectra from collision-induced fragmentation of the [M + H]$^+$ ions of MC-LR (**6**), [Dha$^7$]MC-LR (**5**), [D-Asp$^3$]MC-LR (**4**) and [D-Asp$^3$]MC-ER (**12**).
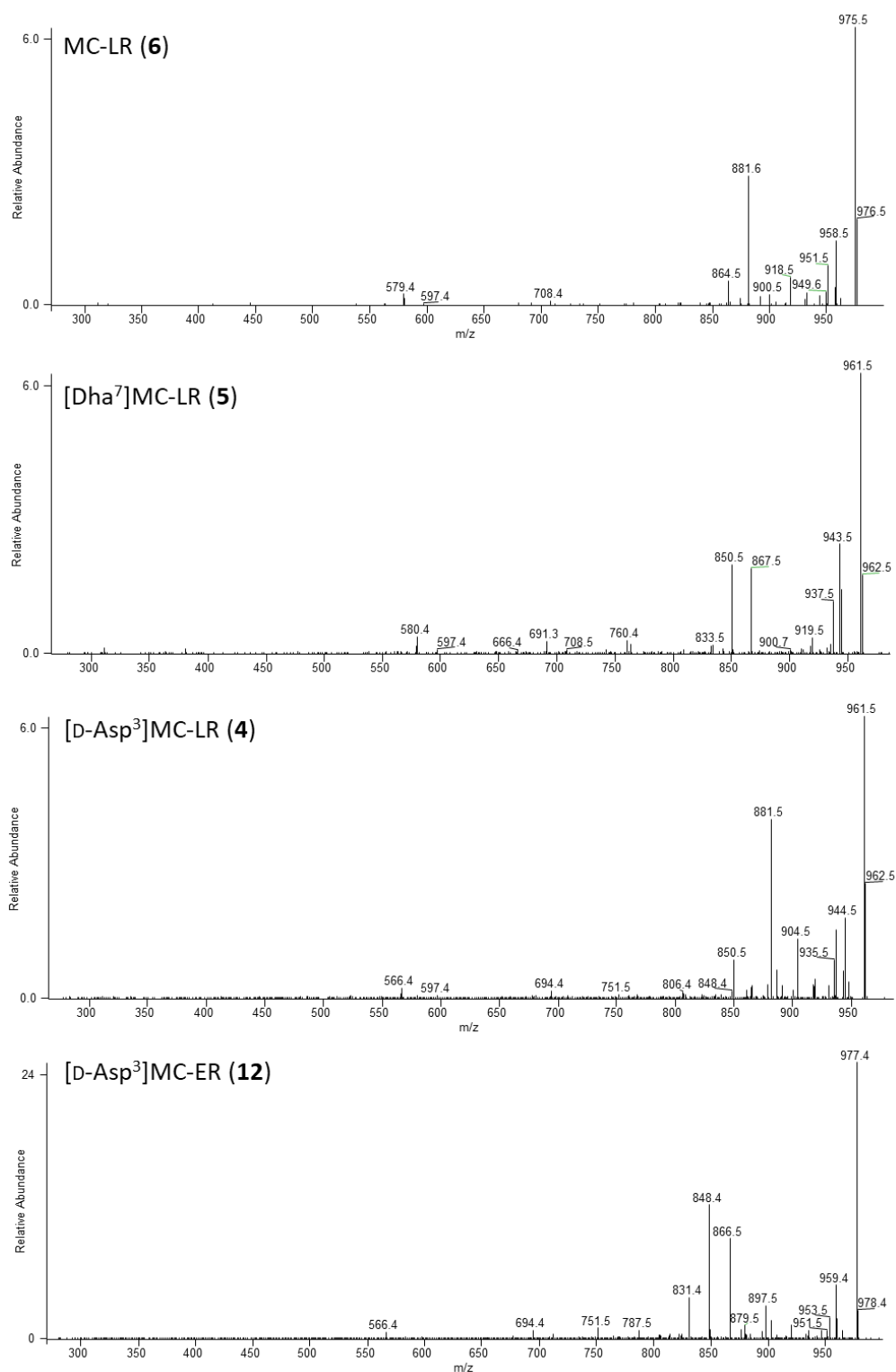
**Figure S14.** LC–MS/MS (method C) negative product ion spectra from collision-induced fragmentation of the [M − H]⁻ ions of MC-LR (**6**), [Dha⁷]MC-LR (**5**), [D-Asp³]MC-LR (**4**) and [D-Asp³]MC-ER (**12**).
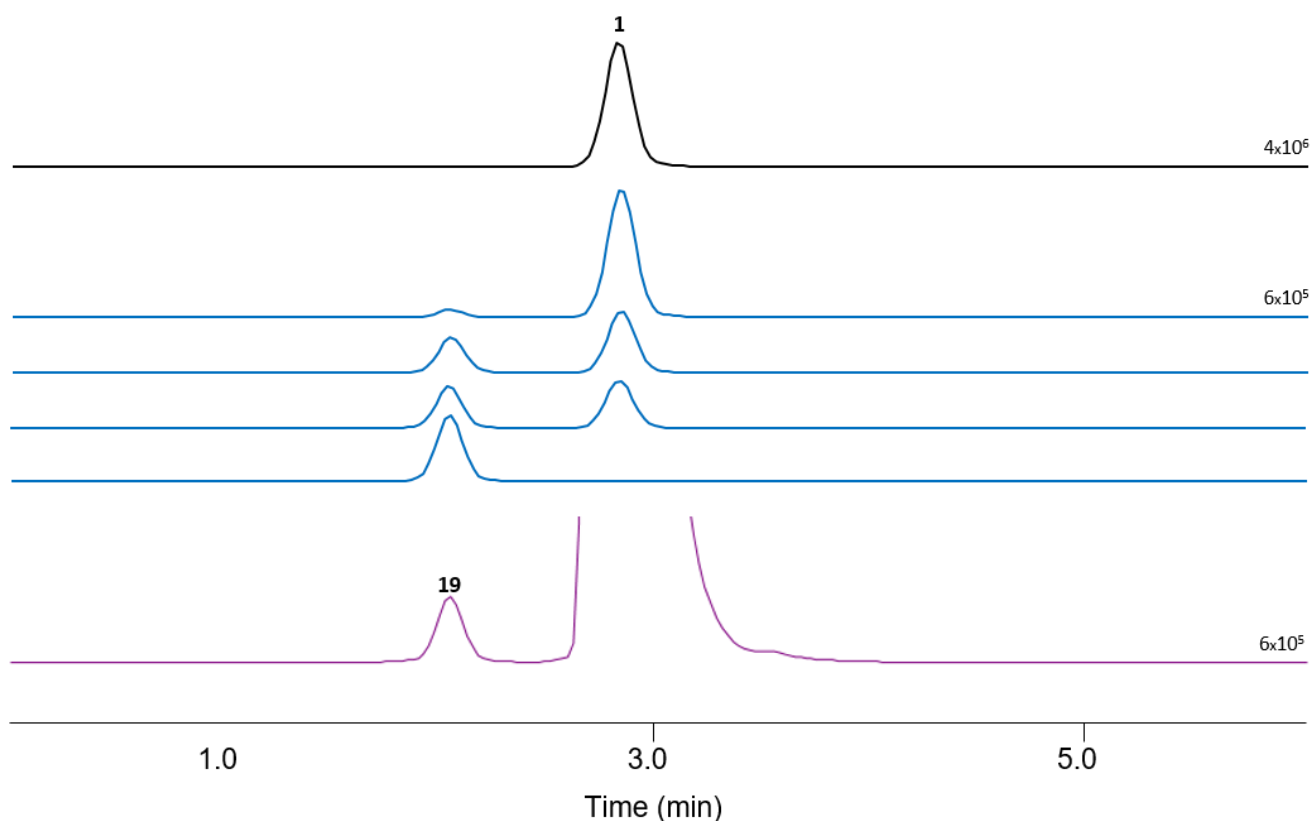
**Figure S15.** Extracted ion (at *m/z* for **1** and **19**) LC−HRMS (method A) chromatograms of: a standard solution of [D-Asp³]MC-RR (**1**) (black); the gradual conversion of standard [D-Asp³]MC-RR (**1**) to the GSH-conjugate of **1** (**19**) by reaction with glutathione in weakly basic solution (blue); an extract of NIVA-CYA 544 showing extracted *m/z* corresponding to [M + H]⁺ for the GSH-conjugate of **1** (**19**) and [D-Asp³]MC-RR (**1**) (purple). Results of the reaction (blue) supported the identification of **19** as the GSH-conjugate of the major microcystin congener **1**, together with elemental composition calculation and comparison of the LC–HRMS characteristics of the products with those of **19** in the culture extract. LC-HRMS/MS spectra of natural **19** in the culture extract and semi-synthetic **19** produced by reaction of **1** with GSH are shown in Figure S39.

**Figure S16.** LC–HRMS/MS PRM spectra (method B) of $[M + 2H]^{2+}$ of $[D-Asp^3]MC-RR$ (**1**) at $m/z$ 512.8 (top), and of nitrogen-15 labelled $[D-Asp^3]MC-RR$ (**1**) at $m/z$ 519.3 (bottom).
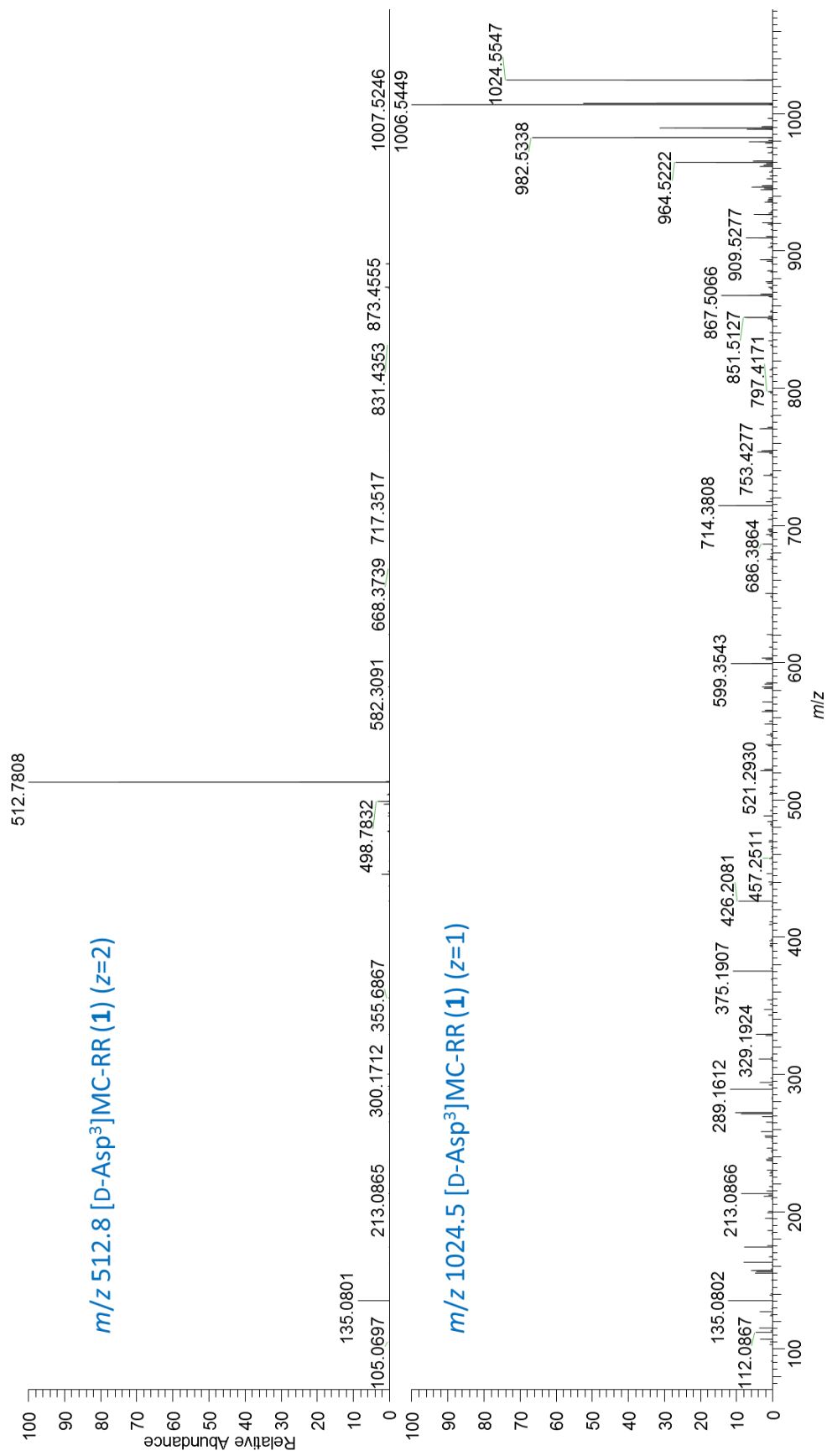
**Figure S17.** LC–HRMS/MS PRM spectra (method B) of $[M + 2H]^{2+}$ of $[D\text{-}Asp^3]MC\text{-}RR$ (**1**) at $m/z$ 512.8 (top), and of $[M + H]^+$ of $[D\text{-}Asp^3]MC\text{-}RR$ (**1**) at $m/z$ 1024.5 (bottom).

*m/z* 981.5 [$^{14}$N$_{10}$][D-Asp$^3$]MC-LR (**4**)

*m/z* 991.5 [$^{15}$N$_{10}$][D-Asp$^3$]MC-LR (**4**)
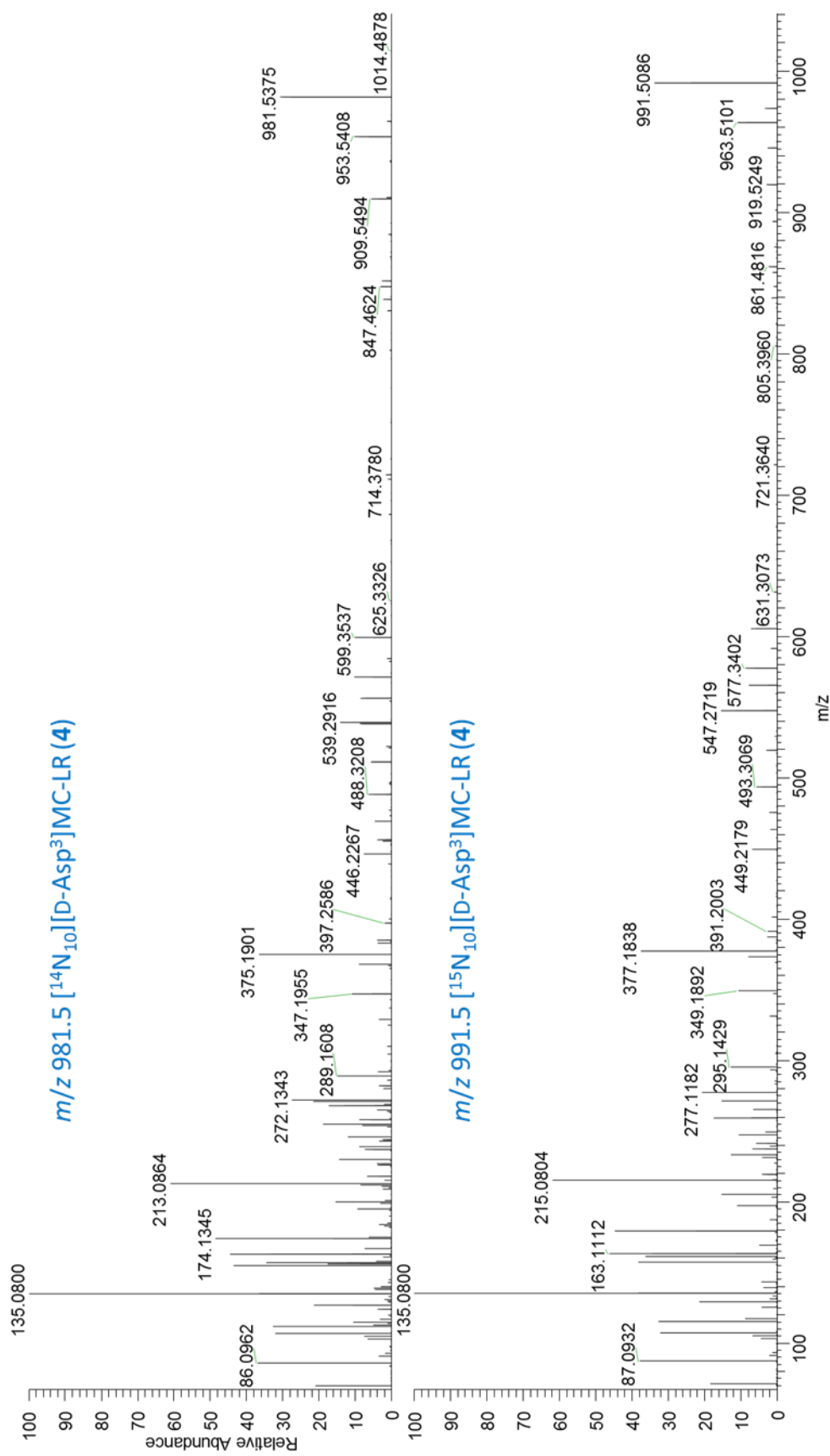
**Figure S18.** LC–HRMS/MS PRM spectra (method B) of [M + H]$^+$ of [D-Asp$^3$]MC-LR (**4**) at *m/z* 981.5 (top), and of nitrogen-15 labelled [D-Asp$^3$]MC-LR (**4**) at *m/z* 991.5 (bottom).
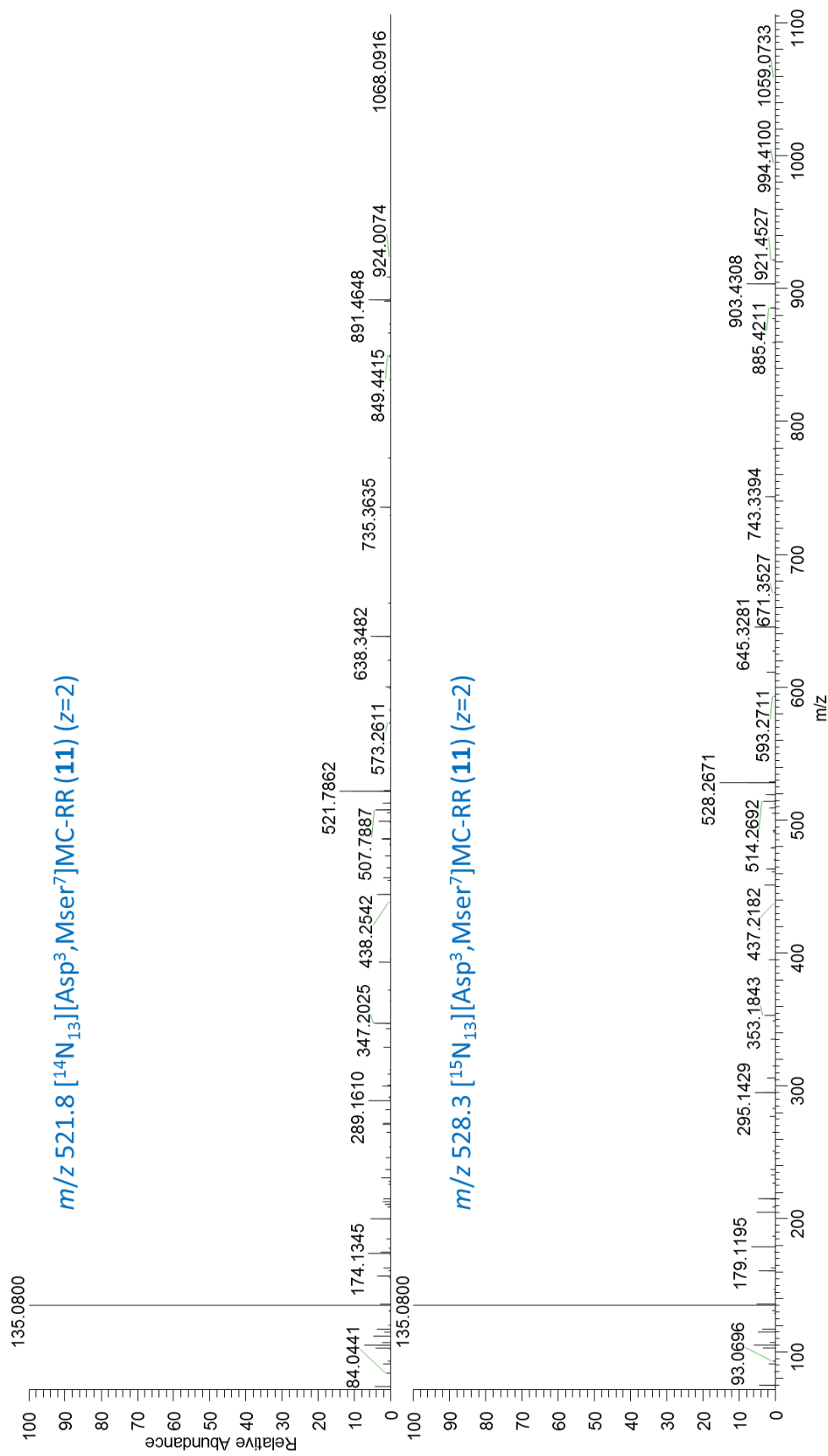
**Figure S19.** LC–HRMS/MS PRM spectra (method B) of [M + 2H]$^{2+}$ of [D-Asp$^3$,Mser$^7$]MC-RR (**11**) at *m/z* 521.8 (top), and of nitrogen-15 labelled [D-Asp$^3$]MC-RR (**11**) at *m/z* 528.3 (bottom).
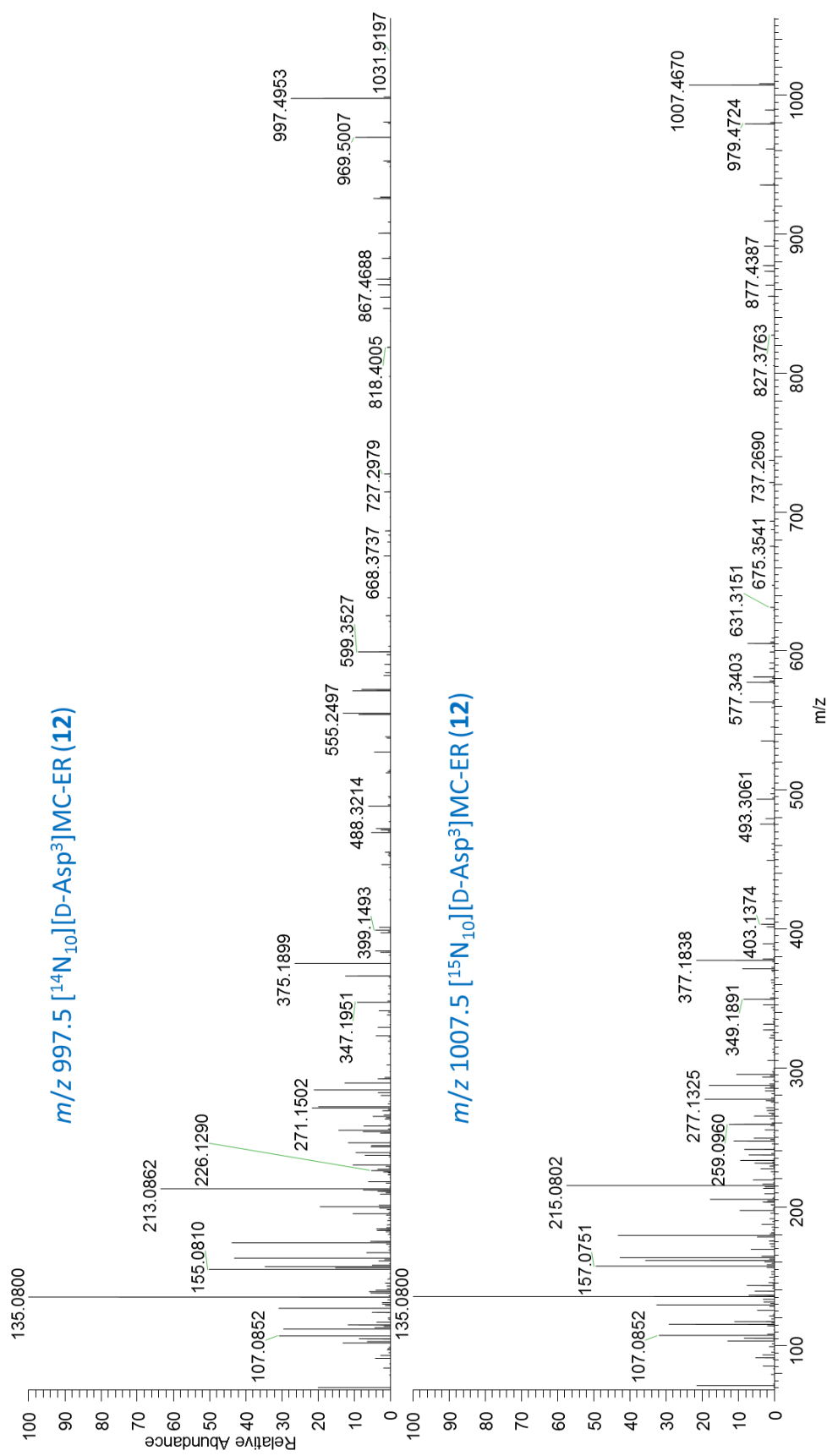
**Figure S20.** LC–HRMS/MS PRM spectra (method B) of [M + H]$^+$ of [D-Asp$^3$]MC-ER (**12**) at $m/z$ 997.5 (top), and of nitrogen-15 labelled [D-Asp$^3$]MC-ER (**12**) at $m/z$ 1007.5 (bottom).

[D-Asp³]MC-LR (**4**)
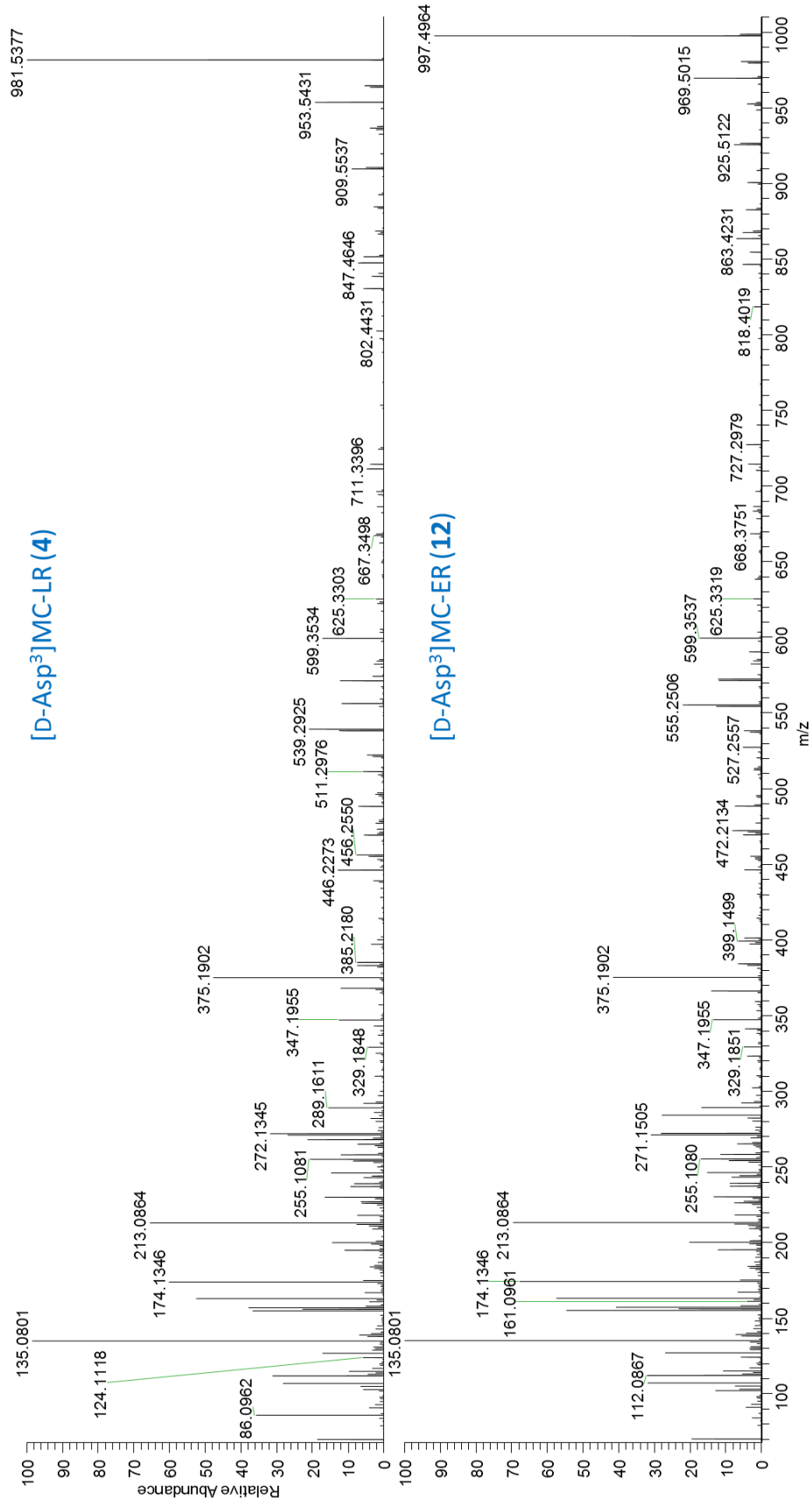
[D-Asp³]MC-ER (**12**)

**Figure S21.** LC–HRMS/MS PRM spectra (method B) of [M + H]⁺ of [D-Asp³]MC-LR (**4**) at *m/z* 981.5 (top), and of [D-Asp³]MC-ER (**12**) at *m/z* 997.5 (bottom).
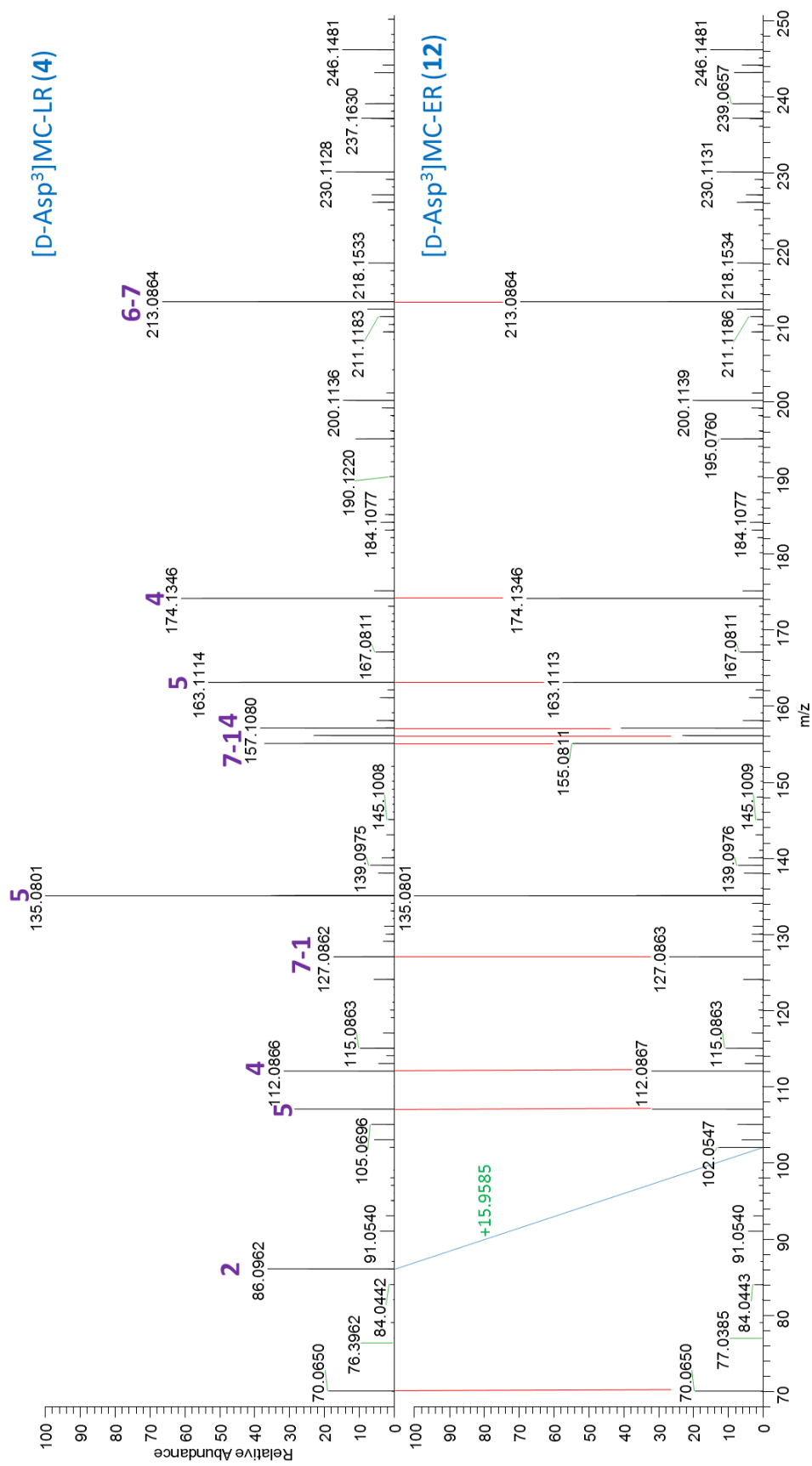
**Figure S22.** Expansion (*m/z* 68–250) of the LC–HRMS/MS PRM spectra (method B) of [M + H]$^{+}$ of [D-Asp$^3$]MC-LR (**4**) at *m/z* 981.5 (top), and of [D-Asp$^3$]MC-ER (**12**) at *m/z* 997.5 (bottom). Blue lines join selected peaks that differ by *m/z* +15.9595, which is the exact mass difference between **4** and **12**, and between leucine and glutamic acid. The bold purple numbers indicate the amino acid residue numbers of the amino acids attributed to selected product ions based on Yilmaz et al.$^l$ The results show that **4** and **12** differ by 15.9595 Da in amino acid-2.
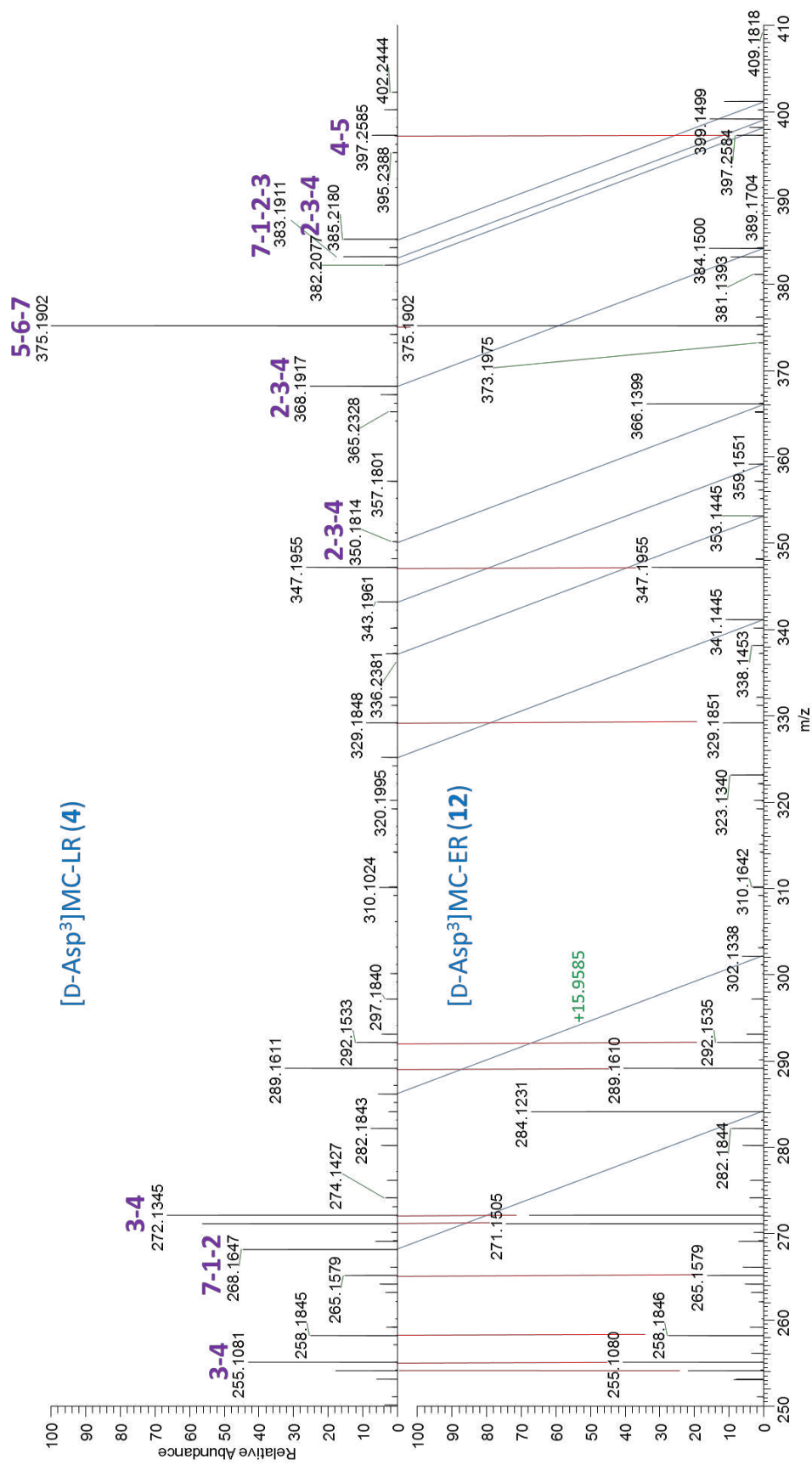
**Figure S23.** Expansion (*m/z* 250–410) of the LC–HRMS/MS PRM spectra (method B) of [M + H]⁺ of [D-Asp³]MC-LR (**4**) at *m/z* 981.5 (top), and of [D-Asp³]MC-ER (**12**) at *m/z* 997.5 (bottom). Blue lines join selected peaks that differ by *m/z* +15.9595, which is the exact mass difference between **4** and **12** (and between leucine and glutamic acid). The bold purple numbers indicate the amino acid residue numbers of the amino acids attributed to selected product ions based on Yilmaz et al. (2019). The results show that **4** and **12** differ by 15.9595 Da in amino acid-2.
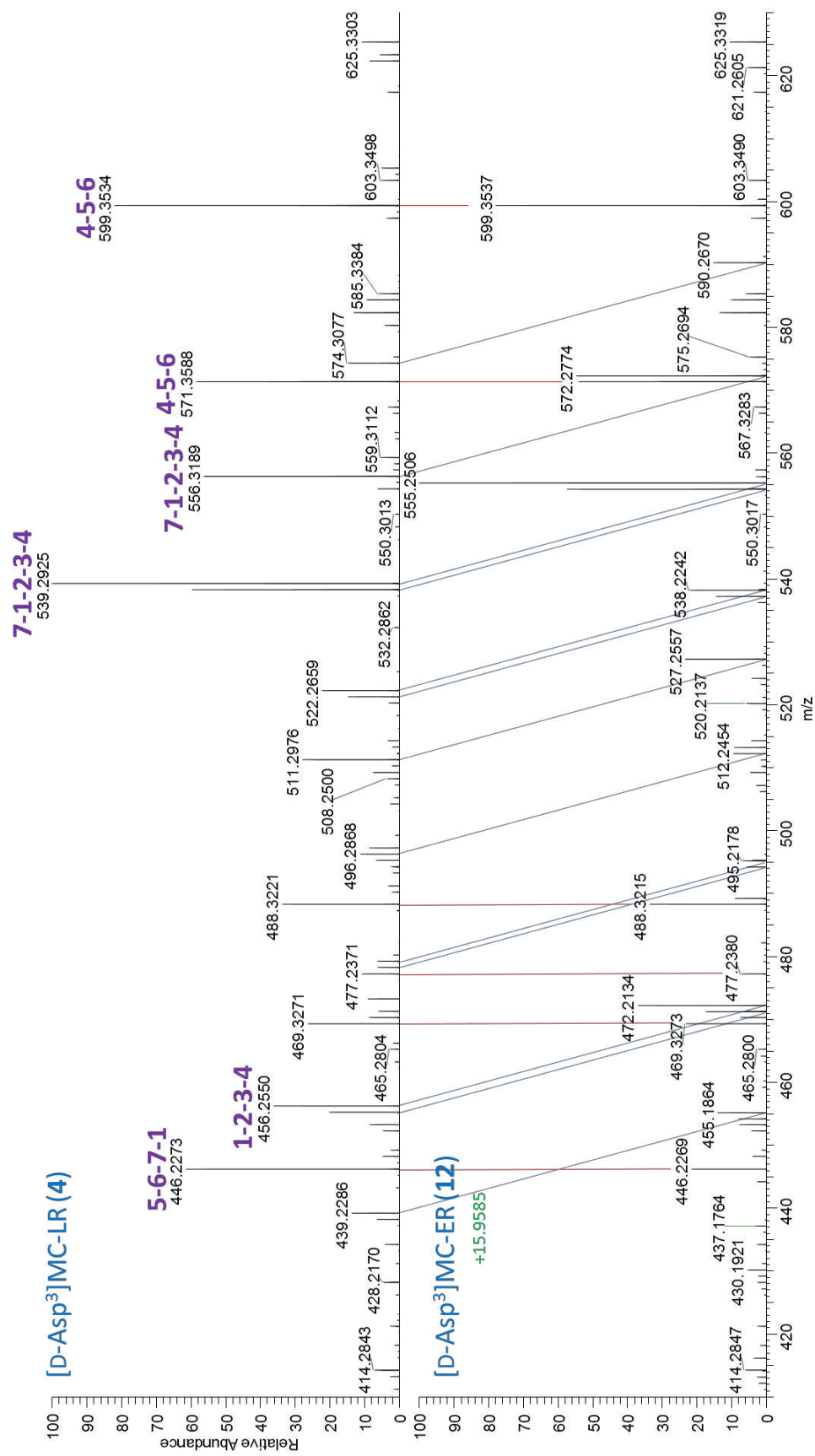
**Figure S24.** Expansion (*m/z* 410–630) of the LC–HRMS/MS PRM spectra (method B) of [M + H]⁺ of [D-Asp³]MC-LR (**4**) at *m/z* 981.5 (top), and of [D-Asp³]MC-ER (**12**) at *m/z* 997.5 (bottom). Blue lines join selected peaks that differ by *m/z* +15.9595, which is the exact mass difference between **4** and **12** (and between leucine and glutamic acid). The bold purple numbers indicate the amino acid residue numbers of the amino acids attributed to selected product ions based on Yilmaz et al. (2019). The results show that **4** and **12** differ by 15.9595 Da in amino acid-2.
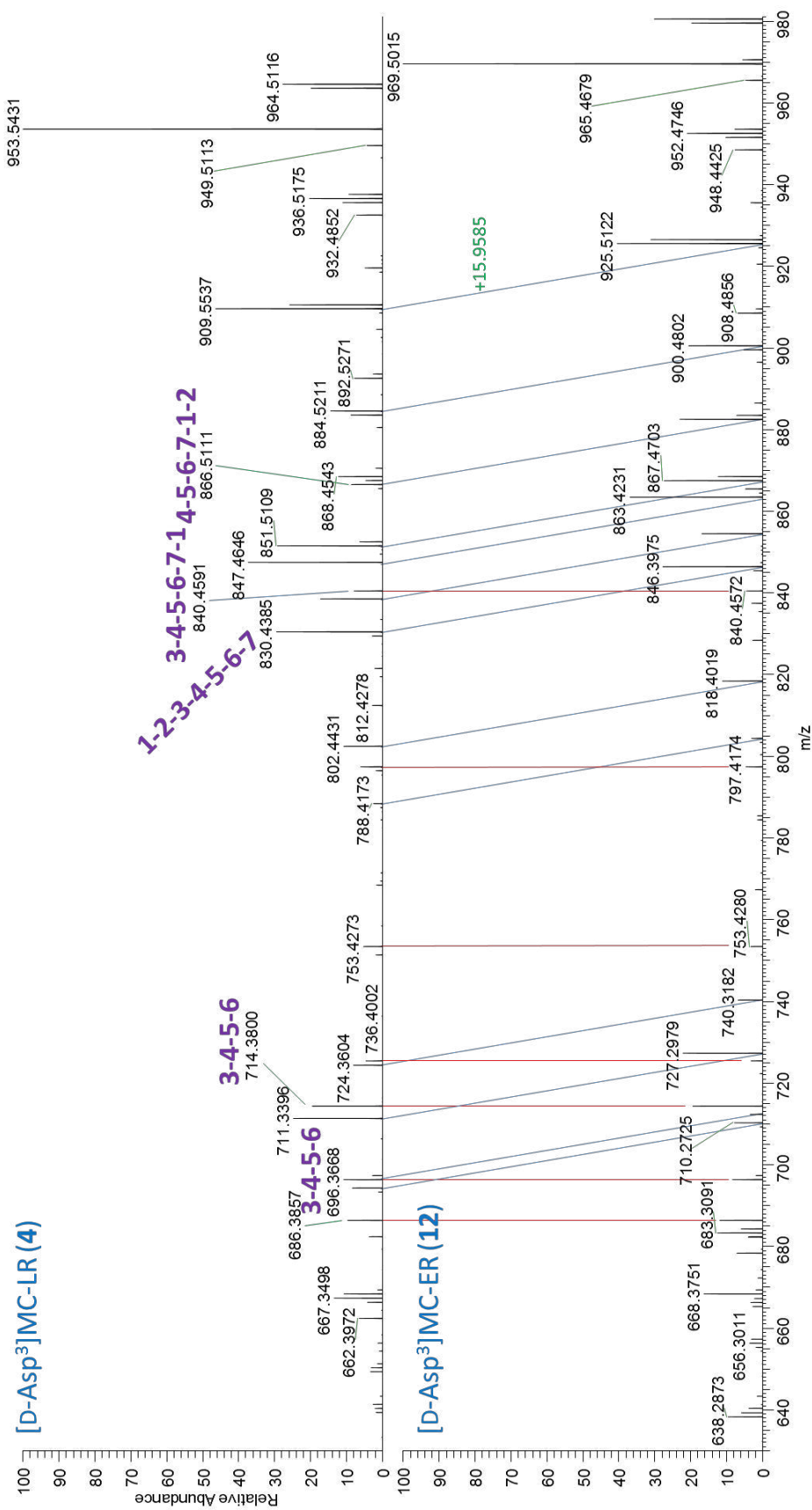
**Figure S25.** Expansion (*m/z* 630–981) of the LC–HRMS/MS PRM spectra (method B) of [M + H]$^+$ of [D-Asp$^3$]MC-LR (**4**) at *m/z* 981.5 (top), and of [D-Asp$^3$]MC-ER (**12**) at *m/z* 997.5 (bottom). Blue lines join selected peaks that differ by *m/z* +15.9595, which is the exact mass difference between **4** and **12** (and between leucine and glutamic acid). The bold purple numbers indicate the amino acid residue numbers of the amino acids attributed to selected product ions based on Yilmaz et al. (2019). T

he results show that **4** and **12** differ by 15.9595 Da in amino acid-2.
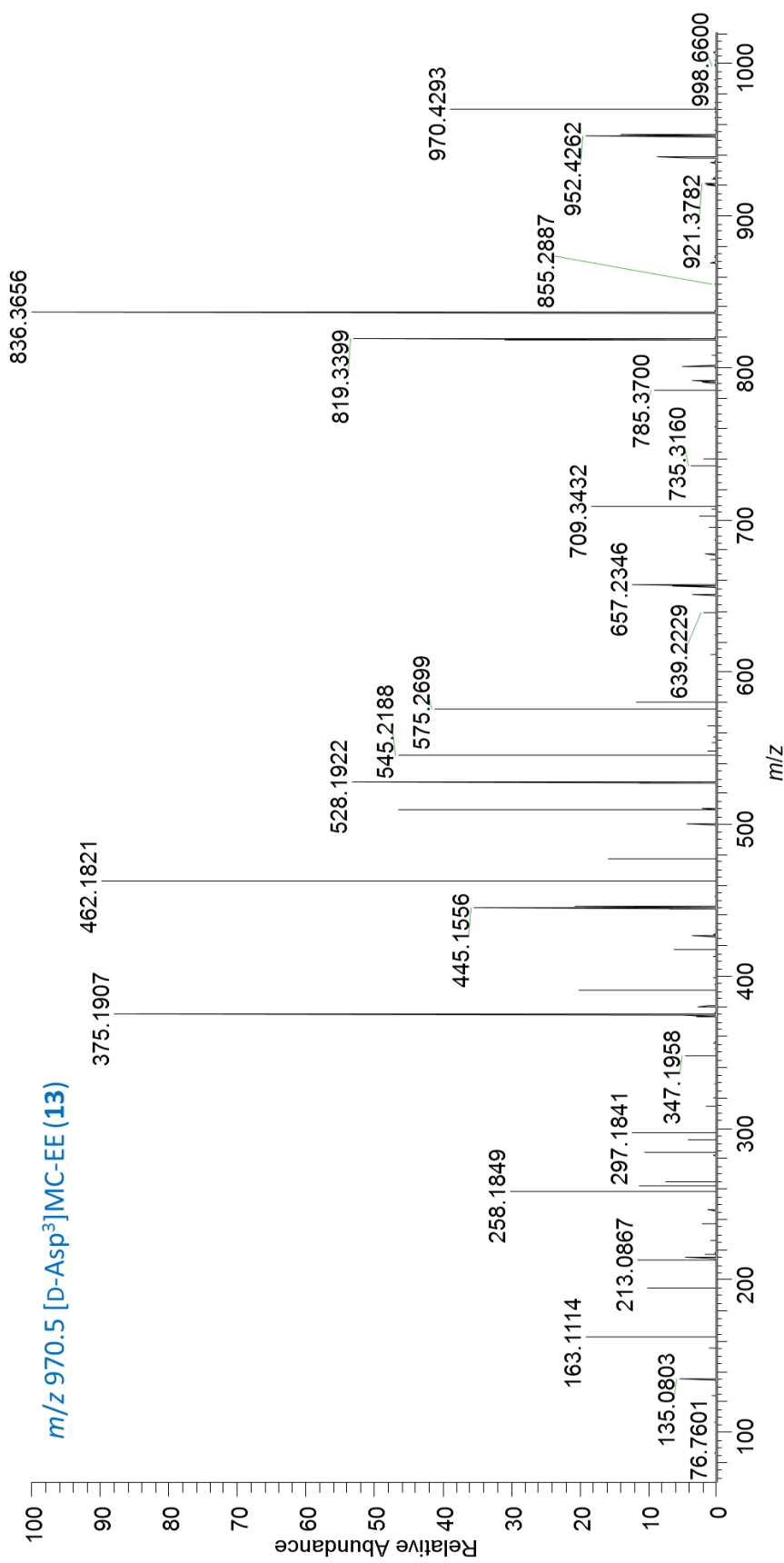
**Figure S26.** LC–HRMS/MS PRM spectrum (method B) of [M + H]$^+$ of [D-Asp$^3$]MC-EE (**13**) at *m/z* 970.5.
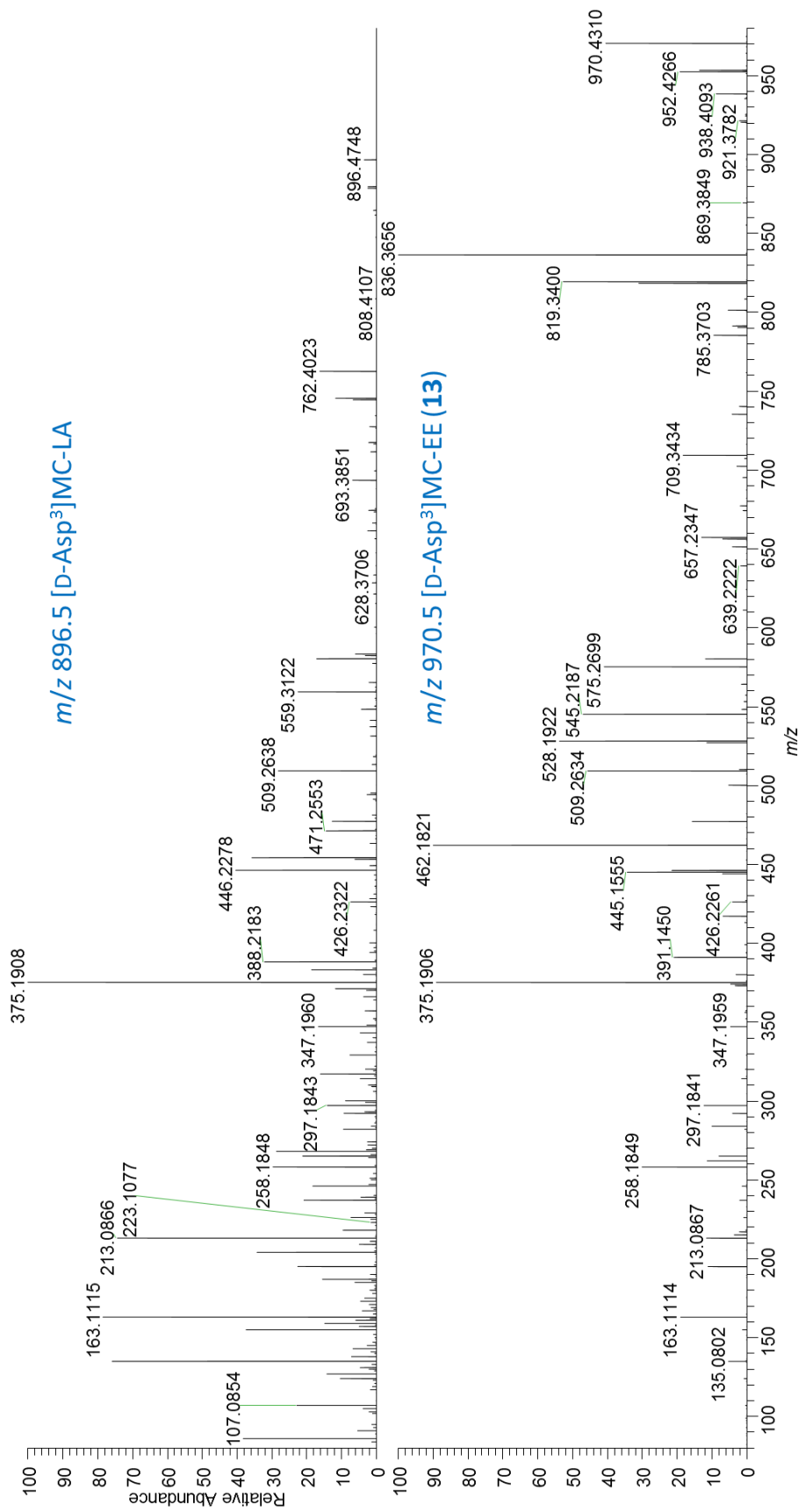
**Figure S27.** LC–HRMS/MS PRM spectra (method B) of [M + H]$^+$ of [D-Asp$^3$]MC-LA at *m/z* 896.5 (top), and of [D-Asp$^3$]MC-EE (**13**) at *m/z* 970.5 (bottom).
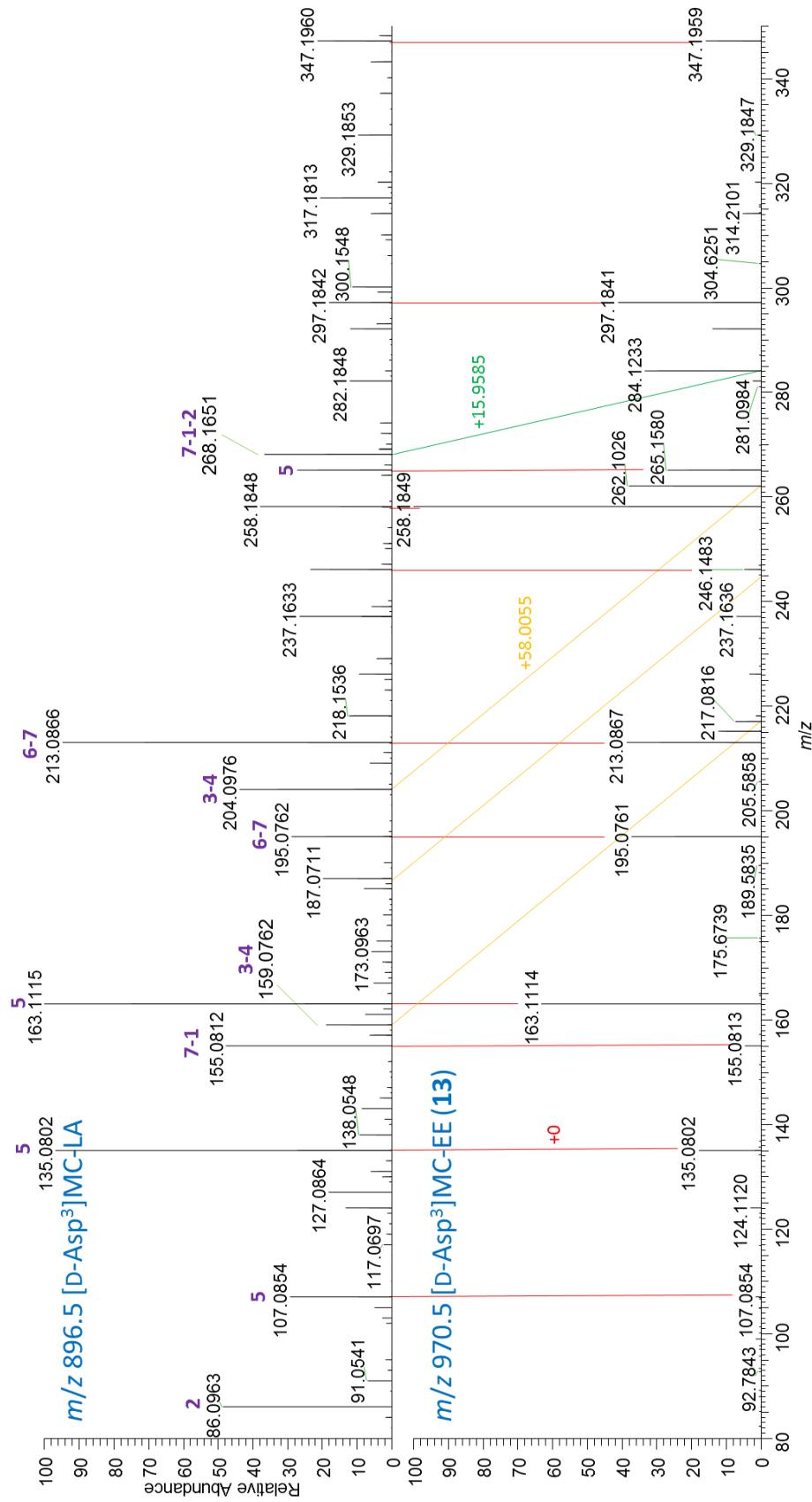
**Figure S28.** Expansion (*m/z* 80–350) of the LC–HRMS/MS PRM spectra (method B) of [M + H]⁺ of [D-Asp³]MC-LA at *m/z* 896.5 (top), and of [D-Asp³]MC-EE (**13**) at *m/z* 970.5 (bottom). Blue lines join peaks differing by *m/z* +73.9640 (the exact mass difference between [D-Asp³]MC-LA and **13**) and contain both amino acid-2 and -4; orange lines join peaks differing by *m/z* +58.0055 (the difference in exact mass between Ala and Glu) and contain amino acid-4 but not -2; green lines join peaks differing by *m/z* +15.9585 (the difference in exact mass between Leu and Glu) and contain amino acid-2 but not -4; red lines join peaks that do not differ between the two compounds, and thus contain neither amino acid-2 nor -4. Bold purple numbers indicate the amino acid residue numbers of the amino acids attributed to selected product ions based on LeBlanc et al.[2] The results show that **13** and [D-Asp³]MC-LA differ by +15.9585 Da in amino acid-2 and by +58.0055 in amino acid-4.

**Figure S29.** Expansion (*m/z* 330–670) of the LC–HRMS/MS PRM spectra (method B) of [M + H]$^+$ of [D-Asp$^3$]MC-LA at *m/z* 896.5 (top), and of [D-Asp$^3$]MC-EE (**13**) at *m/z* 970.5 (bottom). Blue lines join peaks differing by *m/z* +73.9640 (the exact mass difference between [D-Asp$^3$]MC-LA and **13**) and contain both amino acid-2 and -4; orange lines join peaks differing by *m/z* +58.0055 (the difference in exact mass between Ala and Glu) and contain amino acid-4 but not -2; green lines join peaks differing by *m/z* +15.9585 (the difference in exact mass between Leu and Glu) and contain amino acid-2 but not -4; red lines join peaks that do not differ between the two compounds, and thus contain neither amino acid-2 nor -4. Bold purple numbers indicate the amino acid residue numbers of the amino acids attributed to selected product ions based on LeBlanc et al.[2] The results show that **13** and [D-Asp$^3$]MC-LA differ by +15.9585 Da in amino acid-2 and by +58.0055 in amino acid-4.

**Figure S30.** Expansion (*m/z* 560–980) of the LC–HRMS/MS PRM spectra (method B) of [M + H]⁺ of [D-Asp³]MC-LA at *m/z* 896.5 (top), and of [D-Asp³]MC-EE (**13**) at *m/z* 970.5 (bottom). Blue lines join peaks differing by *m/z* +73.9640 (the exact mass difference between [D-Asp³]MC-LA and **13**) and contain both amino acid-2 and -4; orange lines join peaks differing by *m/z* +58.0055 (the difference in exact mass between Ala and Glu) and contain amino acid-4 but not -2; green lines join peaks differing by *m/z* +15.9585 (the difference in exact mass between Leu and Glu) and contain amino acid-2 but not -4; red lines join peaks that do not differ between the two compounds, and thus contain neither amino acid-2 nor -4. Bold purple numbers indicate the amino acid residue numbers of the amino acids attributed to selected product ions based on LeBlanc et al.² The results show that **13** and [D-Asp³]MC-LA differ by +15.9585 Da in amino acid-2 and by +58.0055 in amino acid-4.

**Figure S31.** LC–HRMS/MS PRM spectrum (method B) of [M + H]$^+$ of [D-Asp$^3$]MC-RW (**14**) at $m/z$ 1054.5.
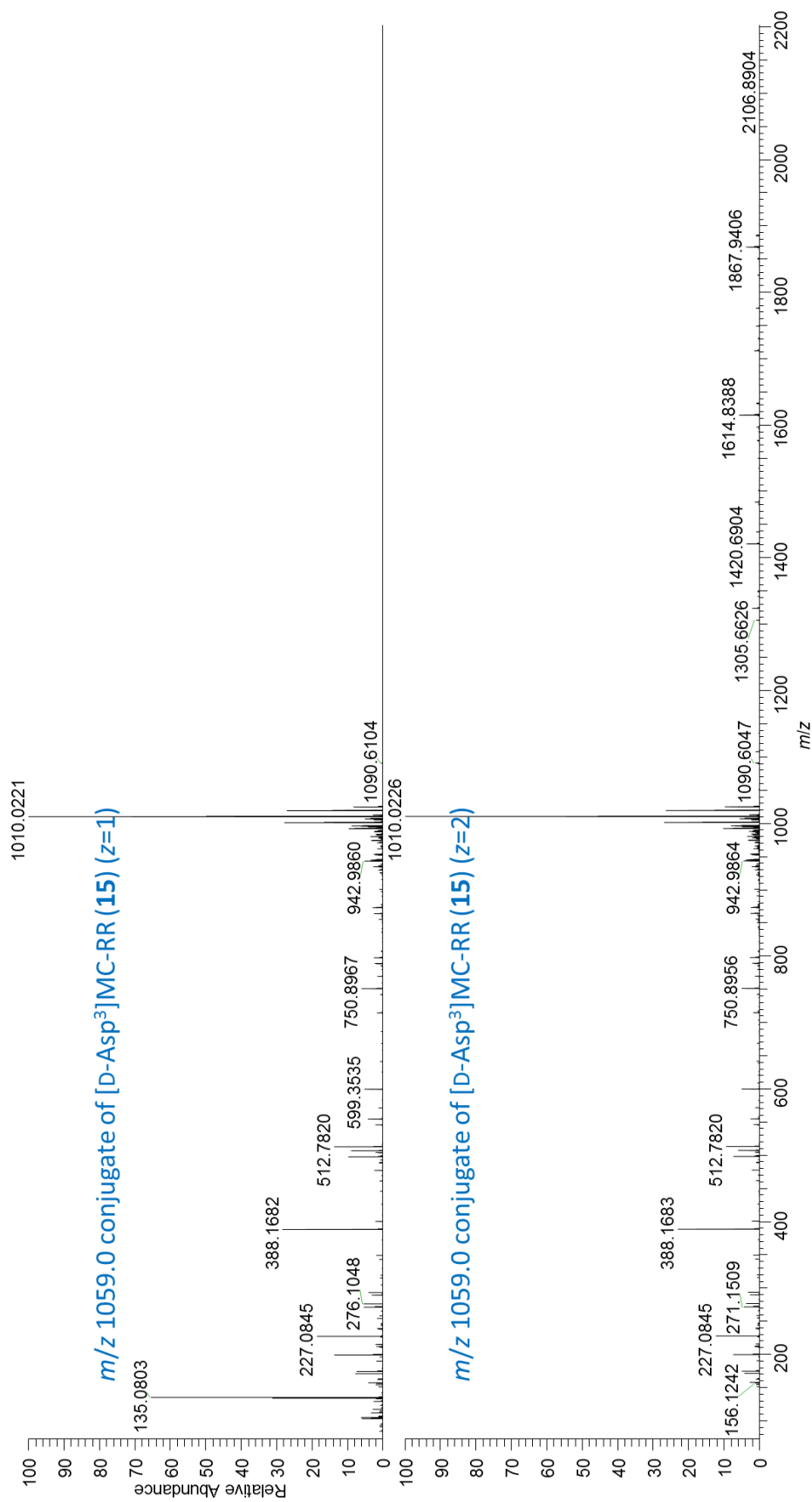
**Figure S32.** LC–HRMS/MS PRM spectra (method B) of $[M + 2H]^{2+}$ of the sulfide conjugate of [D-Asp³]MC-RR (**15**) at *m/z* 1059.0 recorded with setting *z* = 1 (top) leading to scanning from *m/z* 73–1100, and recorded with setting *z* = 2 leading to scanning from *m/z* 145–2180 (bottom).
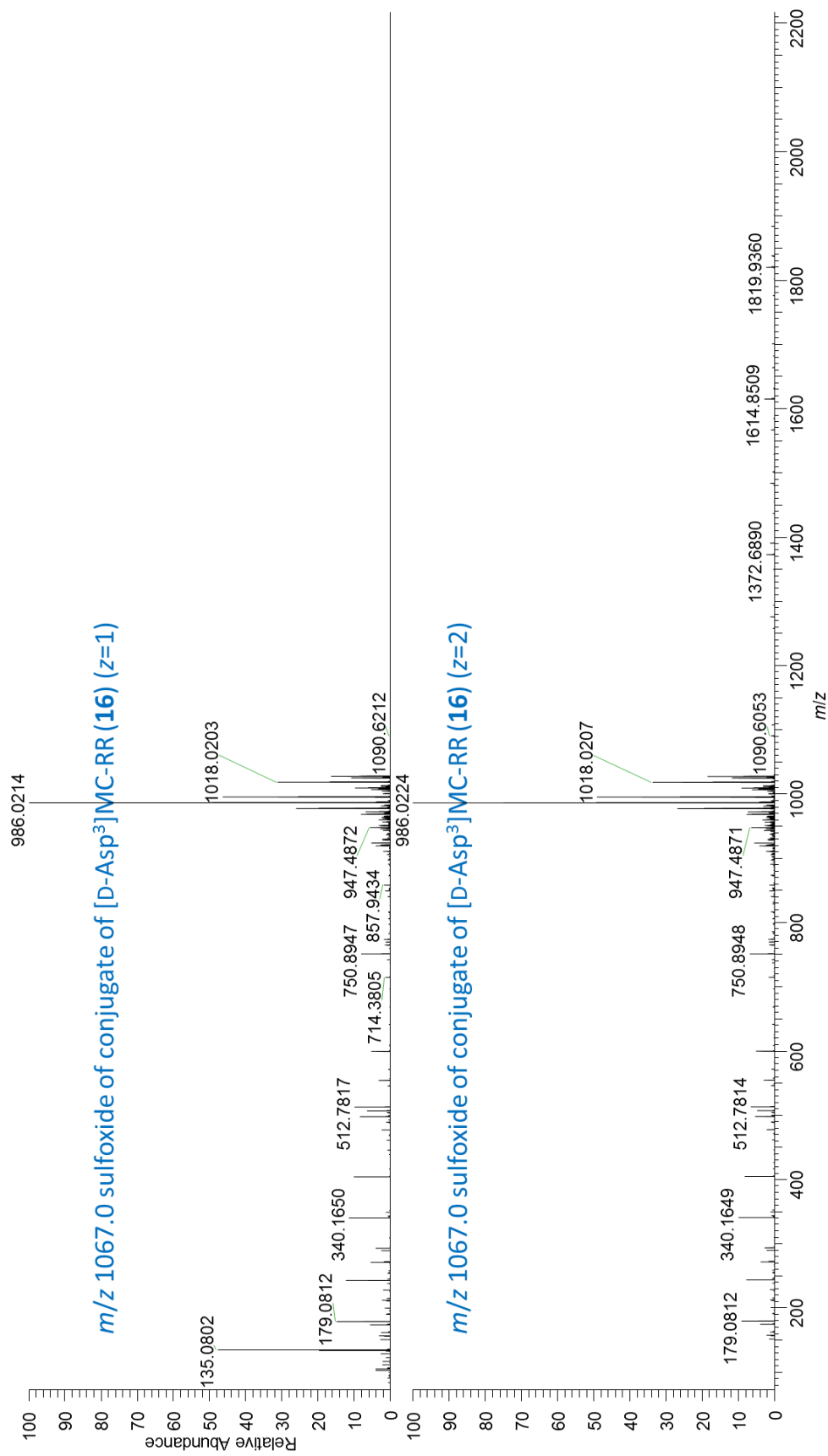
**Figure S33.** LC–HRMS/MS PRM spectra (method B) of [M + 2H]$^{2+}$ of the sulfoxide conjugate of [D-Asp$^3$]MC-RR (**16**) at *m/z* 1067.0 recorded with setting *z* = 1 (top) leading to scanning from *m/z* 73–1105, and recorded with setting *z* = 2 leading to scanning from *m/z* 146–2195 (bottom).
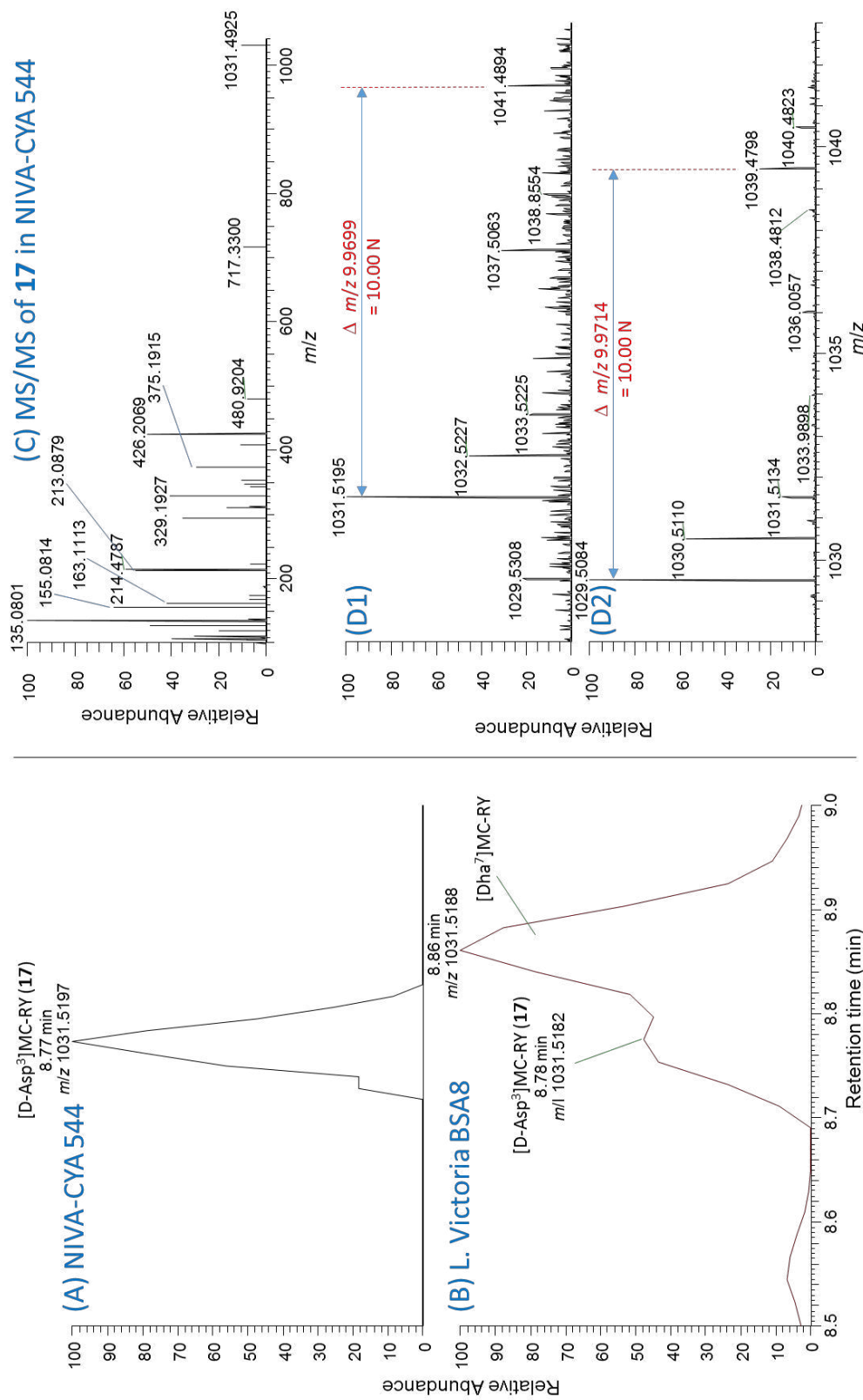
**Figure S34.** Extracted positive ion LC–MS chromatograms (method B) at $m/z$ 1031.5197 an extract of: A, NIVA-CYA 544, and; B, Lake Victoria bloom sample BSA8, showing co-elution of **17** with a sample containing [D-Asp³]MC-RY (**17**). Panel C shows a weak positive ion mode MS/MS spectrum of **17** from NIVA-CYA 544 showing characteristic product ions for an [D-Asp³]MC-RZ congener (*cf.* Figures S31, S35–37). Panels D1 and D2 show positive and negative ion full scan MS spectra of **17** in a mixture of extracts from an unlabelled culture of NIVA-CYA 544 and a culture grown in medium containing 98% ¹⁵N, showing that **17** contains 10 nitrogen atoms (see also Figure S51 for application of the NRC formula calculator to this data).
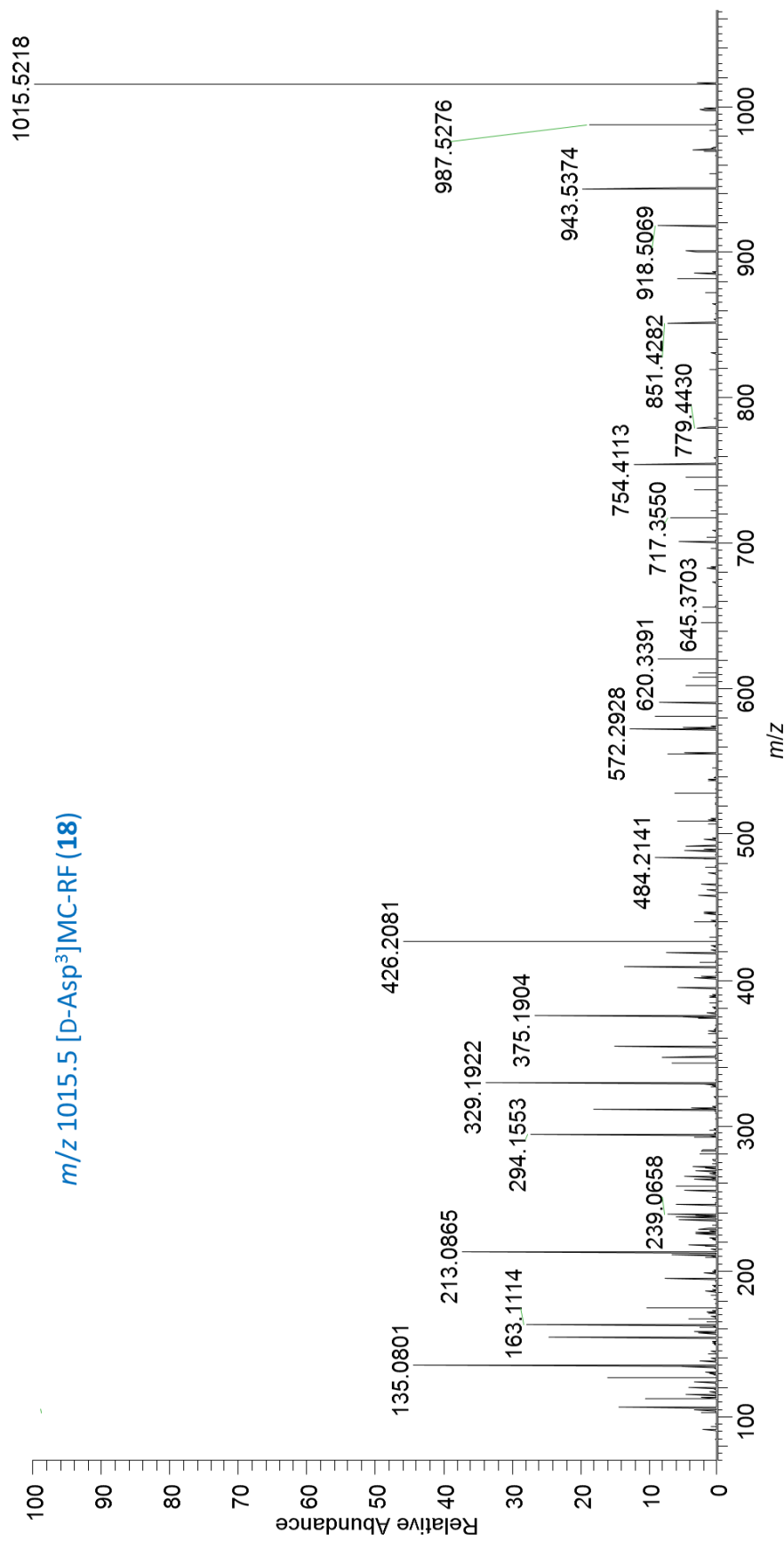
**Figure S35.** LC–HRMS/MS PRM spectrum (method B) of [M + H]$^+$ of [D-Asp$^3$]MC-RF (**18**) at *m/z* 1015.5.
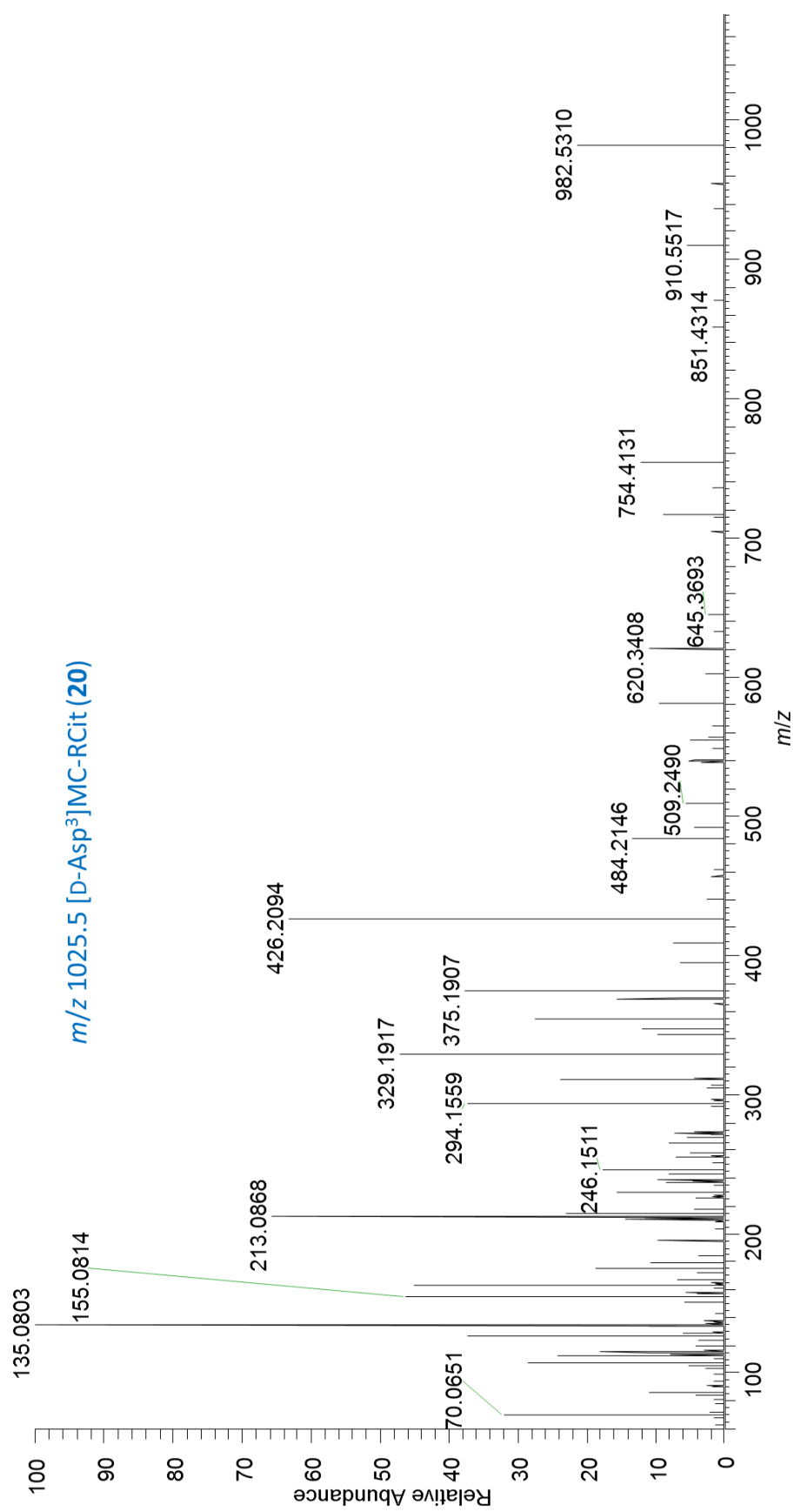
**Figure S36.** LC–HRMS/MS PRM spectrum (method B) of [M + H]$^+$ of [D-Asp$^3$]MC-RCit (**20**) at *m/z* 1025.5.
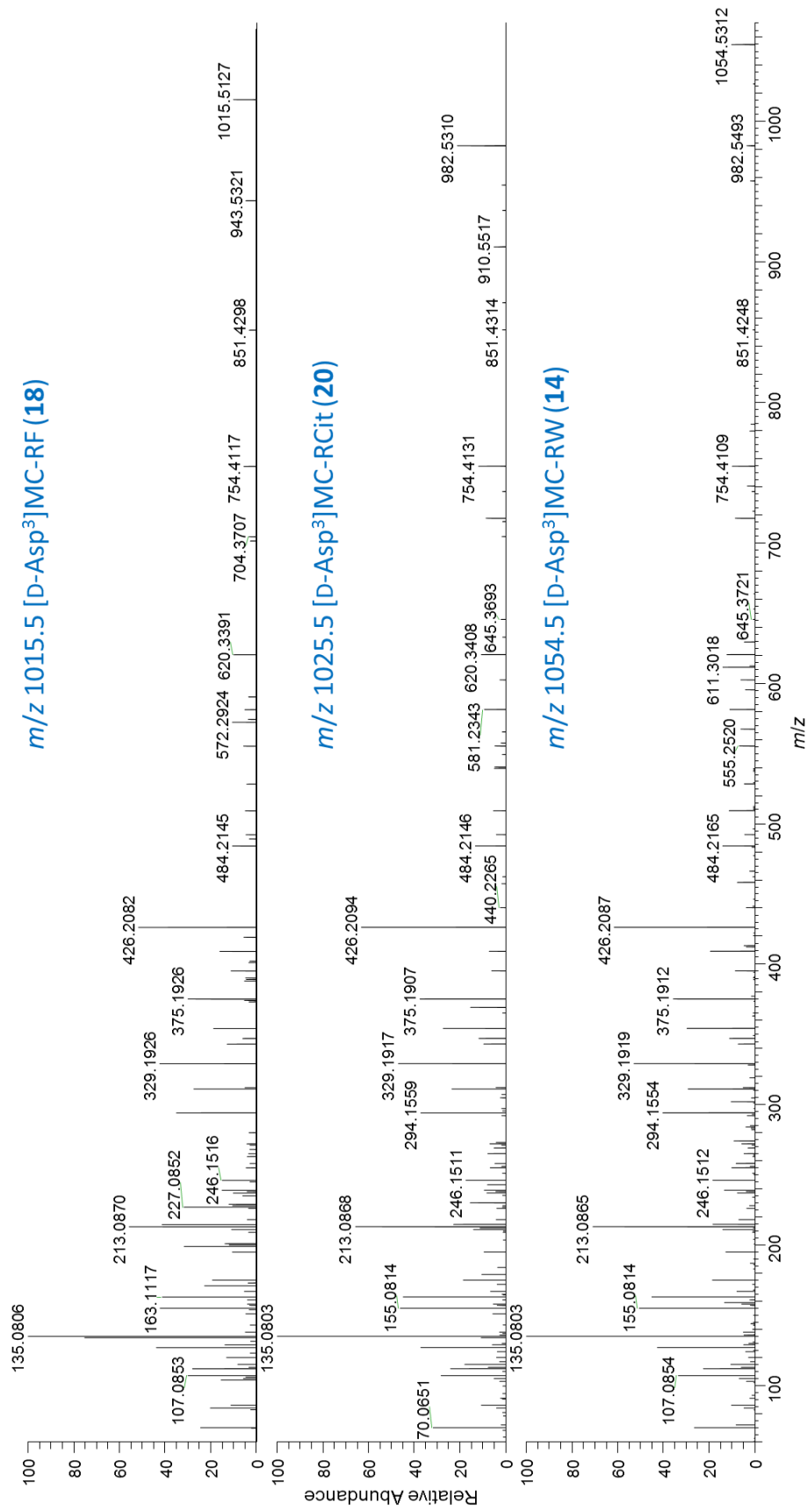
**Figure S37.** LC–HRMS/MS PRM spectra (method B) of [M + H]$^+$ of [D-Asp$^3$]MC-RF (**18**) at *m/z* 1015.5 (top), [D-Asp$^3$]MC-RCit (**20**) at *m/z* 1025.5 (middle), and [D-Asp$^3$]MC-RW (**14**) at *m/z* 1054.5 (bottom). Note the prominent product ions at *m/z* 375.1915 (Adda$^5$–D-Glu$^6$–Mdha$^7$ minus C$_9$H$_{10}$O), and 426.2096 (Dha$^7$–D-Ala$^1$–Arg$^2$–D-Masp$^3$) that are characteristic 3-desmethylated MCs containing Arg at position-2 (i.e. [D-Asp$^3$]MC-RZ) (*cf* also spectra of [D-Asp$^3$]MC-RR (**1**)).
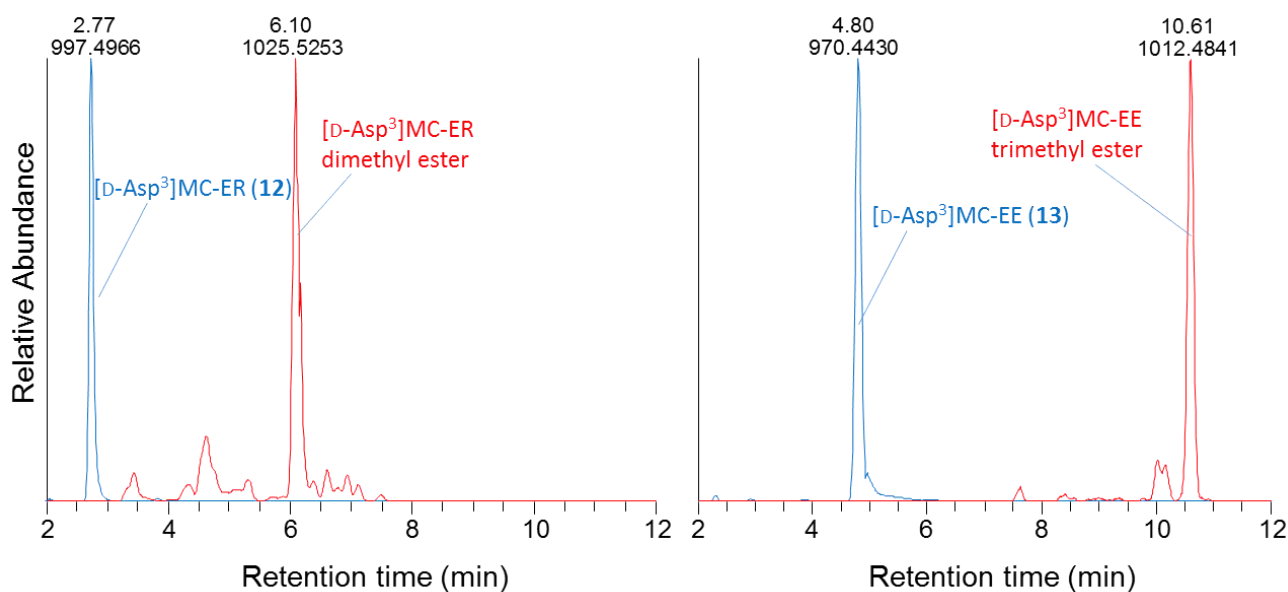
**Figure S38.** Extracted ion LC–HRMS chromatograms (method A) of an extract of NIVA-CYA 544 before (blue) and after (red) esterification with diazomethane. Left, extracted for $m/z$ corresponding to $[M + H]^+$ for [D- Asp$^3$]MC-ER (**12**) and its mono-, di-, and tri-methyl esters; right, extracted for $m/z$ corresponding to $[M + H]^+$ for [D-Asp$^3$]MC-EE (**13**) and its mono-, di-, and tri-methyl esters. Results confirmed the presence of one extra carboxylic acid group in **12**, and two extra carboxylic acid groups in **13**, relative to [D-Asp$^3$]MC-LR (**4**), which was converted almost completely to its mono-methyl ester in the same experiment. Earlier retention times (compared to those ones reported in Table 1 and Table S1) result from use of an older column for monitoring this reaction.
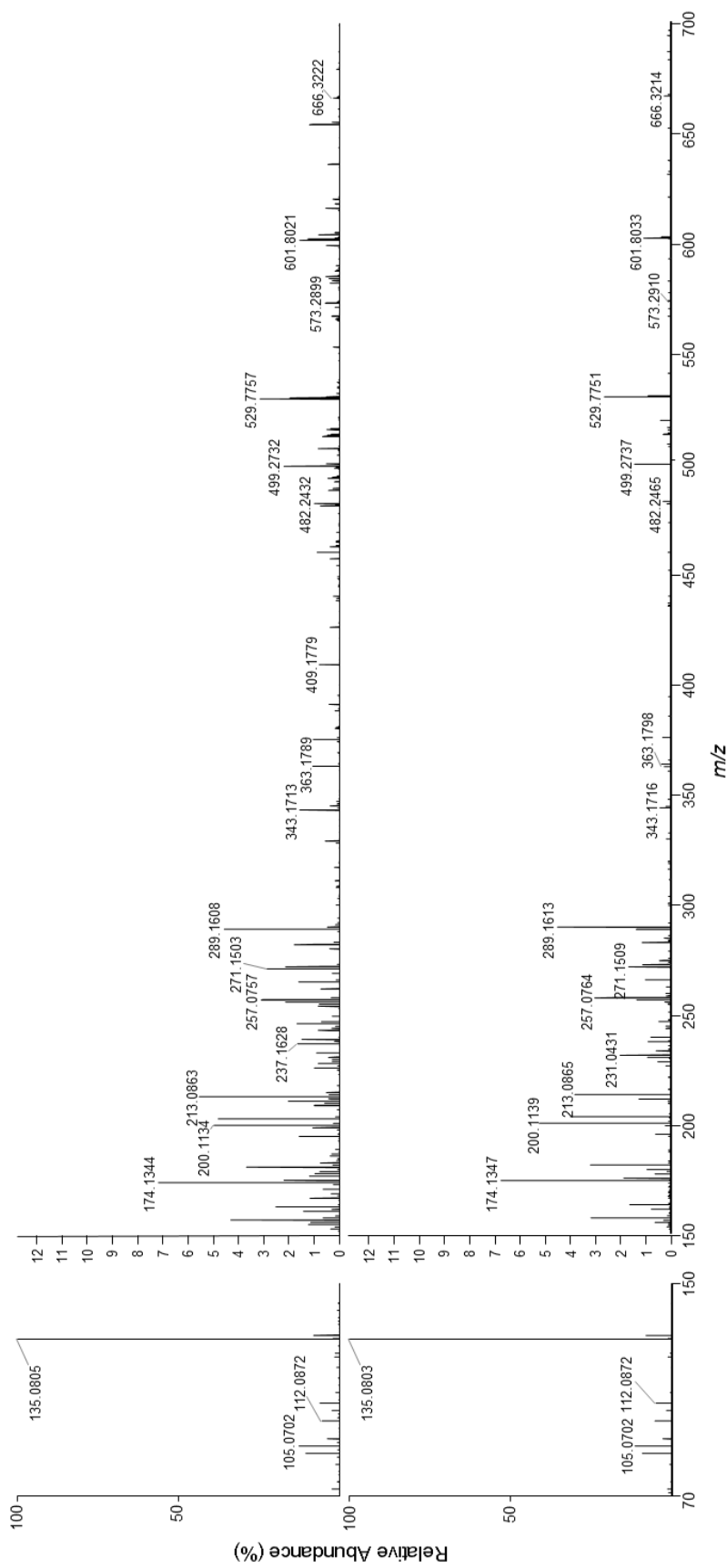
**Figure S39.** LC–HRMS/MS PRM spectra (method A) of $[M + 2H]^{2+}$ of putative GSH-conjugate of **1** (**19**) extracted at *m/z* 666.3. Top, in an extract of NIVA-CYA 544; bottom, in the product obtained from the reaction of a standard of [D-Asp$^3$]MC-RR (**1**) with glutathione (Figure S15). The mass range has been split into two segments with different vertical scales because of the dominance of the Adda-fragment (*m/z* 135.0804) in the spectra. The low mass range (*m/z* 70–150) is shown at full vertical scale (0–100%), whereas an expanded vertical scale (0–13%) was used in the range *m/z* 150–700 to allow visualization of the low-intensity fragments.

LC-HRMS spectrum of unlabeled and $^{15}$N-labelled **1**
Negative ionization mode
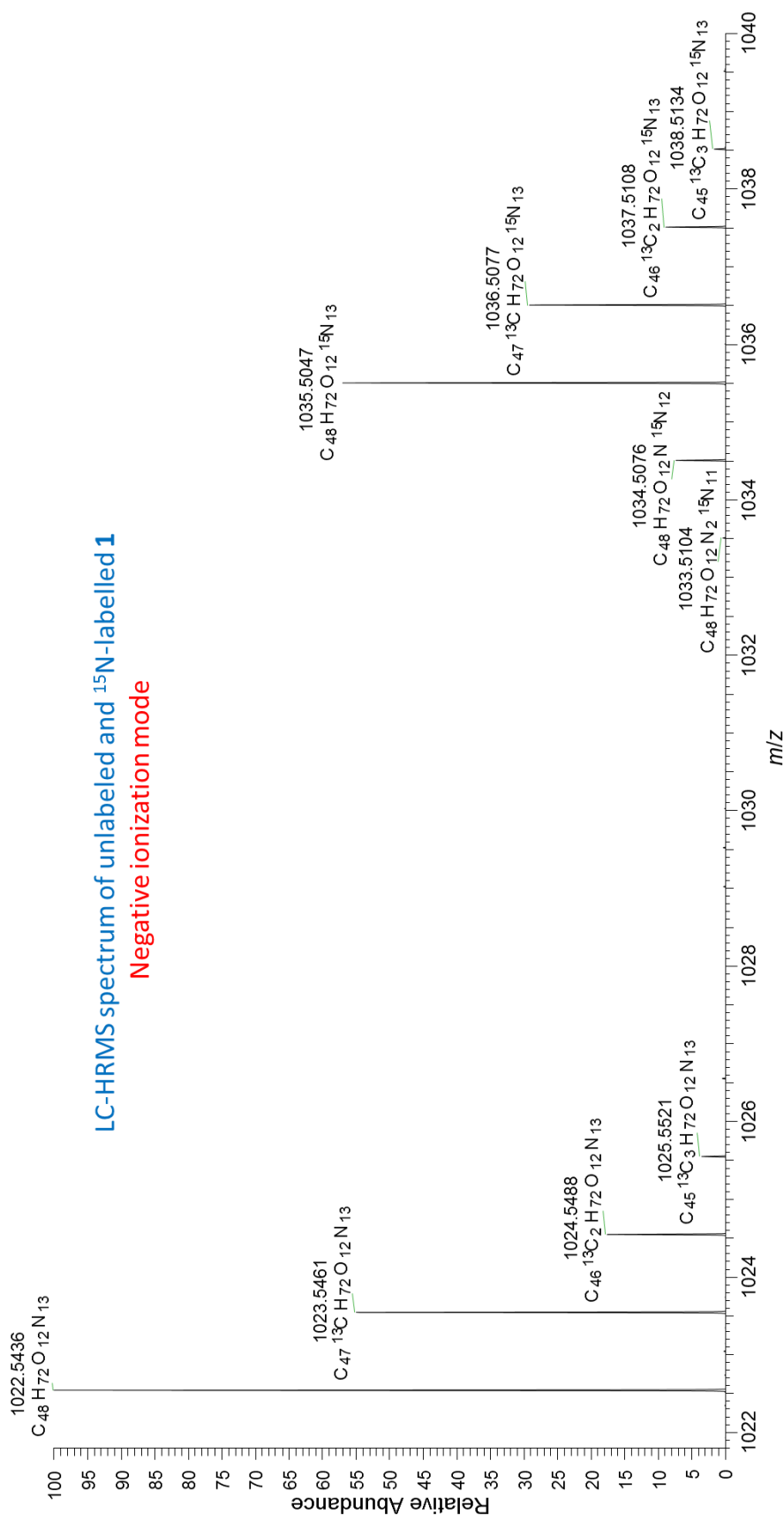
**Figure 40.** LC-HRMS (method B) spectrum of [D-Asp$^3$]MC-RR (**1**) in negative ionization mode ([M − H]$^-$) from a sample containing a mixture of an extract from an unlabelled culture of *P. prolifica* NIVA-CYA 544 and from the same culture grown for an extended period in $^{15}$N-enriched (>98% $^{15}$N) culture medium. Peaks are labelled with their elemental compositions, with all mass errors Δ ≤ 1.0 ppm. The measured level of $^{15}$N-incorporation for the labelled **1** was 98% (see Figure 3). The *m/z* values and isotopomer peak intensities were used in the NRC Molecular Formula Calculator to obtain candidate elemental compositions for **1** (see Figure S42). Similar data was used with the NRC Molecular Formula Calculator to obtain candidate elemental compositions for other microcystins in the culture (see Figures S43–57).

**Figure 41.** LC-HRMS (method B) spectrum of [D-Asp³]MC-RR (**1**) in positive ionization mode ([M +2 H]²⁺) from a sample containing a mixture of an extract from an unlabelled culture of *P. prolifica* NIVA-CYA 544 and from the same culture grown for an extended period in ¹⁵N-enriched (>98% ¹⁵N) culture medium. Peaks are labelled with their elemental compositions, with all mass errors Δ ≤ 2.0 ppm. The measured level of ¹⁵N-incorporation for the labelled **1** was 98% (see Figure 3). The *m/z* values and isotopomer peak intensities were used in the NRC Molecular Formula Calculator to obtain candidate elemental compositions for **1** (see Figure S42). Similar data was used with the NRC Molecular Formula Calculator to obtain candidate elemental compositions for other microcystins in the culture (see Figures S43–57).

$C_{48}H_{72}N_{13}O_{12}$ **score: 1.000**  $C_{48}H_{75}N_{13}O_{12}$ **score: 1.000**

$C_{45}H_{76}N_{13}O_{12}S$ **score: 0.000**  $C_{52}H_{75}N_{13}O_7S$ **score: 0.000**

$C_{49}H_{76}N_{13}O_7S_2$ **score: 0.000**  $C_{49}H_{79}N_{13}O_7S_2$ **score: 0.000**

$C_{53}H_{76}N_{13}O_2S_3$ **score: 0.000**  $C_{53}H_{79}N_{13}O_2S_3$ **score: 0.000**

$C_{50}H_{80}N_{13}O_2S_4$ **score: 0.000**  $C_{50}H_{83}N_{13}O_2S_4$ **score: 0.000**

**[M-H]⁻ ionization**  **[M+2H]²⁺ ionization**

[Asp3]MC-RR

**Figure S42.** Most probable elemental compositions for [D-Asp$^3$]MC-RR (**1**) based on full-scan LC–MS (method B) data for normalized $^{15}$N-labelled (red) and natural abundance (black) cultures in negative (left) and positive (right) ionization modes using the NRC Molecular Formula Calculator. Candidate formulae and their scores are shown above the pairs of spectra in each panel, with the measured *m/z* and intensities indicated by the circles and the calculated values shown with vertical lines. For original data, see Figures S40 and S41.
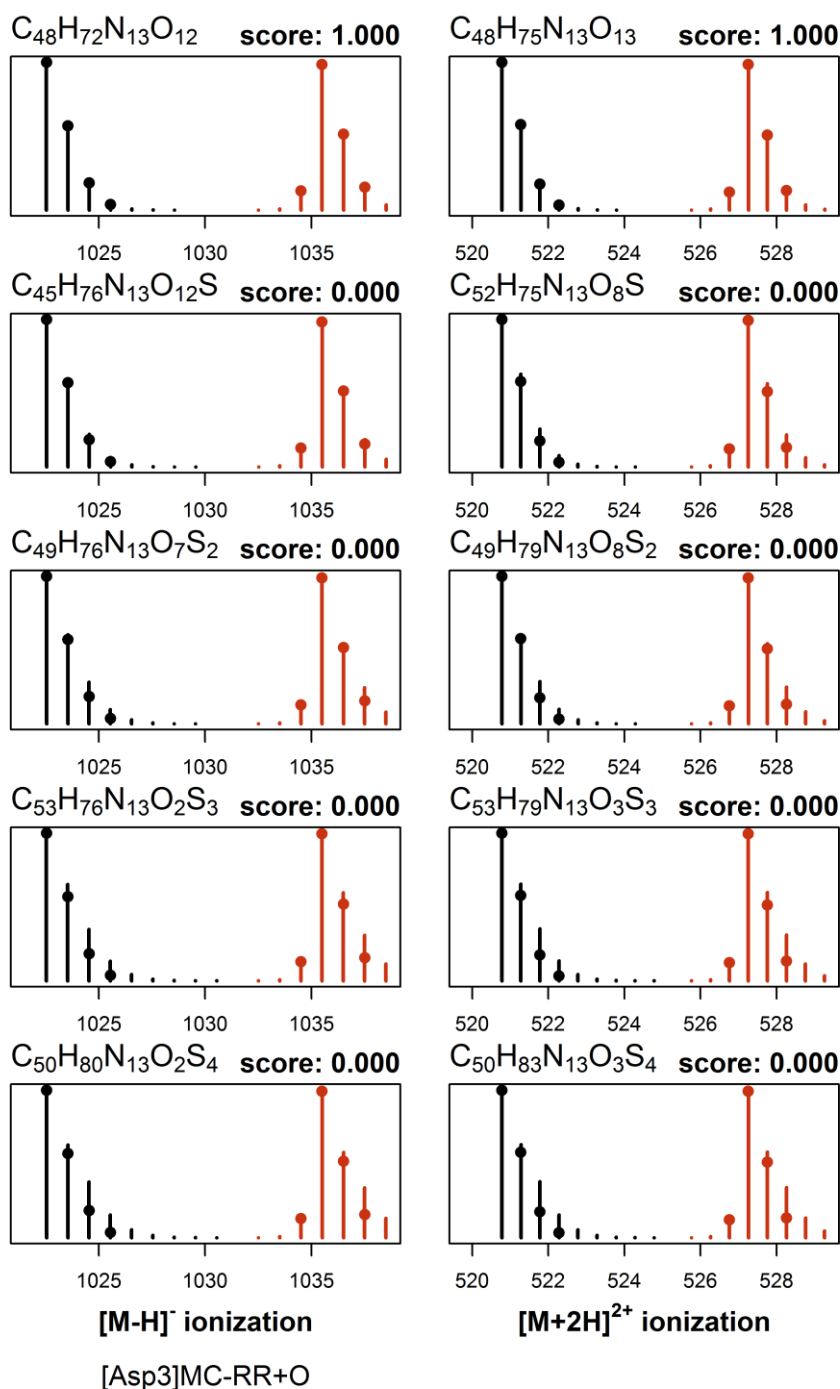
**Figure S43.** Most probable elemental compositions for oxidized [D-Asp³]MC-RR (**1**-oxide) based on full-scan LC–MS (method B) data for normalized ¹⁵N-labelled (red) and natural abundance (black) cultures in negative (left) and positive (right) ionization modes using the NRC Molecular Formula Calculator. Candidate formulae and their scores are shown above the pairs of spectra in each panel, with the measured *m/z* and intensities indicated by the circles and the calculated values shown with vertical lines.
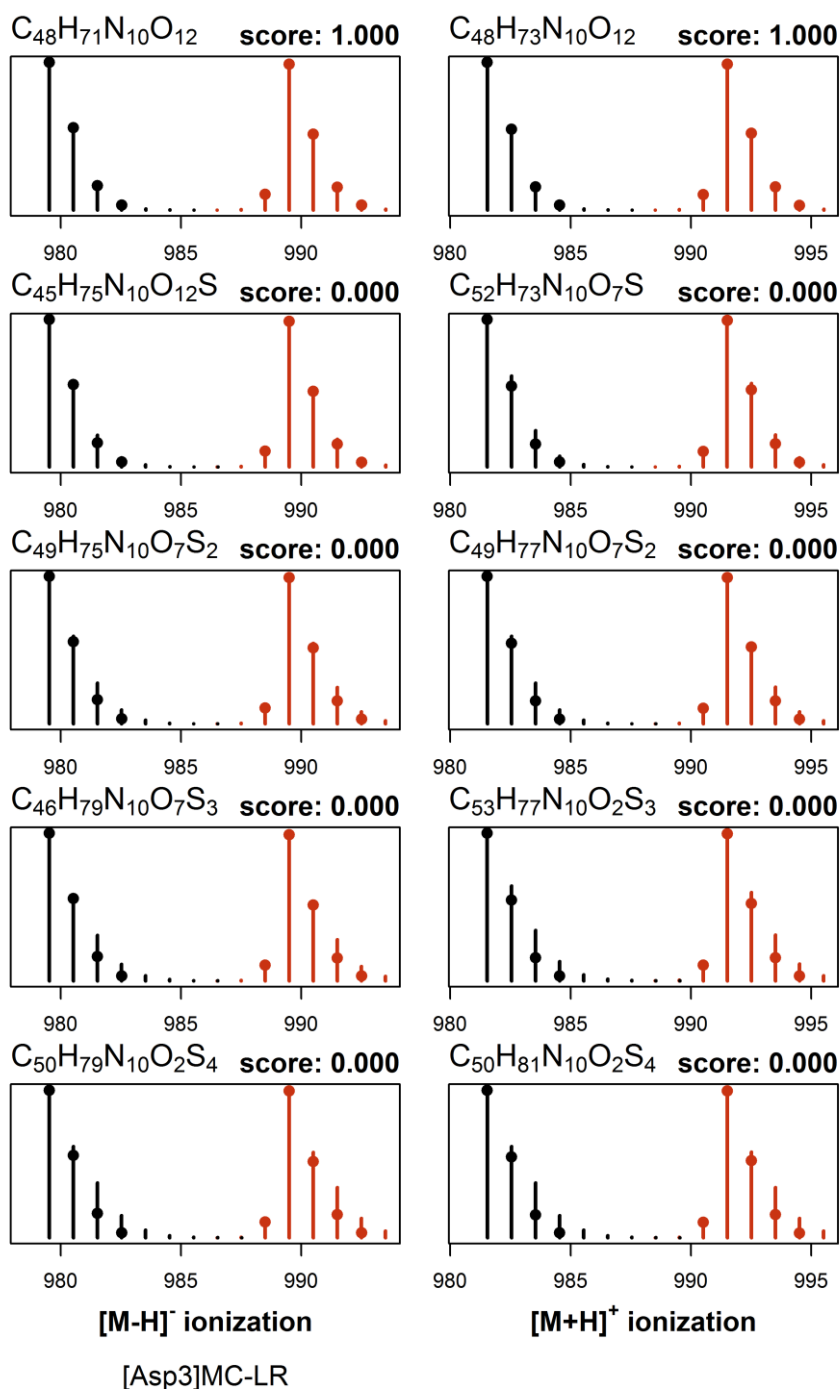
**Figure S44.** Most probable elemental compositions for [D-Asp³]MC-LR (**4**) based on full-scan LC–MS (method B) data for normalized ¹⁵N-labelled (red) and natural abundance (black) cultures in negative (left) and positive (right) ionization modes using the NRC Molecular Formula Calculator. Candidate formulae and their scores are shown above the pairs of spectra in each panel, with the measured *m/z* and intensities indicated by the circles and the calculated values shown with vertical lines.
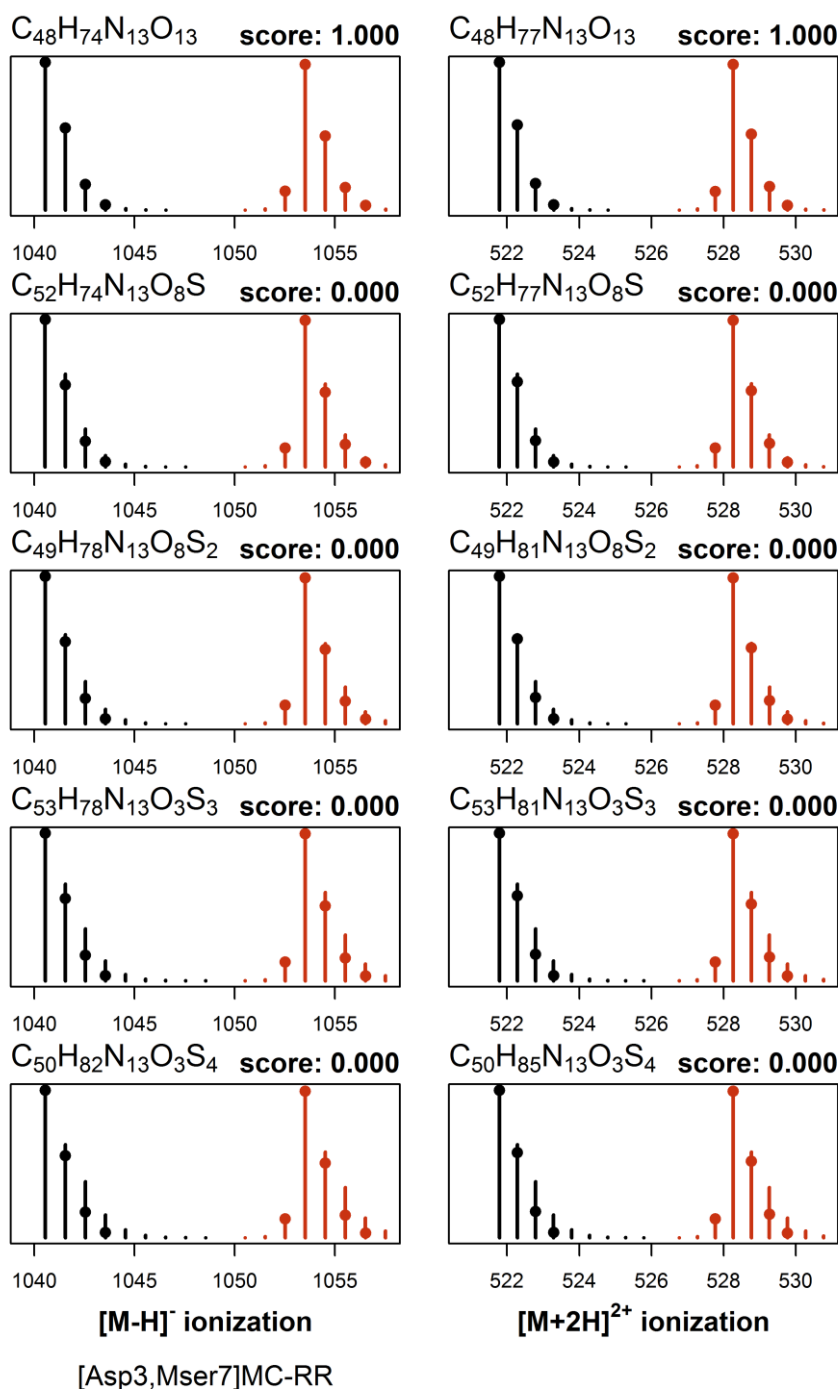
**Figure S45.** Most probable elemental compositions for [D-Asp[3],Mser[7]]MC-RR (**11**) based on full-scan LC–MS (method B) data for normalized ^{15}N-labelled (red) and natural abundance (black) cultures in negative (left) and positive (right) ionization modes using the NRC Molecular Formula Calculator. Candidate formulae and their scores are shown above the pairs of spectra in each panel, with the measured *m/z* and intensities indicated by the circles and the calculated values shown with vertical lines.
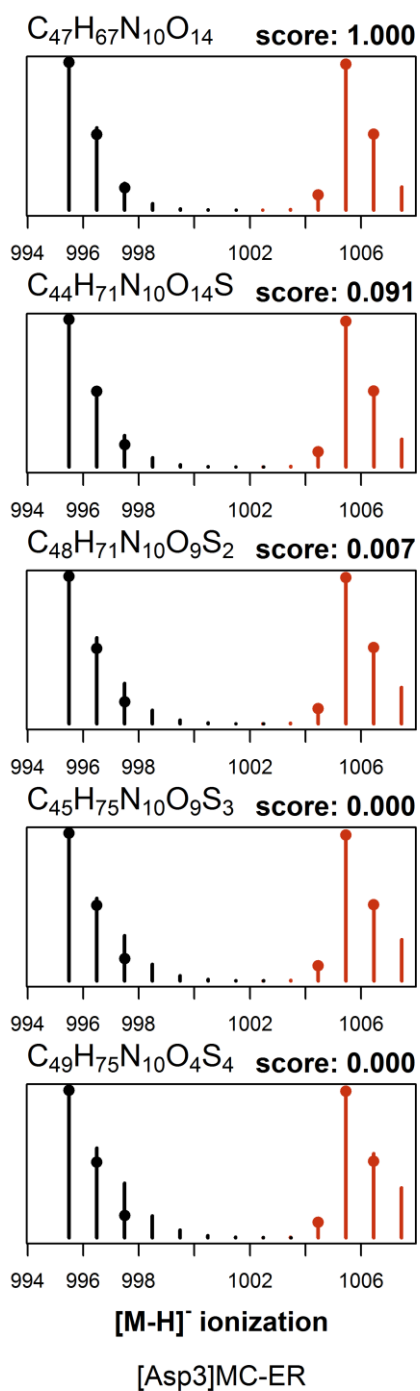
**Figure S46.** Most probable elemental compositions for [D-Asp³]MC-ER (**12**) based on full-scan LC–MS (method B) data for normalized ¹⁵N-labelled (red) and natural abundance (black) cultures in negative (left) ionization mode using the NRC Molecular Formula Calculator. Candidate formulae and their scores are shown above the pairs of spectra in each panel, with the measured *m/z* and intensities indicated by the circles and the calculated values shown with vertical lines.
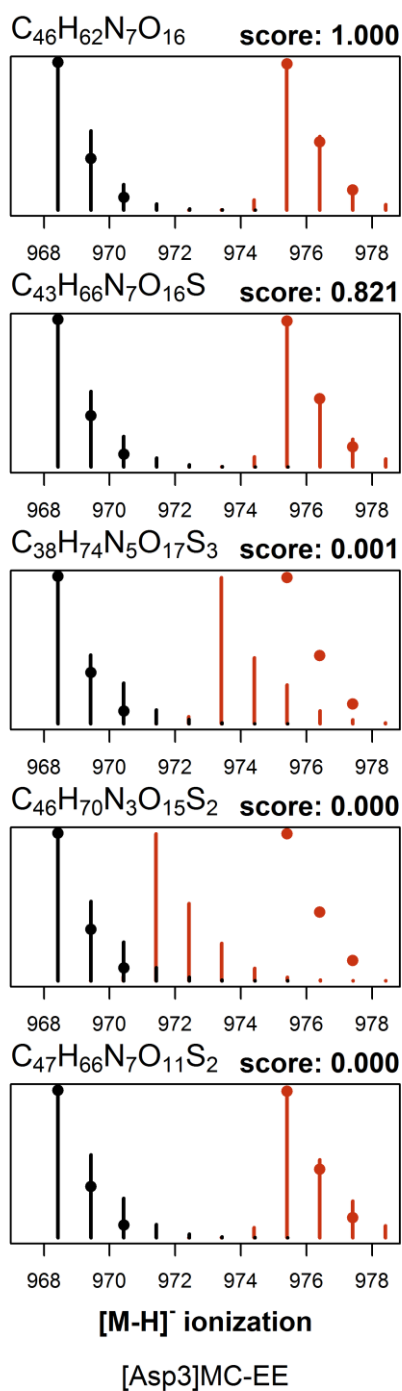
**Figure S47.** Most probable elemental compositions for [D-Asp[3]]MC-EE (**13**) based on full-scan LC–MS (method B) data for normalized ^{15}N-labelled (red) and natural abundance (black) cultures in negative (left) ionization mode using the NRC Molecular Formula Calculator. Candidate formulae and their scores are shown above the pairs of spectra in each panel, with the measured *m/z* and intensities indicated by the circles and the calculated values shown with vertical lines.
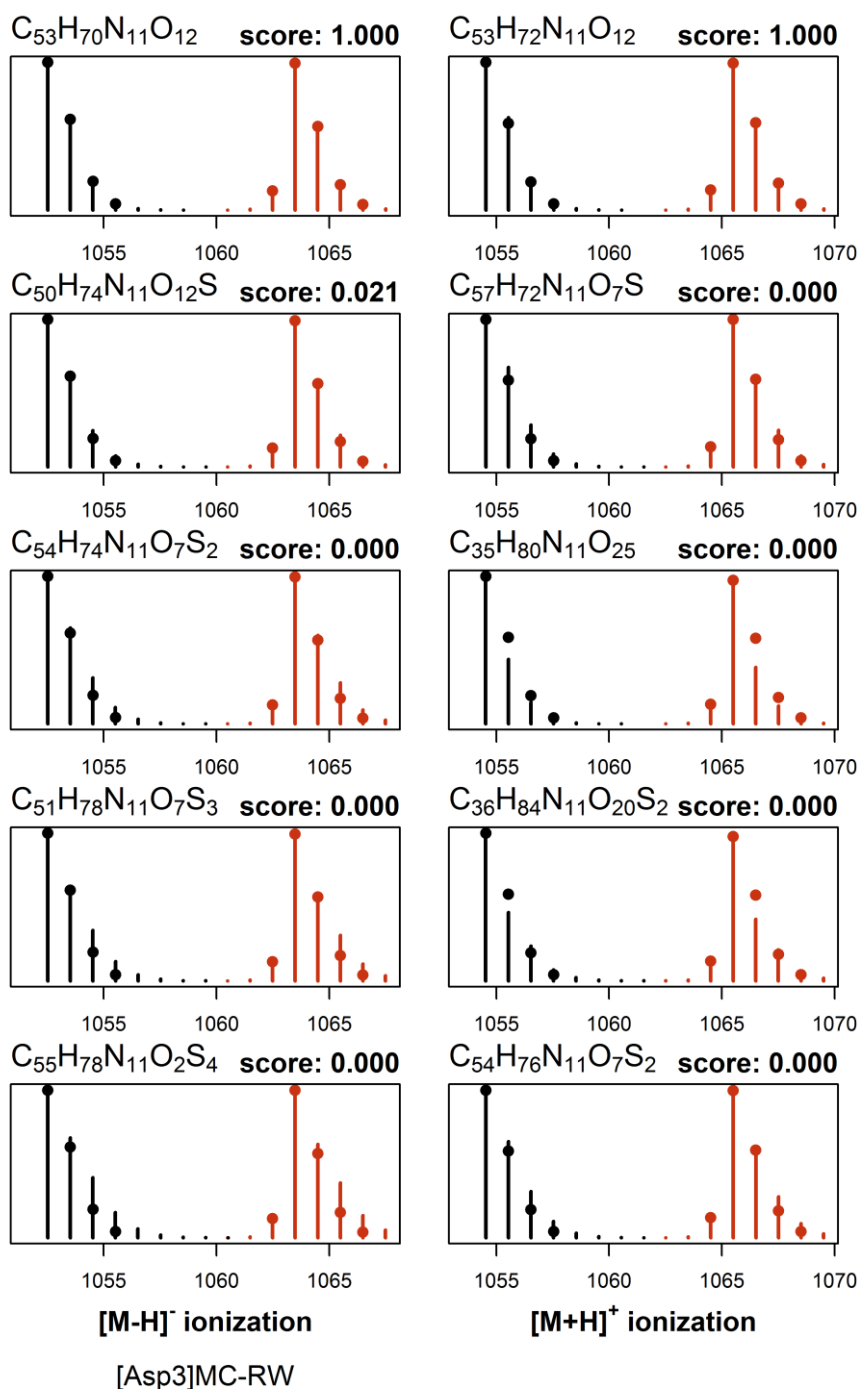
**Figure S48.** Most probable elemental compositions for [D-Asp³]MC-RW (**14**) based on full-scan LC–MS (method B) data for normalized ¹⁵N-labelled (red) and natural abundance (black) cultures in negative (left) and positive (right) ionization modes using the NRC Molecular Formula Calculator. Candidate formulae and their scores are shown above the pairs of spectra in each panel, with the measured *m/z* and intensities indicated by the circles and the calculated values shown with vertical lines.
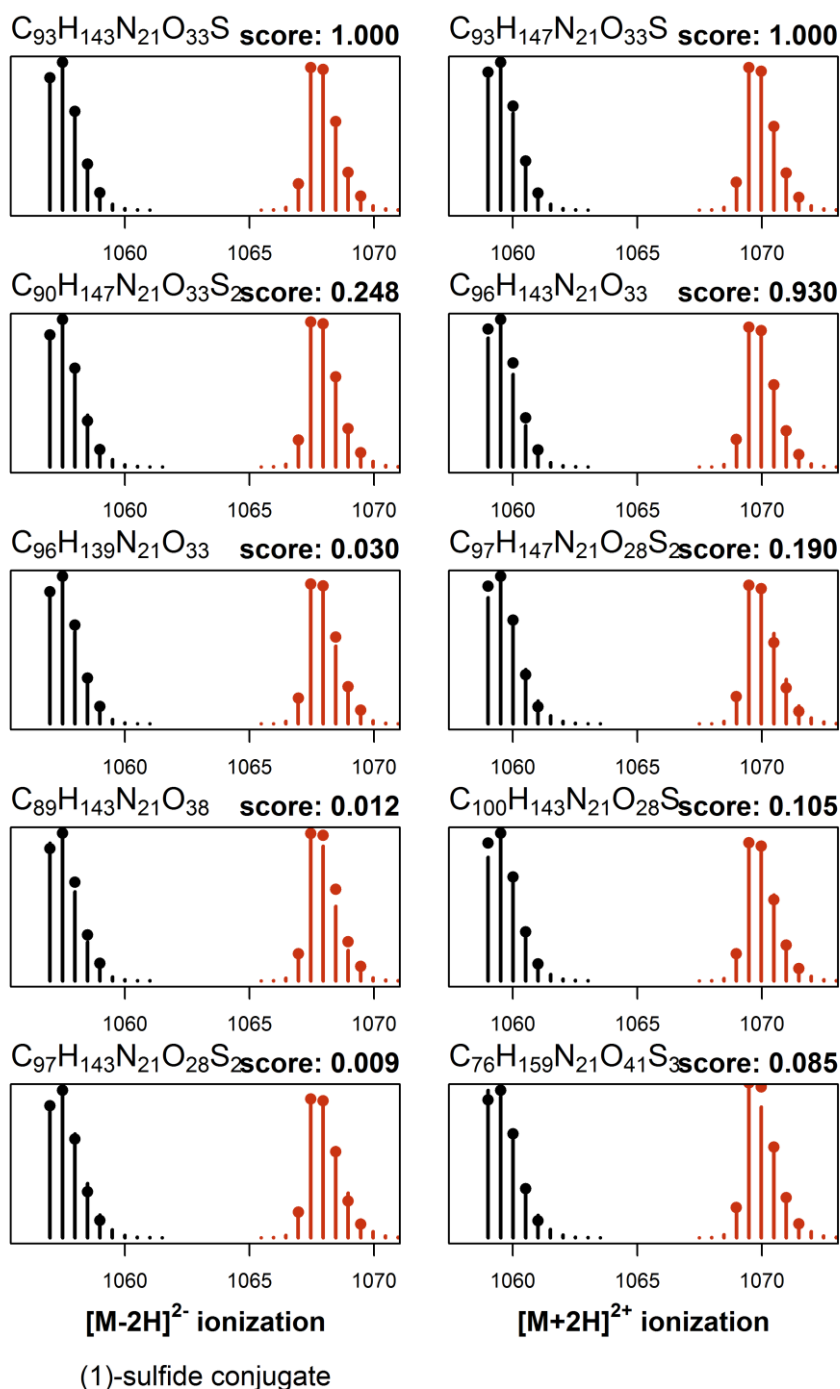
**Figure S49.** Most probable elemental compositions for the sulfide conjugate of [D-Asp[3]]MC-RR (**15**) based on full-scan LC–MS (method B) data for normalized ^{15}N-labelled (red) and natural abundance (black) cultures in negative (left) and positive (right) ionization modes using the NRC Molecular Formula Calculator. Candidate formulae and their scores are shown above the pairs of spectra in each panel, with the measured *m/z* and intensities indicated by the circles and the calculated values shown with vertical lines.
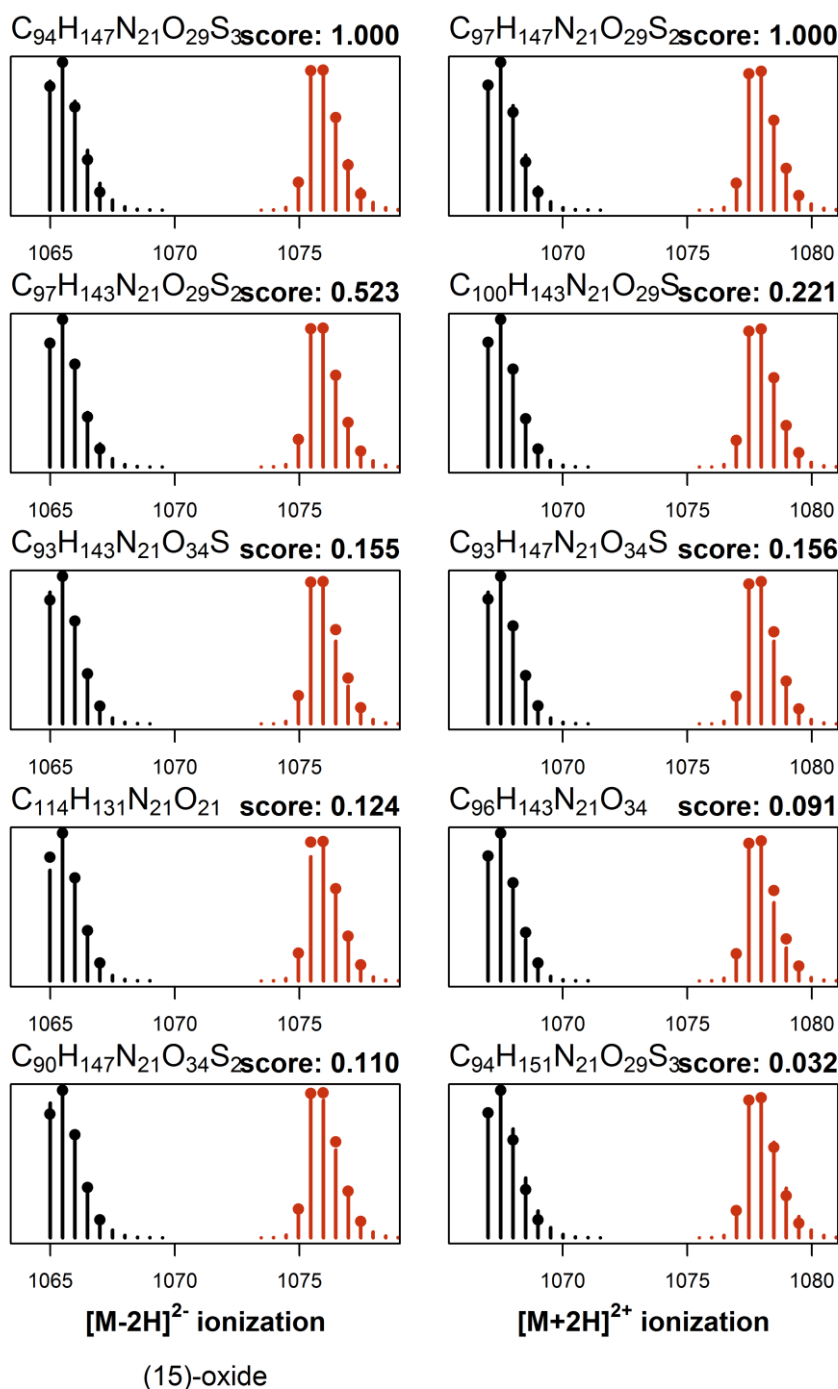
**Figure S50.** Most probable elemental compositions for the sulfoxide conjugate of [D-Asp³]MC-RR (**16**) (i.e. **15**-oxide) based on full-scan LC–MS (method B) data for normalized ¹⁵N-labelled (red) and natural abundance (black) cultures in negative (left) and positive (right) ionization modes using the NRC Molecular Formula Calculator. Candidate formulae and their scores are shown above the pairs of spectra in each panel, with the measured *m/z* and intensities indicated by the circles and the calculated values shown with vertical lines.
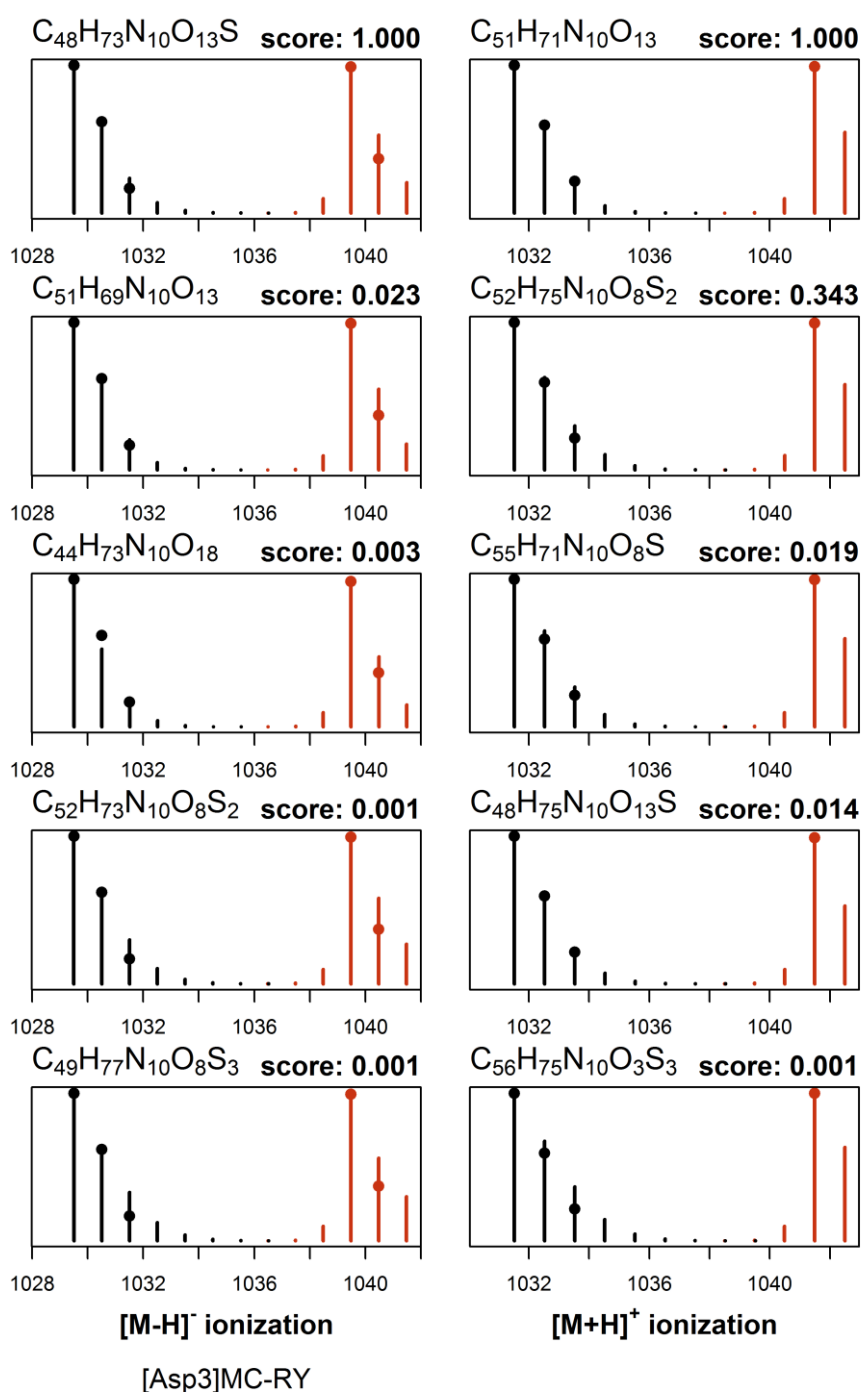
**Figure S51.** Most probable elemental compositions for [D-Asp³]MC-RY (**17**) based on full-scan LC–MS (method B) data for normalized ¹⁵N-labelled (red) and natural abundance (black) cultures in negative (left) and positive (right) ionization modes using the NRC Molecular Formula Calculator. Candidate formulae and their scores are shown above the pairs of spectra in each panel, with the measured *m/z* and intensities indicated by the circles and the calculated values shown with vertical lines.
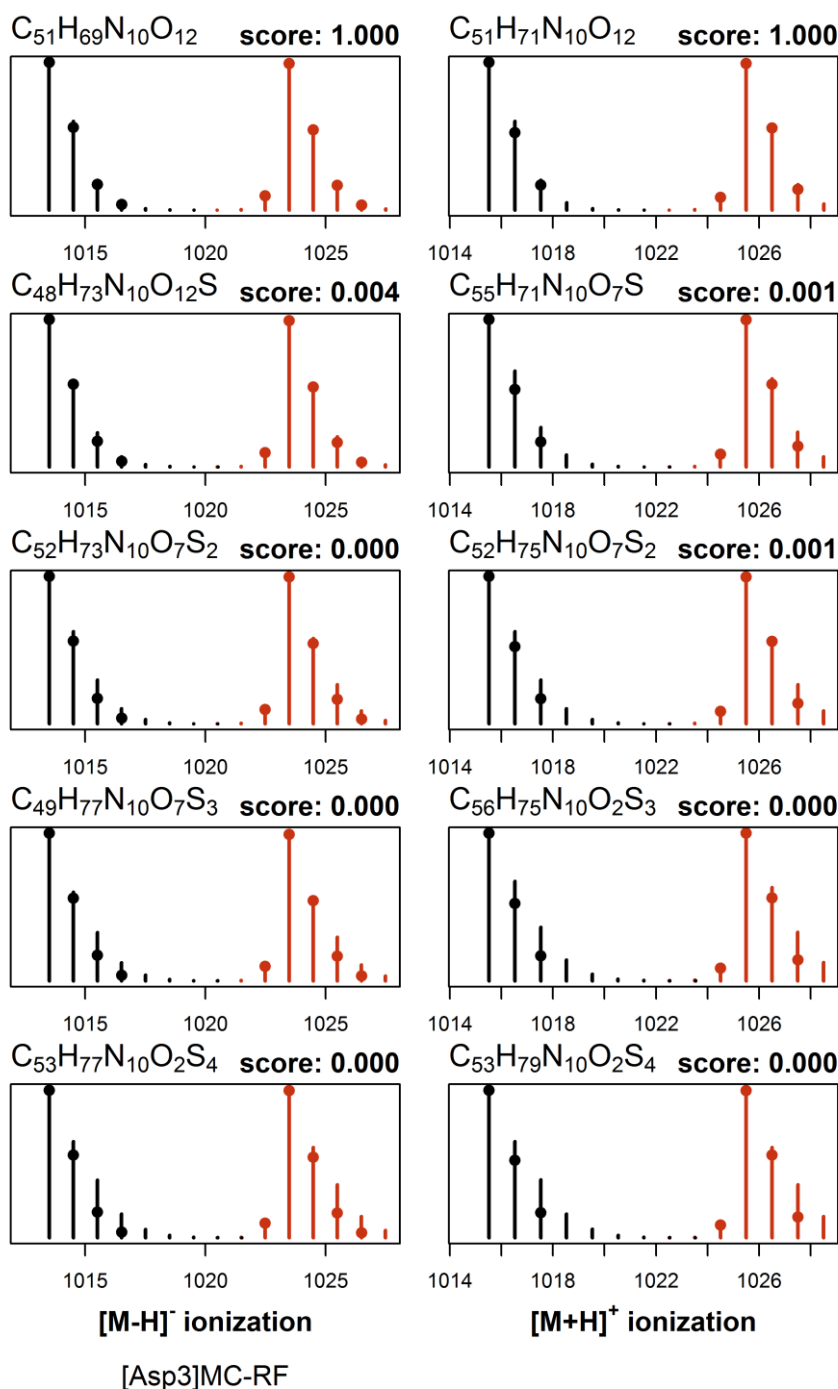
**Figure S52.** Most probable elemental compositions for [D-Asp³]MC-RF (**18**) based on full-scan LC–MS (method B) data for normalized ¹⁵N-labelled (red) and natural abundance (black) cultures in negative (left) and positive (right) ionization modes using the NRC Molecular Formula Calculator. Candidate formulae and their scores are shown above the pairs of spectra in each panel, with the measured *m/z* and intensities indicated by the circles and the calculated values shown with vertical lines.
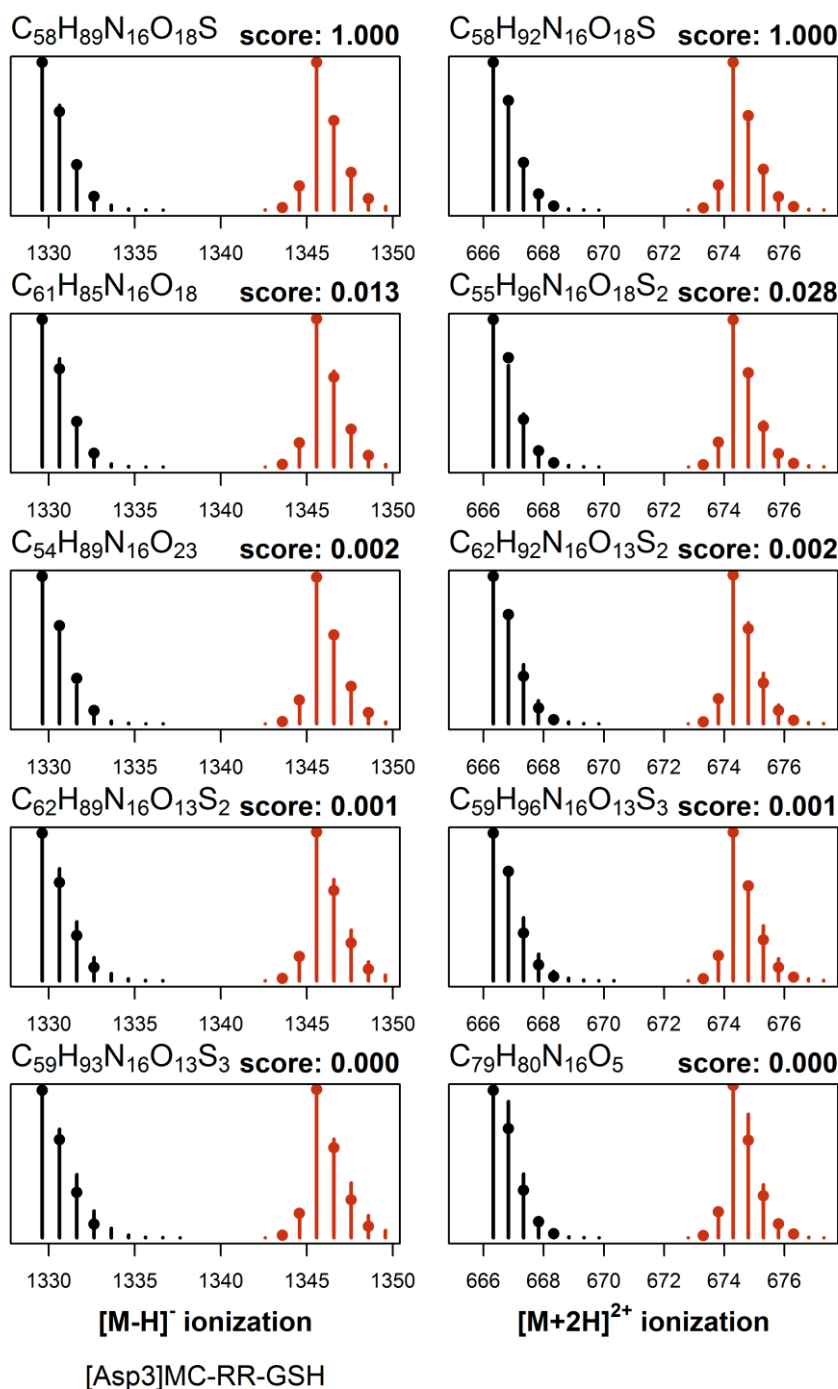
**Figure S53.** Most probable elemental compositions for the glutathione conjugate of [D-Asp$^3$]MC-RR (**19**) based on full-scan LC–MS (method B) data for normalized $^{15}$N-labelled (red) and natural abundance (black) cultures in negative (left) and positive (right) ionization modes using the NRC Molecular Formula Calculator. Candidate formulae and their scores are shown above the pairs of spectra in each panel, with the measured *m/z* and intensities indicated by the circles and the calculated values shown with vertical lines.
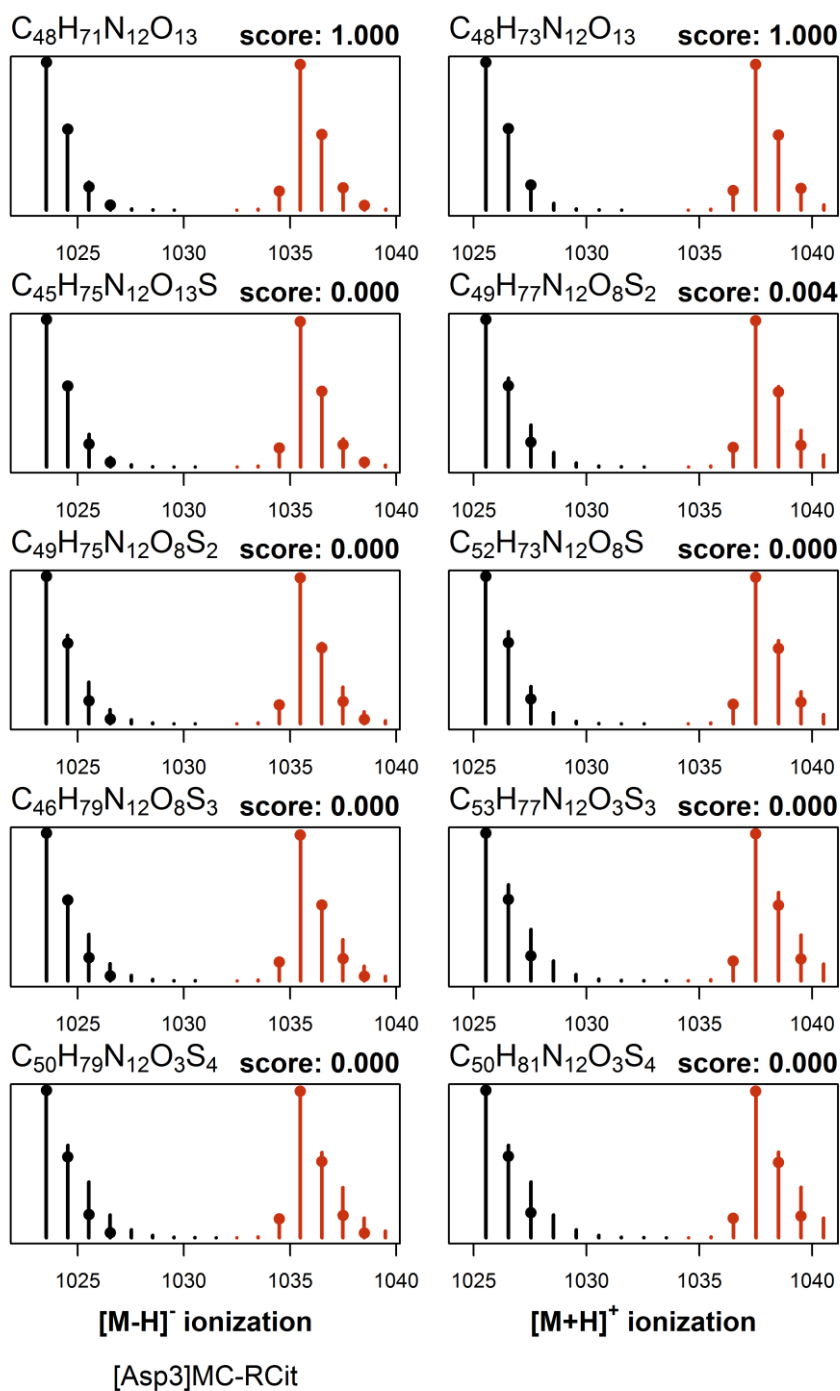
**Figure S54.** Most probable elemental compositions for [D-Asp[3]]MC-RCit (**20**) based on full-scan LC–MS (method B) data for normalized ^{15}N-labelled (red) and natural abundance (black) cultures in negative (left) and positive (right) ionization modes using the NRC Molecular Formula Calculator. Candidate formulae and their scores are shown above the pairs of spectra in each panel, with the measured *m/z* and intensities indicated by the circles and the calculated values shown with vertical lines.
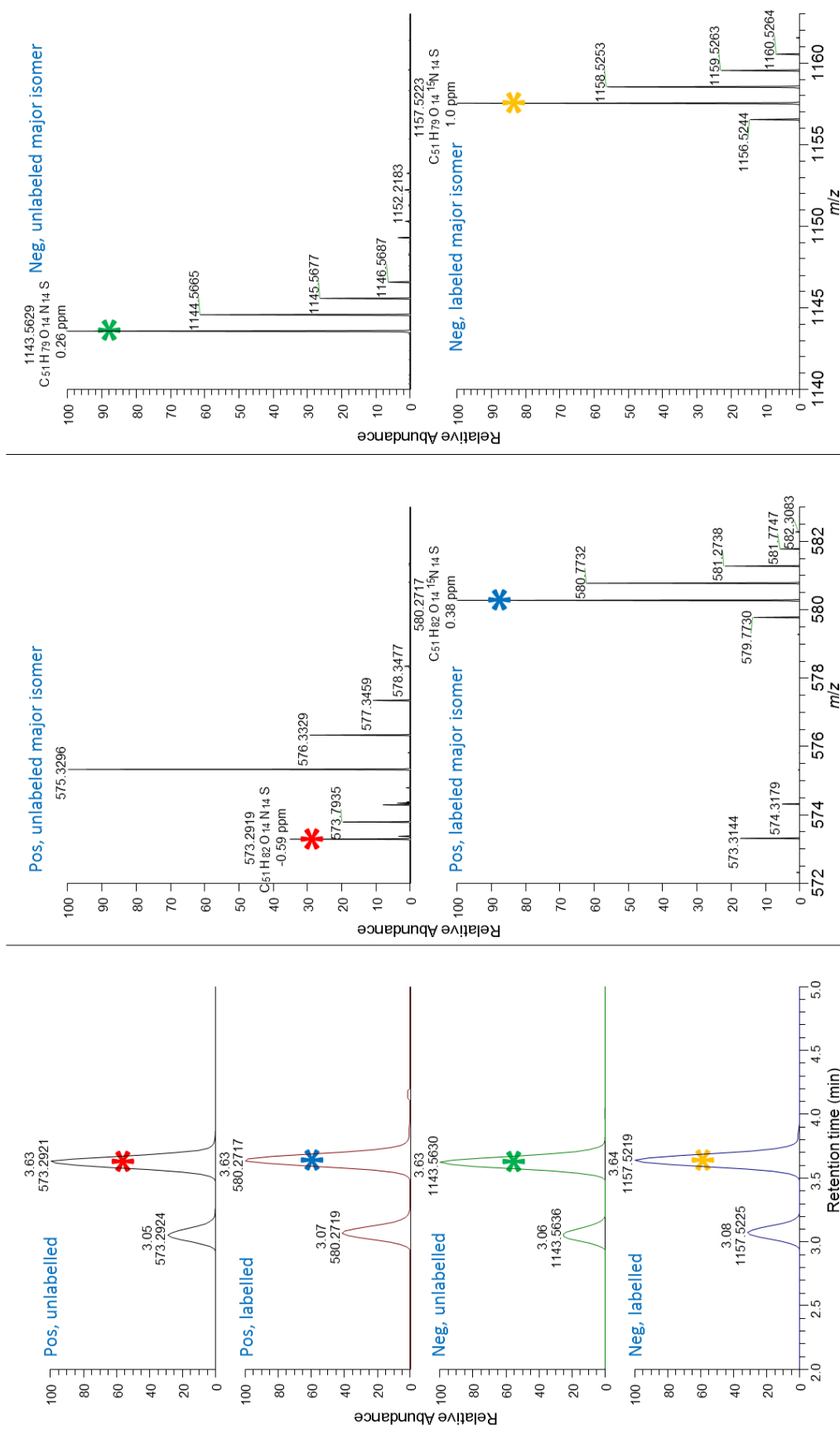
**Figure S55.** Left, LC-HRMS (method B) chromatograms of the [D-Asp³]MC-RR cysteine conjugate in unlabelled and ¹⁵N-labelled cultures of *P. prolifica* NICA-CYA 544 in positive and negative modes extracted at *m/z* for [M + 2H]²⁺ and [M − H]⁻. Note the presence of a major and a minor isomer. Centre, positive mode mass spectra of the major isomer in the unlabelled (top) and ¹⁵N-labelled cultures (bottom). Right, negative mode mass spectra of the major isomer in the unlabelled (top) and ¹⁵N-labelled cultures (bottom). Analysis of the isotope patterns with the NRC Molecular Formula Calculator is shown in Figure S57.
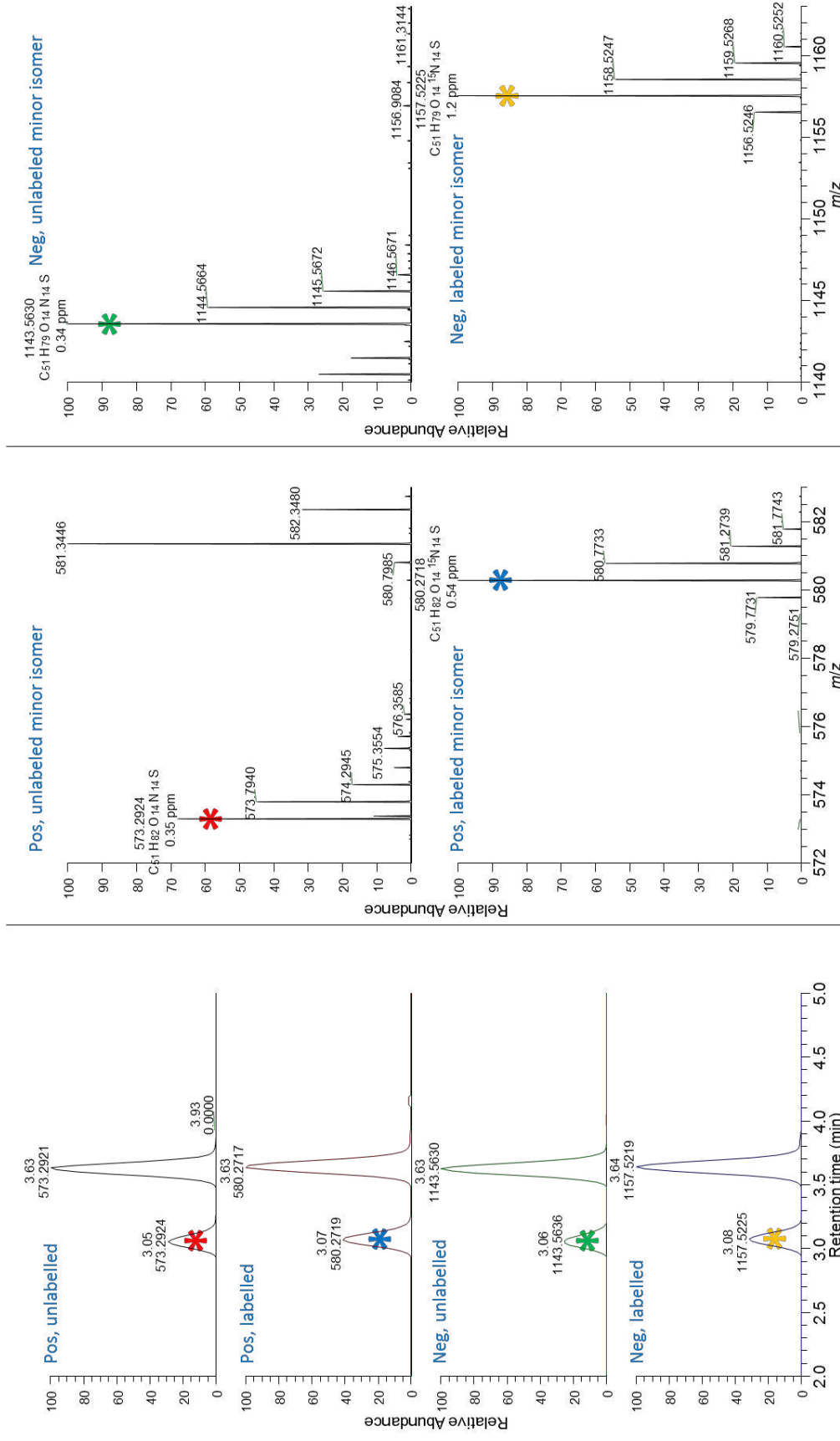
**Figure S56.** Left, LC-HRMS (method B) chromatograms of the [D-Asp³]MC-RR cysteine conjugate in unlabelled and ¹⁵N-labelled cultures of *P. prolifica* NICA-CYA 544 in positive and negative modes extracted at *m/z* for [M + 2H]²⁺ and [M − H]⁻. Note the presence of a major and a minor isomer. Centre, positive mode mass spectra of the minor isomer in the unlabelled (top) and ¹⁵N-labelled cultures (bottom). Right, negative mode mass spectra of the minor isomer in the unlabelled (top) and ¹⁵N-labelled cultures (bottom).

$C_{51}H_{79}N_{14}O_{14}S$ **score: 1.000**

$C_{51}H_{82}N_{14}O_{14}S$ **score: 1.000**

$C_{48}H_{83}N_{14}O_{14}S_2$ **score: 0.000**

$C_{54}H_{78}N_{14}O_{14}$ **score: 0.009**

$C_{55}H_{79}N_{14}O_9S_2$ **score: 0.000**

$C_{52}H_{86}N_{14}O_9S_3$ **score: 0.004**

$C_{72}H_{67}N_{14}O$ **score: 0.000**

$C_{55}H_{82}N_{14}O_9S_2$ **score: 0.003**

$C_{52}H_{83}N_{14}O_9S_3$ **score: 0.000**

$C_{56}H_{86}N_{14}O_4S_4$ **score: 0.000**

**[M-H]⁻ ionization**

**[M+2H]²⁺ ionization**
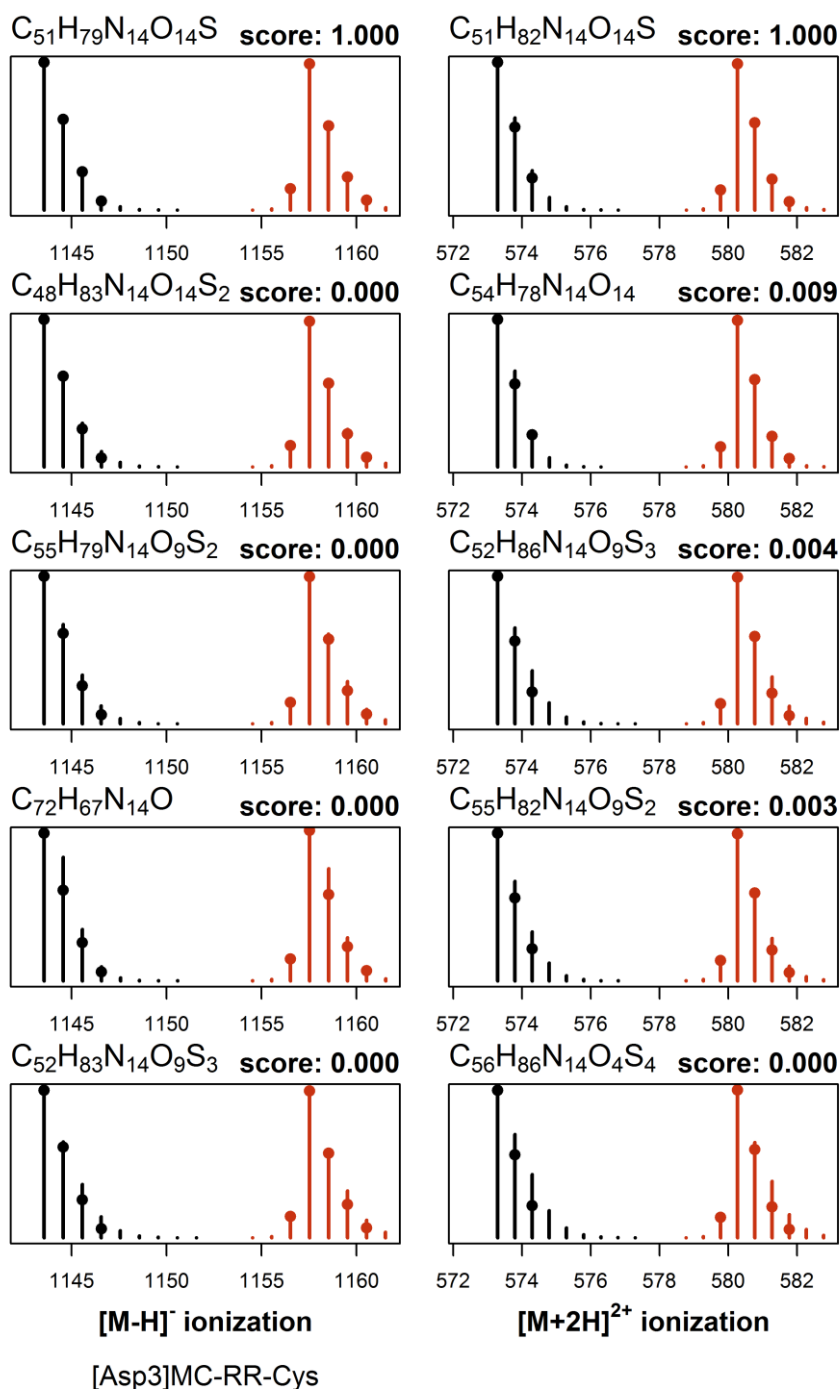
[Asp3]MC-RR-Cys

**Figure S57.** Most probable elemental compositions for the major isomer of the cysteine conjugate of [D-Asp[3]]MC-RR based on the full-scan LC–MS (method B) data shown in Figure S55. The panels show normalized ^{15}N-labelled (red) and natural abundance (black) mass spectra for cultures in negative (left) and positive (right) ionization modes using the NRC Molecular Formula Calculator. Candidate formulae and their scores are shown above the pairs of spectra in each panel, with the measured *m/z* and intensities indicated by the circles and the calculated values shown with vertical lines.
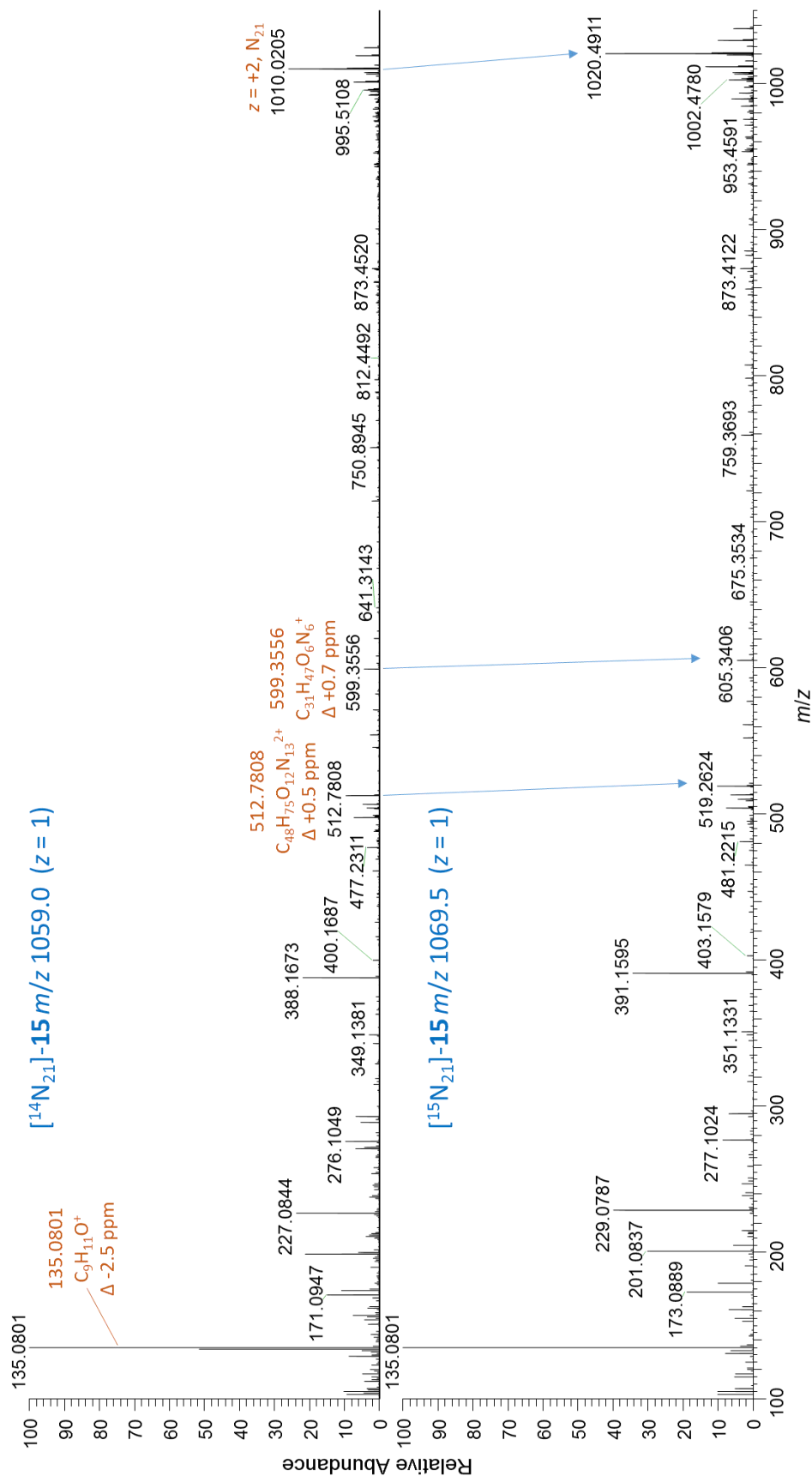
**Figure S58.** LC–HRMS/MS PRM spectra (method B) of [M + 2H]²⁺ of the sulfide conjugate of the: top, unlabelled [D-Asp³]MC-RR (**15**) at *m/z* 1059.0 recorded with setting *z* = 1; bottom, ¹⁵N-labelled **15** at *m/z* 1069.5. Note the characteristic product ions indicating the presence of [D-Asp³]MC-RR (**1**) in conjugate-**15**.
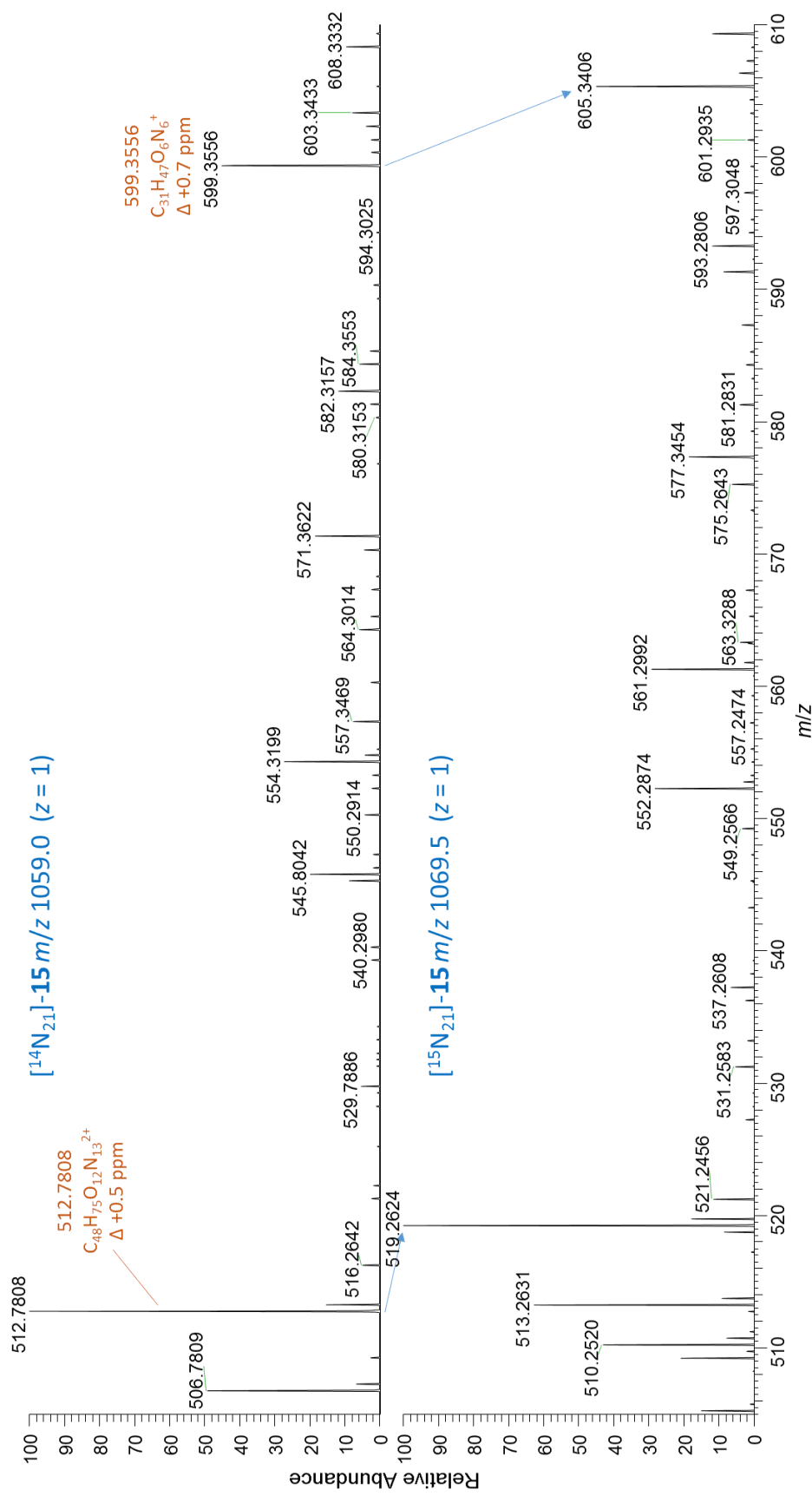
**Figure S59.** Expansion of LC–HRMS/MS PRM spectra (method B) of [M + 2H]$^{2+}$ of the: top, unlabelled [D-Asp$^3$]MC-RR (**15**) at *m/z* 1059.0 recorded with setting *z* =1; bottom, $^{15}$N-labelled **15** at *m/z* 1069.5. Note the characteristic product ions indicating the presence of [D-Asp$^3$]MC-RR (**1**) in conjugate-**15**.

**Figure S60.** Expansion of LC–HRMS/MS PRM spectra (method B) of $[M + 2H]^{2+}$ of the sulfide conjugate (see Figure S58) of the: top, unlabelled [D-Asp³]MC-RR (**15**) at $m/z$ 1059.0 recorded with setting $z=1$; bottom, ¹⁵N-labelled **15** at $m/z$ 1069.5. Note the characteristic product ions indicating the presence of [D-Asp³]MC-RR (**1**) in conjugate-**15**.
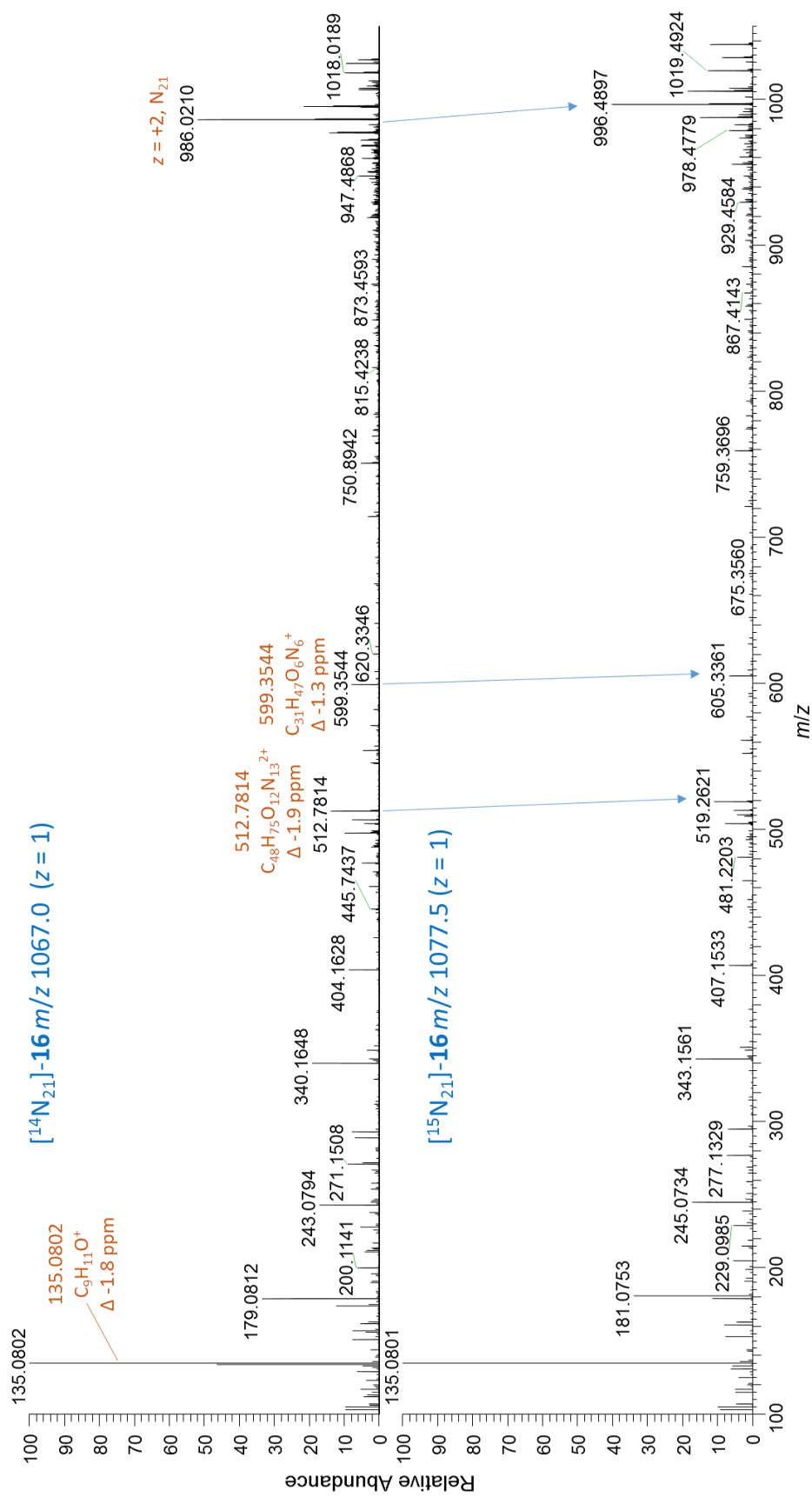
**Figure S61.** LC–HRMS/MS PRM spectra (method B) of $[M + 2H]^{2+}$ of the: top, unlabelled [D-Asp$^3$]MC-RR (**16**) at $m/z$ 1067.0 recorded with setting $z = 1$; bottom, $^{15}$N-labelled **16** at $m/z$ 1077.5. Note the characteristic product ions indicating the presence of [D-Asp$^3$]MC-RR (**1**) in conjugate-**16**.
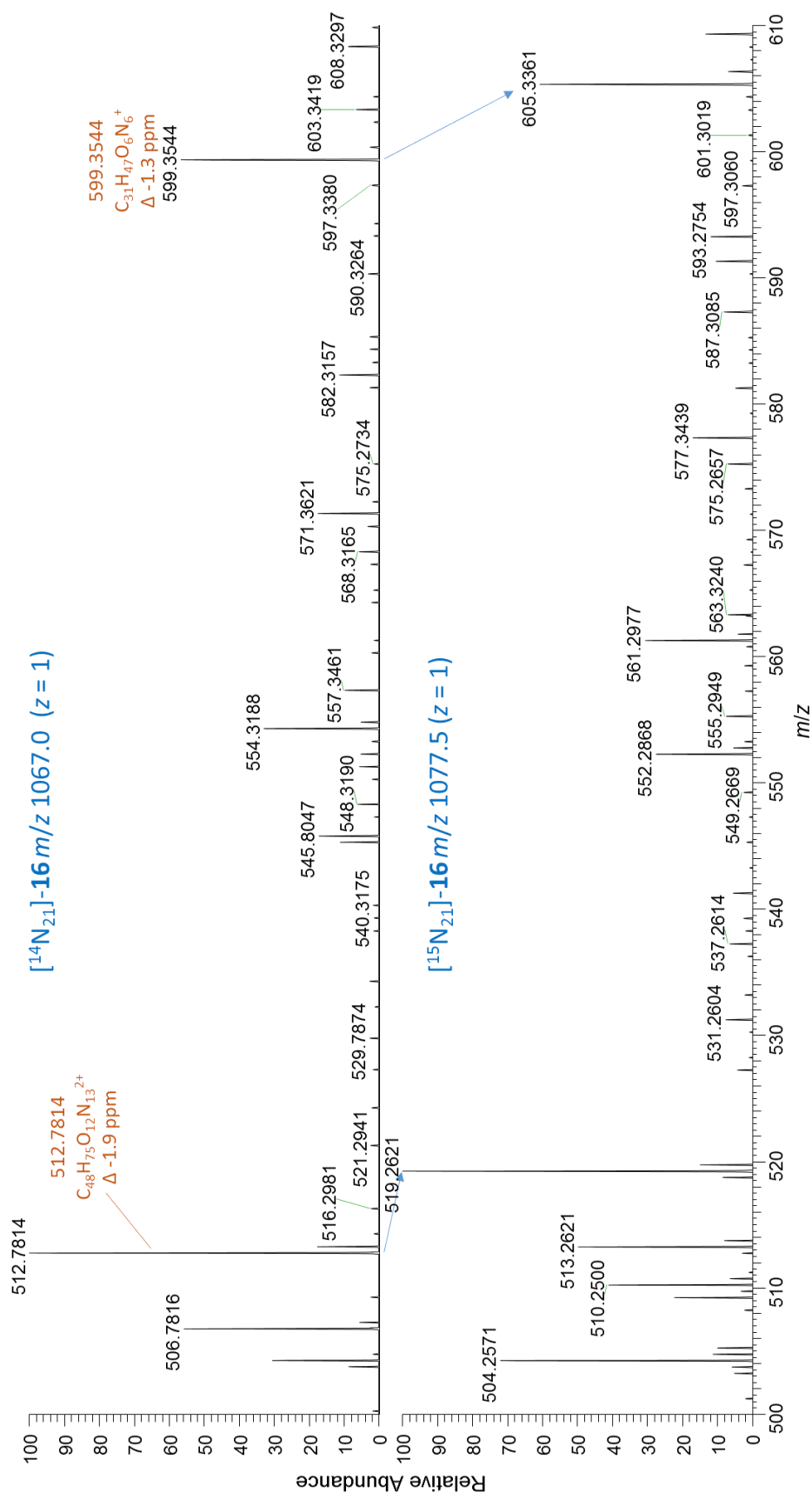
**Figure S62.** Expansion of LC–HRMS/MS PRM spectra (method B) of $[M + 2H]^{2+}$ of the sulfoxide conjugate (see Figure S61) of the: top, unlabelled [D-Asp$^3$]MC-RR (**16**) at $m/z$ 1067.0 recorded with setting $z$ =1; bottom, $^{15}$N-labelled **15** at $m/z$ 1077.5. Note the characteristic product ions indicating the presence of [D-Asp$^3$]MC-RR (**1**) in conjugate-**16**.
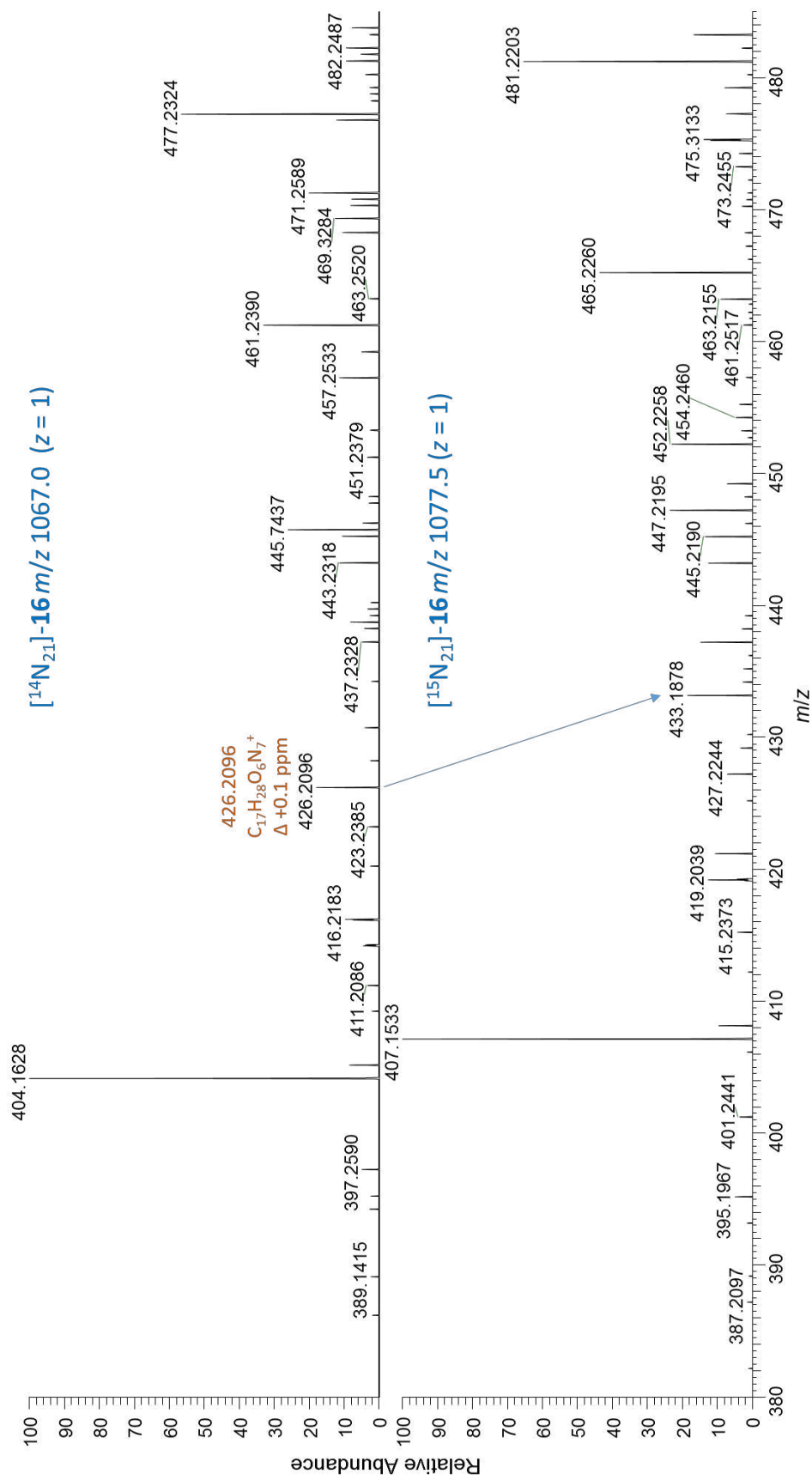
**Figure S63.** Expansion of LC–HRMS/MS PRM spectra (method B) of $[M + 2H]^{2+}$ of the sulfoxide conjugate (see Figure S61) of the: top, unlabelled $[D\text{-Asp}^3]MC\text{-RR}$ (**16**) at $m/z$ 1067.0 recorded with setting $z$ =1; bottom, $^{15}N$-labelled **15** at $m/z$ 1077.5. Note the characteristic product ions indicating the presence of $[D\text{-Asp}^3]MC\text{-RR}$ (**1**) in conjugate-**16**.
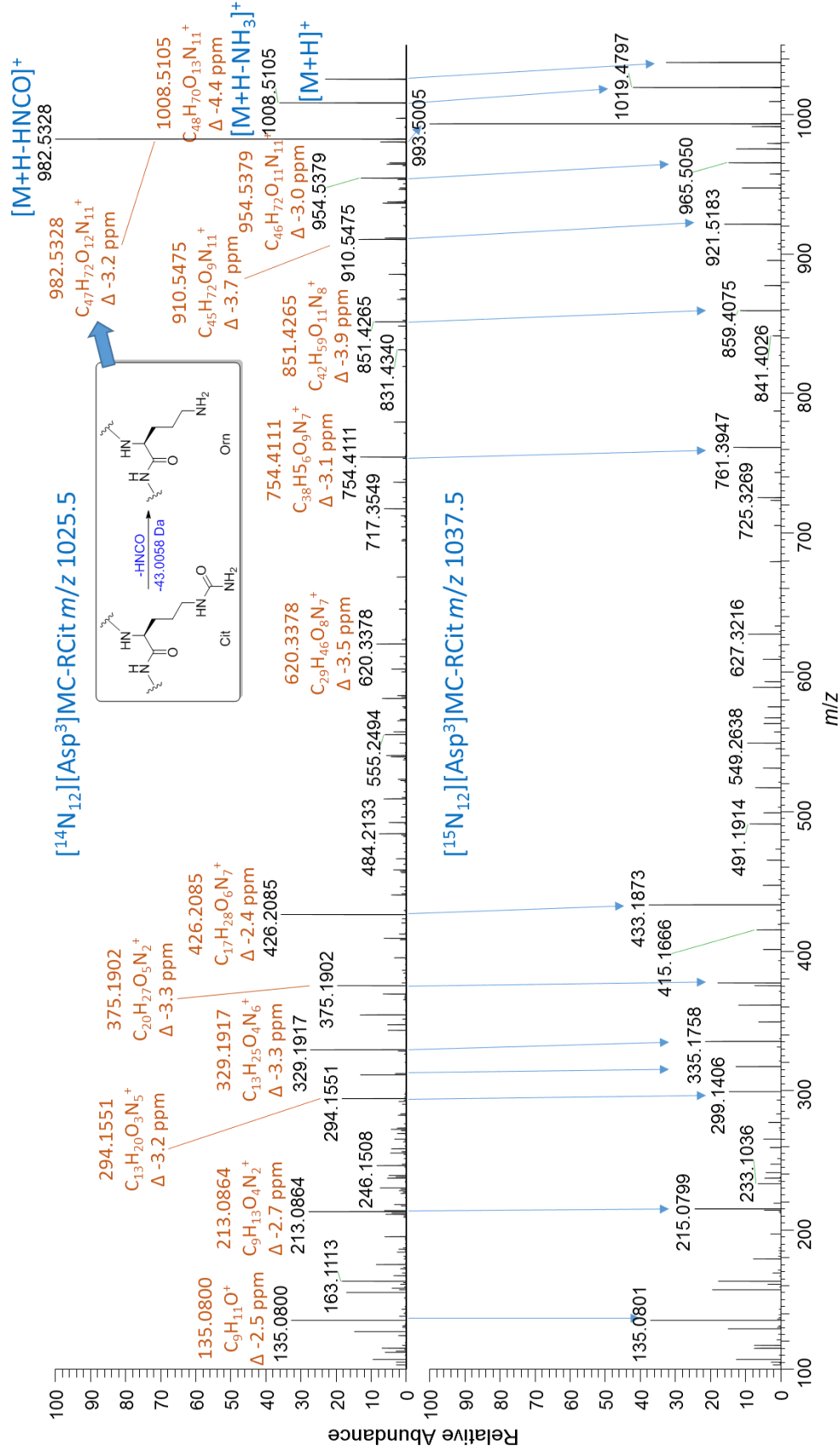
**Figure S64.** LC–HRMS/MS PRM spectra (method B) of $[M + H]^+$ of: top, unlabelled $[D-Asp^3]MC-RCit$ (**20**) at $m/z$ 1025.5, and; bottom, $^{15}N$-labelled **20** at $m/z$ 1037.5. Note the prominent neutral loss of isocyanic acid (HNCO, 43.0058 Da) in unlabelled **20**, which characteristic of citrulline residues in peptides.[4]
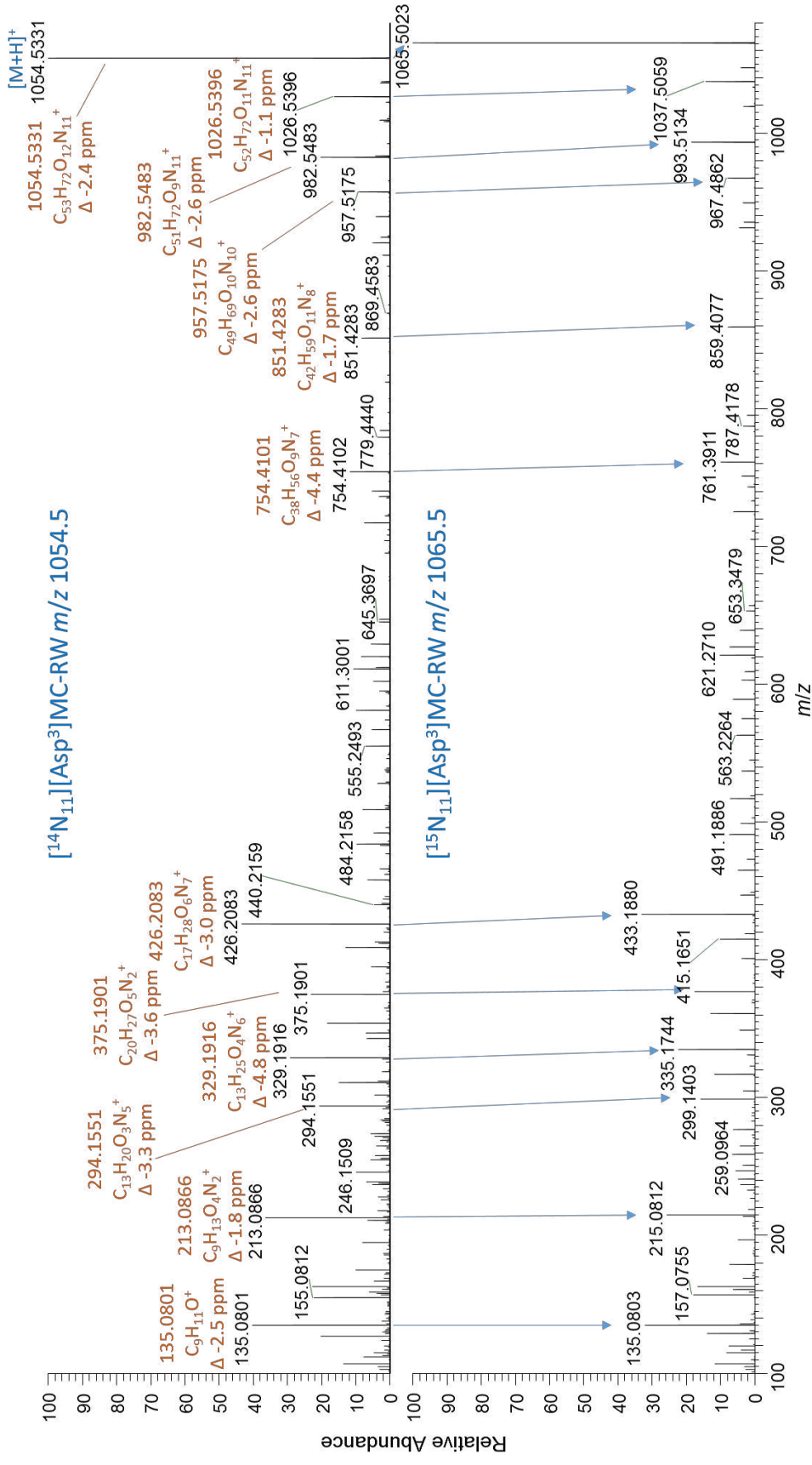
**Figure S65.** LC–HRMS/MS PRM spectra (method B) of [M + H]$^+$ of: top, unlabelled [D-Asp$^3$]MC-RW (**14**) at $m/z$ 1054.5, and; bottom, $^{15}$N-labelled **14** at $m/z$ 1069.5.
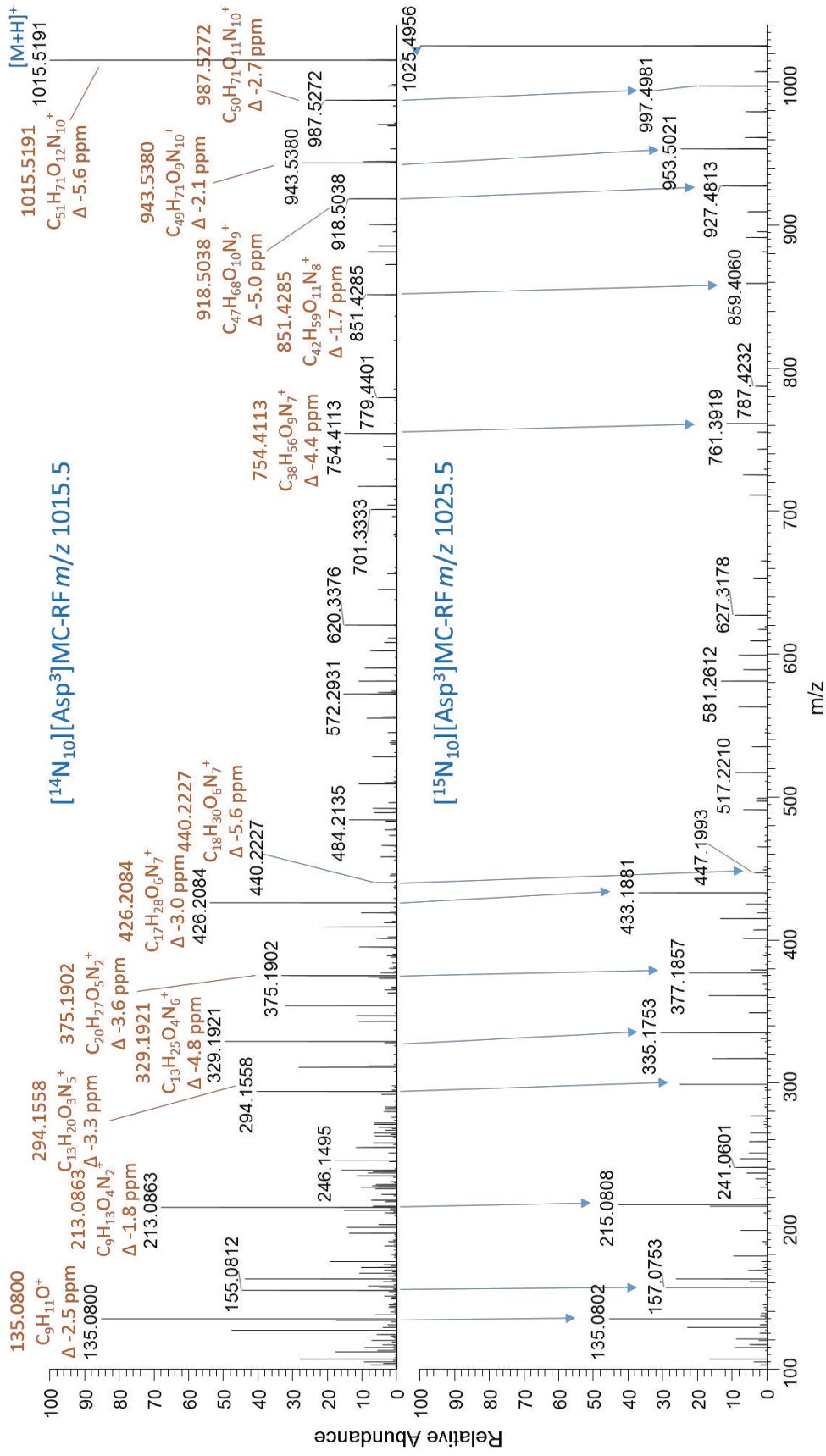
**Figure S66.** LC–HRMS/MS PRM spectra (method B) of $[M + H]^+$ of: top, unlabelled $[D\text{-}Asp^3]MC\text{-}RF$ (**18**) at $m/z$ 1015.5, and; bottom, $^{15}N$-labelled **18** at $m/z$ 1025.5.
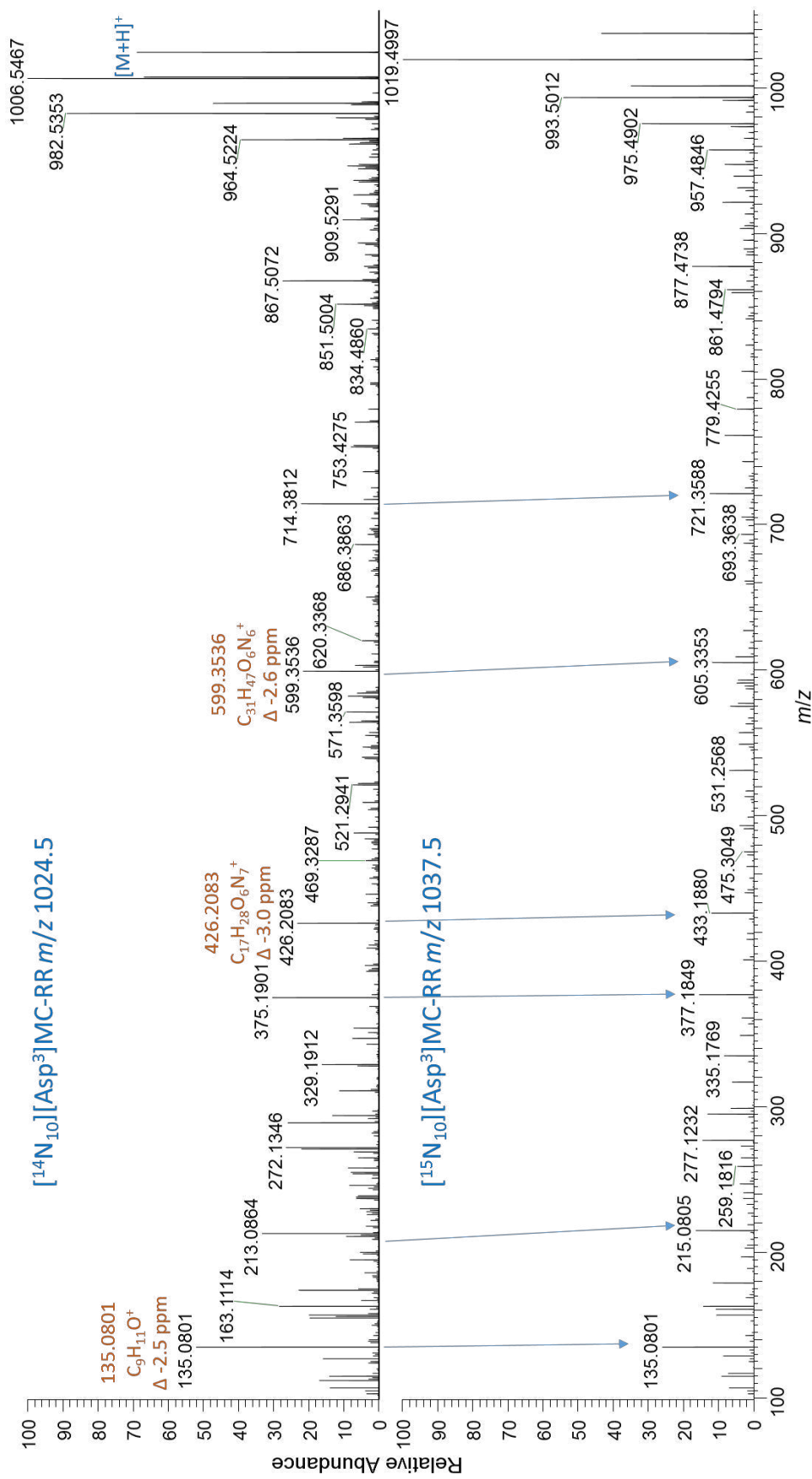
**Figure S67.** LC–HRMS/MS PRM spectra (method B) of [M + H]⁺ of: top, unlabelled [D-Asp³]MC-RR (**1**) at *m/z* 1024.5, and; bottom, ¹⁵N-labelled **1** at *m/z* 1037.5. Note the presence of the characteristic singly-charged product ions at *m/z* 135.0804 (derived from Adda⁵), 426.2096 (derived from Mdha⁷–Ala¹–Arg²–Asp³), and 599.3552 (derived from Arg⁴–Adda⁵–Glu⁶) that were also observed in the MS/MS spectra of **15** and **16** (Figures S32–33 and S58–63).

**Literature Cited**

1.      Yilmaz, Y.; Foss, A. J.; Miles, C. O.; Özen, M.; Demir, N.; Balci, M.; Beach, D. G., Comprehensive multi-technique approach reveals the high diversity of microcystins in field collections and an associated isolate of *Microcystis aeruginosa* from a Turkish lake. *Toxicon* **2019**, *167*, 87–100.

2.      LeBlanc, P.; Merkley, N.; Thomas, K.; Lewis, N. I.; Békri, K.; LeBlanc Renaud, S.; Pick, F. R.; McCarron, P.; Miles, C. O.; Quilliam, M. A., Isolation and characterization of [D-Leu[1]]microcystin-LY from *Microcystis aeruginosa* CPCC-464. *Chem. Res. Toxicol.* **2019**, (submitted).

3.      Miles, C. O.; Sandvik, M.; Nonga, H. E.; Rundberget, T.; Wilkins, A. L.; Rise, F.; Ballot, A., Identification of microcystins in a Lake Victoria cyanobacterial bloom using LC-MS with thiol derivatization. *Toxicon* **2013**, *70*, 21–31.

4.      Hao, G.; Wang, D.; Gu, J.; Shen, Q.; Gross, S. S.; Wang, Y., Neutral loss of isocyanic acid in peptide CID spectra: a novel diagnostic marker for mass spectrometric identification of protein citrullination. *J. Am. Soc. Mass Spectrom.* **2009**, *20*, 723–727.

# PAPER II

# Investigation of In Vitro Endocrine Activities of *Microcystis* and *Planktothrix* Cyanobacterial Strains

**Vittoria Mallia** [1,2,*], **Lada Ivanova** [1], **Gunnar S. Eriksen** [1], **Emma Harper** [3], **Lisa Connolly** [3] **and Silvio Uhlig** [1]

[1] Toxinology Research Group, Norwegian Veterinary Institute, Ullevålsveien 68, N-0454 Oslo, Norway; lada.ivanova@vetinst.no (L.I.); gunnar.eriksen@vetinst.no (G.S.E.); silvio.uhlig@vetinst.no (S.U.)

[2] Department of Chemistry, University of Oslo, P.O. Box 1033, N-0315 Oslo, Norway

[3] Institute for Global Food Security, School of Biological Sciences, Queen's University Belfast, Belfast BT9 5DL, UK; eharper02@qub.ac.uk (E.H.); l.connolly@qub.ac.uk (L.C.)

\* Correspondence: vitt-87@hotmail.it or vittoria.mallia@vetinst.no

**Abstract:** Cyanobacteria are cosmopolitan photosynthetic prokaryotes that can form dense accumulations in aquatic environments. They are able to produce many bioactive metabolites, some of which are potentially endocrine disrupting compounds, i.e., compounds that interfere with the hormonal systems of animals and humans. Endocrine disruptors represent potential risks to both environmental and human health, making them a global challenge. The aim of this study was to investigate the potential endocrine disrupting activities with emphasis on estrogenic effects of extracts from cultures of *Microcystis* or *Planktothrix* species. We also assessed the possible role of microcystins, some of the most studied cyanobacterial toxins, and thus included both microcystin-producing and non-producing strains. Extracts from 26 cyanobacterial cultures were initially screened in estrogen-, androgen-, and glucocorticoid-responsive reporter-gene assays (RGAs) in order to identify endocrine disruption at the level of nuclear receptor transcriptional activity. Extracts from selected strains were tested repeatedly in the estrogen-responsive RGAs, but the observed estrogen agonist and antagonist activity was minor and similar to that of the cyanobacteria growth medium control. We thus focused on another, non-receptor mediated mechanism of action, and studied the 17β-estradiol (natural estrogen hormone) biotransformation in human liver microsomes in the presence or absence of microcystin-LR (MC-LR), or an extract from the MC-LR producing *M. aeruginosa* PCC7806 strain. Our results show a modulating effect on the estradiol biotransformation. Thus, while 2-hydroxylation was significantly decreased following co-incubation of 17β-estradiol with MC-LR or *M. aeruginosa* PCC7806 extract, the relative concentration of estrone was increased.

**Keywords:** cyanobacteria; endocrine disruptor; estrogenic; microcystin; reporter-gene assay; *Planktothrix*; *Microcystis*

**Key Contribution:** Cyanobacterial extracts were tested in estrogen-responsive reporter gene assays (RGAs); while preliminary screening was done using androgen- and glucocorticoid-responsive RGAs. Interference of cyanobacterial extracts or microcystin-LR (MC-LR) with microsomal 17β-estradiol biotransformation was studied.

## 1. Introduction

Cyanobacteria are cosmopolitan photosynthetic prokaryotes, also known as "blue-green algae". In favorable conditions they can form dense blooms (water discoloration due to extended accumulation of biomass) [1], most often in freshwater, but also in brackish and marine water environments [1–3].

During such blooms, cyanobacteria may release a large variety of bioactive metabolites, including well-known cyanotoxins [1,4]. Therefore, they may have negative effects on water safety and quality (drinking, bathing, fishing, and recreational uses) and result in harm to invertebrates and vertebrates including humans [2,5–9]. Different types of cyanobacterial toxins are classified according to their toxicological target as hepatotoxins, neurotoxins, and dermatoxins. The most known and studied cyanotoxins are the microcystins (MCs), potent hepatotoxins produced by several cyanobacterial species, including *Microcystis* and *Planktothrix* spp. [10,11]. MCs are cyclic heptapeptides [12,13], which share a common core structure. Five of the seven amino acids are in general highly conserved while the other two are more variable. Thus, at least 279 different MC-congeners have been reported to date [14]. This enormous structural diversity within the class makes MCs characterization challenging, especially from a toxicological point of view.

The so-called endocrine disrupting compounds (EDCs), or endocrine disruptors (EDs), represent another increasing environmental and health concern. EDCs are exogenous substances or mixtures named by their capability of interfering with normal endocrine (hormonal) system homeostasis. Such interferences can happen through several different mechanisms and by acting on a number of different targets of the endocrine system's components (Figure 1), thereby causing adverse health effects in an intact organism or its progeny, as well as in entire populations [15,16].
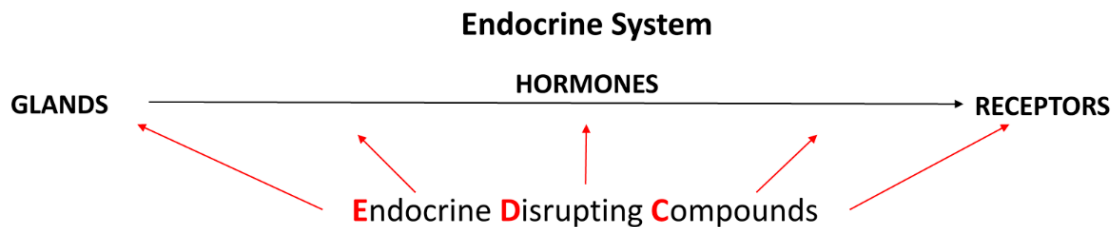


**Figure 1.** Schematic description of main components of the endocrine system. Red arrows symbolize that endocrine disruption may happen at several levels.

Most studies have mainly focused on EDCs of anthropogenic origin without extensively considering those that are naturally-produced in the environment [17,18]. However, it has been reported that cyanobacterial compounds (extracts from blooms and exudates) have ED activity, mainly through activation of the estrogen receptor [19,20]. It is not entirely clear which of the different compounds present in cyanobacterial blooms exert estrogen activity. The net effect may be the result from the interaction of different cyanobacterial metabolites in the bloom, which constitute in themselves a complex mixture of known and unknown compounds, and/or other substances coexisting in the water [18,19,21].

In general, available studies on MCs activity mainly focus on just one congener, microcystin-LR (MC-LR), because of its availability, high occurrence, and high hepatotoxicity. It is, however, well known that although one or two MC-variants (not necessarily including MC-LR) are generally dominant in a single cyanobacterial strain [5,22], the majority of blooming cyanobacteria produce multiple MC-congeners [23], in addition to other bioactive compounds.

Additionally, the few studies supporting the ED potential of MCs are based on MC-LR [24–26]. Some other studies, with a slightly broader approach, have demonstrated ED activities in extracts of cultures from *Microcystis* and *Planktothrix* spp. (which are able to release MCs). However, they seem to contradict, or at least not confirm, the role of MCs in the observed ED activity as the extracts, but not pure MC-LR, had effect in the applied assays, including induction of vitellogenin in zebrafish larvae, an effect associated with exposure to compounds with estrogenic effects [27,28]. The estrogenic effects are frequently a result of activation of the estrogen receptor (agonist) or inhibition of the activation of the androgen receptor (antagonist). Reporter gene assays (RGAs) are excellent tools to measure the agonist or antagonist activity at the receptor levels. Furthermore, Stepankova and collaborators (2011) highlighted that cytotoxicity and estrogenic effects from extracts of blooming cyanobacteria

containing MCs were greater than what would be expected from the extracts of pure laboratory cultures. These studies indicate that cyanobacterial compounds other than MCs are at least partly involved in the reported estrogenic effects. Furthermore, the potential mechanisms of the estrogenic effects of the cyanobacterial metabolites were likewise not studied.

MCs have previously been reported to cause reproductive toxicity [29–31]. Although reproduction is regulated through the endocrine system, it is debated if the reproductive effect of MC exposure is a direct effect on the endocrine system. Furthermore, there are indications that MCs interfere with the endocrine system acting on the hypothalamic–pituitary–thyroid axis in addition to the hypothalamic–pituitary–gonadal axis, which includes the estrogens (endogenous hormones related to reproduction) [32,33].

Based on the previously reported induction of vitellogenin, a clear indication of an estrogenic or anti-androgenic effect, the present study investigated potential ED effects of cyanobacterial extracts from *Microcystis* and *Planktothrix* spp. strains and pure MC-LR, with a main focus on estrogenic activity. We used cell-based models to investigate a direct effect at the receptor level (receptors are natural targets for endogenous hormones). In addition, we used a human liver microsomes (HLM) model to investigate possible interferences with cytochrome P450-mediated 17β-estradiol (herein simply referred to as estradiol) biotransformation. Estradiol is an endogenous hormone belonging to the group of estrogens (steroid hormones). Thus, this study aimed to address the following research questions and null hypotheses:

1. Do cyanobacterial metabolites interfere with hormone receptors, especially with the estrogen receptor? $H_{1-0}$: Extracts from cyanobacterial cultures do not show effects on the estrogen receptor (or other hormone receptors).
2. Are there other modes of action that may result in endocrine disrupting activity of cyanobacterial metabolites, e.g., effects on cytochrome P450 mediated estradiol biotransformation? $H_{2-0}$: Estradiol biotransformation is not affected by the presence of cyanobacterial culture extracts or MCs.
3. If cyanobacterial metabolites show ED activity, are MCs responsible for any of the observed effects? $H_{3-0}$: MCs do not show ED activity.

The different in vitro assays were therefore chosen to take into account that there are a number of processes, receptor-mediated and non-receptor mediated, which could alter endocrine functions [34,35].

## 2. Results

### 2.1. Reporter Gene Assays (RGAs)

We started from a collection of 26 cyanobacterial strains, representative of two common cyanobacterial genera, *Microcystis* and *Planktothrix* (Table S1). They included both MC-producing and non-MC-producing strains. An initial screening was done using RGAs. These assays can measure effects on specific nuclear receptors signaling. It is a high-throughput method for analysis of steroid hormones agonists and antagonists, which are compounds able to mimic or block natural transcriptional activation of steroids by binding to their nuclear receptors. In the first part of the study we focused on effects on estrogen, androgen, and glucocorticoid receptors.

Prior to screening of the 26 cyanobacterial extracts using the RGAs, their cytotoxicity was assessed using the MTT (3-[4,5-dimethylthiazole-2-yl]-2,5-diphenyltetrazolium bromide) cell viability assay. Five assay dilutions of each sample were tested (1:400, 1:800, 1:1600, 1:3200, 1:6400) in order to establish a suitable (i.e., non-toxic) concentration range that could be used in the RGAs (data not shown). In general, there was no substantial cytotoxicity for any of the cell lines, and thus we performed the preliminary screening using the MMV-Luc estrogen-responsive cell line using the two highest concentrations (i.e., dilutions 1:400 and 1:800). However, one of the cyanobacterial extracts (NIVA-CYA 22), which showed weak cytotoxicity at the highest concentration, was therefore tested at 1:800 and 1:1600 dilution in the preliminary RGAs. The 26 cyanobacterial strains were subsequently screened

using the TARM-Luc androgen-responsive, as well as TGRM-Luc glucocorticoid-responsive RGAs using the same extract aliquots and the same dilutions that were used for the estrogen-responsive RGAs.

Six strains were selected for further testing in the estrogen-responsive RGAs because they showed weak activities in the preliminary RGAs (e.g., 14–32% estrogen agonist activity relative to solvent control) (Table S2). Several of the extracts also indicated a possible androgen and glucocorticoid response, but the standard deviation of assay replicates was rather high (Tables S3 and S4). The follow-up of these preliminary results was beyond the scope of the present study and should be pursued in the future.

Another criterion for selection of the six strains to re-test in the estrogen-responsive RGAs was that they should include both MC-producers and non-producers. We aimed also to include representatives of both *Microcystis* and *Planktothrix* spp. In addition, the *M. aeruginosa* PCC7806 strain was selected for further testing because of its extensive use in research including previously reported estrogenic activity [27,36–38]. Thus, the seven strains included five *M. aeruginosa* strains, one *M. novacekii* strain and one *P. prolifica* strain (Table 1). Three of the strains were MC-producers, while four did not produce MCs according to literature data, and our own ELISA (Table 1) [38–41].

**Table 1.** Cyanobacterial strains tested repeatedly in the estrogen-responsive reporter gene assays (RGAs) including information on production of microcystins (MCs).

| Strain ID | Species | MCs [a] |
|---|---|---|
| NIVA-CYA 431 | *Microcystis novacekii* | No |
| NIVA-CYA 476 | *Microcystis aeruginosa* | No |
| NIVA-CYA 22 | *Microcystis aeruginosa* | No |
| PCC7806 | *Microcystis aeruginosa* | Yes |
| NIVA-CYA 544 | *Planktothrix prolifica* | Yes |
| NIVA-CYA 166 | *Microcystis aeruginosa* | No |
| NIVA-CYA 31 | *Microcystis aeruginosa* | Yes |

[a] based on literature data, confirmed by ELISA.

The seven extracts were reanalyzed using the estrogen-responsive RGAs in three independent experiments using new extract replicates that had been concentrated 20:1 (Figure 2). At this stage we also included cyanobacterial growth medium Z8 [42] that was extracted and concentrated using the same protocol as the cyanobacterial cultures, and the effects of the cyanobacterial cultures were expressed as relative to the Z8 growth medium control (which in itself exhibited a low estrogen agonist response). However, the estrogen agonist response for strains NIVA-CYA 431 and 476 was weak but statistically significant ($P \leq 0.05$) compared to that of Z8 medium (Figure 2a). Extracts from two *Microcystis* strains (NIVA-CYA 431 and 166) gave a weak but statistically significant ($P \leq 0.001$) enhancement of the estrogen effect from estradiol (positive control) (Figure 2b). The MTT cell viability assay was always performed in parallel to the RGAs in order to monitor potential cytotoxic effects of the cyanobacterial extracts in the cells (Figure 3). Results for concentrated extracts showed that exposure with NIVA-CYA 166 resulted in about 20% reduction of cell viability at the highest concentration, while the cell viability was little or not affected by exposure with the other six strains or the cyanobacterial growth medium (Figure 3).

*2.2. Interference of Cytochrome P450-Mediated Metabolism of Estradiol Using Human Liver Microsomes (HLM)*

We optimized a human liver microsomes (HLM) assay for the cytochrome P450-mediated biotransformation of estradiol to its main biotransformation product, 2-hydroxyestradiol, as well as 4-hydroxyestradiol (Figure 4) [43]. The levels of estrone and estriol were also monitored. Estrone is a natural weak estrogen which is in equilibrium with estradiol. Estrone can be a metabolic intermediate in the synthesis of estradiol. 17β-hydroxysteroid dehydrogenases (17β-HSD) catalyze interconversion of estradiol and estrone (Figure 4) [44]. The concentration of estradiol was chosen so it was depleted

following first-order kinetics, and assay concentrations of its oxidation products as well as estradiol itself determined using a quantitative LC–MS/MS method (Figure 5). Interference of MCs and/or other *M. aeruginosa* metabolites with cytochrome P450-mediated biotransformation of estradiol was studied by co-incubation of estradiol with either pure MC-LR (0.5 or 5 μM) or an extract of *M. aeruginosa* PCC7806, which produces two main MC-variants, MC-LR and [D-Asp$^3$] MC-LR [38]. The extract concentration of *M. aeruginosa* PCC7806 was adjusted so that the assay-concentration of MCs was about 0.5 μM.



(**a**)

(**b**)
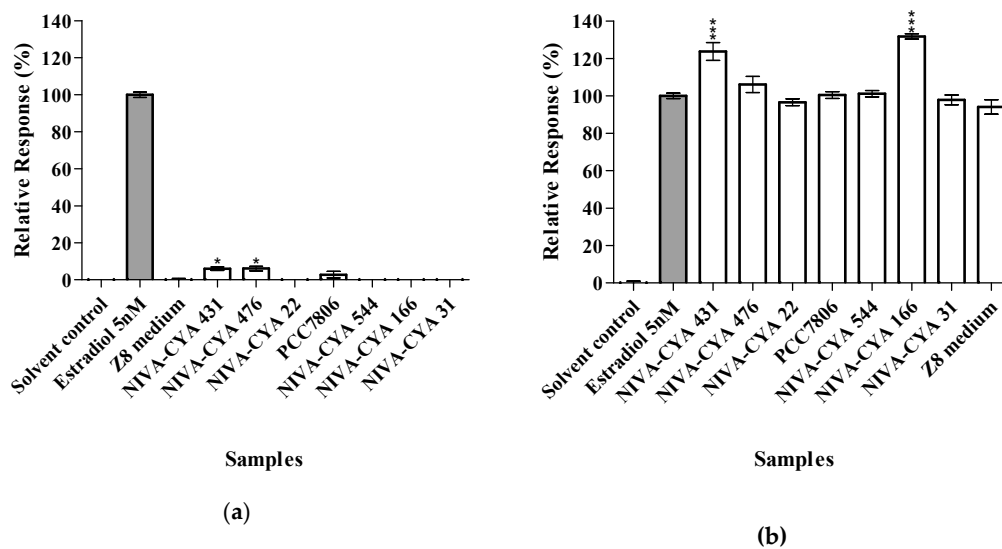
**Figure 2.** Agonistic (**a**) and antagonistic (**b**) responses of repeatedly tested cyanobacterial extracts (shown for highest concentration) and cyanobacterial growth medium (Z8) in the MMV-Luc estrogen-responsive reporter-gene assays (RGAs). Measured responses are presented relative to the cyanobacterial growth medium Z8 (**a**) and estradiol (**b**, 1.36 ng/mL or 5 nM), and expressed as the relative response ± SEM for three independent experiments (each in triplicate). One-way analysis of variance (ANOVA) and Dunnett's multiple comparison test were used. $p \leq 0.05$ (*), $p \leq 0.001$ (***) vs. Z8 medium control (**a**) or positive control (**b**).
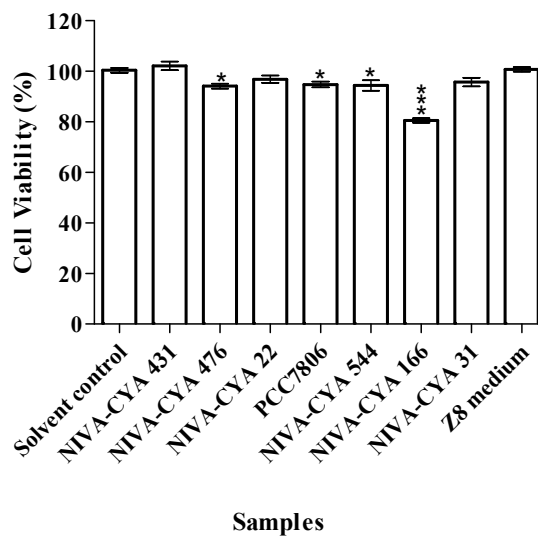


**Figure 3.** Viability of MMV-Luc cells following exposure to the seven concentrated cyanobacterial extracts and cyanobacterial growth medium (Z8) for 48 h, compared to the solvent control. Values are means of the relative viability ± SEM for three independent experiments (n = 3). One-way analysis of variance (ANOVA) and Dunnett's multiple comparison test were used. $p \leq 0.05$ (*), $p \leq 0.001$ (***) vs. solvent control.
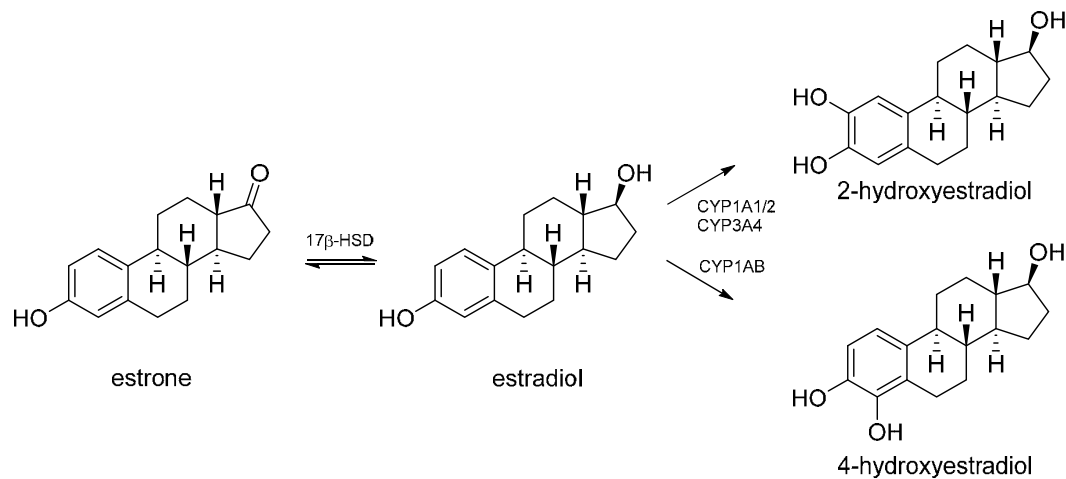
**Figure 4.** Main cytochrome P450-mediated pathways of estradiol to its 2- and 4-hydroxylated metabolites [45,46], as well as interconversion of estradiol and estrone.
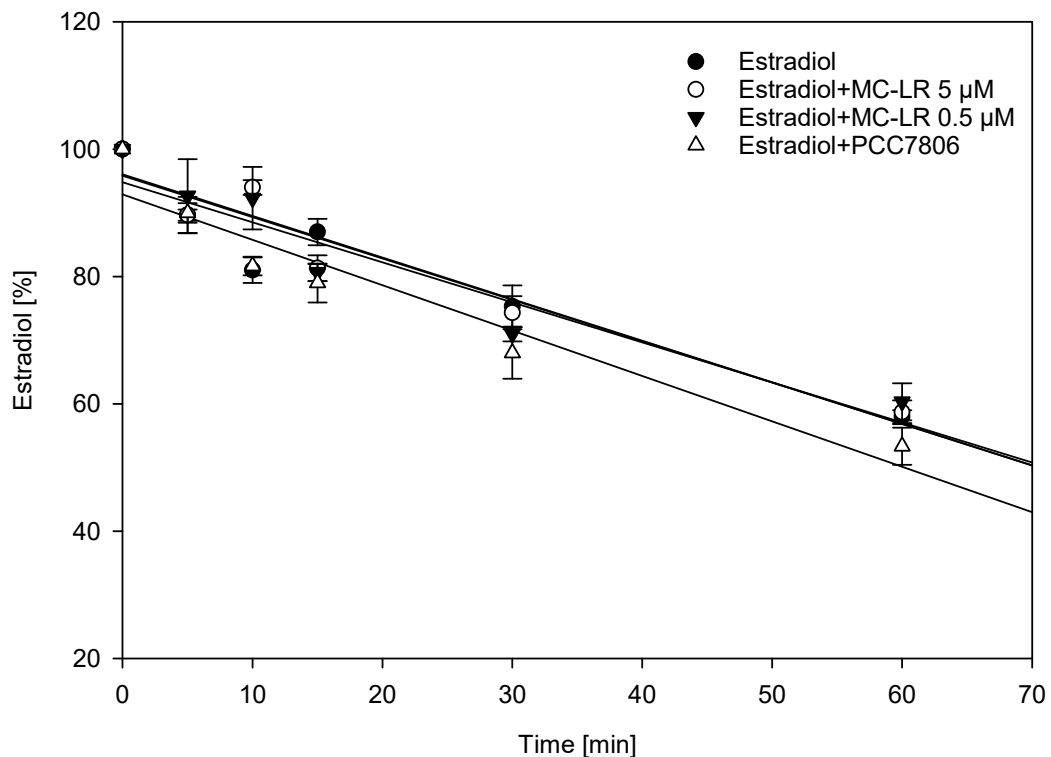


**Figure 5.** Estradiol depletion in human liver microsomes (HLM), either alone or in the presence of microcystin-LR (MC-LR) (0.5 μM and 5 μM) or *M. aeruginosa* PCC7806 extract. Data points are the mean ± SEM (n = 3) of three independent experiments.

Estradiol depletion was not significantly affected by the presence of either MC-LR or the PCC7806 extract at the tested concentrations. However, there was a reproducible trend to higher estradiol depletion when HLM were co-incubated with the PCC7806 extract for one hour (Figure 5).

The major estradiol oxidation products observed in the HLM assay were 2-hydroxyestradiol and estrone, while only traces of 4-hydroxyestradiol and estriol were detected (Figure S1). The concentrations of 2-hydroxyestradiol following co-incubation of estradiol with either 0.5 μM or 5 μM MC-LR, or *M. aeruginosa* PCC7806 extract, were significantly lower compared to when estradiol was incubated with HLM alone (Table 2, Figure S2, Table S5). In contrast, the concentrations of estrone were relatively higher when estradiol was co-incubated with either MC-LR or *M. aeruginosa* PCC7806

extract (Table 2). The relative increase in estrone was only statistically significant when estradiol was co-incubated with *M. aeruginosa* PCC7806 extract (Table 2). All background data from the experiments involving HLM are available in the Supplementary Material.

**Table 2.** Overall relative estrone and 2-hydroxyestradiol concentrations from co-incubation of estradiol with microcystin-LR (MC-LR) or *M. aeruginosa* PCC7806 extract with human liver microsomes (HLM) over 60 min. Numbers are the relative peak areas (in percentage, relative to incubation with estradiol alone) of the individual estradiol metabolites in incubations with or without MC-LR or *M. aeruginosa* PCC7806. Numbers are the grand mean of measurements at six time points and three independent experiments; the standard deviation is shown in parentheses.

| Estradiol Metabolite | 5 µM Estradiol (%) | 5 µM Estradiol + 0.5 µM MC-LR (%) | 5 µM Estradiol + 5 µM MC-LR | 5 µM Estradiol + PCC7806 |
|---|---|---|---|---|
| 2-hydroxyestradiol | 100 | 71 (±5) * | 72 (±11) * | 72 (±12) * |
| estrone | 100 | 115 (±13) | 105 (±10) | 124 (±17) ** |

* significantly different from incubation with estradiol alone based on Dunnett's test with $p < 0.0001$. ** significantly different from incubation with estradiol alone based on Dunnett's test with $p = 0.003$.

## 3. Discussion

Our screening of *Microcystis* and *Planktothrix* spp. culture extracts did not show substantial agonist or antagonist estrogen activity at the estrogen receptor level. Two strains showed statistically significant estrogen agonist activity when compared to Z8 medium. Furthermore, two strains showed a weak but statistically significant enhancement of the estradiol response, but we did not investigate further if this was due to synergism. None of these strains produced MCs, showing that the small but significant activity was not related to these toxins. We did not measure biomass, cell count, or the optical density of the cultures prior to extraction, but acknowledge that such measurements should have been performed. However, with respect to literature data investigating estrogen activity of MCs or *Microcystis* spp., we expected that extracts from visually dense cultures of the cyanobacteria would give a clear response in the estrogen-responsive RGAs provided that there are cyanobacterial metabolites or constituents that induce effects at the receptor level. Other limitations of the RGA-based screening approach were that the production of cyanobacterial metabolites might change over time depending on the growth stage, and metabolite production is also expected to be different in natural environments compared to laboratory conditions [38,47–49]. The reason for the observed agonist activity of the cyanobacterial culture medium Z8 is unclear as it does not contain any chemicals that are expected to possess estrogenic activities [42]. We believe that the origin of its weak biological activity could be due to contaminants from equipment used during the production of the medium, e.g., plastics, but did not investigate this further. However, it emphasizes that the activity of metabolites from the studied cyanobacterial strains on the estrogen receptor was minor. We did thus not aim to trace the relatively low activities in the estrogen responsive RGAs to specific cyanobacterial constituents.

While the study of estrogenic effects of cyanobacteria has been the subject of several reports, androgen- and glucocorticoid-type effects have not been studied in depth so far. However, the limited data did not support such effects from cyanobacterial extracts [19]. We only included androgen- and glucocorticoid-responsive RGAs in preliminary screenings that need further verification. However, the limited data indicated that the cyanobacterial extracts included in this study might induce androgen and glucocorticoid antagonist effects. The replicates variability in these initial screening was high and underlines the need for verification (Tables S1–S3).

MCs and extracts of *Microcystis* cultures reportedly reduce the reproduction in experimental fish [24,50,51]. The exact mechanism behind the effects on reproduction is not known and may involve effects on several endocrine pathways. Earlier work found that lyophilized *M. aeruginosa* but not pure MC-LR increased the expression of vitellogenin genes in zebrafish larvae [28], frequently interpreted as an indication of exposure to estrogenic compounds. Because of the lack of a clear estrogen activity at the receptor level, we investigated another mechanism that may lead to estrogenic effects, i.e.,

the modulation of hormone metabolism and biotransformation. Since we focused on effects of the cyanobacterial extracts on the estrogen receptor, it was natural to investigate the effect of MCs and a cyanobacterial extract on the microsomal biotransformation of estradiol. Since most toxicological studies have been carried out using the major MC-congener MC-LR, we also included this compound in our microsome trials, and co-incubated estradiol with 0.5 μM or 5 μM of the toxin. We also co-incubated estradiol with extract from *M. aeruginosa* strain PCC7806, and adjusted the extract concentration so that the total MCs assay concentration was about 0.5 μM. The PCC7806 strain has previously been shown to induce ED activity and produces MC-LR as principal MC congener. However, it is unknown if the effects were related to the MCs it produces, or other metabolites, but the data indicated that the ED activity was caused by metabolites other than MC-LR [28]. Although estradiol depletion was little affected by co-incubation with MC-LR or *M. aeruginosa* PCC7806, both the pure toxin and the cyanobacterial extract modulated the production of oxidized metabolites similarly (Table 2). Thus, the main product from microsomal cytochrome P450-mediated biotransformation, 2-hydroxyestradiol, was markedly reduced when the liver microsomes were co-incubated with either MC-LR or *M. aeruginosa* PCC7806. This effect was accompanied by an increase in relative estrone concentrations, and therefore overall estradiol depletion remained unaffected.

A large number of estradiol-metabolites have been shown, and they have different estrogenic potency [52,53]. The main hepatic phase-I metabolite 2-hydroxyestradiol has a considerably lower estrogenic potential than estradiol, estrone, 4-hydroxyestradiol, and many other tested estrogen metabolites [52]. Our findings indicate that MC-LR or extracts of a *Microcystis* culture may alter the metabolic transformation of estradiol to other metabolites with different estrogenic potential. It is therefore likely that a decreased formation of 2-hydroxyestradiol could lead to increased occurrence of estradiol or other metabolites with a higher estrogenic potency and hence induce an overall estrogenic effect. The degree of modulation of estradiol biotransformation was similar for co-incubation with 0.5 μM and 5 μM MC-LR (Table 2). However, at present we do not know the underlying mechanism(s) for the apparent modulation. While 2-hydroxylation is one of the principal microsomal biotransformation pathways for estradiol and catalyzed by CYP1A2 and CYP3A4, several other microsomal biotransformation products have been shown [46,54,55]. Future studies should therefore target as many biotransformation products of estradiol as possible, and should also investigate the possible interaction with relevant CYPs in detail. MC-LR and *Microcystis* extracts may also affect other biotransformation enzymes like sulphotransferase and steroid sulfatase. These enzymes are key enzymes in the regulation of the equilibrium between the free active form of estradiol and the much less active conjugates. MCs also affect the hypothalamic-pituitary-thyroid axis and the hypothalamic-pituitary-gonad axis in zebrafish [32,33,50]. Alterations in these pathways may interfere with normal homeostasis and hormone levels and hence explain the observed hormonal effects. Even the well-known inhibition of protein phosphatase PP2A [56–59] may affect the reproduction as the balance of phosphorylation/dephosphorylation of proteins are crucial for the regulation of intracellular signaling pathways and alterations may affect the development of gametocytes.

## 4. Conclusions

The interference of cyanobacterial metabolites from *Microcystis* and *Planktothrix* species with the estrogen receptor appears not to be a major biological effect. Future work should rather concentrate on studying interferences with the lesser-studied androgen and glucocorticoid receptors. Our data indicate that ED activity of MCs and/or other cyanobacterial compounds could arise from modulation of estrogen biotransformation as shown in HLM assays. Thus, MC-LR (and other MCs) may have ED activity.

## 5. Materials and Methods

### 5.1. Chemicals and Reagents

Extraction of cultures: Methanol (MeOH) (gradient quality) was from Romil (Cambridge, UK).

RGAs: Cell culture reagents were supplied by Life Technologies (Paisley, UK). Standards used for RGAs (estradiol, testosterone, progesterone), phosphate buffered saline (PBS), MeOH, dimethyl sulfoxide (DMSO) and 3-(4,5-dimethylthiazol-2-yl)-2,5-diphenyltetrazolium bromide (MTT) were purchased from Sigma-Aldrich (Poole, Dorset, UK). Lysis reagents and luciferase assay system were obtained from Promega (Southampton, UK).

Estradiol biotransformation: $NADP^+$, NADPH, D-glucose 6-phosphate sodium salt, D-glucose-6-phosphate dehydrogenase from baker's yeast (Saccharomyces cerevisiae), HEPES buffer and ammonium formate were purchased from Sigma-Aldrich Norway (Merck Life Science AS, Oslo, Norway). Estradiol, 2-hydroxyestradiol, 4-hydroxyestradiol, estrone and estriol were purchased from Sigma-Aldrich (Millipore-Sigma; St. Louis, MO, USA). All stock solutions were prepared in MeOH at 1 mg/mL (estradiol, estrone, and estriol) or 0.5 mg/mL (2-hydroxyestradiol and 4-hydroxyestradiol). For estradiol, the working solution at 0.25 µg/mL was prepared by appropriate dilution from stock with MeOH. Stock solutions of 2-hydroxyestradiol, 4-hydroxyestradiol, estrone, and estriol were combined for the preparation of the mixed solution containing 2 µg/mL of each compound in 50% acetonitrile (MeCN). The mixture was used to prepare calibration standards in 50% MeCN at 12.5 ng/mL, 15 ng/mL, 75 ng/mL, 150 ng/mL, and 300 ng/mL for quantitative analysis (Table 3).

**Table 3.** Instrument parameters for the LC–MS/MS analysis of estradiol and related metabolites.

| Compound | Transition [a] [*m/z*] | CE [b] | FV [c] | CAV [d] | RT [e] |
|---|---|---|---|---|---|
| estriol | 271.2 → 133.0 (157.0) | 27 | 85 | 2 | 10.5 |
| 2-hydroxyestradiol | 271.2 → 175.0 (149.0) | 19 | 120 | 4 | 11.8 |
| 4-hydroxyestradiol | 271.2 → 175.0 (149.0) | 19 | 115 | 4 | 12.0 |
| estradiol | 255.2 → 159.0 (133.0) | 19 | 100 | 2 | 13.5 |
| estrone | 271.2 → 133.0 (157.0) | 31 | 70 | 4 | 15.1 |

[a] precursor-ion to product-ion transitions, qualifier ion in parentheses. [b] collision energy in eV. [c] fragmentor voltage in V. [d] collision cell accelerator voltage in V. [e] retention time in min.

*ELISA:* Inorganic chemicals and organic solvents were reagent grade or better. MC-LR for the multihapten ELISA was from Enzo Life Sciences Inc. (Farmingdale, NY, USA). For further details refer to Samdal et al. (2014) [60].

### 5.2. Cultivation of Cyanobacterial Strains and Extraction

Twenty-five cyanobacterial strains (19 strains from *Microcystis* spp. and 6 strains from *Planktothrix* spp.) were purchased from The Norwegian Culture Collection of Algae, NORCCA, jointly maintained and owned by the Norwegian Institute for Water Research (NIVA) and the University of Oslo (Table S1). The *M. aeruginosa* PCC7806 strain was purchased from the Pasteur Institute (Paris, France) (Table S1). All strains were cultivated in Z8 medium [42] in 100 mL glass Erlenmeyer flasks in an incubator (IPP110plus, Memmert GmbH + Co.KG, Schwabach, Germany) at 18 °C with a 14/10 h light/dark photoperiod, using 1% of maximum light intensity.

For extract preparation, 3 mL of a cyanobacterial culture was transferred to a glass tube and stored at −20 °C overnight, then allowed to thaw at room temperature, and 3 mL of MeOH was added. The tube was then vortex-mixed for 20 s, sonicated for 5 min and centrifuged for 10 min at 1,000 × *g*. The supernatant was transferred to screw-cap liquid-chromatography (LC) glass vials and stored at −20 °C until use. For concentration of extracts, 1ml aliquots were dried under a gentle stream of nitrogen and re-dissolved in 50 µL of 50%MeOH in screw-cap LC glass vials and stored at −20 °C until use.

### 5.3. Microcystin ELISA

MCs production was assessed using an indirect competitive ELISA as described by Samdal et al. (2014) [60]. All samples and standard dilutions were done in duplicate and performed at ~20 °C. Absorbances were measured at 450 nm using a SpectraMax i3x plate reader (Molecular Devices, Sunnyvale, USA). For further details refer to Samdal et al. (2014) [60].

### 5.4. Cell Culture

Three reporter gene assay (RGA) cell lines were cultivated and used: the MMV-Luc (estrogen responsive), TARM-Luc (androgen responsive), and TGRM-Luc (glucocorticoid responsive). They were previously developed by transforming human mammary gland cell lines using the luciferase gene under the control of a steroid hormone inducible promoter, as reported by Willemsen et al. (2004) [61]. The cells were routinely grown in 75 cm$^2$ tissue culture flasks (Nunc, Roskilde, Denmark), incubated at 37 °C in an atmosphere containing 5% $CO_2$ and at 95% humidity. The MMV-Luc cell culture medium was made up of: Dulbecco's Modified Eagle Medium (DMEM), supplemented with 10% fetal bovine serum (FBS) and 1% L-glutamine (2 mM). The TARM-Luc and TGRM-Luc cell culture medium was made up of DMEM Glutamax, supplemented with 10% FBS. The MMV-Luc culture medium was free from phenol red because of its weak estrogenic activity that may interfere with the assay.

### 5.5. Reporter-Gene Assays (RGAs)

Reporter gene assays (RGAs) are produced by transfecting cell lines with relevant receptors. A transactivation step with a signaling protein (the luciferase) is included. This step allows the measurement of receptor activation, distinguishing at the same time between agonist and antagonist behaviour [61]. The RGA procedures have previously been described by Frizzell et al. (2011) [62]. Briefly, cells were seeded at a concentration of $4 \times 10^5$ cells/mL, 100 mL/well in white walled, clear, and flat bottomed 96-well plates (Greiner Bio-One, Fricken-hausen, Germany). RGA medium differed from that used for maintaining cell cultures in that hormone depleted serum was used instead of common FBS. After 24 h pre-incubation, cyanobacterial extract solutions as well as steroid hormone standards were added in triplicate to the cells at a final methanol concentration of 0.1%. Positive controls for the estrogen-, androgen-, and glucocorticoid-responsive RGAs were estradiol (1.36 ng/mL or 5 nM), testosterone (14.5 ng/mL) and cortisol (181 ng/mL), respectively. A solvent control (0.25% MeOH in deionized water, v/v) was also included. Antagonist tests included co-incubation of test compounds with the positive controls. The cells were incubated for 48 h. Supernatants were then discarded, and the cells were washed once with PBS. Then, 25 μL cell lysis buffer was added to each well. Reading was performed by adding 100 μL of luciferase substrate to each well and measuring luciferase activity with a Mithras Multimode Reader (Berthold, Other, Germany). Agonist response was measured relative to the solvent or cyanobacterial growth medium, and antagonist response was measured relative to the positive controls.

Estrogen-responsive RGAs and connected MTT cell viability assays were performed in triplicate and repeated in three independent exposures, while androgen-responsive and glucocorticoid-responsive RGAs and connected MTT cell viability assays were performed in triplicate, but in only one exposure each.

### 5.6. MTT Cell Viability Assay

Flat-bottomed 96-well plates (Nunc) were seeded with $4 \times 10^5$ cells/well of the appropriate RGA cell line. Cyanobacterial extracts were added to the cells after a pre-incubation period of 24 h at the desired concentration and maintaining a solvent concentration of 0.1% MeOH. Controls and extracts were incubated for 48 h. Supernatants were then discarded, and 50 μL of MTT solution (MTT stock solution/assay media ratio 1:6) added to each well and the cells incubated for another 3 h. Viable cells would convert the soluble and yellow dye MTT into insoluble and purple formazan. Supernatant

were removed and 200 µL of DMSO added to each well to solubilize the formazan crystals. Optical density was measured at 570 nm (630 nm as reference) using a Sunrise spectrophotometer (TECAN, Switzerland). Cell viability was expressed as the relative absorbance of samples compared to the solvent control.

*5.7. Human Liver Microsome (HLM) Incubation*

In vitro metabolism trials were performed using commercially available human liver microsomes (HLM; No. X008067, Lot YAO; Celsis In Vitro Technologies, Baltimore, MD, USA). Estradiol (5 µM assay concentration) was incubated either alone or in presence of MC-LR solutions (0.5 µM and 5 µM assay concentration), as well as in presence of a *M. aeruginosa* PCC7806 extract. The extract was concentrated to obtain an in-assay concentration of MCs (sum of MC-LR and [D-Asp$^3$]MC-LR) of approximately 0.5 µM. Individual incubations were carried out with 2 mg/mL of microsomal protein in a final volume of 1 mL containing a NADPH-generating system (0.91 mM NADPH, 0.83 mM NADP+, 19.4 mM glucose-6-phosphate, 1 U/mL glucose-6-phosphate dehydrogenase and 9 mM magnesium chloride hexahydrate) as well as an incubation buffer (45 mM Hepes, pH 7.4) at 37 °C for 60 min. Enzymatic reactions were stopped by adding aliquots from the individual incubations to ice-cold MeCN (1:1). All samples were vortex-mixed and placed on ice. They were centrifuged at 2,000 × *g* (Eppendorf, Hamburg, Germany) to precipitate proteins, filtered (0.22 µm Corning Costar Spin-X centrifuge tube filters, Corning Inc., NY, USA) and transferred to chromatography vials.

*5.8. Quantification of Estradiol and Biotransformation Products Using LC–MS/MS*

Estradiol and estradiol-related oxidative metabolites were determined by using an Agilent 1290 Infinity Binary UHPLC System with vacuum degasser and thermostatted column compartment (30 °C) coupled via an electrospray ionisation interface (ESI) to an Agilent 6470 TripleQ mass spectrometer (Agilent Technologies, Santa Clara, CA, USA). The instrument's MassHunter Optimizer software (version B 8.0; Agilent) was used to evaluate the fragmentation patterns of the target compounds. The precursor-ion to product-ion transition, mass-to-charge ratio (*m/z*), fragmentor voltage (FV), collision energy (CE), and cell accelerator voltage (CAV) for multiple reaction monitoring (MRM) of all analytes (Table 3) were optimized by infusing a solution of the compounds isocratically with a flow rate of 0.4 mL/min (MeCN:water, 1/1, both containing 0.1% formic acid). Two transitions were monitored for each compound using dynamic multiple reaction monitoring (dMRM) according to Table 3.

The ES interface was operated in positive ion mode including a drying gas temperature of 300 °C, a drying gas flow of 10 L/min, a nebulizer gas pressure of 25 psi, a sheath gas temperature of 375 °C, a sheath gas flow of 12 L/min, a nozzle voltage of 1000 V, and a capillary voltage of 4 kV. A novel separation method was developed using a 150 × 2.1 mm i.d. Kinetex F5 (2.6 µm particles) HPLC column including a 0.5 µm KrudKatcher Ultra pre-column filter (Phenomenex). The target compounds were eluted using a mobile phase gradient consisting of water (A) and MeCN (B), both containing 0.1% formic acid. Chromatographic separation was achieved using isocratic elution at 2% B for 6 min followed by a linear gradient to 35% B over 2 min, and followed by a second linear gradient to 48% B over 10 min. After flushing the column for 3 min with 95% B, the mobile phase was returned to the initial conditions, and the column was eluted isocratically for an additional 2 min. The total run time was 24 min. The flow rate was 0.25 mL/min, the injection volume was 1 µL and the column temperature was maintained at 30 °C.

The biotransformation of estradiol to 2-hydroxyestradiol and estrone in the different groups (i.e., 0.5 µM MC-LR + 5 µM estradiol, 5 µM MC-LR + 5 µM estradiol or *M. aeruginosa* PCC7806 + 5 µM estradiol) was compared to the reference group (5 µM estradiol) using One-Way Analysis of Variance (ANOVA) followed by Dunnett's test (JMP 14.0, SAS Institute Inc., Cary, NC, USA) (Figure S2, Table S4).

**Supplementary Materials:** The following are available online at http://www.mdpi.com/2072-6651/12/4/228/s1, Table S1. Background information for cyanobacterial strains used in this study, including ID, species, origin and production of microcystins (MCs), Table S2. ER RGA summary, Table S3. AR RGA summary, Table S4.

GR RGA summary, Table S5. *P*-values from post-hoc analyses (Dunnett's test and Student's *t* test) of the data set shown in Figure S2. Figure S1. Overlay of total ion chromatograms from LC–MS/MS analyses of estradiol incubations at 0 min and 60 min with human liver microsomes, Figure S2. One-way analysis of the relative production of 2-hydroxyestradiol and estrone in human liver microsomes, including Dunnett's and Student's *t* tests for post-hoc analysis.

## References

1. Huisman, J.; Codd, G.A.; Paerl, H.W.; Ibelings, B.W.; Verspagen, J.M.H.; Visser, P.M. Cyanobacterial blooms. *Nat. Rev. Microbiol.* **2018**, *16*, 471–483. [CrossRef] [PubMed]

2. Carmichael, W.W.; Azevedo, S.M.; An, J.S.; Molica, R.J.; Jochimsen, E.M.; Lau, S.; Rinehart, K.L.; Shaw, G.R.; Eaglesham, G.K. Human fatalities from cyanobacteria: Chemical and biological evidence for cyanotoxins. *Environ. Health Perspect.* **2001**, *109*, 663–668. [CrossRef] [PubMed]

3. Catherine, A.; Bernard, C.; Spoof, L.; Bruno, M. Microcystins and Nodularins. In *Handbook of Cyanobacterial Monitoring and Cyanotoxins Analysis*, 1st ed.; Meriluoto, J., Spoof, L., Cood, G.A., Eds.; John Wiley & Sons Ltd: Chichester, UK, 2017.

4. Janssen, E.M. Cyanobacterial peptides beyond microcystins—A review on co-occurrence, toxicity, and challenges for risk assessment. *Water Res.* **2019**, *151*, 488–499. [CrossRef] [PubMed]

5. Chorus, I.; Bartram, J. *Toxic Cyanobacteria in Water: A Guide to Their Public Health Consequences, Monitoring and Management*; E&FN Spon: New York, NY, USA, 1999.

6. Paerl, H.W.; Hall, N.S.; Calandrino, E.S. Controlling harmful cyanobacterial blooms in a world experiencing anthropogenic and climatic-induced change. *Sci. Total Environ.* **2011**, *409*, 1739–1745. [CrossRef] [PubMed]

7. Paerl, H.W.; Otten, T.G. Harmful cyanobacterial blooms: Causes, consequences, and controls. *Microb. Ecol.* **2013**, *65*, 995–1010. [CrossRef] [PubMed]

8. World Health Organization. Guidelines for Drinking-Water Quality. 2017. Available online: https://www.who.int/water_sanitation_health/publications/drinking-water-quality-guidelines-4-including-1st-addendum/en/ (accessed on 3 April 2020).

9. Falconer, I.R.; Humpage, A.R. Health risk assessment of cyanobacterial (blue-green algal) toxins in drinking water. *Int. J. Environ. Res. Public Health* **2005**, *2*, 43–50. [CrossRef] [PubMed]

10. Buratti, F.M.; Manganelli, M.; Vichi, S.; Stefanelli, M.; Scardala, S.; Testai, E.; Funari, E. Cyanotoxins: Producing organisms, occurrence, toxicity, mechanism of action and human health toxicological risk evaluation. *Arch. Toxicol.* **2017**, *91*, 1049–1130. [CrossRef]

11. Díez-Quijada, L.; Prieto, A.I.; Guzmán-Guillén, R.; Jos, A.; Camean, A.M. Occurrence and toxicity of microcystin congeners other than MC-LR and MC-RR: A review. *Food Chem. Toxicol.* **2019**, *125*, 106–132. [CrossRef]

12. Botes, D.P.; Kruger, H.; Viljoen, C.C. Isolation and characterization of four toxins from the blue–green alga, *Microcystis aeruginosa*. *Toxicon* **1982**, *20*, 945–954. [CrossRef]

13. Botes, D.P.; Viljoen, C.C.; Kruger, H.; Wessels, P.L.; Williams, D.H. Configuration assignments of the amino acid residues and the presence of N-methyldehydroalanine in toxins from the blue-green alga, Microcystis aeruginosa. *Toxicon* **1982**, *20*, 1037–1042. [CrossRef]

14. Bouaicha, N.; Miles, C.O.; Beach, D.G.; Labidi, Z.; Djabri, A.; Benayache, N.Y.; Nguyen-Quang, T. Structural diversity, characterization and toxicology of microcystins. *Toxins* **2019**, *11*, 714. [CrossRef] [PubMed]

15. International Practical Shooting Confederation. *Global Assessment of the State-of-the-Science of Endocrine Disruptors*; IPCS: Geneva, Switzerland, 2002; Available online: https://www.who.int/ipcs/publications/new_issues/endocrine_disruptors/en/ (accessed on 3 April 2020).

16. United Nations Environment Programme; WHO. *State of the Science of Endocrine Disrupting Chemicals–2012*; WHO: Geneva, Switzerland, 2012; Available online: https://www.who.int/ceh/publications/endocrine/en (accessed on 3 April 2020).

17. Giulivo, M.; Lopez de Alda, M.; Capri, E.; Barcelo, D. Human exposure to endocrine disrupting compounds: Their role in reproductive systems, metabolic syndrome and breast cancer. A review. *Environ. Res.* **2016**, *151*, 251–264. [CrossRef] [PubMed]

18. Wee, S.Y.; Aris, A.Z. Endocrine disrupting compounds in drinking water supply system and human health risk implication. *Environ. Int.* **2017**, *106*, 207–233. [CrossRef] [PubMed]

19. Stepankova, T.; Ambrozova, L.; Blaha, L.; Giesy, J.P.; Hilscherova, K. In vitro modulation of intracellular receptor signaling and cytotoxicity induced by extracts of cyanobacteria, complex water blooms and their fractions. *Aquat. Toxicol.* **2011**, *105*, 497–507. [CrossRef] [PubMed]

20. Sychrova, E.; Stepankova, T.; Novakova, K.; Blaha, L.; Giesy, J.P.; Hilscherova, K. Estrogenic activity in extracts and exudates of cyanobacteria and green algae. *Environ. Int.* **2012**, *39*, 134–140. [CrossRef] [PubMed]

21. Jia, Y.; Chen, Q.; Crawford, S.E.; Song, L.; Chen, W.; Hammers-Wirtz, M.; Strauss, T.; Seiler, T.B.; Schaffer, A.; Hollert, H. Cyanobacterial blooms act as sink and source of endocrine disruptors in the third largest freshwater lake in China. *Environ. Pollut.* **2019**, *245*, 408–418. [CrossRef]

22. Douma, M.; Ouahid, Y.; Loudiki, M.; Del Campo, F.F.; Oudra, B. The first detection of potentially toxic *Microcystis* strains in two Middle Atlas Mountains natural lakes (Morocco). *Environ. Monit. Assess.* **2017**, *189*, 39. [CrossRef]

23. Graham, J.L.; Loftin, K.A.; Meyer, M.T.; Ziegler, A.C. Cyanotoxin mixtures and taste-and-odor compounds in cyanobacterial blooms from the Midwestern United States. *Environ. Sci. Technol.* **2010**, *44*, 7361–7368. [CrossRef]

24. Hou, J.; Li, L.; Wu, N.; Su, Y.; Lin, W.; Li, G.; Gu, Z. Reproduction impairment and endocrine disruption in female zebrafish after long-term exposure to MC-LR: A life cycle assessment. *Environ. Pollut.* **2016**, *208*, 477–485. [CrossRef]

25. Oziol, L.; Bouaicha, N. First evidence of estrogenic potential of the cyanobacterial heptotoxins the nodularin-R and the microcystin-LR in cultured mammalian cells. *J. Hazard. Mater.* **2010**, *174*, 610–615. [CrossRef]

26. Zhao, Y.; Xie, L.; Yan, Y. Microcystin-LR impairs zebrafish reproduction by affecting oogenesis and endocrine system. *Chemosphere* **2015**, *120*, 115–122. [CrossRef] [PubMed]

27. Jonas, A.; Scholz, S.; Fetter, E.; Sychrova, E.; Novakova, K.; Ortmann, J.; Benisek, M.; Adamovsky, O.; Giesy, J.P.; Hilscherova, K. Endocrine, teratogenic and neurotoxic effects of cyanobacteria detected by cellular in vitro and zebrafish embryos assays. *Chemosphere* **2015**, *120*, 321–327. [CrossRef] [PubMed]

28. Rogers, E.D.; Henry, T.B.; Twiner, M.J.; Gouffon, J.S.; McPherson, J.T.; Boyer, G.L.; Sayler, G.S.; Wilhelm, S.W. Global gene expression profiling in larval zebrafish exposed to microcystin-LR and *Microcystis* reveals endocrine disrupting effects of cyanobacteria. *Environ. Sci. Technol.* **2011**, *45*, 1962–1969. [CrossRef] [PubMed]

29. Chen, L.; Chen, J.; Zhang, X.; Xie, P. A review of reproductive toxicity of microcystins. *J. Hazard. Mater.* **2016**, *301*, 381–399. [CrossRef] [PubMed]

30. Wu, J.; Shao, S.; Zhou, F.; Wen, S.; Chen, F.; Han, X. Reproductive toxicity on female mice induced by microcystin-LR. *Environ. Toxicol. Pharmacol.* **2014**, *37*, 1–6. [CrossRef] [PubMed]

31. Wang, L.; Wang, X.; Geng, Z.; Zhou, Y.; Chen, Y.; Wu, J.; Han, X. Distribution of microcystin-LR to testis of male Sprague-Dawley rats. *Ecotoxicology* **2013**, *22*, 1555–1563. [CrossRef] [PubMed]

32. Cheng, H.; Yan, W.; Wu, Q.; Liu, C.; Gong, X.; Hung, T.C.; Li, G. Parental exposure to microcystin-LR induced thyroid endocrine disruption in zebrafish offspring, a transgenerational toxicity. *Environ. Pollut.* **2017**, *230*, 981–988. [CrossRef]

33. Liu, W.; Chen, C.; Chen, L.; Wang, L.; Li, J.; Chen, Y.; Jin, J.; Kawan, A.; Zhang, X. Sex-dependent effects of microcystin-LR on hypothalamic-pituitary-gonad axis and gametogenesis of adult zebrafish. *Sci. Rep.* **2016**, *6*, 22819. [CrossRef]

34. Hecker, M.; Newsted, J.L.; Murphy, M.B.; Higley, E.B.; Jones, P.D.; Wu, R.; Giesy, J.P. Human adrenocarcinoma (H295R) cells for rapid in vitro determination of effects on steroidogenesis: Hormone production. *Toxicol. Appl. Pharmacol.* **2006**, *217*, 114–124. [CrossRef]

35. Sanderson, J.T.; Boerma, J.; Lansbergen, G.W.; van den Berg, M. Induction and inhibition of aromatase (CYP19) activity by various classes of pesticides in H295R human adrenocortical carcinoma cells. *Toxicol. Appl. Pharmacol.* **2002**, *182*, 44–54. [CrossRef]

36. Portmann, C.; Blom, J.F.; Gademann, K.; Juttner, F. Aerucyclamides A and B: Isolation and synthesis of toxic ribosomal heterocyclic peptides from the cyanobacterium *Microcystis aeruginosa* PCC 7806. *J. Nat. Prod.* **2008**, *71*, 1193–1196. [CrossRef] [PubMed]

37. Portmann, C.; Blom, J.F.; Kaiser, M.; Brun, R.; Juttner, F.; Gademann, K. Isolation of aerucyclamides C and D and structure revision of microcyclamide 7806A: Heterocyclic ribosomal peptides from *Microcystis aeruginosa* PCC 7806 and their antiparasite evaluation. *J. Nat. Prod.* **2008**, *71*, 1891–1896. [CrossRef] [PubMed]

38. Tonk, L.; Welker, M.; Huisman, J.; Visser, P.M. Production of cyanopeptolins, anabaenopeptins, and microcystins by the harmful cyanobacteria *Anabaena* 90 and *Microcystis* PCC7806. *Harmful Algae* **2009**, *8*, 219–224. [CrossRef]

39. Haande, S.; Ballot, A.; Rohrlack, T.; Fastner, J.; Wiedner, C.; Edvardsen, B. Diversity of *Microcystis aeruginosa* isolates (Chroococcales, Cyanobacteria) from East-African water bodies. *Arch. Microbiol.* **2007**, *188*, 15–25. [CrossRef]

40. Mallia, V.; Uhlig, S.; Rafuse, C.; Meija, J.; Miles, C.O. Novel microcystins from *Planktothrix prolifica* NIVA-CYA 544 Identified by LC–MS/MS, functional group derivatization and $^{15}$N-labeling. *Mar. Drugs* **2019**, *17*, 643. [CrossRef]

41. Rohrlack, T.; Skulberg, R.; Skulberg, O.M. Distribution of oligopeptide chemotypes of the cyanobacterium *Planktothrix* and their persistence in selected lakes in Fennoscandia. *J. Phycol.* **2009**, *45*, 1259–1265. [CrossRef]

42. Kotai, J. *Instructions for Preparation of Modified Nutrient Solution Z8 for Algae*; Norwegian Institute for Water Research: Oslo, Norway, 1972.

43. Yamazaki, H.; Shaw, P.M.; Guengerich, F.P.; Shimada, T. Roles of cytochromes P450 1A2 and 3A4 in the oxidation of estradiol and estrone in human liver microsomes. *Chem. Res. Toxicol.* **1998**, *11*, 659–665. [CrossRef]

44. Labrie, F.; Luu-The, V.; Lin, S.X.; Labrie, C.; Simard, J.; Breton, R.; Belanger, A. The key role of 17β-hydroxysteroid dehydrogenases in sex steroid biology. *Steroids* **1997**, *62*, 148–158. [CrossRef]

45. Lee, A.J.; Cai, M.X.; Thomas, P.E.; Conney, A.H.; Zhu, B.T. Characterization of the oxidative metabolites of 17β-estradiol and estrone formed by 15 selectively expressed human cytochrome P450 isoforms. *Endocrinology* **2003**, *144*, 3382–3398. [CrossRef]

46. Tsuchiya, Y.; Nakajima, M.; Yokoi, T. Cytochrome P450-mediated metabolism of estrogens and its regulation in human. *Cancer Lett.* **2005**, *227*, 115–124. [CrossRef]

47. Briand, E.; Bormans, M.; Gugger, M.; Dorrestein, P.C.; Gerwick, W.H. Changes in secondary metabolic profiles of *Microcystis aeruginosa* strains in response to intraspecific interactions. *Environ. Microbiol.* **2016**, *18*, 384–400. [CrossRef] [PubMed]

48. Rohrlack, T.; Utkilen, H. Effects of nutrient and light availability on production of bioactive anabaenopeptins and microviridin by the cyanobacterium *Planktothrix agardhii*. *Hydrobiologia* **2007**, *583*, 231–240. [CrossRef]

49. Tonk, L.; Visser, P.M.; Christiansen, G.; Dittmann, E.; Snelder, E.O.; Wiedner, C.; Mur, L.R.; Huisman, J. The microcystin composition of the cyanobacterium *Planktothrix agardhii* changes toward a more toxic variant with increasing light intensity. *Appl. Environ. Microbiol.* **2005**, *71*, 5177–5181. [CrossRef] [PubMed]

50. Liu, G.; Ke, M.; Fan, X.; Zhang, M.; Zhu, Y.; Lu, T.; Sun, L.; Qian, H. Reproductive and endocrine-disrupting toxicity of *Microcystis aeruginosa* in female zebrafish. *Chemosphere* **2018**, *192*, 289–296. [CrossRef]

51. Trinchet, I.; Djediat, C.; Huet, H.; Dao, S.P.; Edery, M. Pathological modifications following sub-chronic exposure of medaka fish (*Oryzias latipes*) to microcystin-LR. *Reprod. Toxicol.* **2011**, *32*, 329–340. [CrossRef]

52. Hoogenboom, L.A.P.; de Haan, L.; Hooijerink, D.; Bor, G.; Murk, A.J.; Brouwer, A. Estrogenic activity of estradiol and its metabolites in the ER-CALUX assay with human T47D breast cells. *APMIS* **2001**, *109*, 101–107. [CrossRef]

53. Zhu, B.T.; Han, G.Z.; Shim, J.Y.; Wen, Y.; Jiang, X.R. Quantitative structure-activity relationship of various endogenous estrogen metabolites for human estrogen receptor α and β subtypes: Insights into the structural determinants favoring a differential subtype binding. *Endocrinology* **2006**, *147*, 4132–4150. [CrossRef]

54. Cheng, Z.N.; Shu, Y.; Liu, Z.Q.; Wang, L.S.; Ou-Yang, D.S.; Zhou, H.H. Role of cytochrome P450 in estradiol metabolism in vitro. *Acta Pharmacol. Sin.* **2001**, *22*, 148–154.

55. Lee, A.J.; Kosh, J.W.; Conney, A.H.; Zhu, B.T. Characterization of the NADPH-dependent metabolism of 17β-estradiol to multiple metabolites by human liver microsomes and selectively expressed human cytochrome P450 3A4 and 3A5. *J. Pharmacol. Exp. Ther.* **2001**, *298*, 420–432.

56. Fontanillo, M.; Kohn, M. Microcystins: Synthesis and structure–activity relationship studies toward PP1 and PP2A. *Bioorg. Med. Chem.* **2018**, *26*, 1118–1126. [CrossRef]

57. MacKintosh, C.; Beattie, K.A.; Klumpp, S.; Cohen, P.; Codd, G.A. Cyanobacterial microcystin-LR is a potent and specific inhibitor of protein phosphatases 1 and 2A from both mammals and higher plants. *FEBS Lett.* **1990**, *264*, 187–192. [CrossRef]

58. Runnegar, M.T.; Kong, S.; Berndt, N. Protein phosphatase inhibition and in vivo hepatotoxicity of microcystins. *Am. J. Physiol.* **1993**, *265*, G224–G230. [CrossRef] [PubMed]

59. Yoshizawa, S.; Matsushima, R.; Watanabe, M.F.; Harada, K.; Ichihara, A.; Carmichael, W.W.; Fujiki, H. Inhibition of protein phosphatases by microcystins and nodularin associated with hepatotoxicity. *J. Cancer Res. Clin. Oncol.* **1990**, *116*, 609–614. [CrossRef] [PubMed]

60. Samdal, I.A.; Ballot, A.; Lovberg, K.E.; Miles, C.O. Multihapten approach leading to a sensitive ELISA with broad cross-reactivity to microcystins and nodularin. *Environ. Sci. Technol.* **2014**, *48*, 8035–8043. [CrossRef] [PubMed]

61. Willemsen, P.; Scippo, M.L.; Kausel, G.; Figueroa, J.; Maghuin-Rogister, G.; Martial, J.A.; Muller, M. Use of reporter cell lines for detection of endocrine-disrupter activity. *Anal. Bioanal. Chem.* **2004**, *378*, 655–663.

62. Frizzell, C.; Ndossi, D.; Verhaegen, S.; Dahl, E.; Eriksen, G.; Sorlie, M.; Ropstad, E.; Muller, M.; Elliott, C.T.; Connolly, L. Endocrine disrupting effects of zearalenone, alpha- and beta-zearalenol at the level of nuclear receptor binding and steroidogenesis. *Toxicol. Lett.* **2011**, *206*, 210–217. [CrossRef]

# Supplementary Materials: Investigation of *in Vitro* Endocrine Activities of *Microcystis* and *Planktothrix* Cyanobacterial Strains

**Vittoria Mallia, Lada Ivanova, Gunnar S. Eriksen, Emma Harper, Lisa Connolly and Silvio Uhlig**

**Table S1.** Background information for cyanobacterial strains used in this study, including ID, species, origin and production of microcystins (MCs) according to ELISA.

| Strain ID | Species | Origin and year of isolation | MCs (ELISA) |
|---|---|---|---|
| NIVA-CYA 431* | *M. novacekii* | L. Victoria, Murchison Bay, Uganda, 2000 | no |
| NIVA-CYA 476* | *M. aeruginosa* | L. Victoria, Murchison Bay, Uganda, 2004 | no |
| NIVA-CYA 22* | *M. aeruginosa* | L. Mendota, Madison, WI, 1948 | no |
| PCC7806* | *M. aeruginosa* | Braakman Reservoirs, The Netherlands, 1972 | yes |
| NIVA-CYA 544* | *P. prolifica* | L. Steinsfjorden, Buskerud, Norway, 2004 | yes |
| NIVA-CYA 166* | *M. aeruginosa* | L. Hellesjøvatnet, Akershus, Norway, 1987 | no |
| NIVA-CYA 31* | *M. aeruginosa* | L. Little Rideau, Ontario, Canada, 1954 | yes |
| NIVA-CYA 24 | *P. prolifica* | L. Levrasjön, Kristianstad, Sweden, 1975 | no |
| NIVA-CYA 56/1 | *P. mougeotii* | L. Steinsfjorden, Buskerud, Norway, 1978 | no |
| NIVA-CYA 116 | *P. agardhii* | L. Årungen, Norway,1983 | no |
| NIVA-CYA 123/1 | *M. aeruginosa* | L. Mälaren, Sweden, 1983 | no |
| NIVA-CYA 140 | *M. aeruginosa* | Bendig's Pond, Bruno, Saskatchewan, Canada, 1975 | yes |
| NIVA-CYA 143 | *M. aruginosa* | L. Akersvatnet. Norway, 1984 | no |
| NIVA-CYA 144 | *M. cf. aeruginosa* | L. Borrevatnet, Vestfold, Norway, 1984 | no |
| NIVA-CYA 264 | *M. botrys* | L. Frøylandsvatnet, Rogaland, Norway, 1990 | yes |
| NIVA-CYA 279 | *M. cf. ichthyoblabe* | L. Østensjøvatnet, Oslo, Norway, 1990 | no |
| NIVA-CYA 432 | *Microcistys sp.* | L. Victoria, Murchison Bay, Uganda, 2000 | no |
| NIVA-CYA 475 | *M. aeruginosa* | L. Victoria, Murchison Bay, Uganda, 2000 | no |
| NIVA-CYA 478 | *M. aeruginosa* | L. Victoria, Murchison Bay, Uganda, 2000 | no |
| NIVA-CYA 482 | *M. aeruginosa* | L. Mburo, Uganda, 2004 | no |
| NIVA-CYA 598 | *P. prolifica* | L. Kolbotnvatnet, Akershus, Norway, 2007 | yes |
| NIVA-CYA 613 | *M. botrys* | L. Steinsfjorden, Buskerud, Norway, 2008 | yes |
| NIVA-CYA 632 | *P. rubescens* | L. Lyseren, Østfold, Norway, 2008 | yes |
| NIVA-CYA 754 | *M. aeruginosa* | Roodeplaat, South Africa, 2011 | no |
| NIVA-CYA 842 | *M. aeruginosa* | Hartbeespoort Dam, South Africa, 2013 | no |
| K-0540 | *M. aeruginosa* | Bagsværd Sø, Denmark, ? | no |

*selected strains, concentrated for further reporter gene assays.

<div align="center">**Table S2.** ER RGA summary.</div>

| | | **ESTROGEN RESPONSIVE REPORTER GENE ASSAY** | | |
|---|---|---|---|---|
| **Sample** | **Dilution** | **Agonism % SC\* response (SEM)** | **Antagonism % PC\*\* response (SEM)** | **Cell viability-Cytotoxicity % response rel. to SC\* (SEM)** |
| NIVA-CYA 598 | 1/400 | 8.4 (2.2) | 11.2 (3.0) | -10.3 (1.1) |
| | 1/800 | 4.9 (1.6) | 8.3 (6.1) | -11.5 (3.2) |
| NIVA-CYA 842 | 1/400 | 3.3 (1.1) | 4.6 (1.9) | -16.6 (2.6) |
| | 1/800 | 6.0 (3.0) | 3.4 (1.4) | -18.8 (6.5) |
| NIVA-CYA 613 | 1/400 | 1.9 (1.4) | 7.7 (3.3) | -15.0 (1.9) |
| | 1/800 | 1.7 (0.5) | 8.3 (3.0) | -11.6 (0.5) |
| NIVA-CYA 431 | 1/400 | 15.7 (1.4) | 14.6 (2.8) | 1.8 (0.7) |
| | 1/800 | 5.0 (1.1) | -11.2 (3.9) | 10.0 (3.7) |
| NIVA-CYA 140 | 1/400 | 8.5 (1.6) | 8.4 (1.9) | -6.1 (1.7) |
| | 1/800 | 11.2 (6.4) | 3.1 (4.4) | -8.1 (0.7) |
| K-0540 | 1/400 | 0.8 (1.2) | 9.4 (3.7) | -3.8 (4.0) |
| | 1/800 | 3.3 (1.8) | 8.5 (1.4) | -8.5 (2.3) |
| NIVA-CYA 475 | 1/400 | 2.1 (1.1) | 14.5 (2.0) | -13.2 (0.8) |
| | 1/800 | -0.2 (0.8) | 11.8 (5.1) | -12.5 (3.5) |
| NIVA-CYA 476 | 1/400 | 1.3 (0.8) | 6.4 (2.7) | -0.4 (1.5) |
| | 1/800 | 29.2 (2.8) | 6.4 (3.2) | 12.3 (5.8) |
| NIVA-CYA 22 | 1/800 | 20.5 (1.3) | 11.4 (3.6) | 2.7 (5.7) |
| | 1/1600 | 14.1 (1.3) | 11.3 (5.4) | 11.6 (1.3) |
| NIVA-CYA 632 | 1/400 | 0.7 (0.9) | 24.0 (7.7) | 5.9 (2.8) |
| | 1/800 | 0.1 (0.7) | -4.0 (17.3) | 7.3 (1.7) |
| NIVA-CYA 143 | 1/400 | 3.8 (1.6) | 18.3 (2.8) | -11.3 (2.5) |
| | 1/800 | 8.7 (1.5) | 15.2 (11.0) | -10.1 (1.0) |
| NIVA-CYA 24 | 1/400 | 9.8 (0.6) | 5.8 (23.4) | -5.2 (1.5) |
| | 1/800 | 0.4 (0.3) | -6.9 (11.1) | 4.1 (1.7) |
| PCC7806 | 1/400 | 12.6 (3.9) | -0.3 (22.5) | -11.2 (2.4) |
| | 1/800 | 2.0 (0.7) | -7.3 (15.3) | 25.7 (3.3) |
| NIVA-CYA 478 | 1/400 | 9.3 (1.0) | 6.8 (0.5) | -6.6 (0.6) |
| | 1/800 | -6.8 (1.3) | 15.7 (10.2) | -9.1 (1.3) |
| NIVA-CYA 544 | 1/400 | -2.2 (0.9) | 5.1 (1.6) | 10.6 (1.9) |
| | 1/800 | 23.2 (11.9) | 10.7 (6.8) | 1.2 (3.2) |
| NIVA-CYA 279 | 1/400 | 6.9 (1.0) | -1.5 (4.6) | -6.2 (3.8) |
| | 1/800 | -2.9 (0.8) | 11.5 (2.6) | -5.2 (2.9) |
| NIVA-CYA 144 | 1/400 | 5.2 (0.8) | 9.4 (4.3) | 1.9 (4.1) |
| | 1/800 | 1.6 (0.6) | 9.8 (5.8) | 8.5 (1.6) |
| NIVA-CYA 482 | 1/400 | -1.6 (0.4) | 8.0 (5.6) | 3.4 (1.1) |
| | 1/800 | -4.0 (0.2) | -6.2 (5.1) | 6.8 (2.2) |
| NIVA-CYA 754 | 1/400 | -6.6 (0.9) | 0.1 (9.6) | 1.9 (2.6) |
| | 1/800 | -7.3 (0.6) | 3.1 (7.9) | 9.3 (1.5) |
| NIVA-CYA 166 | 1/400 | 22.3 (1.4) | -2.1 (5.7) | 14.4 (2.3) |
| | 1/800 | -2.2 (2.0) | 4.2 (6.2) | 9.9 (0.4) |
| NIVA-CYA 31 | 1/400 | 32.5 (1.8) | 19.2 (8.6) | 20.1 (2.2) |
| | 1/800 | 0.6 (0.5) | 7.6 (8.9) | 37.1 (8.5) |
| NIVA-CYA 432 | 1/400 | -2.4 (0.6) | -9.0 (2.7) | 18.6 (3.1) |
| | 1/800 | -3.3 (1.0) | -4.1 (4.8) | 13.7 (2.5) |
| NIVA-CYA 56/1 | 1/400 | 11.7 (0.4) | 9.6 (1.1) | 10.6 (2.7) |
| | 1/800 | -2.1 (1.3) | -1.5 (3.4) | 9.8 (1.5) |

| | | | | |
|---|---|---|---|---|
| NIVA-CYA | 1/400 | 0.9 (0.2) | -5.3 (7.2) | 2.1 (1.1) |
| 116 | 1/800 | -1.5 (1.3) | -2.5 (7.0) | 8.3 (2.4) |
| NIVA-CYA | 1/400 | -4.2 (1.4) | 14.0 (9.0) | 10.1 (0.4) |
| 264 | 1/800 | -6.3 (1.0) | 10.0 (17.7) | 9.2 (1.7) |
| NIVA-CYA | 1/400 | -1.0 (1.7) | 5.7 (26.5) | 3.4 (2.7) |
| 123/1 | 1/800 | -3.3 (0.6) | -11.8 (4.0) | 14.8 (5.2) |

*SC= solvent control (0.25% methanol in deionized water, v/v). **PC= positive control (Estradiol 1.36 ng/mL).

**Table S3.** AR RGA summary.

| ANDROGEN RESPONSIVE REPORTER GENE ASSAY | | | | |
|---|---|---|---|---|
| Sample | Dilution | Agonism % SC* response (SEM) | Antagonism % PC** response (SEM) | Cell viability-Cytotoxicity % response rel. to SC* (SEM) |
| NIVA-CYA | 1/400 | 3.9 (1.3) | -61.4 (3.1) | -3.9 (3.8) |
| 598 | 1/800 | 4.0 (0.5) | -54.5 (4.3) | -1.4 (2.9) |
| NIVA-CYA | 1/400 | 4.0 (1.2) | -46.1 (2.7) | -7.1 (3.3) |
| 842 | 1/800 | -0.2 (0.3) | -44.4 (8.1) | -11.0 (1.8) |
| NIVA-CYA | 1/400 | 0.3 (0.6) | -34.6 (13.1) | -6.2 (0.8) |
| 613 | 1/800 | 3.1 (1.2) | -46.0 (2.7) | -3.0 (2.0) |
| NIVA-CYA | 1/400 | 1.6 (1.1) | -54.1 (0.3) | -2.1 (3.9) |
| 431 | 1/800 | 5.1 (4.0) | -88.7 (1.6) | 1.8 (6.7) |
| NIVA-CYA | 1/400 | 2.6 (0.8) | -78.4 (5.2) | 7.0 (1.5) |
| 140 | 1/800 | 3.3 (1.0) | -71.5 (6.2) | 4.4 (1.7) |
| K-0540 | 1/400 | 2.9 (0.8) | -55.4 (7.9) | 1.3 (2.1) |
| | 1/800 | 3.6 (1.4) | -54.3 (4.4) | -4.6 (1.4) |
| NIVA-CYA | 1/400 | 2.7 (1.9) | -47.6 (8.5) | -8.9 (3.2) |
| 475 | 1/800 | 1.2 (0.4) | -47.9 (6.9) | -13.2 (1.3) |
| NIVA-CYA | 1/400 | 4.6 (1.7) | -44.0 (8.4) | -4.7 (2.1) |
| 476 | 1/800 | 3.0 (1.5) | -37.6 (1.9) | 0.8 (3.3) |
| NIVA-CYA | 1/800 | 2.8 (1.1) | -33.4 (4.1) | -10.2 (3.6) |
| 22 | 1/1600 | 1.7 (1.0) | -24.4 (12.6) | 2.0 (0.9) |
| NIVA-CYA | 1/400 | 3.2 (0.5) | -31.2 (5.8) | -4.3 (1.3) |
| 632 | 1/800 | 2.3 (0.5) | -25.5 (7.7) | -3.1 (0.6) |
| NIVA-CYA | 1/400 | 3.1 (1.1) | -36.1 (6.6) | -3.5 (2.4) |
| 143 | 1/800 | 2.2 (0.7) | -21.3 (8.2) | -3.4 (1.2) |
| NIVA-CYA | 1/400 | 3.4 (1.2) | -36.3 (4.4) | -4.3 (1.8) |
| 24 | 1/800 | 3.1 (1.5) | -39.9 (6.9) | 0.7 (3.8) |
| PCC7806 | 1/400 | 2.7 (1.1) | -50.9 (1.3) | 1.3 (1.5) |
| | 1/800 | 1.2 (0.2) | -30.5 (1.0) | 4.0 (0.4) |
| NIVA-CYA | 1/400 | 2.3 (0.3) | -34.6 (10.8) | -6.4 (0.8) |
| 478 | 1/800 | 2.1 (0.9) | -22.7 (1.1) | -6.3 (2.4) |
| NIVA-CYA | 1/400 | 3.9 (0.6) | -17.4 (8.5) | -2.3 (3.2) |
| 544 | 1/800 | 3.7 (0.9) | -20.6 (6.2) | 42.3 (0.8) |
| NIVA-CYA | 1/400 | 2.6 (0.7) | -8.7 (5.5) | 16.8 (17.6) |
| 279 | 1/800 | 4.1 (1.0) | -11.6 (2.9) | -1.9 (6.6) |
| NIVA-CYA | 1/400 | 2.8 (0.9) | -25.9 (14.3) | -2.1(21.6) |
| 144 | 1/800 | 2.7 (0.5) | -34.6 (8.1) | -4.2 (1.8) |
| NIVA-CYA | 1/400 | 1.4 (0.5) | 2.1 (2.3) | 2.8 (2.6) |
| 482 | 1/800 | 3.2 (0.8) | 11.3 (5.6) | -3.5 (2.7) |
| NIVA-CYA | 1/400 | 3.5 (0.5) | 18.1 (14.7) | 1.8 (2.4) |
| 754 | 1/800 | 2.4 (0.5) | 9.9 (6.0) | -3.9 (4.5) |

| NIVA-CYA | 1/400 | 2.8 (0.6) | 20.7 (5.3) | 0.8 (9.8) |
|---|---|---|---|---|
| 166 | 1/800 | 4.0 (0.9) | -1.3 (7.4) | -4.8 (2.1) |
| NIVA-CYA | 1/400 | 3.1 (0.5) | 9.8 (14.3) | -5.7 (1.4) |
| 31 | 1/800 | 2.6 (0.4) | 22.7 (2.5) | 0.5 (4.0) |
| NIVA-CYA | 1/400 | 1.7 (0.2) | 8.8 (14.5) | 7.2 (0.9) |
| 432 | 1/800 | 0.3 (0.4) | 6.1 (7.2) | -0.5 (3.1) |
| NIVA-CYA | 1/400 | 5.2 (0.7) | 3.6 (3.8) | -4.7 (4.7) |
| 56/1 | 1/800 | 1.9 (0.4) | 1.6 (0.5) | 17.2 (11.3) |
| NIVA-CYA | 1/400 | 2.3 (1.3) | 12.3 (7.8) | -9.4 (1.9) |
| 116 | 1/800 | 1.5 (0.6) | 4.6 (14.0) | -7.5 (1.3) |
| NIVA-CYA | 1/400 | 2.6 (0.5) | 15.8 (13.2) | -4.5 (10.7) |
| 264 | 1/800 | 2.9 (0.7) | 5.0 (11.9) | -7.0 (3.6) |
| NIVA-CYA | 1/400 | 2.5 (0.6) | 17.3 (18.2) | -5.3 (0.7) |
| 123/1 | 1/800 | 2.0 (1.4) | 28.3 (8.9) | 9.9 (7.8) |

*SC= solvent control (0.25% methanol in deionized water, v/v). **PC= positive control (Testosterone 14.5 ng/mL).

**Table S4.** GR RGA summary.

| GLUCOCORTICOID RESPONSIVE REPORTER GENE ASSAY | | | | |
|---|---|---|---|---|
| Sample | Dilution | Agonism<br>% SC* response<br>(SEM) | Antagonism<br>% PC** response<br>(SEM) | Cell viability-Cytotoxicity<br>% response rel. to SC*<br>(SEM) |
| NIVA-CYA | 1/400 | 1.9 (0.7) | -7.6 (21.9) | 9.1 (9.3) |
| 598 | 1/800 | 0.4 (0.2) | 30.2 (27.4) | 4.2 (3.9) |
| NIVA-CYA | 1/400 | 0.1 (0.0) | -10.6 (33.3) | 7.9 (7.4) |
| 842 | 1/800 | 0.0 (0.0) | 17.1 (34.0) | 13.0 (7.9) |
| NIVA-CYA | 1/400 | 0.0(0.0) | 14.0 (13.5) | 3.7 (6.1) |
| 613 | 1/800 | -0.1 (0.0) | -39.4 (31.2) | -4.8 (2.3) |
| NIVA-CYA | 1/400 | 0.0 (0.0) | -17.1 (16.6) | -2.8 (2.5) |
| 431 | 1/800 | 0.2 (0.2) | -12.3 (21.3) | -7.0 (7.5) |
| NIVA-CYA | 1/400 | 0.3 (0.2) | -5.7 (26.6) | 17.2 (6.6) |
| 140 | 1/800 | 1.7 (1.6) | 31.6 (37.3) | 7.7 (0.7) |
| K-0540 | 1/400 | 0.2 (0.1) | -52.4 (9.9) | 7.6 (5.4) |
| | 1/800 | 0.0 (0.0) | -23.4 (16.9) | 4.1 (15.7) |
| NIVA-CYA | 1/400 | 0.0 (0.0) | -20.6 (4.8) | 20.4 (20.5) |
| 475 | 1/800 | 2.6 (1.4) | -20.0 (5.1) | 8.7 (8.2) |
| NIVA-CYA | 1/400 | 0.1 (0.0) | -28.0 (11.9) | 8.2 (6.0) |
| 476 | 1/800 | 0.0 (0.0) | 32.4 (25.1) | -4.4 (6.8) |
| NIVA-CYA | 1/800 | 0.0 (0.0) | -19.3 (8.1) | -9.2 (4.5) |
| 22 | 1/1600 | 0.0 (0.0) | 9.9 (54.5) | 4.5 (1.4) |
| NIVA-CYA | 1/400 | 0.0 (0.0) | -39.9 (11.0) | -9.4 (6.2) |
| 632 | 1/800 | 0.0 (0.0) | -25.4 (28.8) | -14.8 (12.2) |
| NIVA-CYA | 1/400 | 0.1 (0.1) | -88.6 (8.2) | -3.7 (8.6) |
| 143 | 1/800 | 0.1 (0.1) | -29.9 (17.5) | -1.0 (7.1) |
| NIVA-CYA | 1/400 | 0.2 (0.2) | 17.8 (9.2) | -6.5 (3.9) |
| 24 | 1/800 | 0.1 (0.1) | -15.2 (30.4) | -10.1 (8.6) |
| PCC7806 | 1/400 | 0.0 (0.0) | 0.7 (19.6) | -15.0 (5.8) |
| | 1/800 | 0.0 (0.0) | -40.0 (18.5) | 7.5 (19.0) |
| NIVA-CYA | 1/400 | 0.7 (0.6) | -7.9 (26.5) | -4.6 (12.7) |
| 478 | 1/800 | 0.2 (0.1) | -11.3 (37.3) | -7.7 (3.1) |
| NIVA-CYA | 1/400 | 0.1 (0.0) | **7.7 (20.5)** | 4.2 (13.1) |
| 544 | 1/800 | 0.0 (0.0) | -76.7 (13.0) | 7.0 (10.3) |

| | | | | |
|---|---|---|---|---|
| NIVA-CYA 279 | 1/400 | 0.0 (0.0) | -54.0(19.3) | -1.3 (16.2) |
| | 1/800 | 0.0 (0.0) | 25.8(14.2) | -2.0 (6.1) |
| NIVA-CYA 144 | 1/400 | 0.0 (0.0) | -79.1 (9.0) | -16.1 (4.8) |
| | 1/800 | 0.1 (0.0) | 26.7 (14.9) | -18.9 (7.3) |
| NIVA-CYA 482 | 1/400 | 0.1 (0.1) | 32.2 (19.8) | -9.2 (5.5) |
| | 1/800 | 0.1 (0.1) | -57.3 (8.5) | -0.4 (14.0 |
| NIVA-CYA 754 | 1/400 | 0.0 (0.0) | -43.3 (15.8) | -5.9 (5.2) |
| | 1/800 | 0.0 (0.0) | -13.0 (10.0) | -3.5 (4.2) |
| NIVA-CYA 166 | 1/400 | 0.0 (0.0) | -23.1 (24.6) | -9.9 (4.3) |
| | 1/800 | 0.6 (0.1) | 28.0 (22.3) | -5.5 (1.3) |
| NIVA-CYA 31 | 1/400 | 9.1 (2.0) | -31.6 (32.1) | -12.6 (1.2) |
| | 1/800 | 0.0 (0.0) | -55.9 (32.0) | -4.2 (4.7) |
| NIVA-CYA 432 | 1/400 | 0.1 (0.1) | -74.1 (19.0) | -5.0 (4.6) |
| | 1/800 | 0.0 (0.0) | -38.9 (18.5) | -2.6 (3.8) |
| NIVA-CYA 56/1 | 1/400 | -0.1 (0.0) | -26.5 (11.5) | -18.9(1.8) |
| | 1/800 | 0.0 (0.0) | -2.5 (25.2) | -10.2 (3.4) |
| NIVA-CYA 116 | 1/400 | 0.2 (0.1) | -40.6 (28.5) | -16.2 (3.0) |
| | 1/800 | 0.3 (0.2) | -20.6 (11.0) | -10.4 (2.4) |
| NIVA-CYA 264 | 1/400 | 0.2 (0.1) | -3.0 (9.5) | -12.1 (4.3) |
| | 1/800 | 0.1 (0.0) | -69.8 (17.1) | -5.4 (3.9) |
| NIVA-CYA 123/1 | 1/400 | 0.1 (0.0) | 17.7 (30.1) | -17.8 (3.4) |
| | 1/800 | 0.1 (0.0) | 39.3 (5.2) | 0.2 (11.4) |

*SC= solvent control (0.25% methanol in deionized water, v/v). **PC= positive control (Cortisol 181 ng/mL).
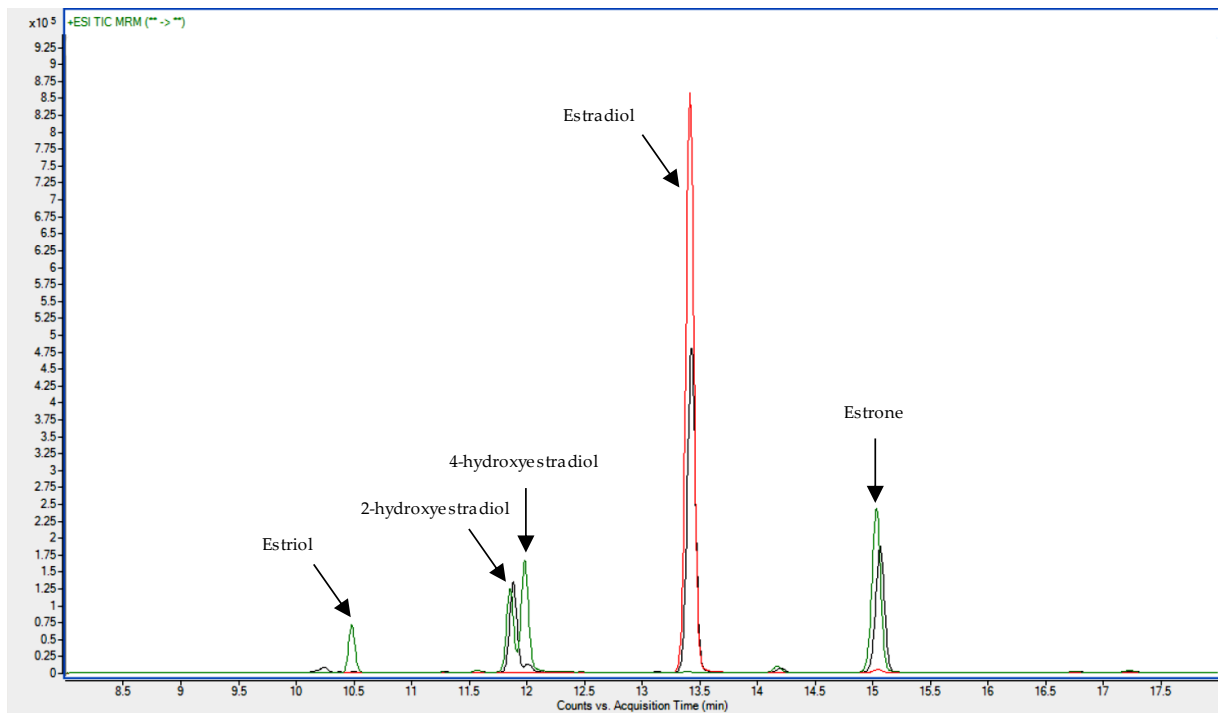
**Figure S1.** Overlay of total ion chromatograms from LC–MS/MS analyses of estradiol incubations at 0 min (red line) and 60 min (black line) with human liver microsomes (HLM). The concentration of individual compounds in the calibration standard was 125 ng/ml (green line).
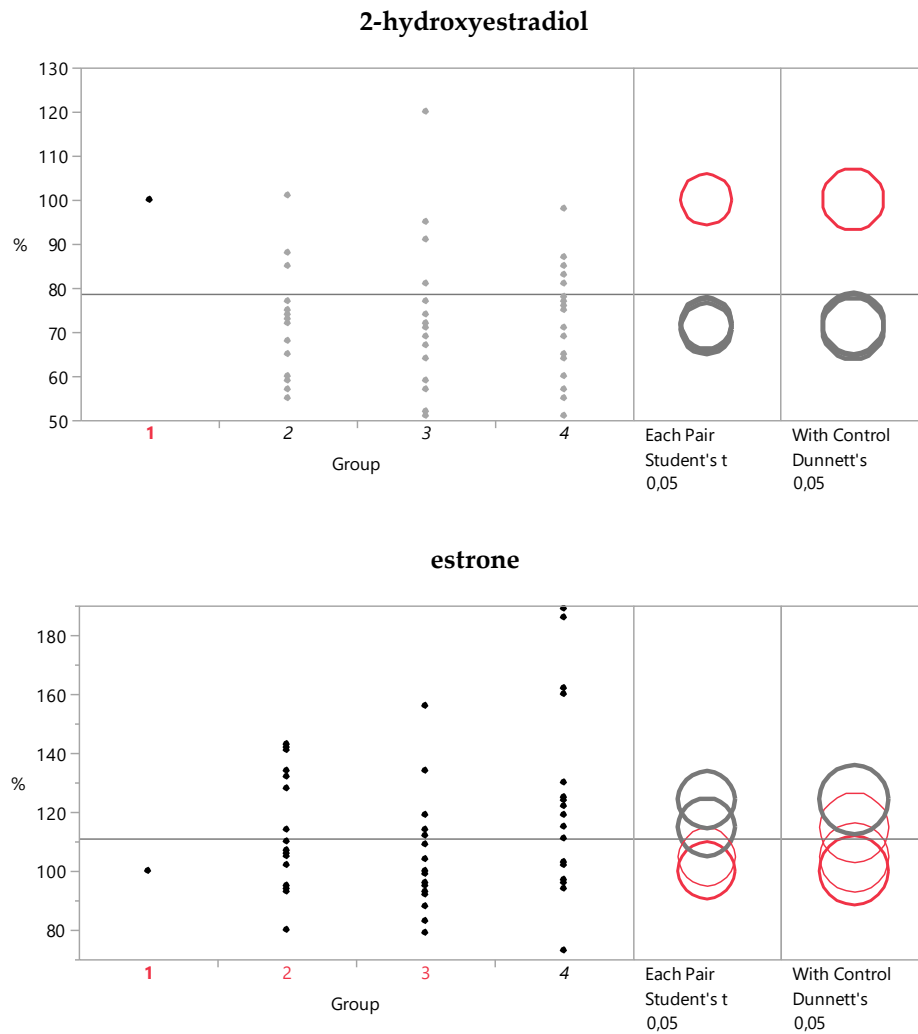
## 2-hydroxyestradiol



## estrone



**Figure S2.** One-way analysis of the relative production of 2-hydroxy-estradiol and estradione in human liver microsomes, including Dunnett's and Student's t tests for post-hoc analysis. The data set consists of the following groups: **1**, 5 µM estradiol only (reference); **2**, 5 µM estradiol + 5 µM MC-LR; **3**, 5 µM estradiol + 0.5 µM MC-LR; **4**, 5 µM estradiol + *M. aeruginosa* PCC7806 containing 5 µM MC-LR.

**Table S5.** *P*-values from post-hoc analyses (Dunnett's test and Student's *t* test) of the data set shown in Figure S2 using estradiol as reference (n=18, i.e. three replicate experiments including six time points). *P*-values that identify statistically significant differences relative to incubations with estradiol alone are shown in bold.

| Estradiol Metabolite | 5 µM estradiol + 0.5 µM MC-LR | | 5 µM estradiol + 5 µM MC-LR | | 5 µM estradiol + PCC7806 | |
|---|---|---|---|---|---|---|
| | *P*-value (Dunnett's) | *P*-value (Student's *t*) | *P*-value (Dunnett's) | *P*-value (Student's *t*) | *P*-value (Dunnett's) | *P*-value (Student's *t*) |
| 2-hydroxyestradiol | <0.0001 | <0.0001 | <0.0001 | <0.0001 | <0.0001 | <0.0001 |
| estrone | 0.096 | 0.038 | 0.845 | 0.508 | 0.003 | 0.001 |

# Paper II_Supplementary Material_HLM background data_revised version_2nd round.xlsx

## estradiol depletion [peak area]

| Time (min) | estradiol rep.1 | estradiol rep.2 | estradiol rep.3 | estradiol + MC-LR 5 µM rep.1 | estradiol + MC-LR 5 µM rep.2 | estradiol + MC-LR 5 µM rep.3 | estradiol + MC-LR 0.5 µM rep.1 | estradiol + MC-LR 0.5 µM rep.2 | estradiol + MC-LR 0.5 µM rep.3 | estradiol + PCC rep.1 | estradiol + PCC rep.2 | estradiol + PCC rep.3 |
|---|---|---|---|---|---|---|---|---|---|---|---|---|
| 0 | 2818305 | 2589076 | 2165125 | 2419903 | 2822546 | 2474766 | 2635306 | 2790213 | 1683638 | 2448156 | 2811977 | 2501352 |
| 5 | 2479295 | 2320766 | 1966051 | 2258482 | 2366570 | 2279441 | 2253174 | 2905069 | 1492987 | 2248364 | 2440827 | 2268398 |
| 10 | 2343393 | 2985822 | 1701035 | 2326423 | 2642784 | 2271869 | 2433522 | 2817625 | 1412545 | 1941662 | 2355063 | 2040420 |
| 15 | 2426110 | 2353843 | 1819236 | 2055824 | 2205236 | 2007373 | 2161926 | 2292735 | 1309336 | 1835768 | 2377226 | 1914181 |
| 30 | 2182191 | 2072039 | 1487070 | 1919373 | 1962561 | 1820134 | 1862578 | 2025586 | 1156234 | 1488561 | 1919787 | 1886242 |
| 60 | 1605646 | 1466948 | 1289649 | 1475836 | 1539327 | 1479977 | 1614856 | 1825063 | 928170 | 1166369 | 1511811 | 1440272 |

## estradiol depletion [%peak area]

| Time (min) | estradiol rep.1 | estradiol rep.2 | estradiol rep.3 | estradiol + MC-LR 5 µM rep.1 | estradiol + MC-LR 5 µM rep.2 | estradiol + MC-LR 5 µM rep.3 | estradiol + MC-LR 0.5 µM rep.1 | estradiol + MC-LR 0.5 µM rep.2 | estradiol + MC-LR 0.5 µM rep.3 | estradiol + PCC rep.1 | estradiol + PCC rep.2 | estradiol + PCC rep.3 |
|---|---|---|---|---|---|---|---|---|---|---|---|---|
| 0 | 100 | 100 | 100 | 100 | 100 | 100 | 100 | 100 | 100 | 100 | 100 | 100 |
| 5 | 88 | 90 | 91 | 93 | 84 | 92 | 85 | 104 | 89 | 92 | 87 | 91 |
| 10 | 83 | 129 | 79 | 96 | 94 | 92 | 92 | 101 | 84 | 79 | 84 | 82 |
| 15 | 86 | 79 | 84 | 85 | 78 | 81 | 82 | 82 | 78 | 75 | 85 | 77 |
| 30 | 77 | 88 | 69 | 79 | 70 | 74 | 71 | 73 | 69 | 61 | 68 | 75 |
| 60 | 57 | 71 | 60 | 61 | 55 | 60 | 61 | 65 | 55 | 48 | 54 | 58 |

## mean estradiol depletion [%peak area] and standard devition

| Time (min) | estradiol Mean | estradiol SD | estradiol + MC-LR 5 µM Mean | estradiol + MC-LR 5 µM SD | estradiol + MC-LR 0.5 µM Mean | estradiol + MC-LR 0.5 µM SD | estradiol + PCC Mean | estradiol + PCC SD |
|---|---|---|---|---|---|---|---|---|
| 0 | 100 | 0 | 100 | 0 | 100 | 0 | 100 | 0 |
| 5 | 89 | 1 | 90 | 4 | 93 | 8 | 90 | 2 |
| 10 | 81 | 2 | 94 | 2 | 92 | 7 | 82 | 2 |
| 15 | 83 | 3 | 81 | 3 | 81 | 2 | 79 | 4 |
| 30 | 78 | 8 | 74 | 4 | 71 | 2 | 68 | 6 |
| 60 | 62 | 6 | 58 | 3 | 61 | 4 | 53 | 4 |

## 2-hydroxy-estradiol production [peak area]

| Time (min) | estradiol | | | estradiol + MC-LR 5 µM | | | estradiol + MC-LR 0.5 µM | | | estradiol + PCC | | |
|---|---|---|---|---|---|---|---|---|---|---|---|---|
| | rep.1 | rep.2 | rep. 3 | rep.1 | rep.2 | rep. 3 | rep.1 | rep.2 | rep. 3 | rep.1 | rep.2 | rep. 3 |
| 0 | 743 | 1671 | 1363 | 751 | 1239 | 811 | 893 | 954 | 1049 | 559 | 1075 | 1159 |
| 5 | 21104 | 43715 | 37070 | 12703 | 31714 | 27621 | 14543 | 41481 | 21794 | 14564 | 33242 | 32318 |
| 10 | 41546 | 111936 | 67862 | 24906 | 72744 | 57548 | 32153 | 79950 | 40116 | 24912 | 63825 | 56163 |
| 15 | 65096 | 135313 | 107705 | 35781 | 92425 | 78002 | 43728 | 97107 | 54536 | 36830 | 95902 | 83601 |
| 30 | 119832 | 261880 | 177163 | 68544 | 178822 | 156030 | 76937 | 194761 | 104597 | 60620 | 171286 | 173331 |
| 60 | 184666 | 382198 | 334127 | 109178 | 287302 | 255716 | 149800 | 345954 | 174670 | 101823 | 293106 | 272280 |

## 2-hydroxy-estradiol production relative to incubation with estradiol alone [%peak area]

| Time (min) | estradiol | | | estradiol + MC-LR 5 µM | | | estradiol + MC-LR 0.5 µM | | | estradiol + PCC | | |
|---|---|---|---|---|---|---|---|---|---|---|---|---|
| | rep.1 | rep.2 | rep. 3 | rep.1 | rep.2 | rep. 3 | rep.1 | rep.2 | rep. 3 | rep.1 | rep.2 | rep. 3 |
| 0 | 100 | 100 | 100 | 101 | 74 | 60 | 120 | 57 | 77 | 75 | 64 | 85 |
| 5 | 100 | 100 | 100 | 60 | 73 | 75 | 69 | 95 | 59 | 69 | 76 | 87 |
| 10 | 100 | 100 | 100 | 60 | 65 | 85 | 77 | 71 | 59 | 60 | 57 | 83 |
| 15 | 100 | 100 | 100 | 55 | 68 | 72 | 67 | 72 | 51 | 57 | 71 | 78 |
| 30 | 100 | 100 | 100 | 57 | 68 | 88 | 64 | 74 | 59 | 51 | 65 | 98 |
| 60 | 100 | 100 | 100 | 59 | 75 | 77 | 81 | 91 | 52 | 55 | 77 | 81 |
| mean | | | | 65 | 71 | 76 | 80 | 77 | 59 | 61 | 68 | 85 |

## grand mean, 2-hydroxy-estradiol production relative to incubation with estradiol alone [%peak area] and standard devition

| | | | | estradiol + MC-LR 5 µM | | | estradiol + MC-LR 0.5 µM | | | estradiol + PCC | | |
|---|---|---|---|---|---|---|---|---|---|---|---|---|
| | | | | Mean | SD | | Mean | SD | | Mean | SD | |
| | | | | 71 | 5 | | 72 | 11 | | 72 | 12 | |

*Numbers are the means of measurements at six time points and three independent experiments*

## estrone production [peak area]

| Time (min) | estradiol | | | estradiol + MC-LR 5 µM | | | estradiol + MC-LR 0.5 µM | | | estradiol + PCC | | |
|---|---|---|---|---|---|---|---|---|---|---|---|---|
| | rep.1 | rep.2 | rep. 3 | rep.1 | rep.2 | rep. 3 | rep.1 | rep.2 | rep. 3 | rep.1 | rep.2 | rep. 3 |
| 0 | 6051 | 4311 | 4355 | 6200 | 6082 | 6186 | 5820 | 5133 | 4948 | 6210 | 5341 | 7061 |
| 5 | 143153 | 133083 | 130034 | 150431 | 146728 | 166365 | 149533 | 178659 | 124577 | 146422 | 153544 | 158672 |
| 10 | 224605 | 338460 | 183984 | 237518 | 271975 | 245697 | 244059 | 280841 | 169689 | 214939 | 245475 | 229141 |
| 15 | 257111 | 266963 | 225350 | 242761 | 252486 | 255995 | 256865 | 264784 | 177199 | 249623 | 295137 | 267870 |
| 30 | 286760 | 269888 | 210398 | 266351 | 286598 | 278613 | 271032 | 303457 | 184167 | 269684 | 337263 | 337115 |
| 60 | 276779 | 236082 | 228382 | 297519 | 311208 | 326436 | 316322 | 368638 | 211479 | 360531 | 439131 | 430545 |

## estrone production relative to incubation with estradiol alone [%peak area]

| Time (min) | estradiol | | | estradiol + MC-LR 5 µM | | | estradiol + MC-LR 0.5 µM | | | estradiol + PCC | | |
|---|---|---|---|---|---|---|---|---|---|---|---|---|
| | rep.1 | rep.2 | rep. 3 | rep.1 | rep.2 | rep. 3 | rep.1 | rep.2 | rep. 3 | rep.1 | rep.2 | rep. 3 |
| 0 | 100 | 100 | 100 | 102 | 141 | 142 | 96 | 119 | 114 | 103 | 124 | 162 |
| 5 | 100 | 100 | 100 | 105 | 110 | 128 | 104 | 134 | 96 | 102 | 115 | 122 |
| 10 | 100 | 100 | 100 | 106 | 80 | 134 | 109 | 83 | 92 | 96 | 73 | 125 |
| 15 | 100 | 100 | 100 | 94 | 95 | 114 | 100 | 99 | 79 | 97 | 111 | 119 |
| 30 | 100 | 100 | 100 | 93 | 106 | 132 | 95 | 112 | 88 | 94 | 125 | 160 |
| 60 | 100 | 100 | 100 | 107 | 132 | 143 | 114 | 156 | 93 | 130 | 186 | 189 |
| mean | | | | 101 | 111 | 132 | 103 | 117 | 93 | 104 | 122 | 146 |

## grand mean, estrone production relative to incubation with estradiol alone [%peak area] and standard devition

| | | | | | Mean | SD | | Mean | SD | | Mean | SD |
|---|---|---|---|---|---|---|---|---|---|---|---|---|
| | | | | | 115 | 16 | | 105 | 12 | | 124 | 21 |

Numbers are the means of measurements at six time points and three independent experiments

# PAPER III

# Microcystins and *Microcystis aeruginosa* extracts modulate steroidogenesis differentially in the human H295R adrenal model *in vitro*

Vittoria Mallia[1,2], Steven Verhaegen[3], Bjarne Styrishave[4], Gunnar S. Eriksen[1], Malene L. Johannsen[4], Erik Ropstad[3], Silvio Uhlig[1]*

[1] Toxinology Research Group, Norwegian Veterinary Institute, Oslo, Norway

[2] Department of Chemistry, University of Oslo, Oslo, Norway

[3] Department of Production Animal Clinical Sciences, Faculty of Veterinary Medicine, Norwegian University of Life Sciences, Oslo, Norway

[4] Toxicology and Drug Metabolism Group, Department of Pharmacy, Faculty of Health and Medical Sciences, University of Copenhagen, Copenhagen, Denmark

* Corresponding author

E-mail: silvio.uhlig@vetinst.no (SU)

# Abstract

The aim of this study was to investigate the potential interference of cyanobacterial metabolites, in particular microcystins (MCs), with steroidogenesis, which is the complex process of steroid hormone biosynthesis. Steroid hormones control many fundamental processes in an organism, thus alteration of their tissue concentrations may affect normal homeostasis. We used liquid chromatography–tandem mass spectrometry (LC–MS/MS) to investigate the modulation of 14 hormones involved in the adrenal steroid biosynthesis pathway using forskolin-treated H295R cells, following exposure with either microcystin-LR (MC-LR) alone, a mixture made up of MC-LR together with eight other MCs and nodularin-R (NOD-R), or extracts from the MC-LR-producing *Microcystis aeruginosa* PCC7806 strain or its MC-deficient mutant PCC7806*mcyB−*. Production of 17-hydroxypregnenolone and dehydroepiandrosterone (DHEA) was increased in the presence of MC-LR in a dose-dependent manner, indicating an inhibitory effect on 3β-hydroxysteroid dehydrogenase (3β-HSD). This effect was not observed following exposure with a MCs/NOD-R mixture, and thus the effect of MC-LR on 3β-HSD appears to be stronger than for other congeners. Exposure to extracts from both *M. aeruginosa* PCC7806 and *M. aeruginosa* PCC7806*mcyB−* had an opposite effect on 3β-HSD, i.e. concentrations of pregnenolone, 17-hydroxypregnenolone and DHEA were significantly decreased, showing that there are other cyanobacterial metabolites that outcompete the effect of MC-LR, and possibly result instead in net-induction. Another finding was a possible concentration-dependent inhibition of CYP21A2 or CYP11β1, which catalyse oxidation reactions leading to cortisol and cortisone, by MC-LR and the MCs/NOD-R mixture. However, both *M. aeruginosa* PCC7806 and *M. aeruginosa* PCC7806*mcyB−* extracts had an opposite effect resulting in a substantial increase in cortisol levels. Our results suggest that

MCs can modulate steroidogenesis, but that the net effect of the *M. aeruginosa* metabolome on steroidogenesis is different from that of pure MC-LR and independent of MC production.

**Keywords:** steroidogenesis; H295R; LC–MS/MS; cyanobacteria**;** endocrine disruptor; microcystin; *Microcystis aeruginosa*

# Introduction

Cyanobacteria, the infamous "blue–green algae", represent an increasing concern for wildlife and human health [1-3]. They are photosynthetic prokaryotic inhabitants of aquatic environments worldwide, mainly in freshwater basins. Under certain conditions (e.g. abundance of nutrients, favorable light and temperature), cyanobacteria may over-accumulate, forming so-called "blooms" [3]. Blooming cyanobacteria may release harmful bioactive metabolites into the water, including potent toxins (cyanotoxins) [1, 2, 4-7].

MCs are likely the most studied among cyanobacterial toxins [8]. They are a large family of cyclic heptapeptides, sharing a common core structure [8-11]. As a result of variations in their amino acid composition and additional structural modifications, the MCs are structurally diverse with at least 279 congeners already reported [9]. Several cyanobacterial genera have the ability to produce MCs, including *Microcystis* [8]. The toxicity of MCs is primarily connected to the inhibition of protein phosphatases PP1 and PP2A [12-14], which are ubiquitously expressed and crucial for regulation of key proteins, which in turn is crucial for key cellular processes [15-17].

MCs are known as hepatotoxins, especially following a well-documented event in 1996, when more than fifty patients died of acute liver failure following hemodialysis with MC-contaminated water in Brazil [18, 19]. However, literature reports several other adverse effects that MCs can exert, both in humans and wildlife, including reproductive toxicity and endocrine disrupting (ED) activity [9, 18, 20-24], which is the interference with normal homeostasis of the endocrine (hormonal) system, at any level of its functioning [25].

It has been reported that extracts and exudates from cyanobacterial blooms have ED activity, in particular estrogenic activity, through activation of the estrogen receptor [26, 27]. However, it is not entirely clear which of the many compounds present in cyanobacterial blooms exert estrogen activity and what role MCs might have. Furthermore, there are several non-receptor-mediated mechanisms, which are less studied but nevertheless important, that may alter endocrine functions [28, 29], including modulation of hormone production at the glandular level [30].

The adrenal cortex, which is the part of the adrenal gland where steroid hormones are produced, has been identified as a major target organ affected by endocrine disruptors (EDs) [31]. Steroid hormones regulate several functions including growth and development, metabolism and reproduction. The overall process of steroid hormone production is called steroidogenesis. It includes several steps and utilizes cholesterol as the common precursor. Cholesterol is transported to the inner mitochondrial membrane by steroidogenic acute regulatory protein (StAR) [32]. Following this rate-limiting step, several key enzymes modify cholesterol into other steroid hormones [33-35].

Most studies into the toxicology of cyanobacteria, including those addressing their ED activity, have focused on microcystin-LR (MC-LR) [13, 20-22, 24, 36], which is considered one

of the most prevalent and toxic MC congeners [8, 9]. Thus, it is the only congener for which the World Health Organization (WHO) has recommended a limit for its concentration in drinking water (1 µg/L) [37]. A recent study by Wang and co-authors showed that persistent MC-LR exposure in adult male zebrafish increased serum cortisol levels by modulating the expression of hypothalamic-pituitary-interrenal (HPI)-axis genes [38]. In an earlier report, Hou et al. [39] indicated that MC-LR could elicit non-dose-dependent estrogenic effects interfering with steroidogenic gene expression. The latter study was performed using the H295R steroidogenesis assay. The adrenocortical human cell line H295R is an *in vitro* model that conserves physiological characteristics of the undifferentiated adrenal cortex gland. Thus, these cells have the unique property of expressing genes that encode for all the key steroidogenesis enzymes [28, 40-44]. The H295R assay has been optimized and validated by the Organization for Economic Co-operation and Development (OECD) to detect substances that affect production of 17β-estradiol and testosterone [45].

In this study, we employed the H295R model, but focused on the modulation of individual steroids rather than gene expression as in Hou et al. [39]. We investigated the production of 14 hormones of the steroidogenesis pathways after exposing the cells to MC-LR in a concentration range that overlapped with that reported by Hou and co-workers [39], and quantified the hormones by liquid chromatography–tandem mass spectrometry (LC–MS/MS). We also investigated exposures to MC-LR in a mixture together with eight other MC congeners and the closely related pentapeptide, nodularin-R (NOD-R) [8, 14, 46]. Furthermore, we included exposures to extracts from the *M. aeruginosa* PCC7806 strain and its MC-deficient mutant PCC7806*mcyB−* [47]. PCC7806 has been widely employed in other research on cyanobacteria, including in studies on their ED activity [7, 23, 48-53]. It produces MC-LR as

the major MC congener, together with lesser amounts of [D-Asp³]MC-LR, including a range of known other bioactive metabolites such as cyanopeptolins, aerucyclamides and aeruginosins, as well as unknown compounds [50-52]. In culture, the *mcyB−* mutant grows similarly to the wild-type, but produces higher concentrations of some compounds other than MCs in a kind of compensatory mechanism [54].

The objective of performing these different exposures was to get a clearer picture of the involvement of MCs in general, and MC-LR in particular, on steroidogenesis, and to clarify whether there are other cyanobacterial metabolites that may modulate hormone concentrations in the H295R model. Thus, the exposure of the cells with pure MC-LR, MC-LR in a mixture with other congeners, an extract from a MC-LR producing cyanobacterial culture or its MC-deficient mutant, was expected to give detailed insight into the role of MC-LR, or other cyanobacterial metabolites, on steroidogenesis.

# Materials and methods

# Chemicals and reagents

Methanol (MeOH, gradient quality) and acetonitrile for extraction of cyanobacteria and protein precipitation, respectively, were from Romil (Cambridge, UK). Water for other purposes than LC–MS was purified and deionized using an ELGA Purelab Maxima system (Vivendi Water Systems, High Wycombe, UK). For H295R cell exposure, the following MC standards (≥ 95% purity) were from Enzo Life Sciences (Enzo Biochem, Inc., Farmingdale, NY, USA): Hepatotox Set 1 (containing MC-LR, MC-RR, MC-LY, MC-YR, MC-LW, MC-LF, MC-

LA, and NOD-R), [D-Asp[3],Dhb[7]]MC-RR (wrongly supplied as [D-Asp[3]]MC-RR) [55]) and [D-Asp[3]]MC-LR. Individual stock solutions of 12.5 µg/mL (MC-LY, MC-LW, MC-LF, MC-LA, [D-Asp[3],Dhb[7]]MC-RR, [D-Asp[3]]MC-LR, 25 µg/mL (MC-RR), and 50 µg/mL (MC-LR, NOD-R), were prepared in 50% MeOH. From those solutions, a pooled working stock solution containing 1 µg/mL of each compound was prepared in 100% MeOH and diluted to the concentrations needed for preparation of samples for cell exposures (Scheme S1). Dulbecco's Modified Eagle Medium/Nutrient Mixture F-12 (DMEM/F-12, Gibco, Thermo Fisher Scientific, Waltham, MA, USA) and trypsin containing 0.25% EDTA (Gibco), were from Fisher Scientific (Trondheim, Norway). Forskolin (from *Coleus forskohlii*, ≥ 98% (HPLC), powder) and charcoal-stripped foetal bovine serum (FBS) were from Sigma-Aldrich (Merck KGaA, Darmstadt, Germany). Alamar Blue solution was purchased from Thermo Fischer Scientific (Waltham, MA, USA). Insulin-transferrin-selenium (ITS 500x) was purchased from BioNordika (Oslo, Norway). For LC–MS analyses, HPLC grade MeOH, acetonitrile and water was from VWR Chemicals (Søborg, Denmark), while formic acid (98–100%) was from Merck KGaA and of EMSURE® quality. Steroid standards were from Sigma-Aldrich and of >96% purity. Deuterated internal standards were either from Toronto Research Chemicals (North York, ON, Canada), CDN isotopes (Pointe-Claire, QC, Canada) or Sigma-Aldrich.

# Cyanobacterial material

## Cultivation of cyanobacteria

*M. aeruginosa* PCC7806 and its MC-deficient mutant PCC7806*mcyB*− were from the Pasteur Institute (Paris, France). They were cultivated in Z8 medium [56] in 100 mL glass

Erlenmeyer flasks in an incubator (IPP110plus, Memmert GmbH + Co.KG, Schwabach, Germany) at 18 °C with a 14/10 h light/dark photoperiod, using 1% of maximum light intensity.

## Cyanobacterial extract preparation

Cultures of *M. aeruginosa* PCC7806 and *M. aeruginosa* PCC7806*mcyB*− were extracted when they were visually dense. For extract preparation, 5 mL of each culture was transferred to a glass tube and stored at −20 °C overnight, then allowed to thaw at room temperature, and 5 mL of MeOH was added. The tube was then vortex-mixed for 20 s, sonicated for 5 min and centrifuged for 10 min at 1,000 rcf. The supernatant was transferred to glass containers and stored at −20 °C until use.

# H295R cell culture and exposure

## Culture conditions

The H295R cell line was from American Type Culture Collection (ATCC). Cells were cultured in 75 cm$^2$ flasks in DMEM/F-12, containing HEPES buffer, L-glutamine and phenol red. Additional supplements were added: FBS at 5% and ITS 500x at 0.2%. H295R cells were incubated at 37 °C, in 5% $CO_2$ under a humidified atmosphere (Air-Jacketed, DH Autoflow Automatic $CO_2$ Incubator; NuAire, Fernbrook, MN, USA), changing the medium every 2–3 days, depending on the density of cells. Cells were passaged when approximately 80% confluent by trypsination using 0.25% trypsin-EDTA. The cells were used for experiments between passages 9 and 10.

## Preparation of test compounds and cyanobacterial extracts

Concentrated stock solutions of individual test compounds were prepared in MeOH. In the assay dilutions, the concentration of MeOH was kept constant at 0.5% to avoid solvent-related cytotoxicity. MC-LR was tested at concentrations of 1, 5, 100, 500, and 1000 ng/mL. The mixture of standard MCs and NOD-R was tested at assay concentrations of 1, 5 and 100 ng/mL (of each toxin, resulting in total toxin concentrations of 10, 50 and 1000 ng/mL, respectively). The MC concentration in the *M. aeruginosa* PCC7806 extract was established using LC–HRMS and adjusted so the total in-assay MC concentration (MC-LR + [D-Asp$^3$]MC-LR]) (in 50% MeOH) was approximately 5 and 500 ng/mL (Scheme S1). The instrumental method used for quantification of MCs against external calibration curves using standards in 50% MeOH was according to method A described by Mallia et al. [57]. The PCC7806*mcyB*− strain was also tested at two different concentrations. These concentrations were obtained by adjusting the overall signal/noise of metabolites observed in full-scan LC–HRMS chromatograms to the same order of magnitude as that observed for the *M. aeruginosa* PCC7806. Cyanobacterial growth medium Z8 [56] was extracted and concentrated using the same protocol as was used for the cyanobacterial cultures, and tested as a separate control sample. More details about samples and exposures can be found in the Supporting Information (Scheme 1).

## H295R steroidogenesis assay and exposure

H295R cells were seeded at a concentration of $3 \times 10^5$ cells/mL, 1 mL/well in white walled, clear and flat-bottomed 24-well plates (Sigma-Aldrich; Merck), and incubated at 37 °C, 5% $CO_2$ in a humidified atmosphere. After 24h, cells were visually inspected under a microscope to ensure there were no unwanted inter and/or intra variations in cell monolayer

morphology. Then, the seeding medium was replaced by fresh medium, which contained forskolin (1.5 μM) to start stimulating cells directly before exposure, in all wells except for medium and solvent controls. Cells were then exposed to test compounds and cyanobacterial extracts, as well as Z8 cyanobacterial growth medium [56] (see below). Each experimental plate included medium control (cell growth medium), solvent control (cell growth medium, containing 0.5% MeOH) and positive control (cell growth medium, containing 0.5% MeOH and 1.5 μM forskolin) in triplicate (Scheme S1). Medium controls and solvent controls were used to verify cell performance during the experiments, ensuring that the cells were not affected by unwanted external effects or technical bias. Positive controls were used as a reference for evaluating how test compounds and extracts impacted hormone production. After 48h of exposure, the medium from each well (~1 mL) was collected in 2-mL Eppendorf tubes and stored at −80 °C until further processing.

## Cell viability

Potential cytotoxicity was evaluated using the Alamar Blue™ assay (Invitrogen). After 48 h of exposure, the medium was removed from the wells and replaced by 1 mL of fresh medium containing 10% Alamar Blue assay solution was added to each well. Plates were incubated for 3 h at 37 °C, in 5% $CO_2$ in a humidified atmosphere, and then 100 μL from each well was transferred into a 96-well plate (Thermo Fisher Scientific), for fluorescence reading using a Spectramax i3x plate reader (Molecular Devices, San Jose, Ca, USA) [58]. Cells with lower viability than 80% compared to solvent control were discarded.

## Steroid extraction of H295R cell culture medium

Protein precipitation was performed according to Weisser et al. [59] before chemical analysis by LC–MS/MS. Internal standard (IS) solution (50 µL, 0.1 µg/mL per compound) was added to each Eppendorf tube containing the following deuterated steroid analogues in MeOH: $d_7$-androstenedione, $d_4$-estrone, $d_5$-17β-estradiol, $d_8$-corticosterone, $d_8$-11-deoxycorticosterone, $d_9$-progesterone, $d_3$-testosterone, $d_4$-cortisol, $d_5$-11-deoxycortisol and $d_6$-dehydroepindrosterone. Hereafter, 900 µL of ice-cold acetonitrile was added and the tubes vortex-mixed for 20 s. The tubes were stored at −20 °C for at least 10 min to allow complete precipitation and then centrifuged at 14800 rpm (24532 rcf) at 4 °C for 20 min. Supernatants were transferred to glass tubes and evaporated at 60 °C under a gentle stream of nitrogen to a volume of about 1 mL. For a second protein precipitation, 900 µL of ice-cold MeOH was added and the tubes vortex-mixed for 20 s. Again, tubes were stored at −20°C for at least 10 min, to allow complete precipitation and then centrifuged at 14800 rpm at 4 °C for 15 min. Supernatants from each tube (approximately 1.9 mL) were transferred to 2 mL chromatography vials and evaporated at 60 °C to approximately 0.7 mL under a gentle stream of nitrogen. Finally, vials were filled up with purified water, to a final volume of 1 mL and stored at −20 °C until hormone analyses.

## LC–MS/MS steroid analyses

The samples collected from the H295R cell assay were analyzed for 14 steroid hormones involved in the steroidogenesis (Fig 1) using LC–MS/MS according to earlier work [59].
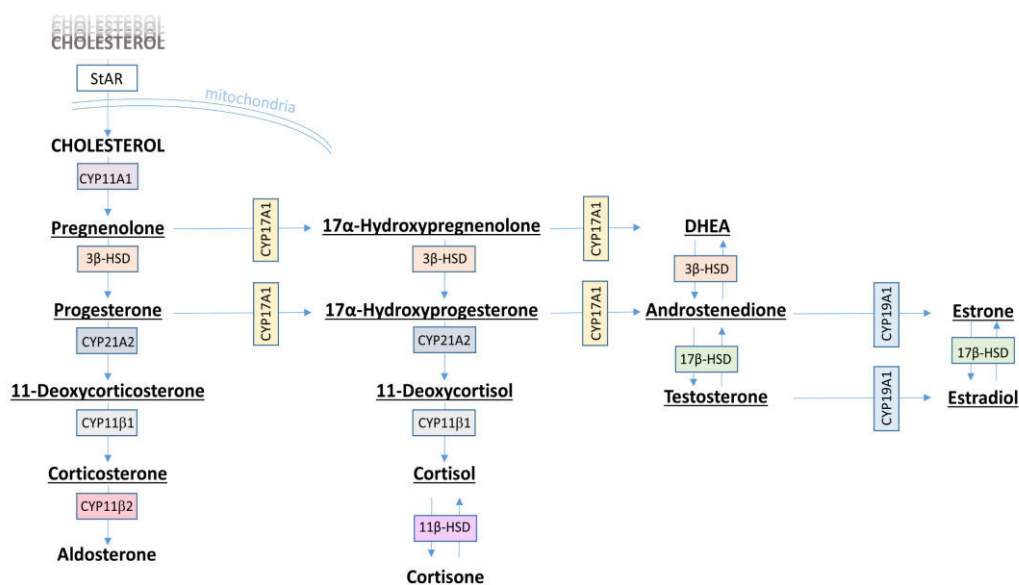
**Fig 1. Steroidogenesis pathway.** Steroidogenesis pathway, including hormones and enzymes involved [32]. The 14 hormones analysed in this study are underlined.

Briefly, a combination of a binary 1290 Agilent Infinity system and a binary 1100 Agilent HPLC pump was used for on-line clean-up and chromatographic separation of steroids. Initially, 100 μL of each sample was injected onto an octadecylsilane column (3.9 x 20 mm, 10 μm) for purification. Steroids were retained while impurities were washed directly into waste. For chromatographic separation, steroids were loaded on to an octadecylsilane analytical column with guard column thermostatted at 40 °C by gradually increasing the proportion of MeOH in acidic water (0.1% (v/v) formic acid in water) utilizing a flow rate of 0.3 mL/min. For the detection and identification of steroids an AB Sciex 4500 QTRAP tandem quadrupole mass spectrometer was used (AB Sciex LLC, Toronto, Canada). The analytes were ionized by atmospheric pressure chemical ionization (APCI) in the positive ionization mode,

and the mass spectrometer operated in the multiple reaction monitoring (MRM) mode. Data collection and processing were performed using the Analyst 1.6.2 software package (AB Sciex).

The analytical method had been validated according to the ICH (2005) guideline [60] on bioanalytical method validation. A standard curve for each steroid was plotted according to Weisser et al. [59]. To evaluate and verify the performance of the instrument, blanks and standards were run for every 6 and 12 samples, respectively.

## Data processing and statistical analysis

The obtained chromatographic peak areas were integrated using MultiQuant 3.0 Software (AB Sciex). The chromatograms from all samples were inspected and, if necessary, integrated manually. The fold-change was calculated for individual steroid concentrations relative to the positive (1.5 µM forskolin) control, and the results plotted in Sigma Plot v. 14 (Systat Software Inc., San Jose, CA, USA).

### Univariate data analyses

Hormone concentrations for all exposures (Supporting information) were normalized prior to statistical analyses by calculating the difference between individual hormone concentrations and the mean hormone concentrations for the positive (1.5 µM forskolin) control using Microsoft Excel 2016. Univariate data analyses were performed using JMP 14.0 (SAS Institute Inc., Cary, NC, USA). Because the data were not normally distributed, we used a two-tailed Wilcoxon signed-rank test to assess whether differences in hormone concentrations deviated from zero. A p-value of <0.05 was considered significant.

## Multivariate data analyses

Missing concentrations for 11-deoxycorticosterone (Supporting information) from one exposure experiment were assumed by taking the mean of the six concentration readings from the two other experiments. The data were log-transformed in order to reduce noise and impact of high variance, and pareto-scaled by dividing each variable by the square root of its standard deviation using Umetrics SIMCA 15.0 (Sartorius Stedim Data Analytics AB, Umeå, Sweden) prior to multivariate analyses using unsupervised and supervised models. Principal component analysis (PCA) was performed for an initial exploration of the data with the main purpose of detecting patterns and potential outliers. Principal component analysis was also performed using the original non-normalized data in order to assess the homogeneity of medium and solvent controls. Orthogonal partial least-squares discriminant analysis (OPLS-DA) was carried out to identify features (i.e. steroids) that discriminate between exposures and the positive (1.5 μM forskolin) control. The discriminant analysis included a default seven-round cross-validation. Furthermore, cross-validation ANOVA (CV-ANOVA) was performed to assess the reliability of the models. Steroid hormones that contributed to class separation in valid OPLS-DA models were inferred from the model S-plots and the predictive variable importance in the projection (VIP) values. Models were rejected if the $P$-value from CV-ANOVA was higher than 0.05. Furthermore, models were regarded as robust when $R^2Y$ and $Q^2X$ were higher than 50% and 40%, respectively [61, 62].

# Results

Of the 14 analysed hormones in the H295R cell culture medium, we were able to acquire quantitative data for 13 steroids. Corticosterone was not detected above the lower limit of detection (0.023 ng/mL) in any of the samples.

## Univariate Analyses

Exposure to the high-concentration extracts of *M. aeruginosa* PCC7806 and *M. aeruginosa* PCC7806*mcyB−*, and to higher concentrations of MC-LR or MCs/NOD-R, were associated with significant changes in several steroids (Fig 2). Steroid hormone profiles following exposure with both high-concentration *M. aeruginosa* PCC7806 and *M. aeruginosa* PCC7806*mcyB−* extracts showed a similar pattern. In both cases, dehydroepiandrosterone (DHEA), 17-hydroxypregnenolone and pregnenolone were detected with significantly lower concentrations relative to the positive forskolin control (Fig 2). In addition, androstenedione levels were significantly lower following exposure to *M. aeruginosa* PCC7806*mcyB−* extract (Fig 2). In the high-concentration exposures with both *M. aeruginosa* strains, concentrations of 11-deoxycorticosterone were significantly higher relative to the positive forskolin control. The steroid 11- deoxycorticosterone was also significantly upregulated following exposure to 1000 ng/mL MC-LR (Fig 2). However, in contrast to the *M. aeruginosa* PCC7806 exposures, production of DHEA and 17-hydroxypregnenolone was significantly higher following exposure with 1000 ng/mL MC-LR (also 100 ng/mL in case of 17-hydroxypregnenolone), compared to the positive control. There was no such concentration-dependent increase in DHEA and 17-hydroxypregnenolone when H295R cells were exposed to MCs/NOD-R (Fig 2).

A second effect of our exposures was on the pathway that leads from 17-hydroxypregnenolone and via 17-hydroxyprogesterone and 11-deoxycortisol to cortisol and cortisone (Fig 2). This effect was strongest for the MCs/NOD-R mixture and culminated in significantly reduced cortisol (fold change 0.16 relative to positive control) at 1000 ng/mL total toxin concentration (including MC-LR at 100 ng/mL) (Fig 2). The same effect was observed for the 500 ng/mL exposure with MC-LR that significantly ($p<0.01$) reduced cortisol and cortisone by 97% and 93%, respectively (Fig 2). Again, both *M. aeruginosa* PCC7806 extracts, i.e. its wild-type and the MC-deficient *mcyB−* mutant, reversed the effect. Thus, the higher-concentration exposures with *M. aeruginosa* PCC7806 and *M. aeruginosa* PCC7806*mcyB−* extracts substantially increased cortisol with fold changes of 2.55 and 2.15, respectively (Fig 2). This effect was not statistically significant due to high variability of cortisol concentrations between experiments.

**Fig 2. Modulation of individual steroids including results from univariate statistical analysis.**
Modulation of hormone production in H295R cells following exposure to different concentrations of MC-LR, a mixture of nine MCs and NOD-R (MCs/NOD-R), the MC-producing strain *M. aeruginosa* PCC7806 or its MC-deficient PCC7806*mcyB*− mutant, or the cyanobacterial growth medium Z8 [56] for 48 h. The in-assay MC concentration (MC-LR + [D-Asp$^3$]MC-LR) in the *M. aeruginosa* PCC7806 exposures were adjusted to approximately 5 ng/mL ("low") and 500 ng/mL ("high"). MC-deficient PCC7806*mcyB*− exposures were adjusted so the LC–HRMS response of metabolites other than MCs were in the same order of magnitude as for corresponding *M. aeruginosa* PCC7806 exposures. Data are presented as fold change relative to the positive (1.5 μM forskolin) control (which is represented by the dashed red line). Error bars represent the standard error of the mean, and asterisks show significant differences from the positive control at a 5% (*) or 1% (**) level of significance based on the Wilcoxon signed-rank test.

## Multivariate Analyses

Principal component analysis (PCA) was carried out in order to visualize data structure within and between exposure experiments. Solvent and medium controls formed a separate and relatively homogeneous cluster across experiments showing the absence of technical bias (S1 Fig). As hormone levels within the same exposure groups varied considerably between experiments (S1 Fig), PCA was limited to the highest exposures only and based on the positive control normalized data (i.e. the identical data set that was used for the univariate analysis). The resulting PCA scores plots show that the first three principal components explained 95% of the variation in the 13 measured hormones (cumulative $Q^2X$ for the three-component model = 43%) (Fig 3). Only the *M. aeruginosa* PCC7806 exposures lead to changes in the hormone profiles that could be visualized in the PCA scores plot (Fig 3). Thus, both the PCC7806 and

the MC-deficient PCC7806*mcyB*− mutant clustered separately from all other exposures, but individual observations were also more dispersed. The 1000 ng/mL MC-LR or MCs/NOD-R exposure groups did not form separate clusters and were partially overlapping with the positive control or the Z8 cyanobacterial growth medium (Fig 3).
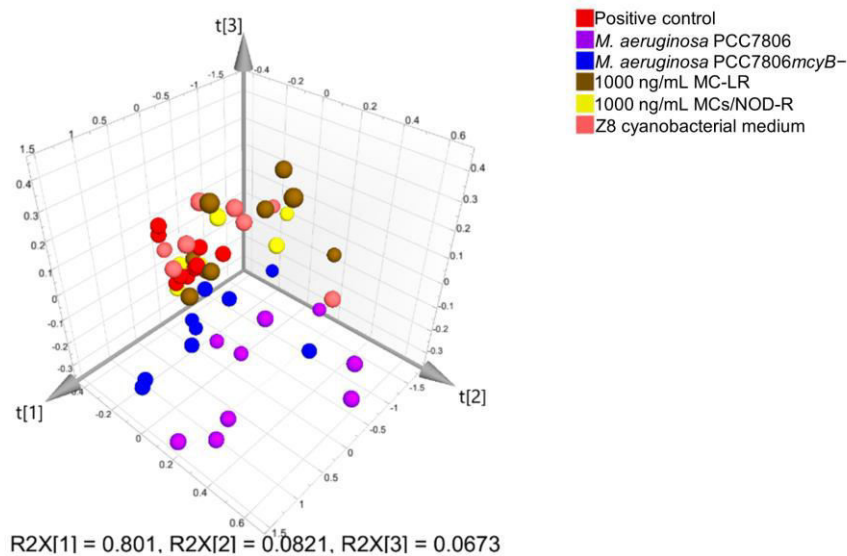


**Fig 3. Principal component analysis scores plot including data from high-concentration exposures.** 3-D scores plot from unsupervised principal component analysis based on pareto-scaled and positive-control-subtracted hormone concentrations, from high-exposure groups only. The first three components explain 95% of the total variation. The plot shows a larger dispersion of the data from *M. aeruginosa* PCC7806 exposures, but individual observations from these exposures also cluster further away from the positive control and microcystin exposures.
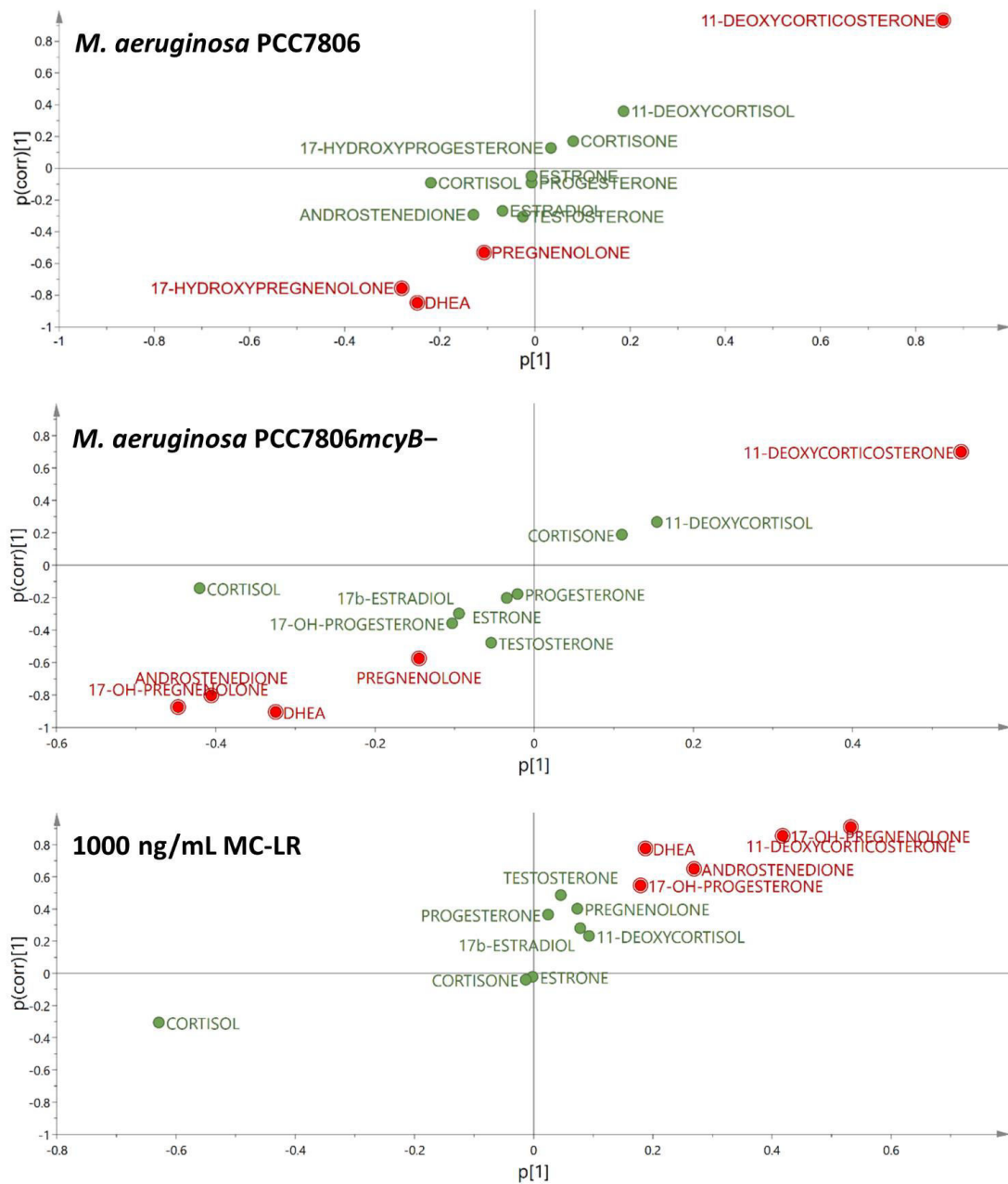
**Fig 4. S-plots from valid orthogonal partial least squares discriminant analysis (OPLS-DA) models.**

S-plots from two-class OPLS-DA models including observations for positive (1.5 µM forskolin) control versus either the wild type of *M. aeruginosa* PCC7806 (upper plot), its MC-deficient mutant PCC7806*mcyB−* (middle plot), or 1000 ng/mL MC-LR (lower plot). The plots show that 11-

deoxycorticosterone was upregulated for all exposures. Dehydroepiandosterone (DHEA) and 17-hydroxypregnenolone were downregulated in exposures for both *M. aeruginosa* PCC7806 strains but upregulated following MC-LR exposure. Related hormones, i.e. androstenedione and pregnenolone followed the same pattern but were not among the main discriminating variables in all three models. Cortisol was not included in the selection of significant variables as it was the major contributing factor to orthogonal variation (oVIP = 3.5).

Subsequently, two-class OPLS discriminant analyses were performed, including the positive (1.5 μM forskolin) control as one of the test groups, with the aim of identifying variables (i.e. steroids) with class-separating power. Three models were robust and met the quality criteria outlined above; these were from discriminant analysis of positive control vs. both of the high-concentration *M. aeruginosa* PCC7806 extracts (i.e. wild-type and *mcyB−*) and from positive control vs. 1000 ng/mL MC-LR (Table 1). Significant models used between two and three components and interpreted at least 91% of the variation in $X$ (i.e. the hormone levels). The predictive value of the models was medium to high with cumulative $Q^2X$ values higher than 52% (Table 1). Hormones that were predictive for the observed class separation were extracted from the OPLS-DA S-plots (Fig 4) [63, 64]. The strongest predictive hormone for class separations was 11-deoxycorticosterone (OPLS-DA predictive VIP=1.9–3.1), which was upregulated in H295R cells following exposure both with 1000 ng/mL MC-LR and the high-concentration *M. aeruginosa* PCC7806 extracts (Fig 4). In contrast, several steroid hormones were downregulated following exposure with the high-concentration *M. aeruginosa* PCC7806 extracts, but upregulated following exposure with 1000 ng/mL MC-LR (Fig 4, Table 1). Thus, both 17-hydroxypregnenolone and DHEA were significantly discriminating variables in all three OPLS-DA models, but with opposite sign in the 1000 ng/mL MC-LR exposure relative to

exposure with the high-concentration *M. aeruginosa* PCC7806 and *M. aeruginosa* PCC7806*mcyB*− extracts. Furthermore, both their direct precursor, pregnenolone, and biosynthetic product, androstenedione, were significantly discriminating variables in two out of the three models (Fig 4, Table 1).

**Table 1.** Characteristics of valid two-class OPLS-DA models based on quantitative hormone concentrations from 13 hormones following H295R cell exposures with either 1000 ng/mL MC-LR, *M. aeruginosa* PCC7806 or PCC7806*mcyB*− extracts, compared to the positive control (1.5 μM forskolin).

| Classes | $R^2(x)$ (cum) | $R^2(y)$ (cum) | $Q^2(x)$ (cum) | CV-ANOVA *P*-value | Steroids predictive for class difference incl. pVIP[a] |
|---|---|---|---|---|---|
| PC vs. MC-LR 1000 ng/mL | 0.93 | 0.58 | 0.52 | 0.039 | 11-deoxycorticosterone (1.9), 17-hydroxypregnenolone (1.5), androstenedione (0.96), DHEA (0.67), 17-hydroxyprogesterone (0.64) |
| PC vs. PCC7806 (high) | 0.97 | 0.89 | 0.83 | $1.1 \times 10^{-3}$ | 11-deoxycorticosterone (3.1), 17-hydroxypregnenolone (1.0), DHEA (0.89) |
| PC vs. PCC7806*mcyB*− (high) | 0.91 | 0.84 | 0.81 | $1.3 \times 10^{-4}$ | 11-deoxycorticosterone (1.9), 17-hydroxypregnenolone (1.6), androstenedione (1.5), DHEA (1.2), pregnenolone (0.52) |

[a] Selection criteria: predictive Variable Importance for the Projection (pVIP) > 0.5; $p[1] > |0.05|$; $p(corr)[1] > |0.5|$

# Discussion

Exposure of H295R cells with either MC-LR, a mixture of MCs (including MC-LR) and NOD-R or *M. aeruginosa* PCC7806 or PCC7806*mcyB*− modulated steroidogenesis in H295R cells in our study (Figs 2-4). A recent study reported the upregulation of testosterone levels in H295R cells following exposure to 10 ng/mL MC-LR, while 17β-estradiol levels were elevated following exposure with 1 and 10 ng/mL MC-LR, but decreased when the cells were exposed

with 500–5000 ng/mL [39]. We did not observe an effect on estrogen levels in any of our exposures (Figs 2 and 4). Testosterone was significantly (p<0.05) increased following exposure to 10 ng/mL MCs/NOD-R mixture, but with a rather small fold change (1.05) relative to the positive control (Fig 2). Thus, the detected difference in this case is likely a result of chance (type I error) rather than a true difference. However, while our cells were treated with 1.5 μM forskolin prior to exposure the cells were not stimulated in the study by Hou et al. [39]. The use of 1.5 μM forskolin for studying effects on steroidogenesis using H295R cells has previously been suggested as it stimulates hormone synthesis without saturating their production [65]. While MC-LR did not affect 17β-estradiol and testosterone concentrations in forskolin-treated H295R cells, the toxin significantly increased 17-hydroxypregnenolone and DHEA in a concentration-dependent manner, as well as 11-deoxycorticosterone (Fig 2). Furthermore, multivariate statistical modelling in addition showed the significant upregulation of androstenedione and 17-hydroxyprogesterone (Fig 4, Table 1). The upregulation effect was most obvious (in terms of fold change) for 17-hydroxypregnenolone and DHEA, which both are substrates for 3β-hydroxysteroid dehydrogenase (3β-HSD) [32]. Thus, MC-LR appears to inhibit 3β-HSD in a dose-dependent manner (Fig 2). This was most clear for DHEA, probably because this hormone has relatively low 3β-HSD affinity and $V_{max}$ conversion rates, allowing for stronger interference by MC-LR [66]. Androstenedione is a substrate of 17β-HSD, and its upregulation could in addition indicate an effect on this enzyme, though much weaker than the effect on 3β-HSD. There was no such concentration-dependent effect for the MCS/NOD-R mixture indicating that the effect of MC-LR on 3β-HSD is stronger than for the other congeners in the tested mixture. The observed significant decrease in estrone levels following exposure with 500 ng/mL MCs/NOD-R mixture or 1000 ng/mL MC-LR supports a possible interaction with 17β-HSD (Fig 2).

The *M. aeruginosa* PCC7806 extract also showed a concentration-dependent effect on 3β-HSD. However, the effect was opposite to that observed for pure MC-LR as both pregnenolone, 17-hydroxypregnenolone and DHEA levels were significantly (p<0.01) downregulated at the higher exposure concentration that contained approximately 500 ng/mL of total MC-LR and [D-Asp³]MC-LR (Fig 2). This effect was also evident in the corresponding supervised OPLS-DA model (Fig 4, Table 1). The *M. aeruginosa* PCC7806*mcyB−* extract exhibited the same downregulation effect on pregnenolone, 17-hydroxypregnenolone and DHEA as the wild-type (Figs 2 and 4, Table 1). This shows that there were other metabolites in the cyanobacterial extracts that had a stronger and opposite effect on 3β-HSD compared to MC-LR. The *M. aeruginosa* PCC7806*mcyB−* extract also resulted in significant downregulation of androstenedione indicating that there are cyanobacterial metabolites that also may induce 17β-HSD, though to a lesser extent than 3β-HSD.

A second effect of our exposures was on enzymes that are involved in the pathway that leads from 17-hydroxypregnenolone and via 17-hydroxyprogesterone and 11-deoxycortisol to cortisol and cortisone (Fig 2). This effect was not revealed by the multivariate statistics. Thus, Fig 2 shows a concentration-dependent inhibition effect of both MC-LR and the MCs/NOD-R mixture on CYP21A2 or CYP11β1 that are responsible for conversion of 17-hydroxyprogesterone to 11-deoxycortisol, and of 11-deoxycortisol to cortisol, respectively [32]. Also this effect was reversed by both high-concentration *M. aeruginosa* PCC7806 extracts, though not with statistical significance (Fig 2). The reversing effect of the cyanobacterial extracts was quite dramatic. Thus, while exposure with 500 ng/mL MC-LR reduced cortisol to 3% relative to the positive forskolin control, exposure with the high-concentration *M. aeruginosa* PCC7806 extract increased it to 255% relative to the positive forskolin control.

A statistically significant and concentration-dependent upregulation of 11-deoxycorticosterone was observed for MC-LR and both *M. aeruginosa* PCC7806 and *M. aeruginosa* PCC7806*mcyB−* extracts, which was evident from both univariate analysis and multivariate modelling. The relative increase was highest for the wild-type *M. aeruginosa* PCC7806 (fold change 1.27 relative to positive control) and supports the interaction of both MC-LR, but also other cyanobacterial metabolites with CYP11β1. This result was further supported by non-detectable concentrations of corticosterone, which is the product of the CYP11β1 catalyzed oxidation of 11-deoxycorticosterone.

Our results show that cyanobacterial compounds have ED activity via modulation of steroid biosynthesis. Furthermore, the results indicated an opposite or at least different effect of MCs relative to other cyanobacterial bioactive metabolites. Different effects may reflect different modes of action. MC congeners have a relatively high molecular weight (ca. 1 kDa) and are relatively hydrophilic, thus they could not be regarded as classical EDs. However, they are known to bind PP1 and PP2A, as main mechanisms of toxicity, leading to hyperphosphorylation and interference with key cellular processes. When in complex with PP1 and PP2A, the MC-cycle is twisted, and blocks potential substrates from entering the active site [9, 67]. The lipophilic group of Adda (3*S*-amino-9*S*-methoxy-2*S*,6,8*S*-trimethyl-10-phenyldeca-4*E*,6*E*-dienoic acid) in position-5 of the heptacyclic core structure, as well as the glutamic acid (Glu) moiety in position-6, which are highly conserved in reported MC congeners [9], are key elements for binding both PP1 and PP2A, giving either hydrophobic interactions or hydrogen bonds in the enzyme's catalytic sites, respectively. Therefore, it could be hypothesized that a similar mechanism of direct interaction with enzymes involved in

steroidogenesis, e.g. HSDs, exist. Alternatively, MCs may act indirectly through affecting gene expression resulting in up- or down-regulating enzyme levels.

# Conclusion

Our results show that MCs and other *Microcystis* metabolites may alter steroidogenesis in a dose-dependent manner. MC-LR increased the levels of 17-hydroxypregnenolone and DHEA, while MC-LR alone and in a mixture with eight other MCs and NOD-R resulted in decreased cortisol and cortisone concentrations *in vitro*. Extracts from a MC-producing *Microcystis* strain and its MC-deficient mutant modulated the same hormones but in opposite direction showing that, although MCs in itself can alter steroidogenesis, the extracts contained other bioactive molecules that affected steroidogenesis independently from MC production. One hormone, 11-deoxycorticosterone, was increased following exposure with either MC-LR, extract from MC-producing or MC-deficient *M. aeruginosa* indicating that there are bioactivities that are shared by MCs and other cyanobacterial metabolites. As steroidogenesis is complex, including branched pathways and reversible reactions, extrapolation of our findings to exposure of a whole organism with MCs or *Microcystis* is difficult or even impossible.

# Supporting information

**Scheme 1.** Experimental plan for H295R cells exposure. (DOCX)

**S1 Fig.** Scores plot from principal component analysis of all raw data from hormone analyses from H295R. (DOCX)

**S1 Table.** Overview over raw data from hormone analyses. (XLSX)

# Acknowledgements

# Data availability statement

All relevant data are within the manuscript and its Supporting information.

# Funding

# Author contributions

**Conceptualization:** Vittoria Mallia, Steven Verhaegen, Gunnar S. Eriksen, Erik Ropstad, Christopher O. Miles, Silvio Uhlig

**Data Curation:** Vittoria Mallia, Malene L. Johannsen

**Formal Analysis:** Vittoria Mallia, Bjarne Styrishave, Malene L. Johannsen, Silvio Uhlig

**Funding Acquisition:** Gunnar S. Eriksen, Christopher O. Miles, Steven Verhaegen, Erik Ropstad

**Investigation:** Vittoria Mallia, Steven Verhaegen, Bjarne Styrishave, Gunnar S. Eriksen, Erik Ropstad, Silvio Uhlig

**Methodology:** Steven Verhaegen, Erik Ropstad, Bjarne Styrishave, Malene L. Johannsen, Silvio Uhlig

**Project Administration:** Gunnar S. Eriksen

**Resources:** Vittoria Mallia, Steven Verhaegen, Bjarne Styrishave, Malene L. Johannsen, Silvio Uhlig

**Validation:** Erik Ropstad, Bjarne Styrishave, Silvio Uhlig

**Visualization:** Vittoria Mallia, Silvio Uhlig

**Writing – original draft:** Vittoria Mallia, Silvio Uhlig

**Writing – review and editing:** Steven Verhaegen, Bjarne Styrishave, Gunnar S. Eriksen, Malene L. Johannsen, Erik Ropstad

# References

1.      Huisman J, Codd GA, Paerl HW, Ibelings BW, Verspagen JMH, Visser PM. Cyanobacterial blooms. Nat Rev Microbiol. 2018;16(8):471–83. doi: 10.1038/s41579-018-0040-1. PubMed PMID: 29946124.
2.      Chorus I, Bartram J. Toxic Cyanobacteria in Water: a Guide to their Public Health Consequences, Monitoring and Management; E&FN Spon: New York, NY, USA. WHO; **1999**.

3.      Merel S, Walker D, Chicana R, Snyder S, Baures E, Thomas O. State of knowledge and concerns on cyanobacterial blooms and cyanotoxins. Environ Int. 2013;59:303–27. Epub 2013/07/31. doi: 10.1016/j.envint.2013.06.013. PubMed PMID: 23892224.

4.     Buratti FM, Manganelli M, Vichi S, Stefanelli M, Scardala S, Testai E, et al. Cyanotoxins: producing organisms, occurrence, toxicity, mechanism of action and human health toxicological risk evaluation. Arch Toxicol. 2017;91(3):1049–130. Epub 2017/01/23. doi: 10.1007/s00204-016-1913-6. PubMed PMID: 28110405.

5.     Carmichael WW, Azevedo SM, An JS, Molica RJ, Jochimsen EM, Lau S, et al. Human fatalities from cyanobacteria: chemical and biological evidence for cyanotoxins. Environ Health Perspect. 2001;109(7):663–8. doi: 10.1289/ehp.01109663. PubMed PMID: 11485863; PubMed Central PMCID: PMCPMC1240368.

6.     Paerl HW, Otten TG. Harmful cyanobacterial blooms: causes, consequences, and controls. Microb Ecol. 2013;65(4):995–1010. Epub 2013/01/15. doi: 10.1007/s00248-012-0159-y. PubMed PMID: 23314096.

7.     Jonas A, Scholz S, Fetter E, Sychrova E, Novakova K, Ortmann J, et al. Endocrine, teratogenic and neurotoxic effects of cyanobacteria detected by cellular in vitro and zebrafish embryos assays. Chemosphere. 2015;120:321–7. Epub 2014/08/30. doi: 10.1016/j.chemosphere.2014.07.074. PubMed PMID: 25170595.

8.     Catherine A, Bernard C, Spoof L, Bruno M. Microcystins and Nodularins.  Meriluoto, J, Spoof, L, Cood, GA Handbook of cyanobacterial monitoring and cyanotoxins analysis**2017**.

9.     Bouaicha N, Miles CO, Beach DG, Labidi Z, Djabri A, Benayache NY, et al. Structural diversity, characterization and toxicology of microcystins. Toxins (Basel). 2019;11(12). Epub 2019/12/11. doi: 10.3390/toxins11120714. PubMed PMID: 31817927.

10.    Botes DP, Kruger H, Viljoen CC. Isolation and characterization of four toxins from the blue–green alga, *Microcystis aeruginosa*. Toxicon. 1982;20(6):945–54. PubMed PMID: 6819659.

11.    Botes DP, Viljoen CC, Kruger H, Wessels PL, Williams DH. Configuration assignments of the amino acid residues and the presence of N-methyldehydroalanine in toxins from the blue-green alga, Microcystis aeruginosa. Toxicon. 1982;20(6):1037–42. Epub 1982/01/01. doi: 10.1016/0041-0101(82)90105-2. PubMed PMID: 6819658.

12.    Fontanillo M, Kohn M. Microcystins: synthesis and structure–activity relationship studies toward PP1 and PP2A. Bioorg Med Chem. 2018;26(6):1118–26. doi: 10.1016/j.bmc.2017.08.040. PubMed PMID: 28893598.

13.    MacKintosh C, Beattie KA, Klumpp S, Cohen P, Codd GA. Cyanobacterial microcystin-LR is a potent and specific inhibitor of protein phosphatases 1 and 2A from both mammals and higher plants. FEBS Lett. 1990;264(2):187–92. PubMed PMID: 2162782.

14.    Yoshizawa S, Matsushima R, Watanabe MF, Harada K, Ichihara A, Carmichael WW, et al. Inhibition of protein phosphatases by microcystins and nodularin associated with hepatotoxicity. J Cancer Res Clin Oncol. 1990;116(6):609–14. PubMed PMID: 2174896.

15.    Tournebize R, Andersen SS, Verde F, Doree M, Karsenti E, Hyman AA. Distinct roles of PP1 and PP2A-like phosphatases in control of microtubule dynamics during mitosis. EMBO J. 1997;16(18):5537–49. Epub 1997/10/06. doi: 10.1093/emboj/16.18.5537. PubMed PMID: 9312013; PubMed Central PMCID: PMCPMC1170186.

16.    Garcia A, Cayla X, Guergnon J, Dessauge F, Hospital V, Rebollo MP, et al. Serine/threonine protein phosphatases PP1 and PP2A are key players in apoptosis. Biochimie. 2003;85(8):721–6. Epub 2003/10/31. doi: 10.1016/j.biochi.2003.09.004. PubMed PMID: 14585537.

17.    Yan Y, Mumby MC. Distinct roles for PP1 and PP2A in phosphorylation of the retinoblastoma protein. PP2A regulates the activities of $G_1$ cyclin-dependent kinases. J Biol Chem. 1999;274(45):31917–24. Epub 1999/11/05. doi: 10.1074/jbc.274.45.31917. PubMed PMID: 10542219.

18.    Li L, Xie P, Chen J. In vivo studies on toxin accumulation in liver and ultrastructural changes of hepatocytes of the phytoplanktivorous bighead carp i.p.-injected with extracted microcystins. Toxicon. 2005;46(5):533–45. Epub 2005/08/09. doi: 10.1016/j.toxicon.2005.06.025. PubMed PMID: 16084552.

19.    Jochimsen EM, Carmichael WW, An JS, Cardo DM, Cookson ST, Holmes CE, et al. Liver failure and death after exposure to microcystins at a hemodialysis center in Brazil. N Engl J Med. 1998;338(13):873–8. doi: 10.1056/NEJM199803263381304. PubMed PMID: 9516222.

20.    Chen L, Chen J, Zhang X, Xie P. A review of reproductive toxicity of microcystins. J Hazard Mater. 2016;301:381–99. doi: 10.1016/j.jhazmat.2015.08.041. PubMed PMID: 26521084.

21.    Liu W, Chen C, Chen L, Wang L, Li J, Chen Y, et al. Sex-dependent effects of microcystin-LR on hypothalamic-pituitary-gonad axis and gametogenesis of adult zebrafish. Sci Rep. 2016;6:22819. Epub 2016/03/11. doi: 10.1038/srep22819. PubMed PMID: 26960901; PubMed Central PMCID: PMCPMC4785373.

22.    Oziol L, Bouaicha N. First evidence of estrogenic potential of the cyanobacterial heptotoxins the nodularin-R and the microcystin-LR in cultured mammalian cells. J Hazard Mater. 2010;174(1-3):610–5. Epub 2009/10/16. doi: 10.1016/j.jhazmat.2009.09.095. PubMed PMID: 19828236.

23.    Rogers ED, Henry TB, Twiner MJ, Gouffon JS, McPherson JT, Boyer GL, et al. Global gene expression profiling in larval zebrafish exposed to microcystin-LR and microcystis reveals endocrine disrupting effects of cyanobacteria. Environ Sci Technol. 2011;45(5):1962–9. Epub 2011/02/02. doi: 10.1021/es103538b. PubMed PMID: 21280650.

24.    Zhao Y, Xie L, Yan Y. Microcystin-LR impairs zebrafish reproduction by affecting oogenesis and endocrine system. Chemosphere. 2015;120:115–22. Epub 2014/07/12. doi: 10.1016/j.chemosphere.2014.06.028. PubMed PMID: 25014902.

25.    International Programme on Chemical Safety (IPCS). *Global assessment of the state-of-the-science of endocrine disruptors* Geneva, Switzerland**2002**.

26.    Stepankova T, Ambrozova L, Blaha L, Giesy JP, Hilscherova K. *In vitro* modulation of intracellular receptor signaling and cytotoxicity induced by extracts of cyanobacteria, complex water blooms and their fractions. Aquat Toxicol. 2011;105(3–4):497–507. Epub 2011/09/10. doi: 10.1016/j.aquatox.2011.08.002. PubMed PMID: 21903046.

27.    Sychrova E, Stepankova T, Novakova K, Blaha L, Giesy JP, Hilscherova K. Estrogenic activity in extracts and exudates of cyanobacteria and green algae. Environ Int. 2012;39(1):134–40. Epub 2012/01/03. doi: 10.1016/j.envint.2011.10.004. PubMed PMID: 22208753.

28.    Hecker M, Newsted JL, Murphy MB, Higley EB, Jones PD, Wu R, et al. Human adrenocarcinoma (H295R) cells for rapid in vitro determination of effects on steroidogenesis: hormone production. Toxicol Appl Pharmacol. 2006;217(1):114–24. Epub 2006/09/12. doi: 10.1016/j.taap.2006.07.007. PubMed PMID: 16962624.

29.    Sanderson JT, Boerma J, Lansbergen GW, van den Berg M. Induction and inhibition of aromatase (CYP19) activity by various classes of pesticides in H295R human adrenocortical carcinoma cells. Toxicol Appl Pharmacol. 2002;182(1):44–54. Epub 2002/07/20. doi: 10.1006/taap.2002.9420. PubMed PMID: 12127262.

30.      La Merrill MA, Vandenberg LN, Smith MT, Goodson W, Browne P, Patisaul HB, et al. Consensus on the key characteristics of endocrine-disrupting chemicals as a basis for hazard identification. Nat Rev Endocrinol. 2020;16(1):45–57. doi: 10.1038/s41574-019-0273-8.

31.      Bergman A, Heindel JJ, Kasten T, Kidd KA, Jobling S, Neira M, et al. The impact of endocrine disruption: a consensus statement on the state of the science. Environ Health Perspect. 2013;121(4):A104–A6. Epub 2013/04/04. doi: 10.1289/ehp.1205448. PubMed PMID: 23548368; PubMed Central PMCID: PMCPMC3620733.

32.      Miller WL. Steroid hormone synthesis in mitochondria. Mol Cell Endocrinol. 2013;379(1-2):62–73. Epub 2013/05/01. doi: 10.1016/j.mce.2013.04.014. PubMed PMID: 23628605.

33.      Payne AH, Hales DB. Overview of steroidogenic enzymes in the pathway from cholesterol to active steroid hormones. Endocr Rev. 2004;25(6):947–70. Epub 2004/12/08. doi: 10.1210/er.2003-0030. PubMed PMID: 15583024.

34.      Stocco DM. StAR protein and the regulation of steroid hormone biosynthesis. Annu Rev Physiol. 2001;63:193–213. Epub 2001/02/22. doi: 10.1146/annurev.physiol.63.1.193. PubMed PMID: 11181954.

35.      Miller WL, Auchus RJ. The molecular biology, biochemistry, and physiology of human steroidogenesis and its disorders. Endocr Rev. 2011;32(1):81–151. Epub 2010/11/06. doi: 10.1210/er.2010-0013. PubMed PMID: 21051590; PubMed Central PMCID: PMCPMC3365799.

36.      Wang L, Wang X, Geng Z, Zhou Y, Chen Y, Wu J, et al. Distribution of microcystin-LR to testis of male Sprague-Dawley rats. Ecotoxicology. 2013;22(10):1555-63. Epub 2013/10/24. doi: 10.1007/s10646-013-1141-2. PubMed PMID: 24150695.

37.      (WHO) WHO. Guidelines for Drinking-Water Quality: Fourth Edition Incorporating the First Addendum, https://www.who.int/water_sanitation_health/publications/drinking-water-quality-guidelines-4-including-1st-addendum/en/ Geneva, Switzerland**2017**.

38.      Wang L, Lin W, Zha Q, Guo H, Zhang D, Yang L, et al. Persistent exposure to environmental levels of microcystin-LR disturbs cortisol production via hypothalamic-pituitary-interrenal (HPI) axis and subsequently liver glucose metabolism in adult male zebrafish (*Danio rerio*). Toxins (Basel). 2020;12(5). Epub 2020/05/02. doi: 10.3390/toxins12050282. PubMed PMID: 32353954.

39.      Hou J, Li L, Wu N, Su Y, Lin W, Li G, et al. Reproduction impairment and endocrine disruption in female zebrafish after long-term exposure to MC-LR: A life cycle assessment. Environ Pollut. 2016;208(Pt B):477–85. Epub 2015/11/11. doi: 10.1016/j.envpol.2015.10.018. PubMed PMID: 26552529.

40.      Gazdar AF, Oie HK, Shackleton CH, Chen TR, Triche TJ, Myers CE, et al. Establishment and characterization of a human adrenocortical carcinoma cell line that expresses multiple pathways of steroid biosynthesis. Cancer Res. 1990;50(17):5488-96. Epub 1990/09/01. PubMed PMID: 2386954.

41.      Gracia T, Hilscherova K, Jones PD, Newsted JL, Zhang X, Hecker M, et al. The H295R system for evaluation of endocrine-disrupting effects. Ecotoxicol Environ Saf. 2006;65(3):293–305. Epub 2006/08/29. doi: 10.1016/j.ecoenv.2006.06.012. PubMed PMID: 16935330.

42.      Hecker M, Giesy JP. Novel trends in endocrine disruptor testing: the H295R Steroidogenesis Assay for identification of inducers and inhibitors of hormone production. Anal Bioanal Chem. 2008;390(1):287–91. doi: 10.1007/s00216-007-1657-5. PubMed PMID: 17957359.

43. Rainey WE, Bird IM, Sawetawan C, Hanley NA, McCarthy JL, McGee EA, et al. Regulation of human adrenal carcinoma cell (NCI-H295) production of C19 steroids. J Clin Endocrinol Metab. 1993;77(3):731–7. Epub 1993/09/01. doi: 10.1210/jcem.77.3.8396576. PubMed PMID: 8396576.

44. Rainey WE, Bird IM, Mason JI. The NCI-H295 cell line: a pluripotent model for human adrenocortical studies. Mol Cell Endocrinol. 1994;100(1-2):45–50. Epub 1994/04/01. doi: 10.1016/0303-7207(94)90277-1. PubMed PMID: 8056157.

45. Organisation for Economic Co-operation and Development (OECD). Revised Guidance Document 150 on Standardised Test Guidelines for Evaluating Chemicals for Endocrine Disruption2018.

46. Janssen EM. Cyanobacterial peptides beyond microcystins — a review on co-occurrence, toxicity, and challenges for risk assessment. Water Res. 2019;151:488–99. Epub 2019/01/15. doi: 10.1016/j.watres.2018.12.048. PubMed PMID: 30641464.

47. Dittmann E, Neilan BA, Erhard M, Von Döhren H, Börner T. Insertional mutagenesis of a peptide synthetase gene that is responsible for hepatotoxin production in the cyanobacterium *Microcystis aeruginosa* PCC 7806. Mol Microbiol. 1997;26(4):779–87. doi: 10.1046/j.1365-2958.1997.6131982.x.

48. Stefanelli M, Vichi S, Stipa G, Funari E, Testai E, Scardala S, et al. Survival, growth and toxicity of *Microcystis aeruginosa* PCC7806 in experimental conditions mimicking some features of the human gastro-intestinal environment. Chem-Biol Interact. 2014;215:54–61. Epub 2014/03/29. doi: 10.1016/j.cbi.2014.03.006. PubMed PMID: 24667652.

49. Mallia V, Ivanova L, Eriksen GS, Harper E, Connolly L, Uhlig S. Investigation of *in vitro* endocrine activities of *Microcystis* and *Planktothrix* cyanobacterial strains. Toxins (Basel). 2020;12(4). Epub 2020/04/09. doi: 10.3390/toxins12040228. PubMed PMID: 32260386; PubMed Central PMCID: PMCPMC7232361.

50. Portmann C, Blom JF, Gademann K, Juttner F. Aerucyclamides A and B: isolation and synthesis of toxic ribosomal heterocyclic peptides from the cyanobacterium *Microcystis aeruginosa* PCC 7806. J Nat Prod. 2008;71(7):1193–6. Epub 2008/06/19. doi: 10.1021/np800118g. PubMed PMID: 18558743.

51. Portmann C, Blom JF, Kaiser M, Brun R, Juttner F, Gademann K. Isolation of aerucyclamides C and D and structure revision of microcyclamide 7806A: heterocyclic ribosomal peptides from *Microcystis aeruginosa* PCC 7806 and their antiparasite evaluation. J Nat Prod. 2008;71(11):1891–6. Epub 2008/11/01. doi: 10.1021/np800409z. PubMed PMID: 18973386.

52. Tonk L, Welker M, Huisman J, Visser PM. Production of cyanopeptolins, anabaenopeptins, and microcystins by the harmful cyanobacteria *Anabaena* 90 and *Microcystis* PCC7806. Harmful Algae. 2009;8:219–24.

53. Tillett D, Dittmann E, Erhard M, von Dohren H, Borner T, Neilan BA. Structural organization of microcystin biosynthesis in *Microcystis aeruginosa* PCC7806: an integrated peptide-polyketide synthetase system. Chem Biol. 2000;7(10):753–64. Epub 2000/10/18. doi: 10.1016/s1074-5521(00)00021-1. PubMed PMID: 11033079.

54. Briand E, Bormans M, Gugger M, Dorrestein PC, Gerwick WH. Changes in secondary metabolic profiles of *Microcystis aeruginosa* strains in response to intraspecific interactions. Environ Microbiol. 2016;18(2):384–400. Epub 2015/05/20. doi: 10.1111/1462-2920.12904. PubMed PMID: 25980449; PubMed Central PMCID: PMCPMC5083810.

55. Mallia V, Uhlig S, Rafuse C, Meija J, Miles CO. Novel microcystins from *Planktothrix prolifica* NIVA-CYA 544 Identified by LC–MS/MS, functional group derivatization and ^{15}N-labeling. Mar Drugs.

2019;17(11). Epub 2019/11/17. doi: 10.3390/md17110643. PubMed PMID: 31731697; PubMed Central PMCID: PMCPMC6891653.

56.     Kotai J. Instructions for preparation of modified nutrient solution Z8 for algae. Norwegian Institute for Water Research, Oslo, Norway, 1972  Contract No.: Publication B-11/69).

57.     Mallia V, Uhlig S, Rafuse C, Meija J, Miles CO. Novel microcystins from *Planktothrix prolifica* NIVA-CYA 544 identified by LC-MS/MS, functional group derivatization and $^{15}$N-labeling. Mar Drugs. 2019;17(11). Epub 2019/11/17. doi: 10.3390/md17110643. PubMed PMID: 31731697; PubMed Central PMCID: PMCPMC6891653.

58.     O'Brien J, Wilson I, Orton T, Pognan F. Investigation of the Alamar Blue (resazurin) fluorescent dye for the assessment of mammalian cell cytotoxicity. Eur J Biochem. 2000;267(17):5421–6. Epub 2000/08/22. doi: 10.1046/j.1432-1327.2000.01606.x. PubMed PMID: 10951200.

59.     Weisser JJ, Hansen CH, Poulsen R, Larsen LW, Cornett C, Styrishave B. Two simple cleanup methods combined with LC–MS/MS for quantification of steroid hormones in *in vivo* and *in vitro* assays. Anal Bioanal Chem. 2016;408(18):4883–95. Epub 2016/05/07. doi: 10.1007/s00216-016-9575-z. PubMed PMID: 27150205.

60.     (EMA) EMA. ICH Q2 (R1) Validation of analytical procedures: text and methodology, h[ttps://www.ema.europa.eu/en/ich-q2-r1-validation-analytical-procedures-text-methodology.](https://www.ema.europa.eu/en/ich-q2-r1-validation-analytical-procedures-text-methodology)

61.     Bradley W, Robert P. Multivariate analysis in metabolomics. Curr Metabolomics. 2013;1(1):92–107. doi: h[ttp://dx.doi.org/10.2174/2213235X11301010092.](http://dx.doi.org/10.2174/2213235X11301010092)

62.     Blasco H, Błaszczyński J, Billaut JC, Nadal-Desbarats L, Pradat PF, Devos D, et al. Comparative analysis of targeted metabolomics: dominance-based rough set approach versus orthogonal partial least square-discriminant analysis. J Biomed Inf. 2015;53:291–9. Epub 2014/12/17. doi: 10.1016/j.jbi.2014.12.001. PubMed PMID: 25499899.

63.     Lee JW, Ji SH, Choi BR, Choi DJ, Lee YG, Kim HG, et al. UPLC-QTOF/MS-based metabolomics applied for the quality evaluation of four processed panax ginseng products. Molecules. 2018;23(8). Epub 2018/08/22. doi: 10.3390/molecules23082062. PubMed PMID: 30126124; PubMed Central PMCID: PMCPMC6222836.

64.     Kellogg JJ, Todd DA, Egan JM, Raja HA, Oberlies NH, Kvalheim OM, et al. Biochemometrics for natural products research: comparison of data analysis approaches and application to identification of bioactive compounds. J Nat Prod. 2016;79(2):376–86. doi: 10.1021/acs.jnatprod.5b01014.

65.     Ahmed KEM, Froysa HG, Karlsen OA, Sagen JV, Mellgren G, Verhaegen S, et al. LC–MS/MS based profiling and dynamic modelling of the steroidogenesis pathway in adrenocarcinoma H295R cells. Toxicol In Vitro. 2018;52:332–41. Epub 2018/07/19. doi: 10.1016/j.tiv.2018.07.002. PubMed PMID: 30017865.

66.     Lee TC, Miller WL, Auchus RJ. Medroxyprogesterone acetate and dexamethasone are competitive inhibitors of different human steroidogenic enzymes. J Clin Endocrinol Metab. 1999;84(6):2104–10. Epub 1999/06/18. doi: 10.1210/jcem.84.6.5646. PubMed PMID: 10372718.

67.     Xu Y, Xing Y, Chen Y, Chao Y, Lin Z, Fan E, et al. Structure of the protein phosphatase 2A holoenzyme. Cell. 2006;127(6):1239–51. doi: [https://doi.org/10.1016/j.cell.2006.11.033.](https://doi.org/10.1016/j.cell.2006.11.033)

# Supplementary Material

# Cyanobacterial microcystins and *Microcystis aeruginosa* extracts modulate steroidogenesis differentially in the human H295R adrenal model *in vitro*

**Vittoria Mallia[1,2], Steven Verhaegen[3], Bjarne Styrishave[4], Gunnar S. Eriksen[1], Malene L. Johannsen[4], Erik Ropstad[3], Silvio Uhlig[1,*]**

[1] *Toxinology Research Group, Norwegian Veterinary Institute, P.O. Box 750 Sentrum, N-0106 Oslo, Norway*

[2] *Department of Chemistry, University of Oslo, P.O. Box 1033, N-0315 Oslo, Norway*

[3] *Department of Production Animal Clinical Sciences, Faculty of Veterinary Medicine, Norwegian University of Life Sciences, P.O. Box 369 Sentrum, 0102 Oslo*

[4] *Toxicology and Drug Metabolism Group, Department of Pharmacy, Faculty of Health and Medical Sciences, University of Copenhagen, 2100 Copenhagen OE, Denmark*

# TABLE OF CONTENTS

**Scheme 1.** Experimental plan for H295R cells exposure.

**S1 Fig.** Scores plot from principal component analysis of all raw data from hormone analyses from H295R.

| MEDIUM CONTROL | MEDIUM CONTROL | MEDIUM CONTROL | SOLVENT CONTROL | SOLVENT CONTROL | SOLVENT CONTROL |
|---|---|---|---|---|---|
| POSITIVE CONTROL | POSITIVE CONTROL | POSITIVE CONTROL | Z8 MEDIUM | Z8 MEDIUM | Z8 MEDIUM |
| PCC7806 low (5ng/ml) | PCC7806 low (5ng/ml) | PCC7806 low (5ng/ml) | PCC7806 high (500ng/ml) | PCC7806 high (500ng/ml | PCC7806 high (500ng/ml |
| PCC7806*mcyB*-low conc. | PCC7806*mcyB*-low conc. | PCC7806*mcyB*-low conc. | PCC7806*mcyB*-high conc. | PCC7806*mcyB*-high conc. | PCC7806*mcyB*-high conc. |

PLATE 1

| MEDIUM CONTROL | MEDIUM CONTROL | MEDIUM CONTROL | SOLVENT CONTROL | SOLVENT CONTROL | SOLVENT CONTROL |
|---|---|---|---|---|---|
| POSITIVE CONTROL | POSITIVE CONTROL | POSITIVE CONTROL | MC-LR 1ng/ml | MC-LR 1ng/ml | MC-LR 1ng/ml |
| MC-LR 5ng/ml | MC-LR 5ng/ml | MC-LR 5ng/ml | MC-LR 100ng/ml | MC-LR 100ng/ml | MC-LR 100ng/ml |
| MC-LR 500ng/ml | MC-LR 500ng/ml | MC-LR 500ng/ml | MC-LR 1000ng/ml | MC-LR 1000ng/ml | MC-LR 1000ng/ml |

PLATE 2

| MEDIUM CONTROL | MEDIUM CONTROL | MEDIUM CONTROL | SOLVENT CONTROL | SOLVENT CONTROL | SOLVENT CONTROL |
|---|---|---|---|---|---|
| POSITIVE CONTROL | POSITIVE CONTROL | POSITIVE CONTROL | mix MCs/NOD-R 1ng/ml | mix MCs/NOD-R 1ng/ml | mix MCs/NOD-R 1ng/ml |
| mix MCs/NOD-R 5ng/ml | mix MCs/NOD-R 5ng/ml | mix MCs/NOD-R 5ng/ml | mix MCs/NOD-R 100ng/ml | *mix MCs/NOD-R 100ng/ml | *mix MCs/NOD-R 100ng/ml |
| | | | | | |

PLATE 3

MEDIUM CONTROL = 100% complete growth medium (D-MEM/F-12 (1x) liquid 1:1 +1% ITS +5% FBS)

SOLVENT CONTROL = growth medium with 0.5% methanol

POSITIVE CONTROL = growth medium with 0.5% methanol and 1.5uM forskolin stimulation

MC-LR = microcystin-LR

mix MCs/NOD-R = standard mix of 9 microcystins including MC-LR + nodularin-R

All exposure samples were prepared as 990uL growth medium + 10uL specific mother solution.

* not included in the 3rd plate of the 3rd run

**Scheme 1.** Experimental plan for H295R exposure in three 24-well plates. This scheme was repeated in three independent runs (Expt1, Expt2, Expt3). Concentrations reported are concentration of samples in the assay (once diluted in the growth medium).
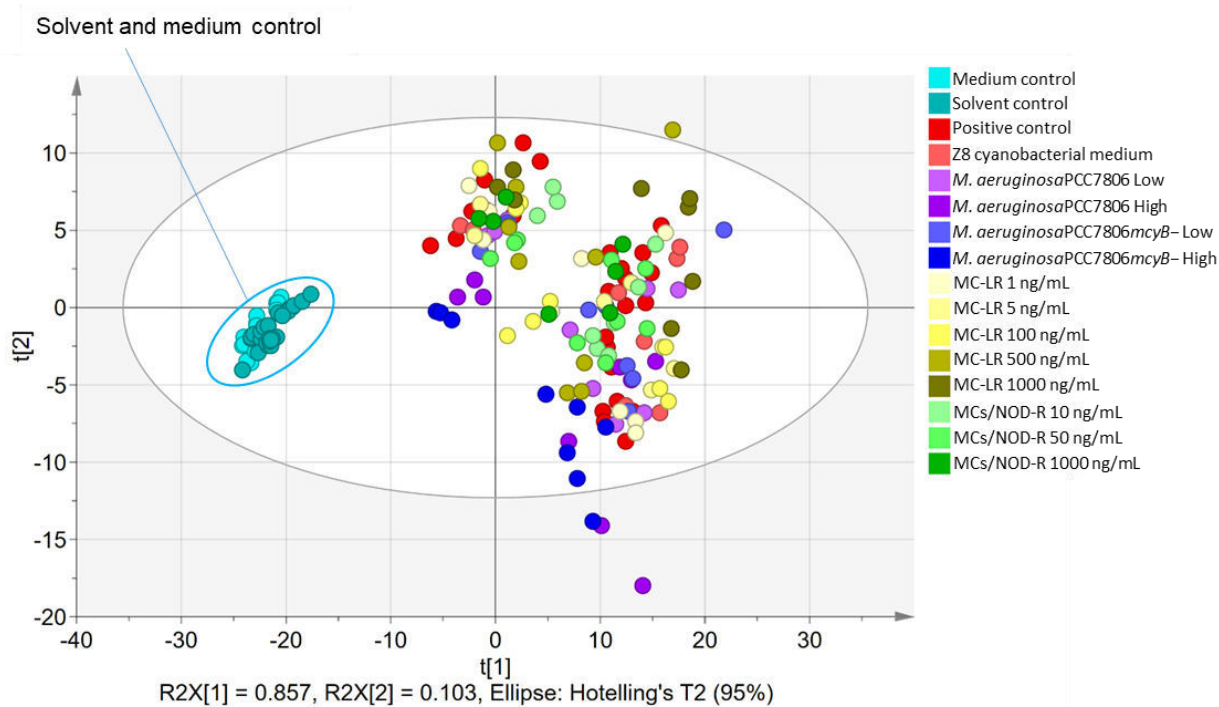
**Fig. S1.** Scores plot from principal component analysis of the pareto-scaled and log-transformed H295R hormone data. The purpose of the figure is to show that hormone concentrations of the solvent and medium control samples were homogeneous across experiments thus confirming the absence of technical bias.

# S1 Table. Overview over raw data from hormone analyses. (XLSX)

| Primary ID | Class ID | 11-deoxycorticosterone (ng/mL) | 11-deoxycortisol (ng/mL) | 17-OH-pregnenolone (ng/mL) | 17-OH-progesterone (ng/mL) | androstenedione (ng/mL) | cortisol (ng/mL) | cortisone (ng/mL) | dehydroepiandrosterone (DHEA) (ng/mL) | estrone (ng/mL) | estradiol (ng/mL) | pregnenolone (ng/mL) | progesterone (ng/mL) | testosterone (ng/mL) |
|---|---|---|---|---|---|---|---|---|---|---|---|---|---|---|
| Medium control_Expt1_1 | MC | 190.4 | 0.66 | 42.61 | 7.75 | 65.90 | 1.94 | 3.50 | 23.24 | 0.14 | 0.11 | 2.98 | 0.22 | 2.47 |
| Medium control_Expt1_2 | MC | 188.5 | 0.64 | 34.01 | 6.21 | 66.99 | 2.06 | 3.49 | 18.78 | 0.13 | 0.10 | 3.84 | 0.09 | 2.29 |
| Medium control_Expt1_3 | MC | 192.8 | 0.62 | 33.71 | 6.00 | 67.22 | 1.97 | 3.49 | 19.53 | 0.15 | 0.11 | 3.91 | 0.08 | 2.24 |
| Medium control_Expt1_4 | MC | 220.5 | 0.63 | 30.03 | 4.26 | 78.62 | 2.15 | 3.52 | 19.64 | 0.16 | 0.12 | 3.94 | 0.05 | 2.80 |
| Medium control_Expt1_5 | MC | 232.7 | 0.73 | 29.96 | 5.06 | 81.41 | 2.41 | 3.54 | 20.94 | 0.19 | 0.14 | 4.05 | 0.05 | 2.98 |
| Medium control_Expt1_6 | MC | 215.8 | 0.62 | 31.59 | 4.49 | 77.44 | 1.98 | 3.43 | 21.98 | 0.18 | 0.13 | 4.79 | 0.10 | 2.77 |
| Medium control_Expt1_7 | MC | 215.9 | 0.57 | 43.28 | 6.21 | 78.93 | 2.30 | 4.06 | 27.67 | 0.17 | 0.11 | 5.38 | 0.08 | 2.56 |
| Medium control_Expt1_8 | MC | 218.9 | 0.52 | 48.47 | 6.80 | 76.29 | 2.54 | 4.10 | 31.88 | 0.16 | 0.11 | 5.21 | 0.08 | 2.62 |
| Medium control_Expt1_9 | MC | 223.4 | 0.57 | 42.52 | 6.11 | 77.61 | 1.81 | 3.94 | 27.26 | 0.09 | 0.08 | 7.14 | 0.14 | 2.61 |
| Medium control_Expt2_1 | MC | 226.9 | 1.03 | 54.49 | 10.55 | 105.64 | 3.67 | 5.38 | 33.85 | 0.21 | 6.55 | 4.88 | 0.12 | 2.91 |
| Medium control_Expt2_2 | MC | 221.2 | 0.94 | 53.96 | 9.78 | 101.75 | 1.71 | 2.82 | 31.33 | 0.23 | 7.12 | 5.30 | 0.13 | 2.62 |
| Medium control_Expt2_3 | MC | 229.9 | 0.97 | 63.46 | 10.80 | 101.92 | 2.18 | 2.62 | 31.77 | 0.22 | 7.35 | 5.48 | 0.14 | 2.87 |
| Medium control_Expt2_4 | MC | 235.7 | 1.30 | 44.19 | 11.41 | 108.72 | 2.30 | 2.35 | 24.76 | 0.23 | 7.11 | 5.29 | 0.13 | 3.04 |
| Medium control_Expt2_5 | MC | 275.3 | 1.21 | 44.71 | 8.98 | 106.40 | 2.42 | 2.55 | 25.95 | 0.24 | 8.49 | 6.32 | 0.16 | 3.05 |
| Medium control_Expt2_6 | MC | 243.7 | 1.02 | 52.05 | 9.61 | 104.00 | 2.17 | 2.41 | 27.23 | 0.19 | 5.81 | 4.33 | 0.16 | 3.17 |
| Medium control_Expt3_1 | MC | data not available | 0.58 | 27.43 | 6.51 | 81.97 | 80.41 | 114.24 | 10.92 | 0.14 | 0.01 | 3.80 | 0.09 | 2.64 |
| Medium control_Expt3_2 | MC | data not available | 0.57 | 32.16 | 6.75 | 75.80 | 49.07 | 72.85 | 12.35 | 0.14 | 0.02 | 3.96 | 0.05 | 2.70 |
| Medium control_Expt3_3 | MC | data not available | 0.61 | 37.70 | 8.27 | 84.94 | 83.34 | 118.35 | 15.16 | 0.13 | 0.04 | 4.34 | 0.07 | 2.87 |

| Label | Type | | | | | | | | | | | | | |
|---|---|---|---|---|---|---|---|---|---|---|---|---|---|---|
| Medium control_Expt3_4 | MC | data not available | 0.72 | 37.69 | 6.28 | 93.76 | 144.55 | 13.78 | 18.64 | 0.22 | 0.13 | 4.73 | 0.06 | 2.96 |
| Medium control_Expt3_5 | MC | data not available | 0.75 | 44.72 | 7.08 | 94.94 | 22.47 | 6.50 | 21.09 | 0.18 | 0.03 | 5.24 | 0.08 | 2.99 |
| Medium control_Expt3_6 | MC | data not available | 0.68 | 33.72 | 5.73 | 101.39 | 34.40 | 7.97 | 16.85 | 0.19 | 0.22 | 4.33 | 0.08 | 2.88 |
| Medium control_Expt3_7 | MC | data not available | 0.56 | 29.37 | 5.71 | 92.66 | 117.19 | 9.72 | 13.67 | 0.13 | 0.09 | 3.90 | 0.06 | 2.82 |
| Medium control_Expt3_8 | MC | data not available | 0.63 | 29.16 | 5.55 | 93.67 | 35.10 | 4.16 | 13.67 | 0.16 | 0.06 | 4.34 | 0.06 | 2.89 |
| Medium control_Expt3_9 | MC | data not available | 0.62 | 32.85 | 6.45 | 98.30 | 69.35 | 24.02 | 15.93 | 0.13 | 0.01 | 4.34 | 0.06 | 2.82 |
| Solvent control_Expt1_1 | SC | 197.7 | 0.75 | 42.67 | 7.62 | 72.92 | 2.08 | 2.78 | 21.95 | 0.16 | 0.12 | 6.26 | 0.13 | 2.78 |
| Solvent control_Expt1_2 | SC | 212.4 | 0.77 | 40.50 | 7.86 | 74.09 | 1.87 | 3.45 | 22.15 | 0.17 | 0.13 | 4.75 | 0.11 | 2.77 |
| Solvent control_Expt1_3 | SC | 246.2 | 0.81 | 43.64 | 8.08 | 80.05 | 1.94 | 3.43 | 22.04 | 0.20 | 0.14 | 4.89 | 0.12 | 3.06 |
| Solvent control_Expt1_4 | SC | 228.2 | 0.82 | 36.20 | 11.60 | 71.93 | 1.65 | 2.61 | 6.51 | 0.12 | 0.09 | 4.14 | 0.21 | 3.36 |
| Solvent control_Expt1_5 | SC | 241.5 | 0.76 | 40.29 | 7.15 | 77.89 | 1.84 | 3.34 | 22.40 | 0.18 | 0.13 | 3.61 | 0.10 | 3.09 |
| Solvent control_Expt1_6 | SC | 260.2 | 0.90 | 33.70 | 6.46 | 86.79 | 2.02 | 3.25 | 18.86 | 0.19 | 0.14 | 6.92 | 0.14 | 3.37 |
| Solvent control_Expt1_7 | SC | 237.4 | 0.66 | 47.59 | 6.77 | 84.83 | 2.32 | 3.32 | 23.15 | 0.14 | 0.12 | 6.98 | 0.12 | 3.05 |
| Solvent control_Expt1_8 | SC | 291.9 | 0.80 | 43.33 | 6.92 | 87.80 | 2.19 | 3.17 | 24.83 | 0.11 | 0.11 | 7.72 | 0.13 | 3.26 |
| Solvent control_Expt1_9 | SC | 291.6 | 0.82 | 50.90 | 6.75 | 92.09 | 2.36 | 4.22 | 24.43 | 0.13 | 0.11 | 7.98 | 0.15 | 3.48 |
| Solvent control_Expt2_1 | SC | 266.8 | 1.53 | 67.72 | 12.82 | 117.14 | 1.94 | 2.47 | 26.61 | 0.23 | 11.42 | 8.50 | 0.18 | 3.54 |
| Solvent control_Expt2_2 | SC | 271.5 | 1.78 | 51.21 | 10.79 | 124.21 | 2.28 | 2.27 | 25.28 | 0.25 | 9.61 | 7.15 | 0.19 | 3.58 |
| Solvent control_Expt2_3 | SC | 264.7 | 1.68 | 50.81 | 10.26 | 119.95 | 2.23 | 2.22 | 24.21 | 0.24 | 9.12 | 6.79 | 0.18 | 3.31 |
| Solvent control_Expt2_4 | SC | 285.9 | 1.56 | 52.63 | 10.69 | 125.17 | 2.23 | 2.50 | 26.24 | 0.23 | 11.09 | 8.25 | 0.20 | 3.44 |
| Solvent control_Expt2_5 | SC | 262.4 | 1.90 | 53.04 | 12.25 | 135.57 | 2.44 | 2.37 | 25.91 | 0.25 | 10.40 | 7.75 | 0.20 | 4.28 |
| Solvent control_Expt2_6 | SC | 271.1 | 1.82 | 52.49 | 12.36 | 147.18 | 2.17 | 2.33 | 26.94 | 0.25 | 9.55 | 7.11 | 0.18 | 4.13 |
| Solvent control_Expt2_7 | SC | 233.6 | 1.65 | 65.15 | 16.21 | 105.87 | 2.18 | 2.03 | 25.94 | 0.32 | 6.46 | 4.81 | 0.49 | 3.36 |
| Solvent control_Expt2_8 | SC | 228.5 | 1.45 | 58.79 | 13.43 | 112.33 | 2.16 | 2.08 | 22.95 | 0.28 | 6.56 | 4.88 | 0.77 | 3.53 |

| Label | Group | | | | | | | | | | | | | |
|---|---|---|---|---|---|---|---|---|---|---|---|---|---|---|
| Solvent control_Expt2_9 | SC | 239.3 | 1.62 | 64.62 | 14.85 | 110.72 | 2.27 | 2.23 | 23.80 | 0.27 | 7.32 | 5.45 | 0.89 | 3.72 |
| Solvent control_Expt3_1 | SC | data not available | 0.72 | 39.17 | 8.47 | 88.97 | 163.66 | 220.06 | 14.30 | 0.16 | 0.02 | 4.74 | 0.08 | 3.33 |
| Solvent control_Expt3_2 | SC | data not available | 1.01 | 37.21 | 8.87 | 100.54 | 76.31 | 86.77 | 14.84 | 0.17 | 0.23 | 4.94 | 0.08 | 3.27 |
| Solvent control_Expt3_3 | SC | data not available | 0.99 | 42.20 | 9.83 | 111.60 | 113.54 | 111.91 | 16.55 | 0.25 | 0.25 | 4.86 | 0.11 | 3.31 |
| Solvent control_Expt3_4 | SC | data not available | 0.90 | 33.98 | 5.95 | 99.49 | 71.56 | 9.98 | 15.94 | 0.23 | 0.01 | 4.99 | 0.06 | 3.50 |
| Solvent control_Expt3_5 | SC | data not available | 0.96 | 28.44 | 5.27 | 105.29 | 63.40 | 4.80 | 12.50 | 0.23 | 0.18 | 5.02 | 0.10 | 3.58 |
| Solvent control_Expt3_6 | SC | data not available | 0.92 | 34.07 | 6.15 | 102.05 | 53.86 | 8.66 | 15.39 | 0.20 | 0.22 | 4.58 | 0.12 | 3.58 |
| Solvent control_Expt3_7 | SC | data not available | 0.79 | 36.14 | 8.76 | 102.34 | 42.53 | 12.55 | 16.43 | 0.17 | 0.14 | 4.64 | 0.07 | 3.28 |
| Solvent control_Expt3_8 | SC | data not available | 0.80 | 35.54 | 8.84 | 105.91 | 37.95 | 15.08 | 16.19 | 0.18 | 0.10 | 4.77 | 0.07 | 3.27 |
| Solvent control_Expt3_9 | SC | data not available | 0.87 | 33.54 | 7.67 | 105.08 | 125.97 | 12.01 | 15.82 | 0.19 | 0.03 | 4.86 | 0.06 | 3.50 |
| Positive control_Expt1_1 | PC | 984.6 | 37.54 | 106.45 | 32.43 | 248.88 | 13.31 | 2.28 | 51.97 | 7.90 | 5.80 | 14.09 | 0.91 | 10.05 |
| Positive control_Expt1_2 | PC | 1085.7 | 40.40 | 115.29 | 33.37 | 274.06 | 16.54 | 2.82 | 54.07 | 8.67 | 5.71 | 20.23 | 1.72 | 10.89 |
| Positive control_Expt1_3 | PC | 1153.9 | 40.57 | 123.26 | 33.87 | 298.43 | 14.78 | 2.62 | 63.01 | 9.20 | 6.41 | 19.86 | 1.03 | 10.95 |
| Positive control_Expt1_4 | PC | 1132.6 | 41.71 | 121.61 | 29.47 | 302.23 | 17.82 | 2.46 | 75.44 | 9.95 | 6.67 | 16.31 | 0.93 | 12.10 |
| Positive control_Expt1_5 | PC | 1159.2 | 38.18 | 119.21 | 31.03 | 290.13 | 13.81 | 2.10 | 62.74 | 9.20 | 6.07 | 22.47 | 1.34 | 10.89 |
| Positive control_Expt1_6 | PC | 1166.4 | 45.55 | 153.41 | 35.84 | 286.86 | 16.15 | 3.09 | 83.94 | 10.22 | 7.17 | 24.20 | 0.98 | 10.50 |
| Positive control_Expt1_7 | PC | 1437.1 | 63.58 | 174.68 | 38.13 | 339.87 | 27.80 | 2.47 | 91.72 | 12.16 | 8.78 | 23.09 | 1.30 | 13.56 |
| Positive control_Expt1_8 | PC | 1371.3 | 63.38 | 160.65 | 37.00 | 316.33 | 19.57 | 2.44 | 70.71 | 10.23 | 8.30 | 24.63 | 1.80 | 12.48 |
| Positive control_Expt1_9 | PC | 1276.2 | 56.29 | 182.83 | 35.37 | 315.76 | 22.59 | 2.30 | 102.13 | 10.79 | 8.14 | 25.86 | 1.57 | 11.62 |
| Positive control_Expt2_1 | PC | 1369.7 | 122.79 | 162.85 | 59.05 | 408.04 | 15.52 | 0.99 | 60.23 | 8.05 | 55.31 | 41.18 | 3.07 | 13.64 |
| Positive control_Expt2_2 | PC | 1282.8 | 135.11 | 174.97 | 67.29 | 396.38 | 16.90 | 1.17 | 57.78 | 7.91 | 58.54 | 43.59 | 3.86 | 13.54 |
| Positive control_Expt2_3 | PC | 1366.5 | 139.87 | 169.99 | 64.31 | 417.72 | 15.71 | 1.13 | 57.77 | 7.37 | 60.94 | 45.37 | 4.56 | 13.34 |
| Positive control_Expt2_4 | PC | 1235.2 | 112.04 | 151.13 | 67.63 | 402.79 | 18.79 | 1.28 | 64.18 | 8.93 | 40.06 | 29.82 | 4.60 | 15.27 |

| Sample | Group | | | | | | | | | | | | | |
|---|---|---|---|---|---|---|---|---|---|---|---|---|---|---|
| Positive control_Expt2_5 | PC | 1322.3 | 125.66 | 154.80 | 74.00 | 391.06 | 16.29 | 0.94 | 57.31 | 7.32 | 44.00 | 32.76 | 3.98 | 14.06 |
| Positive control_Expt2_6 | PC | 1258.2 | 117.48 | 204.30 | 82.75 | 468.98 | 18.22 | 1.19 | 65.80 | 6.94 | 38.21 | 28.45 | 3.83 | 15.64 |
| Positive control_Expt2_7 | PC | 1203.5 | 120.77 | 196.13 | 73.02 | 398.40 | 19.37 | 1.03 | 65.93 | 12.78 | 56.55 | 42.11 | 7.08 | 13.61 |
| Positive control_Expt2_8 | PC | 1325.3 | 124.22 | 232.80 | 88.49 | 427.29 | 17.73 | 0.99 | 67.99 | 12.97 | 50.65 | 37.71 | 8.74 | 14.15 |
| Positive control_Expt2_9 | PC | 1388.3 | 127.03 | 245.27 | 79.69 | 429.55 | 19.43 | 1.02 | 61.98 | 11.93 | 62.58 | 46.59 | 9.15 | 15.38 |
| Positive control_Expt2_1 | PC | data not available | 162.21 | 136.78 | 52.19 | 342.36 | 1068.51 | 44.88 | 40.23 | 26.61 | 2.50 | 48.19 | 3.53 | 16.45 |
| Positive control_Expt2_2 | PC | data not available | 160.86 | 133.37 | 51.31 | 372.60 | 1356.65 | 67.69 | 35.02 | 26.07 | 2.82 | 53.96 | 3.70 | 16.38 |
| Positive control_Expt2_3 | PC | data not available | 178.04 | 129.59 | 49.39 | 355.18 | 3476.08 | 171.26 | 35.23 | 21.91 | 2.99 | 55.86 | 2.98 | 16.64 |
| Positive control_Expt2_4 | PC | data not available | 160.57 | 139.31 | 46.28 | 368.17 | 2681.56 | 33.51 | 37.66 | 22.22 | 2.99 | 45.03 | 2.97 | 17.63 |
| Positive control_Expt2_5 | PC | data not available | 156.35 | 133.88 | 43.31 | 360.02 | 879.10 | 57.64 | 27.36 | 20.15 | 3.40 | 47.13 | 2.98 | 15.54 |
| Positive control_Expt2_6 | PC | data not available | 164.52 | 127.50 | 45.63 | 387.39 | 1879.34 | 75.05 | 31.46 | 18.64 | 2.75 | 46.98 | 3.51 | 17.11 |
| Positive control_Expt2_7 | PC | data not available | 130.12 | 137.23 | 59.15 | 381.19 | 1419.01 | 16.66 | 41.47 | 14.56 | 3.12 | 44.77 | 2.53 | 16.12 |
| Positive control_Expt2_8 | PC | data not available | 125.89 | 178.19 | 72.02 | 383.98 | 2219.91 | 89.14 | 43.63 | 14.86 | 2.51 | 41.67 | 2.55 | 16.33 |
| Positive control_Expt2_9 | PC | data not available | 132.14 | 125.71 | 50.88 | 392.11 | 1163.17 | 45.42 | 31.43 | 14.57 | 2.16 | 45.64 | 2.79 | 15.50 |
| Z8medium_Expt1_1 | Z8 | 1100.0 | 39.18 | 120.39 | 32.47 | 280.98 | 14.46 | 2.57 | 57.55 | 8.64 | 6.06 | 19.77 | 1.49 | 9.69 |
| Z8medium_Expt1_2 | Z8 | 1095.6 | 46.15 | 116.79 | 33.00 | 288.68 | 14.53 | 2.48 | 58.56 | 8.67 | 5.94 | 22.01 | 1.88 | 10.74 |
| Z8medium_Expt1_3 | Z8 | 1141.0 | 45.93 | 132.04 | 36.19 | 305.06 | 15.51 | 2.58 | 63.82 | 9.26 | 6.12 | 19.45 | 2.41 | 11.17 |
| Z8medium_Expt2_1 | Z8 | 1590.9 | 126.94 | 160.15 | 64.24 | 395.76 | 16.95 | 1.31 | 58.74 | 7.75 | 57.04 | 42.47 | 4.12 | 10.89 |
| Z8medium_Expt2_2 | Z8 | 1373.3 | 130.29 | 171.84 | 68.51 | 469.13 | 17.48 | 1.19 | 61.35 | 8.41 | 57.85 | 43.07 | 4.42 | 13.80 |
| Z8medium_Expt2_3 | Z8 | 1389.4 | 126.59 | 161.20 | 67.21 | 476.24 | 17.99 | 1.19 | 63.08 | 9.48 | 55.48 | 41.31 | 4.20 | 14.60 |
| Z8medium_Expt3_1 | Z8 | data not available | 174.50 | 346.80 | 126.85 | 356.14 | 851.55 | 36.66 | 79.99 | 21.95 | 2.63 | 54.98 | 3.93 | 15.62 |
| Z8medium_Expt3_2 | Z8 | data not available | 180.29 | 272.85 | 107.53 | 338.53 | 2038.94 | 107.29 | 57.26 | 22.22 | 3.36 | 54.72 | 4.83 | 16.53 |
| Z8medium_Expt3_3 | Z8 | data not available | 203.20 | 292.60 | 121.52 | 351.52 | 1315.98 | 52.17 | 66.55 | 22.51 | 3.20 | 62.12 | 4.76 | 18.04 |
| PCC7806 low(5ng)_Expt1_1 | PCC_5 | 1052.9 | 53.21 | 115.80 | 35.95 | 304.94 | 14.81 | 2.09 | 56.06 | 9.54 | 6.43 | 19.87 | 0.99 | 12.07 |

| Sample | Group | | | | | | | | | | | | | |
|---|---|---|---|---|---|---|---|---|---|---|---|---|---|---|
| PCC7806 low(5ng)_Expt1_2 | PCC_5 | 1133.5 | 57.02 | 134.27 | 37.88 | 302.85 | 15.46 | 2.27 | 62.27 | 9.65 | 7.31 | 25.05 | 1.44 | 11.49 |
| PCC7806 low(5ng)_Expt1_3 | PCC_5 | 1262.3 | 57.09 | 137.27 | 37.98 | 315.32 | 14.55 | 2.20 | 65.61 | 10.01 | 6.88 | 26.86 | 2.07 | 12.20 |
| PCC7806 low(5ng)_Expt2_1 | PCC_5 | 1290.3 | 146.27 | 150.99 | 66.49 | 463.65 | 17.88 | 1.12 | 55.20 | 9.50 | 48.46 | 36.08 | 5.44 | 16.68 |
| PCC7806 low(5ng)_Expt2_2 | PCC_5 | 1289.4 | 134.05 | 170.65 | 84.32 | 421.92 | 17.31 | 1.25 | 59.50 | 7.70 | 56.96 | 42.41 | 4.96 | 17.16 |
| PCC7806 low(5ng)_Expt2_3 | PCC_5 | 1224.2 | 131.98 | 165.81 | 76.97 | 330.35 | 17.46 | 1.23 | 55.89 | 6.42 | 45.57 | 33.93 | 5.05 | 14.60 |
| PCC7806 low(5ng)_Expt3_1 | PCC_5 | data not available | 163.75 | 268.89 | 110.08 | 308.89 | 1391.30 | 48.66 | 60.94 | 21.18 | 2.62 | 52.80 | 4.16 | 16.65 |
| PCC7806 low(5ng)_Expt3_2 | PCC_5 | data not available | 186.97 | 280.17 | 115.66 | 326.33 | 2187.95 | 108.06 | 53.39 | 22.15 | 2.99 | 49.94 | 4.21 | 15.66 |
| PCC7806 low(5ng)_Expt3_3 | PCC_5 | data not available | 195.40 | 308.66 | 123.61 | 350.92 | 1865.40 | 84.19 | 59.36 | 23.44 | 2.99 | 52.97 | 5.03 | 17.26 |
| PCC7806 high(500ng)_Expt1_1 | PCC_50 | 1345.0 | 54.19 | 71.78 | 26.83 | 286.74 | 36.93 | 2.73 | 29.80 | 9.37 | 6.24 | 14.38 | 2.43 | 9.76 |
| PCC7806 high(500ng)_Expt1_2 | PCC_50 | 1457.9 | 58.82 | 97.82 | 35.26 | 292.03 | 32.86 | 2.34 | 40.76 | 9.12 | 6.39 | 20.42 | 2.56 | 10.24 |
| PCC7806 high(500ng)_Expt1_3 | PCC_50 | 1437.0 | 62.47 | 78.27 | 29.14 | 312.01 | 33.87 | 2.28 | 29.40 | 10.08 | 7.13 | 15.50 | 1.44 | 11.13 |
| PCC7806 high(500ng)_Expt2_1 | PCC_50 | 1734.9 | 167.98 | 112.46 | 65.32 | 402.84 | 41.25 | 1.37 | 36.51 | 5.42 | 36.21 | 26.96 | 4.34 | 13.37 |
| PCC7806 high(500ng)_Expt2_2 | PCC_50 | 1560.5 | 149.14 | 119.36 | 65.50 | 413.36 | 38.61 | 1.15 | 27.68 | 5.73 | 32.04 | 23.85 | 4.40 | 12.52 |
| PCC7806 high(500ng)_Expt2_3 | PCC_50 | 1947.7 | 161.98 | 131.79 | 63.61 | 439.90 | 47.22 | 1.28 | 34.29 | 6.31 | 39.46 | 29.38 | 4.51 | 15.39 |
| PCC7806 high(500ng)_Expt3_1 | PCC_50 | data not available | 217.72 | 137.29 | 77.45 | 316.53 | 2220.97 | 46.36 | 20.19 | 20.03 | 3.09 | 33.58 | 3.96 | 14.61 |
| PCC7806 high(500ng)_Expt3_2 | PCC_50 | data not available | 162.20 | 169.50 | 77.29 | 320.46 | 7974.23 | 184.86 | 27.03 | 20.81 | 3.05 | 33.39 | 1.22 | 13.71 |
| PCC7806 high(500ng)_Expt3_3 | PCC_50 | data not available | 266.25 | 136.36 | 72.44 | 321.94 | 3591.98 | 93.63 | 21.35 | 19.78 | 3.00 | 39.28 | 4.65 | 15.66 |
| PCC7806mcyB-low_Expt1_1 | PCC_MC-LOW | 1154.6 | 57.72 | 108.13 | 32.69 | 329.08 | 15.09 | 1.94 | 58.42 | 9.68 | 6.28 | 15.72 | 1.12 | 12.70 |
| PCC7806mcyB-low_Expt1_2 | PCC_MC-LOW | 1125.2 | 54.88 | 120.34 | 34.87 | 317.21 | 14.85 | 2.03 | 62.72 | 9.41 | 6.51 | 31.90 | 1.39 | 12.36 |
| PCC7806mcyB-low_Expt1_3 | PCC_MC-LOW | 1135.0 | 57.45 | 111.72 | 29.57 | 295.14 | 15.44 | 2.23 | 53.01 | 8.61 | 6.07 | 18.31 | 1.17 | 11.41 |
| PCC7806mcyB-low_Expt2_1 | PCC_MC-LOW | 1401.5 | 142.44 | 206.87 | 70.22 | 512.59 | 17.94 | 1.12 | 72.97 | 10.60 | 54.94 | 40.90 | 4.63 | 18.60 |
| PCC7806mcyB-low_Expt2_2 | PCC_MC-LOW | 1277.8 | 132.82 | 187.99 | 77.30 | 341.65 | 18.28 | 1.13 | 65.48 | 7.50 | 54.81 | 40.81 | 3.85 | 15.30 |
| PCC7806mcyB-low_Expt2_3 | PCC_MC-LOW | 1381.4 | 123.23 | 160.07 | 60.36 | 384.86 | 17.31 | 1.16 | 51.81 | 7.02 | 52.80 | 39.31 | 3.87 | 14.93 |

| Sample | Code | | | | | | | | | | | | | |
|---|---|---|---|---|---|---|---|---|---|---|---|---|---|---|
| PCC7806mcyB-low_Expt3_1 | PCC_MC-LOW | data not available | 176.53 | 289.44 | 104.40 | 344.25 | 1087.66 | 32.33 | 69.24 | 21.54 | 3.05 | 44.90 | 3.93 | 17.95 |
| PCC7806mcyB-low_Expt3_2 | PCC_MC-LOW | data not available | 188.31 | 317.11 | 122.06 | 334.92 | 2074.91 | 98.77 | 74.07 | 18.81 | 2.95 | 48.95 | 4.47 | 17.81 |
| PCC7806mcyB-low_Expt3_3 | PCC_MC-LOW | data not available | 190.82 | 258.05 | 95.25 | 333.87 | 1897.51 | 78.85 | 60.34 | 19.32 | 2.96 | 51.22 | 4.22 | 17.10 |
| PCC7806mcyB-high_Expt1_1 | PCC_MC-HIGH | 1254.3 | 50.73 | 62.70 | 22.30 | 262.36 | 25.80 | 2.02 | 25.94 | 8.19 | 5.58 | 14.12 | 1.64 | 9.83 |
| PCC7806mcyB-high_Expt1_2 | PCC_MC-HIGH | 1229.6 | 53.07 | 66.92 | 26.95 | 264.60 | 23.11 | 1.90 | 26.14 | 8.59 | 6.98 | 15.59 | 1.25 | 9.23 |
| PCC7806mcyB-high_Expt1_3 | PCC_MC-HIGH | 1199.7 | 59.96 | 57.13 | 21.25 | 275.51 | 24.07 | 1.88 | 24.38 | 8.49 | 5.93 | 15.51 | 1.34 | 9.91 |
| PCC7806mcyB-high_Expt2_1 | PCC_MC-HIGH | 1574.0 | 160.17 | 86.90 | 51.45 | 338.89 | 32.94 | 1.21 | 32.31 | 4.85 | 36.24 | 26.98 | 4.52 | 12.46 |
| PCC7806mcyB-high_Expt2_2 | PCC_MC-HIGH | 1350.5 | 135.14 | 95.88 | 57.38 | 315.67 | 27.87 | 1.00 | 28.82 | 5.80 | 38.07 | 28.34 | 9.80 | 15.32 |
| PCC7806mcyB-high_Expt2_3 | PCC_MC-HIGH | 1391.8 | 175.40 | 91.29 | 58.98 | 361.48 | 32.84 | 1.01 | 27.69 | 6.59 | 39.26 | 29.23 | 4.09 | 16.19 |
| PCC7806mcyB-high_Expt3_1 | PCC_MC-HIGH | data not available | 163.94 | 118.84 | 51.92 | 321.99 | 4752.56 | 140.14 | 21.23 | 18.47 | 3.50 | 30.35 | 3.07 | 13.78 |
| PCC7806mcyB-high_Expt3_2 | PCC_MC-HIGH | data not available | 189.72 | 141.72 | 64.44 | 307.96 | 1274.70 | 33.09 | 27.17 | 17.87 | 2.42 | 32.18 | 3.15 | 13.60 |
| PCC7806mcyB-high_Expt3_3 | PCC_MC-HIGH | data not available | 208.14 | 136.34 | 63.61 | 311.78 | 5579.92 | 148.42 | 19.74 | 18.42 | 2.67 | 37.44 | 2.60 | 14.87 |
| MC-LR_1ng/mL_Expt1_1 | MC-LR_1 | 1071.4 | 37.70 | 144.62 | 35.35 | 278.90 | 15.82 | 2.33 | 76.77 | 9.18 | 5.88 | 21.40 | 1.51 | 10.56 |
| MC-LR_1ng/mL_Expt1_2 | MC-LR_1 | 1190.4 | 49.42 | 134.23 | 35.24 | 300.36 | 16.54 | 2.31 | 66.83 | 10.03 | 7.25 | 21.91 | 1.11 | 11.68 |
| MC-LR_1ng/mL_Expt1_3 | MC-LR_1 | 1056.1 | 53.80 | 113.98 | 33.60 | 296.18 | 16.53 | 2.03 | 56.59 | 10.11 | 8.12 | 22.48 | 1.23 | 11.70 |
| MC-LR_1ng/mL_Expt2_1 | MC-LR_1 | 1177.0 | 108.45 | 182.97 | 68.76 | 321.76 | 17.04 | 1.18 | 54.00 | 6.82 | 53.34 | 39.72 | 3.79 | 15.03 |
| MC-LR_1ng/mL_Expt2_2 | MC-LR_1 | 1373.7 | 110.15 | 217.36 | 82.92 | 352.97 | 17.47 | 1.22 | 72.58 | 8.22 | 46.77 | 34.82 | 4.41 | 14.75 |
| MC-LR_1ng/mL_Expt2_3 | MC-LR_1 | 1356.5 | 124.51 | 235.78 | 87.37 | 456.10 | 17.26 | 0.98 | 71.81 | 7.52 | 49.47 | 36.83 | 4.31 | 15.67 |
| MC-LR_1ng/mL_Expt3_1 | MC-LR_1 | data not available | 169.08 | 149.24 | 55.32 | 363.01 | 317.74 | 14.98 | 38.04 | 16.73 | 3.29 | 46.12 | 3.14 | 16.83 |
| MC-LR_1ng/mL_Expt3_2 | MC-LR_1 | data not available | 175.64 | 140.95 | 55.93 | 377.45 | 1403.91 | 50.98 | 35.66 | 18.74 | 3.07 | 47.90 | 3.64 | 17.40 |
| MC-LR_1ng/mL_Expt3_3 | MC-LR_1 | data not available | 181.52 | 139.27 | 55.97 | 372.34 | 1018.72 | 37.90 | 35.08 | 19.16 | 3.46 | 48.60 | 3.51 | 17.70 |
| MC-LR_5ng/mL_Expt1_1 | MC-LR_5 | 1135.6 | 49.33 | 107.43 | 33.62 | 290.53 | 18.50 | 2.41 | 56.94 | 9.51 | 6.92 | 19.88 | 1.15 | 12.04 |
| MC-LR_5ng/mL_Expt1_2 | MC-LR_5 | 1154.1 | 50.07 | 115.85 | 32.60 | 289.72 | 14.87 | 2.11 | 57.28 | 8.90 | 6.02 | 20.18 | 1.10 | 11.44 |

| Sample | Group | | | | | | | | | | | | |
|---|---|---|---|---|---|---|---|---|---|---|---|---|---|
| MC-LR_5ng/mL_Expt1_3 | MC-LR_5 | 1119.6 | 42.38 | 135.12 | 37.61 | 291.65 | 17.41 | 2.57 | 69.21 | 9.48 | 6.95 | 25.07 | 0.98 | 10.46 |
| MC-LR_5ng/mL_Expt2_1 | MC-LR_5 | 1208.4 | 133.21 | 164.97 | 81.29 | 368.03 | 18.89 | 1.14 | 62.70 | 12.19 | 48.33 | 35.99 | 4.18 | 15.62 |
| MC-LR_5ng/mL_Expt2_2 | MC-LR_5 | 1264.6 | 116.22 | 187.13 | 75.87 | 433.91 | 16.81 | 1.00 | 46.68 | 11.97 | 47.74 | 35.55 | 4.96 | 14.64 |
| MC-LR_5ng/mL_Expt2_3 | MC-LR_5 | 1337.4 | 118.58 | 202.61 | 79.94 | 431.32 | 16.62 | 0.98 | 48.65 | 12.41 | 45.42 | 33.82 | 4.76 | 15.97 |
| MC-LR_5ng/mL_Expt3_1 | MC-LR_5 | data not available | 182.69 | 280.76 | 119.24 | 400.50 | 565.65 | 13.97 | 61.76 | 25.02 | 3.29 | 54.51 | 3.90 | 18.04 |
| MC-LR_5ng/mL_Expt3_2 | MC-LR_5 | data not available | 172.56 | 316.30 | 134.05 | 389.76 | 2315.84 | 89.12 | 69.14 | 24.92 | 3.05 | 54.93 | 3.63 | 17.28 |
| MC-LR_5ng/mL_Expt3_3 | MC-LR_5 | data not available | 171.77 | 229.54 | 102.98 | 385.61 | 1822.80 | 66.10 | 49.51 | 20.80 | 3.34 | 57.51 | 3.93 | 16.78 |
| MC-LR_100ng/mL_Expt1_1 | MC-LR_100 | 1159.2 | 41.89 | 158.58 | 43.23 | 278.33 | 14.41 | 2.14 | 89.17 | 9.75 | 7.15 | 25.72 | 1.04 | 10.70 |
| MC-LR_100ng/mL_Expt1_2 | MC-LR_100 | 1247.2 | 57.20 | 149.01 | 43.60 | 323.60 | 15.50 | 2.01 | 73.69 | 11.47 | 8.07 | 31.62 | 1.63 | 12.73 |
| MC-LR_100ng/mL_Expt1_3 | MC-LR_100 | 1392.8 | 61.02 | 151.54 | 39.11 | 322.19 | 18.46 | 2.17 | 71.24 | 10.44 | 7.16 | 24.79 | 1.39 | 11.84 |
| MC-LR_100ng/mL_Expt2_1 | MC-LR_100 | 939.6 | 104.42 | 162.96 | 69.85 | 271.29 | 15.72 | 1.07 | 49.84 | 6.67 | 46.08 | 34.31 | 7.71 | 13.99 |
| MC-LR_100ng/mL_Expt2_2 | MC-LR_100 | 1000.9 | 108.89 | 166.90 | 73.56 | 308.28 | 16.14 | 1.18 | 49.90 | 6.76 | 40.45 | 30.11 | 7.12 | 13.29 |
| MC-LR_100ng/mL_Expt2_3 | MC-LR_100 | 1065.1 | 103.74 | 174.35 | 59.06 | 327.42 | 16.63 | 1.08 | 54.11 | 7.43 | 49.68 | 36.99 | 7.81 | 13.97 |
| MC-LR_100ng/mL_Expt3_1 | MC-LR_100 | data not available | 177.30 | 282.55 | 117.63 | 393.25 | 1845.38 | 62.78 | 69.89 | 25.67 | 3.20 | 50.53 | 3.57 | 17.45 |
| MC-LR_100ng/mL_Expt3_2 | MC-LR_100 | data not available | 174.94 | 250.89 | 105.93 | 395.10 | 4903.40 | 169.55 | 49.84 | 26.72 | 2.95 | 53.32 | 4.08 | 19.27 |
| MC-LR_100ng/mL_Expt3_3 | MC-LR_100 | data not available | 185.20 | 253.62 | 111.39 | 402.98 | 968.93 | 31.65 | 45.77 | 26.92 | 3.05 | 50.44 | 5.00 | 19.09 |
| MC-LR_500ng/mL_Expt1_1 | MC-LR_500 | 1202.8 | 62.16 | 114.23 | 36.02 | 317.51 | 17.20 | 2.04 | 63.63 | 9.29 | 7.23 | 21.59 | 1.38 | 13.42 |

| Sample | Code | | | | | | | | | | | | | |
|---|---|---|---|---|---|---|---|---|---|---|---|---|---|---|
| MC-LR_500ng/mL_Expt1_2 | MC-LR_500 | 1246.8 | 51.77 | 156.71 | 38.95 | 321.99 | 17.92 | 2.08 | 78.09 | 9.37 | 6.27 | 30.60 | 1.30 | 11.91 |
| MC-LR_500ng/mL_Expt1_3 | MC-LR_500 | 1193.5 | 43.67 | 125.31 | 30.10 | 303.50 | 16.77 | 2.26 | 95.20 | 8.64 | 5.97 | 18.23 | 1.05 | 11.54 |
| MC-LR_500ng/mL_Expt2_1 | MC-LR_500 | 983.2 | 105.19 | 190.35 | 88.98 | 271.87 | 17.03 | 1.01 | 84.16 | 8.14 | 36.99 | 27.54 | 4.20 | 13.14 |
| MC-LR_500ng/mL_Expt2_2 | MC-LR_500 | 1188.0 | 111.72 | 208.39 | 66.29 | 372.04 | 16.68 | 1.05 | 70.93 | 10.75 | 51.40 | 38.27 | 4.59 | 13.81 |
| MC-LR_500ng/mL_Expt2_3 | MC-LR_500 | 1338.7 | 109.89 | 406.46 | 110.61 | 452.17 | 17.21 | 1.08 | 113.95 | 9.64 | 50.21 | 37.38 | 5.93 | 15.07 |
| MC-LR_500ng/mL_Expt3_1 | MC-LR_500 | data not available | 145.19 | 140.87 | 48.52 | 332.28 | 22.26 | 1.44 | 32.33 | 9.82 | 2.31 | 28.12 | 5.01 | 17.79 |
| MC-LR_500ng/mL_Expt3_2 | MC-LR_500 | data not available | 148.43 | 144.86 | 51.21 | 348.70 | 22.04 | 1.41 | 31.75 | 9.34 | 2.35 | 29.29 | 5.12 | 17.51 |
| MC-LR_500ng/mL_Expt3_3 | MC-LR_500 | data not available | 136.02 | 139.23 | 51.10 | 354.47 | 21.43 | 1.44 | 38.30 | 9.33 | 1.96 | 33.27 | 5.62 | 19.77 |
| MC-LR_1000ng/mL_Expt1_1 | MC-LR_1000 | 1210.1 | 45.07 | 145.46 | 33.74 | 311.67 | 14.62 | 2.11 | 73.83 | 8.99 | 6.90 | 22.77 | 1.20 | 11.74 |
| MC-LR_1000ng/mL_Expt1_2 | MC-LR_1000 | 1256.5 | 53.69 | 142.65 | 35.44 | 323.24 | 17.39 | 2.26 | 71.86 | 8.81 | 6.63 | 28.21 | 1.25 | 12.08 |
| MC-LR_1000ng/mL_Expt1_3 | MC-LR_1000 | 1428.8 | 53.88 | 161.27 | 38.73 | 309.73 | 18.98 | 2.46 | 89.79 | 8.81 | 6.35 | 28.53 | 1.34 | 10.90 |
| MC-LR_1000ng/mL_Expt2_1 | MC-LR_1000 | 1325.1 | 103.59 | 254.14 | 70.98 | 426.83 | 14.84 | 1.04 | 88.34 | 11.02 | 57.96 | 43.16 | 3.47 | 13.87 |
| MC-LR_1000ng/mL_Expt2_2 | MC-LR_1000 | 1567.5 | 123.27 | 308.24 | 68.41 | 472.94 | 19.41 | 1.25 | 82.00 | 10.79 | 58.54 | 43.58 | 4.94 | 18.22 |
| MC-LR_1000ng/mL_Expt2_3 | MC-LR_1000 | 1464.4 | 122.92 | 231.29 | 58.58 | 481.02 | 17.20 | 1.10 | 82.79 | 10.93 | 52.75 | 39.28 | 4.76 | 16.13 |
| MC-LR_1000ng/mL_Expt3_1 | MC-LR_1000 | data not available | 171.99 | 373.28 | 159.16 | 419.23 | 2017.01 | 67.61 | 92.63 | 16.43 | 2.94 | 48.80 | 4.04 | 19.42 |

| Sample | Code | | | | | | | | | | | | |
|---|---|---|---|---|---|---|---|---|---|---|---|---|---|
| MC-LR_1000ng/mL_Expt3_2 | MC-LR_100 0 | data not available | 166.26 | 256.93 | 105.71 | 415.31 | 1593.53 | 56.07 | 66.65 | 16.76 | 3.07 | 46.48 | 3.82 | 18.55 |
| MC-LR_1000ng/mL_Expt3_3 | MC-LR_100 0 | data not available | 185.88 | 242.09 | 102.55 | 406.93 | 2592.40 | 90.09 | 62.89 | 16.54 | 2.54 | 55.61 | 3.77 | 18.02 |
| nineMCs/NOD-R mix_1ng/mL (each toxin)_Expt1_1 | MC-mix_1 | 1392.5 | 68.85 | 182.51 | 41.56 | 370.36 | 21.26 | 2.25 | 69.44 | 12.89 | 9.89 | 25.68 | 2.28 | 14.45 |
| nineMCs/NOD-R mix_1ng/mL (each toxin)_Expt1_2 | MC-mix_1 | 1399.4 | 64.40 | 161.98 | 41.72 | 370.83 | 19.38 | 2.02 | 72.66 | 10.01 | 7.27 | 21.18 | 2.17 | 14.44 |
| nineMCs/NOD-R mix_1ng/mL (each toxin)_Expt1_3 | MC-mix_1 | 1374.0 | 70.78 | 135.83 | 34.27 | 347.75 | 22.23 | 2.08 | 66.81 | 9.57 | 7.92 | 19.47 | 2.45 | 14.50 |
| nineMCs/NOD-R mix_1ng/mL (each toxin)_Expt2_1 | MC-mix_1 | 1272.6 | 131.83 | 181.89 | 67.31 | 394.65 | 19.50 | 1.05 | 46.38 | 8.00 | 51.61 | 38.42 | 9.26 | 14.18 |
| nineMCs/NOD-R mix_1ng/mL (each toxin)_Expt2_2 | MC-mix_1 | 1449.4 | 129.17 | 200.79 | 72.05 | 420.11 | 18.15 | 1.07 | 56.98 | 8.70 | 53.30 | 39.69 | 10.46 | 15.05 |
| nineMCs/NOD-R mix_1ng/mL (each toxin)_Expt2_3 | MC-mix_1 | 1286.5 | 126.36 | 216.16 | 80.46 | 437.02 | 19.97 | 1.10 | 72.22 | 8.91 | 54.44 | 40.53 | 10.25 | 15.05 |
| nineMCs/NOD-R mix_1ng/mL (each toxin)_Expt3_1 | MC-mix_1 | data not available | 128.61 | 195.25 | 77.90 | 366.18 | 2450.89 | 94.02 | 44.81 | 14.83 | 1.77 | 45.27 | 2.85 | 15.07 |
| nineMCs/NOD-R mix_1ng/mL (each toxin)_Expt3_2 | MC-mix_1 | data not available | 138.90 | 186.97 | 83.94 | 371.44 | 4242.40 | 163.16 | 46.44 | 14.01 | 2.03 | 45.60 | 3.13 | 15.30 |
| nineMCs/NOD-R mix_1ng/mL (each toxin)_Expt3_3 | MC-mix_1 | data not available | 131.70 | 172.53 | 72.95 | 361.06 | 2408.64 | 110.03 | 52.03 | 14.64 | 1.64 | 38.23 | 2.75 | 14.52 |
| nineMCs/NOD-R mix_5ng/mL (each toxin)_Expt1_1 | MC-mix_5 | 1249.6 | 76.06 | 128.06 | 44.37 | 310.87 | 19.73 | 1.86 | 67.60 | 12.30 | 8.76 | 24.58 | 2.05 | 13.63 |
| nineMCs/NOD-R mix_5ng/mL (each toxin)_Expt1_2 | MC-mix_5 | 1116.4 | 73.24 | 144.38 | 45.81 | 315.04 | 18.84 | 2.11 | 63.07 | 11.70 | 8.67 | 22.83 | 2.11 | 12.04 |
| nineMCs/NOD-R mix_5ng/mL (each toxin)_Expt1_3 | MC-mix_5 | 1306.3 | 67.61 | 134.92 | 43.23 | 290.74 | 17.75 | 2.05 | 57.70 | 11.03 | 8.44 | 22.94 | 2.24 | 12.61 |
| nineMCs/NOD-R mix_5ng/mL (each toxin)_Expt2_1 | MC-mix_5 | 1291.0 | 111.97 | 185.48 | 66.53 | 398.54 | 18.55 | 1.03 | 63.65 | 8.04 | 49.32 | 36.72 | 8.75 | 14.24 |

| | | | | | | | | | | | | | | |
|---|---|---|---|---|---|---|---|---|---|---|---|---|---|---|
| nineMCs/NOD-R mix_5ng/mL (each toxin)_Expt2_2 | MC-mix_5 | 1469.4 | 126.30 | 213.32 | 76.81 | 433.87 | 18.76 | 1.03 | 60.10 | 8.59 | 50.01 | 37.23 | 9.52 | 14.87 |
| nineMCs/NOD-R mix_5ng/mL (each toxin)_Expt2_3 | MC-mix_5 | 1374.4 | 154.95 | 189.19 | 79.08 | 406.99 | 18.19 | 0.93 | 56.03 | 7.57 | 55.60 | 41.39 | 10.19 | 15.23 |
| nineMCs/NOD-R mix_5ng/mL (each toxin)_Expt3_1 | MC-mix_5 | data not available | 134.31 | 169.74 | 92.29 | 388.60 | 873.46 | 11.71 | 53.43 | 15.73 | 2.15 | 39.89 | 3.25 | 15.89 |
| nineMCs/NOD-R mix_5ng/mL (each toxin)_Expt3_2 | MC-mix_5 | data not available | 137.61 | 139.07 | 66.39 | 379.76 | 1191.33 | 61.00 | 38.15 | 13.85 | 1.97 | 40.19 | 3.03 | 14.83 |
| nineMCs/NOD-R mix_5ng/mL (each toxin)_Expt3_3 | MC-mix_5 | data not available | 121.55 | 154.58 | 75.61 | 354.46 | 1420.11 | 72.77 | 43.22 | 13.17 | 1.71 | 37.02 | 3.37 | 14.22 |
| nineMCs/NOD-R mix_100ng/mL (each toxin)_Expt1_1 | MC-mix_100 | 1235.2 | 55.83 | 163.22 | 40.50 | 297.59 | 17.60 | 2.51 | 67.60 | 8.16 | 6.00 | 24.01 | 1.50 | 12.70 |
| nineMCs/NOD-R mix_100ng/mL (each toxin)_Expt1_2 | MC-mix_100 | 1159.1 | 51.70 | 122.23 | 30.21 | 292.98 | 10.27 | 1.34 | 64.78 | 7.42 | 7.14 | 17.18 | 1.77 | 10.28 |
| nineMCs/NOD-R mix_100ng/mL (each toxin)_Expt1_3 | MC-mix_100 | 1202.9 | 56.56 | 143.72 | 38.33 | 316.67 | 20.46 | 2.62 | 74.18 | 7.45 | 5.84 | 19.09 | 1.57 | 11.57 |
| nineMCs/NOD-R mix_100ng/mL (each toxin)_Expt2_1 | MC-mix_100 | 1342.4 | 122.47 | 151.84 | 58.04 | 400.21 | 16.73 | 1.07 | 43.17 | 9.58 | 47.75 | 35.55 | 9.72 | 14.71 |
| nineMCs/NOD-R mix_100ng/mL (each toxin)_Expt2_2 | MC-mix_100 | 1349.4 | 114.73 | 184.28 | 68.94 | 411.51 | 17.70 | 1.17 | 55.36 | 6.97 | 43.24 | 32.19 | 8.64 | 14.05 |
| nineMCs/NOD-R mix_100ng/mL (each toxin)_Expt2_3 | MC-mix_100 | 1326.6 | 108.78 | 174.50 | 60.45 | 422.40 | 18.01 | 1.24 | 62.99 | 7.57 | 43.32 | 32.25 | 9.55 | 14.70 |
| nineMCs/NOD-R mix_100ng/mL (each toxin)_Expt3_1 | MC-mix_100 | data not available | 101.63 | 152.59 | 63.11 | 334.21 | 570.55 | 44.85 | 47.74 | 10.94 | 1.69 | 34.91 | 2.20 | 12.23 |